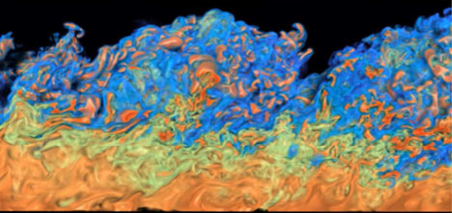
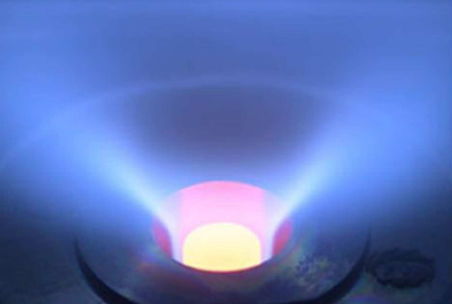
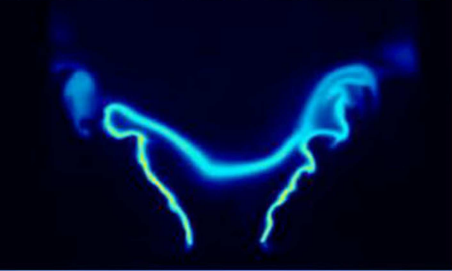
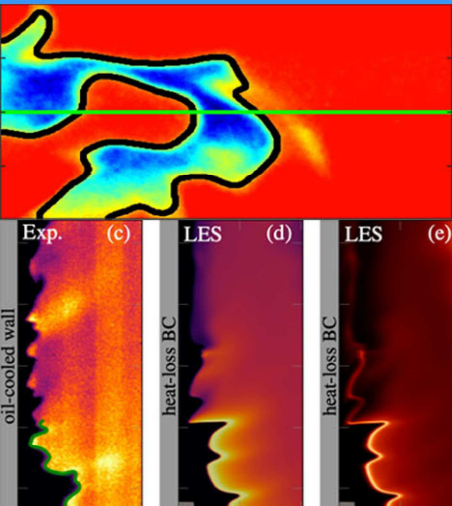
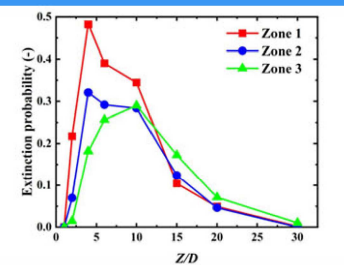
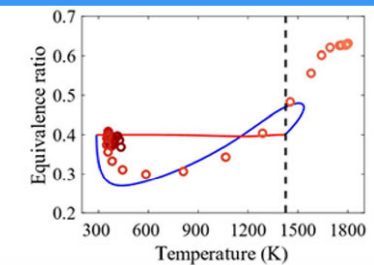
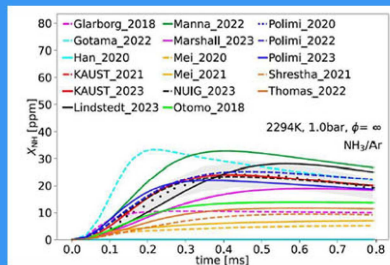
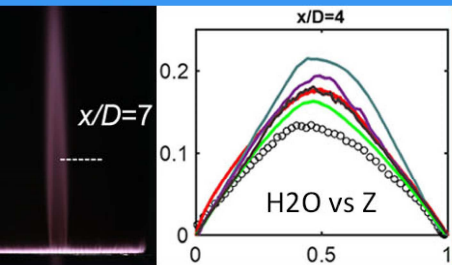


# TNF Workshop

# PTF Workshop



Satellite Workshops of the CI 40<sup>th</sup> International Symposium  
Politecnico di Milano, 20-21 July 2024





## 2024 TNF/PTF Workshop Proceedings – Table of Contents

Cover Page .....	1
Table of Contents .....	2
Workshop Summary .....	6
Workshop Organizers .....	11
Workshop Sponsors .....	12
TNF Registration List .....	13
PTF Registration List .....	15
PTF Workshop Presenters and Titles .....	17
TNF Agenda with Combined TNF/PTF Sessions .....	18
<b>TNF Session: Fundamentals of Premixed Flames of H<sub>2</sub> and H<sub>2</sub> Blends</b> .....	19
<i>Coordinators: Heinz Pitsch and Andy Aspden</i>	
Summary .....	19
Slides – Lean premixed hydrogen flames: Updates since Vancouver – <i>Howarth</i> .....	21
Slides – Sharing of Combustion Data – <i>Rieth, Aspden, Gauding, Dawson, Li</i> .....	30
<b>TNF Session: Chemical Kinetics for Ammonia Combustion</b> .....	38
<i>Coordinator: R. Peter Lindstedt</i>	
Summary (to be added) .....	38
Slides – Chemical kinetics for ammonia combustion – <i>Lindstedt</i> .....	40
Slides – Ammonia kinetics: Can TNF-like experimental tools help– <i>Magnotti</i> .....	56
<b>TNF Session: Comparisons on the HYLON Burner</b> .....	71
<i>Coordinators: Thierry Poinsot and Thierry Schuller</i>	
Summary .....	71
Slides – Introduction to HYLON phase 1 – <i>Poinsot</i> .....	72
Slides – HYLON setup: Hydrogen low NO <sub>x</sub> injector – <i>Schuller</i> .....	74
Slides – CFD results obtained by the participants – <i>Poinsot</i> .....	90
Slides – Main conclusions and HYLON phase 2 – <i>Poinsot</i> .....	111





<b>TNF Session: AI/ML for Turbulence-Chemistry Interaction</b> .....	130
<i>Coordinators: Matthias Ihme and Alessandro Parente</i>	
Summary .....	130
Slides – Introduction .....	132
Slides – ML for Combustion Modeling .....	135
Slides – ML for Experimental Analysis .....	159
Slides – Discussion .....	173
<b>TNF Session: Flame-Wall Interaction</b> .....	178
<i>Coordinators: Christian Hasse and Andreas Dreizler</i>	
Summary .....	178
Slides – Experiments – <i>Dreizler</i> .....	186
Slides – Modeling and Simulation – <i>Hasse</i> .....	210
<b>TNF Session: Partially Premixed NH<sub>3</sub>/H<sub>2</sub>/N<sub>2</sub>/Air Piloted Jet Flames</b> .....	242
<i>Coordinators: Gaetano Magnotti and Hong Im)</i>	
Summary .....	242
Slides – Introduction and experimental overview – <i>Magnotti</i> .....	244
Slides – Joint experimental-numerical comparisons – <i>Guo</i> .....	250
<b>TNF Session: Possible Future TNF Target Cases</b> .....	278
<i>Coordinator: Robert Barlow</i>	
Summary .....	278
Slides – Introduction – <i>Barlow</i> .....	279
Slides – Sydney flames – <i>Dunn</i> .....	280
Slides – KAUST flames – <i>Magnotti</i> .....	293
Slides – DLR, TUD, and All-Candidate Gallery – <i>Barlow</i> .....	310
<b>TNF Session: Final Discussions</b> .....	315
<i>Coordinator: Christian Hasse</i>	
Summary .....	315
Slides – Final TNF Summary and Discussion – <i>Hasse</i> .....	319



<b>TNF Poster Abstracts</b> .....	334
List of first authors and titles .....	334
<i>Al-Kassar</i> Turbulent lean premixed hydrogen flames at high pressure and high temperature .....	335
<i>Berger</i> A priori and a posteriori analysis of an LES combustion model for turbulent hydrogen flames with thermodiffusive instabilities .....	337
<i>Brouzet</i> Effect of sustainable aviation fuel on the direct and indirect noise of a next generation aviation gas turbine.....	339
<i>Cassese</i> Preferential diffusion effects on tabulated chemistry methods for hydrogen/methane and hydrogen/ammonia blends.....	341
<i>Chi</i> Flame thickening during turbulent flame-wall interactions .....	343
<i>Chu</i> Interactions of differential diffusion and mixture inhomogeneities in hydrogen and iso-octane flame kernels under engine conditions ..	345
<i>Cohen</i> Calculating Temperature and Species Concentration from Quasi-2D Combustion Video Data using Physics-Informed Neural Networks	347
<i>Dillon</i> Filtered tabulated chemistry for multi-regime combustion with application to dual-swirl HYLON injector .....	349
<i>Jose</i> ML-augmented diagnostics for feature extraction incorporating deep learning and GPU acceleration methods .....	351
<i>Kaddar</i> Ammonia-hydrogen combustion modelling enabled by high-performance GPU computing .....	353
<i>Kang</i> Effect of swirl-afflicted turbulence on pressure swirl spray in high-momentum jet-stabilised burners .....	355
<i>Niemeitz</i> CO emissions in turbulent premixed methane/hydrogen jet flames interacting with isothermal walls .....	357
<i>Palulli</i> Analysis of NO formation pathways based on extended proper orthogonal decomposition in a swirl-stabilised, hydrogen-fueled gas turbine combustor .....	359
<i>Petry</i> Investigation of hydrogen-air mixing behavior in an atmospheric jet-stabilized single nozzle combustor using 1-D laser Raman spectroscopy .....	361
<i>Richter</i> Measurements of NO in the product gases of laminar premixed NH <sub>3</sub> /H <sub>2</sub> /N <sub>2</sub> -air and NH <sub>3</sub> /CH <sub>4</sub> -air flames using laser induced fluorescence .....	363
<i>Schneider</i> Near-wall H <sub>2</sub> combustion .....	365





<i>Schuh</i>	Model extension for the artificially thickened flame approach for lean hydrogen-ammonia flame ..... 367
<i>Tang</i>	Large eddy simulation of the KAUST piloted ammonia flame with the flamelet-generated manifold method ..... 369
<i>Tian</i>	The impact of mixing models and molecular transport in turbulent non-premixed NH <sub>3</sub> /H <sub>2</sub> /N <sub>2</sub> / jet flames at elevated pressure ..... 371
<i>Walia</i>	Direct Numerical Simulation of flames in high-speed flows ..... 373
<i>Wang</i>	Large eddy simulation of the KAUST piloted ammonia flame with the direct moment closure model ..... 375
<i>Xing</i>	A direct numerical simulation study on the KAUST piloted cracked ammonia flames with detailed chemistry ..... 377

# Summary of TNF16 and Planning for TNF17

*Robert Barlow and Christian Hasse*

The TNF16 workshop (International Workshop on Measurement and Computation of Turbulent Flames) was held at Politecnico di Milano on 20-21 July 2024 as one of five co-located satellite workshops of the Combustion Institute International Symposium. Sessions on the first day were held jointly with the Premixed Turbulent Flames (PTF) workshop, such that the agenda included a blend of TNF-style curated sessions and PTF-style individual talks on connected topics. The combined attendance was of over 150.

This summary briefly outlines the scope and history of the TNF series, the contents of the six TNF-lead topical sessions, some key discussion points as expressed in Christian Hasse's summary from the final TNF session, and steps being undertaken to prepare for TNF17 in 2026.

The TNF16 Proceedings and the proceedings from all previous TNF workshops may be downloaded from [tnfworkshop.org](http://tnfworkshop.org). Summaries and presentation slides for the TNF16 sessions are included, along with TNF poster abstracts, while the slides and abstracts for the PTF contributed talks are available from the [PTF website](#).

**IMPORTANT NOTE:** Results presented at the TNF Workshop may represent work in progress. It would be inappropriate to quote or reference unpublished information from the proceedings without first checking with the authors for permission and for the latest information on results and references.

## **TNF Scope and History**

The TNF workshop focuses on fundamental issues of turbulence chemistry interactions in gaseous flames. The objectives are to:

- Establish a library of well-documented flames that advance fundamental scientific understanding of turbulent combustion and are appropriate for testing and extending models for complex combustion systems.
- Provide a framework for collaborative comparisons of reference data from experiments and DNS with modeled results from LES.
- Identify priorities for further experimental and computational research.

One TNF legacy – among others – is the availability of instantaneous and averaged thermochemical states from Raman/Rayleigh experiments that are crucial for turbulent combustion model development and validation. Up to TNF14 in Dublin (2018), a wide range of flames with different modes (premixed, stratified, partially premixed, non-premixed) and regimes ( $Re$ ,  $Da$ ,  $Ka$  number) were investigated mostly for  $CH_4$ , with only small excursions to DME and very early (before 2000) also to  $H_2$ . TNF sessions evolved around data sets from target flames, and the numerical results from different groups were compared to experimental data. Preliminary and work-in-progress results were submitted. The open workshop atmosphere allowed discussions on the physics of the flames and how the models could be improved. Modeling results usually improved substantially from workshop to workshop, and new experimental configurations were discussed to challenge the models.

In Vancouver (2022), as a practical response to a lower overall attendance due to lingering effects of the COVID pandemic, all sessions were held jointly with the PTF workshop. There were substantially fewer TNF-style discussions on burners and model deficiencies. Interest had decreased for pure hydrocarbon target flames, and there was only one session on the Darmstadt Multi Regime Burner. Despite the large interest in  $H_2$  and  $NH_3$  as carbon-free fuels, experimental data were not yet available; only first DNS data for premixed  $H_2$  flames had been generated. While this did not allow for a TNF-



style comparison, the discussion session on modeling was very intense and engaging. That clearly showed the need for new reference data sets.

## **TNF16 Topical Sessions**

A major development between 2022 and 2024 was that several new data sets for flames of carbon-free fuels became available. This allowed a return to one of the central activities of the TNF workshop series – collaborative comparisons of measured and modeled results for selected target flames. Joint TNF/PTF sessions were also part of the TNF16 program, which combined TNF-style curated sessions with PTF-style contributed individual talks on connected topics. The six TNF-lead topical sessions are briefly outlined below.

### **Fundamentals of Premixed Hydrogen Flames**

This was a return topic from the Vancouver workshop that is of great current interest to the turbulent flame community. The session aimed to give a comprehensive review, assembled by Thomas Howarth, of new research on both laminar and turbulent flames that has occurred since the Vancouver TNF/PTF workshop and to highlight some currently unanswered questions. Corresponding references are listed in the session summary. Brief descriptions of available data sets on turbulent lean premixed hydrogen flames, from both DNS and experiments, were also presented.

The review of turbulent H<sub>2</sub> flames and the subsequent discussion were very engaging and identified several open scientific questions especially for lean H<sub>2</sub> flames. These include among others:

- How does the thermo-diffusive instability (TDI) interact with turbulence? Is the interaction synergistic?
- How does the interaction of turbulence and TDI change for high Ka numbers?
- What are the governing parameters?  $Ze$ ,  $Ka$ ,  $Pe$  and/or others?
- How to model flames under high pressure. Do the observed differences between high- and low-pressure laminar flames carry over to turbulent flames?

This non-exhaustive list clearly demonstrates the need for TNF-style target flames from experiments and DNS to systematically address these scientific questions.

### **Chemical Kinetics for Ammonia Combustion**

Ammonia is a “hot” topic as a potential alternative fuel or hydrogen carrier. However, in spite of the long history of research on the chemical kinetics of ammonia as a NO<sub>x</sub> reduction additive and, more recently, on ammonia as a fuel, there are still significant areas of disagreement among the numerous kinetic models for ammonia combustion that have been published in recent years. This is especially true for the kinetics of pollutant formation, which is a key challenge for ammonia combustion technologies. This is a relevant topic for the TNF community because it is essential to have reliable kinetic models in order to conduct informative comparisons of measurements and simulations of turbulent flames.

In this session, Peter Lindstedt provided some background on ammonia chemistry and an overview of the current state of kinetic mechanisms, with attention to appropriate criteria for assessing kinetic models and areas of uncertainty. The role of flame data in kinetic model validation and some ways in which the TNF community might collaborate with kinetic modelers were also addressed. The second part of the session, presented by Gaetano Magnotti, examined the potential for TNF-type diagnostic tools to contribute toward the development and validation of kinetic models for ammonia, with the main focus being on multi-scalar experiments in laminar flames, including both published examples and possible future experiments.

Looking forward, there are current uncertainties for some key fundamental reaction sequences and these will need to be addressed by the kinetics community. Thus, chemical mechanisms for DNS and LES are likely to evolve over the next years, and needs to be considered in the planning of the numerical work.

### **Comparisons on the HYLON Burner**

The HYLON burner, which was developed under a large EU project, uses a swirled hydrogen-air injection system within a model gas turbine burner geometry. This session, presented by Thierry Poinot and Thierry Schuller, introduced this ongoing project to the TNF/PTF audience by reviewing the burner design features and its extensive experimental characterization, and by summarizing comparisons of those measurements with results from twenty-five modeling groups that had computed two selected flame cases operated at 1 bar and featuring different modes of flame stabilization. The next phase of this project will use a new version of the burner (HYLON2) to extend the studies to elevated pressure up to 10 bar, with experimental measurements being carried out at KAUST.

### **Comparisons on Piloted Ammonia Jet Flames**

The objective of the session was to compare recent experimental measurements (from KAUST) and numerical simulations of a series of turbulent partially-premixed  $H_2/N_2/NH_3$ -air flames stabilized on the Sydney piloted burner. Following the example of the Sandia piloted methane flame series, three cracked-ammonia flames (labeled D, E, F) were measured, with jet Reynolds numbers of 24000, 32000, and 36000, corresponding to 59%, 79%, and 89% of the global blowoff condition. These flames are characterized by varying levels of local extinction and effects of differential diffusion, both of which present challenges to numerical simulations. Nine teams were involved in the simulations, which were preliminary at this stage because the experimental data had been released only a few months before the workshop.

Overall, this dataset was deemed interesting by the TNF community, and the large number of groups involved despite the short time available for the simulation promises that in-depth analysis, conditioned on the type of models used, will be possible. To go further with the analysis, significant improvement of the mixture fraction field will be necessary prior to analyzing the effect of different turbulence-combustion models. Velocity measurements, especially in the near field, would be desirable to help converge to common and more detailed boundary conditions for all the simulations.

### **AI/ML for Turbulence-Chemistry Interaction**

ML for combustion was introduced as a TNF focus topic in 2022. Since then, various ML methods have been adopted and extended by the combustion community to address problems of turbulent combustion modeling and experimental analysis. This session reviewed recent advances with the goal for connecting the broad field of ML to TNF/PTF-related problems. The session was divided into three topics: 1) Background and nomenclature on ML for combustion: 2) Recent developments of ML methods for turbulent combustion modeling: and 3) Applications of ML methods to extract knowledge from experimental data. The presentations included nine contributions from the TNF and PTF community.

The next key challenges involve: data, benchmarks, and metrics; common models, methods, and approaches; and best practice. It was suggested to identify benchmark problems for ML-applications following the TNF approach. This will allow to evaluate ML-based approaches, e.g., for manifold parameterization or combustion modeling in general. There is interest in sharing ML-models through TNF/PTF infrastructure and by this establish best practice guidelines for ML-model selection, ML-training, and ML-evaluation. The need for diverse data sets accessible to the combustion community was also discussed, and the BLASTNet database (<https://blastnet.github.io>) was offered as a repository for data contributed by workshop participants and the broader combustion community.



## Flame-Wall Interaction

Flame-wall interaction (FWI) has been a TNF topic since 2014. Experimental and numerical work initially focused on side wall quenching of laminar and turbulent, premixed CH<sub>4</sub>/air flames. The scope was broadened in 2022 to include interaction of flame with cooling air near a wall and FWI within a crevice. This TNF16 session provided an update on experimental and numerical efforts, identified common findings and key challenges from different FWI studies, and outlined next steps for FWI research. There have been significant recent activities involving H<sub>2</sub> and NH<sub>3</sub>. With these new fuels, an expanded scope with active walls and safety, and the corresponding new configurations, there is a good opportunity to bring experiments and simulations closer together in the spirit of the TNF tradition. With respect to hydrogen, it was noted that the near-wall chemical kinetics of rich hydrogen flames is a key area to be addressed before TNF17. A detailed summary of the FWI session is included in the proceedings.

## Future Target Flames – Experiments and/or DNS

The availability of reference data on carbon-free fuels has substantially improved over the last two years. TNF-style comparisons were presented for the Hylon burner and the KAUST piloted NH<sub>3</sub>/H<sub>2</sub> jet flames, and both HYLON2 and the KAUST piloted flame are likely targets for the next workshop. Several more potential target cases were introduced during the workshop, including experimental data sets from Sydney, KAUST, TU Darmstadt, and others, as well as several DNS datasets, mainly for premixed hydrogen flames. This session simply outlined all the potential candidates for collaborative comparison with simulations, while next steps for selecting specific target cases for TNF 17 were addressed in the final discussion session and are outlined below.

## Key Points and Decisions

Turbulent H<sub>2</sub> and NH<sub>3</sub> flames at atmospheric and pressurized conditions are still poorly understood, and turbulence chemistry interaction models are still in the early stages. The dynamics of hydrogen flames change substantially under pressure, so the extrapolation of atmospheric results to technically relevant conditions is more challenging than previously for hydrocarbon flames. Experiments and DNS for pressurized flames remain a formidable challenge that needs to be coordinated between TNF16 and TNF17. The increasing availability of high-quality experimental and numerical data sets for hydrogen and ammonia flames will allow for TNF-style comparisons at TNF17, aiming to *first break and then advance the models*.

Flashback and flame-wall interaction continue to be relevant topics in the TNF scope. Effusion cooling and active walls are to be considered in the future. The availability of reliable NH<sub>3</sub> kinetics and H<sub>2</sub> near-wall chemistry remain open issues. The selection of chemical mechanisms for TNF target flames should be coordinated to ensure a consistent comparison at TNF17.

The TNF community expressed its strong commitment to return to the more original TNF format with discussion evolving around target flame data sets. In contrast to previous workshops, this will feature not only experimental but also numerical DNS data sets. It is expected that more target flame sessions will be required for TNF17 compared to TNF15 and TNF16.

## Next Steps for TNF17

### 1. Provide an overview of experimental target flames and data sets

Coordinators: Dreizler, Hasse (TU Darmstadt)

TU Darmstadt will prepare brief descriptions (one-pagers) for their experimental configurations as examples. These will include short descriptions of the setup, the employed diagnostics, and the data. Target flame descriptions can include both available data and future data with an approximate date when it can be shared with the TNF community. Data can also include supporting numerical data, e.g., detailed flow conditions from an inflow-LES.

This description can be used as templates for other groups to describe their target flames. These descriptions will be shared among the TNF participants and eventually be published on the TNF website.

Research Data Management has become an important aspect for most funding schemes and recommended data repositories may vary within the TNF community. It was decided that data will be made available by the individual groups using their preferred platform. The data will be assigned a DOI as a unique identifier. New DOIs will be continuously added to the experimental one-pager and published on the TNF website.

## **2. Provide an overview of DNS target flames and data sets**

Coordinator: Attili (University of Edinburgh)

Similarly to the experimental data, University of Edinburgh will prepare a one-pager for the DNS configurations. Following this template, TNF participants working on DNS are invited to provide the description of their own configurations. The aim is to identify a sequences of DNS configurations with increasing complexity, e.g., flame in a box → flame in a temporally evolving shear layer → shear flame.

Sharing the descriptions and the data will follow the approach outlined above for the experimental data.

## **3. Aligning experimental/DNS work with modeling/LES between TNF16 and TNF17**

Coordinators: Dreizler, Hasse (TU Darmstadt)

The one-pagers for experiments and DNS will be shared with the TNF community interested in model turbulent combustion model development and LES. These groups will indicate which flames they will be working on for TNF17. This information will be helpful for both the experimental and DNS groups to better plan their next steps.

The planning should be available spring 2025 and should be updated towards the end of 2025 around the submission deadline for the 41<sup>st</sup> Symposium.

## **4. Chemical kinetics for TNF target flames**

Coordinators: Stagni (Politecnico di Milano), Magnotti (KAUST)

The current uncertainty in NH<sub>3</sub> kinetics and near-wall H<sub>2</sub> kinetics is a challenge for a consistent comparison of experiments/DNS and LES. It is expected that mechanisms will improve in the near future and new versions will be released.

**NH<sub>3</sub>:** When comparing to DNS data, the same mechanism should be used in LES. When comparing to experimental TNF data, a few suitable TNF-preferred mechanisms will be identified and suggested for LES use. The suggestions will be shared with the TNF community and be published on the TNF website. The TNF community can also support the mechanism development with thermochemical states from Raman/Rayleigh/LIF in laminar counterflow flames. This can also include data at higher pressures of up to 5 bars at KAUST.

**H<sub>2</sub> near-wall:** Several TNF participants indicated their interest to discuss the issue with colleagues, e.g. from Material Sciences.

Feedback concerning NH<sub>3</sub> and H<sub>2</sub> near-wall should be given to A. Stagni, who will summarize potential next steps.



## TNF16 Organizing Committee



**Robert Barlow**  
Barlow Combustion Research  
USA



**Andreas Dreizler**  
Technical University of  
Darmstadt  
Germany



**Benoît Fiorina**  
Ecole CentraleSupélec  
France



**Christian Hasse**  
Technical University of  
Darmstadt  
Germany



**Matthias Ihme**  
Stanford University  
USA



**Andreas Kempf**  
University Duisburg-Essen  
Germany



**Peter Lindstedt**  
Imperial College London  
UK



**Gaetano Magnotti**  
King Abdullah University  
of Science and Technology  
Saudi Arabia



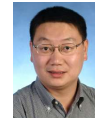
**Asaad Masri**  
University of Sydney  
Australia



**Joseph Oefelein**  
Georgia Tech  
USA



**Heinz Pitsch**  
RWTH Aachen University  
Germany



**Zhuyin Ren**  
Tsinghua University  
China



**Prof. Luc Vervisch**  
INSA Rouen, CORIA  
France

tnfworkshop.org

mission | data archives | proceedings | contacts

TNF/PTF Workshops

Milan, Italy 20-21 July 2024

## PTF Organizers

- Andy Aspden, Newcastle University, UK
- Aaron Skiba, Air Force Research Laboratory, USA
- Sina Kheirkhah, University of British Columbia, Canada



<https://sites.google.com/view/ptf-workshop/home>



TNF/PTF Workshops

Milan, Italy 20-21 July 2024



## SPONSORS



**SFB/Transregio 150**  
Turbulente, chemisch reagierende  
Mehrphasenströmungen in Wandnähe



TECHNISCHE  
UNIVERSITÄT  
DARMSTADT





### TNF Registration List

<b>Surname</b>	<b>Given Name</b>	<b>Affiliation</b>	<b>Country</b>
Akamatsu	Fumiteru	Osaka University	Japan
Aksel	Ånestad	NTNU	Norway
Al Hadi	Zeinab	KAUST	Saudi Arabia
Albalawi	Alfaisal	KAUST	Saudi Arabia
Angelilli	Lorenzo	University of Michigan	United States
Ariemma	Giovanni Battista	STEMS-CNR	Italy
Attili	Antonio	University of Edinburgh	United Kingdom
Balachandran	Achuth Nair	Converge CFD	Austria
Ballotti	Andrea	UNIFI	Italy
Barlow	Robert	Barlow Combustion Research	United States
Basnet	Suman	KAUST	Saudi Arabia
Bathaei	Sayedmehrddad	University of Duisburg-Essen	Germany
Cassese	Biagio	University Federico II Napoli	Italy
Chen	Zhi	Peking University	P.R. China
Chi	Cheng	Otto von Guericke Uni., Magdeburg	Germany
Chu	Hongchao	ITV RWTH Aachen University	Germany
Cohen	Benjamin	University of Southern California	United States
Cuoci	Alberto	Politecnico di Milano	Italy
Dawson	James	NTNU	Norway
De Nardi	Loïc	CERFACS	France
Dillon	Samuel	CentralSupélec	France
Dreizler	Andreas	TU Darmstadt	Germany
Dufitumukiza	Jean Pierre	Saint-Gobain	France
Dunn	Matthew	University of Sydney	Australia
Dupuy	Anthony	CERFACS	France
Eggels	Ruud	Rolls-Royce	Germany
Fang	Xiaohang	University of Calgary	Canada
Fernandez-Galisteo	Daniel	CIEMAT	Spain
Ferrario	Alessandro	D-Orbit Space	Italy
Fiorina	Benoit	CentralSupélec	France
Fortes Soplanes	Emiliano Manuel	Barcelona Supercomputing Center	Spain
Garcia Guillamon	Carlos	Barcelona Supercomputing Center	Spain
Geyer	Dirk	TU Darmstadt	Germany
Ghani	Abdulla	TU Berlin	Germany
Gicquel	Laurent	CERFACS	France
Go	Young Gun	Doosan	South Korea
Gruber	Andrea	SINTEF	Norway
Guiberti	Thibault	KAUST	Saudi Arabia
Gutierrez Sanchez	Sergio	ITV University of Stuttgart	Germany
Hampp	Fabian	ITV University of Stuttgart	Germany



# TNF Workshop

# PTF Workshop

<b>Surname</b>	<b>Given Name</b>	<b>Affiliation</b>	<b>Country</b>
Han	Lei	Tianjin University	P.R. China
Hasse	Christian	TU Darmstadt	Germany
Hawkes	Evatt	University of New South Wales	Australia
Hernandez-Perez	Francisco Emanuel	KAUST	Saudi Arabia
Hiestermann	Marian	MTU Aero Engines	Germany
Ho	Jen Zen	Stanford University	United States
Ihme	Matthias	Stanford University	United States
Jiangkuan	Xing	Kyoto University	Japan
Kaddar	Driss	TU Darmstadt	Germany
Kang	Yeonse	IVLR University of Stuttgart	Germany
Karakaya	Yasin	Paderborn University	Germany
Karaminejad	Sadrollah	University of Duisburg-Essen	Germany
Kawanabe	Hiroshi	Kyoto University	Japan
Kempf	Andreas	University of Duisburg-Essen	Germany
Kildare	Jordan	University of Adelaide	Australia
Kinaci	Mustafa Efe	Converge CFD	Austria
Kyupeli	Shenol	Converge CFD	Austria
Laera	Davide	Politecnico di Bari	Italy
Li	Han	Peking University	P.R. China
Lim	Joonghyun	Doosan	South Korea
Lindstedt	Peter R	Imperial College London	United Kingdom
Luo	Kun	Zhejiang University	P.R. China
Macfarlane	Andrew	University of Sydney	Australia
Magnotti	Gaetano	KAUST	Saudi Arabia
Mao	Runze	Peking University	P.R. China
Marragou	Sylvain	KAUST	Saudi Arabia
Masri	Assaad	University of Sydney	Australia
Massey	James	Cambridge University	United Kingdom
Mercier	Renaud	Safran Group	France
Michael	Gauding	ITV RWTH Aachen University	Germany
Mira	Daniel	Barcelona Supercomputing Center	Spain
Morii	Youhi	Tohoku University	Japan
Moureau	Vincent	CORIA	France
Navid	Ali	IWTT TU Freiberg	Germany
Niemietz	Kai	ITV RWTH Aachen University	Germany
Palulli	Rahul	KTH	Sweden
Parente	Alessandro	Universite Libre de Bruxelles	Belgium
Peterson	Brian	University of Edinburgh	United Kingdom
Petry	Niklas	DLR-Stuttgart	Germany
Poinsot	Thierry	Institute of Fluid Mechanics of Toulouse	France
Ren	Zhuyin	Tsinghua University	P.R. China
Richter	Martin	NTNU	Germany
Rosati Opazo	Vincenzo	STEMS CNR	Italy



<b>Surname</b>	<b>Given Name</b>	<b>Affiliation</b>	<b>Country</b>
Ruan	Jiangheng	ONERA	France
Schiavone	Francesco Gabriele	Politecnico di Bari	Italy
Schneider	Max	TU Darmstadt	Germany
Scholtissek	Arne	TU Darmstadt	Germany
Schuh	Vinzenz	TU Darmstadt	Germany
Schuller	Thierry	Institute of Fluid Mechanics of Toulouse	France
Sekularac	Nikola	CERFACS	France
Shehab	Hazim	AIST	Japan
Shi	Shuguo	TU Darmstadt	Germany
Shoraka	Yashar	University of Sydney	Australia
Song	Wonsik	NTNU	Norway
Sorrentino	Giancarlo	STEMS CNR	Italy
Stein	Oliver T.	Karlsruhe Institute of Technology	Germany
Taileb	Said	Safran Group	France
Vargas Ruiz	Hector Jose	CERFACS	France
Walia	Gunvir Singh	Indian Institute of Technology Kanpur	India
Wang	Xingjian	Tsinghua University	P.R. China
Wehrfritz	Armin	University of Turku	Finland
Wu	Bin	KAUST	Saudi Arabia
Xinguang	Luo	KAUST	Saudi Arabia
Zhou	Bo	Southern Univ. of Science and Tech.	P.R. China
Zhou	Hua	Tsinghua University	P.R. China
Zhou	Yuchen	Lund University of Technology	P.R. China
Æsøy	Eirik	NTNU	Norway

### PTF Registration List

<b>Surname</b>	<b>Given Name</b>	<b>Affiliation</b>	<b>Country</b>
Aspden	Andy	Newcastle University	United Kingdom
Bai	Xue-Song	Lund University	Sweden
Bajrami	Julian	ITV University of Hannover	Germany
Chaudhuri	Swetaprovo	University of Toronto	Canada
Chen	Jacqueline	Sandia	United States
Creta	Francesco	Sapienza University of Rome	Italy
Dinkelacker	Friedrich	ITV University of Hannover	Germany
Driscoll	James	University of Michigan	United States
Egolfopoulos	Fokion	University of Southern California	United States
Frederick	Mark	Purdue University	United States
Grenga	Temistocle	University of Southampton	United Kingdom





# TNF Workshop

# PTF Workshop

Surname	Given Name	Affiliation	Country
Hayakawa	Akihiro	Tohoku University	Japan
Hochgreb	Simone	Cambridge University	United Kingdom
Hori	Tsukasa	Osaka University	Japan
Howarth	Thomas	ITV RWTH Aachen University	Germany
Jozsa	Viktor	Budapest Uni. of Technol. & Econ.	Hungary
Khamedov	Ruslan	KAUST	Saudi Arabia
Kheirkhah	Sina	University of British Columbia	Canada
Koch	Lars	ITV University of Hannover	Germany
Lapenna	Pasquale Eduardo	Sapienza University of Rome	Italy
Lefkowitz	Joseph	Technion	Israel
Li	Tao	TU Darmstadt	Germany
Lipatnikov	Andrei	Chalmers University	Sweden
Matsumoto	Ryotaro	Tohoku University	Japan
Miyazaki	Shogo	Tohoku University	Japan
Moriyama	Hinata	Tohoku University	Japan
Nista	Ludovico	ITV RWTH Aachen University	Germany
Novoselov	Alex	University of Utah	United States
Okada	Haru	Tohoku University	Japan
Porcarelli	Alessandro	TU Delft	Netherlands
Quentin	Douasbin	CERFACS	France
Rieth	Martin	Sandia	United States
Ronney	Paul	University of Southern California	United States
Savard	Bruno	Polytechnique Montréal	Canada
Senior-Tybora	Weronika	Technion	Israel
Sharma	Priybrat	KAUST	Saudi Arabia
Shen	Si	Technion	Israel
Skiba	Aaron	Air Force Research Laboratory	United States
Steinberg	Adam	Georgia Tech	United States
Tsunoda	Akira	Tohoku University	Japan
Vabre	Martin	Polytechnique Montréal	Canada
Wang	Haiou	Zhejiang University	P.R. China
Wang	Shixing	KAUST	Saudi Arabia
Wen	Xu	Hefei Univ. Science & Technol.	P.R. China
Xia	Yu	Tohoku University	Japan
Yao	Matthew	Princeton University	United States
Zhang	Min	Peking University	P.R. China
Zisen	Li	Polytechnique Montréal	Canada

## PTF Workshop – Contributed Titles

20 – 21 July 2024, Politecnico di Milano, Milan, Italy

Presentation slides are available on the [PTF website](#)

### Joint TNF/PTF Session Talks on Saturday:

Mathew Yao	Decomposition of the turbulent flame speed in lean premixed hydrogen flames
Francesco Creta	Modeling aspects of thermodiffusive instabilities in filtered simulations
Martin Rieth	Premixed hydrogen-enriched flames in intense sheared turbulence and their scaling
Andrei Lipatnikov	Experimental support of leading point concept (lean H <sub>2</sub> /NH <sub>3</sub> /O <sub>2</sub> /N <sub>2</sub> )
Jackie Chen	DNS study of NO <sub>x</sub> formation and flame structure in low-emission ammonia rich-quench-lean combustion
Haiou Wang	Rayleigh-Taylor instability induced turbulence in lean hydrogen/air premixed flames
Sina Kheirkhah	Effects of combustion progress variable, Lewis number, and Karlovitz number on the scalar dissipation rate models of turbulent premixed flames: An experimental study
Bruno Savard	DNS of a laboratory lean H <sub>2</sub> /CH <sub>4</sub> low-swirl flame impinging on a wall
Swetaprovo Chaudhuri	Introducing two novel combustors: a fuel-flex combustor (burning H <sub>2</sub> and/or CH <sub>4</sub> ) and a self-decarbonizing combustor (burning H <sub>2</sub> generated in-situ from CH <sub>4</sub> )

### Separate PTF Session Talks on Sunday Morning:

Thomas Howarth	Role of enthalpy transport in premixed hydrogen flames
Fokion Egolfopoulos	Local Effects in Turbulence-Flame Interactions: Assessing the Validity of Fundamental Assumptions
Andy Aspden	Premixed regime diagram revisited
Hai Wang	Detonation cells arise from microscopic jetting
Mark Frederick	Reactive Transverse Waves in Near-Limit Detonations
Jackie Chen	DNS of nonequilibrium chemistry effects in planar detonation waves, and on pressure scaling of turbulent burning rate in premixed hydrogen blends
Aaron Skiba	High-Fidelity Measurements of Local Induction Lengths in Ethylene-Air Detonations at Atmospheric Conditions
Adam Steinberg	Supersonic swirl flames

### PTF Talks on Sunday Afternoon (Open to TNF Participants):

Vishal Acharya	Turbulent burning velocity measurements of lean CH <sub>4</sub> /H <sub>2</sub> blended flames
Paul Ronney	Jet-stirred reactors for turbulent premixed flame and chemical kinetics studies
Friedrich Dinkelacker	Ignition of a biogas engine with an active pre-chamber - numerical and experimental study
Swetaprovo Chaudhuri	How "mixing" affects propagation and structure of intensely turbulent, lean, hydrogen-air premixed flames
Simone Hochgreb	Simultaneous OH PLIF and Rayleigh measurements in hydrogen-methane-air flames: quantifying the role of instabilities and turbulence.  Analysis of characteristics obtained from 3D measurements of spherically expanding turbulent flames

## TNF2024 Workshop – Agenda

20 – 21 July 2024

Politecnico di Milano, Milan, Italy

### **Saturday, July 20: Joint Sessions of the TNF and PTF Workshops**

8:00 – 8:30	Registration
8:30 – 8:35	Introduction and Announcements
8:35 – 10:30	Fundamentals of Premixed Hydrogen Flames (Coordinators: Heinz Pitsch, Andy Aspden) PTF Talks*: Yao, Creta, Rieth
10:30 – 11:00	<i>Coffee Break (Poster Session)</i>
11:00 – 12:30	PTF Talks: Lipatnikov, Chen Chemical Kinetics for Ammonia Combustion (Coordinator: Peter Lindstedt)
12:30 – 13:30	<i>Lunch (all workshops)</i>
13:30 – 15:30	PTF Talks: Wang, Kheirkhah Comparisons on the HYLON Burner (Coordinator: Thierry Poinso)
15:30 – 16:00	<i>Coffee Break (Poster Session)</i>
16:00 – 18:00	PTF Talks: Savard, Chaudhuri AI/ML for Turbulence-Chemistry Interaction (Coordinator: Matthias Ihme)
18:00 – 21:00	<i>Poster Session, Networking Dinner and Drinks (all workshops)</i>

### **Sunday, July 21: Joint TNF/PTF Session and Separate TNF Sessions**

8:00 – 8:30	Registration
8:30 – 9:30	Flame-Wall Interaction (Joint TNF/PTF) (Coordinators: Andreas Dreizler, Christian Hasse) <i>PTF Transition to Separate Lecture Hall</i>
9:30 – 10:30	Comparisons on KAUST Piloted NH <sub>3</sub> /H <sub>2</sub> Jet Flames (Coordinators: Gaetano Magnotti, Hong Im)
10:30 – 11:00	<i>Coffee Break (Poster Session)</i>
11:00 – 12:30	Possible Future TNF Target Cases (Coordinator: Rob Barlow) TNF Summary and Closing Discussion (Coordinator: Christian Hasse)
12:30 – 13:30	<i>Lunch (all workshops)</i>
13:30 – 15:00	PTF Talks: Acharya, Ronney, Dinkelacker, Chaudhuri, Hochgreb (Open to TNF participants)

\* PTF titles attached. Talks are nominally 10 minutes plus 5 minutes for discussion.

# Lean premixed hydrogen flames - some updates since Vancouver

Thomas Howarth, Michael Gauding, Xu Wen, Hongchao Chu, Lukas Berger, Edward Hunt, Martin Rieth, Andy Aspden, Heinz Pitsch

Lean premixed hydrogen flames are of great interest to the turbulent flame community, and this presentation aims to give a comprehensive review and of new research that has occurred since the last TNF/PTF workshops in Vancouver in 2022 and give some ideas of currently unanswered questions.

## Laminar flames

In 2D lean premixed hydrogen flames, domain confinement limits the overall consumption speed of the flame [2] up to domain sizes of  $l_x \approx 100l_F$ . Mean local flame speed enhancement (i.e. stretch factor) is unaffected by the confinement. In 3D flames [12], a similar effect is seen, with confinement also causing larger curvature values locally in the flame. Reaction rates are also increased, due to larger fluctuations in mixture fraction compared to the equivalent 2D flames. Due to strong fluctuations in local species concentrations and temperature compared to the representative 1D flamelet, thermodiffusive instability can strongly impact chemistry. In the case of nitrogen oxides, experiments observed trace amounts of  $\text{NO}_x$  even when the adiabatic flame temperature was far below temperatures associated with thermal NO production [3]. This was demonstrated to be related to the effect that thermodiffusive instability has on the NNH pathway, with thermal NO essentially not contributing to the production [13]. Lean premixed hydrogen flames experience both hydrodynamic instability and thermodiffusive instability. Hydrodynamic instability in these flames only serves to enhance flame surface area generation, whereas thermodiffusive instability enhances both flame surface area and local flame speed fluctuations [1]. When combined, the instabilities act together to generate both additional flame surface and enhanced local flame speeds.

To model mean local flame speeds (i.e. stretch factors), a few different approaches by different groups have been suggested. Firstly, based on a second-order coefficient ( $\omega_2 = -(B_1 + \beta(L_{\text{eff}} - 1)B_2 + PrB_3)$ ) from linear stability analysis [10], the stretch factor can be modelled in 2D and 3D flames through [7, 8]

$$I_0^{2D} = \frac{s_F}{s_L} = \begin{cases} \exp(0.057\omega_2) & \text{if } \Pi < \Pi_c \\ 1 + 0.22\omega_2 & \text{otherwise} \end{cases} \quad I_0^{3D} = \begin{cases} \exp(0.08\omega_2) & \text{if } \Pi < \Pi_c \\ 1 + 0.47\omega_2 & \text{otherwise} \end{cases} \quad (1)$$

for a critical normalised pressure  $\Pi_c$ . Alternatively, the flame speeds could be modelled through a Peclet number [11]

$$Pe = \frac{|\frac{\partial Y_{\text{H}_2}}{\partial x} u|_{1\text{D},\text{max}}}{|\frac{1}{\rho} \frac{\partial}{\partial x} \left( \rho \frac{W_{\text{H}_2}}{W_m} D_{\text{H}_2} \frac{\partial X_{\text{H}_2}}{\partial x} \right)|_{1\text{D},\text{max}}} \quad (2)$$

which, when combined with the Zel'dovich number, also demonstrates a satisfactory correlation with both overall consumption flame speed and stretch factor. Peclet number also identifies a similar low- and high-pressure regime to the  $\omega_2$  formulation.

## Turbulent flames

Given that freely-propagating flames propagate locally with a different flame speed to the 1D equivalent flamelet, non-dimensional quantities relating to the turbulent flame (e.g. Damköhler and Karlovitz number) should also be constructed using these values [8]. By doing so, flame structure is far more consistent and suitable for modelling than with quantities normalised through 1D speeds and thicknesses. Turbulence enhances the mean local flame speed even further, and this can be modelled through a combination of  $\omega_2$  and freely-propagating Karlovitz number

$$\frac{I_0^{\text{turb}}}{I_0^{3D}} = 1 + 0.26 \exp(-0.038\omega_2) \sqrt{Ka_F} \quad (3)$$

Effects on mean local flame speed originate from turbulence-flame interaction on the flame scale, and so Karlovitz number satisfactorily parameterises this. This can be demonstrated through simulations with larger integral length scales, and correspondingly larger Damköhler number, which permit the same mean local flame speed but larger turbulent flame speed through area enhancement. Having a low fuel Lewis number does increase the flame area, however the effect is far smaller than the converse effect found at high Lewis number which drastically suppresses flame surface area.

In hydrogen flame kernels at engine relevant conditions, the stretch factor is seen to stabilise at a value similar to that found in the planar flame under laminar conditions. However, the addition of turbulence triggers the thermodiffusive response of the flame much sooner in time, but at a similar radius. Additionally, hydrogen flame kernels experience a much larger throughput of surface area compared to the iso-octane equivalent, i.e. more area was both generated and destroyed [6]. For these flames, ignition in different regions of turbulence resulted in different behaviour, and this originates from the difference in small-scale motion, and not local flow intensity or large scale motion, in agreement with other studies [5]. Tangential strain rate is seen as an important quantity for the understanding and modelling of turbulent flames, and seems to naturally scale with Kolmogorov length scale in both non-reacting and reacting flows. The alignment of said strain rate with the flame had previously been shown to be sensitive to the Lewis number. However, it was found that once dilatation was considered, that tangential strain rate values and alignments in the solenoidal component of the velocity field are insensitive to the Lewis number [4].

## References

- [1] L. Berger, M. Grinberg, B. Jürgens, P. E. Lapenna, F. Creta, A. Attili, and H. Pitsch. Flame fingers and interactions of hydrodynamic and thermodiffusive instabilities in laminar lean hydrogen flames. *Proceedings of the Combustion Institute*, 39(2):1525–1534, 2023.
- [2] L. Berger, K. Kleinheinz, A. Attili, and H. Pitsch. Characteristic patterns of thermodiffusively unstable premixed lean hydrogen flames. *Proceedings of the Combustion Institute*, 37(2):1879–1886, 2019.
- [3] R. Cheng, D. Littlejohn, P. Strakey, and T. Sidwell. Laboratory investigations of a low-swirl injector with H<sub>2</sub> and CH<sub>4</sub> at gas turbine conditions. *Proceedings of the Combustion Institute*, 32(2):3001–3009, 2009.
- [4] H. Chu, L. Berger, M. Gauding, A. Attili, and H. Pitsch. Effects of dilatation and turbulence on tangential strain rates in premixed hydrogen and iso-octane flames. *Journal of Fluid Mechanics*, 981:A5, 2024.
- [5] H. Chu, L. Berger, T. Grenga, M. Gauding, L. Cai, and H. Pitsch. Effects of turbulence on variations in early development of hydrogen and iso-octane flame kernels under engine conditions. *Combustion and Flame*, 255:112914, 2023.
- [6] H. Chu, L. Berger, T. Grenga, Z. Wu, and H. Pitsch. Effects of differential diffusion on hydrogen flame kernel development under engine conditions. *Proceedings of the Combustion Institute*, 39(2):2129–2138, 2023.
- [7] T. Howarth and A. Aspden. An empirical characteristic scaling model for freely-propagating lean premixed hydrogen flames. *Combustion and Flame*, 237:111805, 2022.
- [8] T. Howarth, E. Hunt, and A. Aspden. Thermodiffusively-unstable lean premixed hydrogen flames: Phenomenology, empirical modelling, and thermal leading points. *Combustion and Flame*, 253:112811, 2023.
- [9] E. Hunt and A. Aspden. Thermodiffusively-unstable lean premixed hydrogen flames: Length scale effects and turbulent burning regimes. *Submitted to Combustion and Flame*, 2024.
- [10] M. Matalon, C. Cui, and J. Bechtold. Hydrodynamic theory of premixed flames: effects of stoichiometry, variable transport coefficients and arbitrary reaction orders. *Journal of fluid mechanics*, 487:179–210, 2003.
- [11] M. Rieth, A. Gruber, and J. H. Chen. The effect of pressure on lean premixed hydrogen-air flames. *Combustion and Flame*, 250:112514, 2023.
- [12] X. Wen, L. Berger, L. Cai, A. Parente, and H. Pitsch. Thermodiffusively unstable laminar hydrogen flame in a sufficiently large 3D computational domain—Part I: Characteristic patterns. *Combustion and Flame*, 263:113278, 2024.
- [13] X. Wen, L. Berger, L. Cai, A. Parente, and H. Pitsch. Thermodiffusively unstable laminar hydrogen flame in a sufficiently large 3D computational domain—Part II: NO<sub>x</sub> formation mechanism and flamelet modeling. *Combustion and Flame*, 265:113497, 2024.



## Outline of the Session: Fundamentals of Premixed Flames of H<sub>2</sub> and H<sub>2</sub> Blends

---

- Update on thermodiffusive instabilities of hydrogen flames (Howarth)
- PTF talks (Yao, Creta)
- TNF talks: Sharing of combustion data (Rieth, Aspden, Gauding, Li, Dawson)
- Discussion

---

Institute for Combustion Technology |  
Source: L. Berger et al (2022) Comb. Flame (244)



## Lean premixed hydrogen flames – some updates since Vancouver

**Thomas Howarth**, Michael Gauding, Xu Wen, Hongchao Chu, Lukas Berger,  
Edward Hunt, Martin Rieth, Andy Aspden, Heinz Pitsch

Institute for Combustion Technology  
RWTH Aachen University



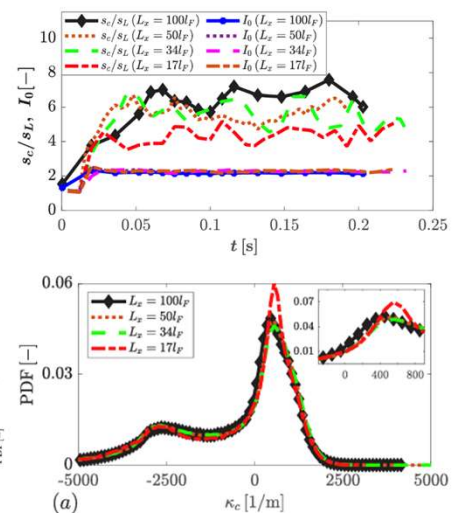
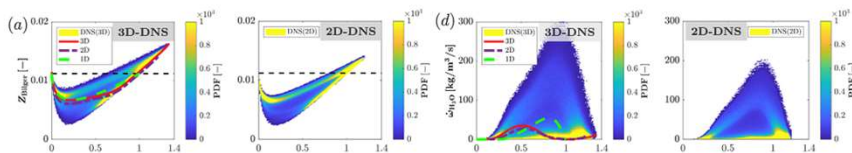
## Outline

What's new since the last workshop? Focussing on physics, rather than modelling

- Laminar flames
  - 2D vs. 3D
  - NOx formation
  - Interaction between hydrodynamic and thermodiffusive instability
  - Flame speed scaling in laminar flames
- Turbulent flames
  - Karlovitz number definition
  - Flame speed scaling in turbulent flames
  - Turbulent length scale effects
  - Lewis number effects
  - Flame kernel behaviour
  - Role of tangential strain rate
- Some open questions

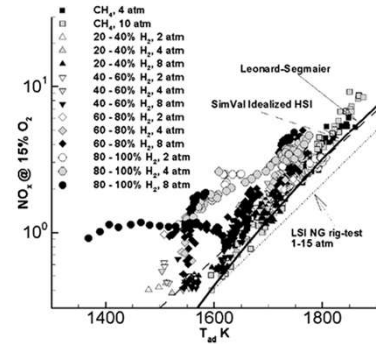
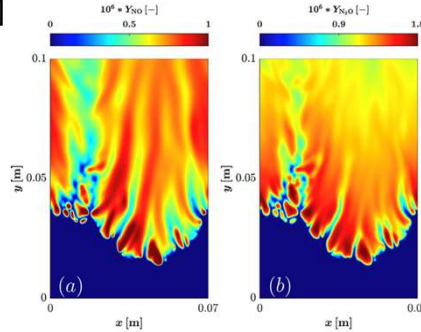
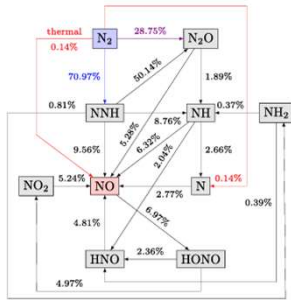
## Laminar flames – 2D vs. 3D

- In 2D, domain confinement limits overall consumption speed of the flame [1]
- For  $\varphi = 0.4$ ,  $T_u = 298K$ ,  $p = 1atm$ , this is seen up to  $L_x \approx 100l_L$
- In 3D, similar effect seen [2]
- Stretch factor (mean local flame speed) unaffected
- Domain confinement also causes larger curvature values
- Reaction rates increased, but trends nearly identical to 2D
- Higher mixture fraction values found



## Laminar flames – NOx formation

- Thermodiffusive instability influence NNH reaction pathway due to accumulation of H radical [1,2]
- 90% of NO formed in positively-curved regions [2]
- For  $\varphi = 0.4, T_u = 298K, p = 1atm$ :
- Thermal NO produces less than 1% of NO
- Overall NOx production very low ( $< 1ppm$ )
- In agreement with experiments [3]

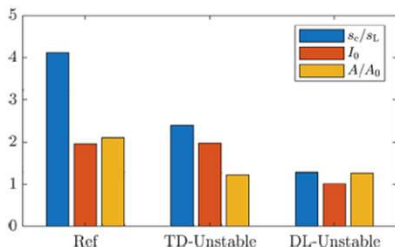
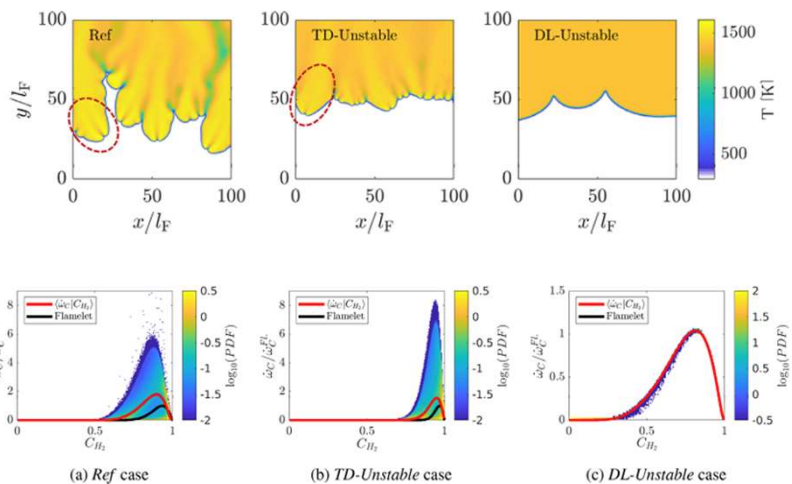


5 Institute for Combustion Technology | Thomas Howarth | TNF/PTF joint session  
 [1] Day, Bell, Gao & Glarborg PCI 33 (2011) 1591-1599 [3] Cheng, Littlejohn, Strakey & Sidwell PCI 32 (2009) 3001-3009  
 [2] Wen, Berger, Cai, Parente & Pitsch CNF 265 (2024) 113497



## Laminar flames – DL and TD instability interaction

- Hydrodynamic and thermodiffusive instability act together to generate flame surface area
- Reaction rates unaffected by hydrodynamic instability
- Mean local flame speed only affected by TDI



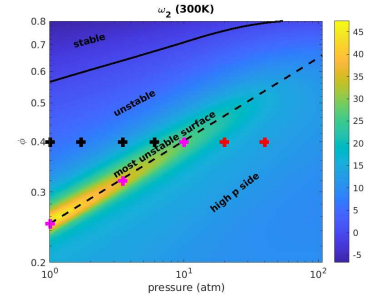
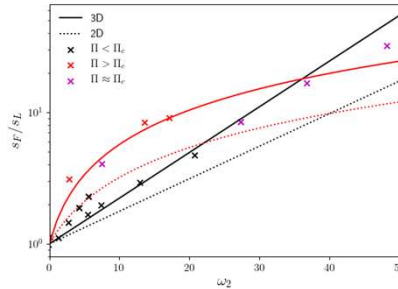
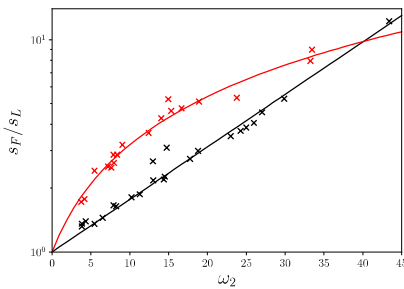
6 Institute for Combustion Technology | Thomas Howarth | TNF/PTF joint session  
 [1] Berger, Grinberg, Jürgens, Lapenna, Creta, Atilli & Pitsch PCI 39 (2023) 1525-1534



## Laminar flames – Mean local flame speed models

- Categorically different behaviour each side of the most-unstable-surface
- Same function form, but higher coefficients in 3D
- Consistent with findings from earlier

$$\omega_2 = -(B_1 + \beta(Le_{\text{eff}} - 1)B_2 + PrB_3)$$



$$I_0 = \frac{s_F}{s_L} = \begin{cases} \exp(0.057\omega_2) & \text{if } \Pi < \Pi_c \\ 1 + 0.22\omega_2 & \text{otherwise} \end{cases} \quad [1]$$

$$I_0 = \frac{s_F}{s_L} = \begin{cases} \exp(0.08\omega_2) & \text{if } \Pi < \Pi_c \\ 1 + 0.47\omega_2 & \text{otherwise} \end{cases} \quad [2]$$

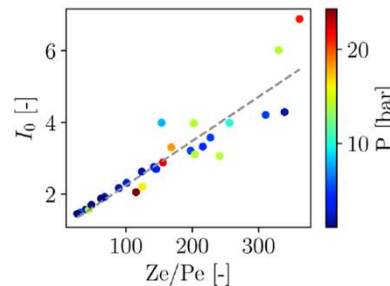
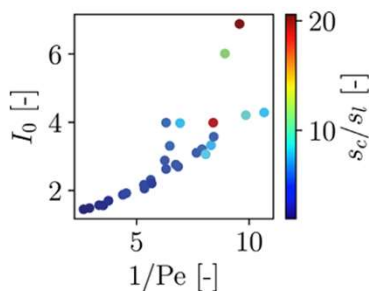
7 Institute for Combustion Technology | Thomas Howarth | TNF/PTF joint session  
 [1] Howarth & Aspden, CNF 237 (2022) | 11805  
 [2] Howarth, Hunt & Aspden, CNF 253 (2023) | 112811



## Laminar flames – Mean local flame speed models

- An alternative to  $\omega_2$  is a Peclet number [1]
- Quantifies disparity between convective and diffusive fluxes
- Suggests a quantity relating to underlying thermo-chemistry to improve correlation
- Multiplication by Zel'dovich number improves correlation
- Tested across many conditions (laminar and turbulent)

$$Pe = \frac{\left| \frac{\partial Y_{H_2}}{\partial x} \right|_{1D, \max}}{\left| \frac{1}{\rho} \frac{\partial}{\partial x} \left( \rho \frac{W_{H_2}}{W_m} D_{H_2} \frac{\partial X_{H_2}}{\partial x} \right) \right|_{1D, \max}}$$

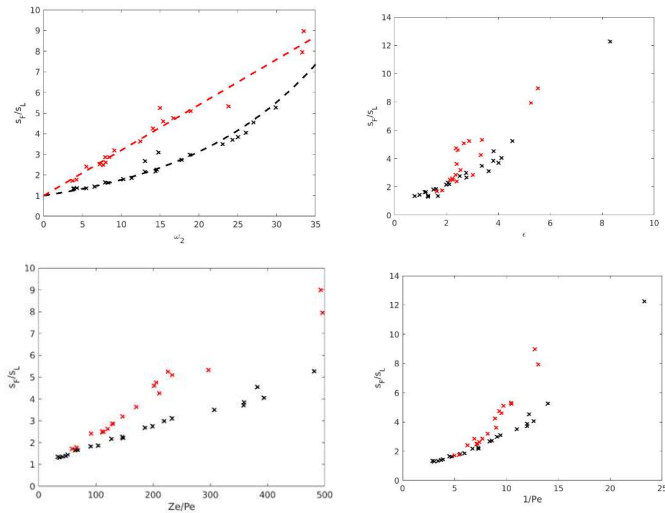


8 Institute for Combustion Technology | Thomas Howarth | TNF/PTF joint session  
 [1] Rieth, Gruber & Chen, CNF 250 (2023) | 112514



## Laminar flames – Mean local flame speed models

- How do different models compare?
- Cases from [1] considered
- Considering  $\omega_2$  [1],  $1/Pe$ ,  $Ze/Pe$  [2] and  $\epsilon$  [3].
- Closely correlated
- All identify two regimes (low/high-pressure)



9

Institute for Combustion Technology | Thomas Howarth | TNF/PTF joint session

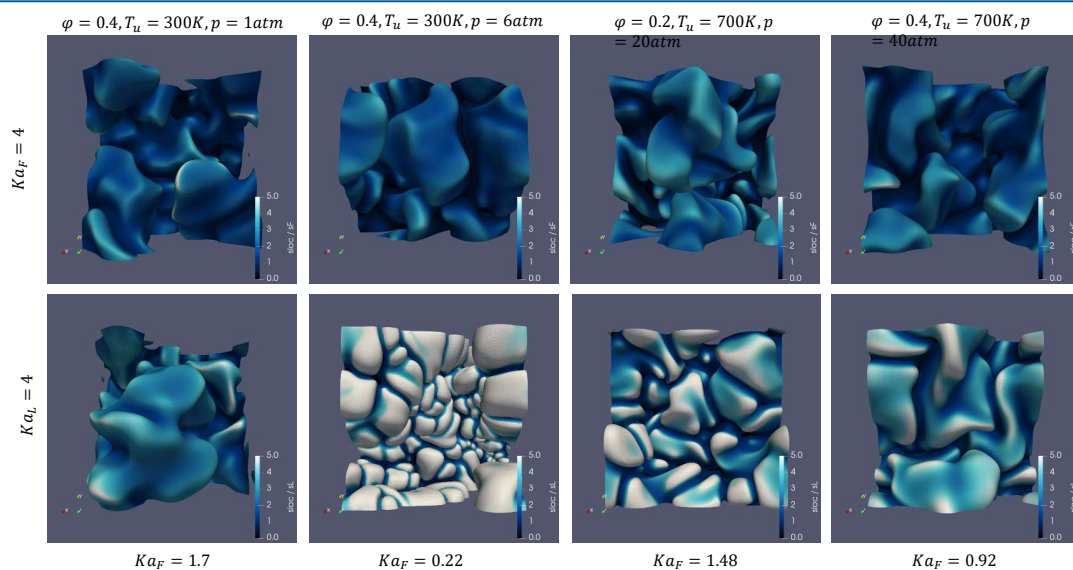
[1] Howarth & Aspden, CNF 237 (2022) | 11805

[3] Creta, Lapenna, Lamioni, Fogla & Matalon CNF 216 (2020) 256-270

[2] Rieth, Gruber & Chen, CNF 250 (2023) | 112514



## Turbulent flames – Karlovitz number definition



10

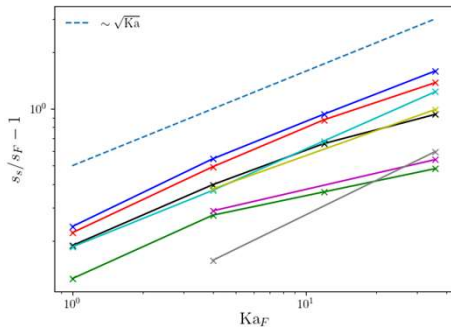
Institute for Combustion Technology | Thomas Howarth | TNF/PTF joint session

[1] Howarth, Hunt & Aspden, CNF 253 (2023) | 112811

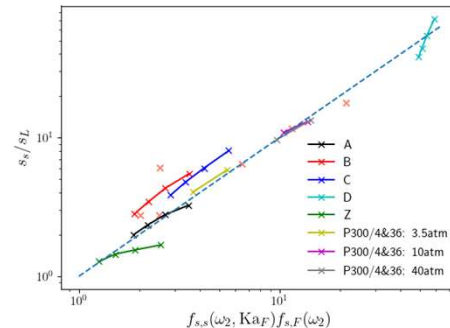




## Turbulent flames – mean local flame speed



a) Function of  $Ka_F$

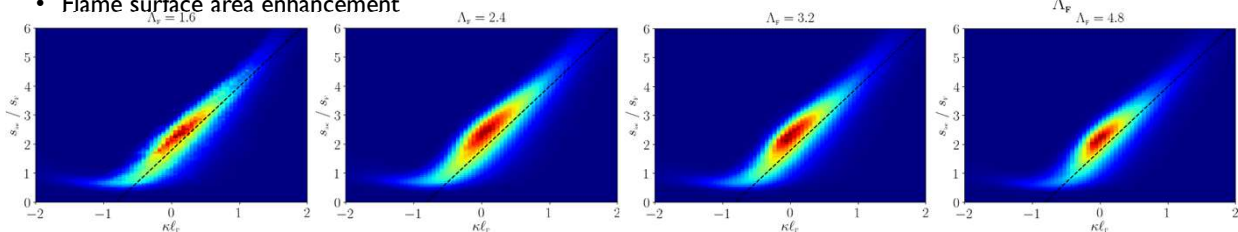
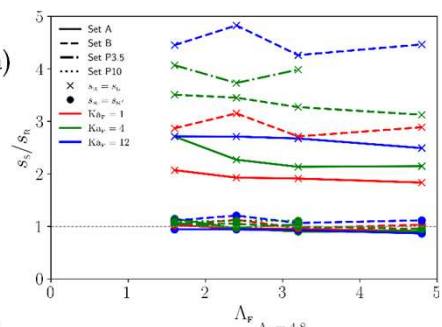


b) Model  $s_s$  in terms of  $s_L$

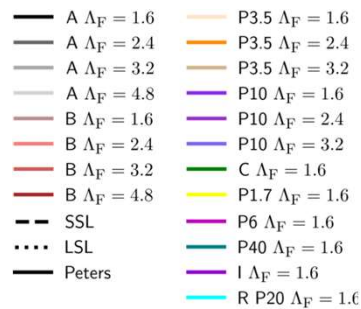
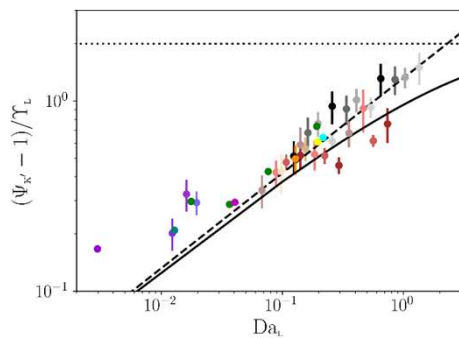
- Apparent  $\sqrt{Ka_F}$  dependence; can formulate empirical model local flame speed accounting for  $\omega_2$  and  $Ka_F$
- Some uncertainty in  $s_F$ ; better to measure reference speed and scale through  $\sqrt{Ka_F}$

## Turbulent flames – turbulent length scale effects

- Study: Fix Karlovitz number and move to larger length scales (i.e.  $Da$ )
- Right: local flame speed; Below: flame-speed/curvature JPDFs
- Local flame properties depend on  $\omega_2$  and  $Ka_F$ 
  - Independent of length scale
- General premise:  $s_T = s_s \psi$ 
  - Reference flame speed  $s_s(\omega_2, Ka_F)$
  - Flame surface area enhancement



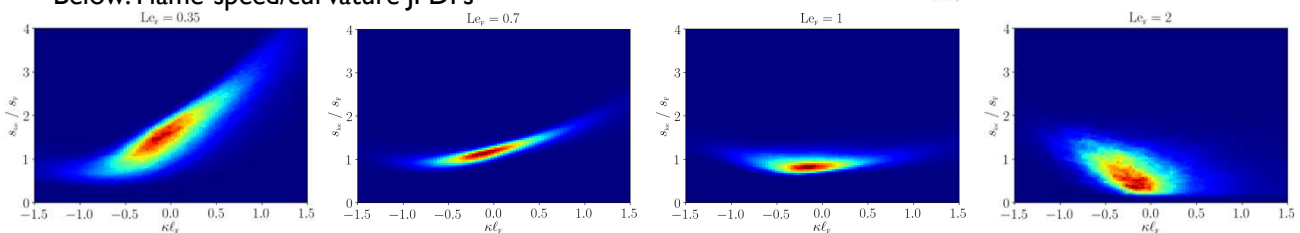
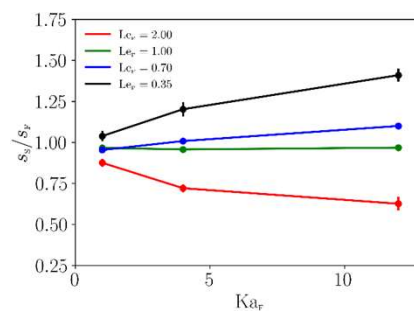
## Turbulent flames – turbulent length scale effects



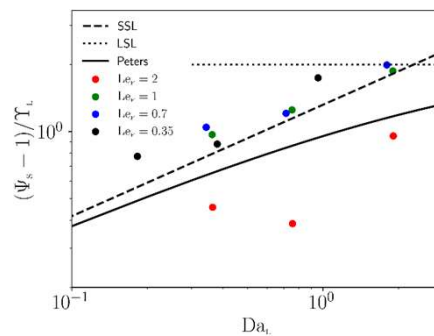
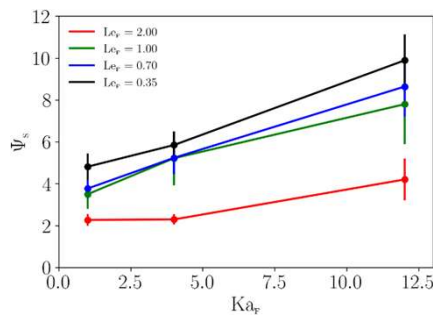
- Good agreement with Damköhler's small-scale turbulence limit (dashed line)
- Considered different reference quantities
  - L most compelling, but F (and S) give similar measures of error
  - DNS lacks range of scales necessary (all  $Da \sim 1$ )
- Model constants different to the literature
  - Is it hydrogen? Or just the way quantities are measured?

## Turbulent flames – Lewis number effects

- Using the same mechanism
- Artificially alter the Lewis number of the fuel
- Four constant values  $Le = 0.35, 0.7, 1.0, 2.0$
- $Ka = 1, 4, 12$
- Fixed length scale ratio  $\Lambda_F = 2.4$
- Local flame properties
- Right: Mean local flame speed
- Below: Flame-speed/curvature JPDFs



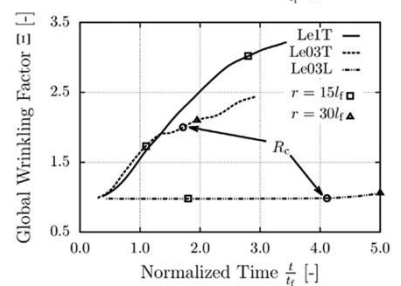
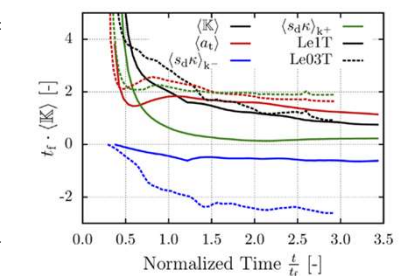
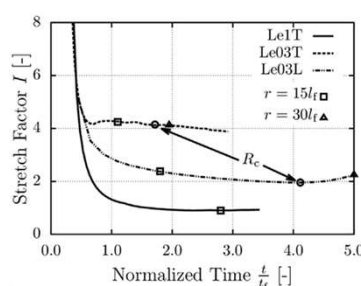
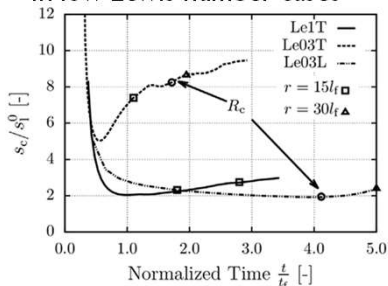
## Turbulent flames – Lewis number effects



- There is a Lewis number effect; area increases with decreasing Lewis number
- Not that much different for  $Le \lesssim 1$ ; more pronounced for  $Le > 1$
- Interpretation is a volume-filling-surface concept
  - There's only so much flame surface are can fit in a given volume

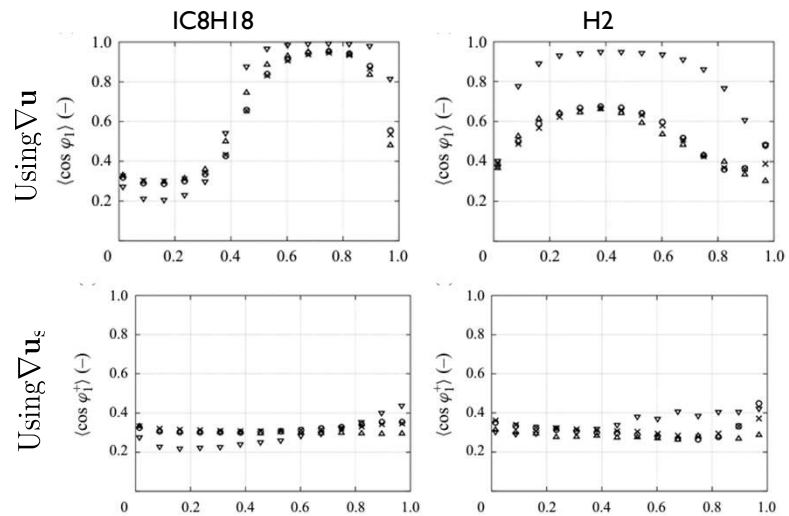
## Turbulent flames – Flame kernel behaviour

- At engine relevant conditions  $\phi = 0.4, T_u = 800K, p = 40bar, Ka_L = 4.4$
- Stretch factor (mean local flame speed enhancement) of 4
- Stretch factor in equivalent laminar case 1.5 – 2
- Intense burning triggered earlier by turbulence
- Larger throughput for area – more production and destruction of area in low Lewis number cases



## Turbulent flames – Tangential strain rate insensitivity

- Tangential strain rate of material surfaces in incompressible turbulence scales with Kolmogorov time scale,  $a_t t_\eta \approx 0.28$  [1], aligns with most compressive strain rate
- Driven by solenoidal component of turbulence [2]
- This result is insensitive to the choice of fuel – the same for iso-octane (high Le) and hydrogen (low Le)



17

Institute for Combustion Technology | Thomas Howarth | TNF/PTF joint session

[1] Yeung, Girimaji & Pope, CNF 79(1990) 340-365

[2] Chu, Berger, Gauding, Atilli & Pitsch, JFM 981 (2024)



## Open questions

- Laminar flames:
  - Why is there a high-pressure and low-pressure regime?
  - Why are characteristic length scales in high-pressure laminar flames smaller than in low-pressure flames, even after normalisation by mean local thicknesses?
- Turbulent flames:
  - Range of validity of  $I_0 \sim \sqrt{Ka_F}$  - decrease seen at extreme turbulence level
  - An empirical model of  $I_0 \sim \sqrt{Ka_F}$  suggests that the mean local enhancement is proportional to speed scales on the Kolmogorov scale, however, this is inconsistent with a strain-based argument that it should be proportional to time scale ratios instead. How can this be addressed?
- Both laminar and turbulent flames:
  - What happens near  $\omega_2 = 0$ ?
  - How much faith can we have in mechanisms where the effects are very strong?

18

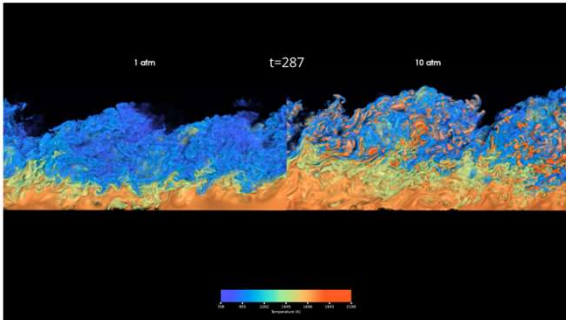
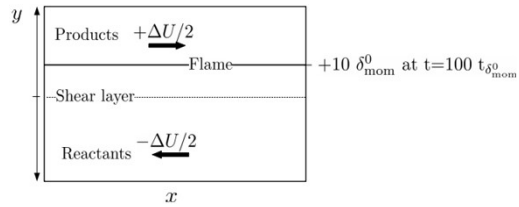
Institute for Combustion Technology | Thomas Howarth | TNF/PTF joint session



## Sandia/SINTEF DNS Data

Temporally evolving shear layer ammonia/hydrogen

	NH <sub>3</sub> /H <sub>2</sub> /N <sub>2</sub> -air	
Fuel	40% NH <sub>3</sub> , 45% H <sub>2</sub> , 15% N <sub>2</sub>	
Pressure	1 atm	10 atm
$\phi$	0.45	
$T_u$	750	
Ka	300-600	
Re <sub>t</sub>	500-1100	



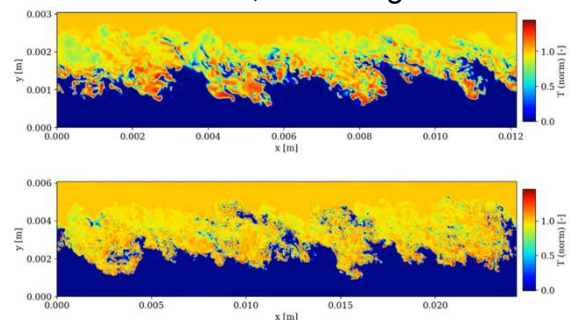
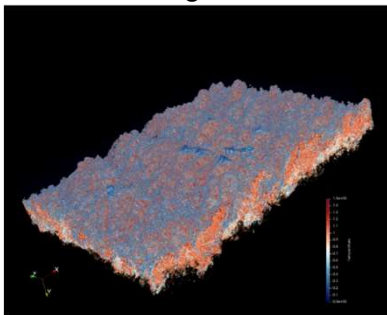
### Publications

1. Rieth et al., *Enhanced burning rates in hydrogen-enriched turbulent premixed flames by diffusion of molecular and atomic hydrogen*, C&F 2022.
2. Rieth et al., *A direct numerical simulation study on NO and N<sub>2</sub>O formation in turbulent premixed ammonia/hydrogen/nitrogen-air flames* PROCI 2023.

## Sandia/SINTEF DNS Data

Temporally evolving shear layer hydrogen (new data not yet published)

	H <sub>2</sub> -air					
Pressure	1 atm			10 atm		
	low Re	med Re	high Re	low Re	med Re	high Re
$\phi$	0.3					
$T_u$	750					
Ka	90	130	180	90	130	180
Re <sub>t</sub>	300	700	1200	300	700	1200
	10 atm, high Re			10 atm, low vs high Re		

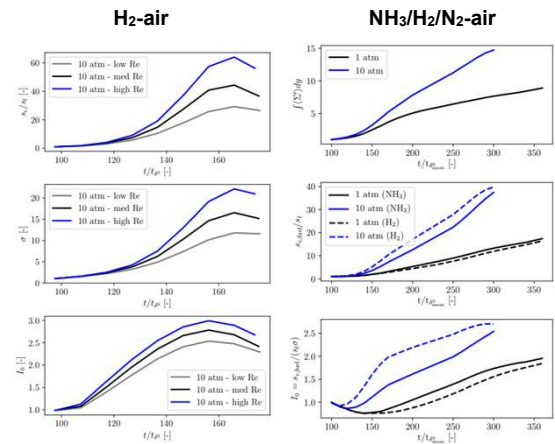




## Sandia/SINTEF DNS Data

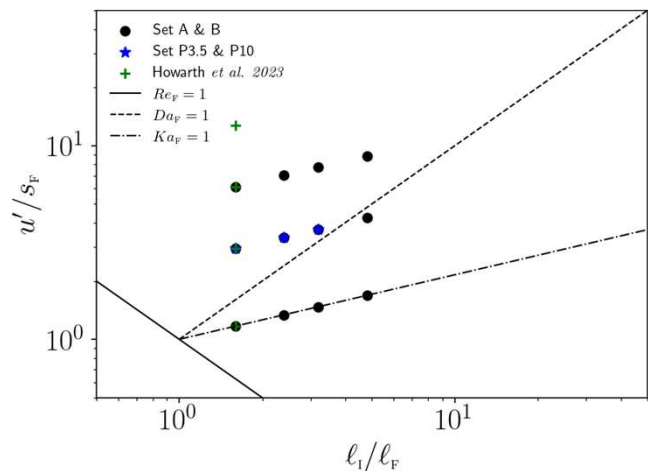
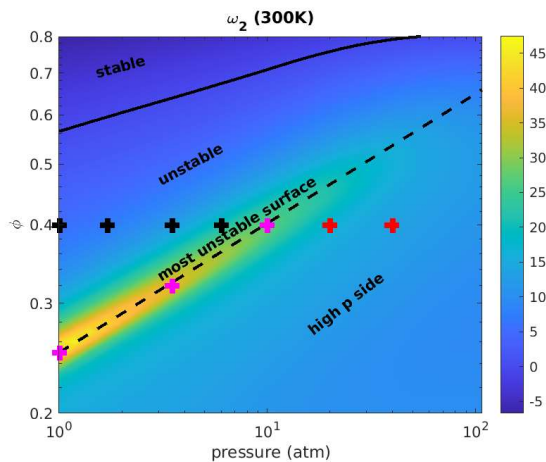
### Statistics

- Characterization of initial conditions (velocity statistics, flame location, etc.)
- Global quantities vs time ( $l_0$ ,  $s_c$ , FSD)
- 1D statistics as function of  $y$  at different times (e.g.,  $T$ , HRR profiles,  $U'$ )
- Conditional means as function of progress variable at different times
- PDFs of flame features (e.g.,  $|C|$ , curvature) at different times

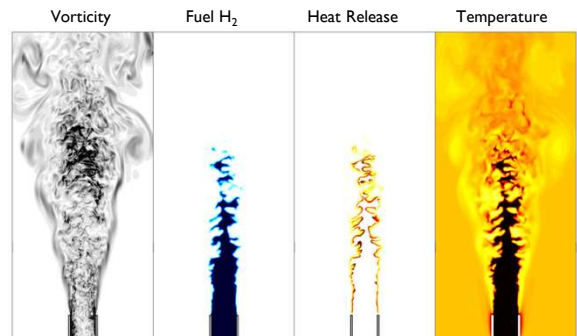


## DNS turbulent flame-in-a-box

- Turbulent premixed flames in maintained turbulence
- Howarth *et al.* CNF 111805 (2022) & 112811 (2023)



# Direct numerical simulations of turbulent premixed hydrogen/air flames in a slot burner configuration [1]



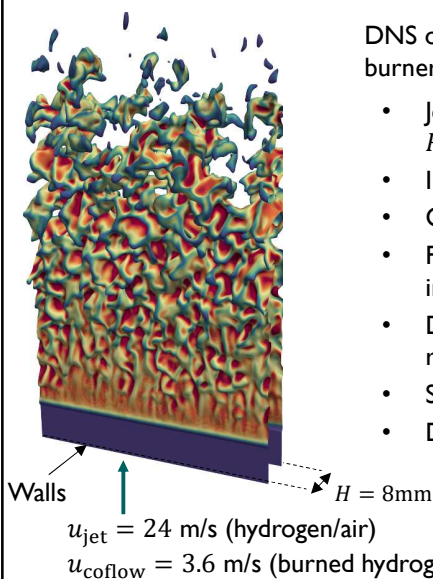
M. Gauding, L. Berger, T. Howarth, H. Pitsch

Institute for Combustion Technology  
RWTH Aachen University, Germany  
m.gauding@itv.rwth-aachen.de

[1] L. Berger et al. (2022), Combustion and Flame 244

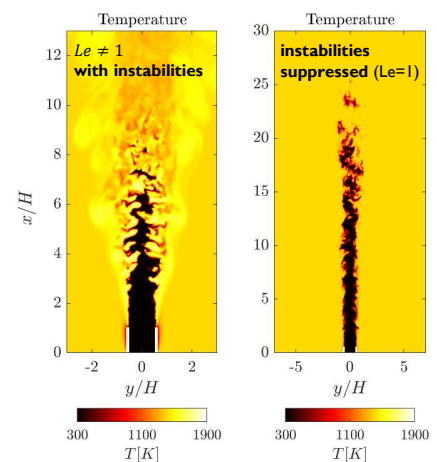


## Turbulent premixed hydrogen flames: case setup



DNS of turbulent hydrogen/air flames in slot burner configuration

- Jet flow:  $\phi = 0.4$ ,  $T_u = 298$  K,  $p = 1$  bar,  $Re = 11,000$ ,  $Ka = 25$
- Inflow: auxiliary turbulent channel flow
- Coflow: burned gas (laminar)
- Flow solver CIAO: higher-order semi-implicit finite difference code
- Detailed chemistry (9 species, 46 reactions)
- Soret effect considered
- Different Lewis numbers for each species



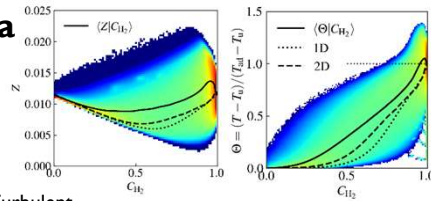
Two cases [1]:  
 $Le \neq 1$  (left) and  $Le = 1$  (right)  
→ Analysis of thermo-diffusive instabilities

24 Institute for Combustion Technology | M. Gauding, L. Berger, T. Howarth, H. Pitsch  
[1] L. Berger et al. (2022), Combustion and Flame 244



# Turbulent premixed hydrogen flames: data available

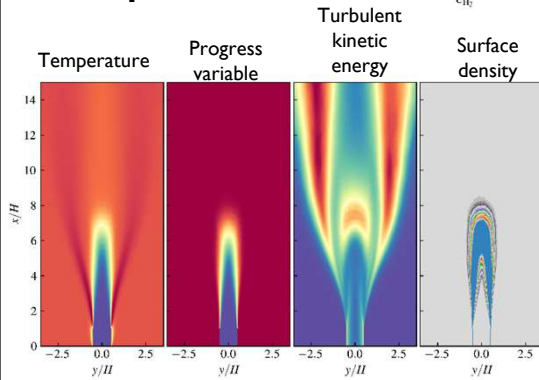
## Post-processed data



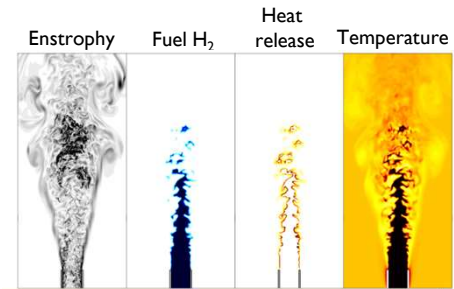
- Velocity, temperature, density, species, etc.
- Processed fields ( $S_d, \kappa, K, K_T$ , etc.)
- 60 independent snapshots
- 80 TB of data, shared via s3 identifier on Coscine [1]



## Mean quantities



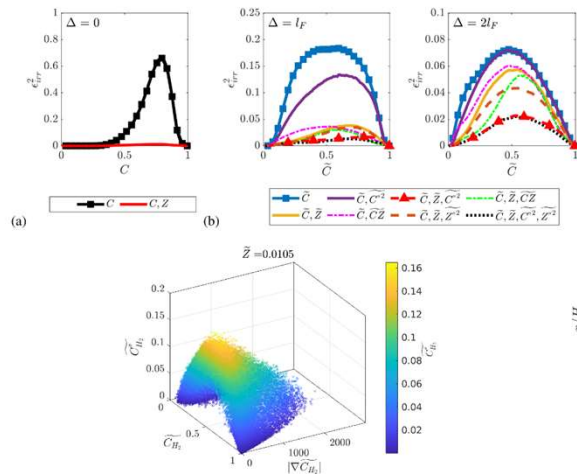
## Instantaneous three-dimensional fields



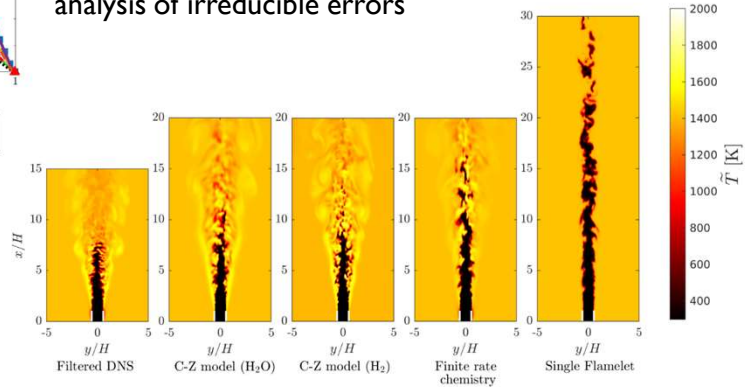
25 Institute for Combustion Technology | M. Gauding, L. Berger, T. Howarth, H. Pitsch  
 [1] coscine.rwth-aachen.de  
 [2] L. Berger et al. (2022), Combustion and Flame 244



# Turbulent premixed hydrogen flames: case studies



## Model development: analysis of irreducible errors



## Optimal estimator analysis: modeling the progress variable variance [1]

LES: a posteriori analysis of combustion models [1]  
 → Analysis and modeling of thermo-diffusive instabilities

26 Institute for Combustion Technology | M. Gauding, L. Berger, T. Howarth, H. Pitsch  
 [1] L. Berger et al. (2024) submitted to the Journal of Fluid Mechanics



## Turbulent premixed hydrogen flame: case setup

	$Le = 1$	$Le \neq 1$
$H$ (mm)	8	4
$U_{\text{jet}}$ (m/s)	24	48
$U_{\text{coflow}}$ (m/s)	3.6	7.2
$s_L$ (m/s)	0.17	0.24
$l_F$ ( $\mu\text{m}$ )	714	374
$\eta$ ( $\mu\text{m}$ )	180	90
$\Delta_{\text{mesh}}$ ( $\mu\text{m}$ )	70	35
$L_{\text{flame}}/H$	8.5	26.3
$Re_{\text{jet}}$	11,000	
$\frac{L_x}{H}, \frac{L_y}{H}, \frac{L_z}{H}$	15, 12.5, 4.6	30, 20, 4.6
$N_x, N_y, N_z$	1792, 1024, 512	3300, 1062, 512

27 Institute for Combustion Technology | M. Gauding, L. Berger, T. Howarth, H. Pitsch



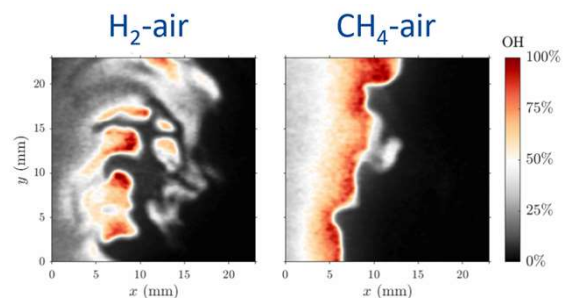
## Dataset:

### Turbulent bluff-body stabilised $\text{H}_2$ -flame(s)

James Dawson and Eirik  $\text{\AA}$ esøy  
Norwegian University of Science and Technology

Email:

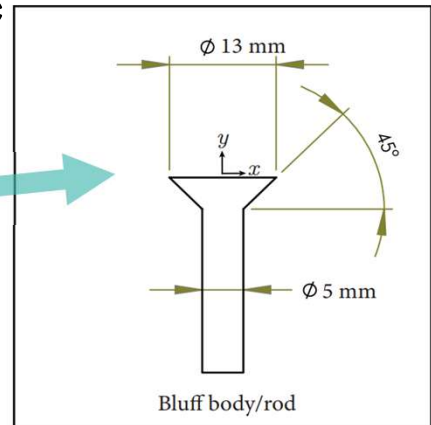
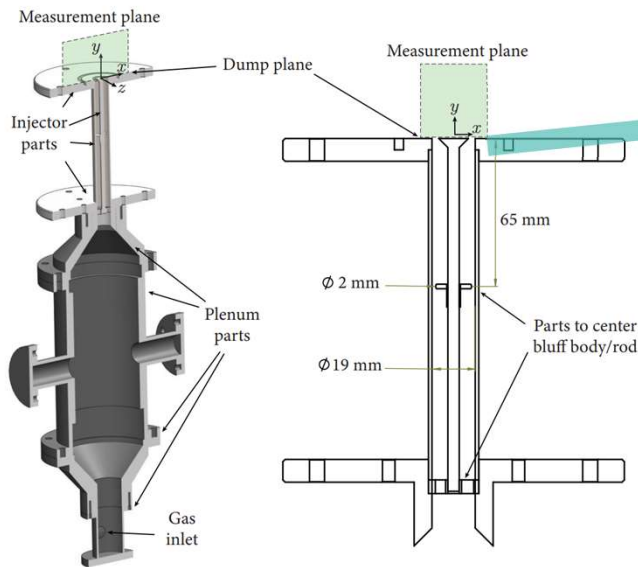
[james.dawson@ntnu.no](mailto:james.dawson@ntnu.no)  
[eirik.asoy@ntnu.no](mailto:eirik.asoy@ntnu.no)



25 mm x 25 mm FoV



## Current dataset: Geometry\*



### For new datasets:

- Vary bluff body diameter
- Open or confined flames
- Add swirl

29

\* CAD drawings available



NTNU

## Current dataset: Operating conditions

Mean reactants velocity: $U$	15 m/s
Reynolds number, $Re_D$ – based on bluff body diameter, $D$ .	13,000
Equivalence ratio, $\Phi$	0.4
Air mass flow: $m_{air}$	2.258 g/s
Fuel mass flow: $m_{H_2}$	0.0292 g/s
Unburned reactant temperature, $T_u$	298 K
Pressure, $P$	1 bar
Power	3.5 kW

30



NTNU



# Current dataset: Measurements

## 2D-PIV (cold and hot)

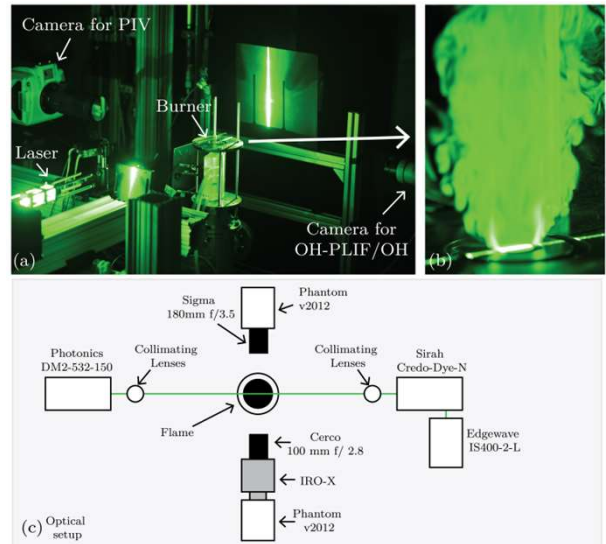
- 2000 vector fields, sampled at 1kHz (cold), 10 kHz (hot)
- Resolution (window size)  $dx = 0.25$  mm (cold), 0.4 mm (hot)
- FoV approx. 45 x 55 mm

## OH-PLIF (high speed YAG, Sirah credo dye)

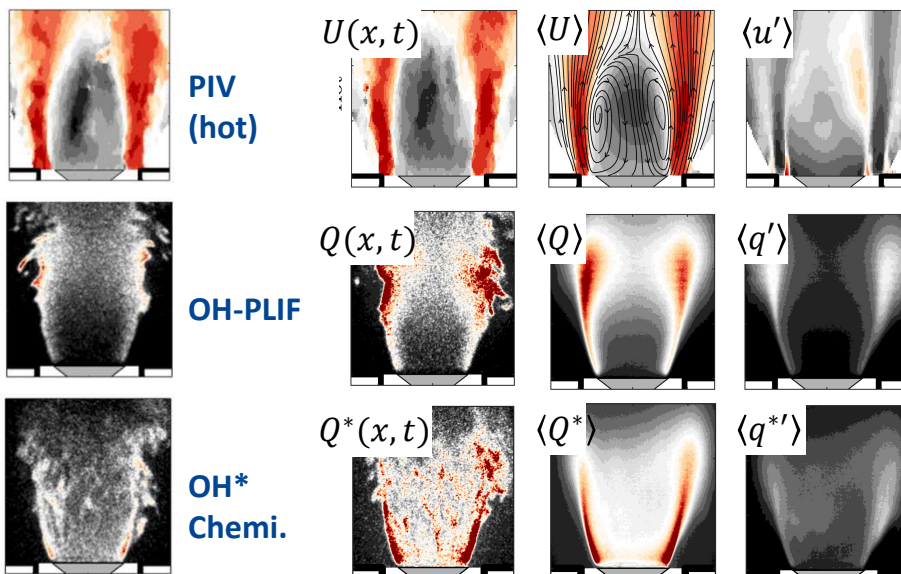
- 2000 images, sampled at 10kHz, resolution  $dx = 0.089$  mm
- Excitation frequency: 283.57 nm
- FoV approx. 45 x 55 mm

## OH\*-Chemiluminescence

- Line-of-sight OH\*, same specs as OH-PLIF



# Current dataset: Example data



**Note:**  
We have not yet analysed the data in detail.

**Simulation cases:**  
Four groups have been in contact about the data.

No results that we are aware of yet.



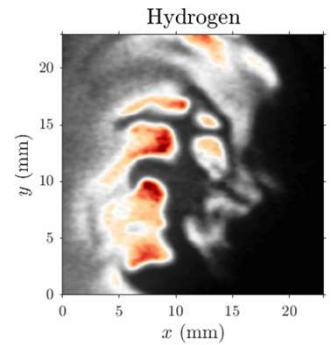
# New datasets: Feedback/suggestions?

## Planned for August:

- Two equiv. ratios: 0.4, 0.35?, two Re (or vary Ka?)
- Maximise resolution (eg. FoV: 25 x 25 mm) to capture thermodiffusive effects

## Planned for late 2025/early 2026:

- Effect of pressure
- Ze/Pe scaling



$$u = 13\text{m/s} \quad \Phi = 0.35$$

33



DARMSTADT HYDROGEN FLAMES

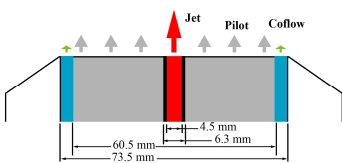


## TURBULENT JET BURNER

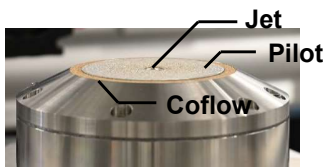
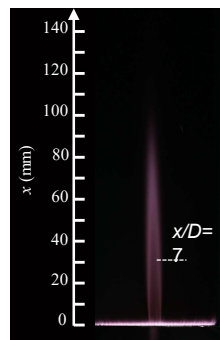
2D09

4H03

### Geometry



### H<sub>2</sub> Flames



S. Shi et al. *Combustion and Flame*, under review

### Lean H<sub>2</sub>/air jet flames

Case	$\Phi_{\text{jet}}$	$U_{\text{jet}}$ (m/s)	$Ka_F$	OH-LIF	PIV	Raman
H100P040U050	0.4	50	50	✓	✓	✓
H100P040U100	0.4	100	260	✓	✓	✓
H100P040U150	0.4	150	545	✓	✓	✓
H100P040U200	0.4	200	730	✓	✓	✓
H100P030U100	0.3	100	7690	✓	✓	✓
H100P045U100	0.45	100	100	✓	✓	✓

### Lean and rich NH<sub>3</sub>/H<sub>2</sub>/N<sub>2</sub>-air jet flames

Case	NH <sub>3</sub> :H <sub>2</sub> :N <sub>2</sub>	$\Phi_{\text{jet}}$	$U_{\text{jet}}$ (m/s)	OH-LIF	PIV	Raman
AHNA45P080U50	40:45:15	0.8	50			✓
AHNA45P120U50	40:45:15	1.2	50			✓
AHNA45P160U50	40:45:15	1.6	50	✓	✓	✓



Mechanical Engineering | Rea

**TNF Session: Chemical Kinetics for Ammonia Combustion**

*Coordinator: Peter Lindstedt*

(Summary to be added)

TNF/PTF Workshops

Blank Page

**IMPERIAL**

## **Chemical Kinetics for Ammonia Combustion**

TNF2024 Workshop  
Politecnico di Milano, July 20-21, 2024

**Contributions from Rob Barlow, Peter Glarborg, Andrea Gruber, Gaetano Magnotti, Heinz Pitsch, Martin Richter and others are gratefully acknowledged.**

R. P. Lindstedt  
19/07/2024

**IMPERIAL**

### **Background**

Ammonia is the current “hot” topic when it comes to alternative fuels. It is also a “terrible” fuel with exceptionally low reactivity typically requiring hydrogen enhancement to use even in a laboratory environment.

The aim of the current talk is to explore:

- What are the challenges?
- Current state of chemical mechanisms.
- Comments on what criteria are sensible.
- Some – not extensive - current uncertainties in key fundamental rate parameters.
- What role for validation data and what types?
- How can we move this forward and can the TNF community help?

# IMPERIAL

## Challenges

### Andrea Gruber

- What is the pressure effect on NO & N<sub>2</sub>O formation in premixed and non-premixed flames? Which minimal set of elementary reactions are needed to accurately predict this?
- What is the origin of ammonia slip observed in experiments (less so in simulations) of ammonia flames, either premixed or non-premixed, at globally fuel-rich conditions? Is there a chemical kinetics pathway that leads to ammonia slip even at idealized adiabatic-flame conditions or ammonia slip is just the result of local extinction and/or wall heat loss / quenching?
- *Are presently available chemical kinetics schemes able to accurately predict HCN formation in ammonia-methane flames? Which minimal set of elementary reactions are needed to accurately predict this?*

*Background for this: in a set of high-pressure experiments that we recently conducted for a customer on lab-scale GT combustor fired with a methane-ammonia blend, we measured (FTIR) 100-200 ppm HCN in the exhaust gases at certain operating conditions!*

# IMPERIAL

## Background Ammonia Chemistry

Work on ammonia in a combustion context can arguably be divided into three time periods based on the discovery of Selective Non-Catalytic Reduction (SNCR) of nitric oxide (NO):

1. The pre-SNCR era leading up to 1975.
2. The SNCR era spanning the period from 1975 to 2011.
3. The post-SNCR era spanning the period from 2011 onwards.

The above is, of course, highly approximate and only serves to illustrate the rather intermittent progress made.

The dividing dates stem from the original SNCR patent by Lyon (US3900554A) in 1975 and the study of SNCR by Klippenstein et al. (2011)<sup>1</sup>.

<sup>1</sup> Klippenstein et al., The role of NNH in NO formation and control, Combust. Flame 158 (2011) 774-789.

# IMPERIAL

## Background Ammonia Chemistry

Taking a big risk in attempting to attribute motivation:

- The pre-SNCR era was driven by curiosity.
- The SNCR era by a desire to understand how it works, to determine applicability limits and process optimization.
- The current era is aimed at figuring out if and how we can use ammonia as a hydrogen rich fuel.
- The stoichiometric reaction is simple:  $2\text{NH}_3 + 1.5\text{O}_2 = 3\text{H}_2\text{O} + \text{N}_2$

Property	NH <sub>3</sub> -O <sub>2</sub>	NH <sub>3</sub> -Air	CH <sub>4</sub> -Air
T [K]	2845	2070	2226
N <sub>2</sub>	0.225	0.688	0.709
H <sub>2</sub> O	0.559	0.304	0.183
O <sub>2</sub>	0.027	0.0013	0.0046
OH	0.054	0.0014	0.0029
NO	0.0079	0.00072	0.0020
N <sub>2</sub> O	2.15*10 <sup>-7</sup>	3.39*10 <sup>-8</sup>	---
CO	---	---	0.0090
CO <sub>2</sub>	---	---	0.0850

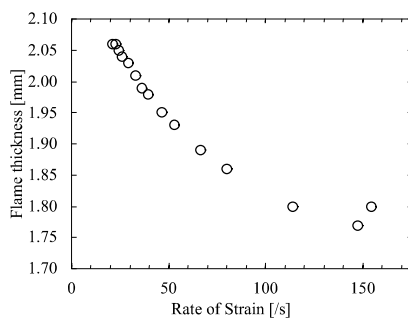
Table shows chemical equilibrium products for stoichiometric ammonia combustion compared to methane at atmospheric pressure<sup>1</sup>.

<sup>1</sup>Kobayashi et al. (2019) point out that NO levels in flames can reach 4000 ppm even with 5% NH<sub>3</sub> added.

# IMPERIAL

There are (at least) three main challenges:

1. Oxides of nitrogen present a significant problem with **the chemistry of ammonia is particularly complex** as it can be used to reduce NO through the SNCR chemistry as well as providing wholly unacceptable levels if not mitigated.
2. How to model the poor reaction dynamics as the hydrogen content is reduced – this will lead to increased/intense turbulence-chemistry interactions.
3. A direct consequence is that the accuracy of the applied chemistry matters to an even higher degree than for hydrocarbon-based fuels.



Laminar flame thicknesses based on the 5 to 95 % temperature rise in counterflow back-to-back stoichiometric ammonia-air flames.

Accounting for the low burning velocities (peak around 7 cm/s) a characteristic chemical timescale for ammonia combustion around 27 ms.

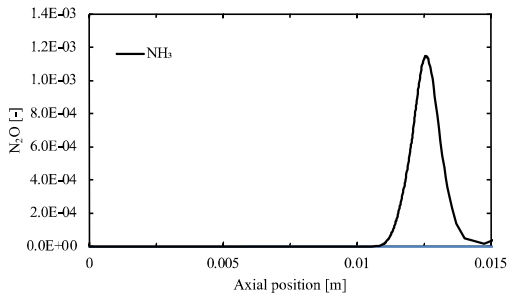
The corresponding methane flame timescale is around 1.3 ms.



# IMPERIAL

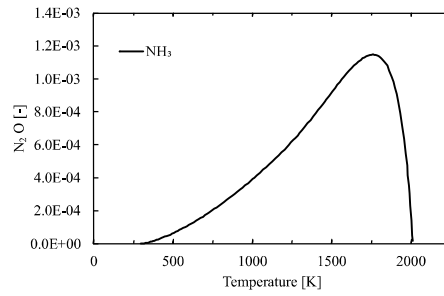
Nitrous oxide can become an issue.

Nitrous oxide has a greenhouse gas potential that is around 300 times that of carbon dioxide and is formed in large concentrations as an intermediate.



The flame is pushed towards the stagnation plane due to the low burning velocity even at the low rate of strain of 81 /s.

The nitrous oxide formation start at low temperatures in a manner that is consistent with nitric oxide.



Can local extinction and incomplete combustion give rise to nitrous oxide emissions?

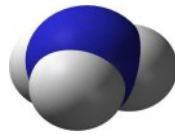
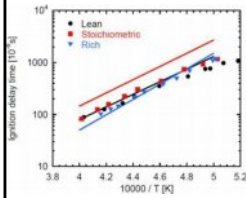
Slide provided by Peter Glarborg



## NH<sub>3</sub> oxidation modeling status 2018

Shock tube IDT

(Mathieu and Petersen, 2015)

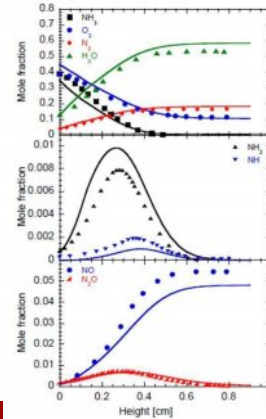


Model:

Glarborg et al. (2018)

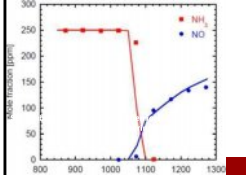
Flame structure

(Bian et al., 1986)



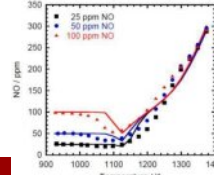
reactor: CO/NH<sub>3</sub>

(Wargadalam et al., 2000)



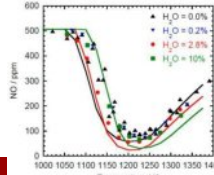
NH<sub>3</sub>+trace NO

(Vikas and Glarborg, 2004)



Thermal DeNO<sub>x</sub>

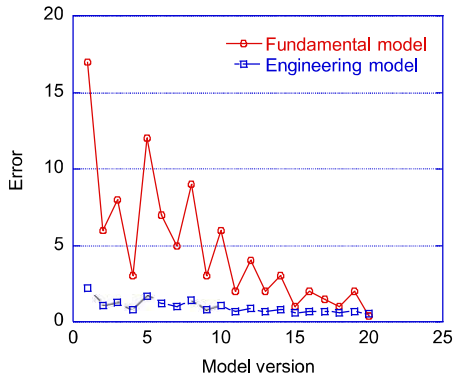
(Duo et al., 1990)







## First-principles versus engineering models



### First-principles model

- Scientifically solid
- Represents the present understanding of the chemistry
- Often lower accuracy compared to engineering models

### Engineering model

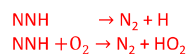
- Optimized to improve agreement
- Often impressive predictive capabilities (within optimized regime)
- Tends to disguise scientific issues

11

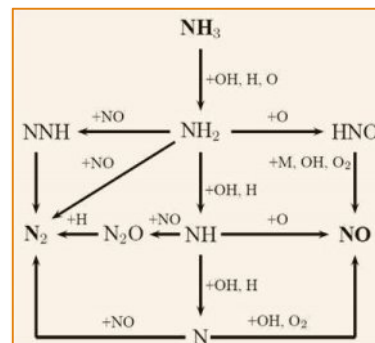
Slide adapted from Rob Barlow

### Thermal DeNOx (SNCR)

- Key step has two product channels:
  - $\text{NH}_2 + \text{NC} \rightleftharpoons \text{NNH} + \text{OH}$  (sustains process via  $\text{NNH} \rightarrow \text{N}_2 + \text{H}$ )
  - $\text{NH}_2 + \text{NC} \rightleftharpoons \text{N}_2 + \text{H}_2\text{O}$  (does not sustain process)
- Effective in narrow temperature range centered around 1250 K (too slow below 1100 K;  $\text{NH}_2 \rightarrow \text{HNO} \rightarrow \text{NO}$  above 1400 K)
- Early work done with low  $\text{NH}_3$  levels (additive, not fuel)
- The two crucial steps controlling the SNCR behaviour are linked to the NNH radical as shown by Greenblatt et al. (2023).



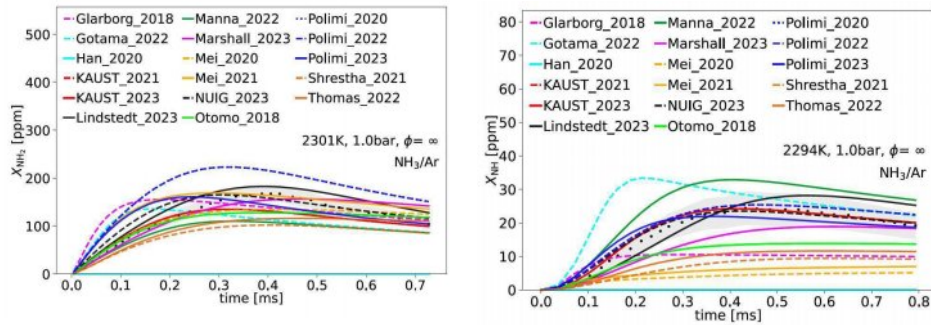
The two steps are intrinsically linked and cannot be independently specified if the SNCR performance of a model is to be maintained.



Glarborg et al., Prog. Energy Combust. Sci. 67 (2018) 3168

## IMPERIAL

Graphs provided by Heinz Pitsch and correspond to Girhe et al. (2024) accepted for publication (Combust. Flame) Experimental data from Davidson et al. (1990).



The  $\text{NH}_2$  chemistry, crucial for SNCR, is better reproduced than the subsequent  $\text{NH}$  pathways.  
The  $\text{NH}$  radical plays an important role in  $\text{N}_2\text{O}$  formation.

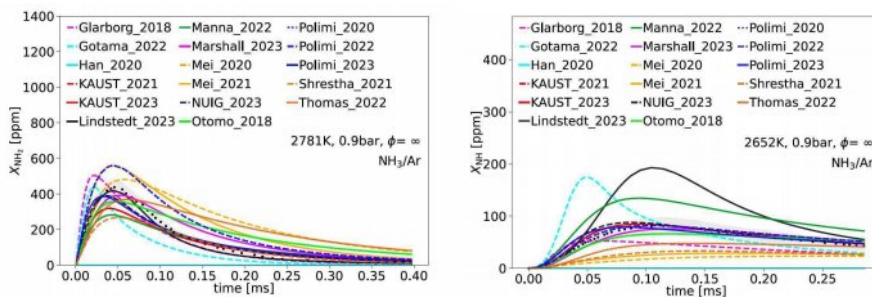
Imperial College London

13

02/08/2024

## IMPERIAL

Graphs provided by Heinz Pitsch and correspond to Girhe et al. (2024) accepted for publication (Combust. Flame). Experimental data from Davidson et al. (1990).



One particular issue that causes the over-prediction of  $\text{NH}$  with the Greenblatt and Lindstedt (2023) mechanism is caused by a single pyrolysis reaction  $\text{NH} + \text{H} = \text{N} + \text{H}_2$  which was increased by a factor of 3.3 by Alturaifi et al. (2022) from the Davidson et al. (1990) value.

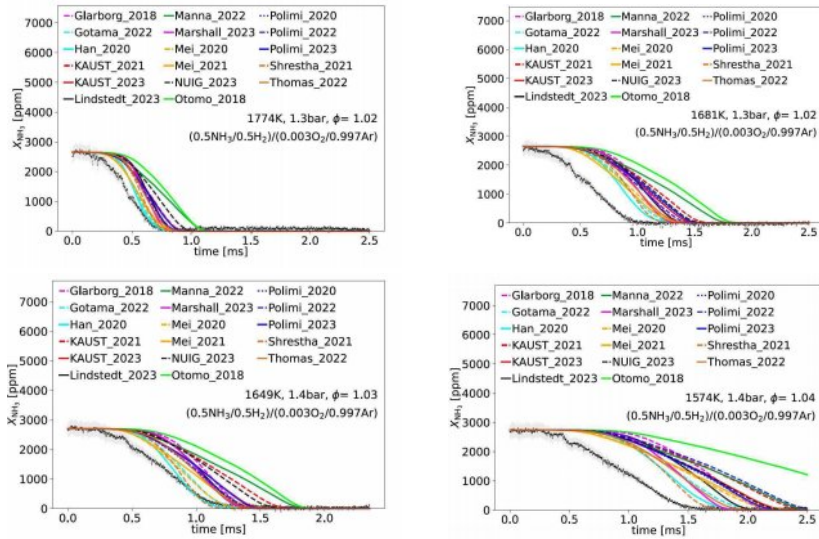
Imperial College London

14

02/08/2024

# IMPERIAL

Graphs provided by Heinz Pitsch and correspond to Girhe et al. (2024) accepted for publication (Combust. Flame). Experimental data from Altuarifi et al. Proc. Combust. Inst. (2023).



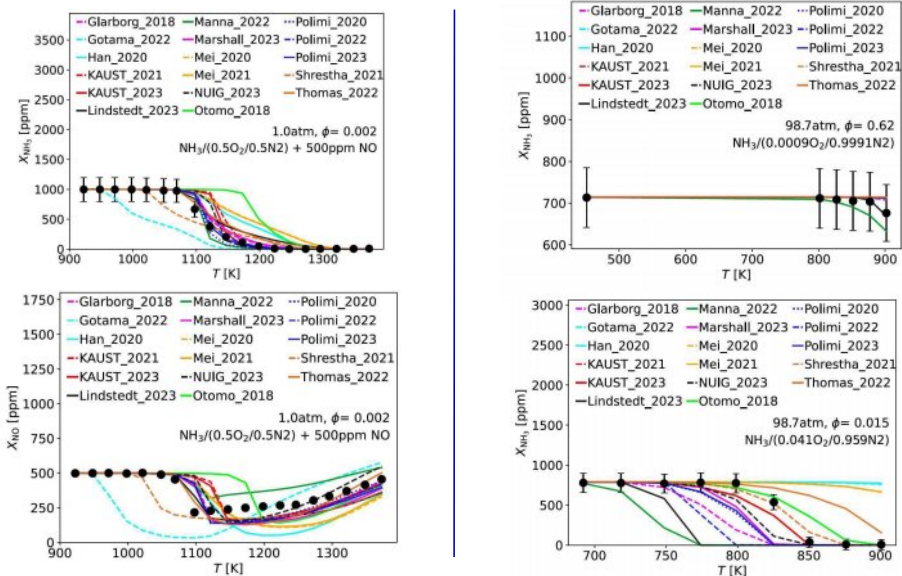
Imperial College London

15

02/08/2024

# IMPERIAL

Graphs provided by Heinz Pitsch and correspond to Girhe et al. (2024) accepted for publication (Combust. Flame). Experimental data from (left) Kasuya et al., Chem. Eng. Sci. 50 (1995) 1455-1466 and (right) Song et al., Fuel 181 (2016) 358-365.



Imperial College London

16

1/2024

# IMPERIAL

## Thermal DeNOx (SNCR)

### Rate comparisons:

**Top:**  $\text{NNH} = \text{N}_2 + \text{H}$

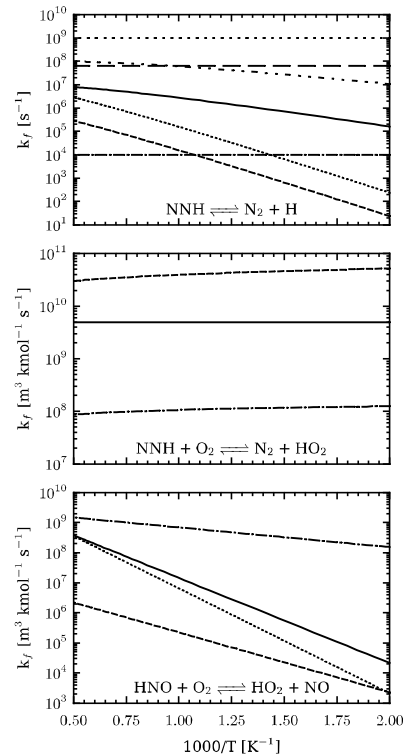
Lindstedt et al. (1994) (solid line); Miller and Bowman (dot-dashed line); Vandooren et al. (1991) (dotted line), Bozzelli and Dean (1995) (dot-dot-dash line); Miller and Glarborg (1999) (long dashed line) and Klippenstein et al. (2011) (sparse dotted line).

**Middle:**  $\text{NNH} + \text{O}_2 = \text{N}_2 + \text{HO}_2$

GRI-Mech 3.0 (solid line), Klippenstein et al. (2011) (dashed line) and Dean and Bozzelli (dot-dashed line).

**Bottom:**  $\text{HNO} + \text{O}_2 = \text{HO}_2 + \text{NO}$

GRI-Mech 3.0 (solid line), Bryukov et al. (1993) (dashed line), Fujii et al. (1981) (dot-dashed line) and Dean and Bozzelli (2000) (dotted line).



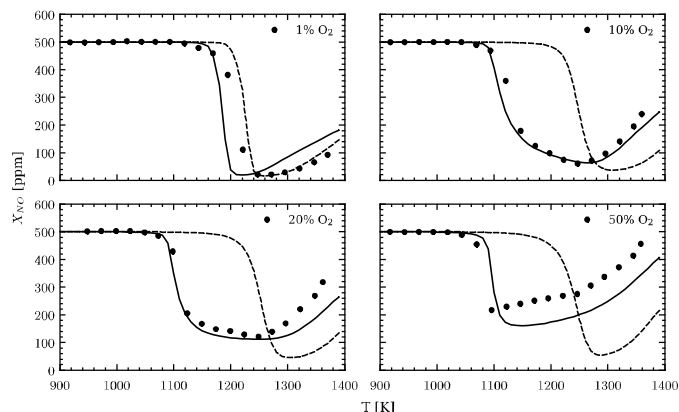
Imperial College London

17

02/08/2024

# IMPERIAL

## Thermal DeNOx (SNCR)



Flow reactor calculations comparing the impact on the SNCR behaviour of an inappropriate balancing of the NNH destruction reactions. From Greenblatt et al. (2023).

Experimental data from Kasuya et al. (1995) showing the impact of  $\text{O}_2$  on the SNCR behaviour with inlet concentrations:  $\text{NH}_3 = 1000$  ppm,  $\text{NO} = 500$  ppm,  $\text{O}_2 = 1, 10, 20$  and  $50\%$ ,  $\text{H}_2\text{O} = 5\%$  with a residence time (s) =  $88,0/T(\text{K})$  at a pressure of 101 kPa and mole fractions balanced with  $\text{N}_2$ .

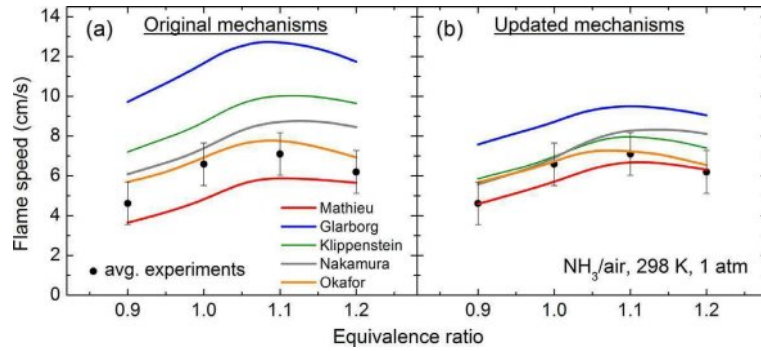
Imperial College London

18

02/08/2024

# IMPERIAL

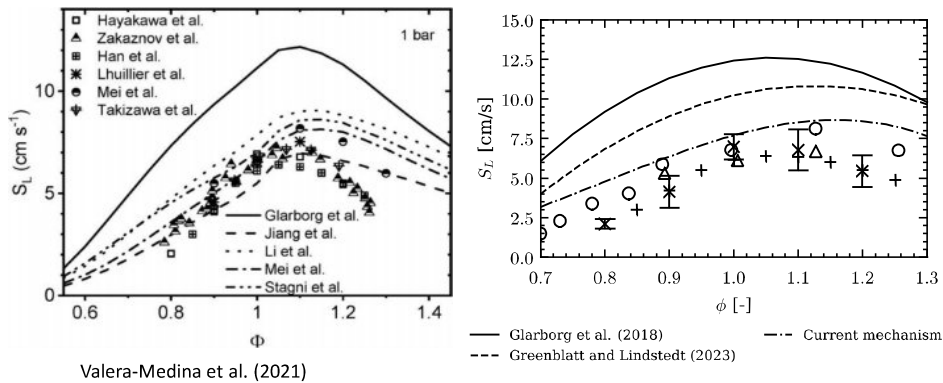
Importance of pyrolysis reactions – a key feature of ammonia combustion dynamics Alturaifi et al. (2022)



Prediction of  $\text{NH}_3$  / air laminar flame speed showing the effect of updating selected detailed chemical kinetics mechanisms with the  $\text{NH}_3$  pyrolysis sub-mechanism of Alturaifi et al. (2022). Experiments were averaged at each equivalence ratio from the studies of Takizawa et al. (2008), Hayakawa et al. (2015), Mei et al. (2019) and Han et al. (2019).

# IMPERIAL

The burning velocity discrepancies are probably close to being removed.

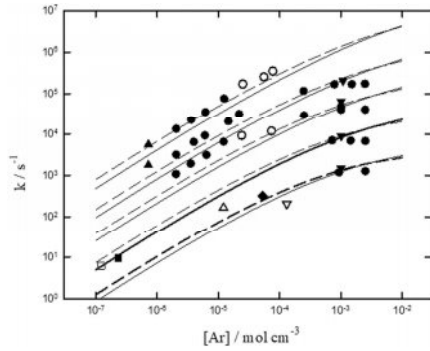


Valera-Medina et al. (2021)



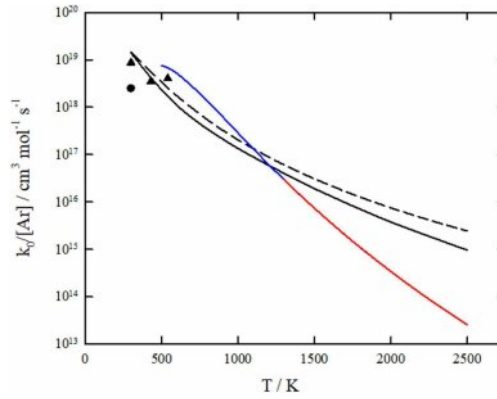
## IMPERIAL

A key reaction:  $\text{N}_2\text{H}_4 (+ \text{Ar}) \rightarrow \text{NH}_2 + \text{NH}_2 (+ \text{Ar})$  from Cobos et al. *Combust Flame* 257 (2023) 112374.



Falloff curves for  $\text{N}_2\text{H}_4 (+ \text{Ar}) \rightarrow \text{NH}_2 + \text{NH}_2 (+ \text{Ar})$ . Representations from bottom to top, for 1110, 1200, 1300, 1400 and 1550 K. Theoretical curves: (dashed line) Klippenstein et al. (2009); (solid line) Cobos et al. (2023).

Imperial College London



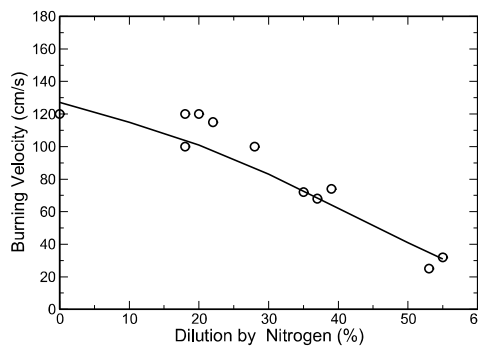
Limiting low-pressure rate constants  $k_0$  for  $\text{N}_2\text{H}_4 (+ \text{Ar}) \rightarrow \text{NH}_2 + \text{NH}_2 (+ \text{Ar})$ . Red curve and blue curves experimental data and theoretical calculations by Klippenstein et al. (2009) with  $\langle \Delta E \rangle_{\text{down}}/hc = 150 (T/300 \text{ K})^{0.85} \text{ cm}^{-1}$  (dashed black line) and from Cobos et al. (2023) with  $\langle \Delta E \rangle_{\text{total}}/hc = -100 \text{ cm}^{-1}$  (solid black line).

21

02/08/2024

## IMPERIAL

Hydrazine decomposition flames (no oxidant) are exceptionally sensitive to the  $\text{N}_2\text{H}_4/\text{N}_2\text{H}_3$  system Cobos et al. (2023) amongst others.



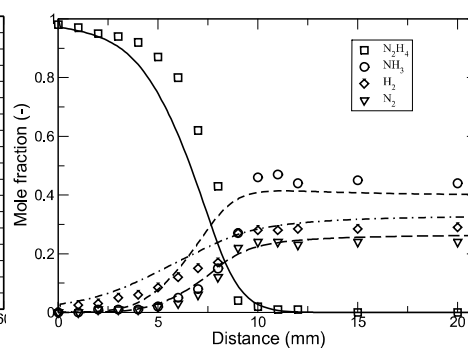
Burning velocities of  $\text{N}_2$  diluted hydrazine decomposition flames. Circles: mixtures with  $\text{N}_2$  at 1 atm pressure and an initial temperature of 383 K.

Experimental data from Karpov and Sokolik, *Russ. J. Phys. Chem.* 38 (1964) 903 (c.f., Konnov and De Ruyck 2001). Computations; Lindstedt (2024).

Imperial College London

22

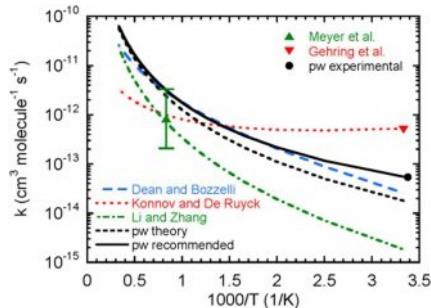
02/08/2024



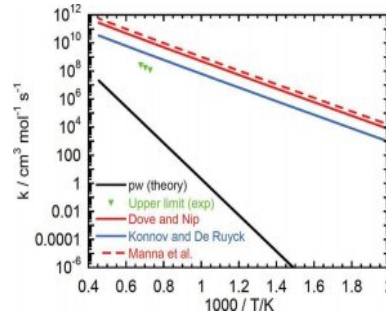
Hydrazine decomposition flame structure. Experimental results from MacLean and Wagner (1967). Initial temperature 353 K, pressure 14 Torr (0.0184 atm). Computations Lindstedt (2024).

## IMPERIAL

The  $\text{N}_2\text{H}_4/\text{N}_2\text{H}_3$  system is critical for hydrazine combustion with an impact on ammonia.



Arrhenius plot of some evaluations of the rate coefficient for  $\text{NH}_2 + \text{N}_2\text{H}_4$  (Gao et al., *Proc. Combust. Inst.* 39 (2023) 571-579). ▲ Meyer et al. (1969), ▼ Gehring et al. (1971), dotted red line Konnov and De Ruyck [6], green dash-dot line Li and Zhang (2006), blue dashed line Dean and Bozzelli (2000), dashed black line present quantum calculations, ● Gao et al. (2023) measurement and solid black line their recommendation.



Arrhenius plot for the reaction  $\text{NH}_3 + \text{NH}_2 \rightleftharpoons \text{N}_2\text{H}_3 + \text{H}_2$  (Marshall and Glarborg, *J. Phys. Chem. A* 127 (2023) 2601-2607). The calculated value, assumed to be an upper limit, is compared to estimates from Dove and Nip (1979), Konnov and De Ruyck (2001) and Manna et al. (2020). Also shown is upper limit values derived from modeling the flow reactor results of Benes et al. (2021).

Imperial College London

23

02/08/2024

## IMPERIAL

### Some critical reaction steps

- The pyrolysis chemistry has a huge impact due to the scarcity of H radicals during the combustion of  $\text{NH}_3$  – in particular in the absence of additional  $\text{H}_2$  as part of the fuel stream. How much  $\text{H}_2$  is appropriate?
- Girhe et al. (2024) recommend that the reaction  $\text{NH}_2 + \text{NH} = \text{N}_2\text{H}_3$  be studied further. The lack of stabilisation reported by Klippenstein et al., *J. Phys. Chem. A* 113 (2009) 10241 could usefully be confirmed.
- Greenblatt et al. (2023) adopts the NNH chemistry for decomposition and oxidation according to Klippenstein et al. (2011). This is not universal and good SNCR results can be obtained using very different rate combinations. The uncertainties in the reaction  $\text{NNH} + \text{O}_2$  could usefully be further established. The same applies to the reaction  $\text{HNO} + \text{O}_2$ .
- Gao et al. (2023) makes a forceful argument that the that the pyrolysis chemistry of  $\text{N}_2\text{H}_3$  is in urgent need of clarification.
- How accurate is the low-pressure limit for the reaction  $\text{N}_2\text{H}_4 (+ \text{M}) = \text{NH}_2 + \text{NH}_2 (+ \text{M})$ ? The reaction has been studied by Cobos et al. (2023) and Klippenstein et al. (2009) amongst others. Computed results can be exceptionally sensitive to both chaperon efficiencies (c.f., Glarborg et al. 2021) and the actual value (e.g., in Ar bath gas).

Imperial College London

24

02/08/2024

## Model improvements

### Reaction mechanism performance (Girhe et al. 2024)

Kinetic model	Species concentration							Ignition delay time	Laminar burning velocity	Overall mean
	Pyrolysis	Oxidation			Thermal DeNO <sub>x</sub>	Mean				
		High <i>T</i>	Intermediate <i>T</i>	Low <i>T</i>						
NUIG_2023	0.741	0.778	0.841	0.894	0.909	0.833	0.842	0.888	0.854	
KAUST_2023	0.734	0.763	0.903	0.890	0.910	0.840	0.820	0.897	0.852	
KAUST_2021	0.734	0.759	0.887	0.890	0.901	0.834	0.823	0.894	0.851	
Polimi_2023	0.687	0.769	0.850	0.883	0.908	0.819	0.822	0.888	0.843	
Polimi_2020	0.715	0.737	0.848	0.885	0.906	0.818	0.817	0.892	0.842	
Mei_2021	0.673	0.759	0.848	0.850	0.921	0.810	0.818	0.882	0.837	
Polimi_2022	0.715	0.736	0.848	0.869	0.906	0.815	0.801	0.892	0.836	
Thomas_2022	0.636	0.769	0.848	0.834	0.898	0.797	0.814	0.889	0.833	
Mei_2020	0.633	0.736	0.851	0.811	0.917	0.790	0.819	0.891	0.833	
Manna_2022	0.708	0.720	0.887	0.848	0.910	0.814	0.823	0.833	0.823	
Lindstedt_2023	0.707	0.689	0.832	0.865	0.898	0.798	0.821	0.841	0.820	
Shrestha_2021	0.678	0.685	0.815	0.797	0.712	0.737	0.818	0.890	0.815	
Gotama_2022	0.589	0.748	0.825	0.845	0.731	0.748	0.804	0.880	0.810	
Marshall_2023	0.718	0.712	0.829	0.840	0.892	0.798	0.793	0.831	0.807	
Glarborg_2018	0.624	0.699	0.809	0.816	0.892	0.768	0.823	0.810	0.801	
Han_2020	0.095	0.752	0.843	0.831	0.859	0.676	0.810	0.899	0.795	
Otomo_2018	0.652	0.591	0.808	0.858	0.819	0.746	0.805	0.818	0.790	

25



## IMPERIAL

### Summary

- Chemical kinetic mechanisms for ammonia are advancing rapidly and increasingly based on the much-improved understanding of fundamental kinetic rate data and pathways.
- An exceptionally wide range of chemical mechanisms have been produced. Some of these are not based on best available data and/or not subject to comprehensive validation.
- There are current uncertainties for some key fundamental reaction sequences and these need to be addressed. However, very useful “engineering” models can certainly be formulated on “best” available current data.

#### Peter Glarborg:

“While there are still some unresolved issues to solve (luckily!), it looks like we are converging towards a mechanism that is useful over a broader range of conditions (without optimizing). Stephen’s theoretical work on several of the key steps has had a large impact.”

Imperial College London

26

02/08/2024

# IMPERIAL

## Summary

- Accurate validation data remains essential and not all data sets available appear to have been subject to a thorough accuracy assessment.
- Inaccurate validation data poses a problem when assessing model performance. Put simply – to assess model performance vs questionable data is at best futile and at worst misleading.
- **Accurate speciation data is king** and the prospects for fundamental “chemistry experiments” featuring time resolved shock tube data are gradually improving.
- Stirred reactor data can be affected by imperfect mixing, heat losses and, if mixtures are not sufficiently dilute, heat release effects. Still such data also has a major role provided conditions are well-defined. Flow reactor data may also suffer some of these disadvantages.
- Flames are not suitable for determining chemical kinetic data. There is, however, a major role for accurate flame data use in the context of validation. This opens the possibility of assessing the overall performance of a model under more complex conditions.

Imperial College London

27

02/08/2024

# IMPERIAL

Richter et al. (2024)

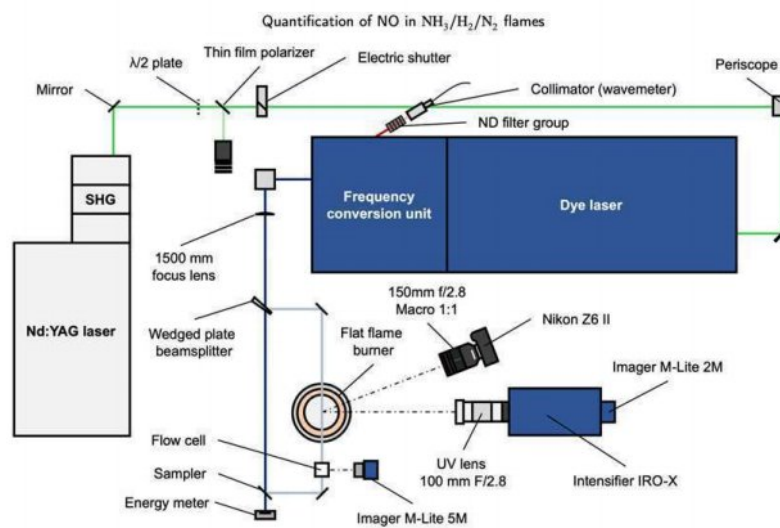


Figure 1: Experimental setup (NO-LIF, absorption and chemiluminescence).

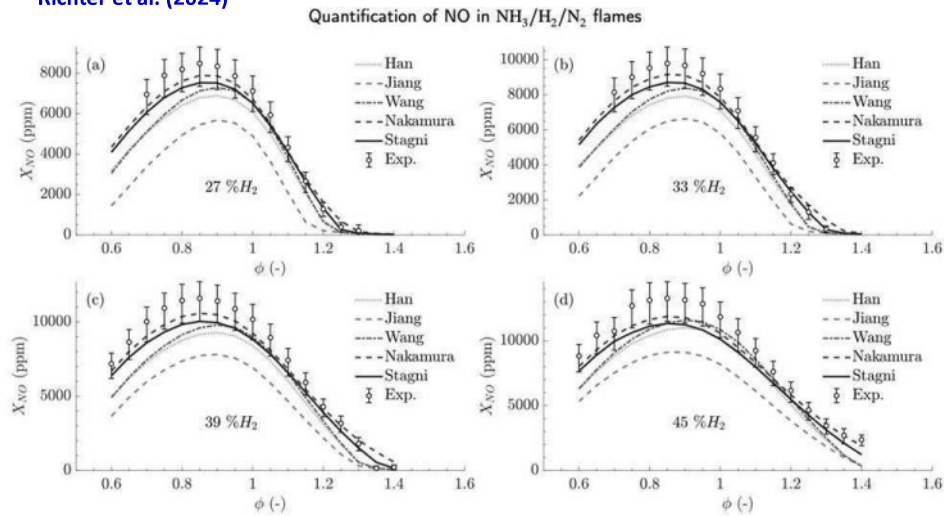
Imperial College London

28

02/08/2024

# IMPERIAL

Richter et al. (2024)



Imperial College London

29

02/08/2024

# IMPERIAL

## What can TNF do in collaboration with others?

- Is there scope for a chemical kinetic data evaluation/advisory group featuring contributions from practitioners and dedicated to recommend the best chemical kinetic data currently available (c.f., Baulch et al. 1992, 1994, 2005)?
- If so, the development of accurate ammonia mechanisms can usefully be considered in two parts: pyrolysis and oxidation. Perhaps with a further focus on high pressure.
- The success of TNF has to a large extent relied upon accurate experimental data. Can an experimental data evaluation group be convened that assesses the accuracy of validation data sets and their appropriate use?
- Is there any prospect for the exceptionally useful formal accuracy assessment developed by Pitsch and co-workers (Girhe et al. 2024) to be made available to model developers to help analyse their efforts?
- If so, can that framework evolve to account for new and more comprehensively evaluated data sets? Can RWTH Aachen be a custodian for the benefit of the community?
- Most of the above activities would probably be a community effort of the type supported by TNF members in the past.

Imperial College London

30

02/08/2024

**IMPERIAL**

**Thank you!**

**Gaetano has kindly offered to provide a perspective on  
experimental data and techniques.**



# Ammonia chemical kinetics

## Can TNF-like experimental tools help?

TNF 16, Milan July 20 2024

Presenter: Gaetano Magnotti

Acknowledgement: Alessandro Stagni

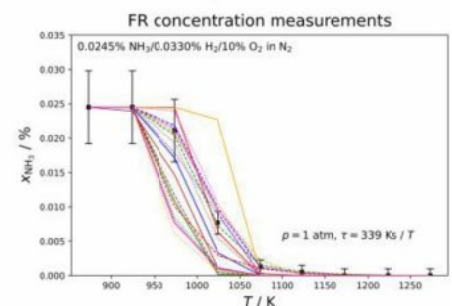
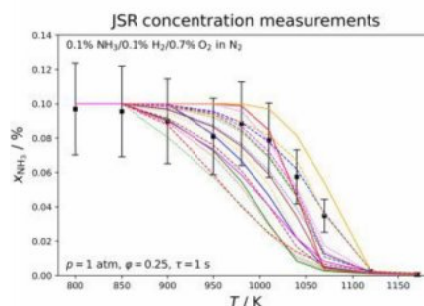
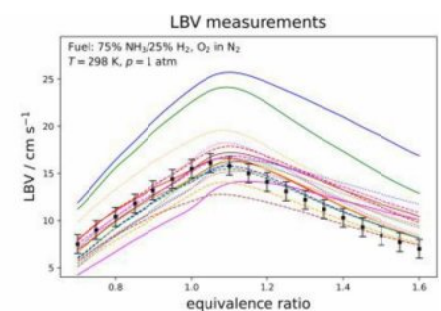
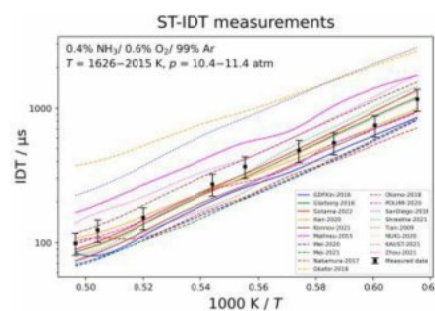


1



## Are chemical kinetic models sufficiently accurate ?

- Despite large effort and apparently simpler chemistry, kinetics mechanisms have not converged yet.
- No model is able to match satisfactorily all data
- Visual comparison between experimental and numerical data can be misleading





## A more comprehensive metric

Curve Matching (CM) score as a metric to indicate agreement between experimental data and their counterpart (*Ramalli et al. Chem. Eng. J., 454 (2023), Article 140149*) and **Gireh, 2024 CNF, 267, 113560**

Essential to have high-quality data. Bad data can be highly detrimental!

Kinetic model	Species concentration					Mean	Ignition delay time	Laminar burning velocity	Overall mean
	Pyrolysis	Oxidation			Thermal DeNO <sub>x</sub>				
		High T	Intermediate T	Low T					
NUIG_2023	0.947	0.941	0.860	0.889	0.865	0.900	0.930	0.876	0.902
KAUST_2023	0.951	0.901	0.872	0.884	0.869	0.895	0.914	0.884	0.898
KAUST_2021	0.951	0.902	0.872	0.886	0.859	0.894	0.915	0.882	0.897
POLIMI_2023	0.922	0.912	0.861	0.869	0.856	0.884	0.921	0.879	0.895
Mei_2021	0.899	0.930	0.862	0.844	0.872	0.881	0.921	0.880	0.894
Mei_2020	0.882	0.922	0.866	0.834	0.869	0.875	0.920	0.885	0.893
POLIMI_2020	0.941	0.891	0.863	0.854	0.842	0.878	0.917	0.882	0.893
Thomas_2022	0.911	0.929	0.857	0.843	0.854	0.879	0.918	0.879	0.892
POLIMI_2022	0.941	0.892	0.864	0.847	0.842	0.877	0.912	0.883	0.891
Marshall_2023	0.959	0.883	0.842	0.830	0.863	0.875	0.915	0.835	0.875
Han_2020	0.677	0.929	0.860	0.832	0.824	0.824	0.916	0.884	0.875
Manna_2022	0.931	0.900	0.876	0.837	0.865	0.882	0.911	0.827	0.873
Gotama_2022	0.848	0.910	0.848	0.836	0.707	0.830	0.911	0.872	0.871
Shrestha_2021	0.926	0.865	0.853	0.816	0.692	0.830	0.905	0.876	0.870
Glarborg_2018	0.872	0.887	0.841	0.833	0.859	0.859	0.915	0.809	0.861
Otomo_2018	0.924	0.805	0.832	0.833	0.756	0.830	0.910	0.816	0.852

## Experimental data used for the score

### 36 dataset used in Gireh exercise

#### Jet Stirred reactors (10/36)

- Homogenous mixture,
- Excellent temperature control.
- Pressure < 1.5 bar
- 500 < T < 1450 K, suitable for **low to intermediate temperature oxidation, thermal denox**
- He as diluent, containing ~1000 ppm of NH<sub>3</sub>
- Speciation measurements available

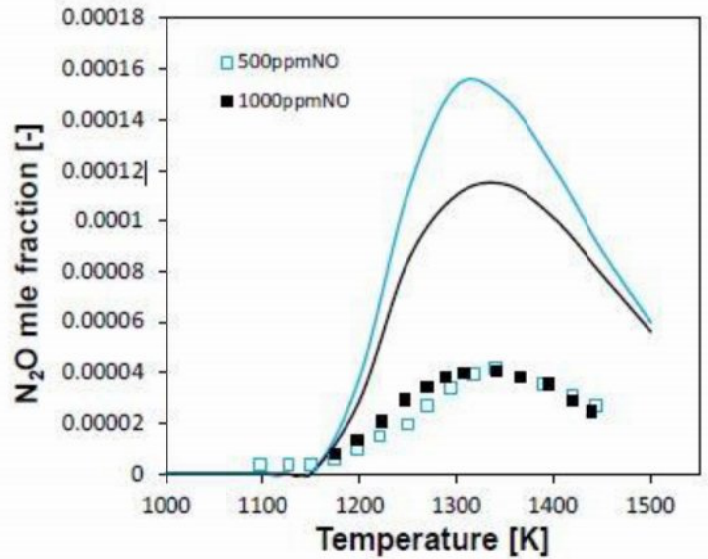
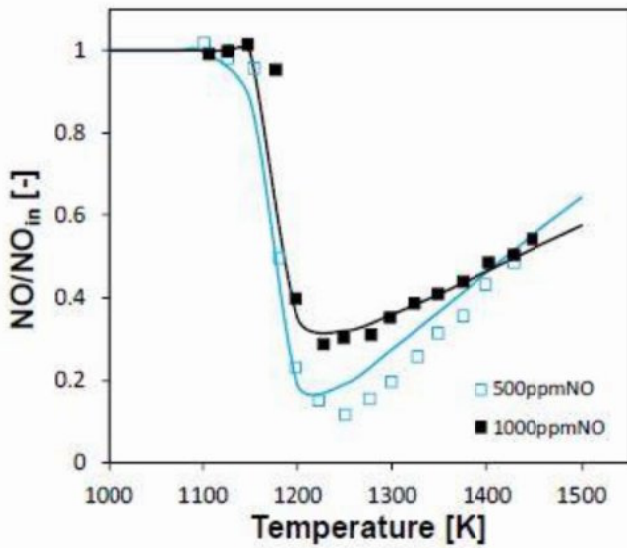
#### Flow reactors (7/36)

- Homogenous mixture,
- Generally 1 bar, but one study at 30 and 100 bar
- 500 < T < 1970 K, suitable for **low to intermediate temperature oxidation, denox**
- Speciation measurements available



## Experimental data used for the score

36 dataset used in Gireh exercise



Stagni, 2023 React. Chem. Eng., 2020,5, 696

5

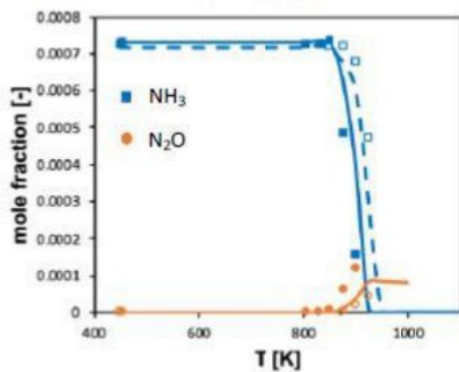


## Experimental data used for the score

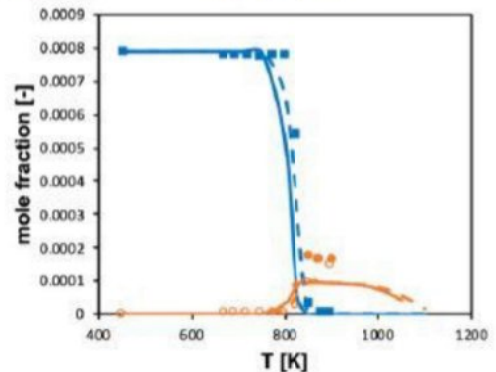
Stagni, 2023 React. Chem. Eng., 2020,5, 696

Caution ! Surface effects can be very important

a,b) P = 30 bar



c,d) P = 100 bar



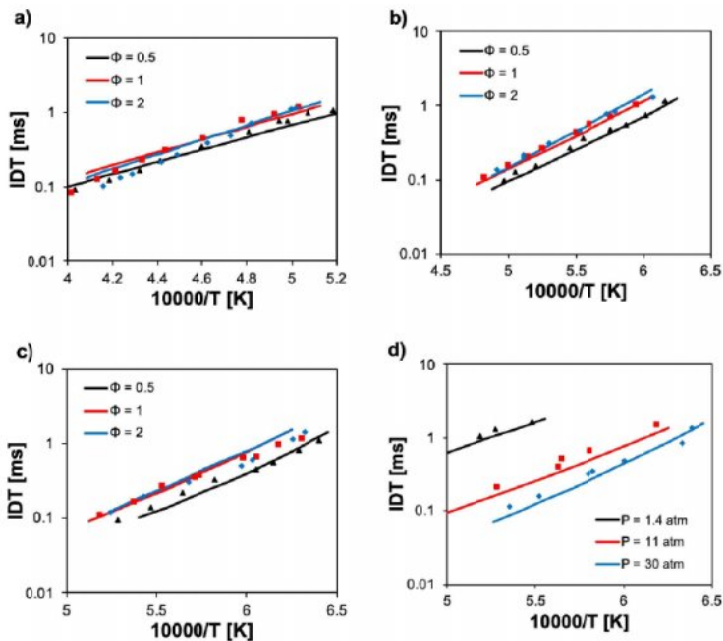
■ — Quartz    □ - - Alumina

6



## Experimental data used for the score

### 36 dataset used in Gireh exercise



### Constant volume vessel and heat flux burners (12/36)

- Temperature 290:500 K
- Pressure 1-5 bar
- Laminar burning velocity measurements

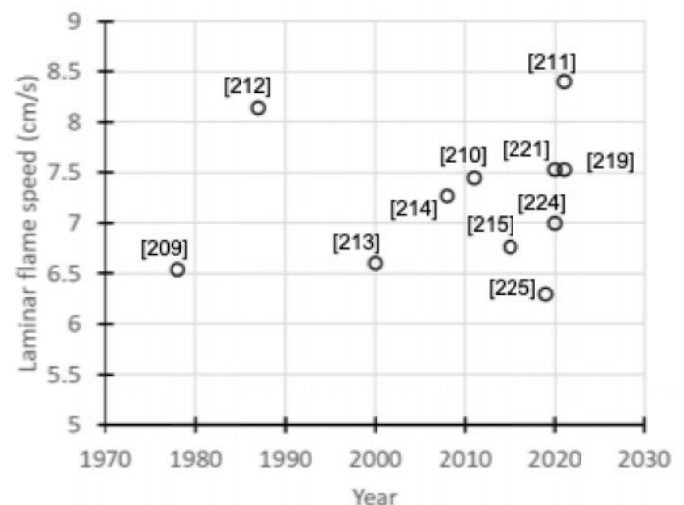
7



## Chemical Kinetics development: a wish list

Too many data can become a problem. We need good data

- Effect of bath gas.
- Effect of pressure
- Species at practical pressure and temperatures
- **Low temperature data (focus on  $HNO$  and  $N_2O$ )**
- $O_2$  rich environment
- New diagnostics for unstable intermediates
- Ammonia/Hydrocarbons blends
  - **Soot-ammonia interaction**

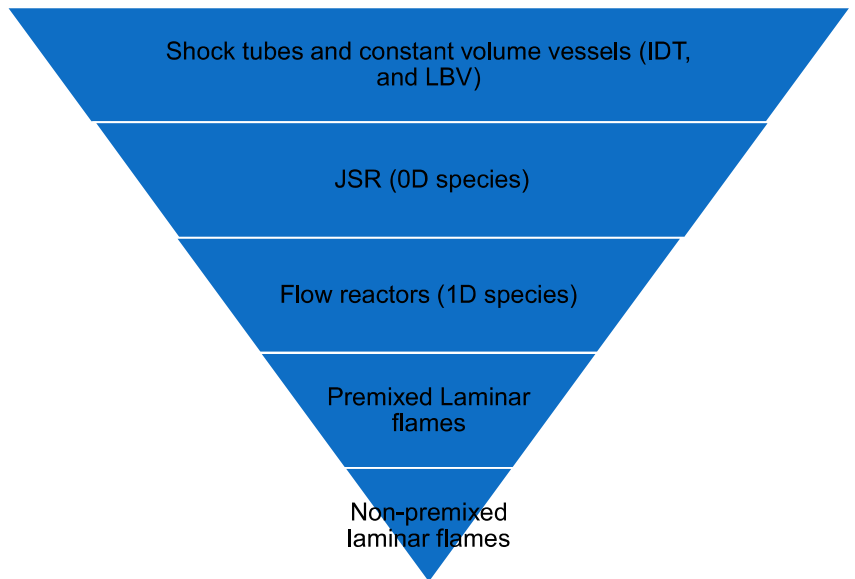


8

# What about flame data?

## Measurements in laminar flames are still fairly rare

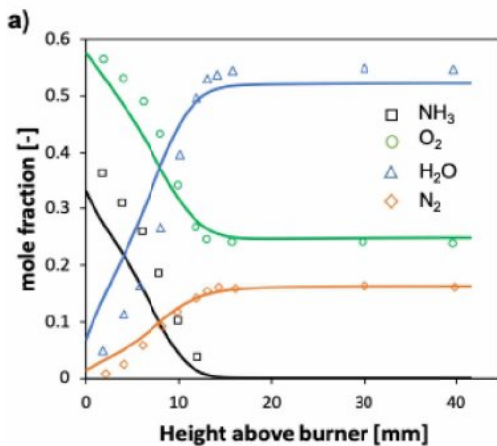
- Increasing complexity principle.
- Why we need it:
  - Include transport in the problem
  - Useful to remove surface effects
  - Chemical kinetics models that cannot match laminar flames, cannot work correctly in turbulent flames



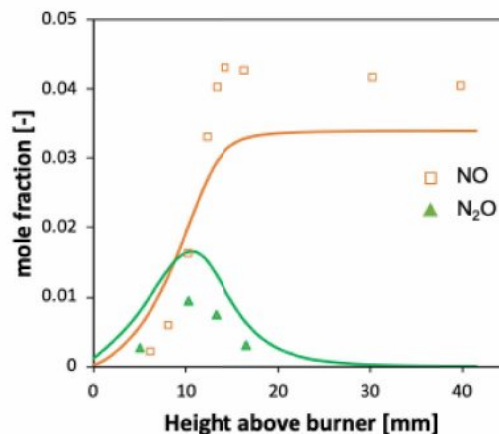
9

## Laminar flames for chemical kinetics development

- Several measurements in flames stabilized over a porous plug burner from the 70's



Stagni, 2023 React. Chem. Eng.,  
2020,5, 696



(1970)

t. Flame 20

19.

on

iation of an

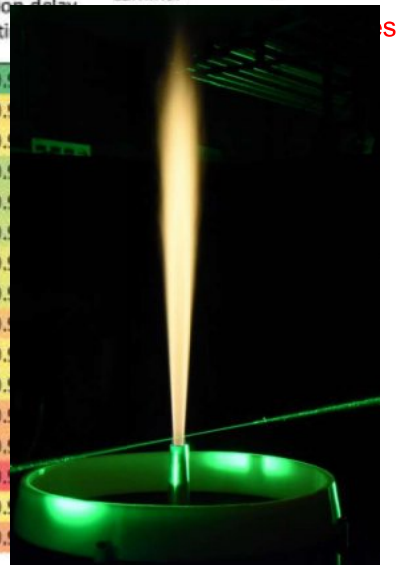
and CH<sub>4</sub>

Brackmann et al. CNF Vol 163  
pp 370, 2016



# A TNF prospective

Kinetic model	Species concentration						Ignition delay time	Laminar burning velocity
	Pyrolysis	Oxidation			Thermal DeNO <sub>x</sub>	Mean		
		High T	Intermediate T	Low T				
NUIG_2023	0.947	0.941	0.860	0.889	0.865	0.900	0.930	0.876
KAUST_2023	0.951	0.901	0.872	0.884	0.869	0.895	0.914	0.884
KAUST_2021	0.951	0.902	0.872	0.886	0.859	0.894	0.915	0.882
POLIMI_2023	0.922	0.912	0.861	0.869	0.856	0.884	0.921	0.879
Mei_2021	0.899	0.930	0.862	0.844	0.872	0.881	0.921	0.880
Mei_2020	0.882	0.922	0.866	0.834	0.869	0.875	0.920	0.885
POLIMI_2020	0.941	0.891	0.863	0.854	0.842	0.878	0.917	0.882
Thomas_2022	0.911	0.929	0.857	0.843	0.854	0.879	0.918	0.879
POLIMI_2022	0.941	0.892	0.864	0.847	0.842	0.877	0.912	0.883
Marshall_2023	0.959	0.883	0.842	0.830	0.863	0.875	0.915	0.835
Han_2020	0.677	0.929	0.860	0.832	0.824	0.824	0.916	0.884
Manna_2022	0.931	0.900	0.876	0.837	0.865	0.882	0.911	0.827
Gotama_2022	0.848	0.910	0.848	0.836	0.707	0.830	0.911	0.872
Shrestha_2021	0.926	0.865	0.853	0.816	0.692	0.830	0.905	0.876
Glarborg_2018	0.872	0.887	0.841	0.833	0.859	0.859	0.915	0.809
Otomo_2018	0.924	0.805	0.832	0.833	0.756	0.830	0.910	0.816



- CO, H<sub>2</sub>, NO, NH<sub>3</sub>, ... profiles
- Computational cost?

# A TNF prospective

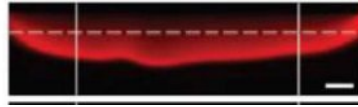
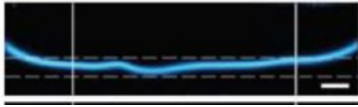
Kinetic model	Species concentration						Ignition delay time	Laminar burning velocity	Pilot flames
	Pyrolysis	Oxidation			Thermal DeNO <sub>x</sub>	Mean			
		High T	Intermediate T	Low T					
NUIG_2023	0.947	0.941	0.860	0.889	0.865	0.900	0.930	0.876	?
KAUST_2023	0.951	0.901	0.872	0.884	0.869	0.895	0.914	0.884	?
KAUST_2021	0.951	0.902	0.872	0.886	0.859	0.894	0.915	0.882	?
POLIMI_2023	0.922	0.912	0.861	0.869	0.856	0.884	0.921	0.879	?
Mei_2021	0.899	0.930	0.862	0.844	0.872	0.881	0.921	0.880	?
Mei_2020	0.882	0.922	0.866	0.834	0.869	0.875	0.920	0.885	?
POLIMI_2020	0.941	0.891	0.863	0.854	0.842	0.878	0.917	0.882	?
Thomas_2022	0.911	0.929	0.857	0.843	0.854	0.879	0.918	0.879	?
POLIMI_2022	0.941	0.892	0.864	0.847	0.842	0.877	0.912	0.883	?
Marshall_2023	0.959	0.883	0.842	0.830	0.863	0.875	0.915	0.835	?
Han_2020	0.677	0.929	0.860	0.832	0.824	0.824	0.916	0.884	?
Manna_2022	0.931	0.900	0.876	0.837	0.865	0.882	0.911	0.827	?
Gotama_2022	0.848	0.910	0.848	0.836	0.707	0.830	0.911	0.872	?
Shrestha_2021	0.926	0.865	0.853	0.816	0.692	0.830	0.905	0.876	?
Glarborg_2018	0.872	0.887	0.841	0.833	0.859	0.859	0.915	0.809	?
Otomo_2018	0.924	0.805	0.832	0.833	0.756	0.830	0.910	0.816	?

# Flat flame burner(Lund)

$\Phi = 0.9$

$\Phi = 1.0$

$\Phi = 1.2$

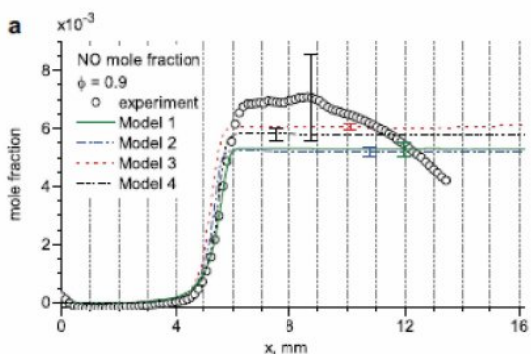
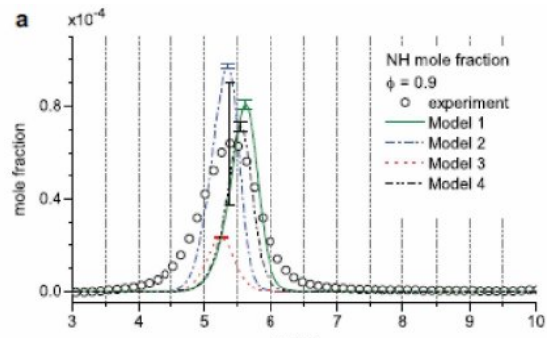
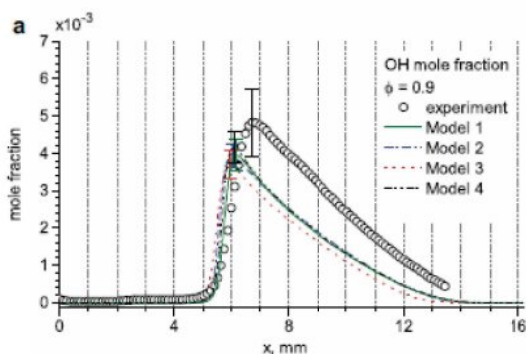
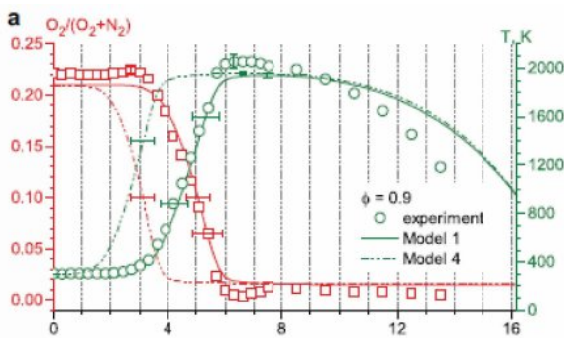


- Premixed ammonia-air flames stabilized over a porous plug burner
- Steel disc 16.2 mm from the porous plug,
- Flames stabilized 5 mm above porous plug
- Dual broadband CARS for temperature and relative O<sub>2</sub> concentration
- Saturated PLIF for OH, NH (308.7 nm) and NO (225.5 nm) (not simultaneous)
- Bidirectional LIF for calibration

Brackmann et al. CNF Vol 163  
pp 370, 2016

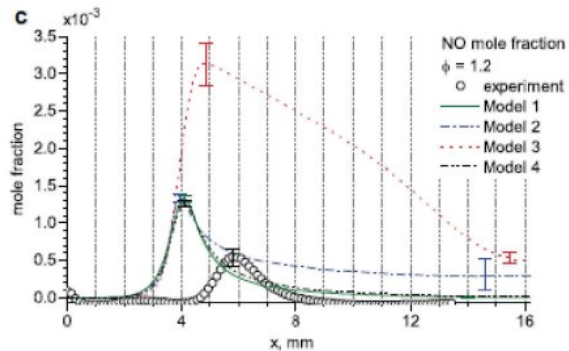
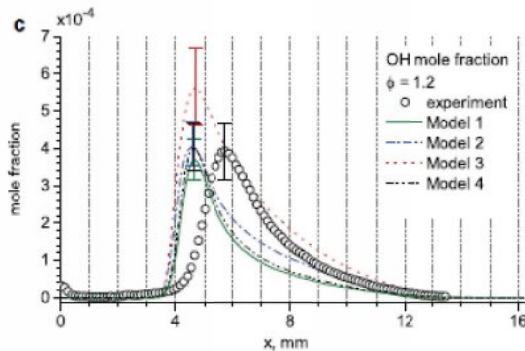
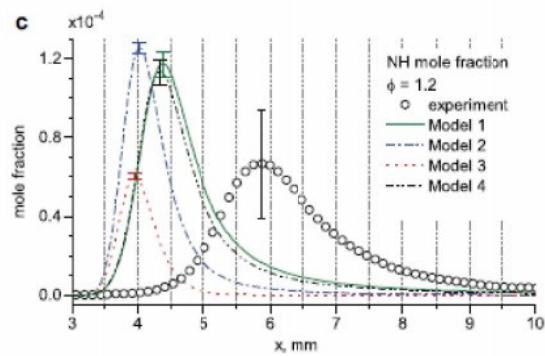
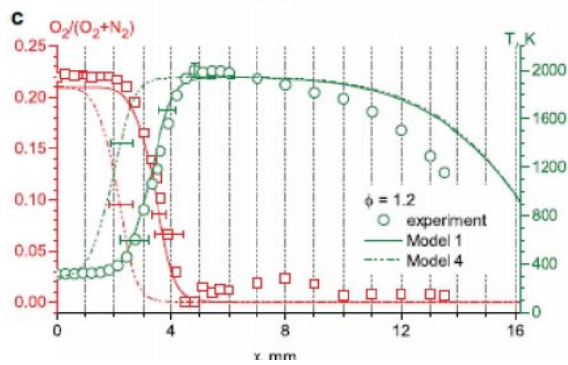
## Flat flame burner: $\Phi = 0.9$

Brackmann et al. CNF Vol 163  
pp 370, 2016



# Flat flame burner: $\Phi = 1.2$

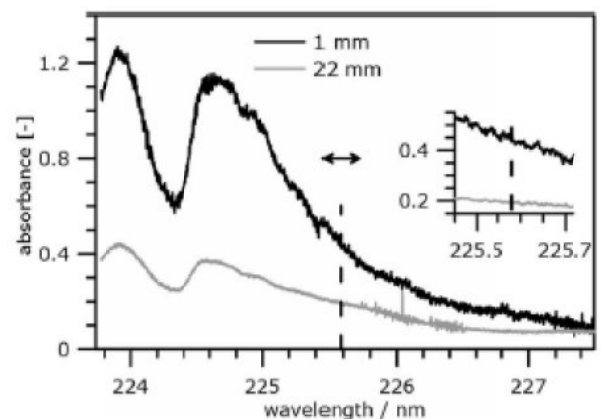
Brackmann et al. CNF Vol 163  
pp 370, 2016



15

## Challenges in flat-flames

- 1D model struggle to match the temperature and species profiles
- Flame aerodynamically stabilized and very sensitive to small disturbances
- Difficult to extend to high-pressure or high O<sub>2</sub> content
- Measurements are not simultaneous
- Spatial resolution (300-500 microns) introduces bias
- Strong ammonia absorption at selected NO excitation wavelength
- Need to use different line as already discussed in Wang et al. (PROCI 2023)



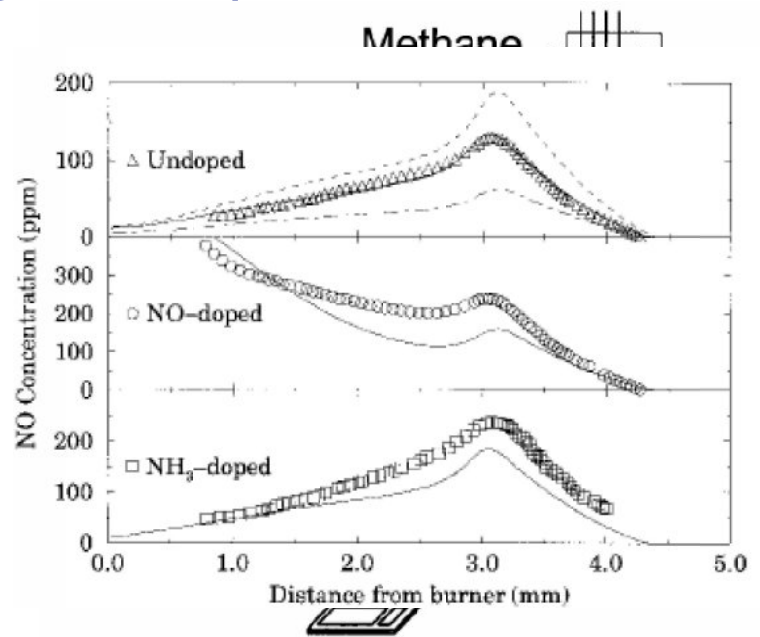
El Baba et al. Combustion and  
Flame 264 (2024) 113424

16



## Counterflow flame (Michigan, 1998)

- Tsuji burner at fixed flow velocity
- NO in CH<sub>4</sub>-air flames, with no seeding, NO and NH<sub>3</sub> seeding
- Planar LIF for NO and OH
- Temperature from previous CARS measurements

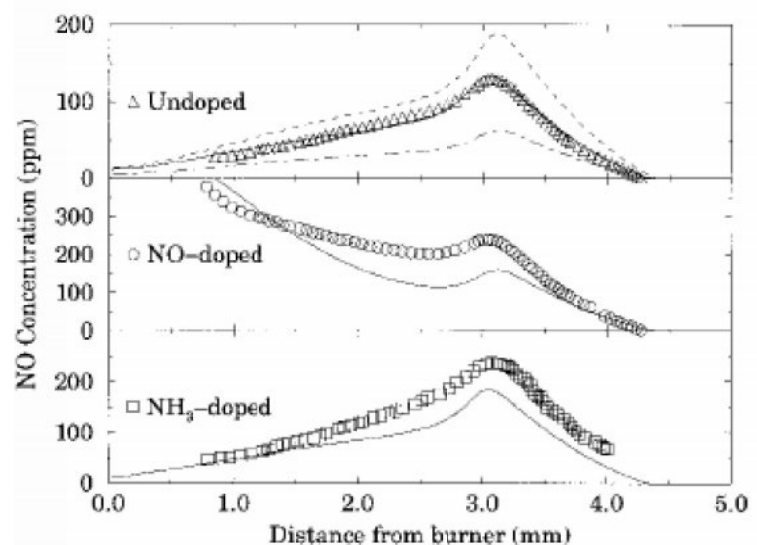


Sick, PROCI 1998, pp 1401

17

## Counterflow flame (Michigan, 1998)

- Tsuji burner at fixed flow velocity
- NO in CH<sub>4</sub>-air flames, with no seeding, NO and NH<sub>3</sub> seeding
- Planar LIF for NO and OH
- Temperature from previous CARS measurements



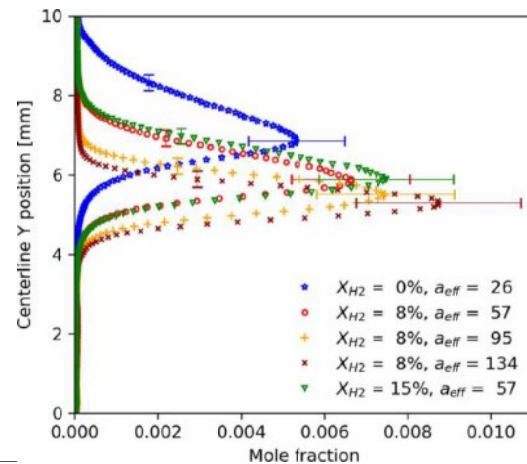
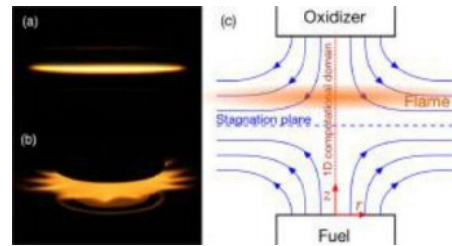
Sick, PROCI 1998, pp 1401

18

# Counterflow flame (Minnesota)

Thomas et al. *PROCI* Vol.39 1803, 2023

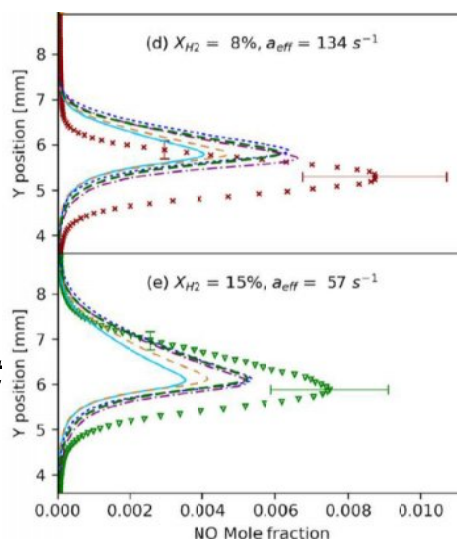
- 10 mm separation, 22.2 mm diameter. Mesh to generate plug-flow
- 5 non-premixed NH<sub>3</sub>/H<sub>2</sub>/air flames
- Saturated planar NO LIF with NO excitation at 225.5 nm (Absorption from ammonia a potential issue)
- Calibration based on bidirectional absorption. Temperature from model ( $\pm 150K$  uncertainty)
- NO increases with increasing H<sub>2</sub> and increasing strain rate, Attributed to reduction in NO destruction via reactions with NH<sub>2</sub> and NH



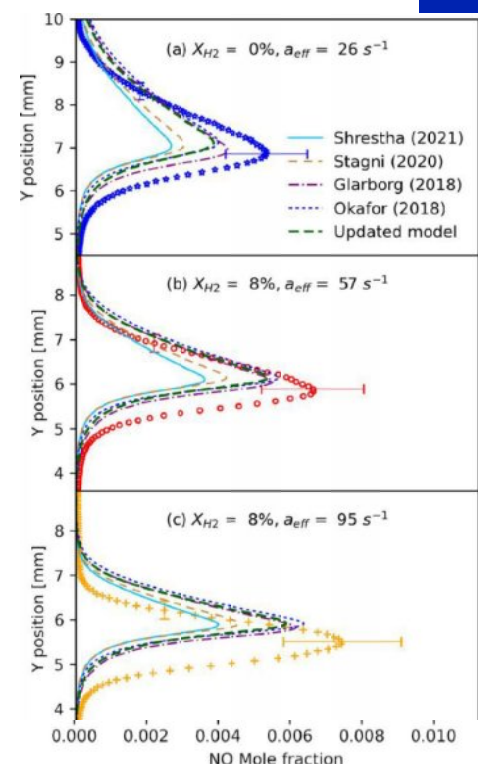
19

# Counterflow flame (Minnesota)

- None of the model able to provide sufficiently accurate results
- Significantly underpredicted NO concentrations
- Used by Mauss to upgrade coefficients in 10 reaction
- **Potential issues:**
  - **Ammonia absorption at 225**
  - **Deviation from saturation**
  - **Temperature from model, not measured**



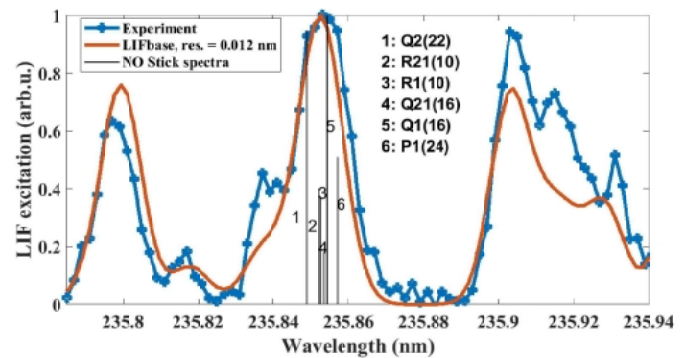
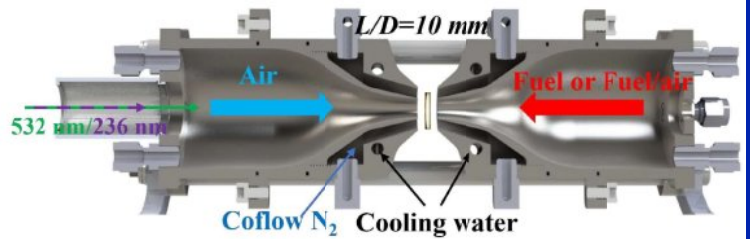
Thomas et al. *PROCI* Vol.39 1803, 2023



## Counterflow flame at KAUST

- 1D quantitative Raman/LIF of major species, temperature and NO
- NO excitation at 235.85 nm to avoid  $\text{NH}_3$  absorption
- Operated in the saturated regime
- Full thermochemical structure for each laser shot
- Comparison in mixture fraction space to minimize sensitivity to boundary conditions
- Large dataset of 15 counterflow flames made available to modelers.

Tang et al. CNF, 267, 113556, 2024

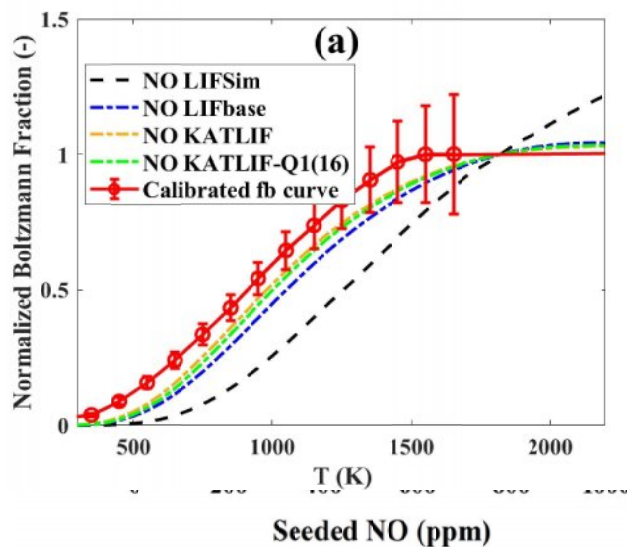


21

## Counterflow flame at KAUST

- Calibration in product of  $\text{H}_2/\text{N}_2/\text{air}$  McKenna burner flame seeded with NO
- Excellent agreement between chemical kinetics mechanism in predicting NO in the products
- Experiments within 80 ppm of prediction
- Empirical calibration of the normalized Boltzmann function based on  $\text{N}_2/\text{H}_2/\text{air}$  counterflow flames seeded with NO

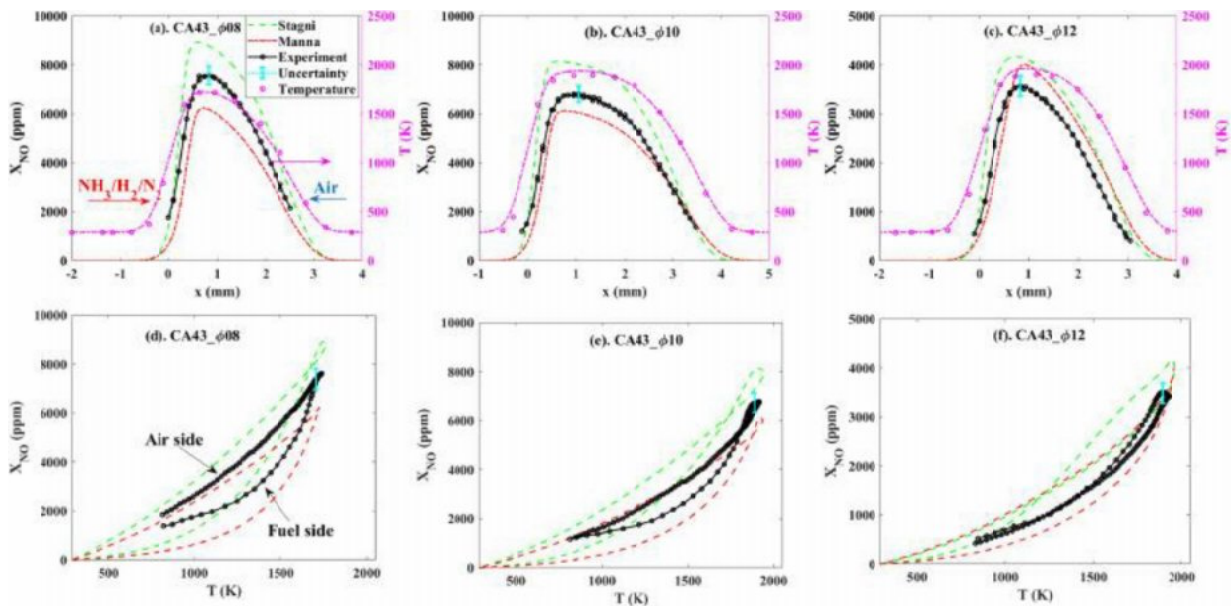
Tang et al. CNF, 267, 113556, 2024



22

# NOx in premixed flames

Tang et al. CNF, 267, 113556, 2024

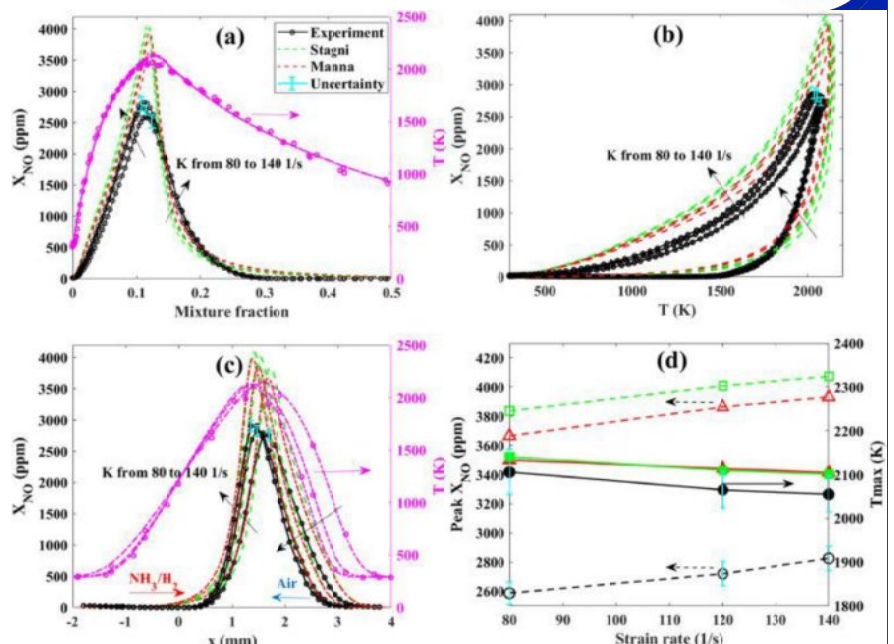


- Experiments show NO concentration in between models for non-premixed flames

23

# NOx in non-premixed flames: effect of strain

- Small effect of strain
  - ~20 K on Temperature
  - NO increase by 162 ppm (% 6%)
- Models
  - Greatly overestimate (35-40%) the NO peak values
  - Underpredict NO in the rich region
  - Correctly predict the observed trends in T and NO



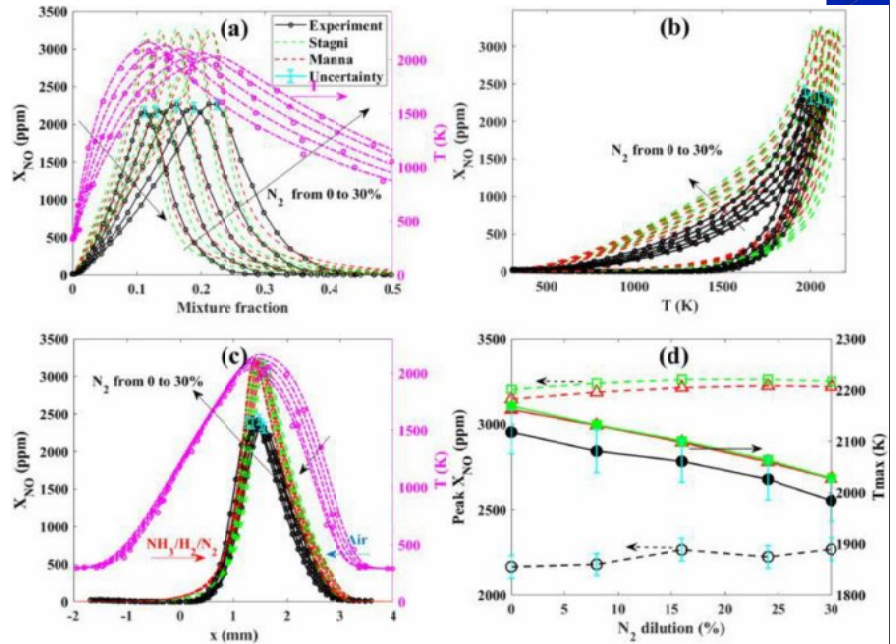
24



# NOX in non-premixed flames: N2 addition

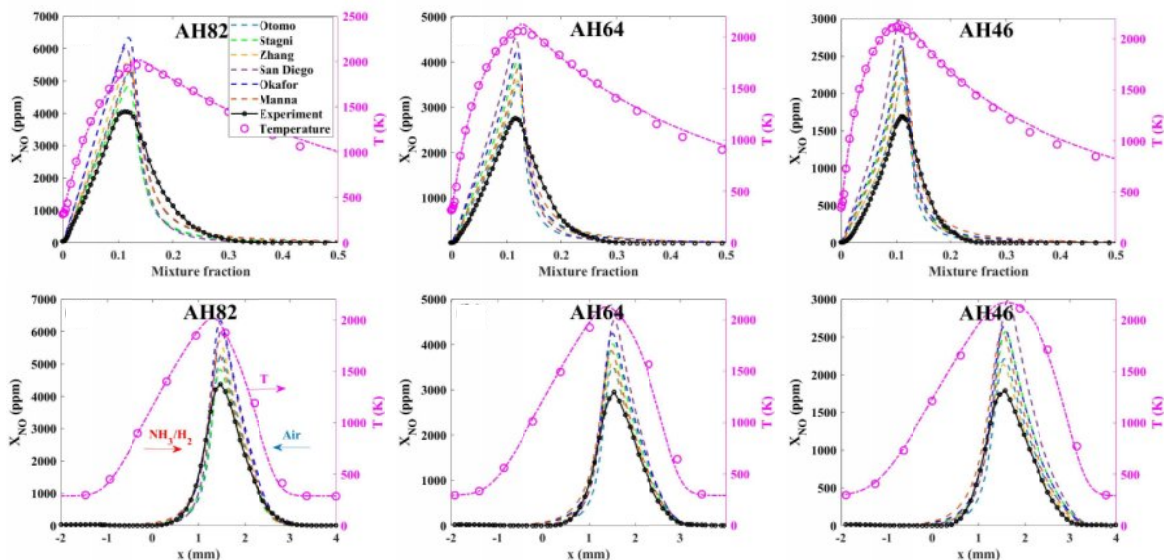


- N2 addition:
  - Temperature drops from 2160 K to 2023 K
  - NO increase by 50 ppm (~2%)
- Models
  - Correctly predict temperature variation
  - Similar trend in NO increase (1.5%-2.5%)
  - Peak NO overestimated by 42%.



25

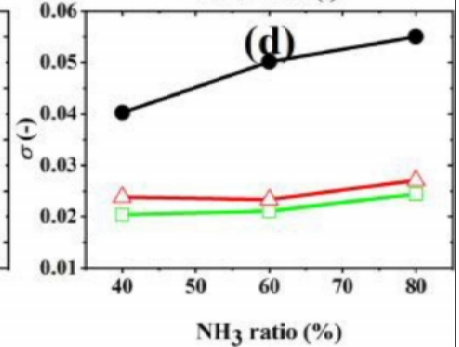
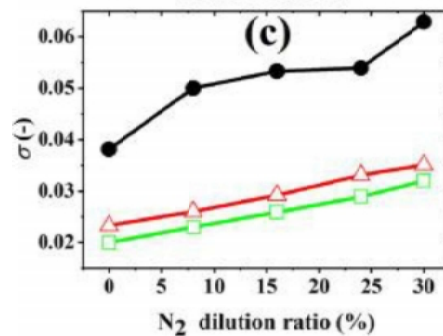
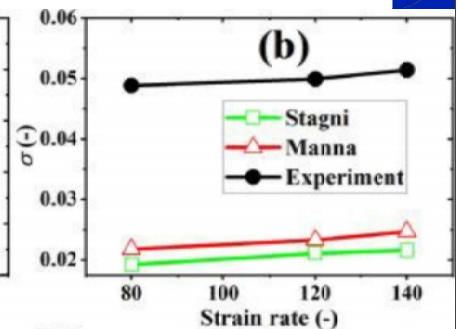
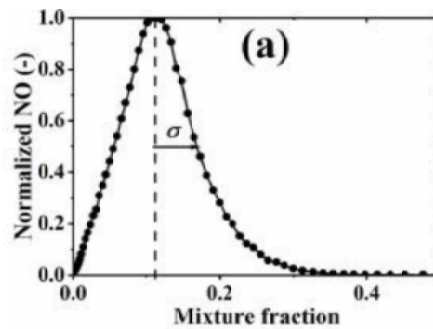
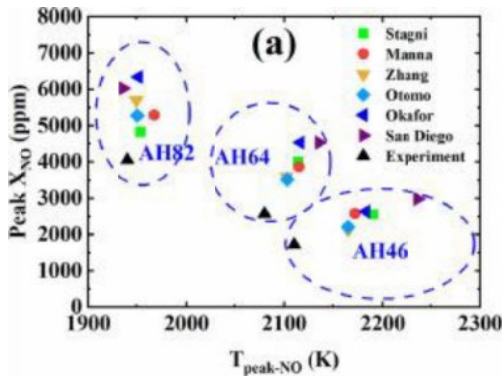
# NOX in non-premixed flames: H2 addition



- Qualitative trend captured, with NO decreasing with H<sub>2</sub> addition
- NO peak overestimated by all models
- NO underestimated by all models in the rich region

26

# NOX in non-premixed flames: summary



- Models overpredict peak NO
- Models underpredict NO in the rich region
  - Width of the NO profile in mixture fraction is underestimated

## Conclusions



- Detailed temperature and species measurements in flames can complement 0D and 1D reactors
- Define ad-hoc subset of data for CM coefficient more relevant to turbulent flames simulations
- Counterflow flames well suited for this task
  - Raman/Rayleigh/LIF for minor species profiles in temperature and mixture fraction space
  - Optically accessible counterflow flames already extensively tested at elevated pressures (5-bar)
  - No intrinsic challenge in varying the inlet temperature and O2 content, and bath gas (water vapor addition?)
  - Flexible platform to develop LIF of additional species (NH, N2O, NO2)

TNF/PTF Workshops

Blank Page



## **TNF Session: Comparisons on the HYLON Burner**

*Coordinators: Thierry Poinsot and Thierry Schuller*

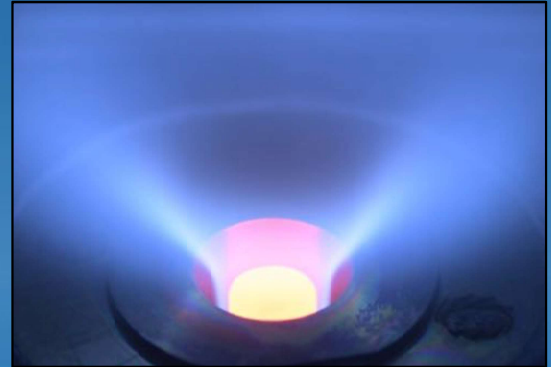
### **Summary**

The HYLON experimental set up uses a swirled hydrogen-air injection system, developed during the ERC SCIROCCO ([cerfacs.fr/scirocco](http://cerfacs.fr/scirocco)) EU project at Institut de Mécanique des Fluides de Toulouse and CERFACS. It is a potential technology for future injection systems in gas turbines. In TNF, it was used as a benchmark for CFD methods. Twenty-five groups have computed two typical flames of HYLON at 1 bar in 2023 and 2024. The two regimes correspond to a low-power anchored flame and a high-power lifted flame, respectively. The first one burns mainly in a diffusion mode, while the second one features both diffusion and premixed flames, making modeling more complicated.

During the TNF workshop, the structures of the HYLON flames were discussed, and the results of the various CFD groups were compared to PIV measurements, H<sub>2</sub> Raman data, and OH\* two-dimensional images. Conclusions were drawn in terms of code capacities, subgrid models, chemistry and transport models, heat transfer approaches near walls. The future data to be obtained on a HYLON type geometry by IMFT together with KAUST were also discussed: NO<sub>x</sub>, Raman data for more species, and temperature measurements should be available in 2025 up to 10 bar. These data will be provided to TNF to be used by all groups interested in H<sub>2</sub> air simulations. The transition to high pressure cases was discussed extensively and identified as one of the major difficulties for CFD codes, since resolving all scales at high pressures will become much more difficult than it has been at 1 bar in the past HYLON exercise.



# HYLON 2023-2024



Organization: S. MARRAGOU, A. ANIELLO, H. MAGNES, M. VILESPY, H. PANIEZ,  
T. RIOU, K. CHAPLET, T. SCHULLER, L. SELLE, T. POINSOT

Institut de Mécanique des Fluides de Toulouse

Presentation by *T. Schuller and T. Poinso*

IMFT – Institut de Mécanique des Fluides de Toulouse  
UMR 5502 – CNRS / Toulouse INP / UT3 – 2 allée du Pr Camille Soula 31400 Toulouse

## CAW H2 CFD workshop: Introducing new flames in TNF —> H2-air, complex geometry flames

The CAW-H2-CFD workshop was initiated in 2022 to test CFD codes for H2-air flames ‘relevant for gas turbines’, organized by E. Mastorakos, T. Poinso and H. Pitsch. Integrated in TNF and distributed to CFD groups for tests in 2023. Three experiments were included:

- TU Berlin -> Pr Paschereit
- NTNU Trondheim -> Pr Dawson
- HYLON IMFT Toulouse -> Pr Schuller

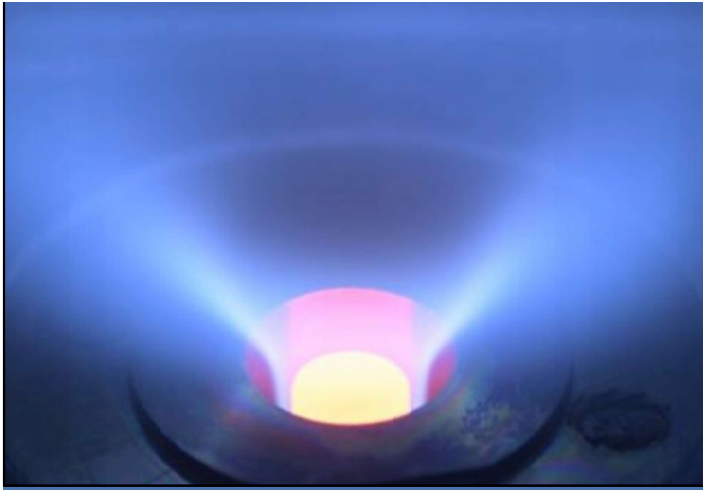
26 groups computed HYLON over the last year. HYLON is a setup developed thanks to the ERC SCIROCCO of IMFT and CERFACS ([cerfacs.fr/scirocco](http://cerfacs.fr/scirocco))

**TODAY DISCUSS RESULTS OBTAINED FOR HYLON at 1 bar in Toulouse (IMFT).**

**WE CALL IT ‘HYLON PHASE 1’. THIS IS THE DATA AVAILABLE ON THE TNF WEB SITE**

**A first discussion of results took place in Toulouse in February 2024 during the ‘HYDROGEN WEEK’ ->**





**THANKS TO ALL  
CONTRIBUTORS !**

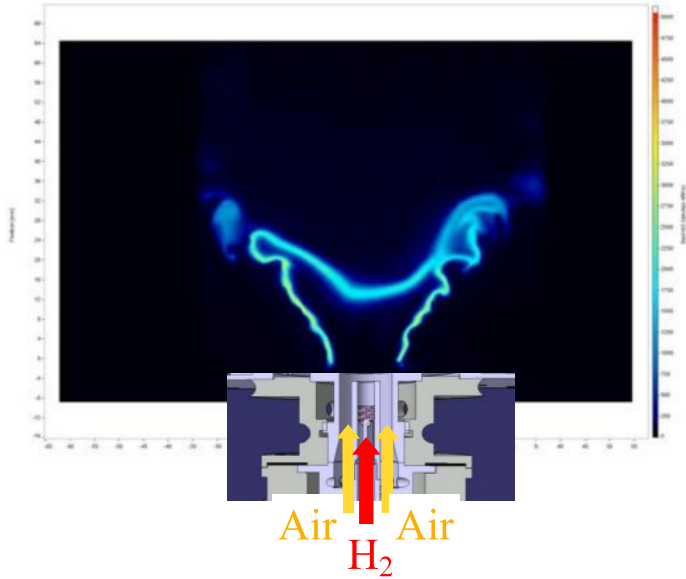
Ergon research	L. Palanti, L. Mazzei
Czestochowa Un. Technology	A. Tyliszczak, A. Boguslawski, K. Wawrzak, A. Wawrzak
Marseille Univ M2P2	S. ZHAO, P. Boivin, I. Mir
Loughborough	A. van Bruygom, A. Duncan Walker, A. Garmory
Safran Tech, CORIA, EM2C	S. Dillon, R. Mercier, V. Moureau, B. Fiorina
General Electric	V. Raj, V. Sukumar, K. Vasudevarao, Y. Zhang
UTSI, Berkeley	X. Gan
POLITECNICO DI MILANO	F. Ghioldi, S.M. Aithal, F. Piscaglia
ANSYS	D. Bessette, I. Verma, S. Orsino, R. Yadav
CONVERGE	S. Nambully, S. Liu, E. Pomraning, D. Lee
CIRA	A. French
Hopkinson Lab., Cambridge	J. Massey
ONERA	N. Bertier, L. Rua
Imperial college	W. P. Jones, W. Liu
Imperial college	S. Navarro
KTH	C. Duwig
Georgia Tech	V. Acharya
Honeywell	V. Verma
RWTH	X. Wen
IFPEN	I. Sikic, C. Mehl, V. Giuffrida
Destinus	J. Marrero
DARMSTADT	S. Balmaseda
BSC	C. Guillamón, D. Mira, A. Moure Sabater, M. Cans Cugat
Pekin Uni.	Z. X. Chen, M. Zhang, G. Dang
IMF Toulouse and CERFACS	M. Vilesny, N. Rouland
UNIFI	A. Ballotti, A. Andreini

## OUTLINE

**Presentation of the HYLON SETUP**

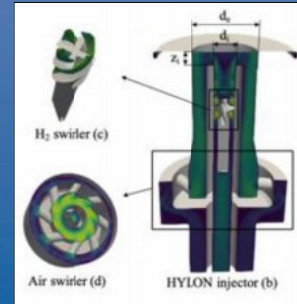
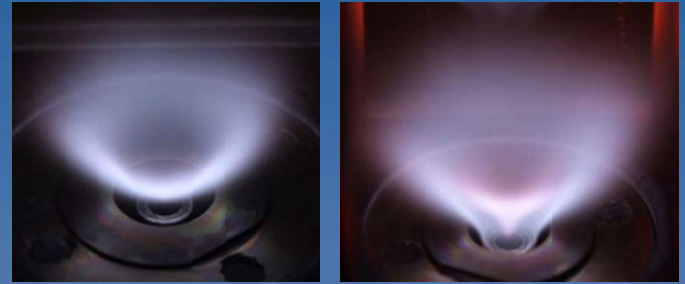
**CFD results obtained by the participants**

**Main conclusions: where are the main problems and solutions ?**



# HYLON: Hydrogen Low NOx injector

*H. Magnes, S. Marragou, T. Schuller*



IMFT – Institut de Mécanique des Fluides de Toulouse  
UMR 5502 – CNRS / Toulouse INP / UT3 – 2 allée du Pr Camille Soula 31400 Toulouse

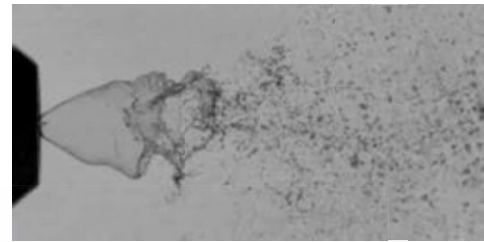
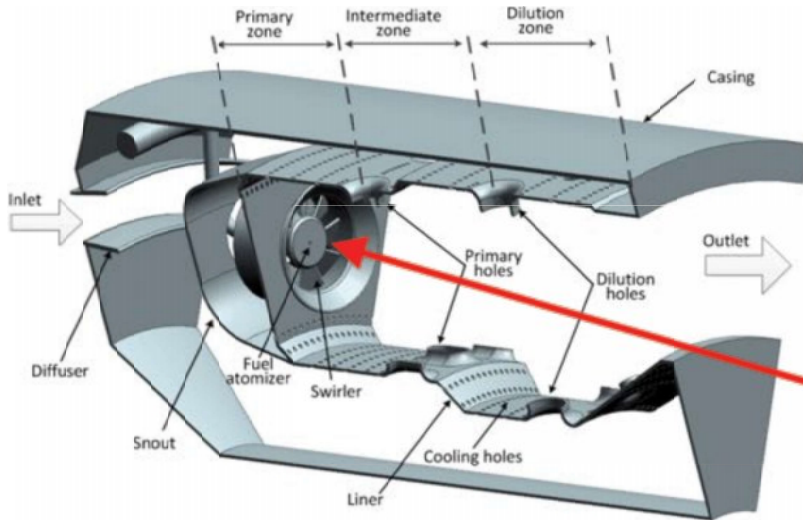
## Summary

1. HYLON: how does it work?
2. New generations of HYLON burner
3. Current scientific issues explored with HYLON

# Aerojet engine gas turbine

Powered by kerosene

Hollow cone fuel spray injector



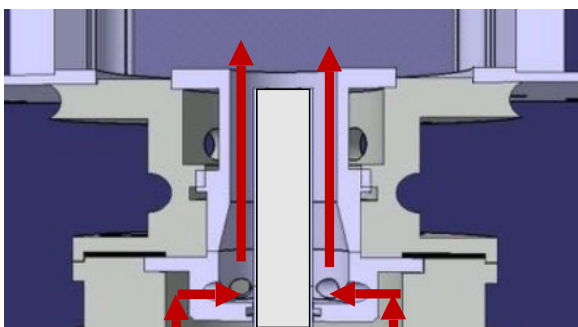
2x10<sup>5</sup> frames/s

Swirled injector

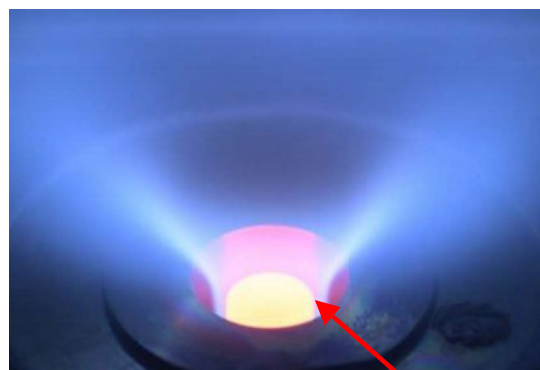
## How to switch to hydrogen?



# Fully premixed H<sub>2</sub>-air swirled flames



H<sub>2</sub>/air H<sub>2</sub>/air



T ~ 900°C

Turbulent premixed H<sub>2</sub>-air swirled flames are extremely sensitive to flashback



## Requirements for hydrogen injectors for aeronautical gas turbines

### 1. Large operability domain

- Flashback resistant
- Blow-off resistant
- Resilience to rapid changes of fuel flow rate

### 2. High combustion efficiency: No unburned fuel

### 3. Long life span: No flame anchoring on injector lips

### 4. Low pressure losses

### 5. Low pollutant emissions: Low NOx emissions.

### 6. Easy chamber integration

### 7. Smooth ignition and altitude relight capabilities

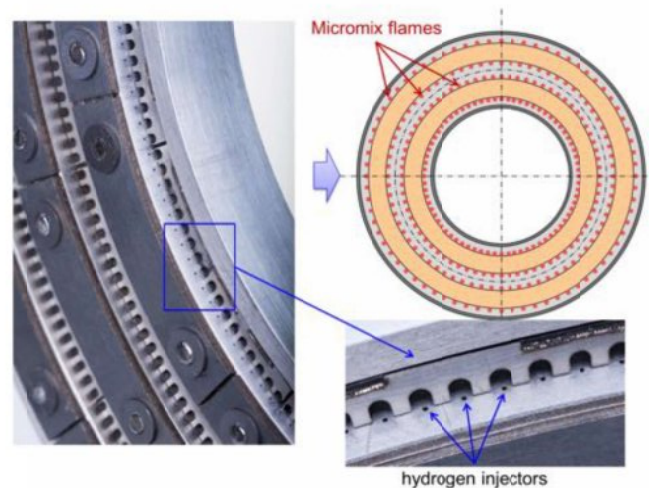
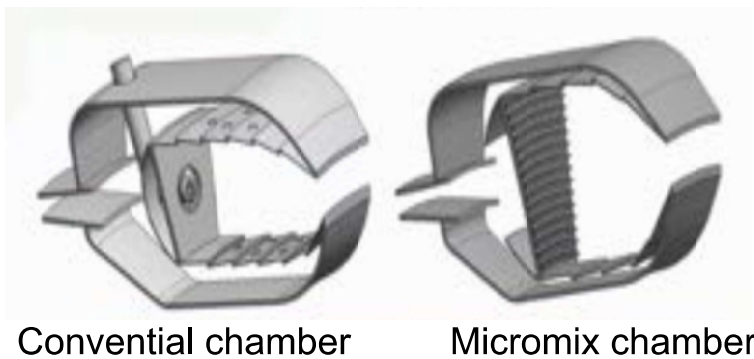
### 8. Weak susceptibility to trigger thermo-acoustic instabilities



## Aerojet gas turbine MICROMIX concept

Disruptive technology with deep modification of combustion chamber architecture

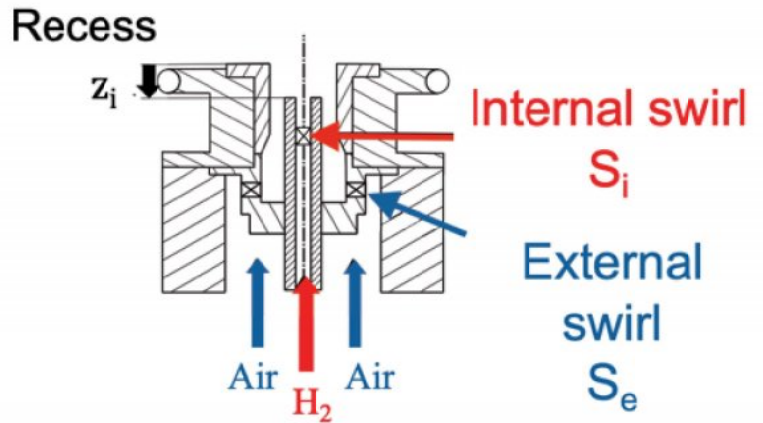
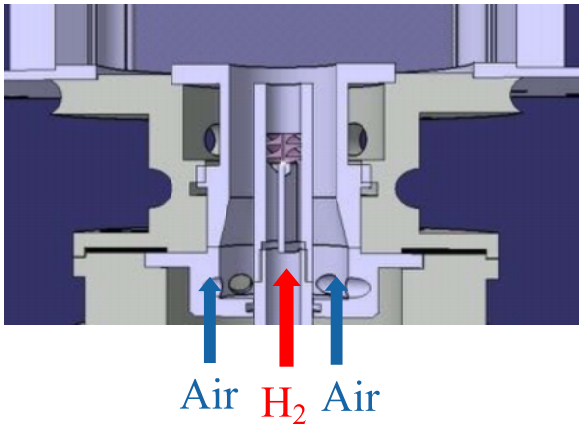
MICROMIX injectors : many small hydrogen jets in air cross-flow





# HYLON : Hydrogen Dual Swirl Low NOx burner

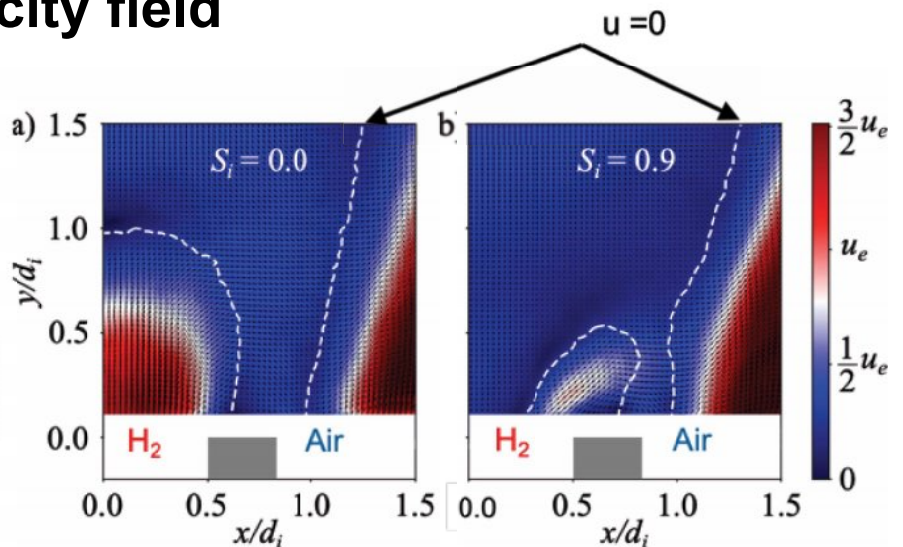
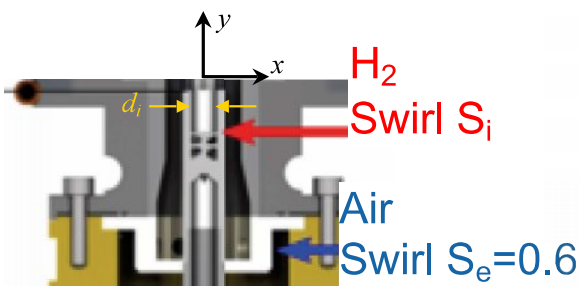
- Late hydrogen injection *eliminate the flashback risk*
- Swirled hydrogen injection *improve mixing rate*



Richard, Viguier, Marragou, Schuller, FR Patent No FR21111267, 2021

## Impact of $S_i$ on velocity field

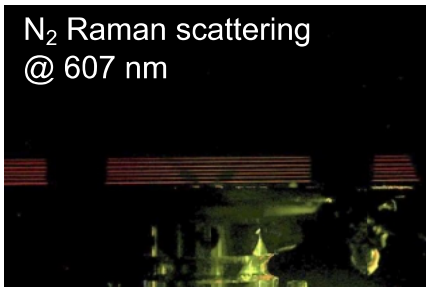
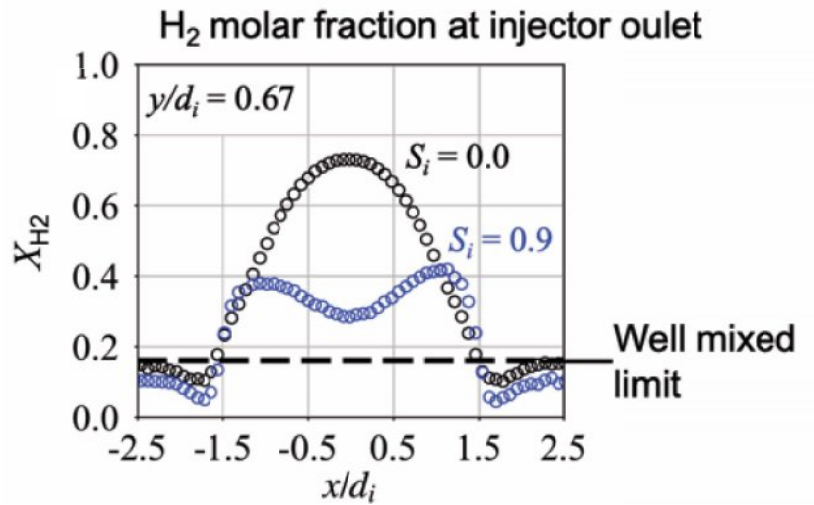
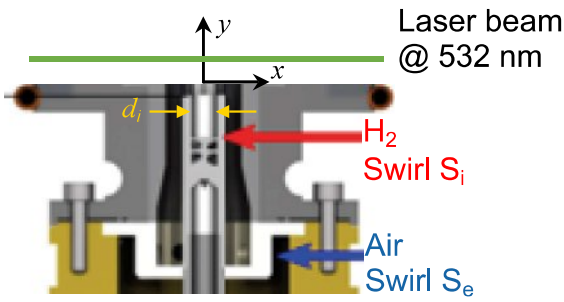
Cold flow velocity field (PIV)



1. Flow blockage at the hydrogen injector outlet
2. Deflection of hydrogen towards air
3. Higher hydrogen flow velocities close to the external nozzle lip

Marragou et al. Proc. Combust. Inst (2023) 39:4345

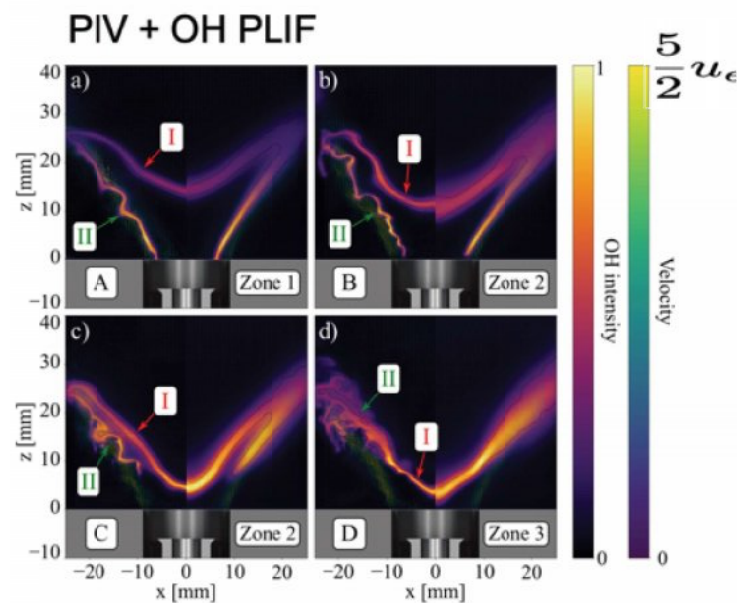
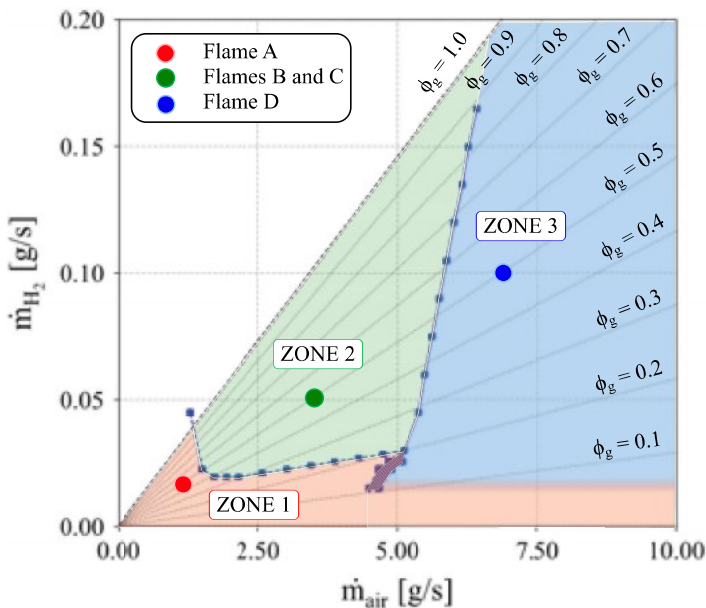
# Impact of $S_i$ on H<sub>2</sub>/air mixing rate



Swirling hydrogen improves the mixing rate at the burner outlet

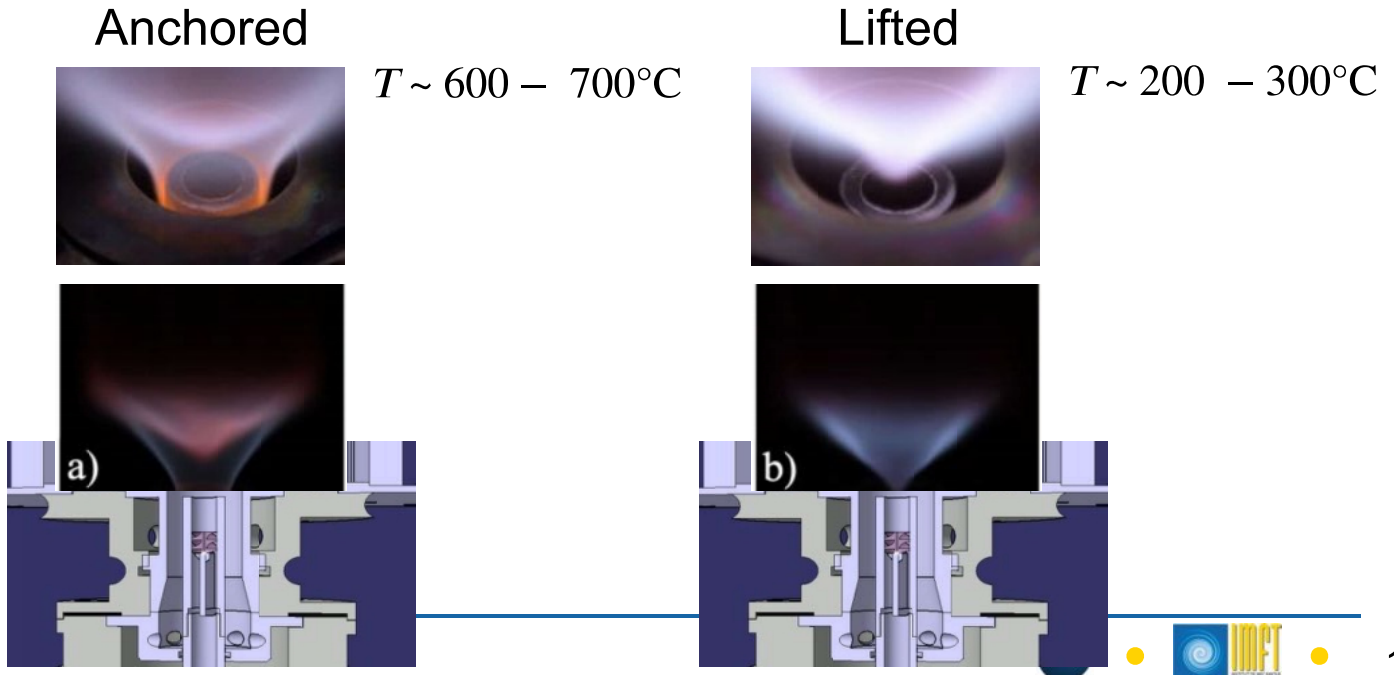
Marragou et al. (2024) Flow Turb. Combust., in revision

# Stabilization chart @ p=1 bar, T=300 K

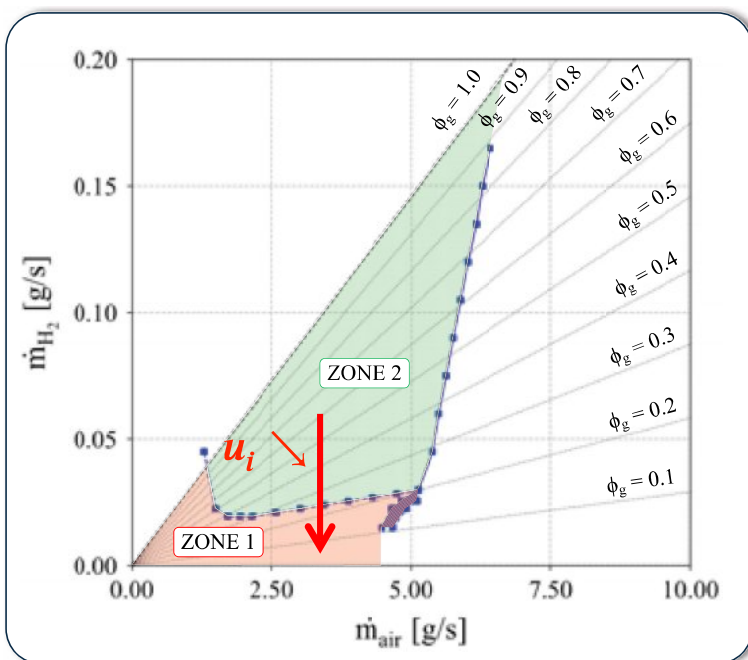


Magnes et al. (2024) JEGTP 145:051004

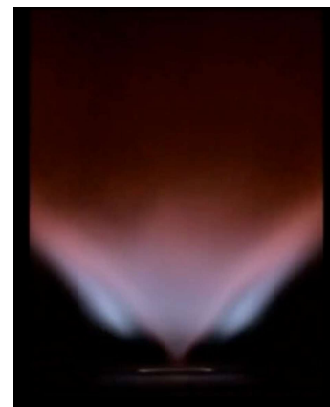
# Injector thermal load



# Analysis of flame re-anchoring



**Zone 2:** Reduction of the hydrogen injection velocity  $U_i$

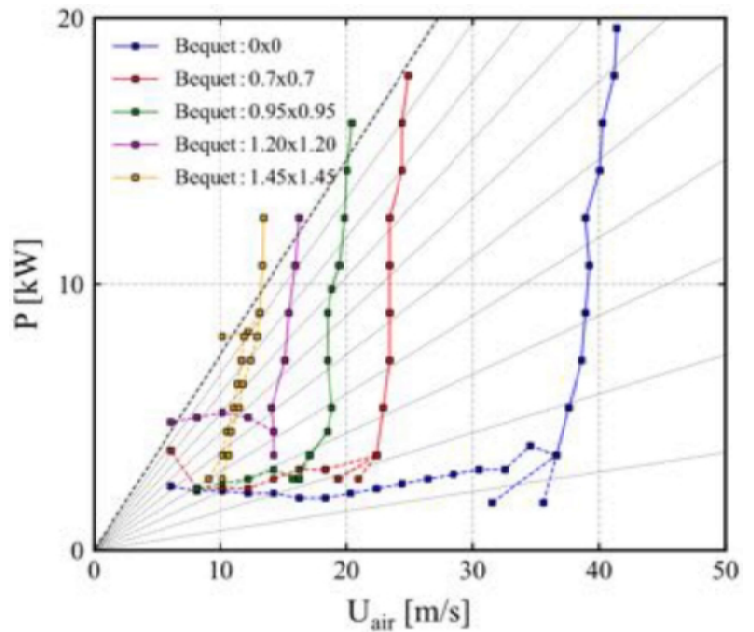


**Abrupt flame re-anchoring**  
**Hysteresis when  $U_i$  is re-increased**

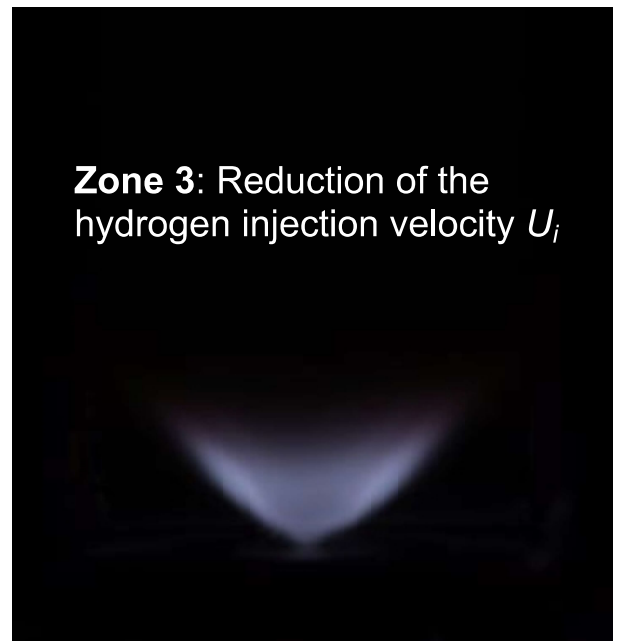
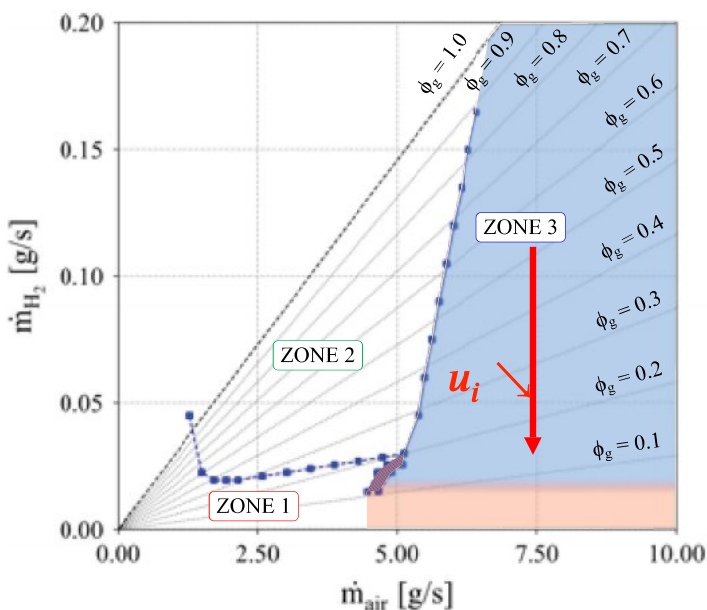
# Impact of hydrogen injector spoiler



Stabilization map is very sensitive to geometry of the hydrogen injector



# Analysis of flame re-anchoring



Zone 3: Reduction of the hydrogen injection velocity  $U_i$

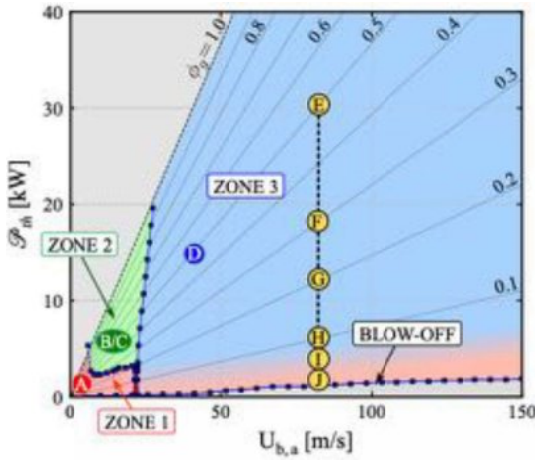
Smooth and progressive shrink  
No hysteresis when fuel is re-increased



# Blow off

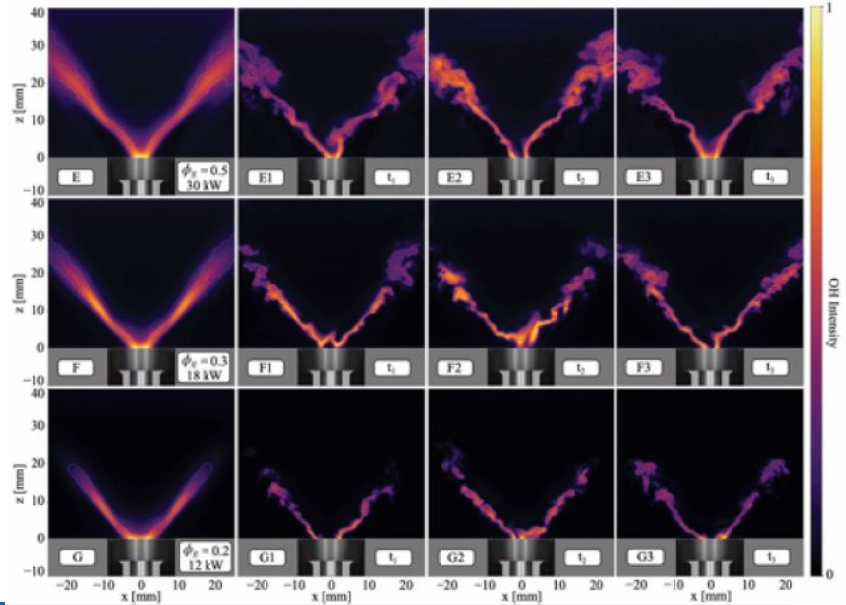
Magnes et al. (2024) GT2024-128817

$p=1 \text{ atm}, T_0=300 \text{ K}$

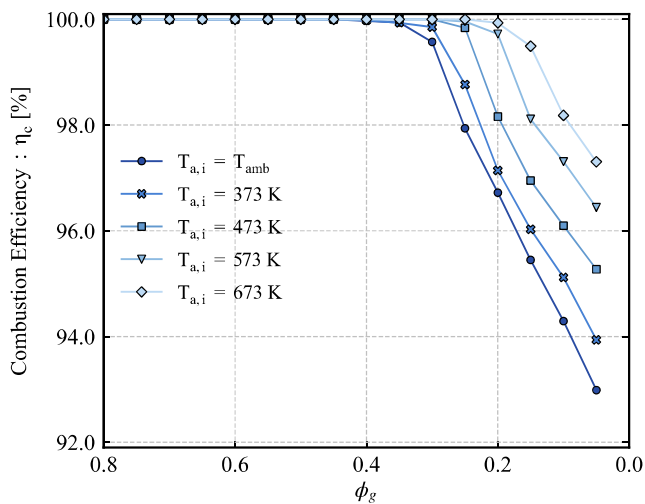


Local fragmentation of the flame front as the fuel is reduced

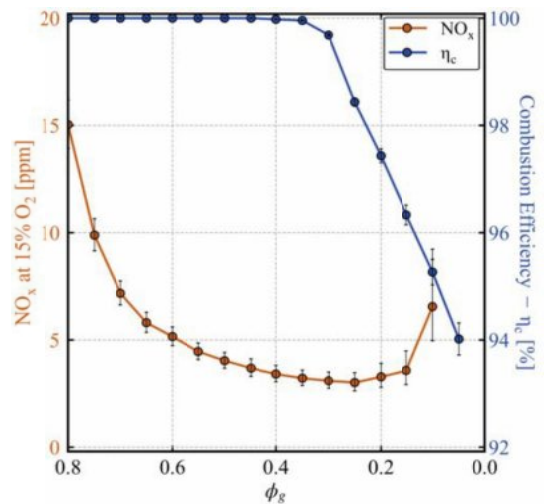
Mean OH Instantaneous OH snapshots



# Interplay between unburnt and NOx emissions



Operability range increases with air preheat temperature

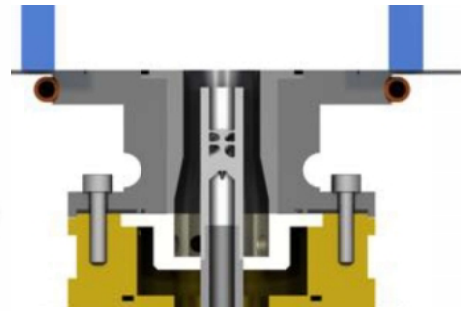
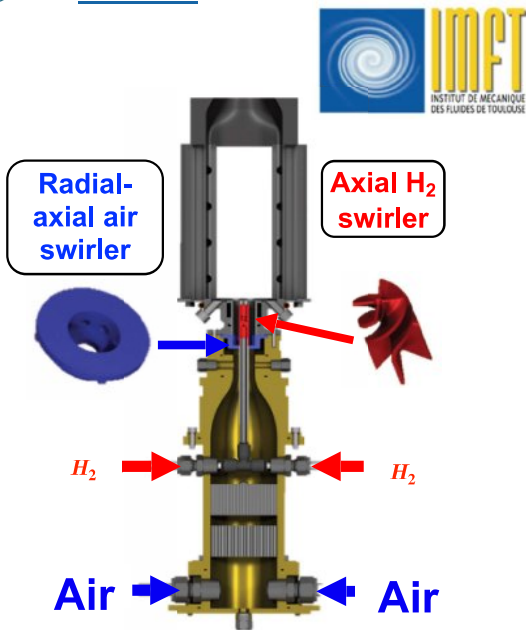


Compromise between NOx and unburnt emissions

Magnes et al. (2024) GT2024-128817

# HYLON injector generations

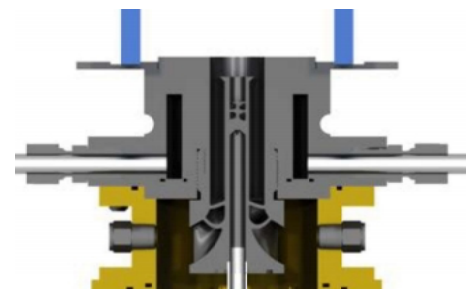
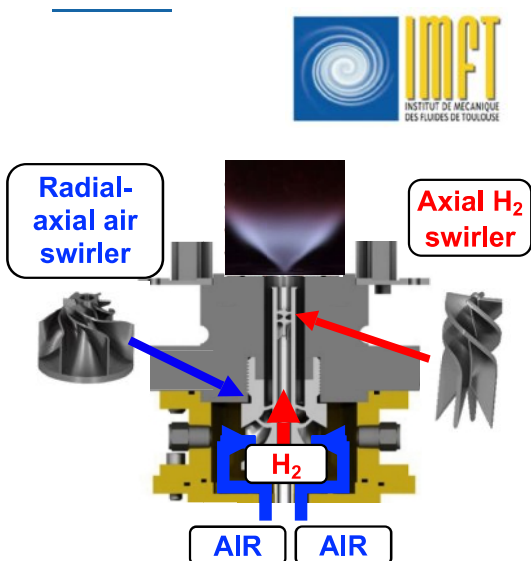
TNF phase 1: 2024



Pressure	$p_a = 1 \text{ atm}$
Temperature	$T = T_a \text{ ambient}$
Air mass flow range	$< 330 \text{ NL/min}$
thermal power range	$< 21 \text{ kW}$

Database available @ [TNF – Hydrogen Flames](#)

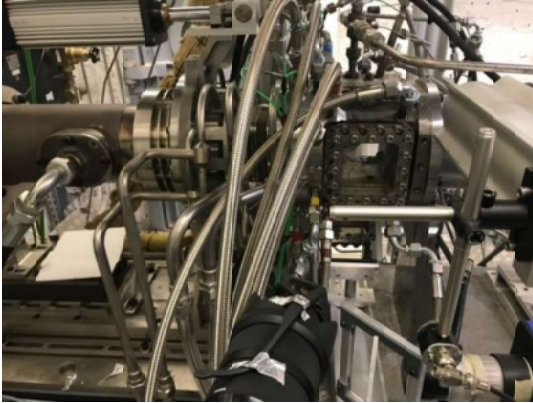
# HYLON injector generations



Pressure	$p_a = 1 \text{ atm}$
Temperature	$T_a < T < 800 \text{ K}$
Air mass flow range	$< 800 \text{ NL/min}$
thermal power range	$< 21 \text{ kW}$
Air dilution	Yes



# HYLON injector generations



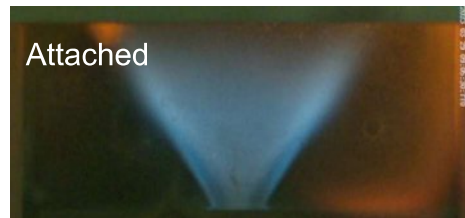
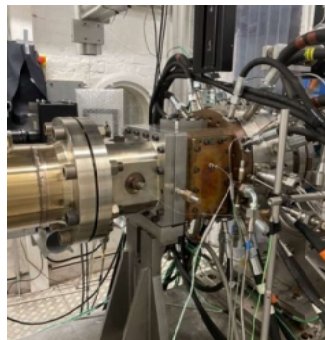
Pressure	$p_a < p < 15 \text{ bar}$
Temperature	$T_a < T < 700 \text{ K}$
Air mass flow range	10000 NI/min
thermal power range	< 250 kW

# High pressure test @ ONERA



High pressure ONERA Palaiseau Micado test rig

Test at engine relevant thermodynamic conditions



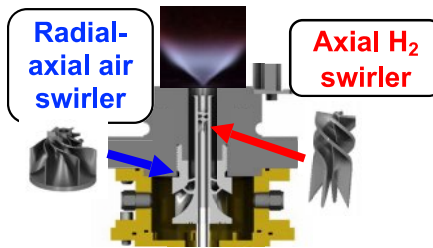
# HYLON injector version and bench implementation



Clean Combustion Research Center

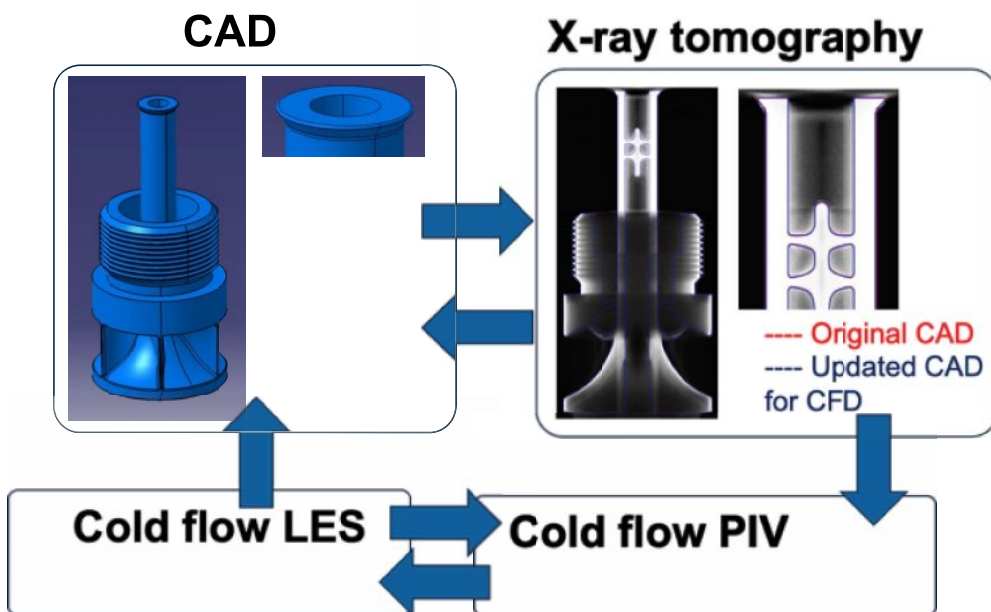
TNF Phase 2

High Pressure Combustion Lab

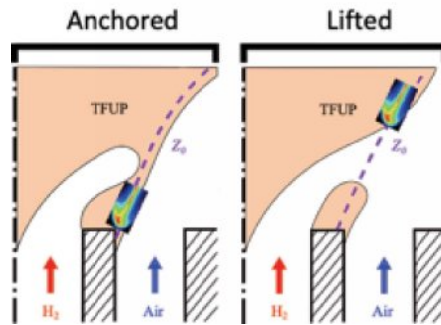
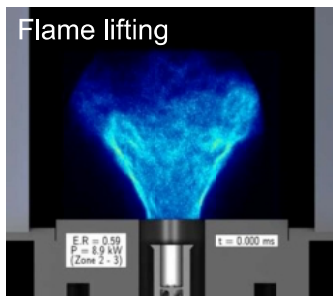
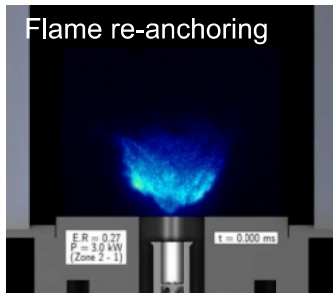


Pressure	P < 10 bar
Temperature	T < 800 K
Air mass flow range	4000 NI/min
thermal power range	< 75 kW

# Geometry crosscheck



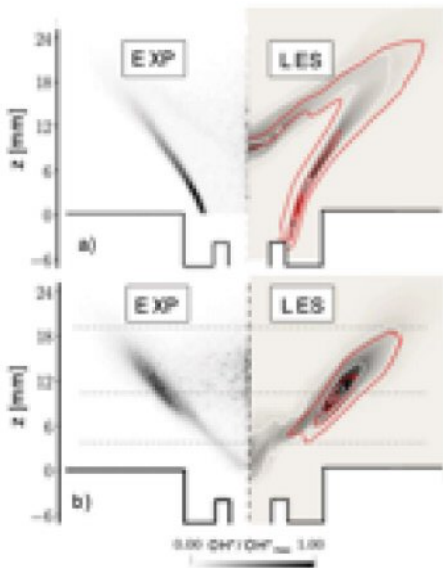
# Current issues explored with HYLON



Marragou et al. Proc. Combust. Inst (2023) 39:4345

Marragou et al. CNF (2023) 255:112908

# OH\* and NOx formation mechanisms

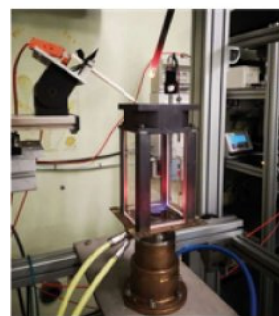


**CERFACS**  
CENTRE EUROPEEN DE RECHERCHE ET DE FORMATION AVANCEE EN CALCUL SCIENTIFIQUE

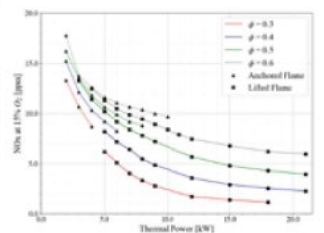


Schiavone et al. Proc. Combust. Inst. (2024) 40:105248

Thursday, 25/07/2024  
Poster H18  
2PM « Silver Room »



NOx measurements in burnt gas



Ongoing NO LIF measurements

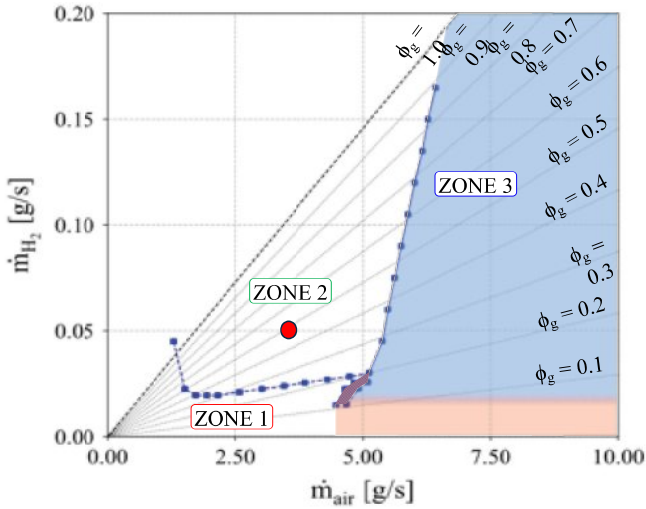
جامعة الملك عبد الله  
للعلوم والتقنية  
King Abdullah University of  
Science and Technology

Clean Combustion  
Research Center

**TNF Phase 2**

# Ignition dynamics

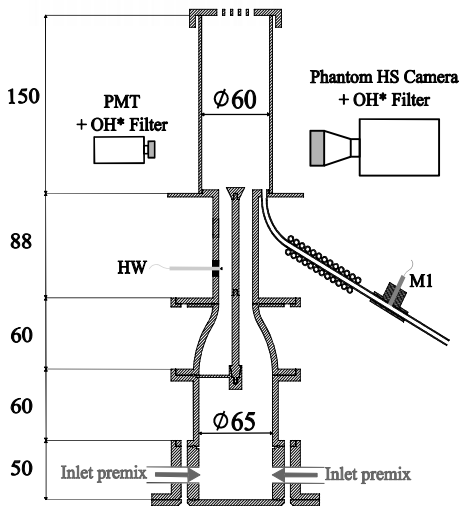
## Spark ignition in Zone 2



# Ignition dynamics : fully premixed



Yahou et al. Proc. Combust. Inst. (2023) 39:4641  
 Yahou et al. J. eng. Gas Turb. Power (2024) 146:011023

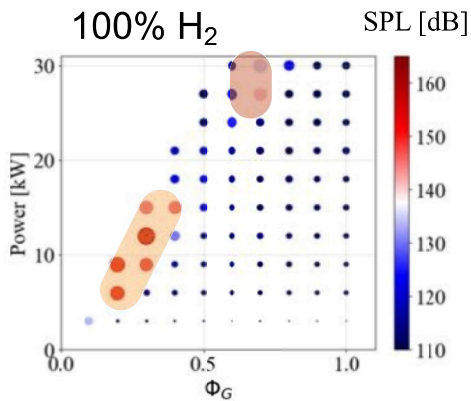


**5E01: The role of preferential diffusion on the ignition dynamics of lean premixed hydrogen flames**  
 Yahou et al.

**Friday 26, 9h40**  
**Propulsion session, Room Yellow 1**

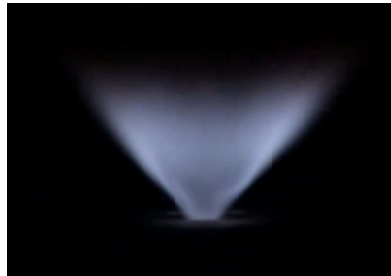


# Thermo-acoustic instabilities



Low frequency TAI, 590 Hz

High frequency TAI, 5 kHz



1C09: High frequency thermo-acoustic instability in a dual swirl H2 burner Paniez et al.

Monday 22, 16:00, Room Blue 1  
Flame dynamics and transport processes

- Low frequency TAI ~ 500 Hz
- High frequency TAI ~ 5 kHz

# Future experiments with HYLON

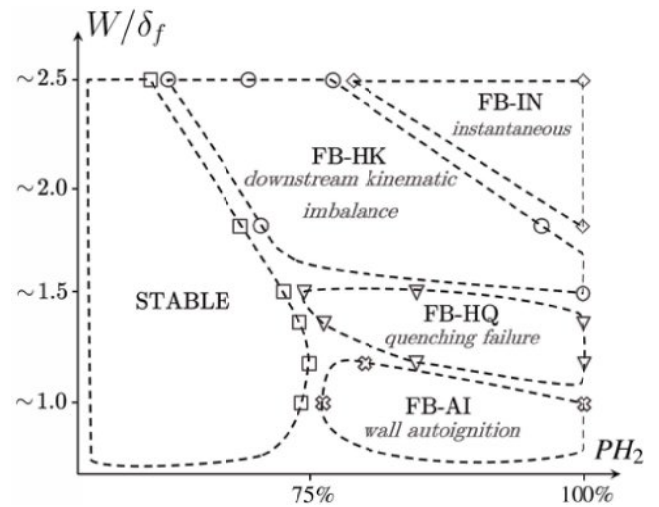
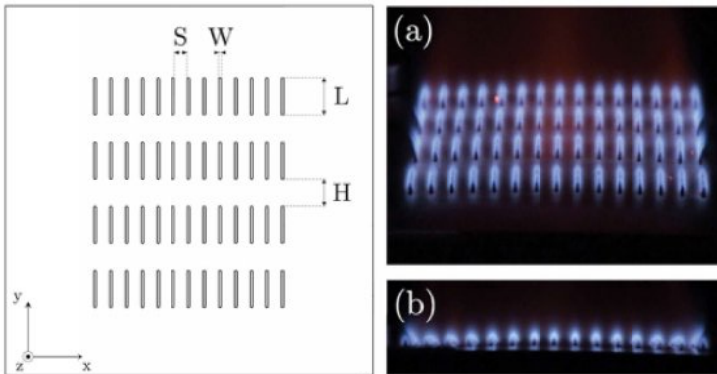
New examples of HYLON burner will be used

- KAUST, Saudi Arabia
- ONERA, France
- Poliba, Italy
- Firenze, Italy
- NTNU, Norway
- TU Darmstadt, Germany
- ETH Zurich, Switzerland



ERC SYNERGY HYROPE

# Flashback in laminar premixed hydrogen flames



T16: Effect of quenching on flashback of hydrogen-enriched laminar premixed flames

Pers et al.

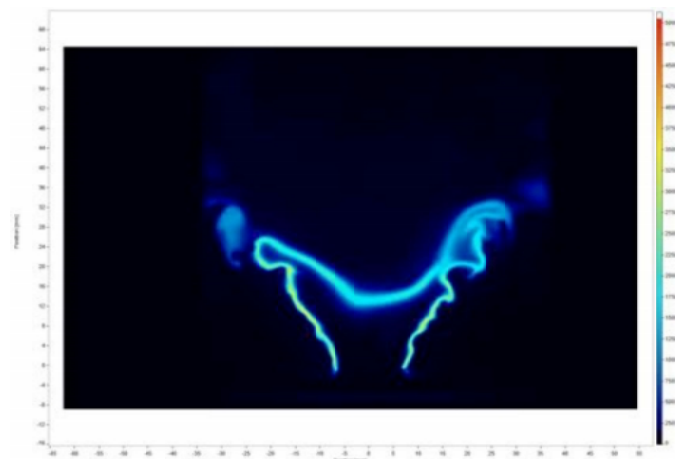
Tuesday 23, Poster session, Silver room, 14:00

## OUTLINE

Presentation of the HYLON SETUP

CFD results obtained by the participants

Main conclusions: where are the main problems and solutions ?



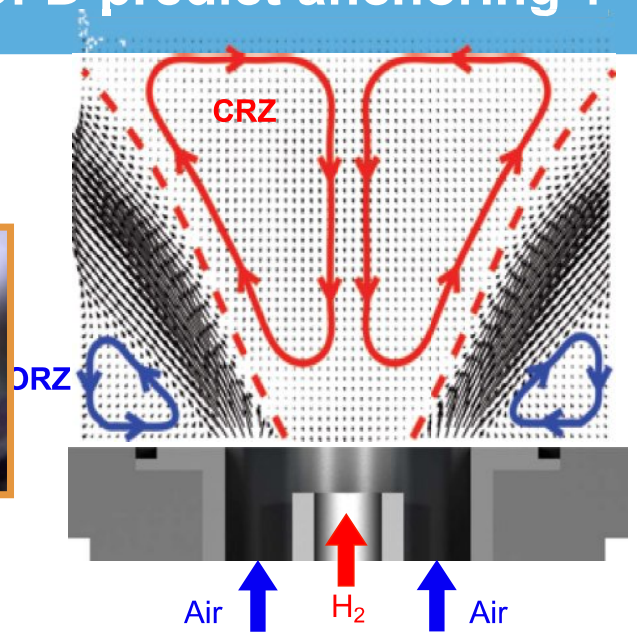


# « Anchored vs lifted »: Can CFD predict anchoring ?

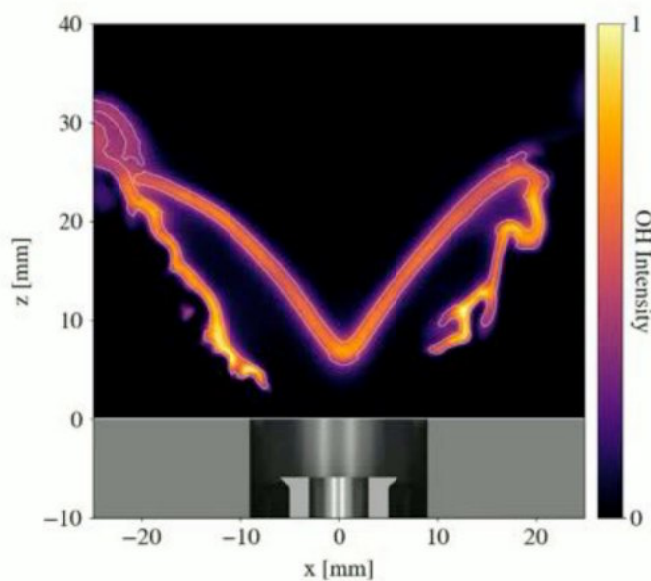
**ANCHORED**  
Diffusion



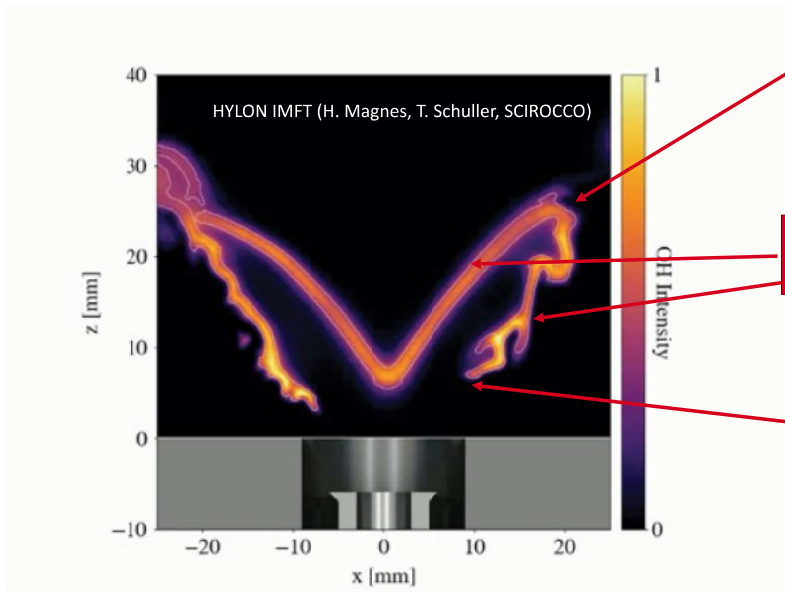
**LIFTED**  
Diffusion/premixed



## Experimental data (courtesy: H. Magnes, IMFT)



# MULTI REGIME FLAME: tough for CFD



PREMIXED FLAMES

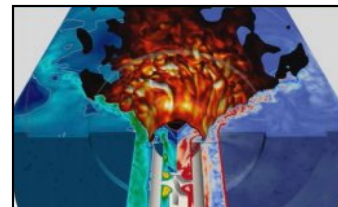
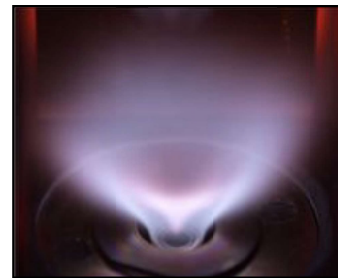
DIFFUSION FLAMES

EDGE FLAMES



37

PRESENTATION OF RESULTS  
OBTAINED BY PARTICIPANTS



TNF16 Workshop Proceedings



90



20-21 July 2024, Milan, Italy

# LIST OF PARTICIPANTS

Nbr	Name	Country	INSTITUTION
1	Lorenzo Mazzei	Italy	Ergon research
2	Artur Tyliszczak	Poland	Czestochowa University of Technology
3	Pierre Boivin	France	Marseille Univ M2P2
4	Andrew Garmory	UK	Loughborough
5	R. Mercier	France	Safran Tech, CORIA, EM2C
6	Zhang Yu	USA	General Electric
7	Xiao Gan	USA	UTSI, Berkeley
8	Federico Piscaglia	ITALY	POLITECNICO DI MILANO
9	Sunil Patil	USA	ANSYS
10	Daniel Lee	USA	CONVERGE
11	Ainslie French	Italy	CIRA
12	James Massey	UK	Hopkinson Laboratory, Cambridge
13	Nicolas Bertier	France	ONERA
14	William Jones	UK	Imperial college
15	Salvador Navarro	UK	Imperial college
16	Christophe Duwig	SWE	KTH
17	Vishal Acharya	USA	Georgia Tech
18	Vishwas Verma	USA	Honeywell
19	Xu Wen	GER	RWTH
20	Olivier Colin	France	IFPEN
21	Javier Marrero	SPAIN	Destinus
22	Sandra Recio Balmaseda		DARMSTADT
23	Daniel Mira	SPAIN	BSC
24	Zhi Chen	CHINA	Pekin Uni.
25	Martin Vilespy	France	IMF Toulouse
26	Andrea Ballotti	ITALY	UNIFI

## CASES PROPOSED FOR COMPUTATIONS

**COLD FLOW PIV DATA FOR TWO REGIMES (mean and RMS):**

- ONE FOR AN ANCHORED FLAME CASE (CALLED 'A')

## ALL INFORMATION FOR THESE RESULTS AVAILABLE ON THE TNF WEB SITE

- ONE FOR A LIFTED FLAME (CALLED 'L')

**HOT FLOW PIV DATA FOR TWO REGIMES (mean and RMS):**

- ONE FOR AN ANCHORED FLAME CASE (CALLED 'A')
- ONE FOR A LIFTED FLAME (CALLED 'L')

**DIRECT VIEW OF OH FIELD FOR:**

- ANCHORED FLAME CASE (CALLED 'A')
- LIFTED FLAME (CALLED 'L')

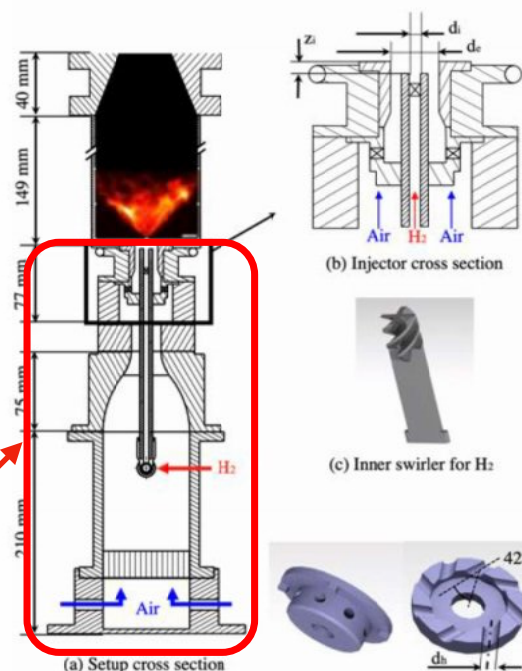
# WHAT IS DIFFERENT IN HYLON TYPE FLAMES COMPARED TO CLASSICAL TNF FLAMES ?

Not only a combustion (kinetics and flame/ turbulence models): the mean and turbulent flow in the whole burner must be captured, including near swirler walls: the swirler must be resolved.

This eliminates many usual i-j-k DNS codes and requires codes able to handle complex geometries.

Now the results depend on the combustion models AND on the specifics of the numerical method.

Example of question: how well do we need to predict the turbulent flow upstream of the flame ?



## WHO DID WHAT ?

Nbr	Name	Country	INSTITUTION	COLD FLOW ATTACHED	COLD FLOW LIFTED	COLD FLOW MIXING	REACTING ATTACHED	REACTING LIFTED
1	Lorenzo Mazzei	Italy	Ergon research					
2	Artur Tyliczszak	Poland	Ceasochowa University of Technology					
3	Pierre Boivin	France	Marseille Univ M2P2					
4	Andrew Garmory	UK	Loughborough					
5	R. Mercier	France	Safran Tech, CORIA, EM2C					
6	Zhang Yu	USA	General Electric					
7	Xiao Gan	USA	UTSI, Berkeley					
8	Federico Piscaglia	ITALY	POLITECNICO DI MILANO					
9	Sunil Patil	USA	ANSYS					
10	Daniel Lee	USA	CONVERGE					
11	Ainslie French	Italy	CIRA					
12	James Massey	UK	Hopkinson Laboratory, Cambridge					
13	Nicolas Bertier	France	ONERA					
14	William Jones	UK	Imperial college					
15	Salvador Navarro	UK	Imperial college					
16	Christophe Duwig	SWE	KTH					
17	Vishal Acharya	USA	Georgia Tech					
18	Vishwas Verma	USA	Honeywell					
19	Xu Wen	GER	RWTH					
20	Olivier Colin	France	IFPEN					
21	Javier Marrero	SPAIN	Destinus					
22	Sandra Recio Balmaseda		DARMSTADT					
23	Daniel Mira	SPAIN	BSC					
24	Zhi Chen	CHINA	Pekin Uni.					
25	Martin Vilesny	France	IMF Toulouse					
26	Andrea BALLOTTI	Italy	UNIFI					



## WITH WHICH CODE ?

Nbr	Name	Country	INSTITUTION	COLD FLOW ATTACHED	COLD FLOW LIFTED	COLD FLOW MIXING	REACTING ATTACHED	REACTING LIFTED	Code
1	Lorenzo Mazzei	Italy	Ergon research						ANSYS Fluent
2	Artur Tyliczszak	Poland	Czestochowa University of Technology						ANSYS Fluent
3	Pierre Boivin	France	Marseille Univ M2P2						ProLB LBM
4	Andrew Garmory	UK	Loughborough						STAR-CCM+
5	R. Mercier	France	Safran Tech, CORIA, EM2C						YALES2
6	Zhang Yu	USA	General Electric						
7	Xiao Gan	USA	UTSI, Berkeley						
8	Federico Piscaglia	ITALY	POLITECNICO DI MILANO						OpenFoamGPU im
9	Sunil Patil	USA	ANSYS						ANSYS Fluent
10	Daniel Lee	USA	CONVERGE						CONVERGE CFD
11	Ainslie French	Italy	CIRA						
12	James Massey	UK	Hopkinson Laboratory, Cambridge						OpenFOAM v7
13	Nicolas Bertier	France	ONERA						CEDRE
14	William Jones	UK	Imperial college						BOFFIN-LESc
15	Salvador Navarro	UK	Imperial college						
16	Christophe Duwig	SWE	KTH						
17	Vishal Acharya	USA	Georgia Tech						
18	Vishwas Verma	USA	Honeywell						
19	Xu Wen	GER	RWTH						
20	Olivier Colin	France	IFPEN						CONVERGE CFD
21	Javier Marrero	SPAIN	Destinus						
22	Sandra Recio Balmaseda		DARMSTADT						
23	Daniel Mira	SPAIN	BSC						Alya (FEM)
24	Zhi Chen	CHINA	Pekin Uni.						DeepFlame Ope
25	Martin Vilespy	France	IMF Toulouse						AVBP
26	Andrea BALLOTTI	Italy	UNIFI						ANSYS Fluent

## WITH WHICH MESH TYPE ?

Nbr	Name	Country	INSTITUTION	COLD FLOW ATTACHED	COLD FLOW LIFTED	COLD FLOW MIXING	REACTING ATTACHED	REACTING LIFTED	Code	MESH
1	Lorenzo Mazzei	Italy	Ergon research						ANSYS Fluent	Polyhedra
2	Artur Tyliczszak	Poland	Czestochowa University of Technology						ANSYS Fluent	Tetrahedra
3	Pierre Boivin	France	Marseille Univ M2P2						ProLB LBM	
4	Andrew Garmory	UK	Loughborough						STAR-CCM+	Polyhedra
5	R. Mercier	France	Safran Tech, CORIA, EM2C						YALES2	Tetrahedra
6	Zhang Yu	USA	General Electric							
7	Xiao Gan	USA	UTSI, Berkeley							
8	Federico Piscaglia	ITALY	POLITECNICO DI MILANO						OpenFoamGPU im	Polyhedra
9	Sunil Patil	USA	ANSYS						ANSYS Fluent	Polyhedra
10	Daniel Lee	USA	CONVERGE						CONVERGE CFD	Polyhedra
11	Ainslie French	Italy	CIRA							
12	James Massey	UK	Hopkinson Laboratory, Cambridge						OpenFOAM v7	Tetrahedra
13	Nicolas Bertier	France	ONERA						CEDRE	Tetrahedra
14	William Jones	UK	Imperial college						BOFFIN-LESc	Tetra Polyhedra
15	Salvador Navarro	UK	Imperial college							
16	Christophe Duwig	SWE	KTH							
17	Vishal Acharya	USA	Georgia Tech							
18	Vishwas Verma	USA	Honeywell							
19	Xu Wen	GER	RWTH							
20	Olivier Colin	France	IFPEN						CONVERGE CFD	Polyhedra
21	Javier Marrero	SPAIN	Destinus							
22	Sandra Recio Balmaseda		DARMSTADT							
23	Daniel Mira	SPAIN	BSC						Alya (FEM)	Tetra Pentahedra
24	Zhi Chen	CHINA	Pekin Uni.						DeepFlame Ope	Polyhedra
25	Martin Vilespy	France	IMF Toulouse						AVBP	Tetrahedra
26	Andrea BALLOTTI	Italy	UNIFI						ANSYS Fluent	Polyhedra

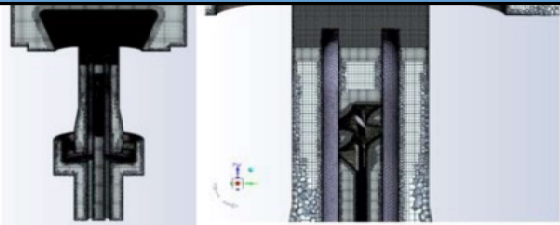
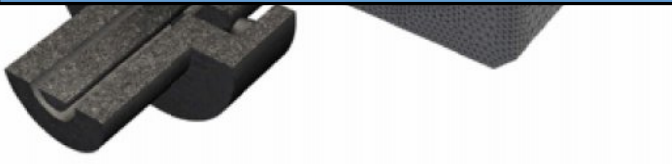
**TETS**

**HEXAS**

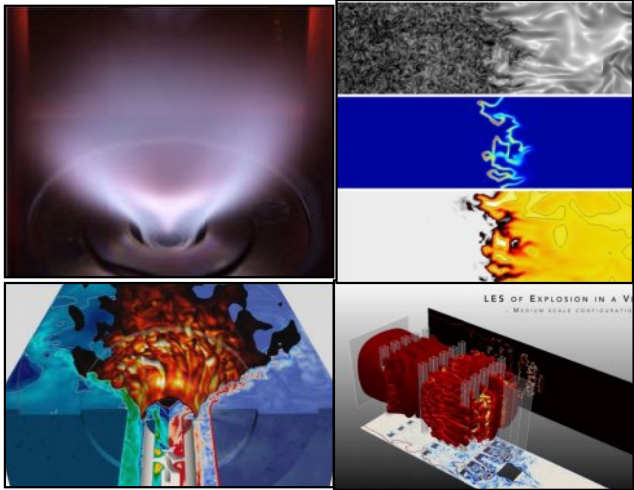


Static mesh 28 millions

**YES, THE MESH TYPE ALSO PLAYS A ROLE...**



**CFD FOR H2:  
comparison of results**



With the support of:  
ERC advanced grant SCIROCCO (2019-2024), SELECT-H (2023-2028), SYNERGY ERC grant HYROPE (2024-2030),  
SAFRAN, AIRBUS, ALSTOM, AIR LIQUIDE, GRTGAZ, TOTALENERGIES, SAINT-GOBAIN

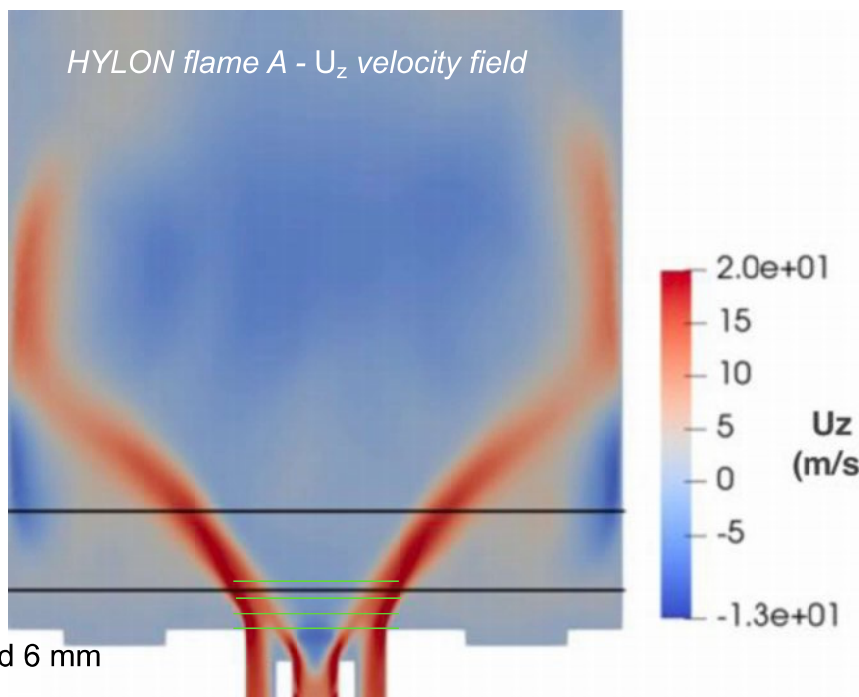




## Location of measurements:

For velocities  $\left\{ \begin{array}{l} Z = 15 \text{ mm} \\ Z = 5 \text{ mm} \end{array} \right.$

For RAMAN  $X_{H_2}$ :  $Z = 1, 2, 4$  and  $6 \text{ mm}$

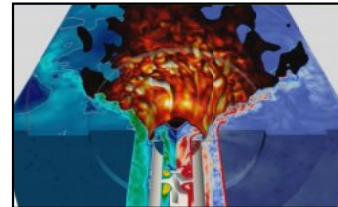
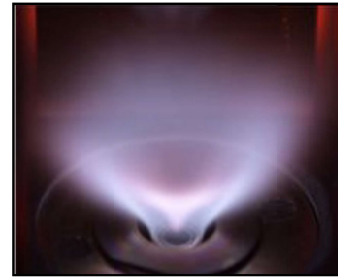


## Color codes

- CZESTOCHOWA
- BSC
- PEKING
- ANSYS
- ONERA
- CONVERGE
- IFPEN
- EM2C
- ERGON
- UNIFI
- M2P2
- IMPERIAL
- UCAM
- POLIMI
- AVBP
- LOUGHBOROUGH
- PIV

EXPERIMENT →

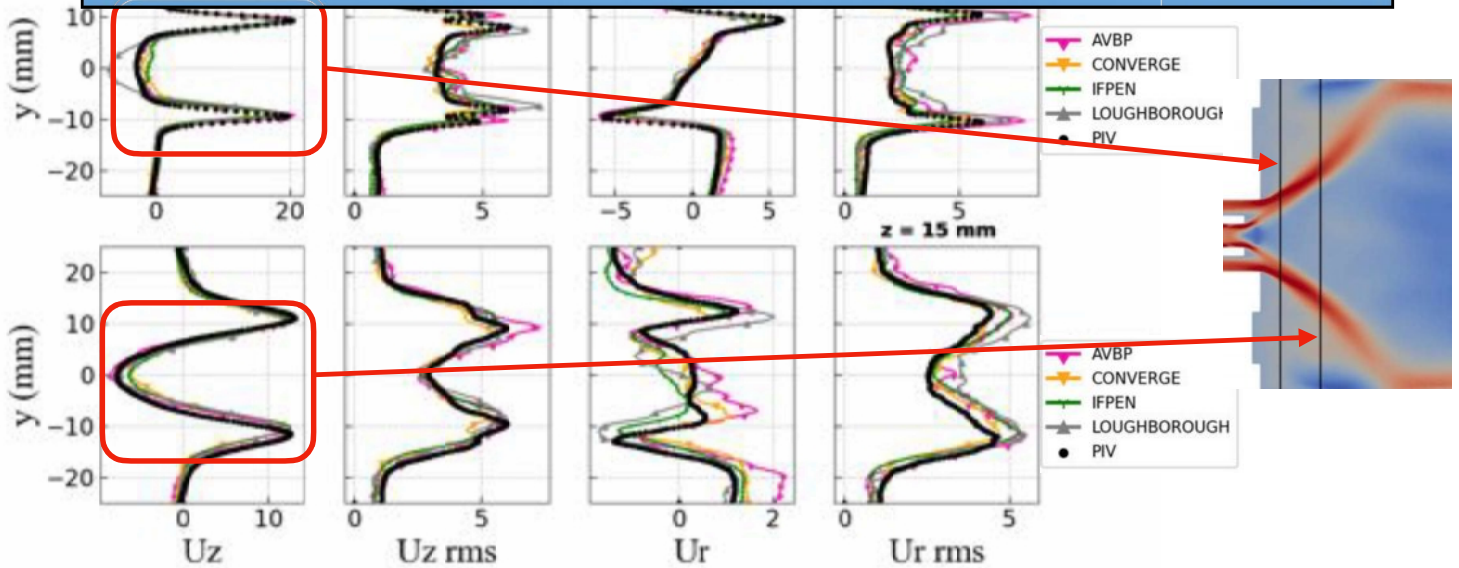
# COLD FLOW RESULTS FOR CASES A AND L



With the support of:  
 ERC advanced grant SCIROCCO (2019-2024), SELECT-H (2023-2028), SYNERGY ERC grant HYROPE (2024-2030),  
 SAFRAN, AIRBUS, ALSTOM, AIR LIQUIDE, GRTGAZ, TOTALENERGIES, SAINT-GOBAIN

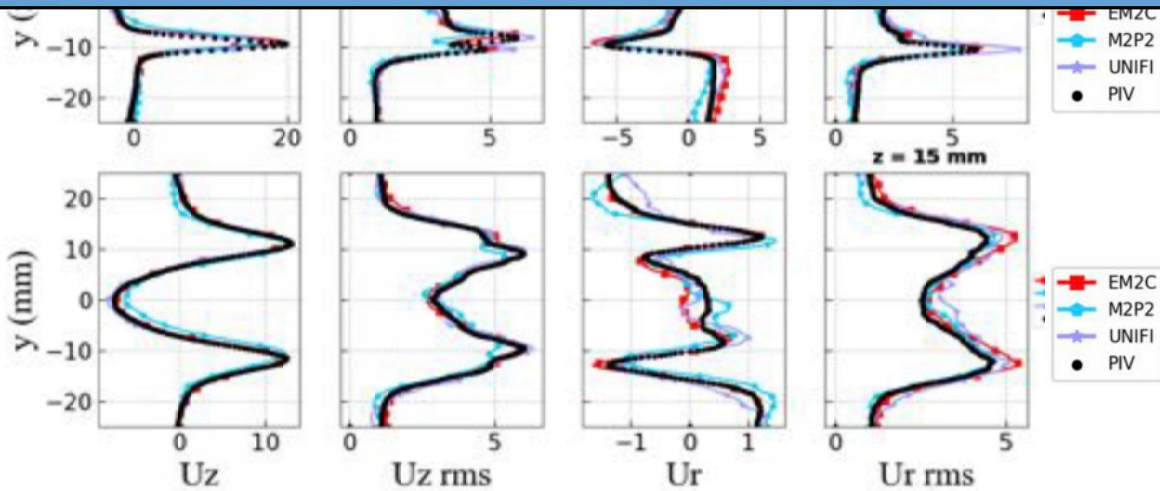


## ANOTHER SPECIFICITY OF THESE FLAMES: IMPORTANCE OF RECIRCULATED ZONES

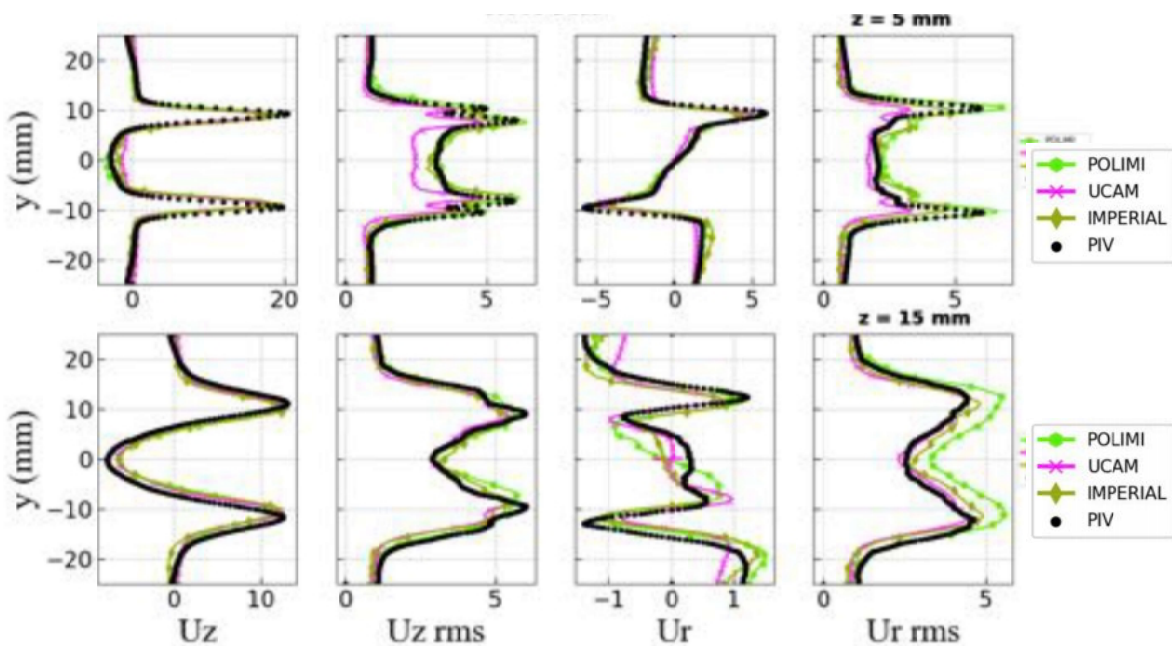


Ve

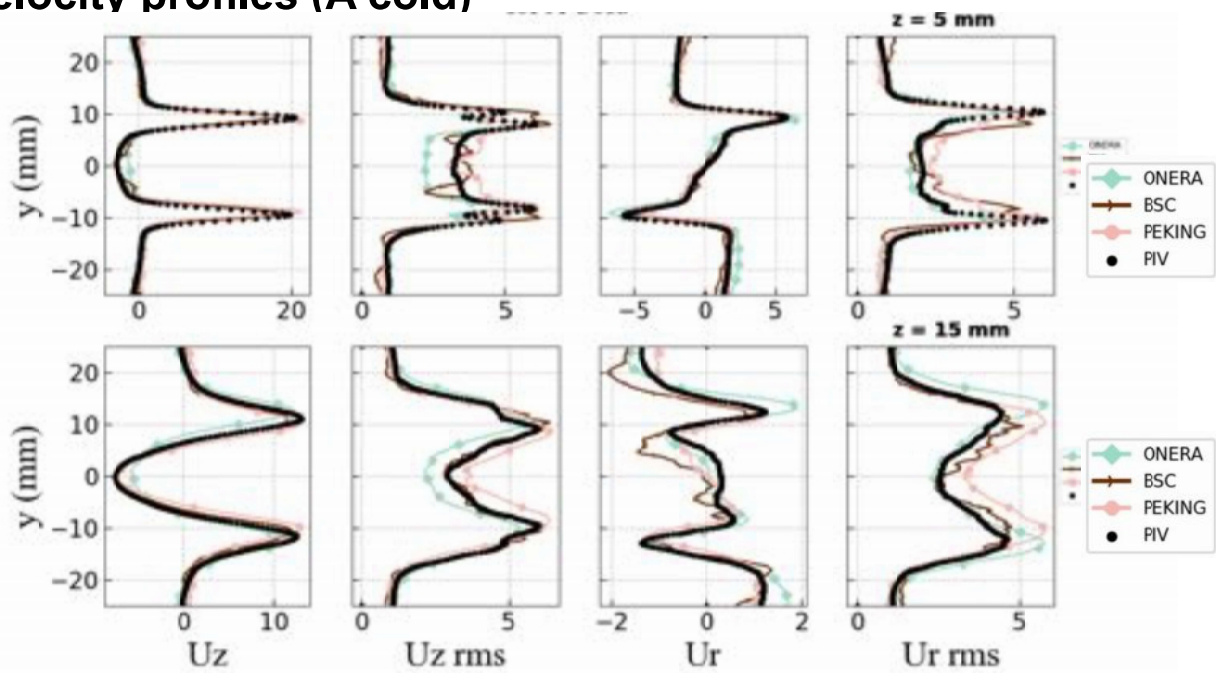
**TYPICAL OF STATE-OF-THE-ART LES CODES TODAY: WITHOUT COMBUSTION, THEY USUALLY DO VERY WELL FOR MEAN AND RMS FIELDS**



### Velocity profiles (A cold)



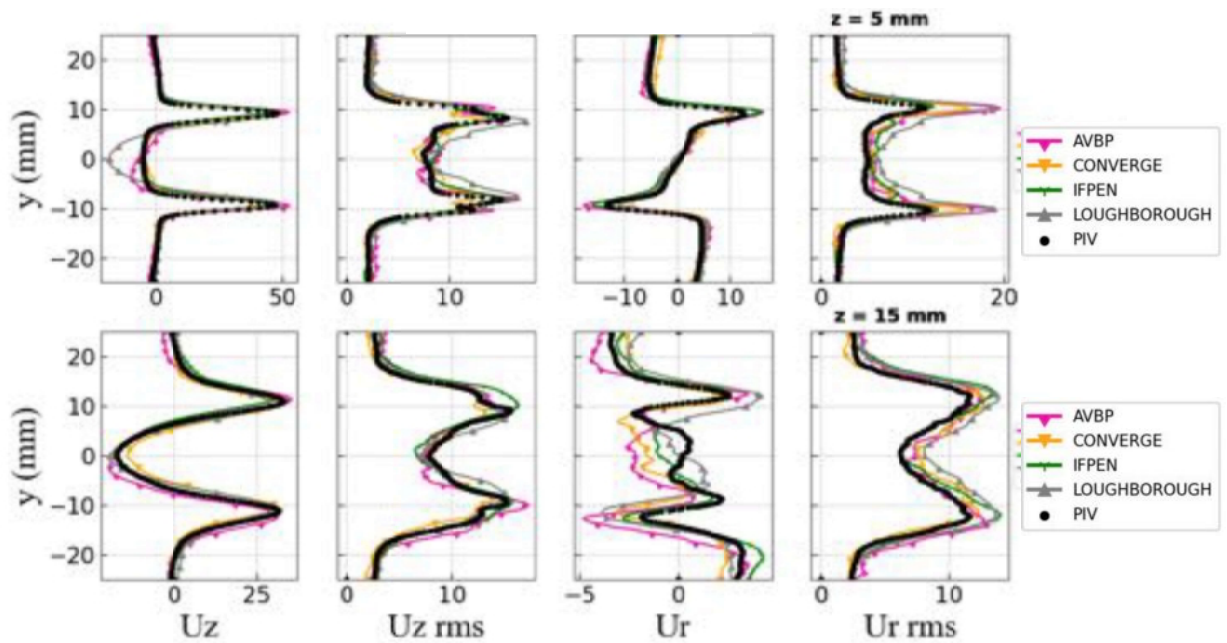
## Velocity profiles (A cold)



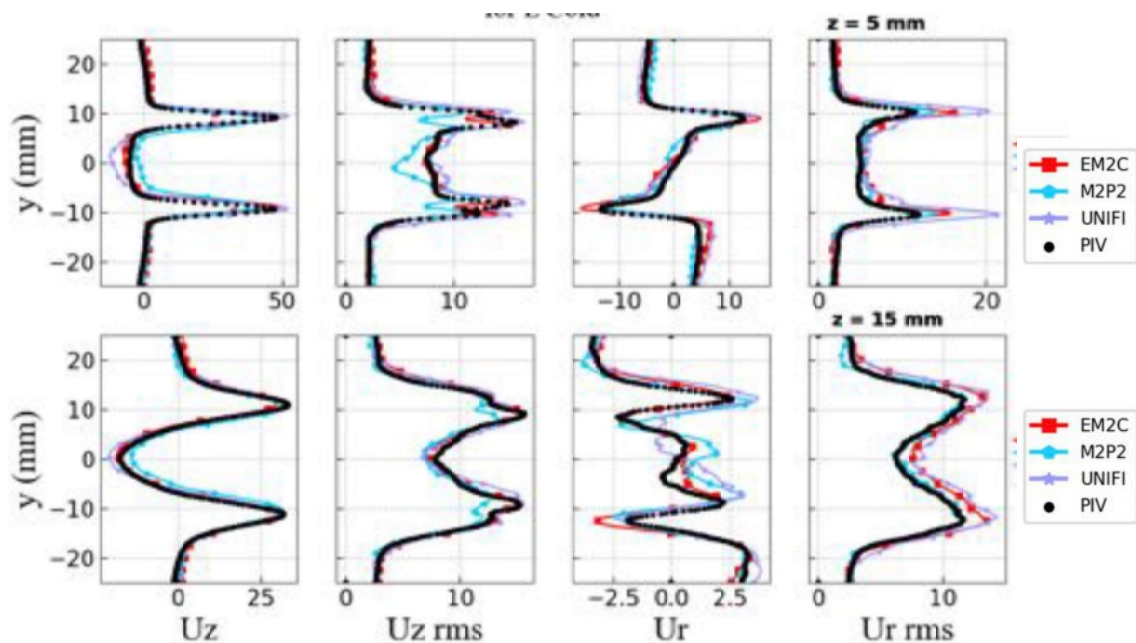
**LET US GO TO CASE L  
(LIFTED): The Reynolds  
number increases !**



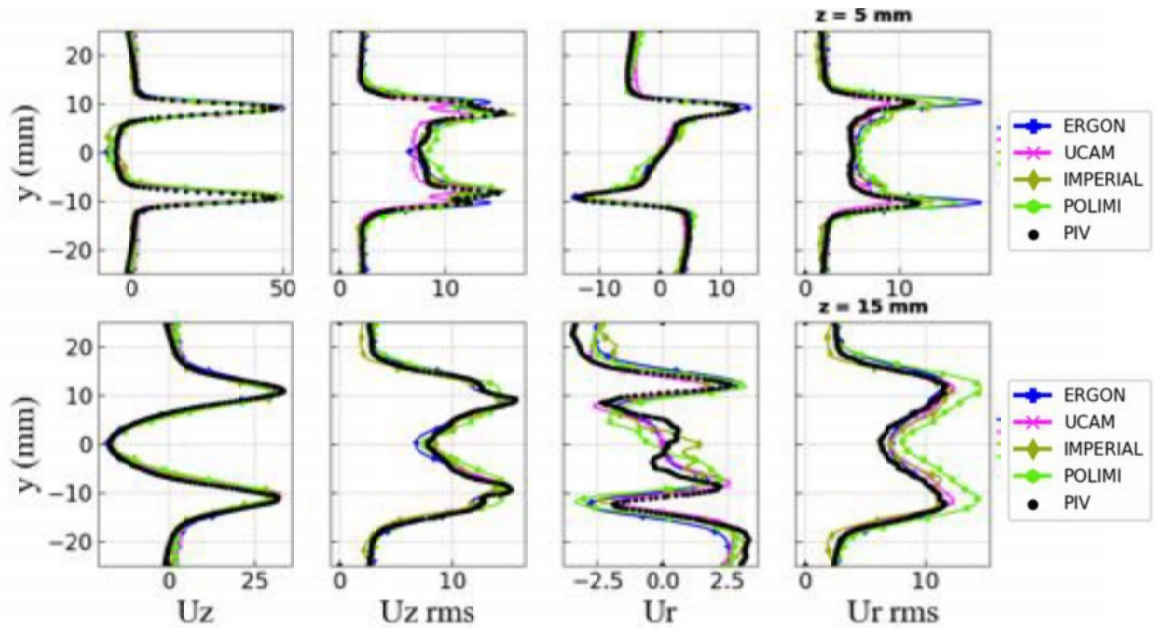
## Velocity profiles (L cold)



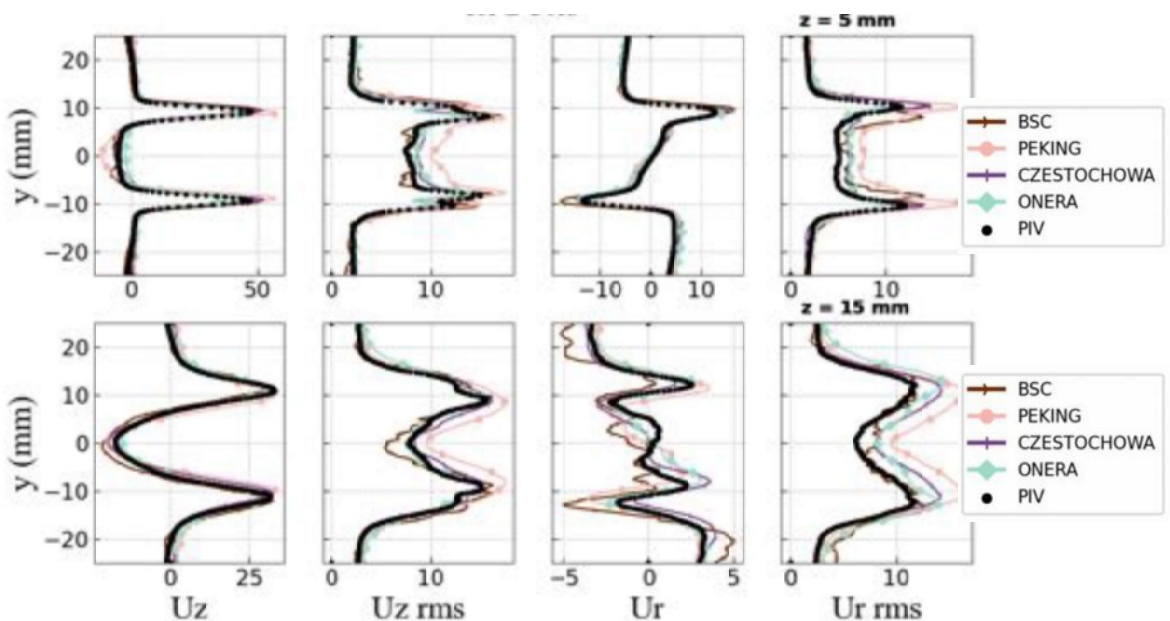
## Velocity profiles (L cold)



## Velocity profiles (L cold)

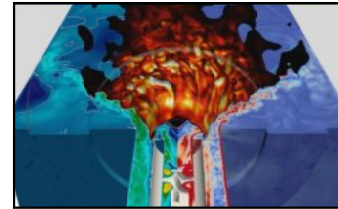
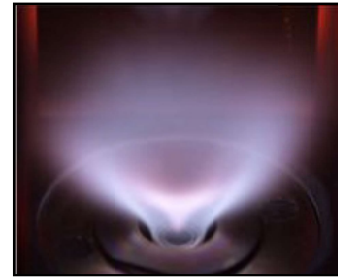


## Velocity profiles (L cold)





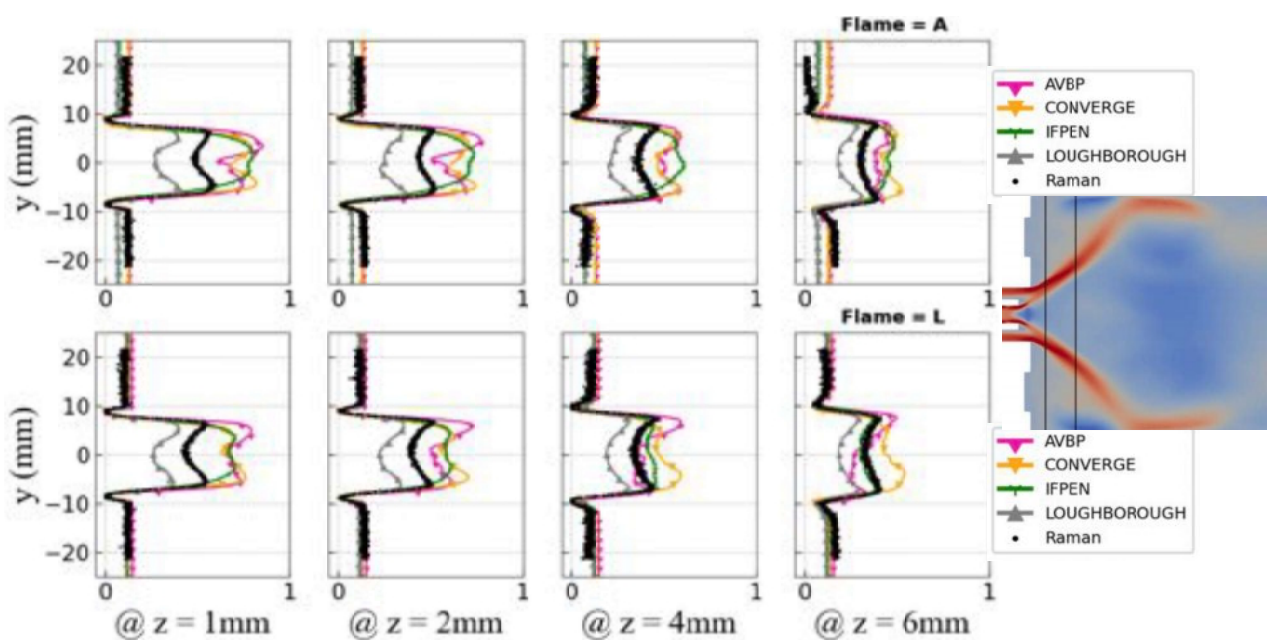
# COLD FLOW RESULTS FOR MIXING IN CASES A AND L (RAMAN ON H2)



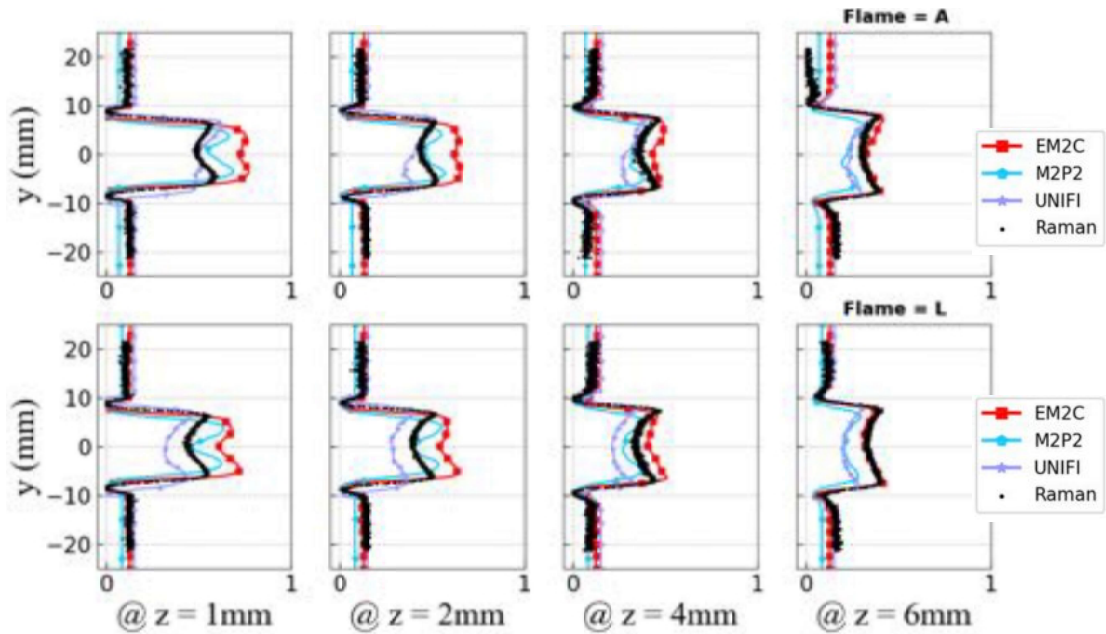
With the support of:  
 ERC advanced grant SCIROCCO (2019-2024), SELECT-H (2023-2028), SYNERGY ERC grant HYROPE (2024-2030),  
 SAFRAN, AIRBUS, ALSTOM, AIR LIQUIDE, GRTGAZ, TOTALENERGIES, SAINT-GOBAIN



## Mixing: $X_{H_2}$ profiles (A and L cold)



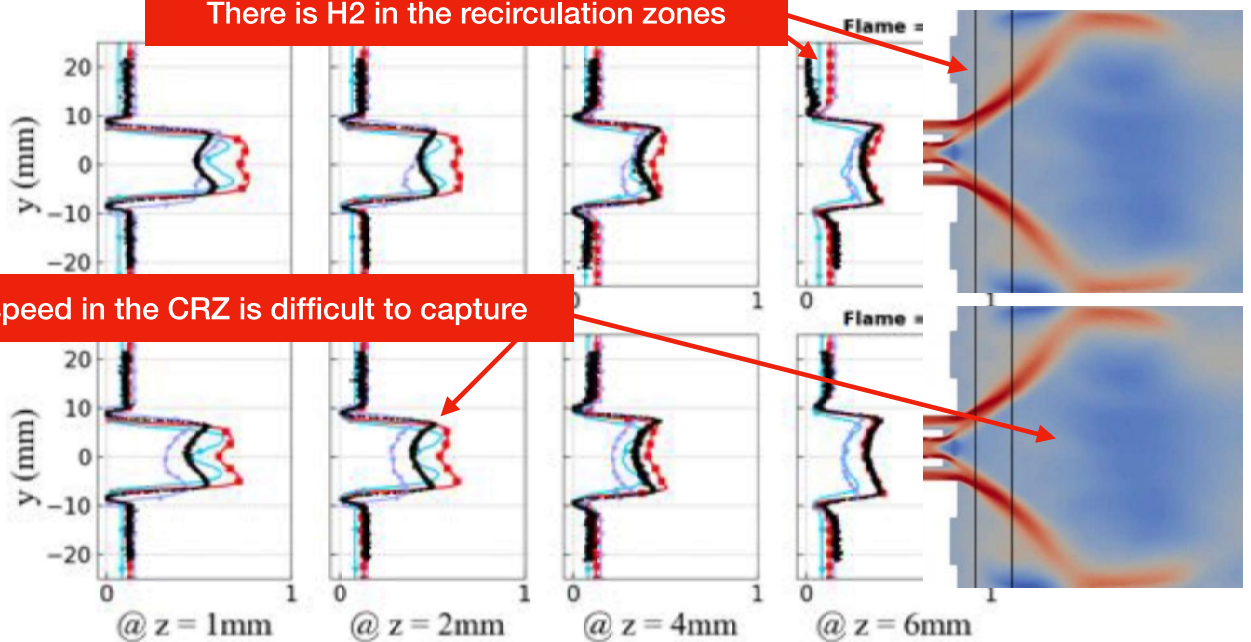
## Mixing: $X_{H_2}$ profiles (A and L cold)



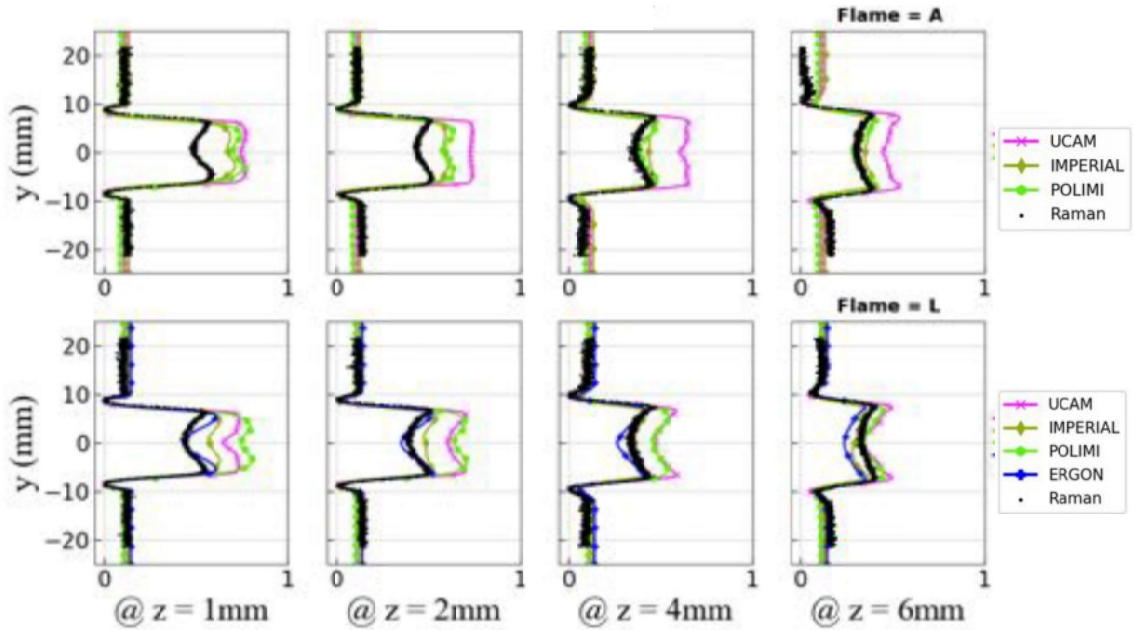
## Mixing: $X_{H_2}$ profiles (A and L cold)

There is  $H_2$  in the recirculation zones

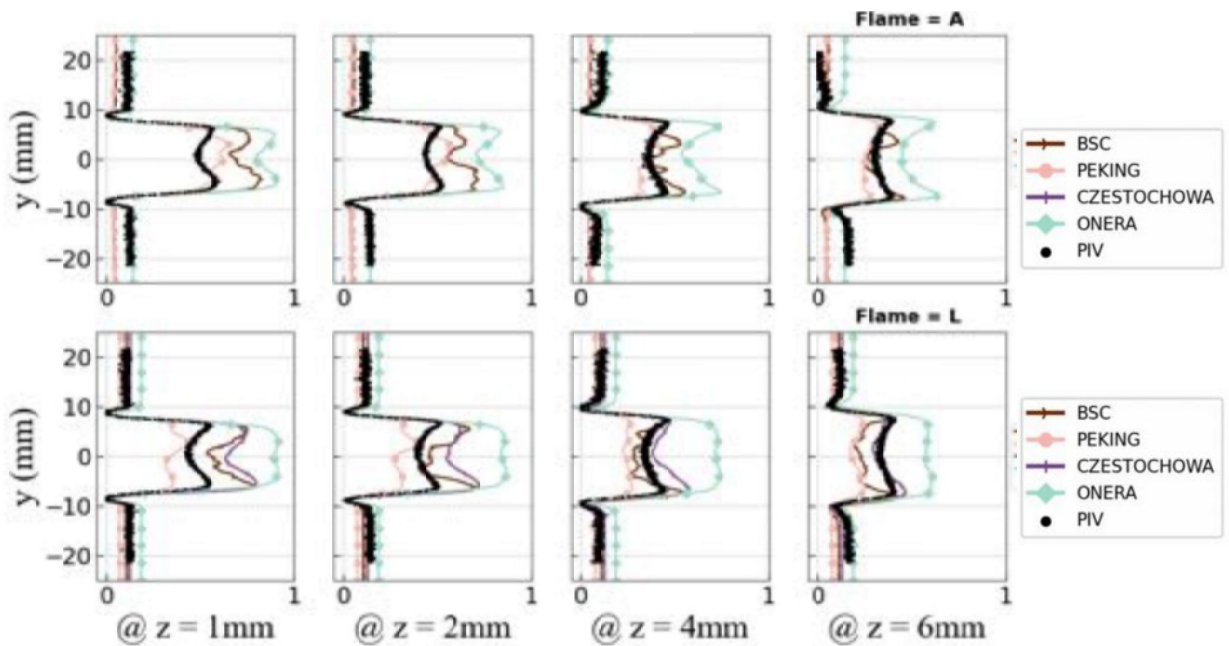
The mixing speed in the CRZ is difficult to capture



## Mixing: $X_{H_2}$ profiles (A and L cold)

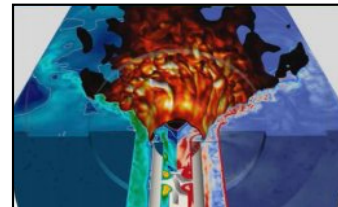


## Mixing: $X_{H_2}$ profiles (A and L cold)





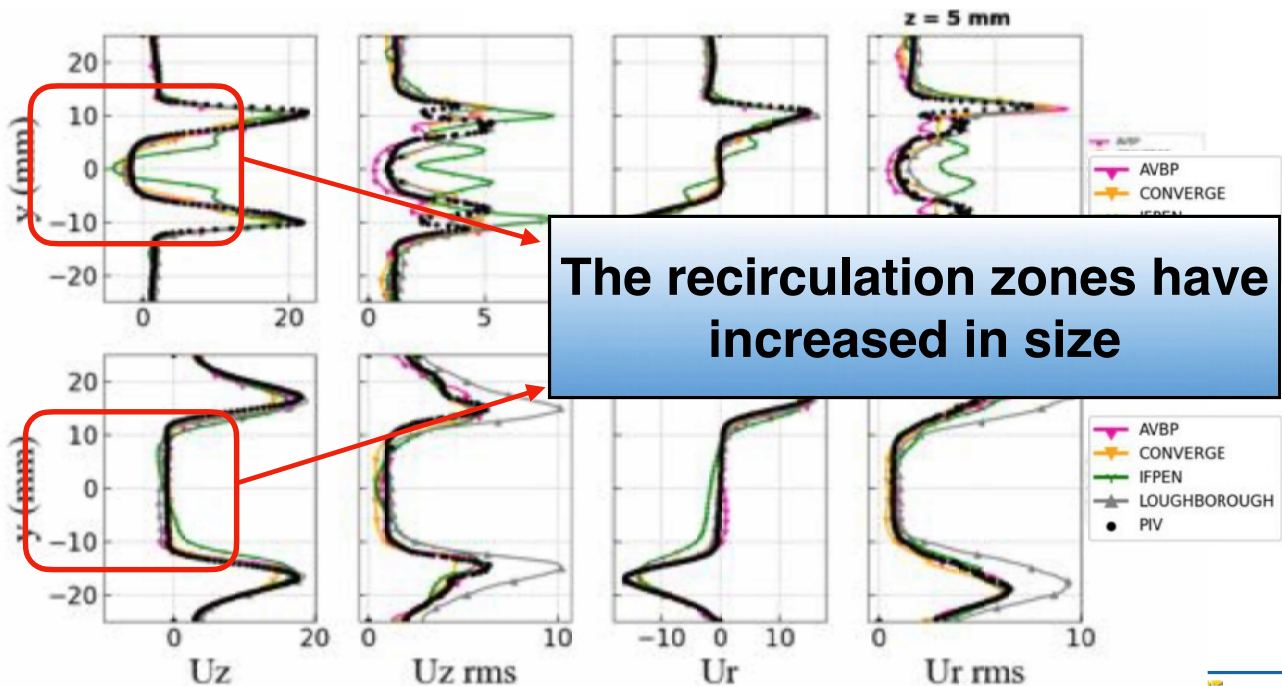
# REACTING FLOW RESULTS FOR CASES A AND L: VELOCITY FIELDS



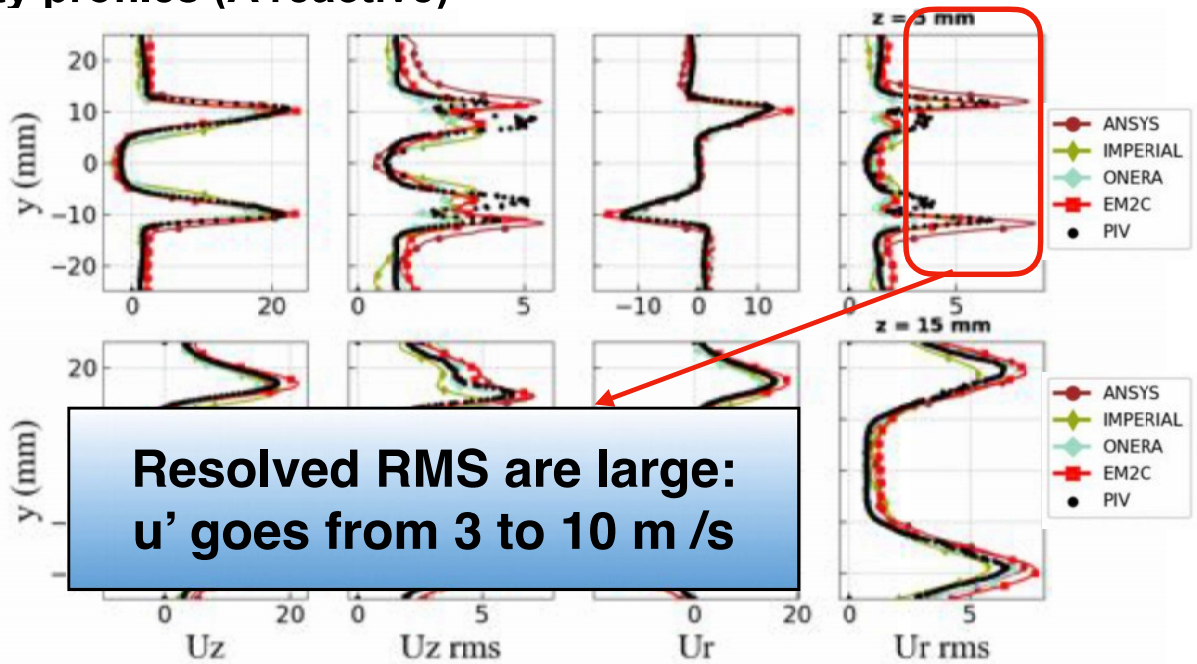
With the support of:  
 ERC advanced grant SCIROCCO (2019-2024), SELECT-H (2023-2028), SYNERGY ERC grant HYROPE (2024-2030),  
 SAFRAN, AIRBUS, ALSTOM, AIR LIQUIDE, GRTGAZ, TOTALENERGIES, SAINT-GOBAIN



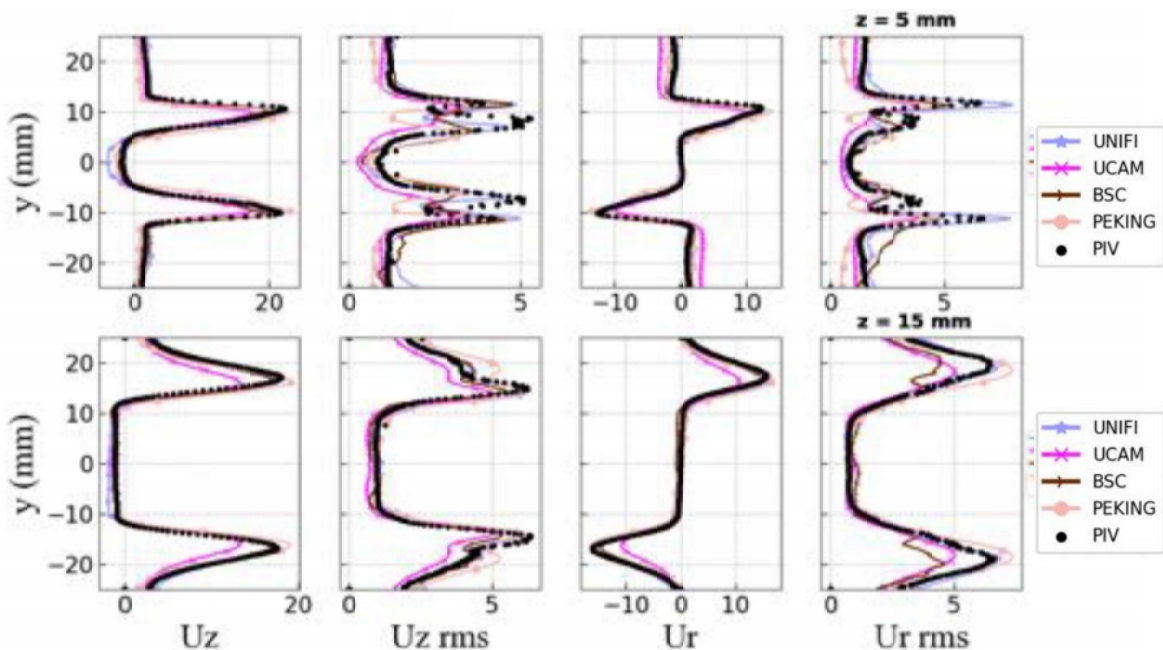
## Velocity profiles (A reactive)



## Velocity profiles (A reactive)



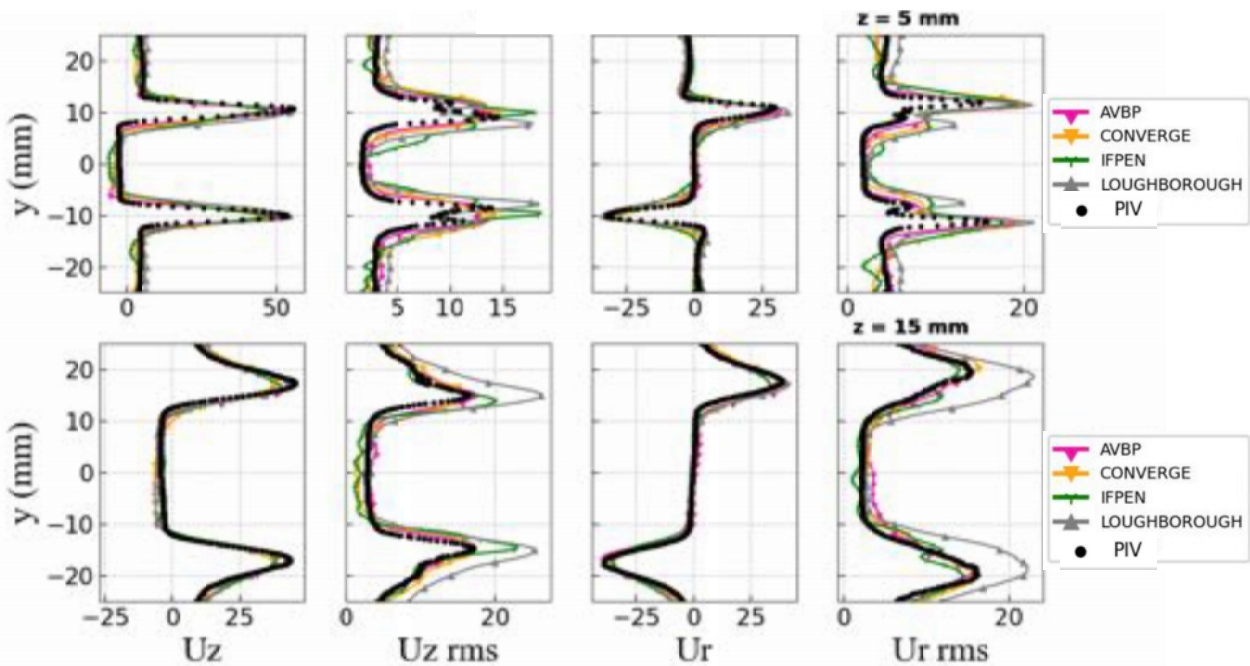
## Velocity profiles (A reactive)



**LET US GO TO REACTING CASE L (LIFTED):  
The Reynolds number increases !  
The flame lifts off from the injector lips**

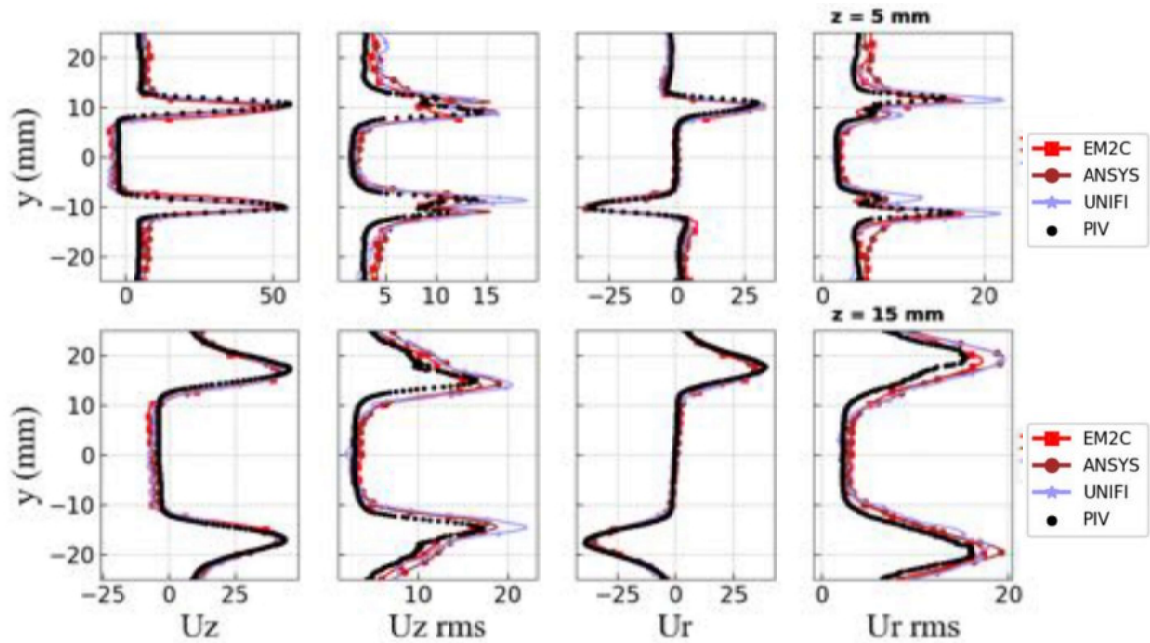


**Velocity profiles (L reactive)**

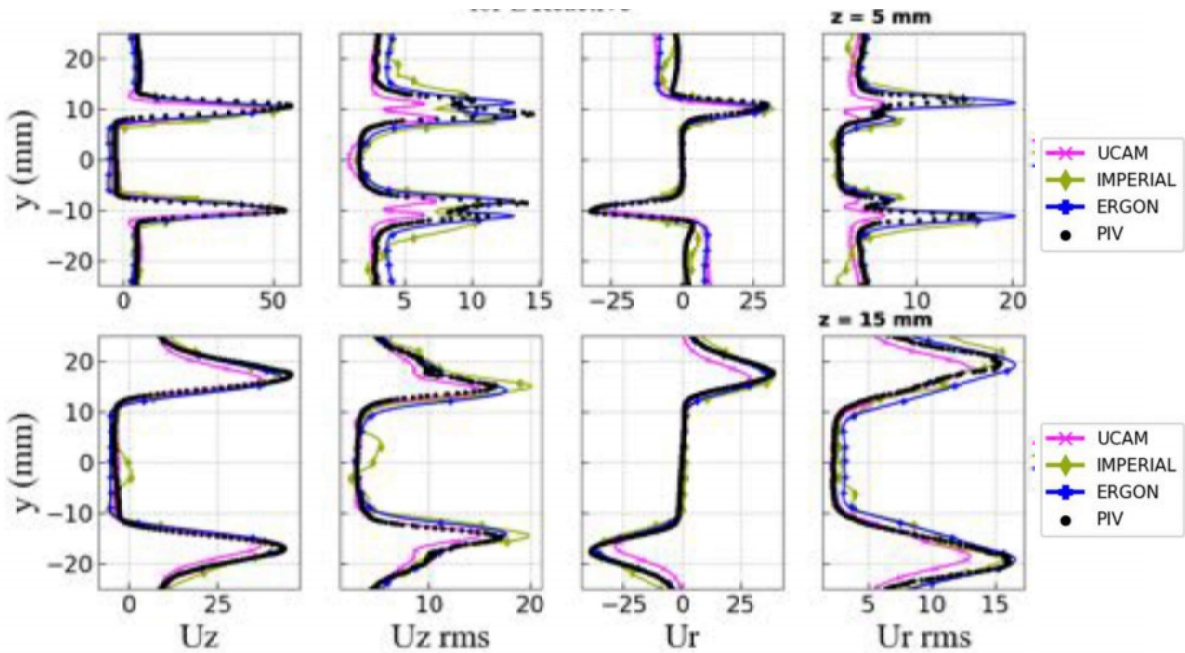




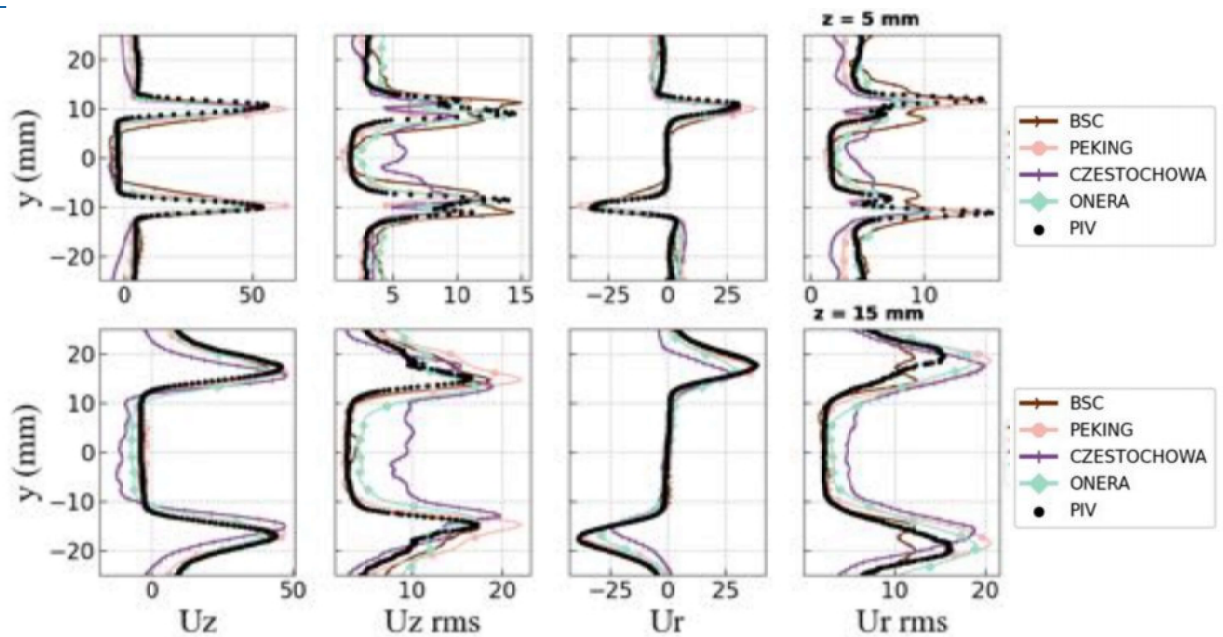
## Velocity profiles (L reactive)



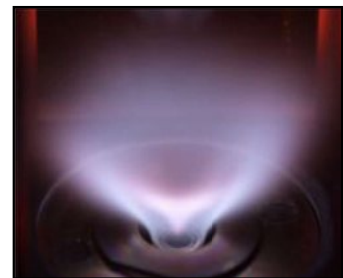
## Velocity profiles (L reactive)



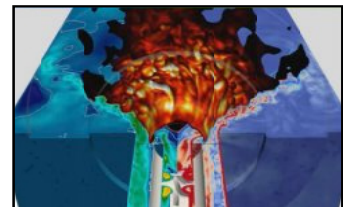
## Velocity profiles (L reactive)



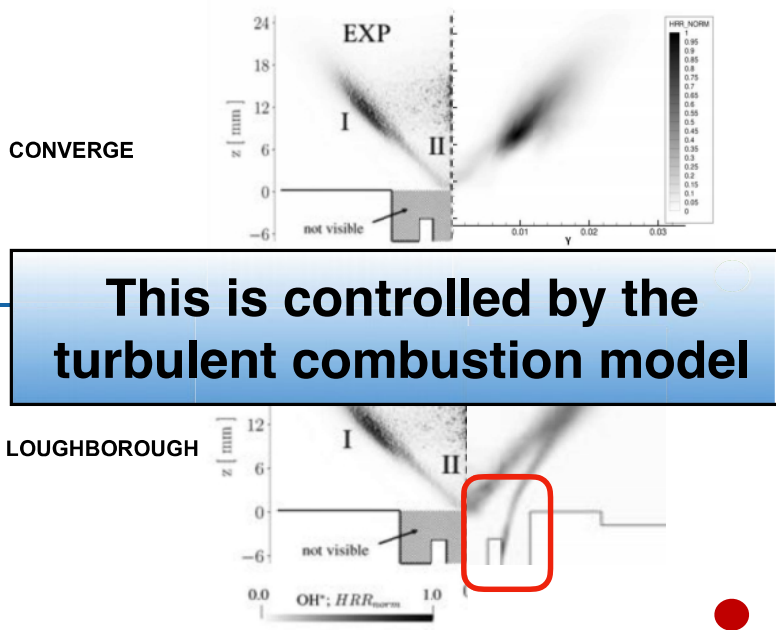
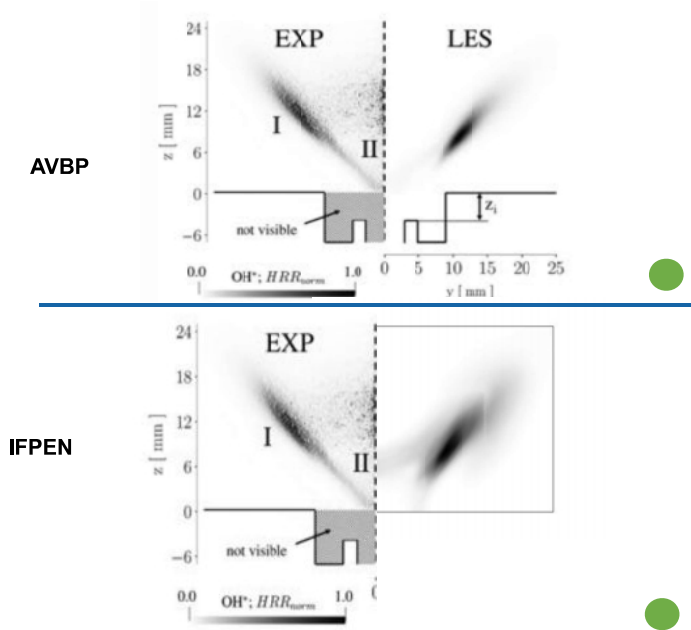
**REACTING FLOW RESULTS  
FOR CASES A AND L:  
OH FIELDS -> is the flame  
anchoring captured or not ?**



**Let us look at OH\* fields**



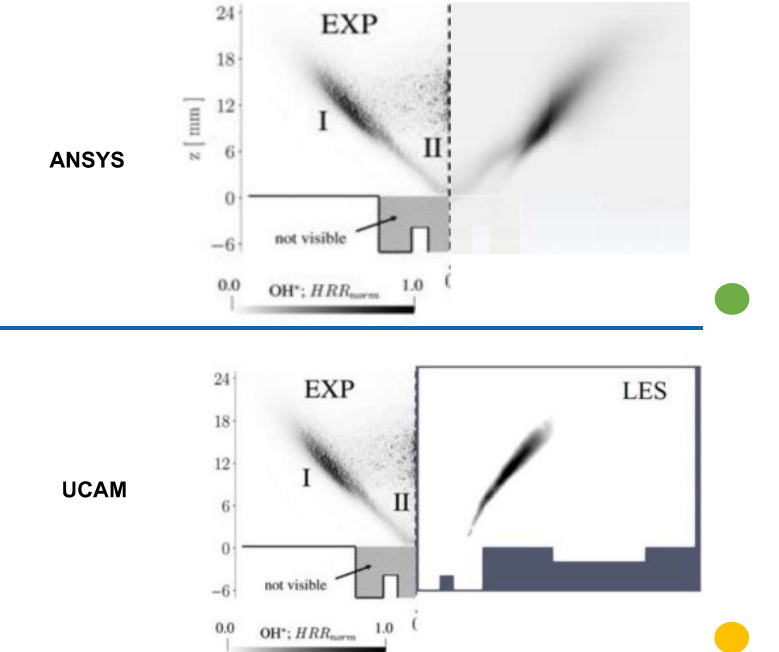
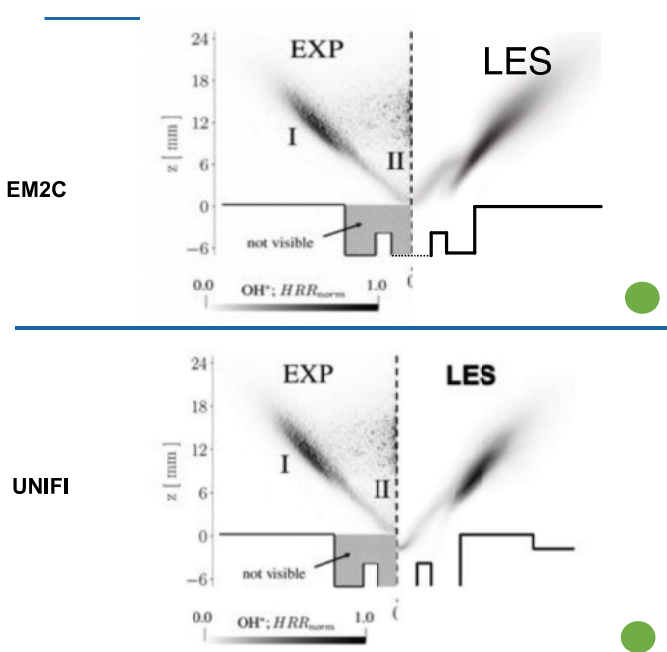
# OH\* profiles for L reactive



This is controlled by the turbulent combustion model

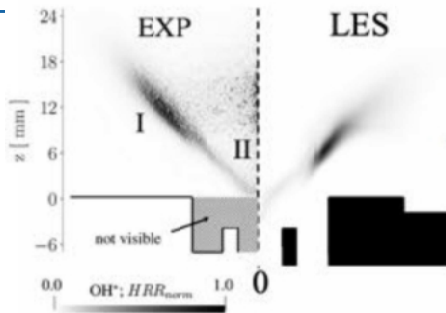


# OH\* profiles for L reactive

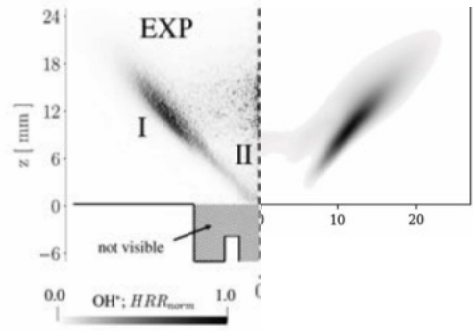


# OH\* profiles for L reactive

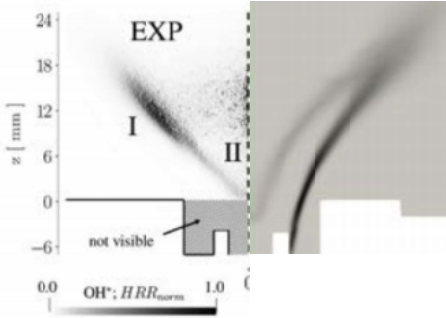
IMPERIAL



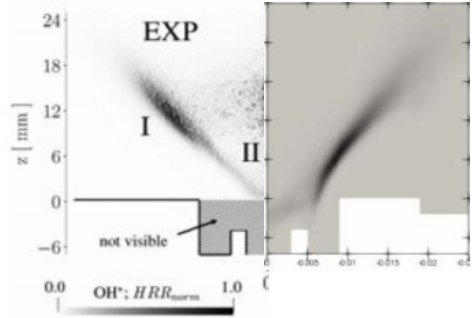
ERGON



BSC



PEKING

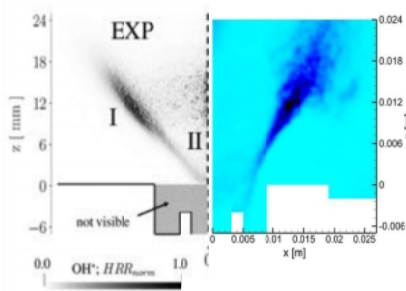


SCIROCCO

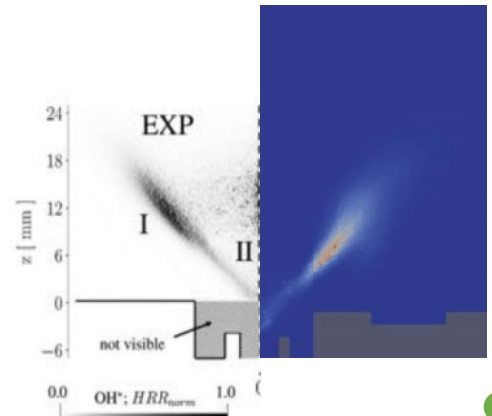
CERFACS IMPT

# OH\* profiles for L reactive

CZESTOCHOWA



ONERA

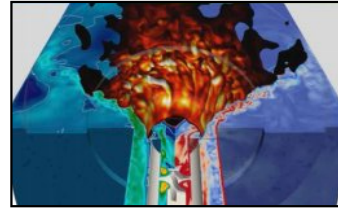


SCIROCCO

CERFACS IMPT



## Overall conclusions from HYLON PHASE 1



**MAIN OUTPUT:** capturing the velocity fields was not that difficult: most codes do it. In fact the flame position being more or less imposed by the recirculation within the chamber, the velocity field cannot vary that much as long as we have the right temperature field. So far, so good

**IS IT THAT SIMPLE?** Let us discuss the essential ingredients which the CFD codes should have to achieve the TRUE objectives:

- go to high pressure
- predict NO<sub>x</sub> and unburnt H<sub>2</sub> when this happens
- study flame dynamics: ignition, blow-off, flashback

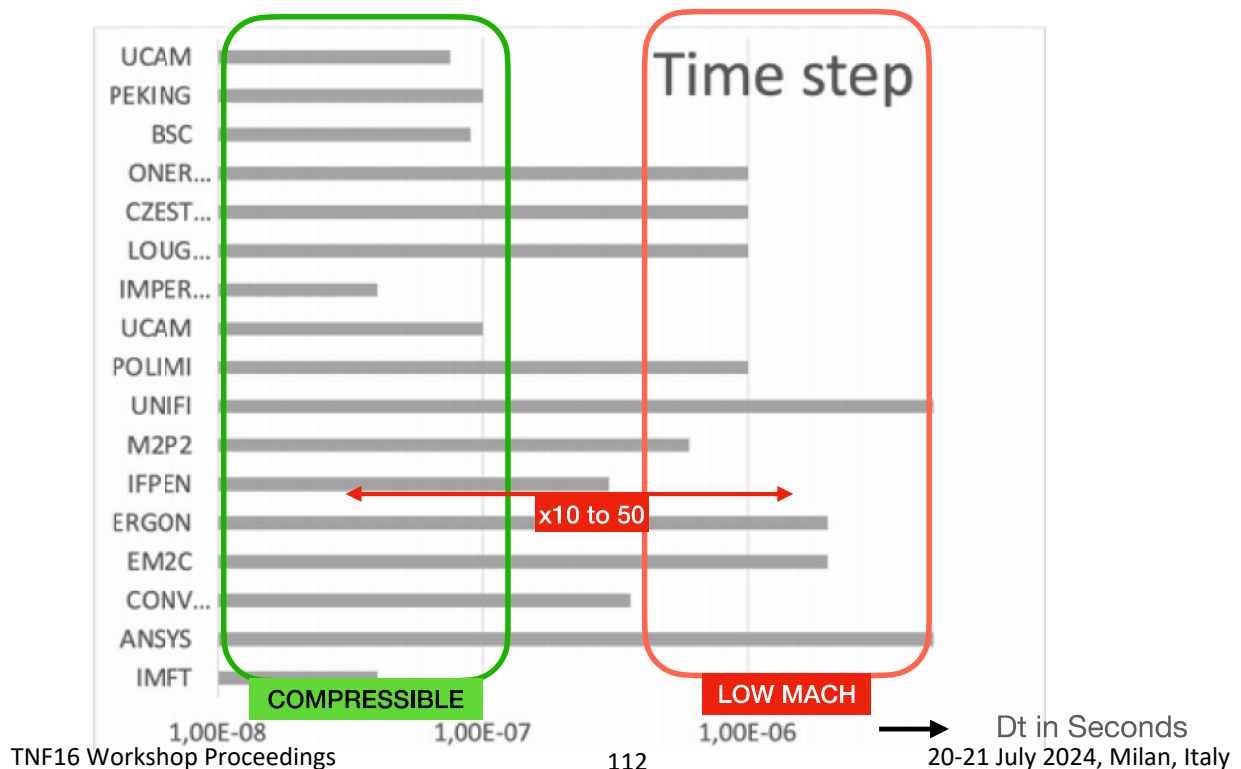


# 1. CODE ORDER: DOES ACCURACY MATTER ?

**SPACE ACCURACY:** Many groups (especially coming from aerodynamics and DNS) argue that high-order codes ( $>4$ ) are needed for LES in CFD. It does not seem to be the first worry of most groups in the present exercise: most codes have a spatial accuracy close to 2.

**TIME ACCURACY:** more complex issue. Very wide range of time steps. Compressible solvers use time steps close to 10 ns. Low Mach solvers go up to microseconds. That does not seem to affect results much

## Time steps are vastly different !



## 2 MESH, STATIC AND DYNAMIC REFINEMENTS

Smallest mesh: generally from 75 to 250 microns

Noone used dynamic Mesh Refinement where the mesh follows the flame in real time: not needed here because the flame does not move that much

Some groups used static Mesh Refinement

What imposes the mesh size ? The flame OR the flow in the swirler ? Most of us are combustion guys so we think that the flame is the controlling factor: we must resolve the flame front.

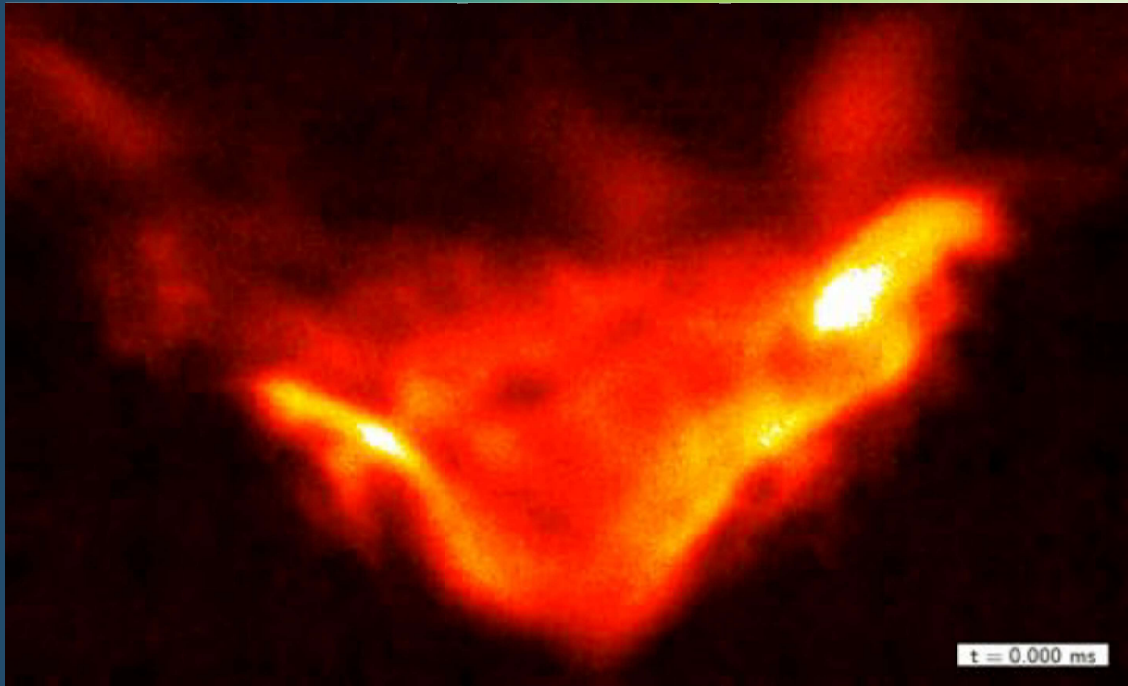
BUT...

Let us look at the transition from lifted to attached flame. Can do it experimentally and numerically

Experiment (real time)

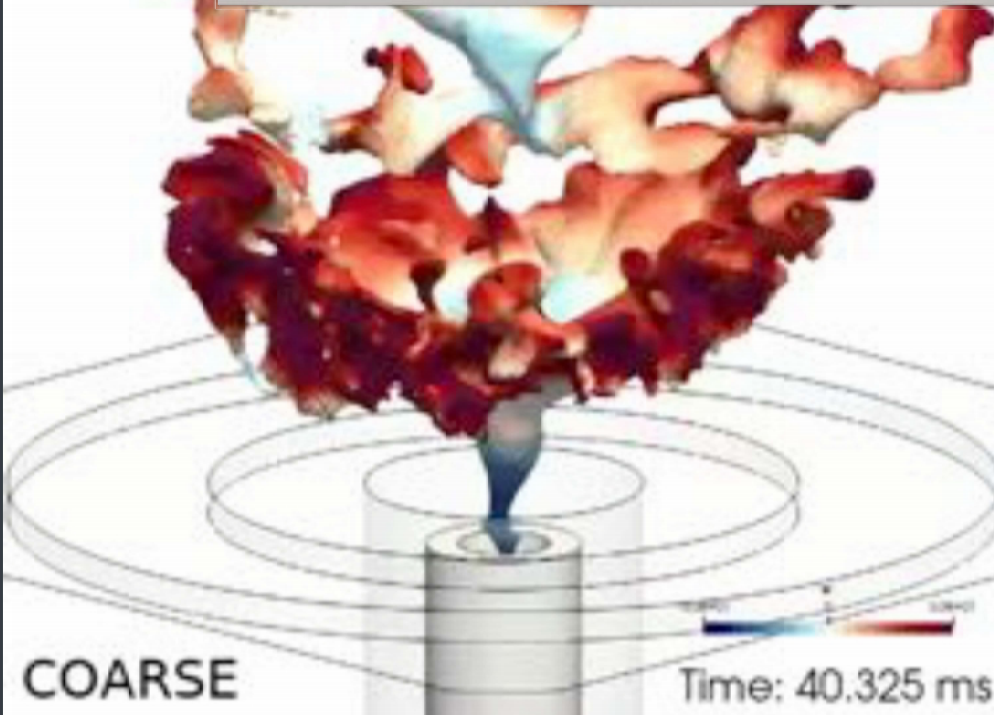


# Experiment (16 kHz camera)



AIR ↑ | H<sub>2</sub> ↑ | AIR ↑

## LES transition



C. Perez Arroyo

# The dangerous question

Does this transition depend on the mesh of the swirler ?

SIMPLE TEST: refine

- the swirler mesh only and
- not the flame zone...

COARSE MESH LES  
reattaches

FINE MESH LES  
does not reattach

Capturing a flame like HYLON might require more points in the swirler than in the flame: the velocity profile at the burner lips is crucial.

The *velocity gradients* at the lip may actually be a key ingredient: we know for example that flashback is controlled by the velocity gradients at the wall of the lip

COARSE

Time: 40.325 ms FINE

Time: 40.775 ms

C. Perez Arroyo

## 3 TURBULENT COMBUSTION MODEL

### TFLES:

- AVBP (CERFACS)
- CONVERGE (IFPEN)
- FLUENT (UNIFI)
- FLUENT (ERGON)
- ProLB (M2P2)
- OPENFOAM (POLIMI)

### FGM:

- STARCCM (LOUGHBOROUGH)

### F TACLES:

- YALES2 (CORIA, EM2C, ST)

### PDF models:

- OPENFOAM (UCAM)
- BOFFIN (IMPERIAL COLLEGE)

No model at all, just chemical scheme with no SGS correction

- FLUENT (ANSYS)
- CONVERGE (CSI)

## 3 TURBULENT COMBUSTION MODEL

- Why no model at all ?

Good reasons for this: ?:

- we don't have a clear single model which can do premixed and diffusion at the same time. Might as well use finite rate chemistry (except we know it is wrong)
- pressure is low so maybe we are not so far from DNS -> we'll come back to this



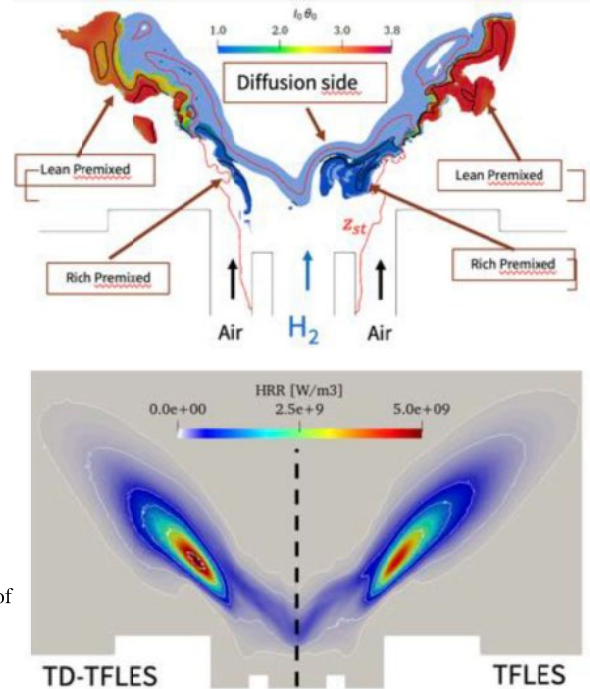
## 4 - DO WE NEED TO ACCOUNT FOR THERMODIFFUSIVE INSTABILITIES ?

There are premixed flamelets in HYLON when the flame is lifted (Flame L)

But no-one took them into account in this exercise because a large part of the flame is a diffusion flame or a rich premixed one

One model for TD effects was tested in 2022 using the  $l_0$  correlation of RWTH at the Stanford Summer program and did not show significant changes

A. Aniello, D. Laera, L. Berger, A. Attili and T. Poinso. Introducing thermodiffusive effects in large-eddy simulation of turbulent combustion for lean hydrogen-air flames. Proceedings of the Summer Program. Center for Turbulence Research, Stanford, 267-276, 2022.



## 5 - ARE OUR CHEMICAL SCHEMES SUFFICIENT ?

Chemical schemes used for HYLON:

- San Diego
- Burke
- C3 reduced to 10 species
- Boivin

For HYLON:

- all groups used reasonably accurate schemes
- we did not see a major influence of the scheme

## 5 - ARE OUR TRANSPORT MODELS SUFFICIENT ?

Many groups use multicomponent transport models for  $D_k, \lambda, \mu$

In practice this is an overkill in most LES because in our codes, we never use:

$D_k, \lambda, \mu$

but

$D_k = D_{k, \lambda, \mu}$

where the

- VERY LARGE compared to the laminar values

- VERY WRONG: these are models for turbulent transport

**Not an issue for LES: results don't change when the laminar diffusivities models change.**

**Careful: conclusion valid only for LES. Accurate**

$$\overline{\rho u'' \Theta''} = -\frac{\mu_t}{Sc_t} \frac{\partial \tilde{\Theta}}{\partial x}$$

## 6 - WHAT ABOUT NO<sub>x</sub> AND TEMPERATURE

NO<sub>x</sub> was NOT considered up to now. It will be soon. This will require a proper computation of the temperature field

This raises the question of the boundary conditions to give to the CFD groups:

1/ We measure the wall temperature and use it as boundary condition for CFD. How much data do we need ? temperature field on all walls for all flames ??

OR

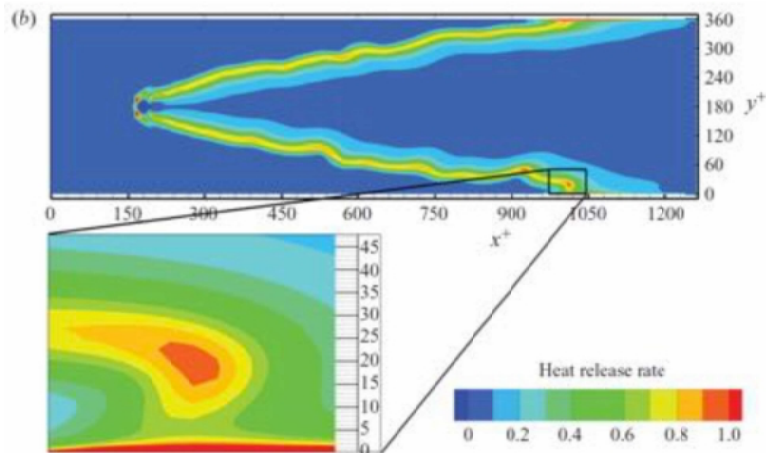
2/ We ask the CFD groups to do the full Conjugate Heat Transfer simulation of the whole setup

UNSOLVED ISSUE...

## 7 - WHAT ABOUT WALL TREATMENTS

Most solvers used inert walls: no chemistry at the walls. However, we know that strange things occur at walls... very large heat release on walls due to H<sub>2</sub> radical

AVBP uses a treatment called IFHC (Comb Flame 2024): we still believe something must be done at the walls (see other presentation on FWI during the TNF workshop by C. Hasse)



[1] Gruber et al. (JFM, 2010)

## 8 - HIGH PRESSURES

HYLON PHASE 1 was at 1 bar. Imagine we want to go to 20 bar now.

At 1 bar, we picked a smallest mesh size between 100 and 250 micrometers and created a mesh

This choice was not guided by physics: we only did what we could... Now, at 1 bar, a typical flame thickness was 400 microns. So with the mesh we created, we are almost good: 4 points in the flame. For the flow, the Reynolds number in the air swirler is 8000.

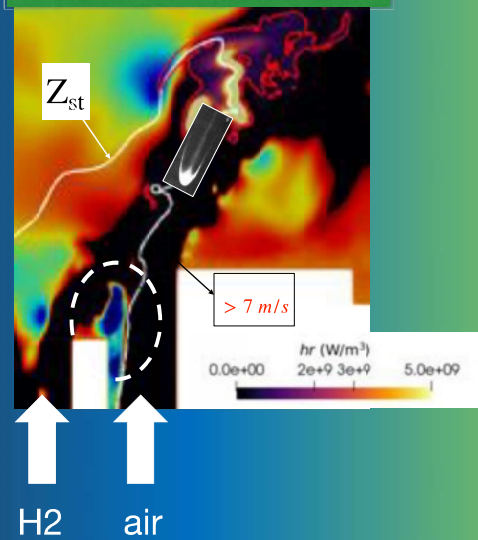
**THIS IS A NICE COINCIDENCE. DONT TAKE IT FOR GRANTED...**

At 20 bar, the flame thickness will be 30 microns instead of 400 microns: no-one will use 10 microns meshes in 3D. The Reynolds number of the air channel is 100 000. Brute force approach will fail even when using Mesh Refinement.

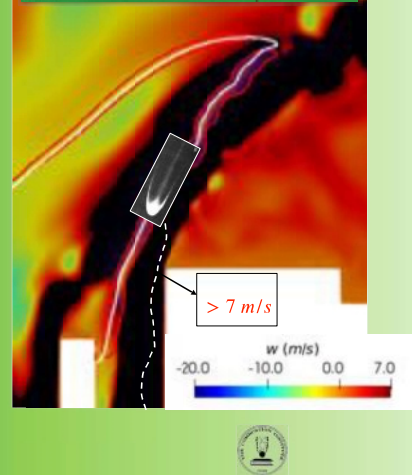
We will need LES models: for the flame but also for near wall turbulence in the swirler

EDGE FLAMES: NEAR THE INJECTOR LIPS: WE WILL NEED TO RESOLVE TRIPLE FLAMES WHICH ARE ESSENTIAL INGREDIENTS CONTROLLING DIFFUSION FLAME STABILIZATION

Attached flame.



Lifted flame.

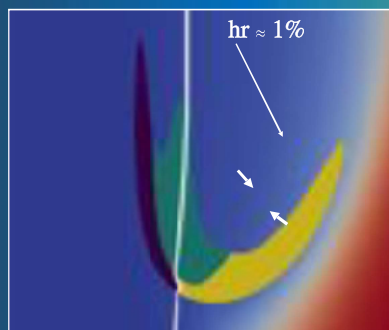


8



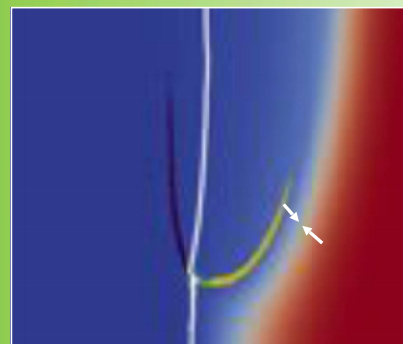
These triple flames are extremely thin.  
DNS is not so easy at high pressures even in 2D...

$\Delta x = 25 \mu\text{m}$



T = 300 K , P = 1 bar

$\Delta x = 8 \mu\text{m}$



T = 300 K , P = 5 bar



14

Aniello's PhD unpublished results

# These edge flames induce flashback



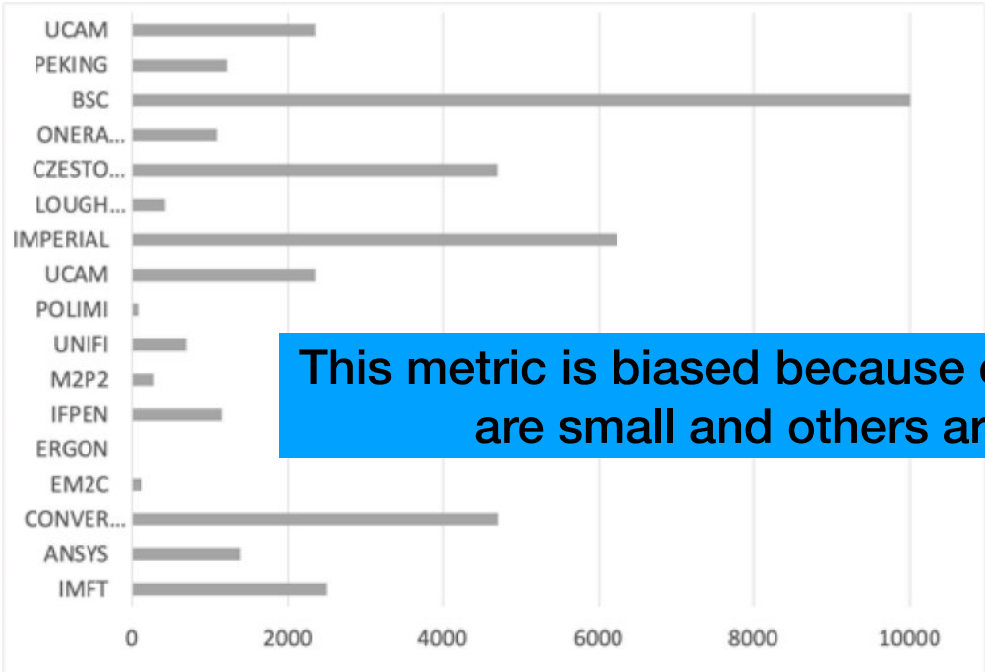
## 9 - CPU TIMES

Noone really tried hard during the HYLON PHASE 1 to use all possible options to optimize CPU time  
Everyone used a different mesh so that comparisons are also difficult

Still, we can have a look at orders of magnitude for the High Performance Computing aficionados !

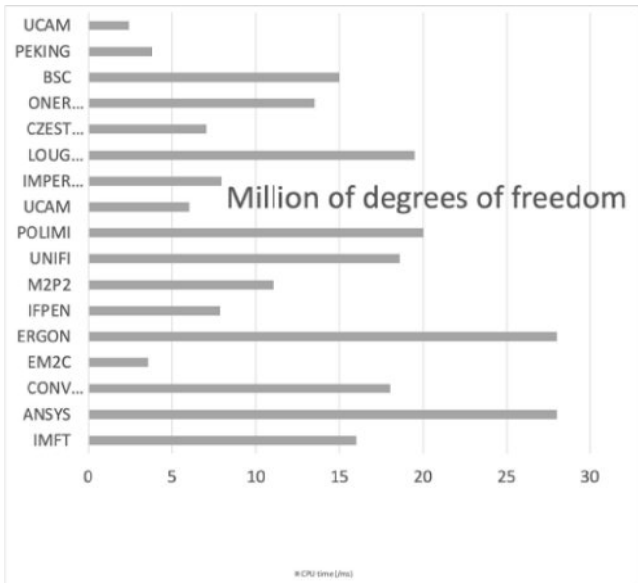
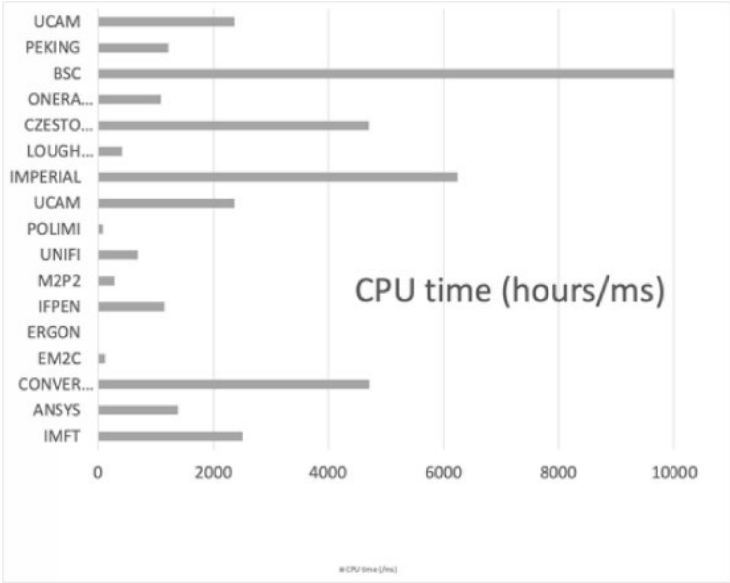


# 9 - CPU TIMES: CPU hours for one ms of physical time in HYLON

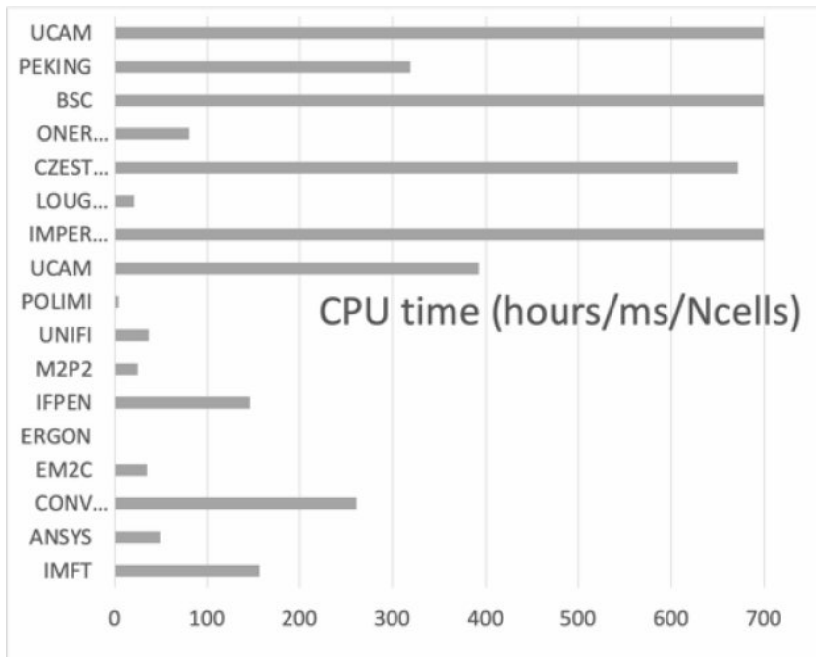


This metric is biased because certain meshes are small and others are... big

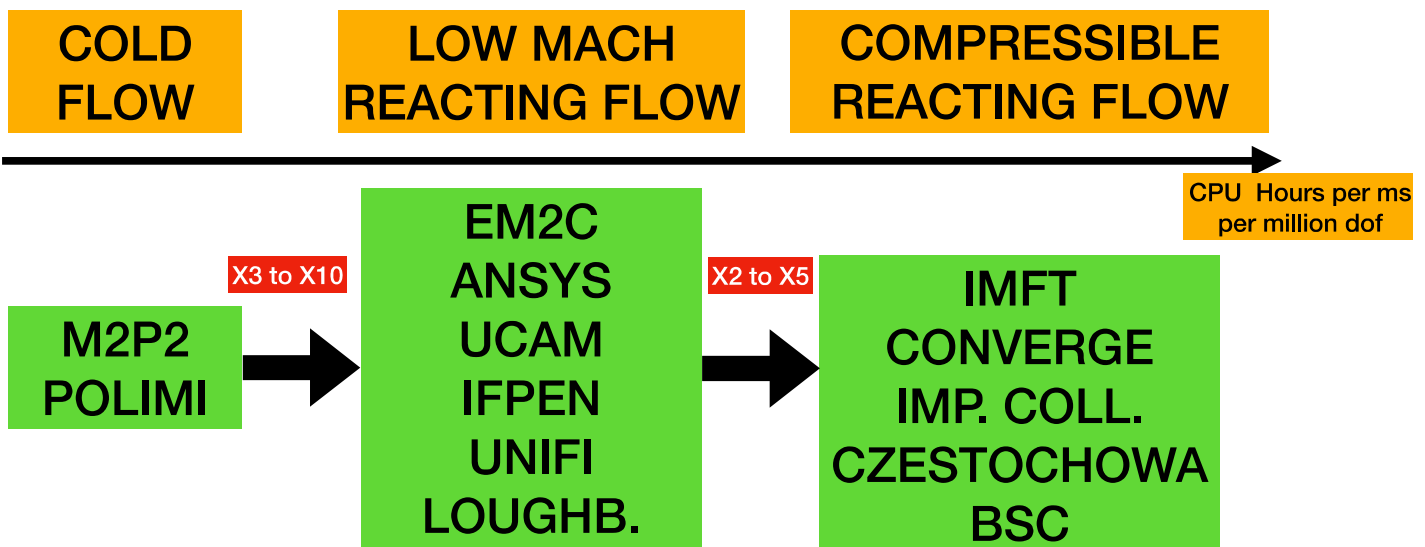
# 9 - CPU TIMES and mesh sizes (nbr of degrees of freedom)



## 9 - CPU TIMES scaled by number of degrees of freedom: hrs for 1 ms of physical time and 1 Million mesh points



## 9 - CPU TIMES: a summary - you have what you pay for



## WHAT IS NEXT ? Going for the really tough cases

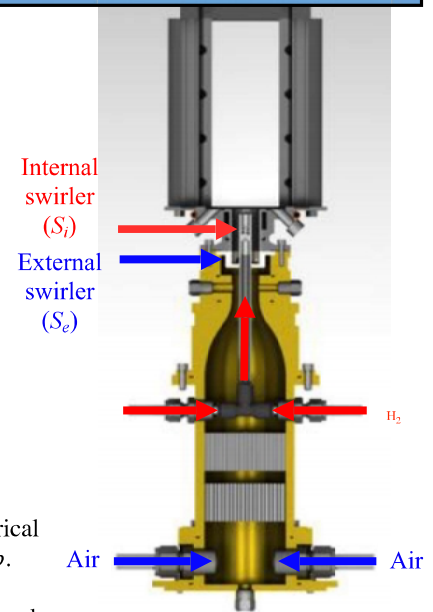
There are actually 3 versions of HYLON:

- HYLON TNF: the one we discuss today. 1 bar at IMFT (papers below and TNF)
- HYLON HP: will start in 2024 at IMFT and operate up to 3 bar
- HYLON KAUST: operates up to 10 bar. Working now

S. Marragou, H. Magnes, A. Aniello, T. Guiberti, L. Selle, T. Poinso, T. Schuller. Modeling of H<sub>2</sub>/air flame stabilization regime above coaxial dual swirl injectors. *Comb. Flame* 255, 112908, 2023.

Aniello, D. Laera, S. Marragou, H. Magnes, L. Selle, T. Schuller, T. Poinso. Experimental and numerical investigation of two flame stabilization regimes observed in a dual swirl H<sub>2</sub>-air coaxial injector. *Comb. Flame* 249, 112595, 2023.

A. Aniello, T. Poinso, L. Selle, T. Schuller. Hydrogen substitution of natural-gas in premixed burners and implications for blow-off and flashback limits. *Int. J. Hydrogen Energy*. 2022.



105

## WHAT IS NEXT ? Going for the really tough cases

You have seen the results of the HYLON PHASE 1 exercise at 1 bar

IMFT and KAUST propose to collaborate to provide more data within the TNF workshop for a HYLON-type configuration **at higher pressures: HYLON PHASE 2**

Caveats:

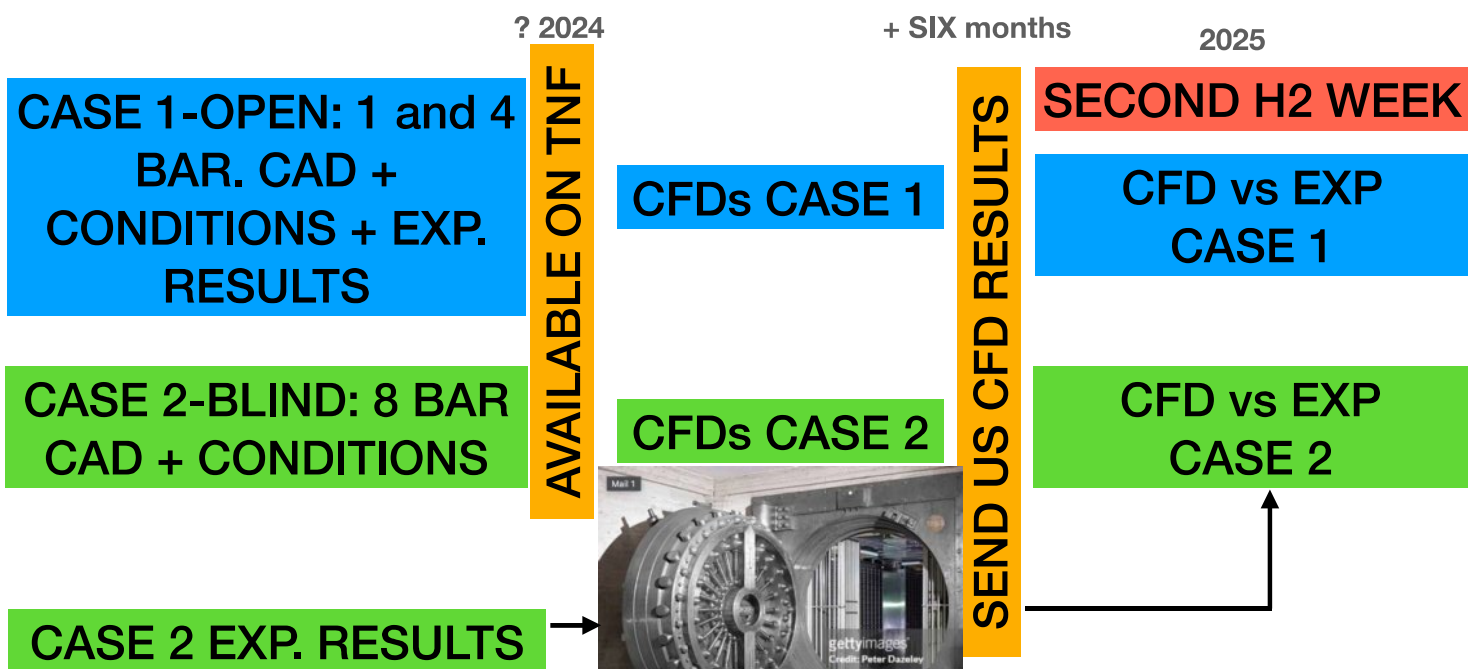
- the KAUST burner geometry will not be exactly HYLON: new meshes will need to be created by you. It will be very close, however...but CFD guys will need to redo their meshes
- Provide velocity profiles + pressure losses + **NOx profiles + main species profiles**
- **Data at 1 bar and** two higher pressure results (4 and 8 bar)
- this is NOT ready yet
- if we distribute results, it will be done « **almost** » exactly like for TNF HYLON PHASE 1

**« Almost » :**  
**HYLON PHASE 2 MIGHT CONTAIN A BLIND TEST**

We propose to split the data used in HYLON PHASE 2 coming out in the next year in two parts:

- experimental results available for everyone right away. For ex: measurements at 4 bar
- experimental results kept 'secret' until CFD runs are finished. For ex, measurements at 8 bar

**Summary of time line for HYLON PHASE 2:**



## PHASE 2 : IN PRACTICE

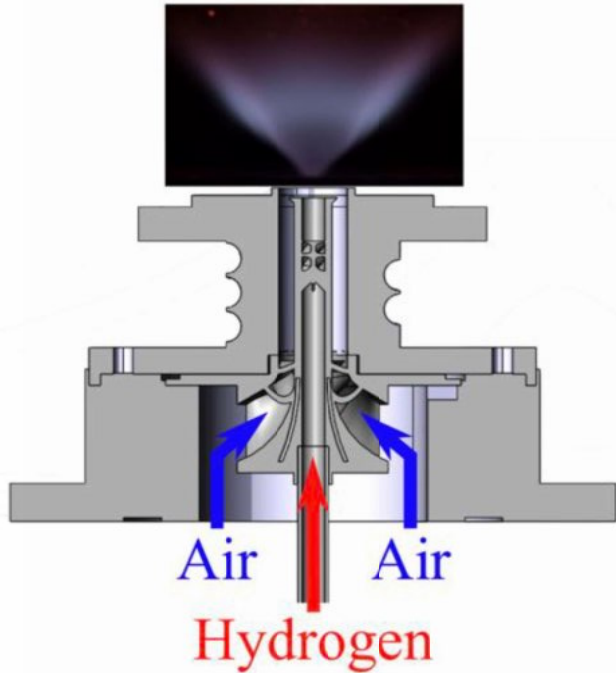
IMFT and KAUST need a few months to make sure that we can provide the experimental data  
Then, we will invite the community to participate as done for HYLON PHASE 1.



## Hylon 2 IMFT/KAUST



## Final geometry of the HYLON TNF PHASE 2 injector

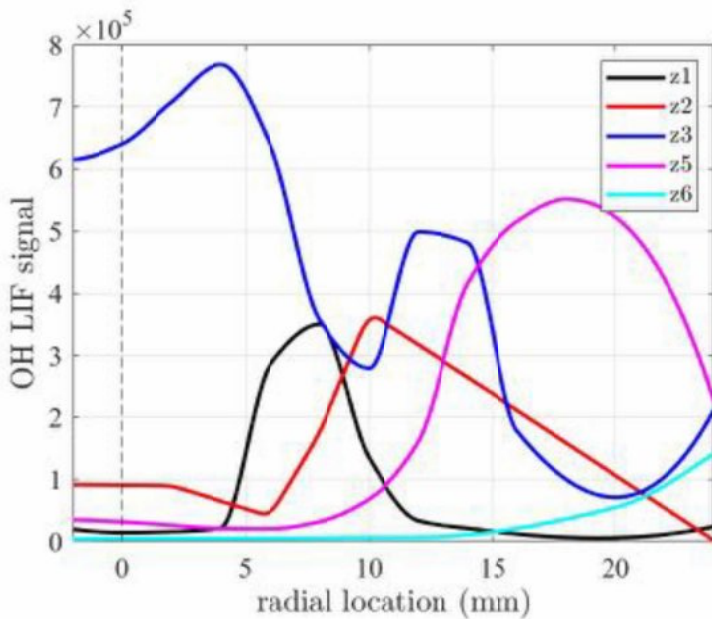


- Diameter annular channel: 18 mm
- Diameter central channel: 6 mm
- Thickness central channel: 2 mm
- Size central channel deflector: 1.5 mm
- Recess central injector: 4.3 mm
- Swirl number air flow: 0.9
- Swirl number hydrogen flow: 0.9
- Width combustion chamber: 78 mm
- Length combustion chamber: 149 mm
- Contraction ratio exhaust: 0.51

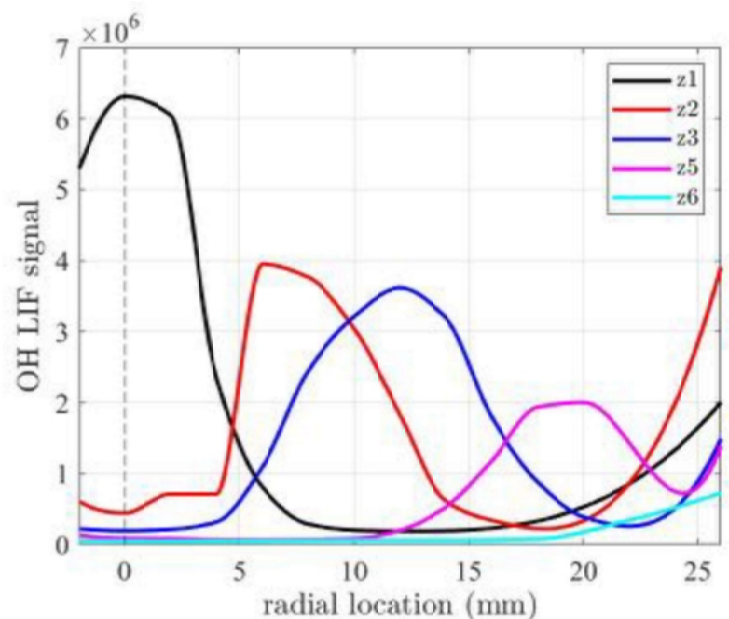
111

## Preliminary results: OH LIF profiles

Flame A

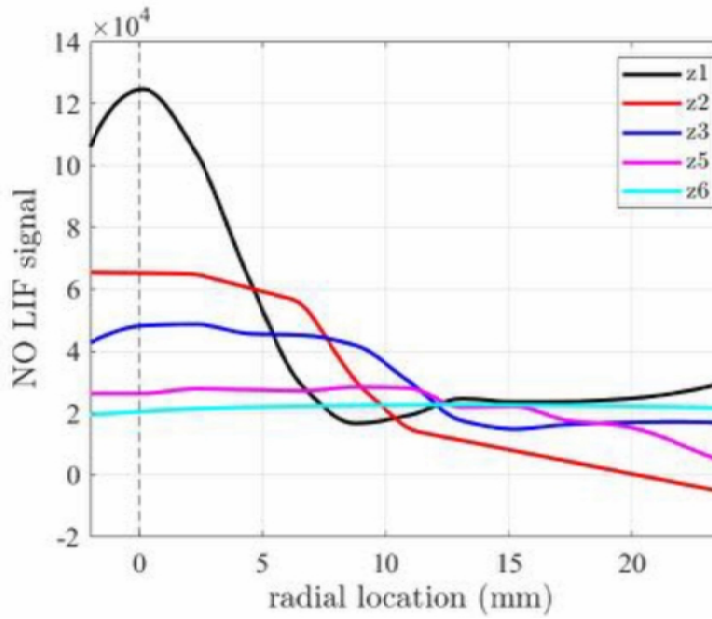


Flame L

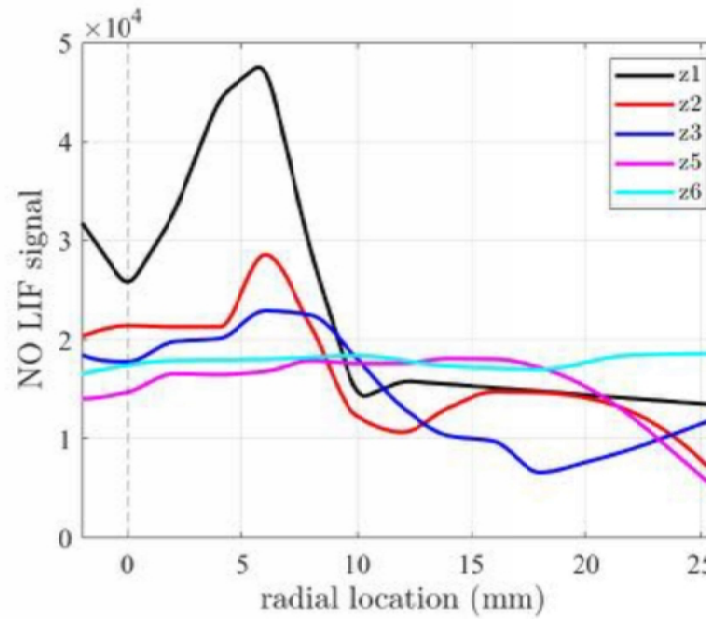


# Preliminary results: NO LIF profiles

Flame A

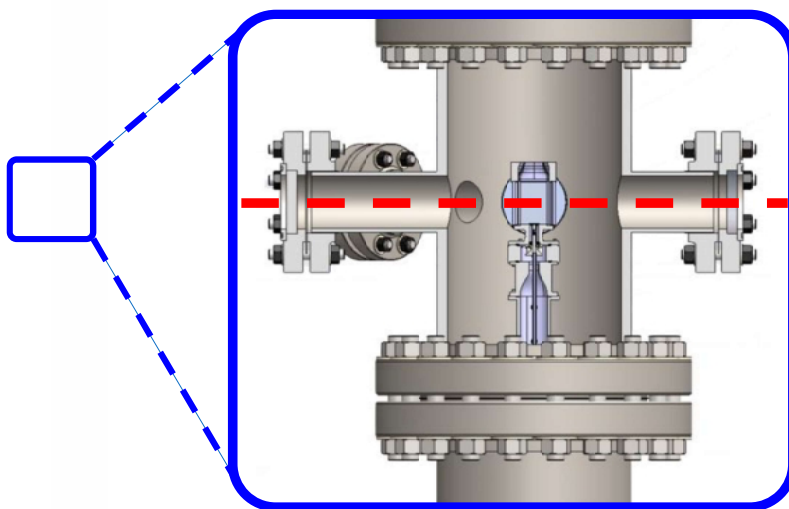


Flame L

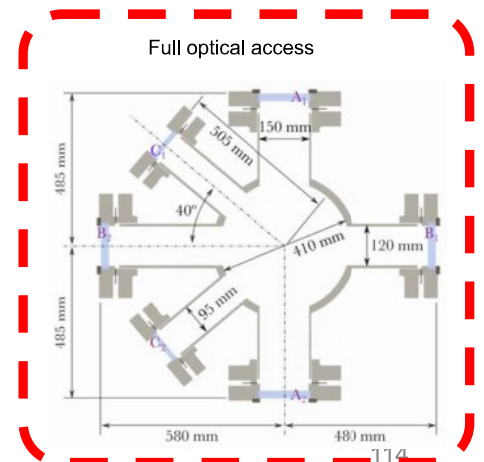


113

# Installation inside the HPCD test bench



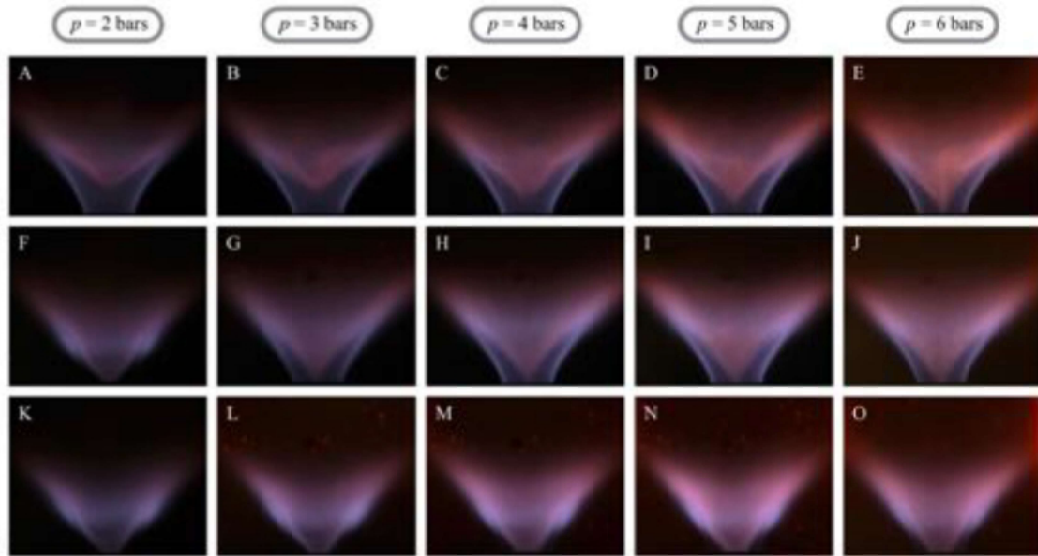
- Thermal power range: 0 to 70 kW
- Overall pressure range: 1 to 15 bars
- Pre-heated air system: currently in implementation



114



# High-pressure flames



The injector both anchored and lifted flame stabilization regimes (and some other interesting cases!)

115

**THANK YOU**

ERC  
IMFT  
CERFACS  
TNF members for having us here

IMFT team:

Martin Vilespy, Theo Riou, Marc Chen, Kennie Chaplet, Herve Magnes, Hugo Paniez, Thierry Schuller, Laurent Selle, Matthieu Durand, Dilay Guleryuz, Nathanael Rouland, Muriel Sabater, Enrique Flores Montoya



## Summary: AI/ML for Turbulence-Chemistry Interaction

Matthias Ihme, Stanford University, [mihme@stanford.edu](mailto:mihme@stanford.edu)

Alessandro Parente, Université libre de Bruxelles, [Alessandro.Parente@ulb.be](mailto:Alessandro.Parente@ulb.be)

Following the 2022 TNF workshop, the session on AI/ML for Turbulence-Chemistry Interaction was the second TNF session on the topic intersecting machine learning and artificial intelligence with turbulent combustion. Since 2022, various ML methods have been adopted and extended by the combustion community to address problems of turbulent combustion modeling and experimental analyses. The main applications of ML for combustion tasks involve:

- Accelerating combustion simulations and experimental analysis
- Creating knowledge and gain physical insight
- Formulating hybrid closures for improved fidelity simulations
- Developing reduced-order models and digital twins

In this session, we reviewed recent advances with the specific goal of connecting the broad field of ML to TNF/PTF-related problems. We solicited contributions from the TNF and PTF research community, resulting in a total of nine contributions.

The session was split into three topics: (i) background on ML for combustion, (ii) ML for turbulent combustion modeling, and (iii) ML for experimental combustion analysis. The first section provided a succinct overview of the different ML techniques to find a common nomenclature within or combustion community.

The second section reviewed recent developments of ML-methods for application to turbulent combustion modeling, focusing on integrating supervised ML methods for regressing multi-dimensional reaction-transport manifolds, the use of ML techniques to accelerate turbulent reacting flow simulations, the construction of reduced-order manifolds, and embedding uncertainty quantification into ML combustion models. Other model developments included the identification of reduced manifolds that are either obtained from principal component analysis or derived as latent spaces from auto encoder projections, which provide access to non-linear parameterization of reduced state-spaces. The acceleration of high-fidelity combustion simulations (DNS and LES) was also addressed by employing on-the-fly reduced-order state-space representations using time-dependent basis functions and in-situ closure models for flame-surface density using high-order terms in the parameterization of filtered flame front displacement terms.

The third section was concerned with discussing applications of ML methods to extract knowledge from experimental data and the use of ML methods for experimental analysis. Supervised and unsupervised learning methods were applied to a comprehensive set of data from Adelaide's jet-in-hot-coflow experiments, which has been a benchmark dataset of TNF, to generate temperature fields from OH/CH<sub>2</sub>O PLIF measurements. These results showed that standard ML architectures have matured to the point where these techniques can be utilized to extract physical information about fuel sensitivities and flow conditions from sparse data. Other presentations discussed progress towards developing ML-augmented diagnostics for feature extraction as open-source tools to accelerate the analysis of experimental measurements.

In regard to developing foundational ML models for turbulent premixed and non-premixed combustion applications, the need for diverse data accessible to the broader combustion community was discussed. A community-driven effort towards achieving this

goal was discussed through the BLASTNet database (<https://blastnet.github.io>), which offers access to several terabytes of data from high-quality DNS to support various ML tasks. Contributions from workshop participants and the broader combustion community were encouraged with the incentive of joint co-authorship of this community-driven enterprise that has been supported through the NSF Pathways to Enable Open-Source Ecosystems program.

**References:**

- Ihme, Chung, Mishra, “Combustion machine learning: Principles, progress and prospects.” *Progress in Energy and Combustion Science*, 91, 101010, 2022, <https://doi.org/10.1016/j.pecs.2022.101010>
- Ihme, Chung, “Artificial intelligence as a catalyst for combustion science and engineering.” *Proceedings of the Combustion Institute*, 40, 105730, 2024, <https://doi.org/10.1016/j.proci.2024.105730>
- Chung, Akoush, Sharma, Tamkin, Jung, Chen, Guo, Brouzet, Talei, Savard, Poludnenko, Ihme, Turbulence in Focus: Benchmarking Scaling Behavior of 3D Volumetric Super-Resolution with BLASTNet 2.0 Data, *Advances in Neural Information Processing Systems 36 (NeurIPS 2023) Datasets and Benchmarks Track*.



# TNF Machine Learning

*Coordinator: Matthias Ihme and  
Alessandro Parente*

## Contributions

- Imperial College (Stelios Rigopoulos)
- Université Libre de Bruxelles (Alessandro Parente)
- TU Magdeburg (Cheng Chi, Dominique Thevenin)
- University of Stuttgart (Fabian Hampp)
- Tsinghua University (Zhuyin Ren)
- University of Melbourne (JenZen Ho, Mohsen Talei)
- University of Adelaide/University of South Australia (Jordan Kildare, Paul Medwell, Michael Evans)
- NREL (Shashank Yellapantula)
- KAUST (Hong Im)

# Overview and objecties

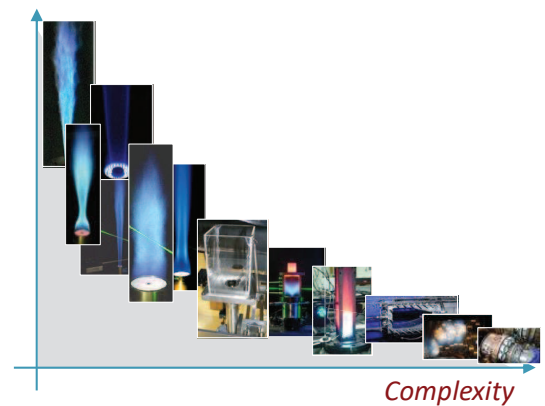
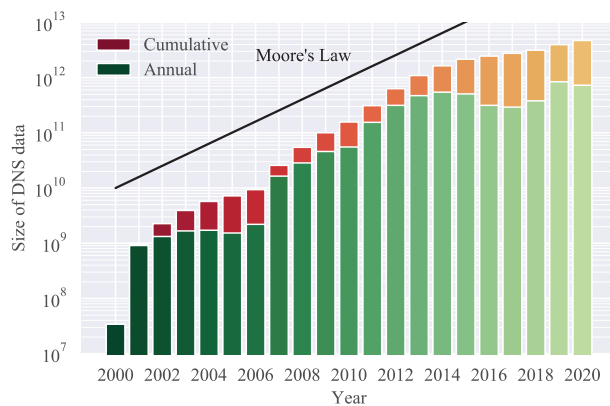
- Machine learning for Combustion @ TN/PF
  - Background on Combustion ML
  - ML for turbulent combustion modeling
    - Stelios Rigopoulos
    - Cheng Chi, Dominique Thevenin
    - Hong Im
    - Shashank Yellapantula
    - Alessandro Parente
    - Jackie Chen [presentation]
    - JenZen Ho [presentation]
  - ML for experimental analysis
    - Jordan Kildare [presentation]
    - Fabian Hampp [presentation]
- Discussions

3

# Machine learning methods for combustion

Supervised learning	Unsupervised learning	Semi-supervised learning
<p>Relate labeled input to unknown output</p>	<p>Identify pattern and discover structures</p>	<p>Learn from partially labeled data or through interaction with environment</p>
Classification      Regression	Clustering      Dimensional reduction	Reinforcement learning      Generative approaches
<i>Logistic regression</i> <i>Classification trees</i> <i>Random forests</i> <i>Neural networks</i> <i>Support vector machines</i>	<i>Gaussian mixture models</i> <i>K-means</i> <i>Mean shift</i> <i>Spectral clustering</i>	<i>Q-learning</i> <i>State-action-reward-state-action</i> <i>Deep Q-learning</i> <i>Deep deterministic policy gradient</i>
<i>Linear regression</i> <i>Regression trees</i> <i>Random forests</i> <i>Neural networks</i> <i>Gaussian processes</i>	<i>Principal component analysis</i> <i>Factor analysis</i> <i>Autoencoder</i> <i>Stochastic neighbor embedding</i>	<i>Generative adversarial network</i> <i>Variational autodecoders</i> <i>Boltzmann machine</i>
Applications	Applications	Applications
- Representation of fuel properties, thermochemical response functions, and potential energy surfaces - Parameterization of combustion manifolds - Prediction of risk occurrence and critical events - Combustion-closure modeling	- Characterization of combustion regimes - Identification of low-dimensional manifolds - Discovery of structures and coherent features - Detection of anomalies and faults - Signal processing	- Optimization and control of combustion systems - Data augmentation and data generation - Generative combustion modeling - Robust combustion modeling - Operation with incomplete data

# Data in combustion science and engineering



## Challenges

Sparse data (limited to specific operating conditions, fuels, and geometries)

Lack of data for complex combustion conditions

Data accessibility

Ihme, Chung, and Mishra, Prog. Energy Combust. Sci. 91, 101010, 2022

5

## Combustion ML Tasks

- Accelerate combustion simulations and experimental analysis
- Create knowledge and gain physical insight
- Formulate hybrid closures for improved fidelity simulations
- Develop reduced-order models and digital twins

# Combustion ML Tasks

## ML for experimental analysis

- Physical understanding
- Discovery of structures, combustion regime, and coherent features
- Construction of low-order models for control-oriented applications
- Data-generation

## ML for combustion modeling

- Parameterization of combustion manifolds
- Data augmentation and data generation
- Combustion-closure models
- Physical embedding to reduce computational cost

## ML for combustion modeling



# ML for combustion-model closure and accelerating simulations

- Stelios Rigopoulos
- Cheng Chi, Dominique Thevenin
- Hong Im
- Shashank Yellapantula
- Zhuyin Ren
- Jackie Chen [presentation]
- JenZen Ho [presentation]

Accelerating combustion simulations

Identification and parameterization of combustion manifolds

Model developments

Combustion regime Classification

Uncertainty quantification

9



Imperial College  
London

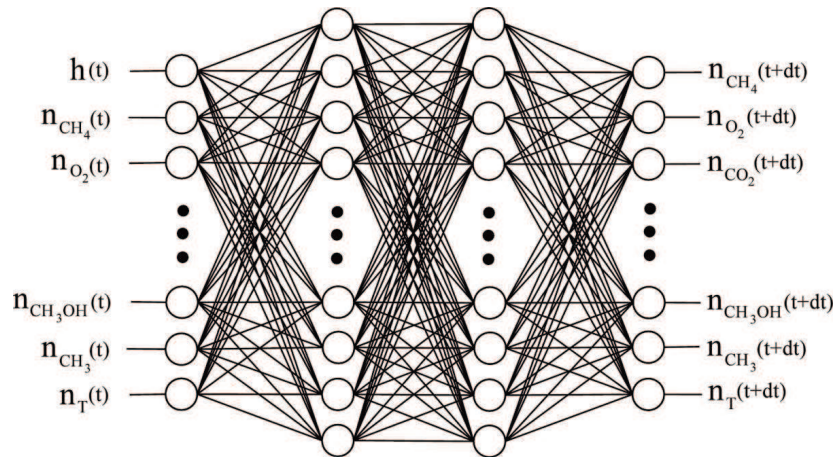
## Machine Learning Tabulation of Chemical Kinetics for Turbulent Combustion Simulations

Stelios Rigopoulos, Thomas Readshaw,  
Tianjie Ding, William P. Jones



## ANN Tabulation of Chemical Kinetics

- Real-time integration of chemical kinetics can consume the majority of the required computational time in many methods for reacting flow simulation, including:
- ANNs are trained with an abstract problem and attain generalization sufficient for application to families of turbulent flames



11

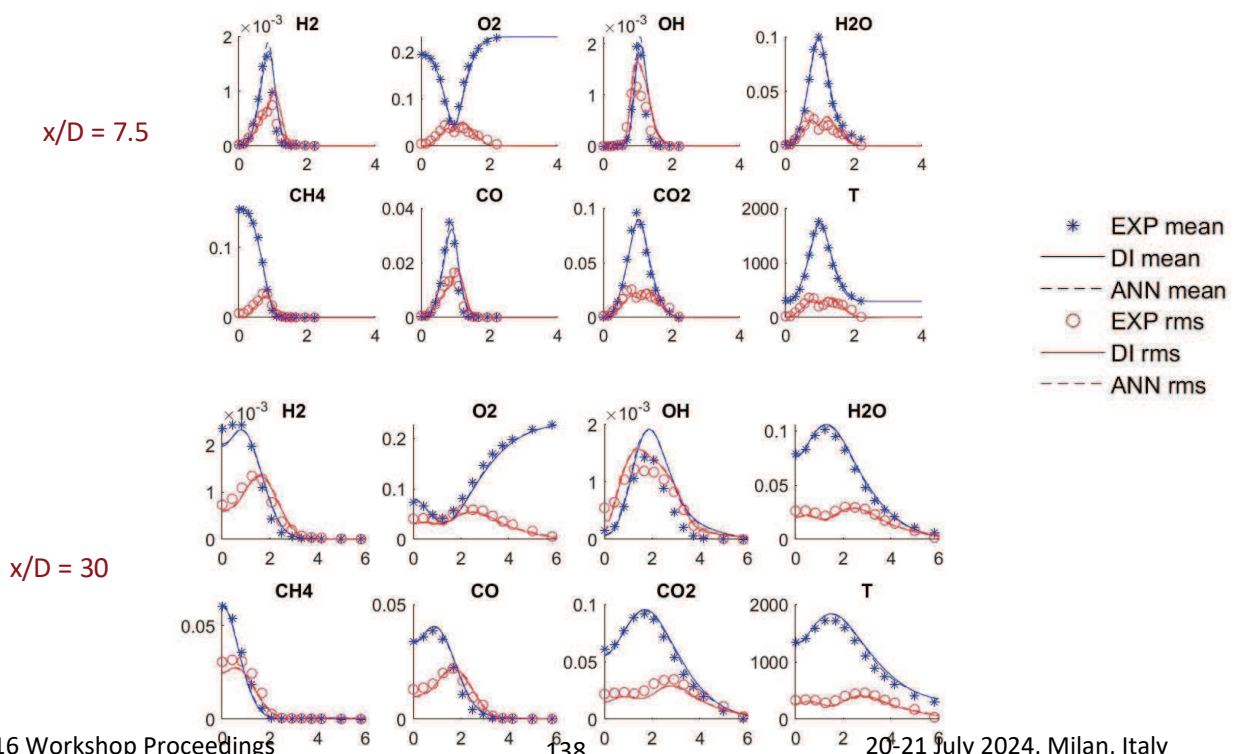
Case study	Single species MLPs	HFRD	Dataset origin	MMLP	Element cons.	Main objective / feature
Laminar flamelets	X	X	flamelet	X		Whole range of strain rates
1D premixed flames	X	X	flamelet	X		Premixed flames, whole range of equiv. ratios, differential diffusion
Sandia flames D-F	X	X	flamelet	X		Turbulent diffusion flames, local extinction
Sydney flame L	X	X	flamelet			Single vs. multiple species MLPs
Sydney flame HM1	X	X	flamelet	X		Varying fuel composition, heat loss
Cambridge/Sandia Swirl Burner, cases 5-6	X	X	premixed	X		Turbulent premixed flame (stratified)
1D premixed flames (CH <sub>4</sub> , C <sub>3</sub> H <sub>8</sub> )	X	X	premixed		X	Test element conservation method
Sydney swirl flame SMA2	X	X	flamelet	X		NO <sub>x</sub> prediction, recirculation
Sandia DME flames	X	X	flamelet	X		Biofuel

# Case 1: Sandia flames D-F

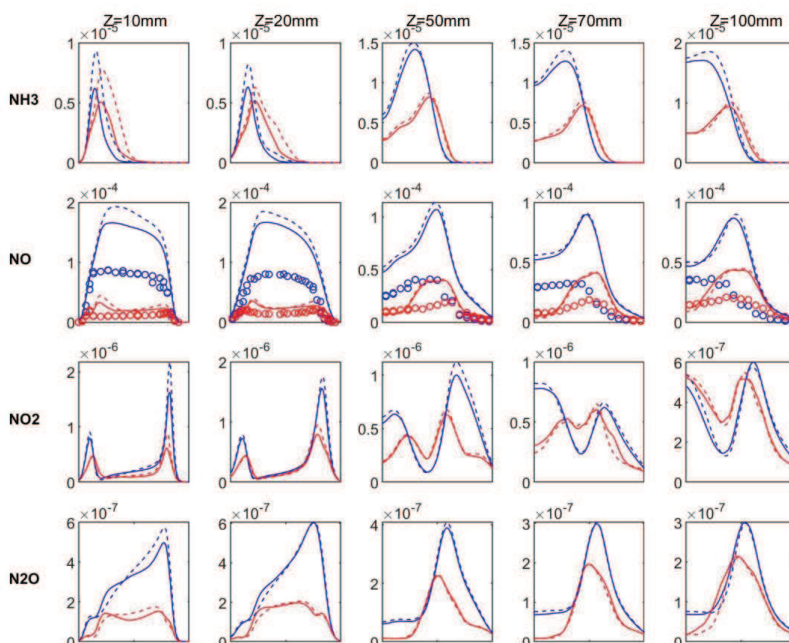
Flame and simulation details:

- Partially-premixed, piloted turbulent CH<sub>4</sub>/Air flame.
- LES-PDF simulation, 8 stochastic fields, 3 million cells,  $\Delta t = 1\mu s$ .
- Full GRI 1.2 mechanism, 31 species
- ANNs vs VODE solver

## Sandia D



### Case 3: Bluff body swirl flame SMA2 (NO<sub>x</sub> formation)



Speed-up ratio for the reaction step ranging from 12x – 56x, depending on size and stiffness of the mechanism, complexity of ANN architecture and method elements involved (MMLP, element conservation)

15



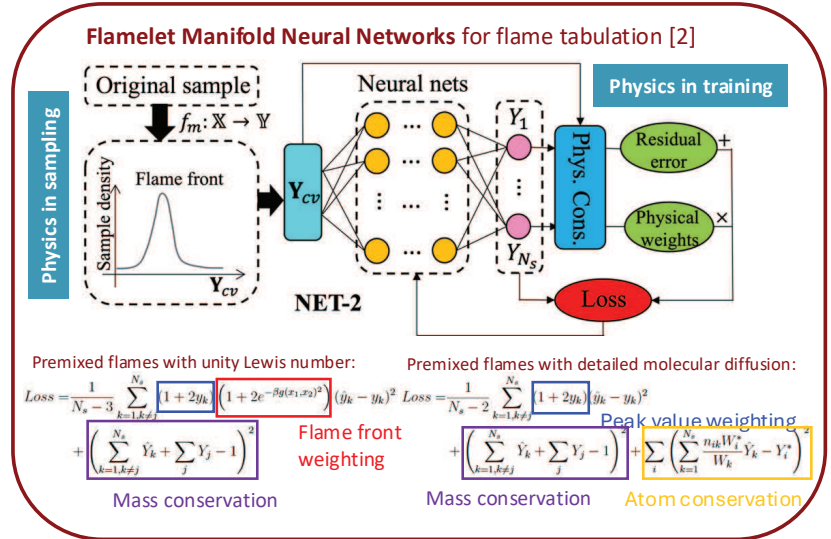
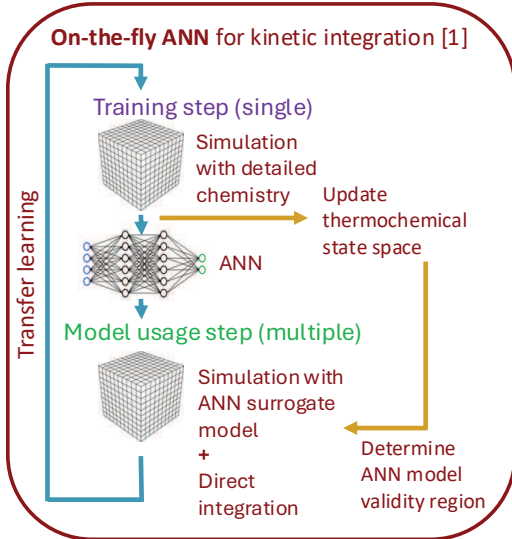
Scientific machine learning for combustion simulation acceleration, model development, and combustion modes classification

Cheng Chi, Dominique Thevenin

# ML for combustion simulation acceleration

Problems with detailed kinetic mechanism:

- Reduced time step is needed for stiff reactions (ODEs)
- Transport equations increase with species number.



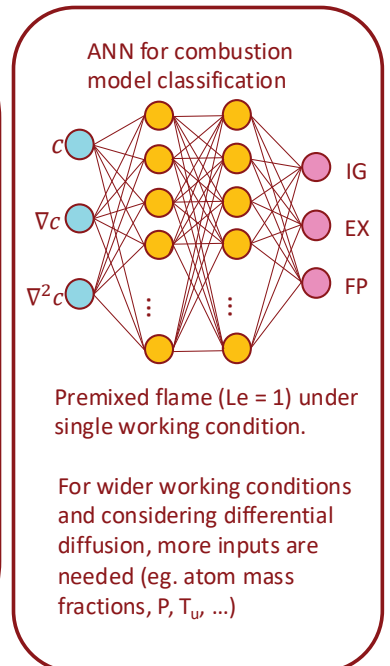
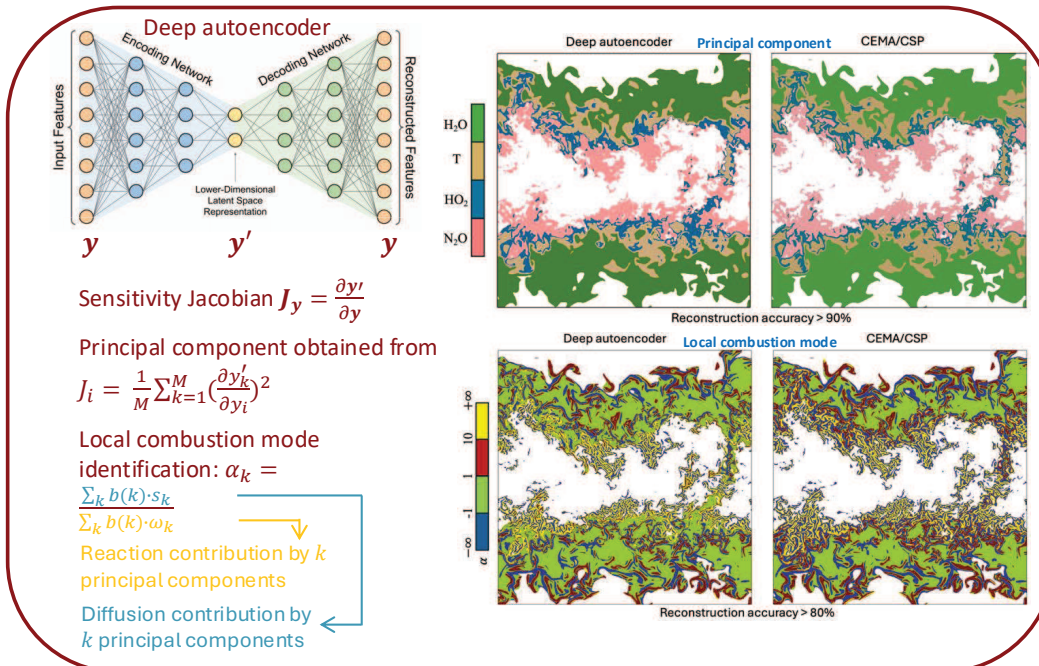
[1] Chi et al., *Combust. Flame* 226 (2021) 467-477.

[2] Chi et al., *Combust. Flame* 245 (2022) 112325.

cheng.chi@ovgu.de

17

# ML for classifying local combustion mode



\* Work in progress



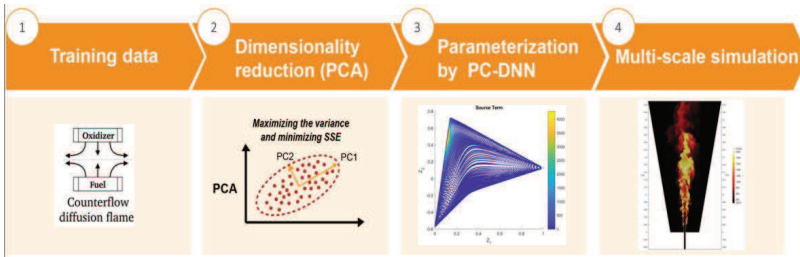
# Construction of Reduced order modeling through ML methods

Hong Im

19

## PCA-DNN for LES Application

- Principal Component Analysis (PCA) allows for identifying the direction of maximum variance in the data



### PC-transport Approach:

$$\frac{\partial}{\partial t}(\rho \mathbf{Y}_k) + \nabla(\rho \mathbf{u} \mathbf{Y}_k) = \nabla(\rho \mathbf{D}_k \nabla \mathbf{Y}_k) + \mathbf{R}_k \quad k = 1, \dots, n_s \quad (\text{ns transport equations})$$

$$\mathbf{Z} = \mathbf{Y} \mathbf{A}_q \quad (q \ll n_s)$$

$$\frac{\partial}{\partial t}(\rho \mathbf{z}) + \nabla(\rho \mathbf{u} \mathbf{z}) = \nabla(\rho \mathbf{D}_z \nabla \mathbf{z}) + \mathbf{s}_z \quad (\text{q transport equations})$$

$\mathbf{A}$  is the basis matrix (ns PCs)  
 $\mathbf{A}_q$  is the truncated basis matrix (q PCs)  
 $\mathbf{z}$  principal component scores

J.C. Sutherland and A. Parente, Proc. Combust. Inst., 32 (2009)

## Extended manifold

- To account for the NH<sub>3</sub>/H<sub>2</sub> ratio change

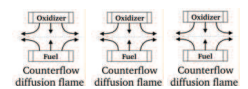
Baseline manifold



Single NH<sub>3</sub>/H<sub>2</sub> ratio (1.716)

NH <sub>3</sub> (Vol.)	H <sub>2</sub> (Vol.)	N <sub>2</sub> (Vol.)
0.563	0.328	0.109

Extended manifold



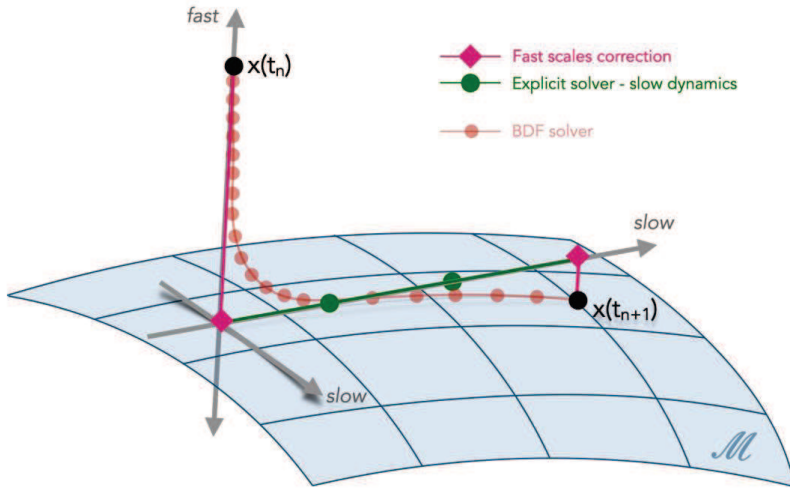
Different NH<sub>3</sub>/H<sub>2</sub> ratios (1.716, 1.802, and 1.886)

- Only 2 PCs are required in the extended manifold as well



# The CSP Solver: Principles

## Physics-based adaptive solver (CSP)



local ROM free of fast scales

explicit integration with large time steps

system evolves on a slow manifold

...but projection basis requires the eigensystem of Jacobian

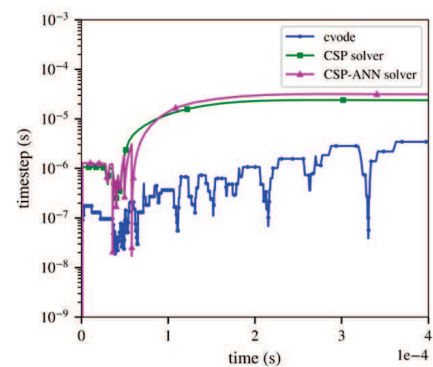
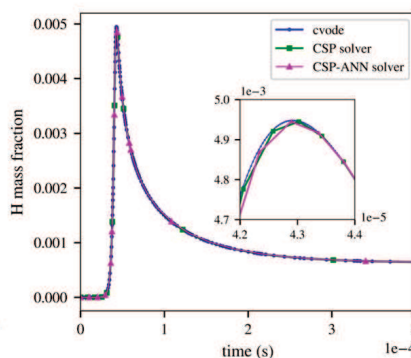
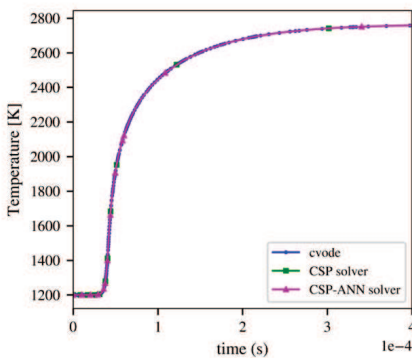
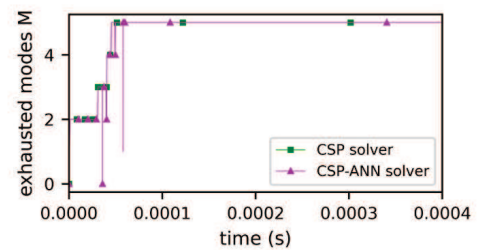
expensive if N is large

Malpica Galassi et al., 2022, J. Comp. Phys., 451, 110875

21

# CSP-ANN solver

- ANN used to retrieve the Jacobian eigenvectors
- Integration accuracy is high
- Only the slow dynamics is resolved
- $M$  represents the adaptivity (how many fast scales, locally)
- Timesteps are larger compared to CVODE



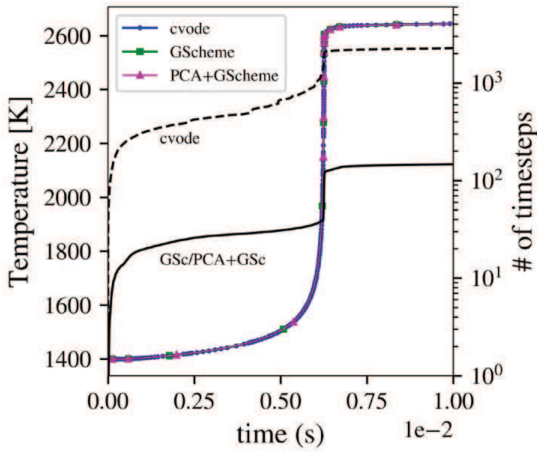
22

Malpica Galassi et al., 2022, J. Comp. Phys., 451, 110875

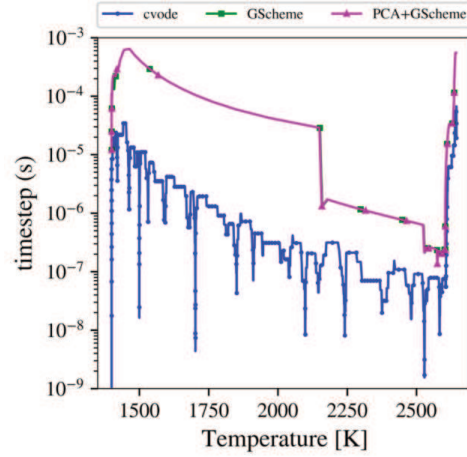
# Combined CSP-PCA Solver – Latent Jacobian

Homogeneous reactor, NH<sub>3</sub> (36 species mechanism)

Full system: N = 37 (species + T)  
Latent system: q = 27 (PCA scores)



PCA/G-Scheme is accurate despite not explicitly resolving the fast/slow scales and the PCA truncation error.



Two orders-of-magnitude improvement in time step size, absence of initialization overhead.

Malik et al., 2024, 40th PROCI, PPP (M08)

23≈

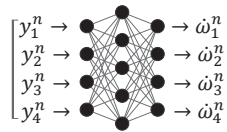
# Neural ODE for stiff chemical kinetics

Neural ODE for chemical kinetics:

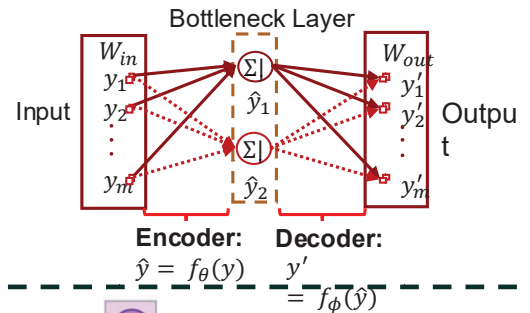
$$\frac{dy(t)}{dt} = \dot{y} = f_{\theta}(y(t), t) = NN(y(t))$$

$$y^1, y^2, \dots, y^n = \text{ODE Solve}(y^0, f_{\theta}, t_1, t_2, \dots, t_n)$$

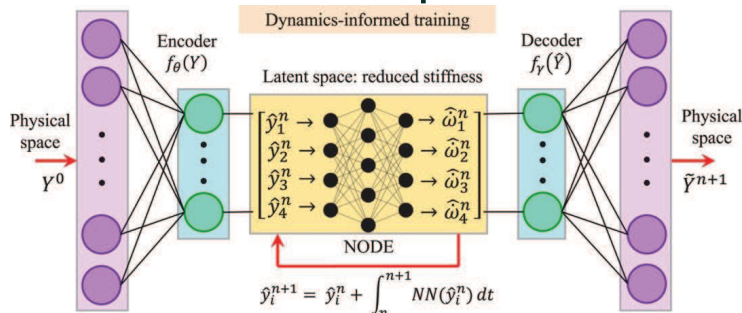
$$y_i^{n+1} = y_i^n + \int_n^{n+1} NN(y_i^n) dt$$



AutoEncoder:



AutoEncoder + Neural ODE for chemical kinetics:

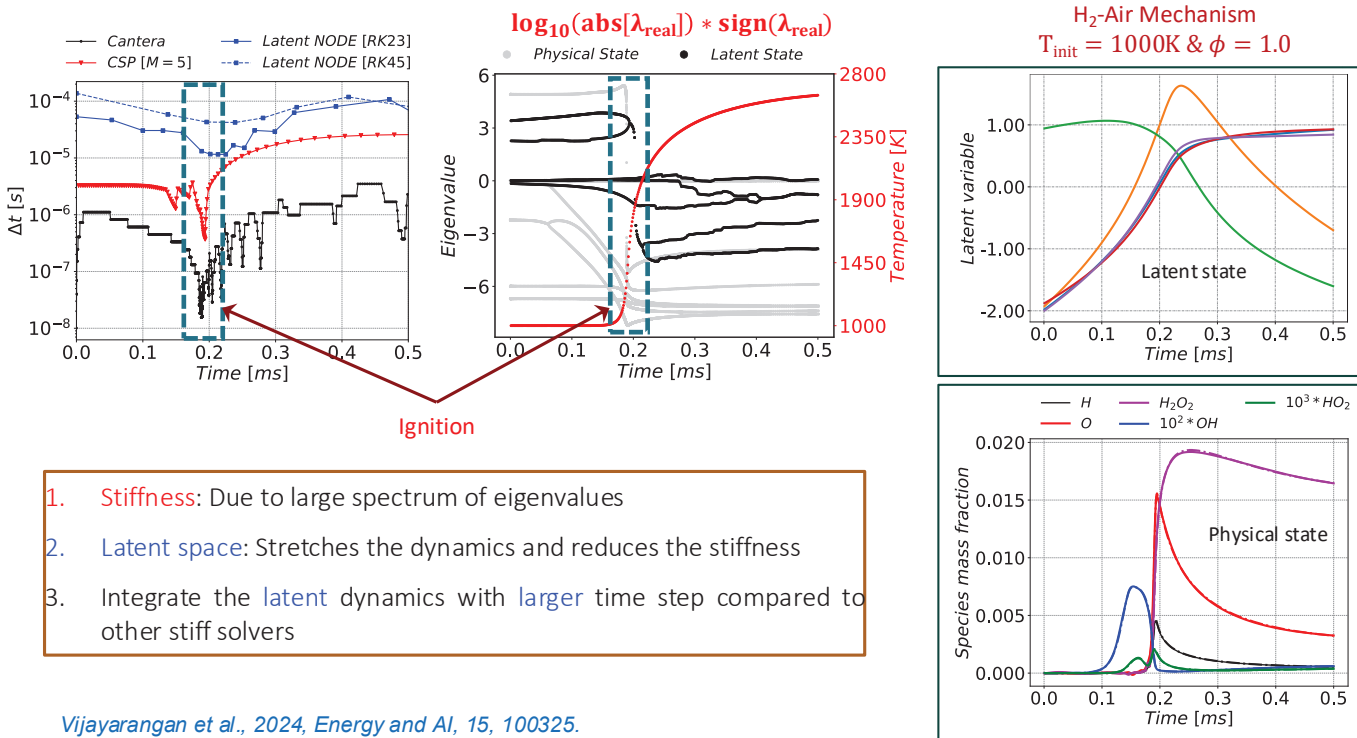


$$\mathcal{L} = \epsilon_1 \|Y - \tilde{Y}\|_2^2 + \epsilon_2 \|f_{\phi}(f_{\theta}(Y)) - \tilde{Y}\|_2^2 + \epsilon_3 \|f_{\theta}(Y) - \hat{Y}\|_1$$

24

Vijayarangan et al., 2024, Energy and AI, 15, 100325.

# Stiffness Reduction & Time Step Improvement



25



## Quantifying Uncertainty in ML Combustion Models

Graham Pash, Malik Hassanaly, Bruce Perry, Michael Mueller & Shashank Yellapantula

# Progress Variable Dissipation Model

- Unresolved progress variable dissipation rate

$$\tilde{\chi}_{C,sgs} = 2D_C \overline{|\nabla \tilde{C}|^2} - 2\tilde{D}_C |\nabla \tilde{C}|^2$$

- Sink term in  $C_{var}$  equation
- Parameterizes strain in some strained FGM models

- Simple “linear relaxation” models are inaccurate for reacting flows;  $\tilde{\chi}_{C,sgs} = c_\chi |\tilde{S}| C_{var}$

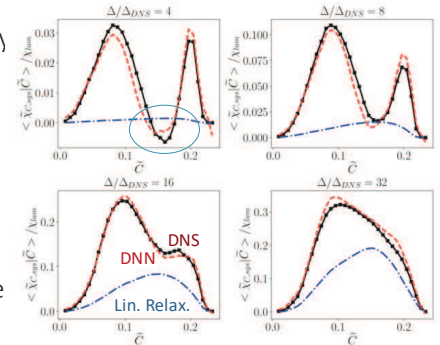
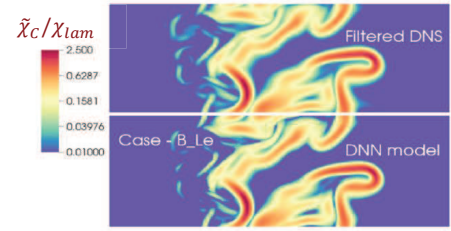
- Approach [1]: use a deep neural network to regress  $\tilde{\chi}_{C,sgs}$  against known physically important inputs:

$$\tilde{\chi}_{C,sgs} = \text{DNN}(\tilde{C}, C_{var}, \tilde{D}_C, 2D_C \overline{|\nabla \tilde{C}|^2}, |\nabla \tilde{C}|^2, \alpha, \beta, \gamma, \dots)$$

- Data from filtered DNS of planar premixed flames at varied Ka [2]

- DNN provides robust predictions across conditions and fuels in a-priori tests**

- Even correctly predicting negative values that are impossible in physical mode



[1] S. Yellapantula, B. A. Perry, R. W. Grout. *Proceedings of the Combustion Institute* 38 (2020) 2929-2938.

[2] B. Savard, G. Blanquart, *Combustion and Flame* 180 (2017) 77-87.

# Progress Variable Dissipation Model

- Unresolved progress variable dissipation rate

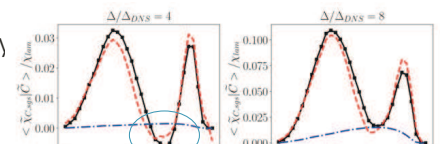
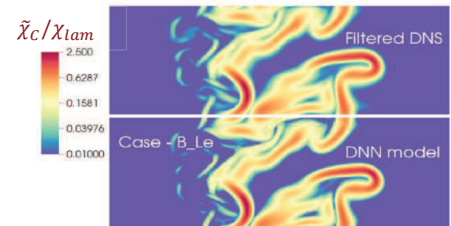
$$\tilde{\chi}_{C,sgs} = 2D_C \overline{|\nabla \tilde{C}|^2} - 2\tilde{D}_C |\nabla \tilde{C}|^2$$

- Sink term in  $C_{var}$  equation
- Parameterizes strain in some strained FGM models

- Simple “linear relaxation” models are inaccurate for reacting flows;  $\tilde{\chi}_{C,sgs} = c_\chi |\tilde{S}| C_{var}$

- Approach [1]: use a deep neural network to regress  $\tilde{\chi}_{C,sgs}$  against known physically important inputs:

$$\tilde{\chi}_{C,sgs} = \text{DNN}(\tilde{C}, C_{var}, \tilde{D}_C, 2D_C \overline{|\nabla \tilde{C}|^2}, |\nabla \tilde{C}|^2, \alpha, \beta, \gamma, \dots)$$



1. How universal is this model across regimes & fuels

2. Can we quantify uncertainty in the predictions made by this ML model?

3. How do we propagate this uncertainty through forward reacting flow simulations?

[1] S. Yellapantula, B. A. Perry, R. W. Grout. *Proceedings of the Combustion Institute* 38 (2020) 2929-2938.

[2] B. Savard, G. Blanquart, *Combustion and Flame* 180 (2017) 77-87.

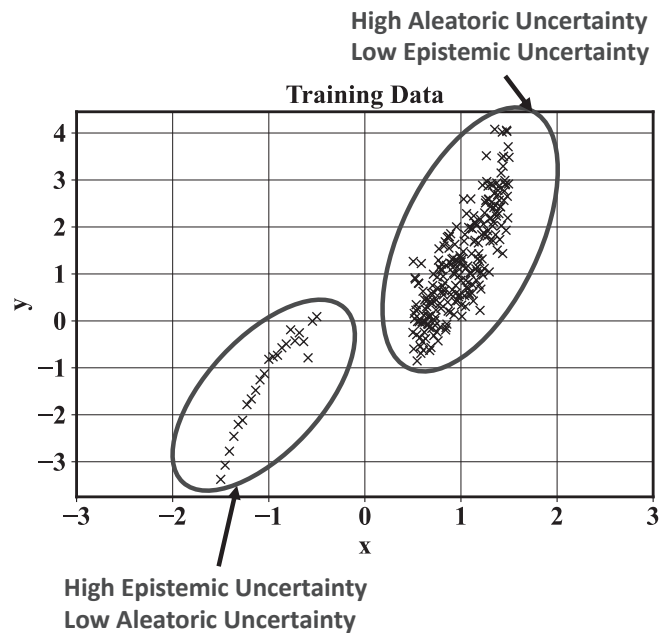
# Forms of Uncertainty

## Epistemic

- Reducible with additional data
- DNS data availability in phase space
- Extrapolatory uncertainty

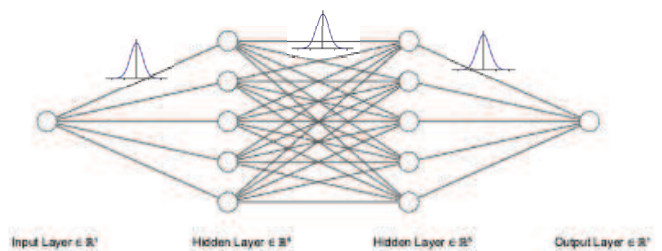
## Aleatoric

- Irreducible with additional data
- Dependent on model features that we include
- Influenced by coarse-graining/filtering

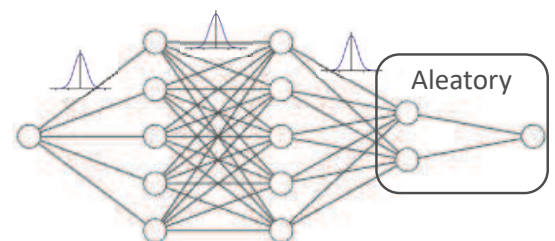


# Bayesian Neural Network (BNN)

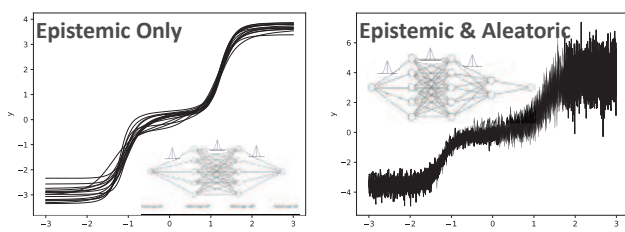
- Typically, Gaussian processes modeling is used
  1. Intractable  $\mathcal{O}(n^3)$  training and  $\mathcal{O}(n^2)$  prediction
- Bayesian neural networks (BNNs) are an attractive alternative
  1. Flexible model form
  2. Training amenable to big data regime
  3. Quick to evaluate on-line



BNN modeling *epistemic* uncertainty.



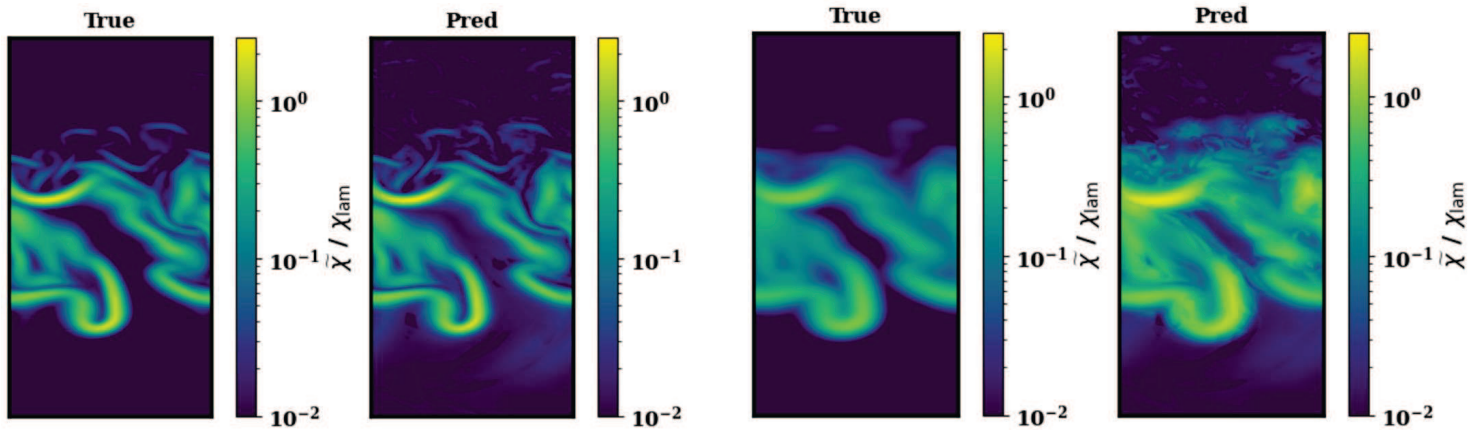
BNN modeling *epistemic* and *aleatoric* uncertainty.





# Results – Physical Space

Lower Karlovitz Number Flame

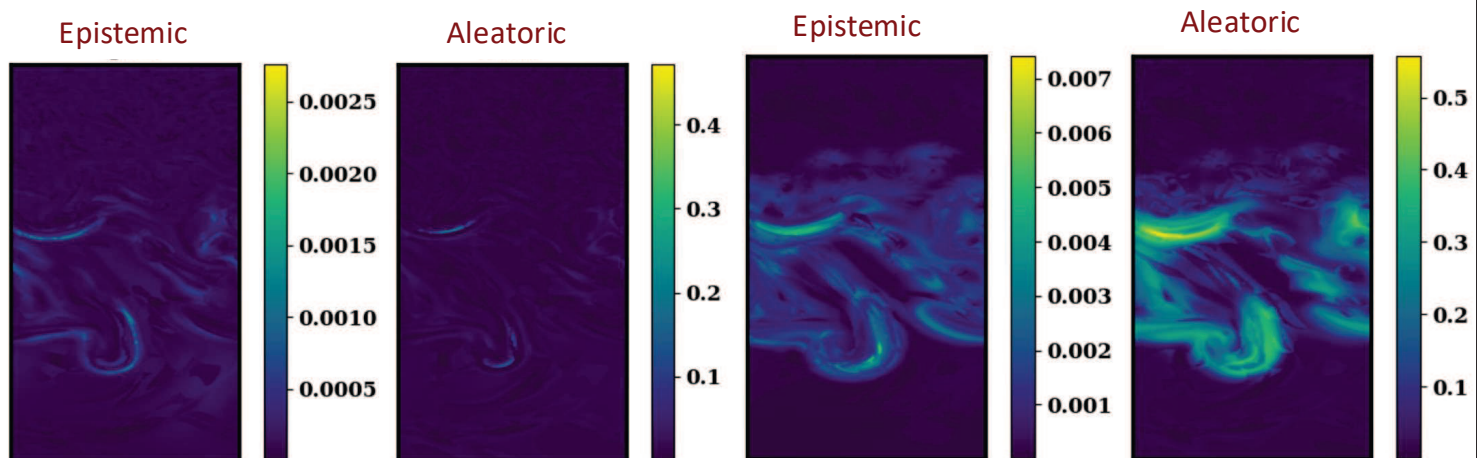


Filter width =  $4 \Delta_{DNS}$

Filter width =  $16 \Delta_{DNS}$

# Results – Physical Space

Lower Karlovitz Number Flame



Filter width =  $4 \Delta_{DNS}$

Filter width =  $16 \Delta_{DNS}$

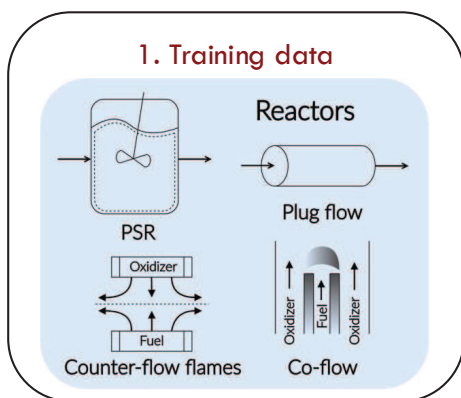
1. Higher Uncertainty at larger filter widths
2. Higher Epistemic and Aleatoric uncertainty for higher Karlovitz number flames

# Augmenting filtered flame front displacement models for LES using machine learning with a posteriori simulations

Kamila Zdybał, James Sutherland,  
Alessandro Parente

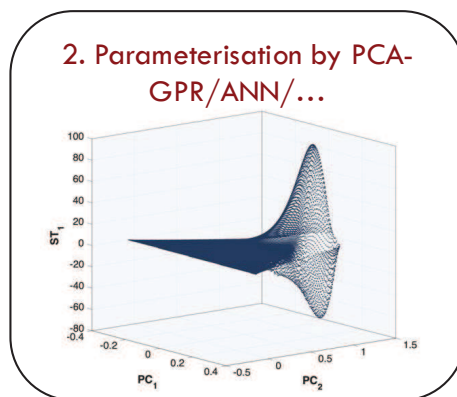
## PC transport framework

### 1. Training data

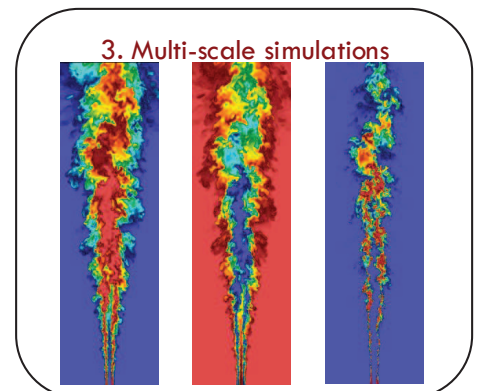


Cheap function evaluations

### 2. Parameterisation by PCA-GPR/ANN/...

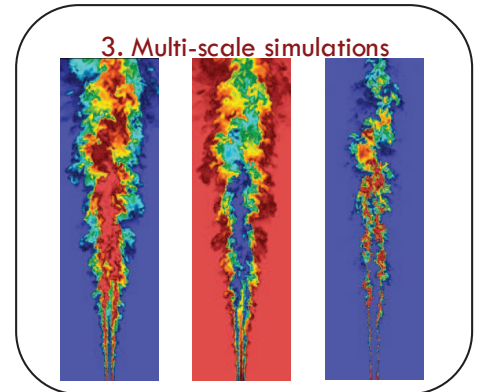
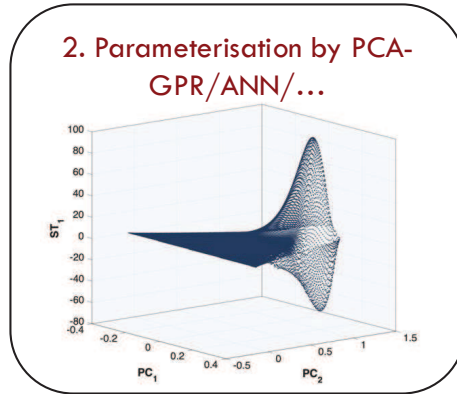
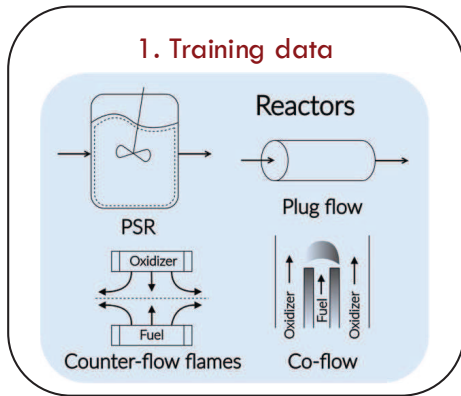


### 3. Multi-scale simulations



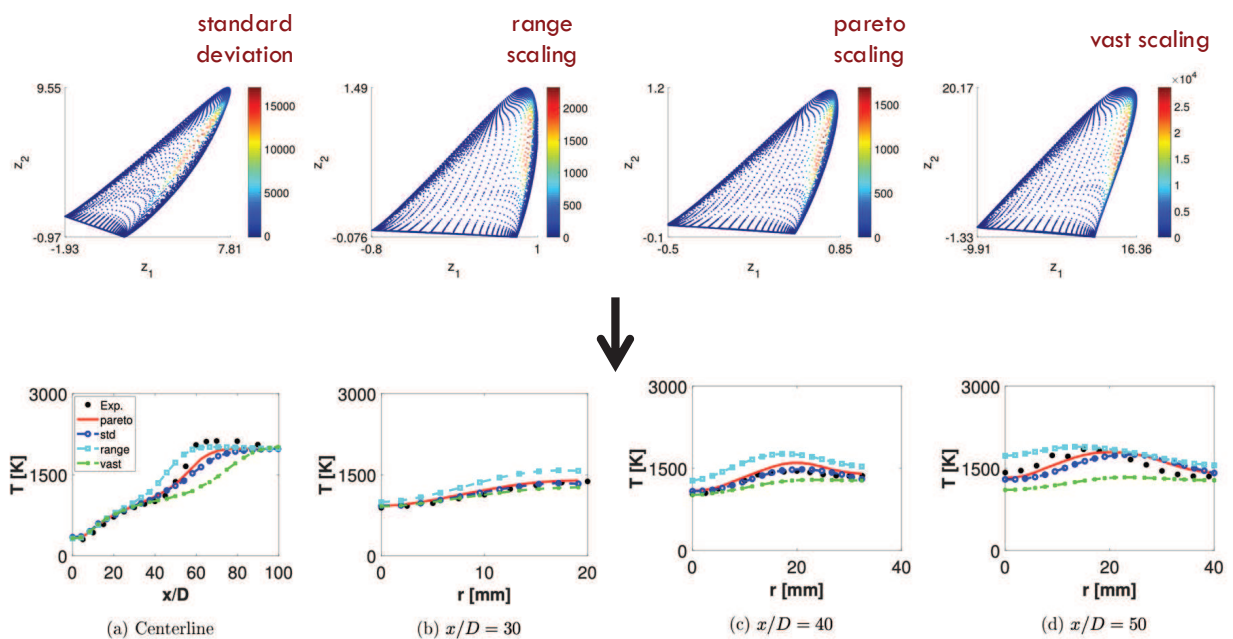
Expensive function evaluations

# PC transport framework

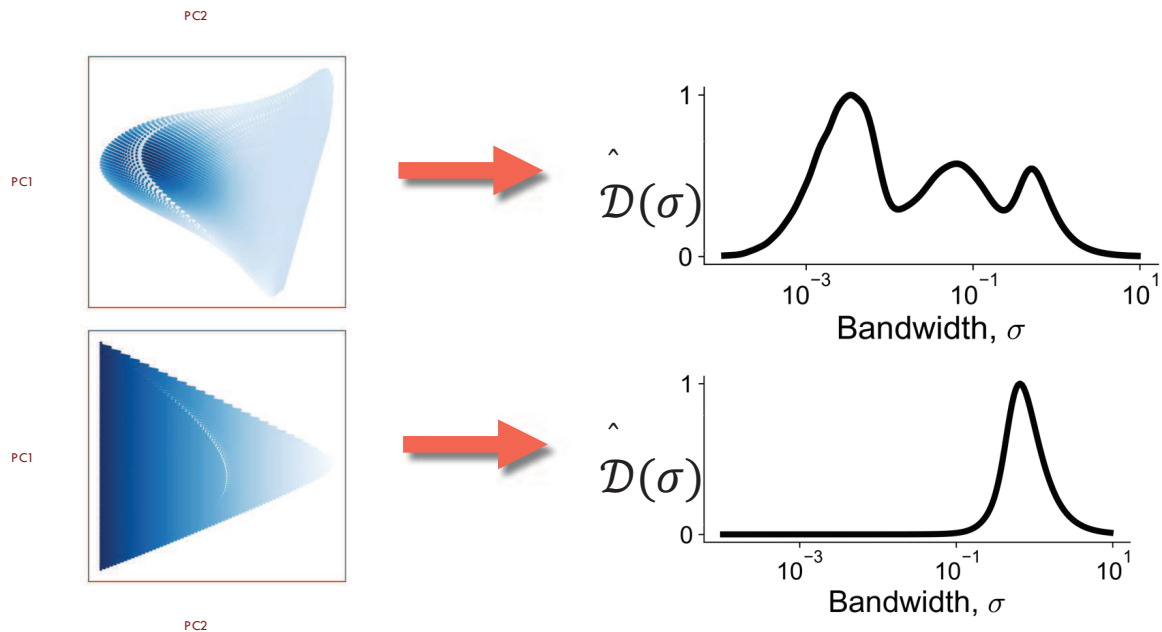


The quality of the manifold is key

The manifold changes significantly with the scaling, and so the results



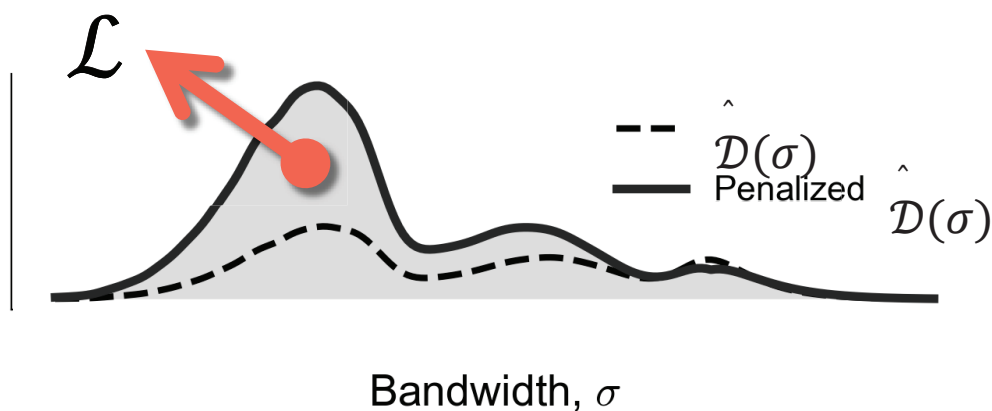
# How can we assess the quality of the manifold $\alpha$ priori?



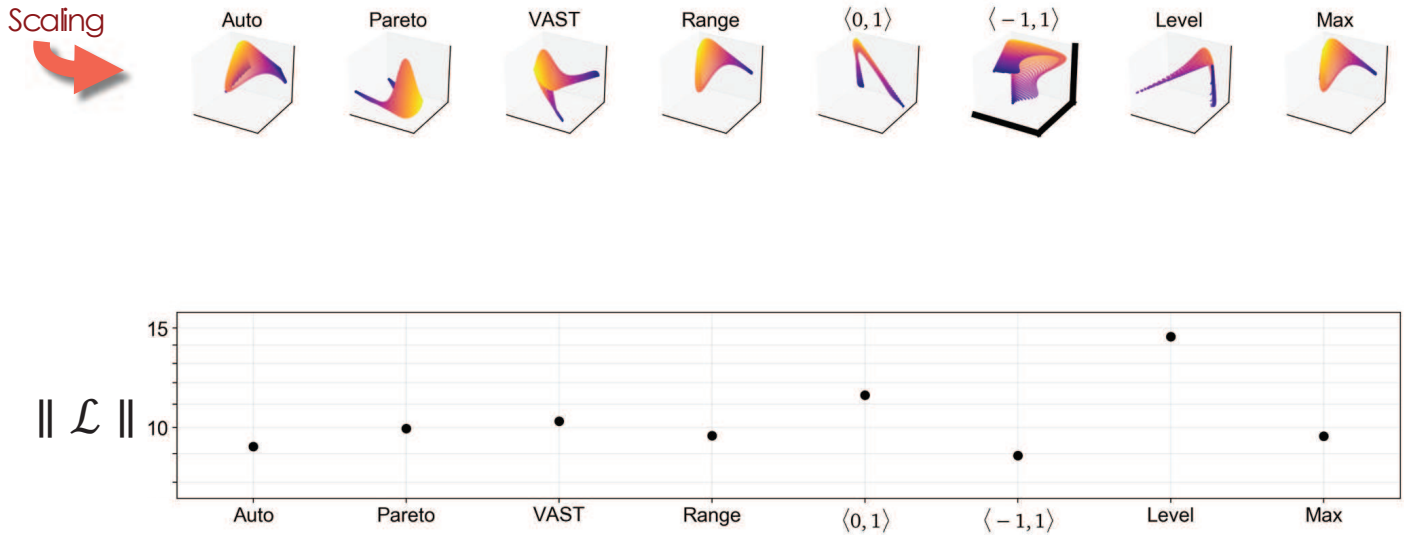
E. Armstrong, J.C. Sutherland, CTM 25 (2021) 646-668

37

We have constructed a cost function based on integrating the penalized  $\hat{\mathcal{D}}(\sigma)$  curve

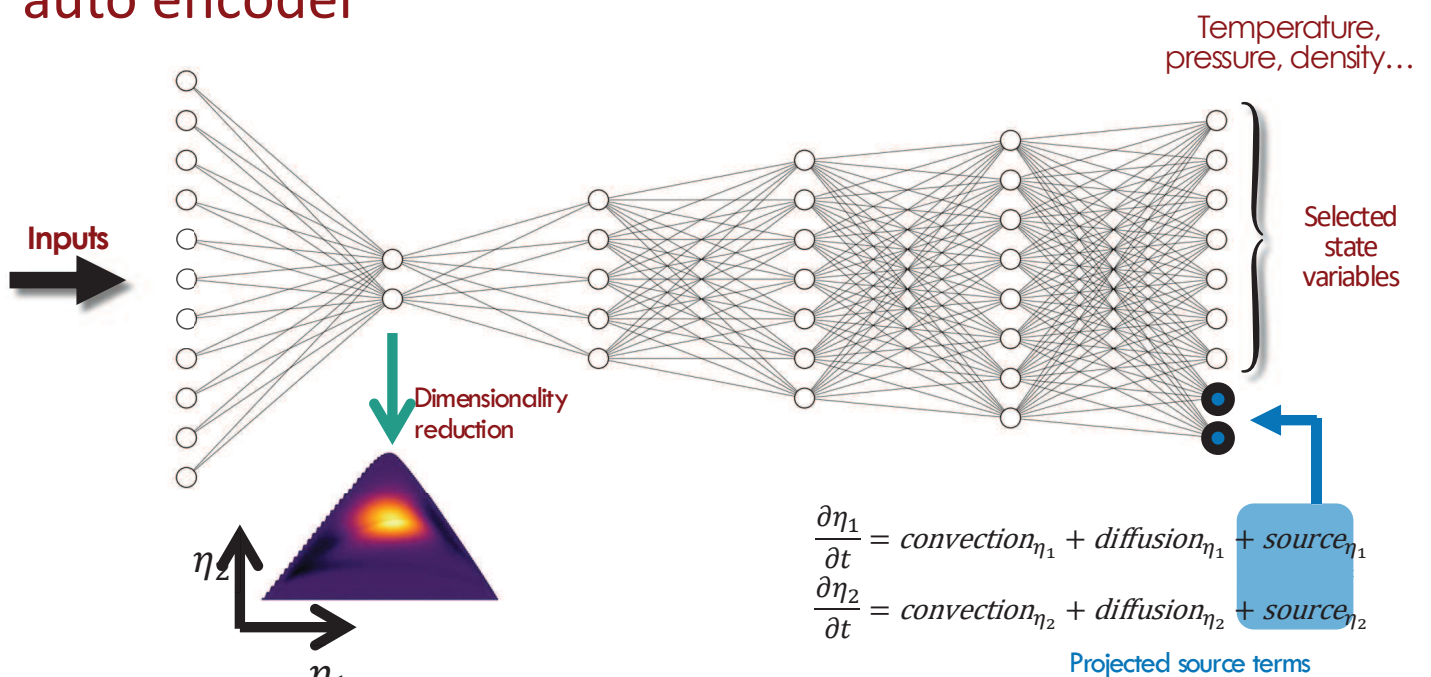


# A priori assessment of the effect of scaling on manifold quality



39

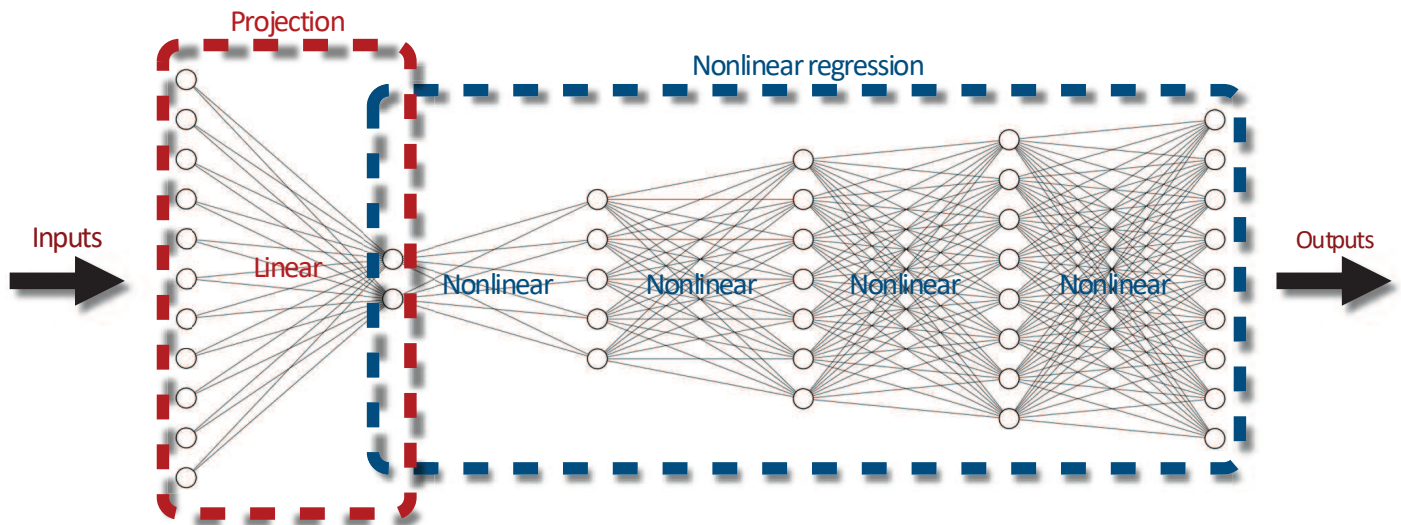
# We can build QoI-aware projections using a QoI-aware auto encoder



K. Zdybal, A. Parente, J.C. Sutherland, Patterns 11 (2023) 100859.

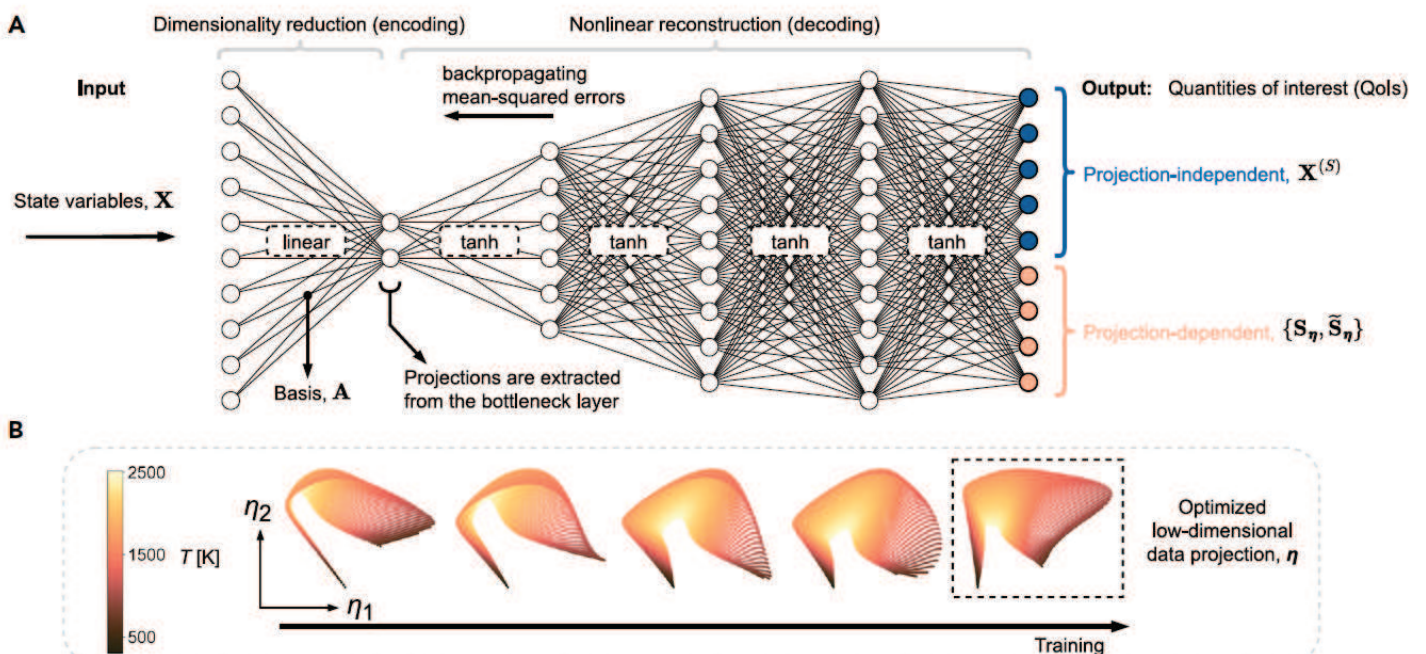


# The combination of linear and non-linear projections results in “better” manifolds

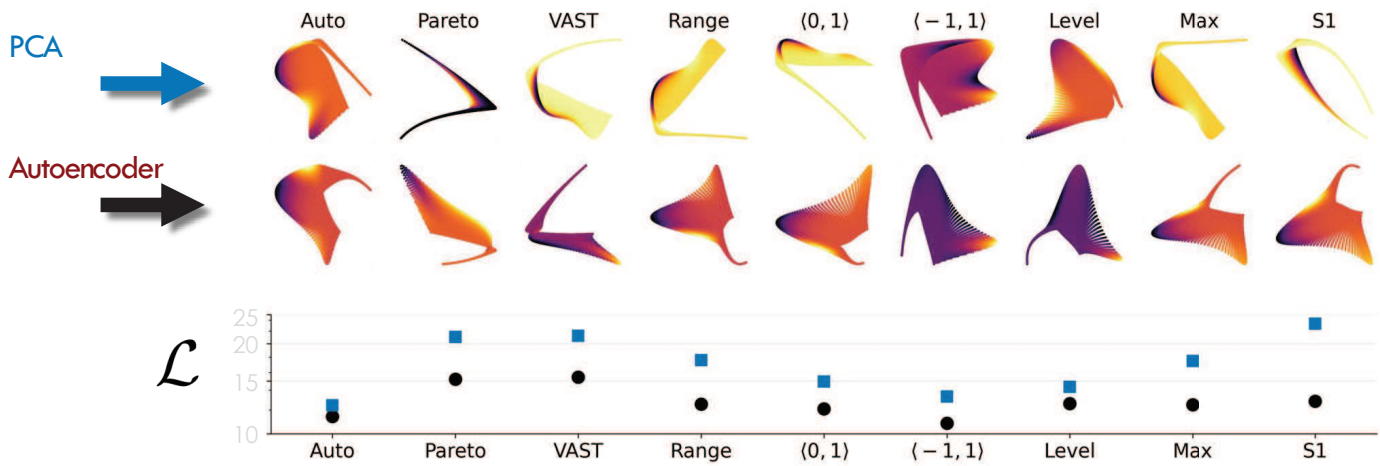


41

# The combination of linear and non-linear projections results in “better” manifolds

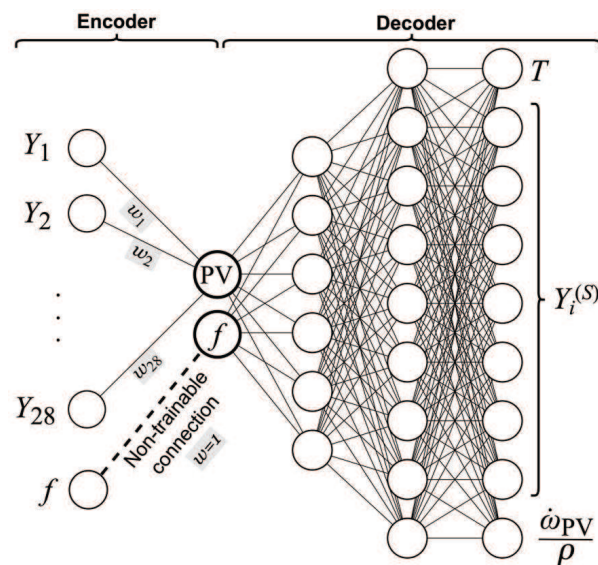


# The auto-encoder projections show higher quality compared to PCA-based ones

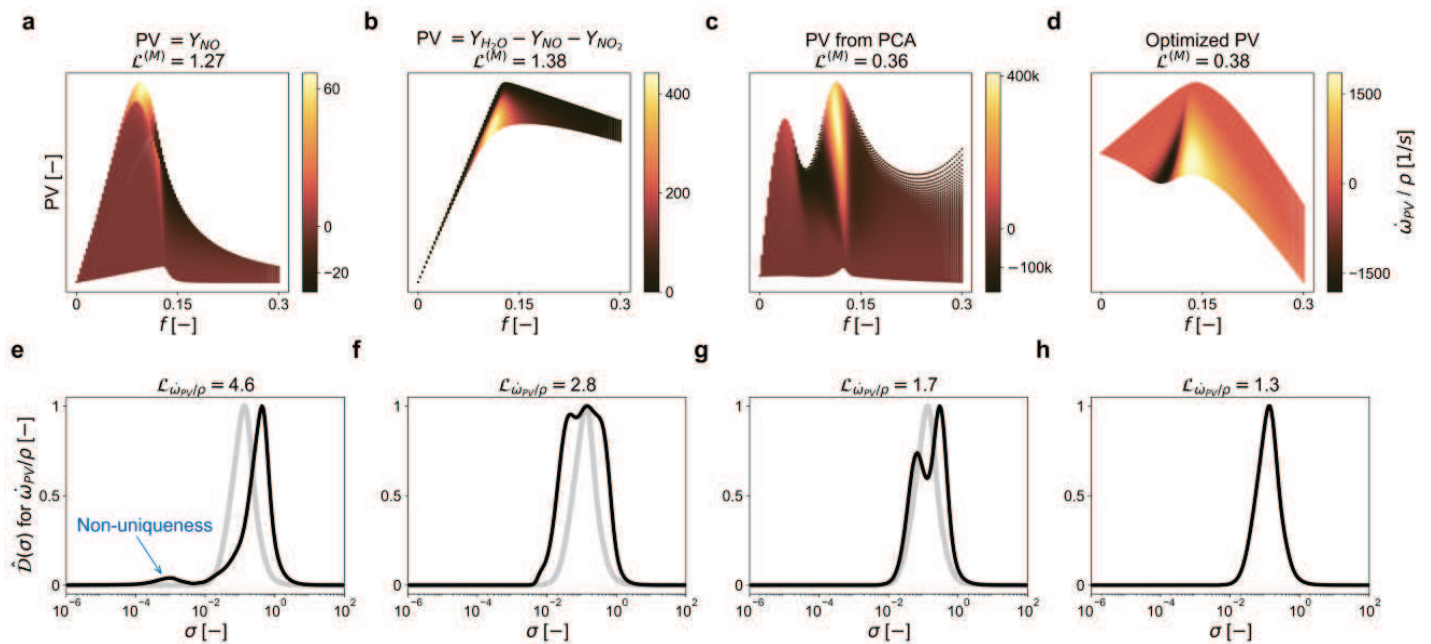


43

# The QoI-aware autoencoder shows potential for optimal PV definition, variable selection, ...



# The QoI-aware autoencoder shows potential for optimal PV definition, variable selection, ...



45



## Accelerating DNS of reacting flows with on-the-fly ROM: time-dependent bases with CUR decomposition (TDB-CUR)

Jackie Chen, Kisung Jung, Cristian Lacey, Hessam Babaei

# Augmenting filtered flame front displacement models for LES using machine learning with a posteriori simulations

Jen Zen Ho, Mohsen Talei, Davy Brouzet,  
Wai Tong Chung, Pushan Sharma,  
Matthias Ihme

47



## FFFD Fundamentals

For LES, the filtered transport equation for  $c$  can be written as:

$$\frac{D(\bar{\rho}\tilde{c})}{Dt} + \nabla \cdot (\bar{\rho}\tilde{\mathbf{u}}\tilde{c} - \bar{\rho}\tilde{u}\tilde{c}) = \bar{\omega}_c + \nabla \cdot \overline{\rho D_c \nabla c},$$

The RHS is modelled by the Filtered Flame Front Displacement (FFFD) term:

$$\begin{aligned} \bar{\omega}_c + \nabla \cdot \overline{\rho D_c \nabla c} &= \overline{\rho s_d |\nabla c|} \\ &= \overline{(\rho s_d)_s |\nabla c|} \end{aligned}$$

For algebraic models of FSD,  $\overline{|\nabla c|}$ , we model FSD using wrinkling factor,  $\Xi = \frac{\overline{|\nabla c|}}{|\nabla \tilde{c}|}$ .

Generally,

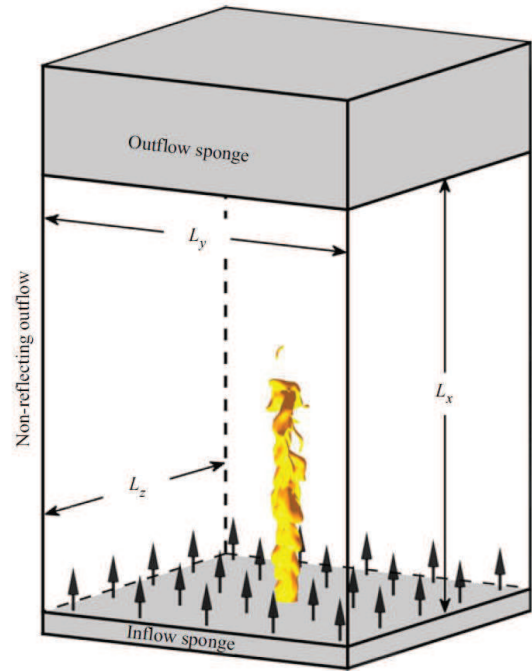
$$\Xi = f(u'_\Delta, \Delta).$$





## Methods

- A turbulent jet case with  $Re = 5,300$  [1] was filtered using a Gaussian filter with  $\Delta = [0.5, 1.0, 2.0]\delta$ , where  $\delta$  is the thermal flame thickness.
- Dataset: 550 cross-sections through the midplane.
- The models were trained on 0.8 flowthrough times:  $\tau_{ft}$ , worth of data. After  $0.5\tau_{ft}$ ,  $0.2\tau_{ft}$  was used as the testing dataset.
- Only points from  $0.29 < c < 0.68$  were extracted ( $> 50\%$  maximum HRR in 1D) to avoid bias towards the unburned and burnt gas region.



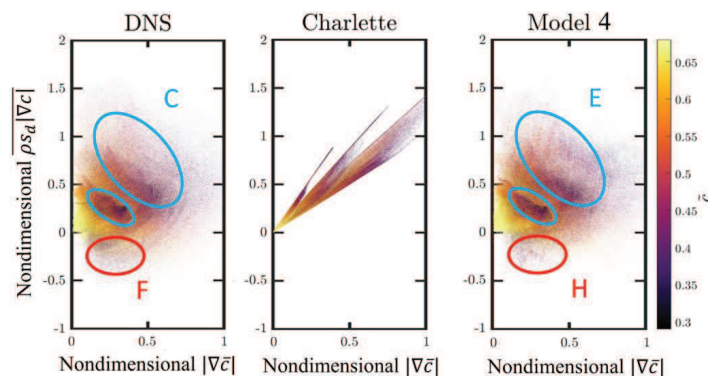
Turbulent jet DNS domain [1].

[1] D. Brouzet, M. Talei, M. Brear, B. Cuenot (2021). The impact of chemical modelling on turbulent premixed flame acoustics, Journal of Fluid Mechanics, 1-33, 915.



## Direct FFFD Modelling

- In FFFD –  $|\nabla\bar{c}| - \bar{c}$  space, Region C (high FFFD and  $|\nabla\bar{c}|$ , low  $\bar{c}$ ) appears from the large spread of  $\rho s_d$ .
- Region F shows that the FFFD can be negative, which cannot be predicted by any FSD model since  $|\nabla\bar{c}| \geq 0$  and  $\rho_u s_L > 0$ .
- Model 4, which uses a random forest ML algorithm to direct model FFFD shows that it is capable of predicting these regions.

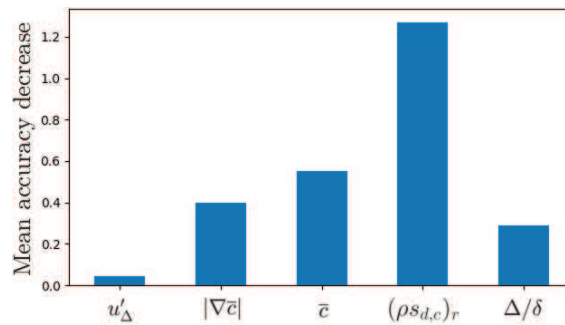






## Importance of variables

- Importance of each variable can be found by randomly permuting a single feature value and finding the decrease in accuracy.
- Resolved curvature term is most important, followed by filtered progress variable,  $|\nabla\bar{c}|$ , filter size, and subgrid turbulence intensity. The top two features are not usually used in algebraic FSD models.

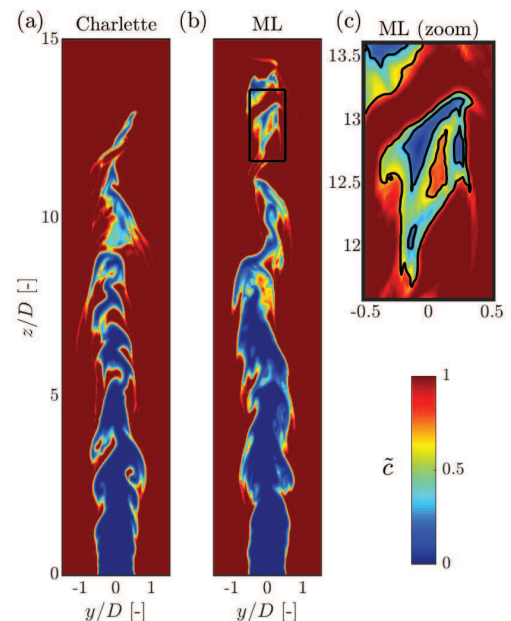


51



## *A posteriori* simulations

- LES of the turbulent jet is run using the ML model for the flame location ( $0.29 < c < 0.68$ ) and Charlette model otherwise.
- Two simulations were run:
  - $\frac{\Delta}{\delta} = 0.125$  (DNS-like)
  - $\frac{\Delta}{\delta} = 0.25$
- Ran for 2 flowthrough times with no stability issues or visible physical inconsistencies.

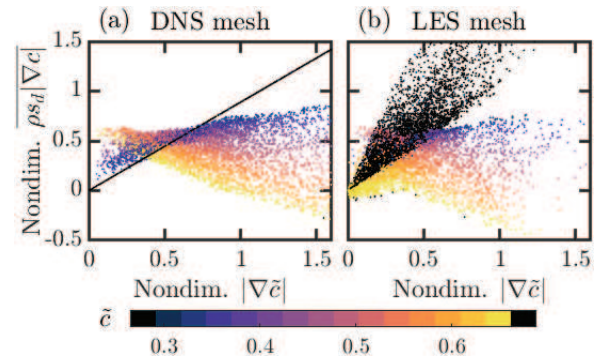


DNS-like mesh results



## A posteriori simulations

- The scatter plot shows the distribution of points in the FFFD -  $|\nabla\tilde{c}|$  space. The black points are the results from the points using Charlette's model.
- ML model predicts lower FFFD for large  $|\nabla\tilde{c}|$  values, and is able to predict the high FFFD, high  $|\nabla\tilde{c}|$ , and low  $\tilde{c}$  region in the *a priori* plots
- However, the negative FFFD regions are less well-predicted and will be the subject of future work.



53



## Conclusions

- ML models have been used to model and study FFFD.
- *A priori* study show
  - The resolved curvature term and  $\bar{c}$  is important
  - Modelling FFFD directly gives a better flame representation in the  $\overline{|\nabla c|} - |\nabla \bar{c}| - \bar{c}$  space.
- *A posteriori* simulations show
  - The ML model trained on predicting FFFD directly preserves the better flame representation in the  $\overline{|\nabla c|} - |\nabla \bar{c}| - \bar{c}$  space, though some discrepancies occur from *a priori* to *a posteriori*.
  - ML models for the combustion source term can be stable even for relatively simple ML models.

## ML for experimental analysis



Stanford University

## Presentation

- ML-methods for experiment analysis
  - Jordan Kildare: Intrinsic flame characteristic encoding through temperature prediction from combustion scalar measurements
  - Fabian Hampp: Transferable and general DNN-based object detection models to segregate signal from background in imaging-based diagnostic data
- Discussion

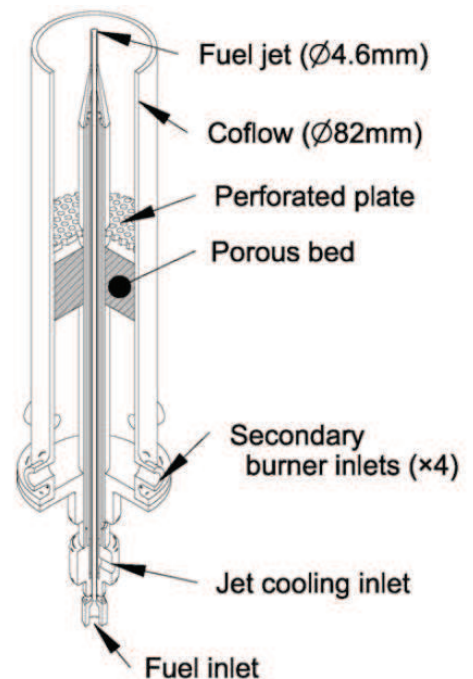
# Intrinsic flame characteristic encoding through temperature prediction from combustion scalar measurements

Jordan Kildare, Paul Medwell, Michael Evans

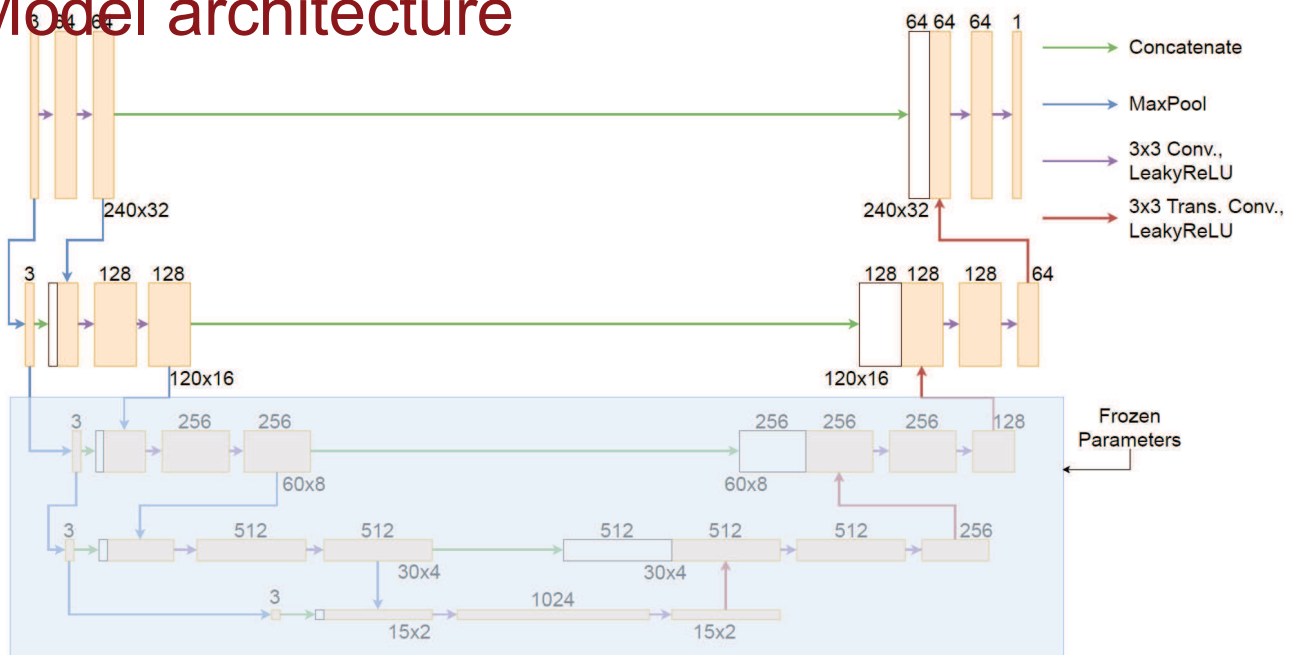
57

## Jet-in-hot-coflow burner

- Subject of numerous studies
  - >35 unique flame conditions
- Emulates recirculation of exhaust gases required to achieve MILD combustion
- Measurements include:
  - OH planar laser-induced fluorescence (PLIF)
  - CH<sub>2</sub>O-PLIF
  - Temperature (via Rayleigh scattering)



# Model architecture



59

# Model details

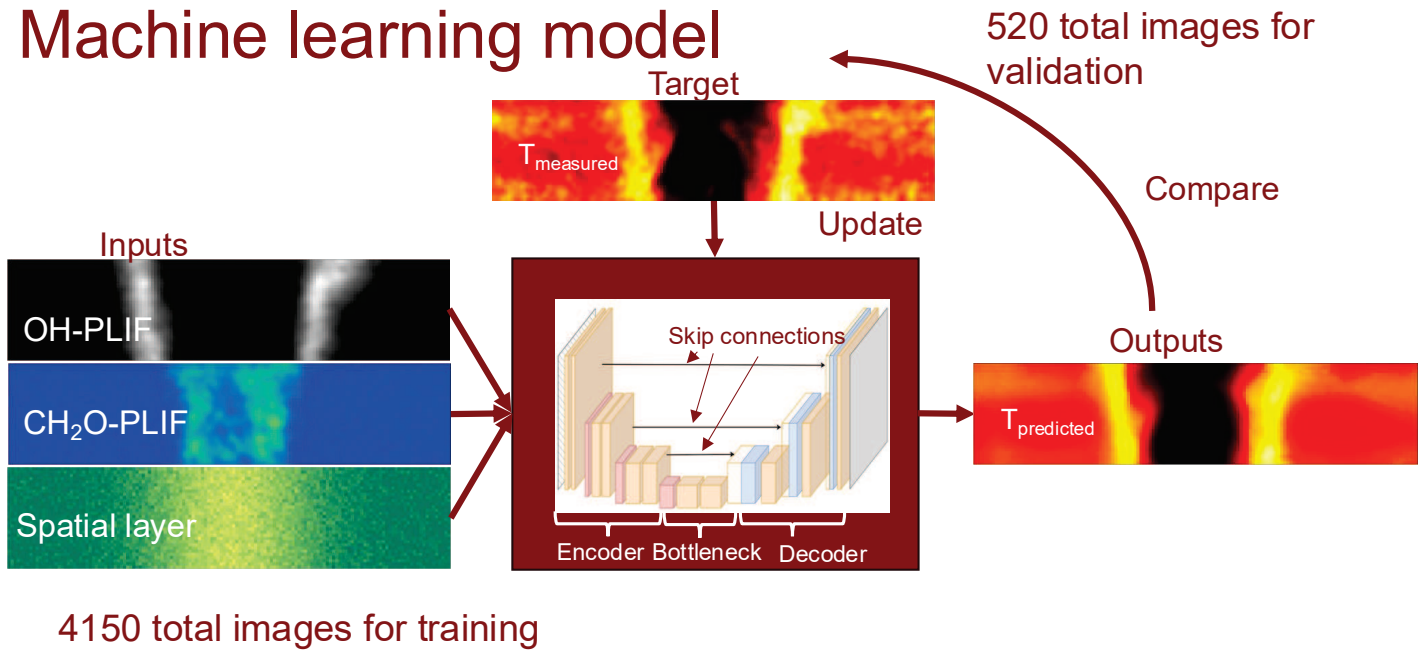
- Multi-scale U-Net architecture
- Leaky rectified linear unit (LeakyReLU) activation functions:

$$L(x) = \begin{cases} x, & x \geq 0 \\ -mx, & x < 0 \end{cases}$$

- Adam optimizer
  - Ideal for attention models
- L2 regularization
  - Reduces over-fitting and increases robustness
- Learning rate scheduling
  - Manages learning rate to ensure convergence

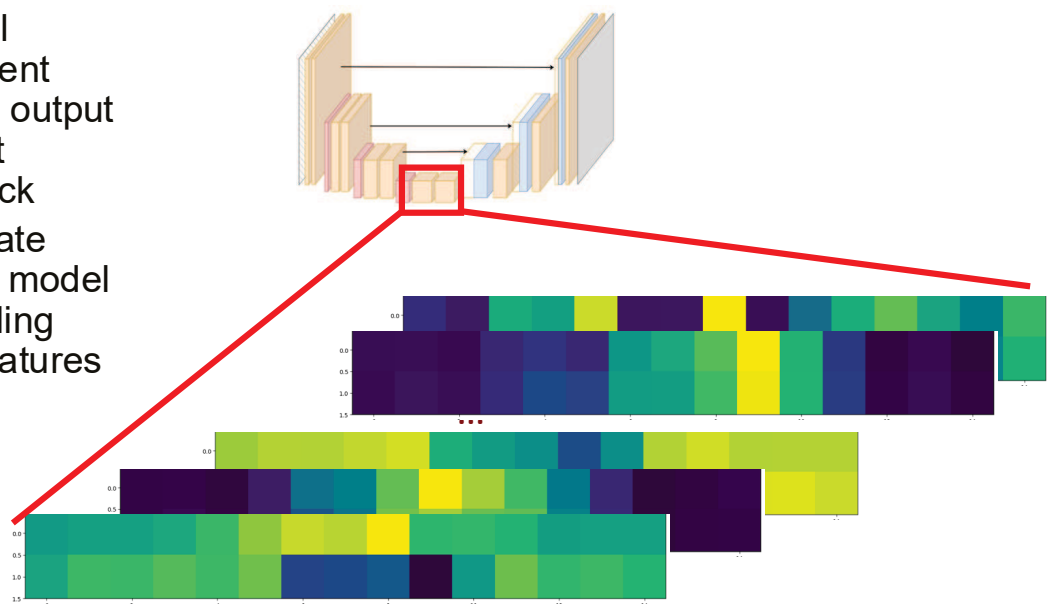


# Machine learning model



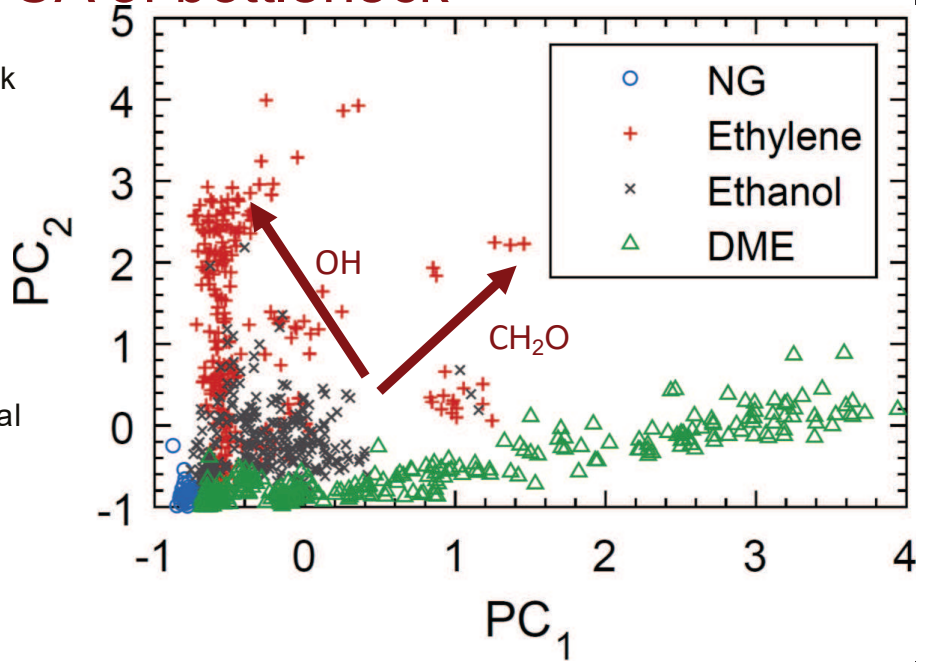
# Model analysis – PCA of bottleneck

- Principal component analysis output at U-Net bottleneck
- Investigate whether model is encoding flame features



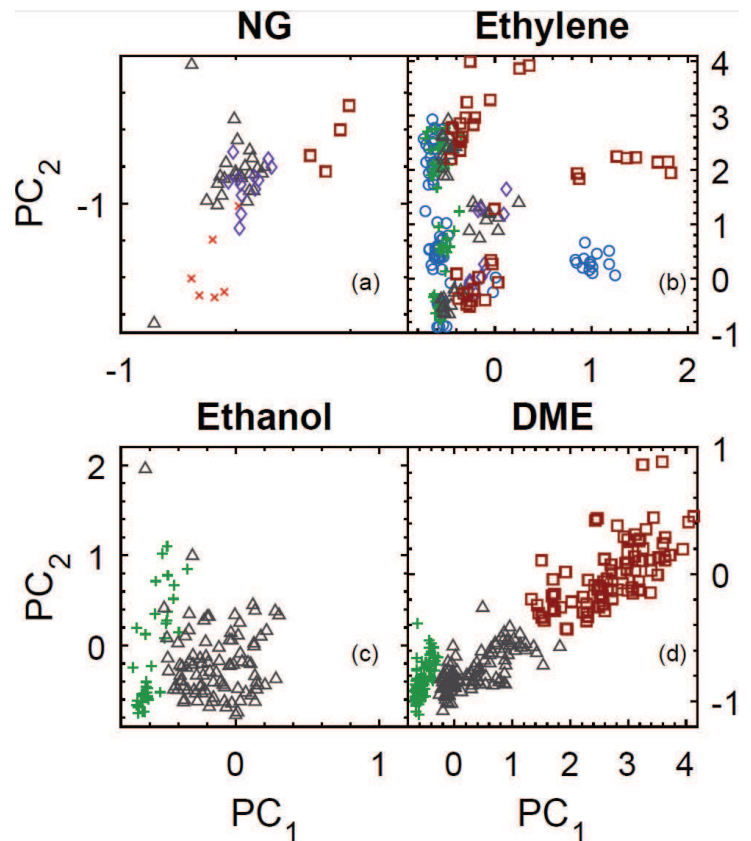
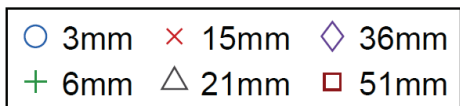
# Model analysis – PCA of bottleneck

- First two PCs of bottleneck
- Distinct clustering of fuels in PC space
- Based on dummy inputs:
  - PC<sub>1</sub> CH<sub>2</sub>O signal dominated
  - PC<sub>2</sub> OH signal dominated
- Ethylene and methane clusters affected more by OH than other fuels
- DME strongly CH<sub>2</sub>O signal dominant



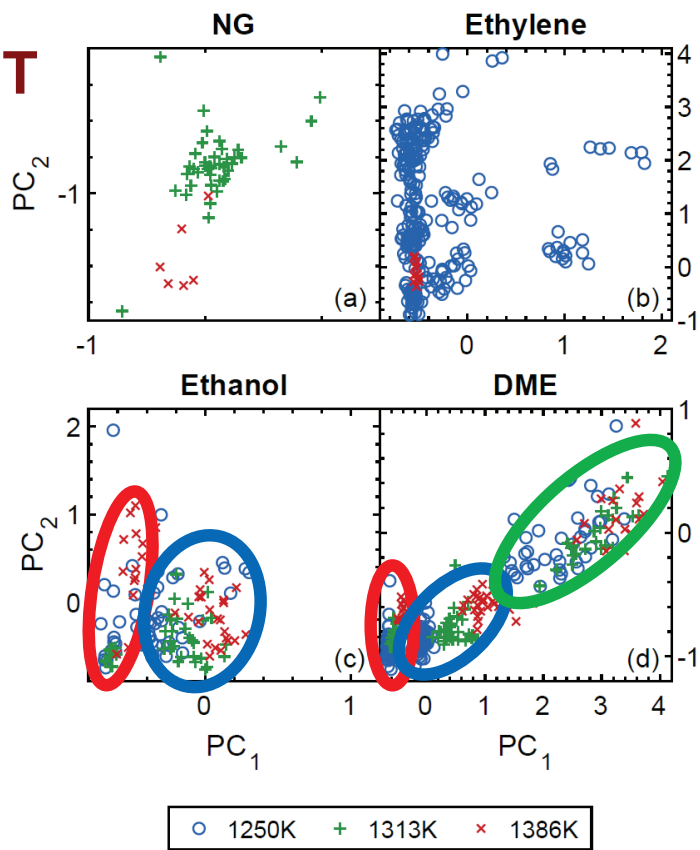
# Clusters by height

- Downstream precursor development notable for DME and ethanol
- Little to distinguish non-oxygen containing fuels



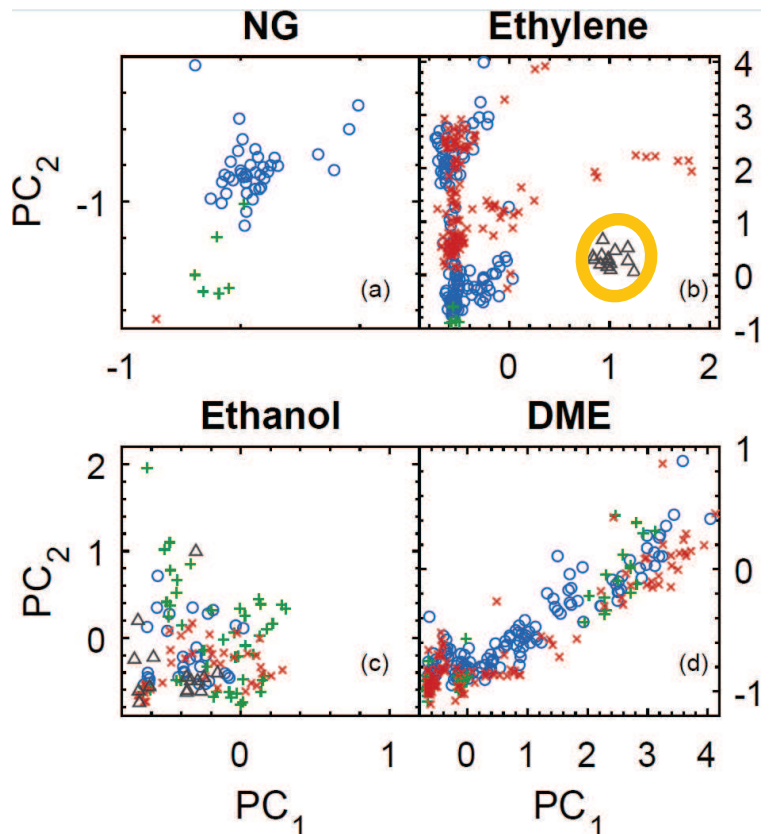
# Clusters by coflow T

- Distinct clusters for DME within height regions
- Suggestive of unique flame features upstream
- Dependence on precursor development for flame characteristics
- Predominantly 1250K cases in ethylene
  - Uniqueness of 1386K cases not apparent



# Clusters by O<sub>2</sub> level

- Minimal differences in ethanol and DME
- Two branch appearance for 9% ethylene
- 11% ethylene isolated
  - Distinct difference in flame phenomenology
- 3% shows minor branching, but primarily constant PC<sub>1</sub>



# Classification of flame features via MLP

- Classification based on different experimental conditions
- 3 hidden layer multi-layer perceptron, 4-16-4 size
- Classification performance consistent with experimental observations
  - Ethanol low dependence on  $O_2$  for flame features
  - Ethylene low dependence on axial location for flame features

Fuel	Species	$T_{co}$ (K)	Coflow $O_2$	$Re_{jet}$	x/D
All	99%	91%	76%	98%	93%
Ethylene	-	100%	93%	89%	71%
Ethanol	-	91%	67%	-	100%
DME	-	90%	93%	-	100%

Classification accuracy in testing dataset

67

## Conclusions

- Model capable of predicting temperature fields with accuracy comparable to experimental methods
- Principal component analysis of latent space reveals coherent patterns related to each fuel
- Patterns in PC space are supported by experiments
- Classification of points in PC space also in agreement with experimental observations

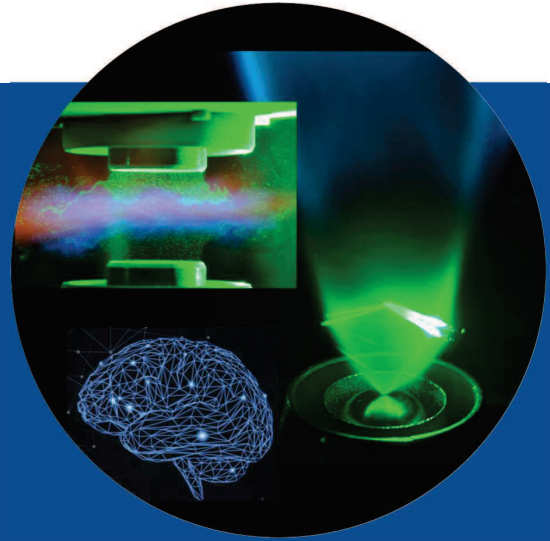


University of Stuttgart

# ML-augmented diagnostics for feature extraction

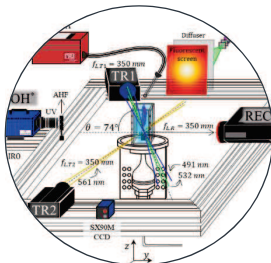
Fabian Hampf

16th TNF, Milan, Italy, 20-21.07.2024

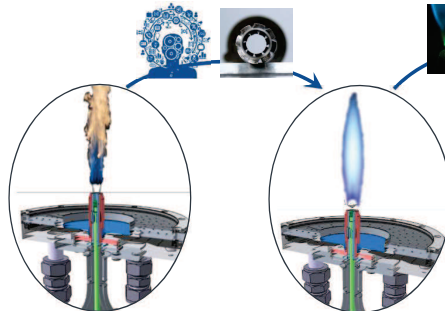


## Research Field

Realising clean and fuel-flexible combustion from  $H_2$ ,  $NH_3$  to liquid fuels



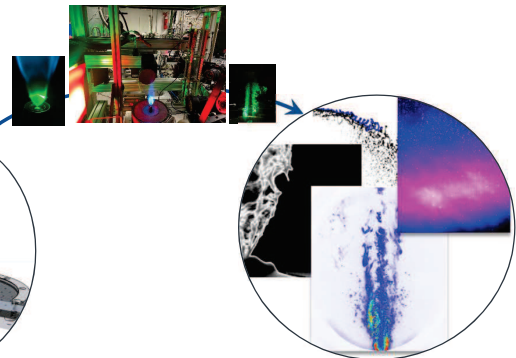
Fundamental understanding and advanced manufacturing to optimise injector and burner hardware



Sooting flame

Clean and fuel flexible combustion

Laser-based diagnostics



TBs of Data



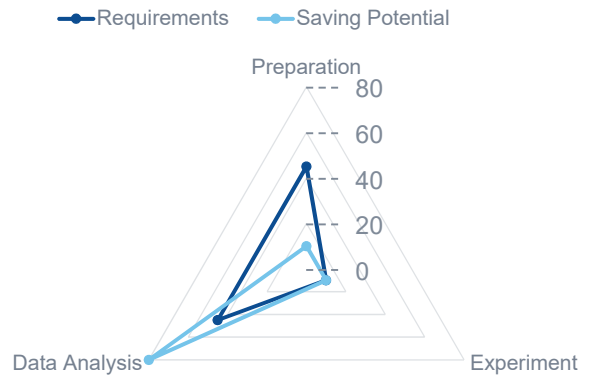
## Problem Definition and Motivation

Common time requirements for laboratory work

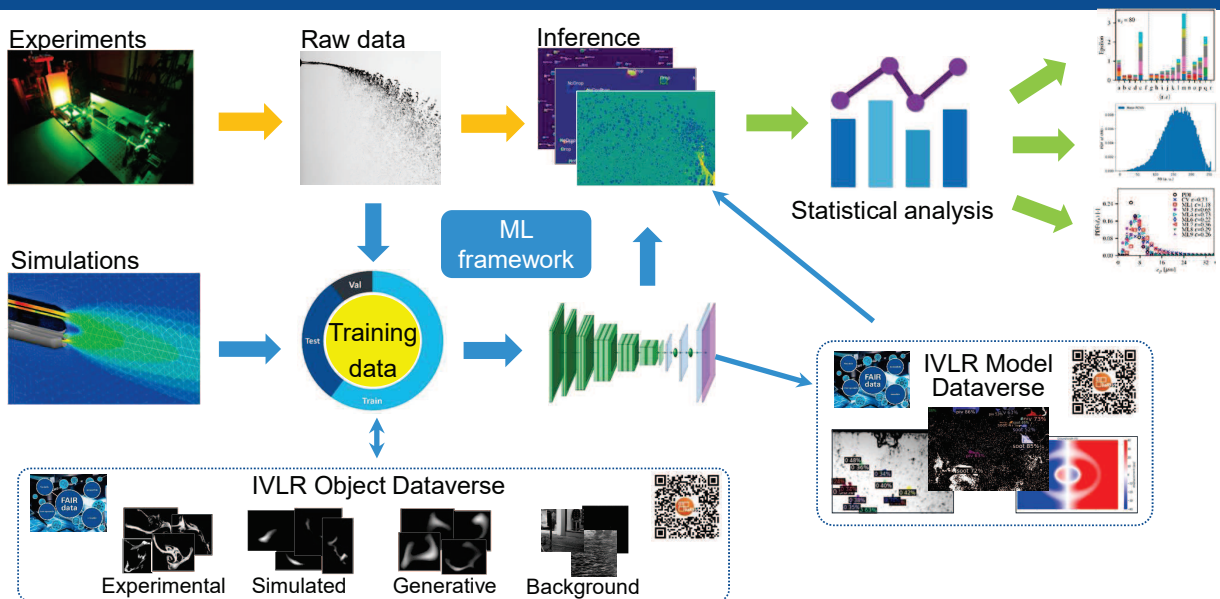
- ❑ High-level statistics: Object detection, binarization and conditional statistics
- ❑ Preparation time difficult to reduce
- ❑ Experiments are rather efficient
- ❑ Data analysis is usually extensive
  - ❑ More powerful hardware / resources
  - ❑ Autonomous / hands-off data analysis
  - ❑ General applicable & transferable tools

➤ Rethink data analysis equivalent to open source CFD Tools (e.g. OpenFoam)

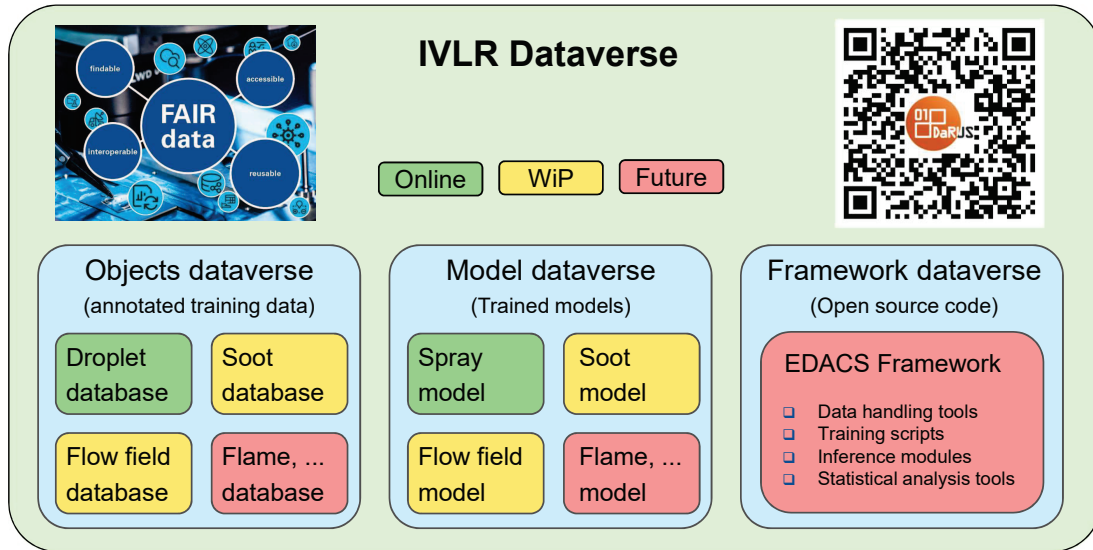
### Estimated Time Saving Potential



## ML-augmented Diagnostics | Framework



## ML-augmented Diagnostics | IVLR Dataverse



Fabian Hampf - ML-augmented diagnostics for feature extraction - University of Stuttgart - IVLR

20/07/2024

5

## Towards Open Source Data Analysis Framework (for Combustion Science)

Vision: „OpenFOAM equivalent“ for Data Analysis

Next steps:

- Continue building-up data and model repositories
- Seek funding (DFG - Research Software Infrastructure, phase I):
  - Object repositories with annotated training data
  - Model repositories for ML-augmented segregation
  - Develop software from (re-)train models, over evaluation tools to implementable software module
- Phase II → Vision

Needs analysis questionnaire  
(2-5 min)



Fabian Hampf - ML-augmented diagnostics for feature extraction - University of Stuttgart - IVLR

20/07/2024

6



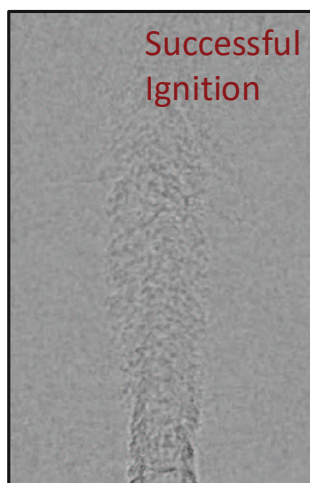
# ML-enabled ensemble predictions for forced ignition with hybrid stochastic physics-embedded deep-learning framework

Wai Tong Chung, Charlelie Laurent,  
Donatella Passiatore, Matthias Ihme

75

## ML-enabled ROMs for forced ignition

- Reliable ignition for space propulsion
  - Stricter success criteria
  - Repeatable ignition sequence
  - Laser ignition
- Stochastic ignition
  - Turbulent mixing
  - Variations in laser energy



Successful  
Ignition



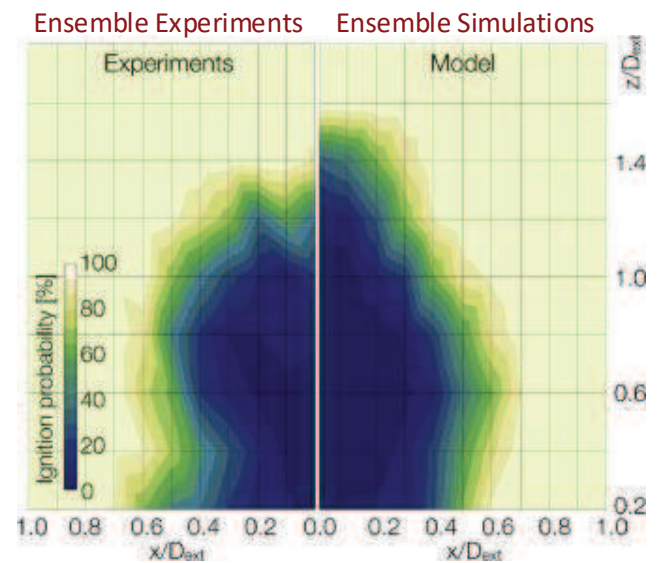
Failed  
Ignition

Mastorakos, Prog. Energy Combust. Sci., 35, 2009  
Strelau et al., AIAA 2023

WT Chung, C Laurent, D Passiatore, M Ihme Ensemble predictions of laser ignition with a hybrid stochastic physics-embedded deep-learning framework  
Proceedings of the Combustion Institute 40 (1-4), 105304

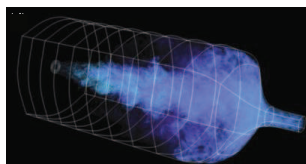
# Background: reliable ignition

- Reliable ignition for space propulsion
  - Stricter success criteria
  - Repeatable ignition sequence
  - Laser ignition
- Stochastic ignition
  - Turbulent mixing
  - Variations in laser energy
- Challenge
  - Statistical characterization needed for robust deployment
  - Expensive testing/modeling

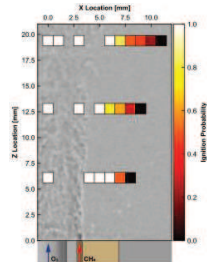


# ML-SDE for Reduced-Order Modeling

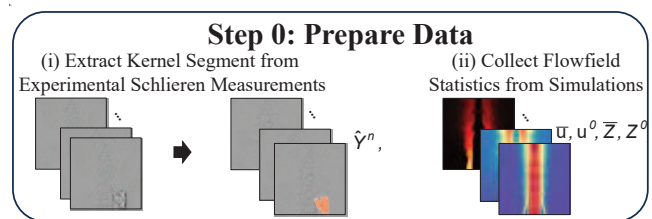
Single, Inert Simulations



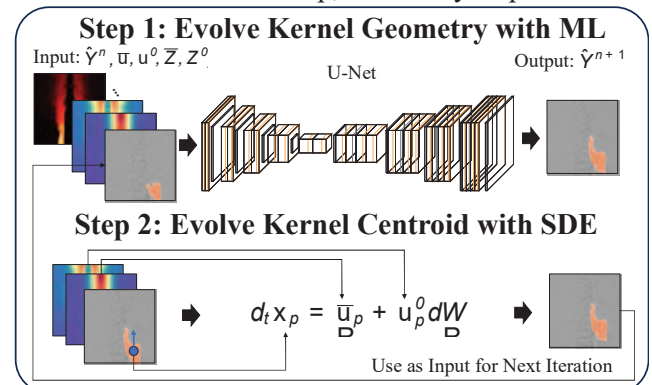
Sparse Measurements



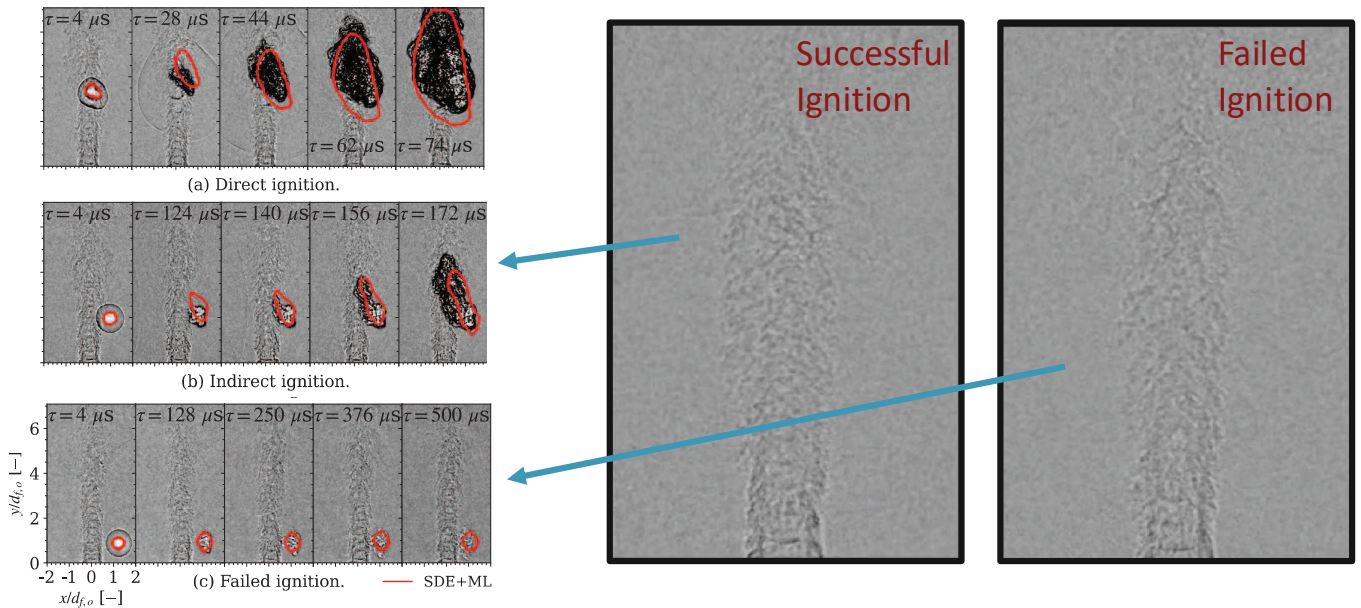
- Sparse (153) ignition tests
  - ~19,000 frames of 2D Schlieren measurements
- 3D Inert LES data
  - 220M-Cell Grid, Smagorinsky Model
- Instead of learning ensemble behavior, focus on learning **kernel growth behavior**



For Each Timestep, Iteratively Repeat:



# Instantaneous Results

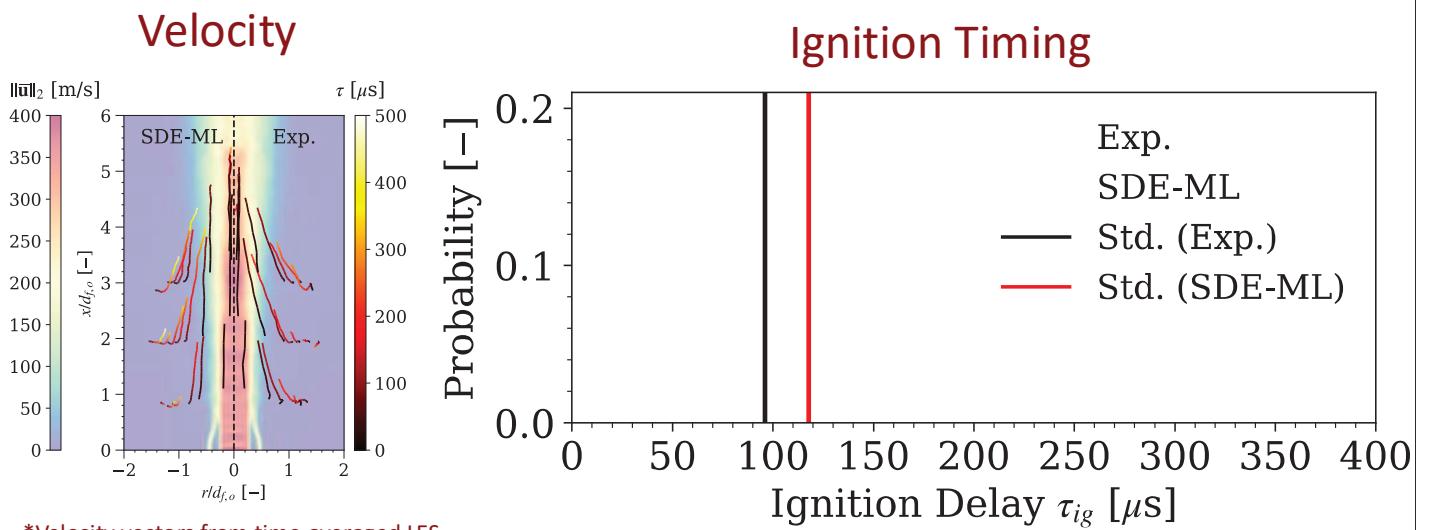


SDE+ML approach can model indirect ignition and consider kernel geometry

Strelau et al., AIAA 2023

79

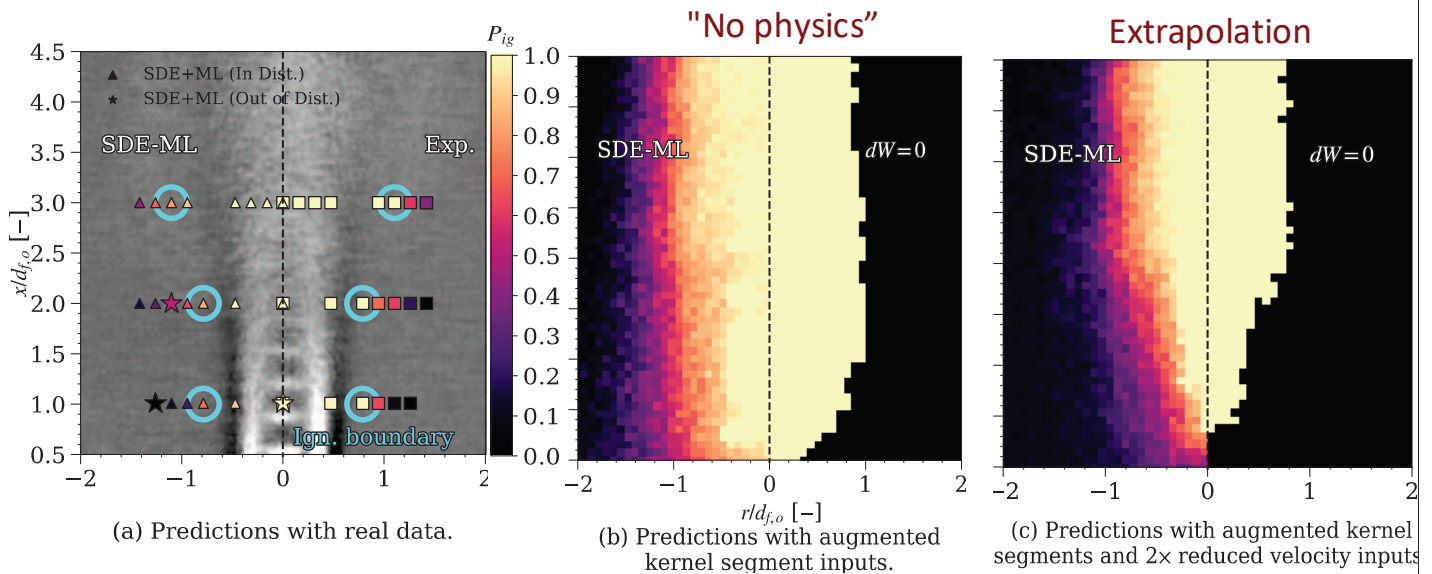
# Ensemble Results



\*Velocity vectors from time-averaged LES



# Probability Maps – out-of-distribution



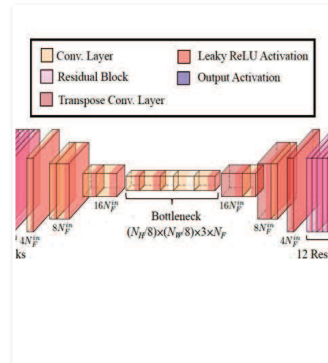
\*Ignition boundaries are where  $P_{ig}$  transitions below 1

## Summary

- In presence of sparse datasets, employ domain knowledge to define suitable learning tasks
- Hierarchical SDE-ML model
  - Only learn ignition kernel growth behavior as a function of mixture and velocity fields
  - Model ignition kernel transport with SDE
- Opportunities
  - Use ML-model to statistically characterize ignition in presence of sparse ensemble data
  - Captures distinct ignition modes and kernel geometry effects, as well as ignition timing and kernel trajectory
  - SDE-ML model can generate a spatially coherent ignition probability map at affordable cost: 9 s for inference per trajectory, 2 hours of training on 4 V100 GPUs

## Discussion

RESEARCH OPPORTUNITIES  
AND NEEDS

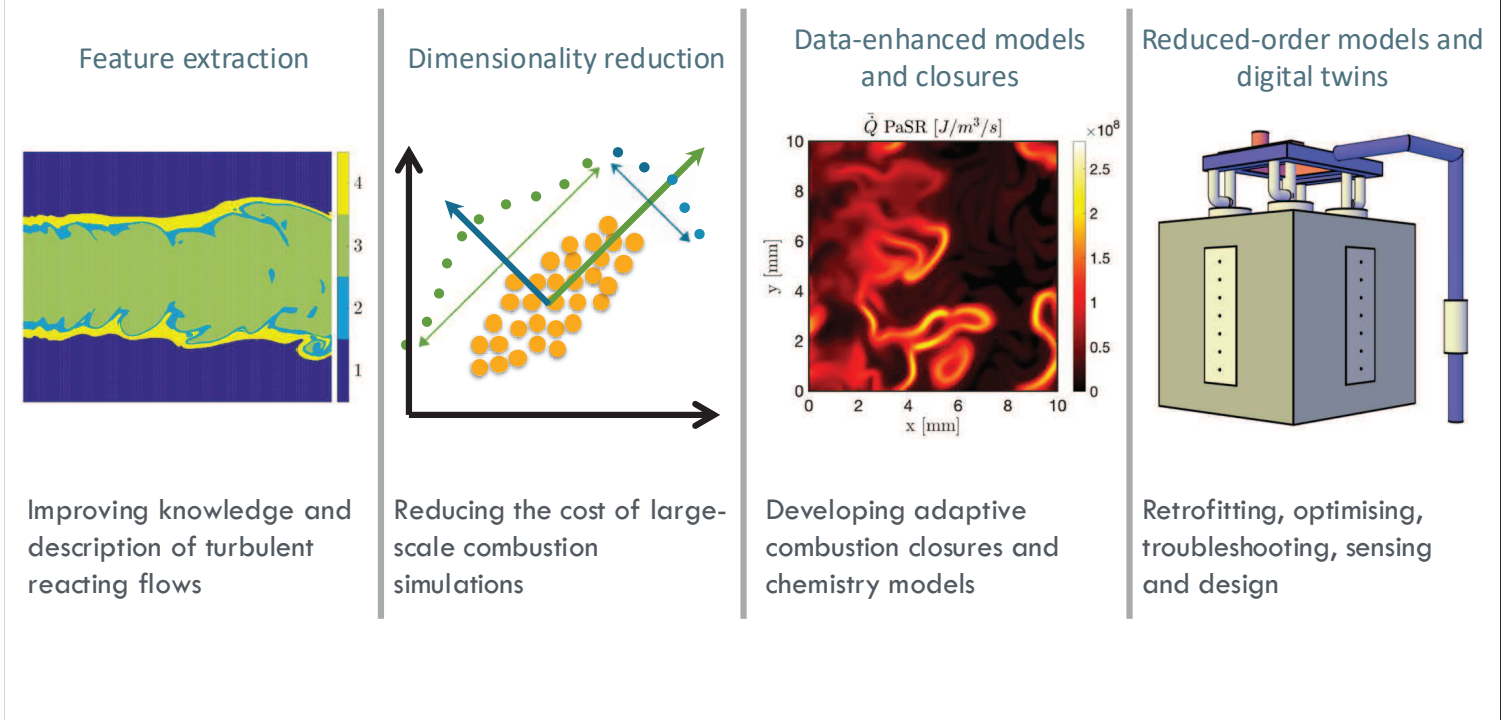


Stanford University

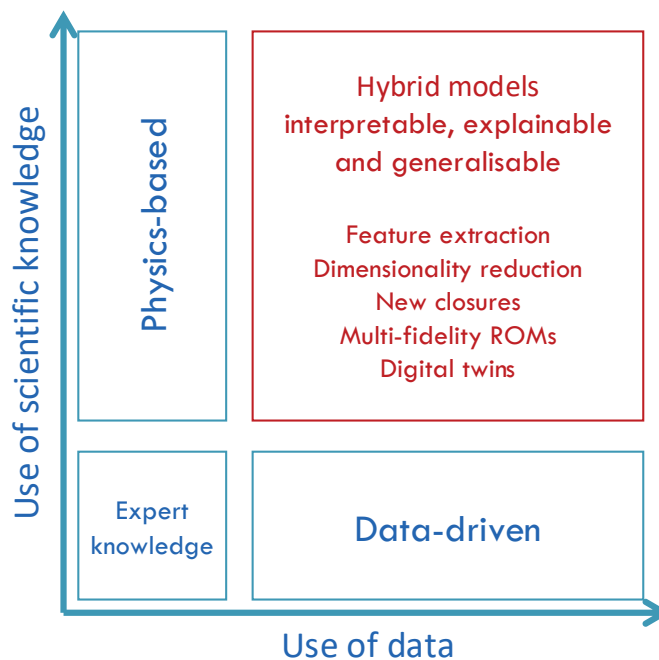
## Discussions: Combustion ML @ TN/PF

- Key challenges
  - Data, benchmarks, and metrics
  - Common models, methods, and approaches
  - Best practice
- How to integrate ML in TN/PF?
  - Establish database and metrics
  - Experimental configurations to consider
- TNF configurations and problems
- Tools, methods, best practice
  - Foundational ML models
  - Develop best practice for ML-model selection, ML-training, ML-evaluation
  - Integrate domain-knowledge into Combustion ML

# Machine learning for combustion



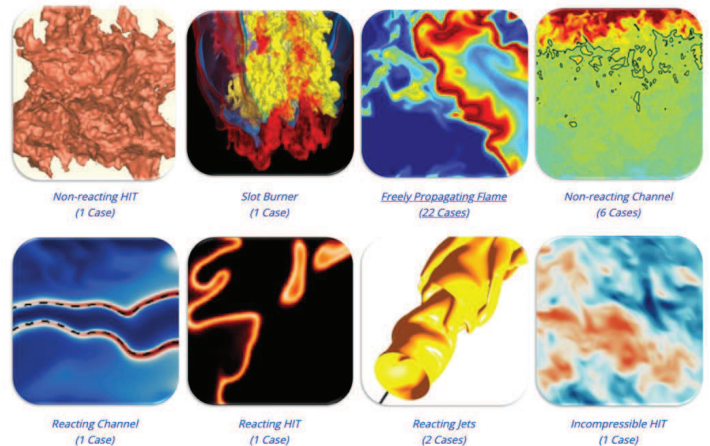
# Physics-based, data-driven approaches



# BLASTNet Dataset

- Addresses gap in 3D multi-physics turbulent flow physics data.
- Latest version:
  - 35 configurations
  - 4.8 TB
  - 44 full-domain samples
  - 6 to 29 channels (velocity, pressure, temperature, and chemical species)
- ML-ready format
- Shared on Kaggle

Data contributed by numerous institutions:



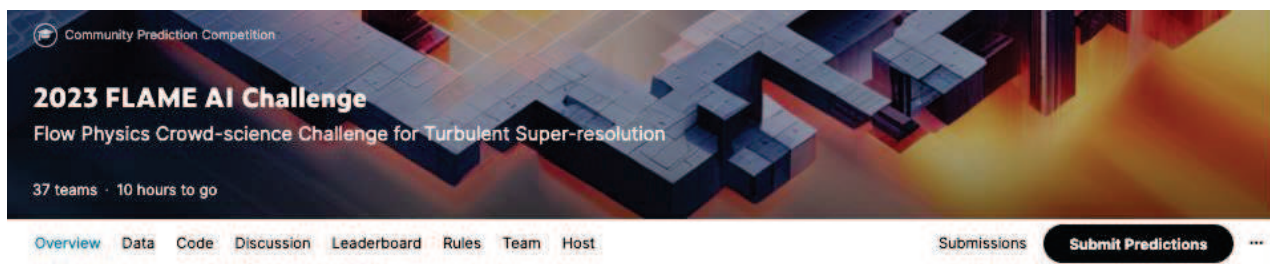
<https://blastnet.github.io>

# Community-driven ML-enabled dataset

- BLASTNet aims to curate 100 different reacting DNS flow configurations
- Extension to incorporate experimental data
- Provides tutorials for sharing and accessing data, ML-samples
- Stores metadata in consistent JSON format
- Provides standards and guidelines for shared data
- Hosts discussion forum for user support and community feedback
- BlastNet should be built out even more, including data from TNF/PTF
- better lossy data reduction tools that guarantee error bounds on PD and QoI are needed.
- More high-quality data with greater diversity is needed that is accessible to train and assess ML-based models.
- include statistical quantities (means, variances, etc.) associated with a given dataset for validating ML-based models

<https://blastnet.github.io>

# 2023 FLAME AI Challenge



## Participants

- 49 Competitors
- 37 Teams
- 673 Entries

#	Team	Members	Score	Entries	Last	Join
1	Louis & ThomasX		0.00557	65	9h	
2	Anas Jini		0.00625	16	1h	
3	nithin sekhar		0.00767	32	17m	
4	Thivin & Divij		0.00839	62	2m	
5	Varun Hiremath		0.00860	40	1d	
6	Jordan & David		0.00898	29	19h	
7	Abu Bucker		0.00930	18	9h	
8	mcolo		0.00931	4	3d	
9	Adib Bazgir		0.00949	69	3h	
10	Abhinay		0.00969	37	1d	

89

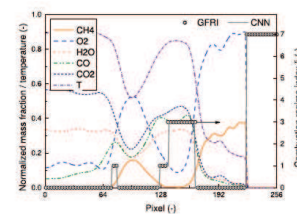
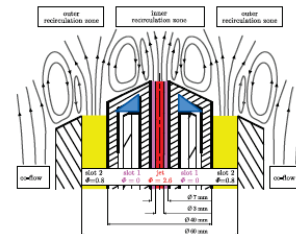
# Combustion ML @ TN/PF

- Combustion ML-specific challenges
  - Interpretability and explainability
  - Quantifying uncertainties of combustion ML models
  - Evaluation out-of-distribution predictions
  - Integrating domain knowledge in combustion ML
  - Computational complexity and accuracy



# Combustion ML @ TN/PF

- Benchmark problems for ML-applications
  - Combustion-regime identification
  - Manifold parameterization
  - Combustion modeling
- TN/PF participation
  - ML-model benchmark
  - Share ML-models through TN/PF infrastructure
  - Establish best practice



91

# Discussions: Combustion ML @ TN/PF

- Key challenges
  - Data, benchmarks, and metrics
  - Common models, methods, and approaches
  - Best practice
- How to integrate ML in TN/PF?
  - Establish database and metrics
  - Experimental configurations to consider
- TNF configurations and problems
- Tools, methods, best practice
  - Foundational ML models
  - Develop best practice for ML-model selection, ML-training, ML-evaluation
  - Integrate domain-knowledge into Combustion ML

## Flame-Wall Interaction -- Summary

*Coordinators: Andreas Dreizler and Christian Hasse*

Flame-wall interaction (FWI) has been a topic since TNF12 in 2014. A side wall quenching (SWQ) geometry was introduced in TNF13 in 2016 as a first target flame, for which the available experimental data has been continuously expanded for laminar and turbulent flow conditions. A fully premixed flame is anchored at a ceramic rod generating a V-shaped flame brush where one of the two branches is interacting with a temperature-controlled wall. This setup has been investigated in a series of experimental and numerical studies. Based on the SWQ configuration, further, especially numerical, setups for high-resolution simulations were devised.

In 2022 during TNF15, the scope of the FWI session was broadened. Investigations of the interaction of flames with cooling air near walls (FCAI – flame cooling air interaction) and FWI in a crevice were integrated, going beyond generic SWQ configurations. FWI for zero-carbon fuels ( $H_2$ ,  $NH_3$ ) and their mixtures with hydrocarbons are gaining more and more interest. Safety aspects such as flashback, which is inextricably linked to flame-wall interaction, are also becoming increasingly important.

The primary aim of FWI and FCAI studies is to gain a deeper understanding of the near-wall dynamics of laminar and turbulent flames. Combustion in enclosed chambers, in many cases cooled by near-wall air flows, is of great technical relevance, as the walls represent boundary conditions that have a significant impact on the physico-chemical processes and the micro- and macrostructure of the flame in the boundary layer. Strong heat losses lead to thermal flame quenching and incomplete combustion results in the formation of primary pollutants such as carbon monoxide (CO) and unburned hydrocarbons (UHC). Mixing with cooling air needs to be considered in many applications. To understand these processes, the influence of walls and effusion cooling on the flame dynamics and in particular turbulence-chemistry interaction as one of the primary fields of interest in the TNF workshop must be studied.

Based on the previous TNF workshops and recent research efforts, the objective of the FWI session at TNF16 was threefold:

1. Provide an update on recent numerical and experimental efforts
2. Identify common challenges and findings from the different FWI studies
3. Identify the next steps for further studies of FWI

### 1. Update on experimental efforts

Results were provided by three groups (Coria Rouen, France; University of Edinburgh, UK; TU Darmstadt, Germany).

The **Coria group** provided an update on measurements on the test case introduced at TNF15. The scope is to study the interaction between premixed flames and cooling air near walls (FCAI). At atmospheric pressure, a rod-stabilized  $CH_4$ /air V-flame interacts with an oil-cooled wall that is shielded by a cooling air film. Blowing ratios between film and main flow are varied between 0.1 and 4. The experimental data base contains wall temperatures, CO imaging, flow velocities, and flame visualization. Post-processed data include information on

near-wall flame stretch. Investigations have been expanded to investigate more realistic FCAI configurations and to study the durability of metallic walls exposed to realistic thermochemical conditions imposed by flames.

The **Edinburgh Group** contributed four studies. The first is in cooperation with TU Darmstadt using the generic SWQ burner, operated at 1 bar and turbulent lean DME-air conditions. Using highly resolved velocimetry, the flame vortex interaction is studied in detail that was identified to transport hot exhaust gases very close to the wall upstream into the yet unburned mixture. Using Reynolds decomposition, it is shown how vortical structures interact with the premixed flame during a HOQ-scenario. The vortex presses the flame very close to the wall enhancing heat transfer. In turn the flame quenches and transitions into a SWQ-scenario. During this flame vortex interaction, the afore-mentioned transport mechanism is active, causing locally high CO<sub>2</sub> mole fractions at rather low temperatures.

Using the same burner in the second study recent advances of the 1D CARS approach were highlighted. Combined with thermographic phosphor thermometry and OH-PLIF, instantaneous wall-normal temperature gradients are now available. Combined with PIV, for the turbulent case, scalar fluxes become accessible, which is a great step forward.

The third study is on SWQ-like FWI in a fixed volume chamber, mimicking a geometry similar to an IC engine. Using cinematographic chemiluminescence and wall temperature imaging, the differences between stoichiometric methane and lean hydrogen-air combustion are highlighted. The hydrogen case shows clear evidence of thermodiffusive instabilities evolving during flame propagation in the crevice.

Finally, as a potential new topic for the TNF, FWI during flame spread on PMMA surfaces was discussed. In first of its kind experiments, wall temperatures were measured by thermographic phosphor imaging showing the onset of pyrolysis ~1 mm ahead of the flame front. Temperature measurements were possible even beneath flame in the burning region.

The **Darmstadt Group** contributed studies classified into passive and active walls. For passive walls, the generic SWQ configuration was extended to an enclosed setup. Pressure effects were compared between 1 and 3 bar. The study was finalized and documented in three publications (see slides). Data are available upon request. As continuation of the generic SWQ configuration, lean hydrogen/air flames are currently investigated but no data was shown at the TNF16.

For active walls, the generic SWQ facility was equipped with a wall providing effusion cooling through different holes. This is as well ongoing work, and results are expected for TNF17. Like the Edinburgh group, the Darmstadt group started work on boundary layer flames and pyrolysis/combustion of polymer samples. As a starting point, different variants of active walls have been designed mimicking the pyrolysis of a polymer. Secondary fuel is injected at very low momentum ratios upstream or downstream of the quenching point of a rod-stabilized V-flame quenched at the wall. In contrast to the pyrolysis of a polymer, this configuration provides much better-defined boundary conditions (secondary fuel flow rate, fuel composition, thermal boundary conditions) as needed for comparison to numerical simulations. Compared to the previous FWI studies, as an additional complexity the local

equivalence ratio varies, and depending on the configuration, a near-wall boundary layer flame develops. This is new ground for the FWI discussed in the TNF.

### **Key Messages and Challenges for experiments close to passive and active walls**

The experimental investigations are summarized in the following key messages.

**KM1-exp:** For passive walls and hydrocarbon fuels, many studies exist for laminar and turbulent flow conditions under atmospheric conditions and for elevated pressures. In addition to extensive experimental data sets, individual phenomena such as flame vortex interaction in the region of the extinction point have been investigated. Experimental FWI studies for H<sub>2</sub>/NH<sub>3</sub> mixtures are currently being investigated in a similar way as previously for hydrocarbon fuels, such that new data for TNF17 can be expected.

**KM2-exp:** The investigation of flames on active walls has been intensified. Two main directions have developed: 1) Flame Cooling Air Interaction (FCAI); and 2) flame propagation or boundary layer flames in the context of fire safety. For FCAI, data exist for generic and complex geometries, which are available in publications. With regard to fire safety, experiments are at an early stage, and it needs to be decided whether this is an appropriate future topic for the TNF.

**KC1-exp:** The challenge for laser optical measurement techniques, particularly for partially premixed flames, is to measure the local mixture fraction as an additional variable. This is equally important for FCAI and boundary layer flames.

**KC2-exp:** Regarding canonical FWI/FCAI geometries, there is a need to further develop these for the requirements resulting from H<sub>2</sub> or H<sub>2</sub>/NH<sub>3</sub> fuel mixtures. This should include the aspect of flashback for H<sub>2</sub>-containing mixtures.

**KC3-exp:** Experimental and numerical studies are usually carried out separately. In the future, in the spirit of the TNF tradition, a closer exchange should take place and experimental configurations with the corresponding data sets should be used more intensively for comparison with numerical simulations.

## **2. Update on numerical efforts**

In total, there were 13 contributions from 12 groups for various configurations: RWTH Aachen University (Germany), Aalto University (Finland), Beihang University (China), TU Berlin (Germany), CERFACS (France), TU Darmstadt (Germany), SINTEF/NTNU (Norway), University of Magdeburg (Germany), University of Melbourne (Australia), Newcastle University (UK). In several cases, the work from different groups included collaborations with other universities and industrial partners. Only the affiliation of the main PI is listed here.

Considering the increased variety of fuels and configuration studied, the numerical contributions were categorized as shown in Figure 1. On the one hand, a distinction was made between three **FWI configurations (abscissa)**: 1) classic head on quenching (HOQ) and side wall quenching (SWQ) for passive walls; 2) active walls; and 3) safety. These configurations were considered for a **variety of fuels divided into three categories (ordinate)**:

1) CH<sub>4</sub> and other hydrocarbons; 2) NH<sub>3</sub>/H<sub>2</sub> as non-carbon fuels; and 3) mixtures of (1) and (2).

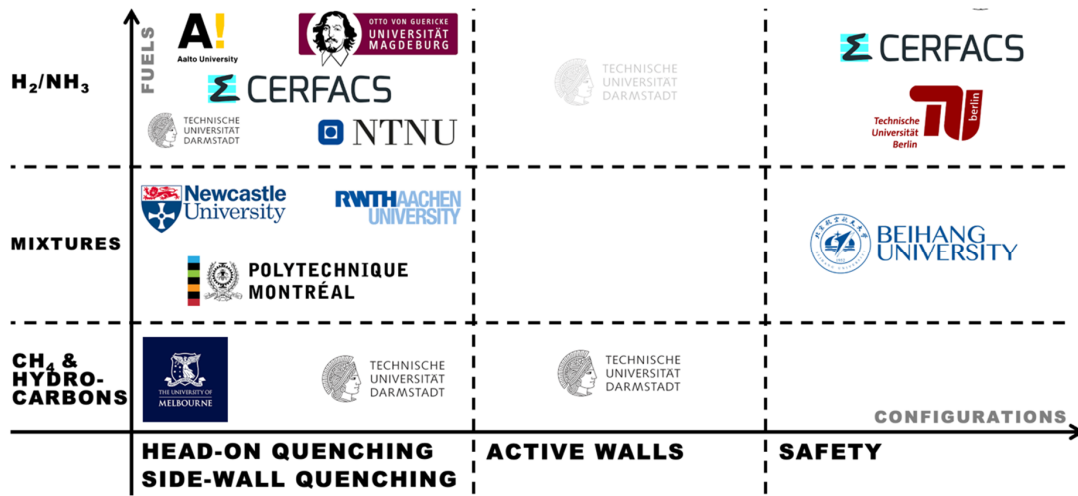


Figure 1: Classification of numerical contributions for the TNF16 FWI session. The different configurations are placed on the abscissa, the fuels investigated are indicated on the ordinate.

This wide scope of FWI did not allow for a direct “TNF-style” comparison due to the lack of an isolated aspect such as multi regime combustion. But several findings and challenges (see below) could be identified based on the following key observations

1. **New fuels and mixtures:** FWI for H<sub>2</sub>/NH<sub>3</sub> and their mixtures with hydrocarbons differs significantly from hydrocarbons, even in simple geometries.
2. **Beyond standard FWI:** There is significant interest in technically relevant FWI/FACI scenarios that are more complex than previously considered HOQ/SWQ setups. These include effusion cooling and active walls with polymers. New areas such as safety, especially flashback, are particularly challenging for zero-carbon fuels.
3. **Increase in number of DNS studies:** Most of the numerical contributions used DNS rather than LES. This reflects the current lack of knowledge on FWI and FCAI, especially for new fuels. DNS as a numerical experiment is crucial for model development.

In the following a brief summary of the individual contributions is given structured along the configurations, see the abscissa in the above figure. The ordering corresponds to the attached slides.

## 2.1 Head-on Quenching/Side-wall Quenching

The TU Darmstadt group performed turbulent direct chemistry (DC) simulations of FWI of a side-wall quenching flame in a channel flow. A stoichiometric CH<sub>4</sub>/air flame was considered. The focus was on the flame vortex interaction mechanism that appears at the flame tip close



to the wall in the boundary layer. The vortex pushes burnt gas to the wall and the flame propagates over the burnt gases. This leads to a mixing of fresh and (cooled down) burnt gases and to the characteristic near wall flame dynamics with finger formation. This mixing process can be included in a flamelet model. When used in a fully coupled manner, considering this mixing process improves LES predictions substantially. Part of the work is published in *Combustion and Flame* (10.1016/j.combustflame.2023.112923).

The **Melbourne group** performed turbulent DNS of CH<sub>4</sub>/air FWI in channel flows under intense turbulence. The focus of this study was the comparison of different wall temperatures, here 300 and 800 K. They could show that turbulence has a substantial influence on FWI. Another aspect was the flame orientation during quenching, concluding that 1D head on quenching can be largely representative of the FWI in terms of flame orientation in the presence of intense turbulence.

The **Montréal group** performed DNS of a laboratory lean H<sub>2</sub>/CH<sub>4</sub>/air low-swirl flame impinging on an inclined wall. The DNS is derived from an experimental setup. They could demonstrate a complex flame wall interaction scenario, where the wall heat flux influences the flame structure. Very lean flames can be sustained, potentially by back-support. The products are not fully reached and more CH<sub>4</sub> slip is observed compared to H<sub>2</sub>.

The **Newcastle group** provided a database for turbulent oblique flame-wall interaction, the focus is on a parametric variation of the fuel Lewis number  $Le_F$ . Three different mixtures were studied: pure CH<sub>4</sub> ( $Le_F = 1.0$ ), a 25%/75% mixture of H<sub>2</sub> and CH<sub>4</sub> ( $Le_F = 0.6$ ) as well as a mixture of 90% C<sub>2</sub>H<sub>6</sub> and 10% CH<sub>4</sub> ( $Le_F = 1.4$ ). A second DNS database has been made available for turbulent head-on quenching at different Reynolds numbers for stoichiometric CH<sub>4</sub>/air flames. Both isothermal and adiabatic walls were considered.

The **RWTH Aachen group** performed a turbulent DC simulation of a lean premixed CH<sub>4</sub>/H<sub>2</sub>/air turbulent jet flame with FWI, considering 0%, 10%, and 20% H<sub>2</sub>. The jet Reynolds number of the simulation is 5500, the pressure is 4 bar, and the considered wall temperature 1000 K. An increased H<sub>2</sub> content leads as expected to shorter flame lengths. The joint PDF of the progress variable and the CO mass fraction shows that the conditional mean gets closer to the unstretched flame limit with increasing H<sub>2</sub>. This needs to be further explored in the future.

The **CERFACS groups** studied the influence of chemical schemes for H<sub>2</sub> flames impacting on cold walls. Previous studies observed for **rich** flames substantial heat release near the wall. In the CERFACS implementation, the maximum heat release at the wall increases with refined meshes and there seems to be no limit. They could show that in their simulations this heat release is directly coupled to the H radical at the wall. They introduced the Infinitely Fast Heterogeneous Catalysis Model (IFHC), which adds three wall reactions and brings the H radical to zero at the wall. The heat release is substantially lowered. The group stresses that this is problem should be revisited by chemistry and catalysis experts. The work is published in *Combustion and Flame* ([10.1016/j.combustflame.2024.113328](https://doi.org/10.1016/j.combustflame.2024.113328))

The **NTNU/SINTEF group** in collaboration with the TU Darmstadt group showed first results of the DNS of a turbulent anchored V-flame, two lean H<sub>2</sub> flames at 2 bar were considered.

Differential diffusion plays an important role and superadiabatic conditions are observed near the wall. The analysis of the turbulent dataset is still ongoing.

The **Aalto group** studied FWI of premixed laminar  $\text{NH}_3/\text{air}$  flames enriched with  $\text{H}_2$ . They could show that the quenching distance decreases and maximum absolute wall heat flux increases with increasing the blending ratio, the equivalence ratio, the wall temperature, and the pressure. More details can be found in their *Combustion and Flame* paper (10.1016/j.combustflame.2024.113444). This work is currently extended to 2D scenarios, where also the formation of pollutants ( $\text{NO}$  and  $\text{N}_2\text{O}$ ) is analyzed.

The **Magdeburg group** contributed a database on head-on quenching of  $\text{H}_2/\text{air}$  and  $\text{NH}_3/\text{H}_2/\text{air}$  flames in a turbulent channel flow. The focus is on differential diffusion effects, the near-wall pollutant formation and the flame dynamics. Selected results show that flame/wall and flame/flame interactions result in an accumulation of  $\text{N}_2\text{O}$  and consumption of  $\text{NO}$ . Results for the flame dynamics reveal that the major reason for flame thickening is the zero-diffusion flux boundary condition. For turbulent flames with high  $\text{Da}$  numbers, the effect of wall turbulence is negligible, while for flames with low  $\text{Da}$  number, the flame thickness decreases due to the laminarization near the wall. The results are partially published in the *Proceedings of the Combustion Institute* (10.1016/j.proci.2024.105276) and the *European Journal of Mechanics – B/Fluids* (10.1016/j.euromechflu.2023.05.008).

## 2.2 Active Walls

The **TU Darmstadt group** performed DC simulations of laminar flame-wall (FWI)/Flame-effusion-cooling-air (FCAI) interaction considering stoichiometric methane/air flames. A simplified numerical setup was developed, and a variable volumetric cooling air inflow was studied. Depending on the inflow rate, superposition of FWI and FCAI effects occurs. Three different interaction regimes have been identified: 1) Heat loss dominated, i.e. FWI is the main mechanism; 2) mixing dominated, i.e. dilution by air is the main mechanism for FCAI; 3) both FWI and FCAI are relevant. The work has been published in the *Proceedings of the Combustion Institute* (10.1016/j.proci.2024.105453).

## 2.3 Safety

The **Beihang group** performed an LES for flashback of a lean  $\text{H}_2/\text{CH}_4$  flame. In a previous study with a thickened flame approach, they could show that two flashback scenarios can occur, a large-scale flame tongue and flashback due to flame bulges. The focus of this work is the influence of differential diffusion. To this end, two flamelet tables with unity and non-unity Lewis number were built and employed in the LES. The flashback speed predicted with differential diffusion is close to the experimentally observed one while the unity Lewis number prediction is substantially lower. Further, the flame tongue with differential diffusion is more wrinkled and the flow field is inversed at an upstream location. This wrinkling is argued to be responsible for the higher flame speed.

The **CERFACS group** contributed their initial results for the studies of high-pressure hydrogen jet flames impacting on walls. This work is complementary to experimental studies conducted

at IMFT. The LES of the choked  $H_2$  jet is currently work in progress and aims to investigate the auto ignition, the flame stabilization in the shock system, the effect of the crossflow and FWI. Since this is a high-speed flow, the wall treatment will be another topic of interest.

The **TU Berlin group** looked at flashback of lean turbulent hydrogen flames, the corresponding experimental data was provided by TU Delft (not published yet). They looked at the transition process from an unconfined flame to confined boundary layer flashback. Curvature plays a substantial role in the transition; another finding is that the adverse pressure gradient in the confined state facilitates the upstream propagation. A more detailed analysis revealed that flashback is triggered by a low velocity streak caused by a lift-up mechanism, which transports low velocity fluid away from the wall.

### **Key Findings and Challenges – numerical FWI and FCAI**

The reported numerical results can be summarized in one key message (KM1-num) and three key challenges (KC1-num, KC2-num, KC3-num).

**KM1-num: Advanced near-wall combustion models for hydrocarbon are available for laminar and turbulent FWI.** Flamelets for hydrocarbon fuels show good results if properly chosen; the parameterization depends on the complexity of the configuration, e.g. active vs. passive walls. Reduced order models can be constructed from canonical flames - but these are more complex, e.g. head on quenching (HOQ). If near-wall turbulent mixing is resolved in LES, extended flamelet models are adequate.

**KC1-num: Near-wall chemistry for  $H_2/NH_3$  and mixtures.** While there is a substantial body of knowledge for hydrocarbon fuels, homogeneous and heterogenous (catalytic) reactions at/close to the wall should be (re)visited for  $H_2$ . This also applies for  $NH_3$  where even less is known. To this end, cooperation with materials science and chemistry is being sought.

**KC2-num: Near-wall combustion and pollutant models for  $H_2/NH_3$  and mixtures.** In contrast to hydrocarbons, reduced order models for  $H_2/NH_3$  are not yet available. These will be developed based on DNS datasets. Further validation requires experiments that are not yet available.

Several open scientific questions can be identified including:

- Can canonical configurations such as HOQ be used for reduced order models?
- Near-wall stratification/superadiabatic conditions/pollutants: Are these imposed by the main flame or are these caused by near-wall processes or both?
- What are the main processes that lead to CO and NO<sub>x</sub> (incl. N<sub>2</sub>O) near wall emissions?

**KC3-num: Safety and especially flashback for  $H_2/NH_3$  and mixtures.** Turbulent flashback scenarios for  $H_2$  are only partially understood.

- Differential diffusion was shown to be highly relevant near the wall. The impact on the occurrence of flashback requires further research.
- Multiple flashback scenarios could be identified for the laminar case. Current DNS and experimental data do not allow to draw definite conclusion about the turbulent case. This is an area where further research is urgently needed.
- The impact of several phenomena on flashback needs to be understood, this includes at least the uncertainty in the near wall chemistry (see above) and conjugate heat transfer.

### **3. Towards TNF17**

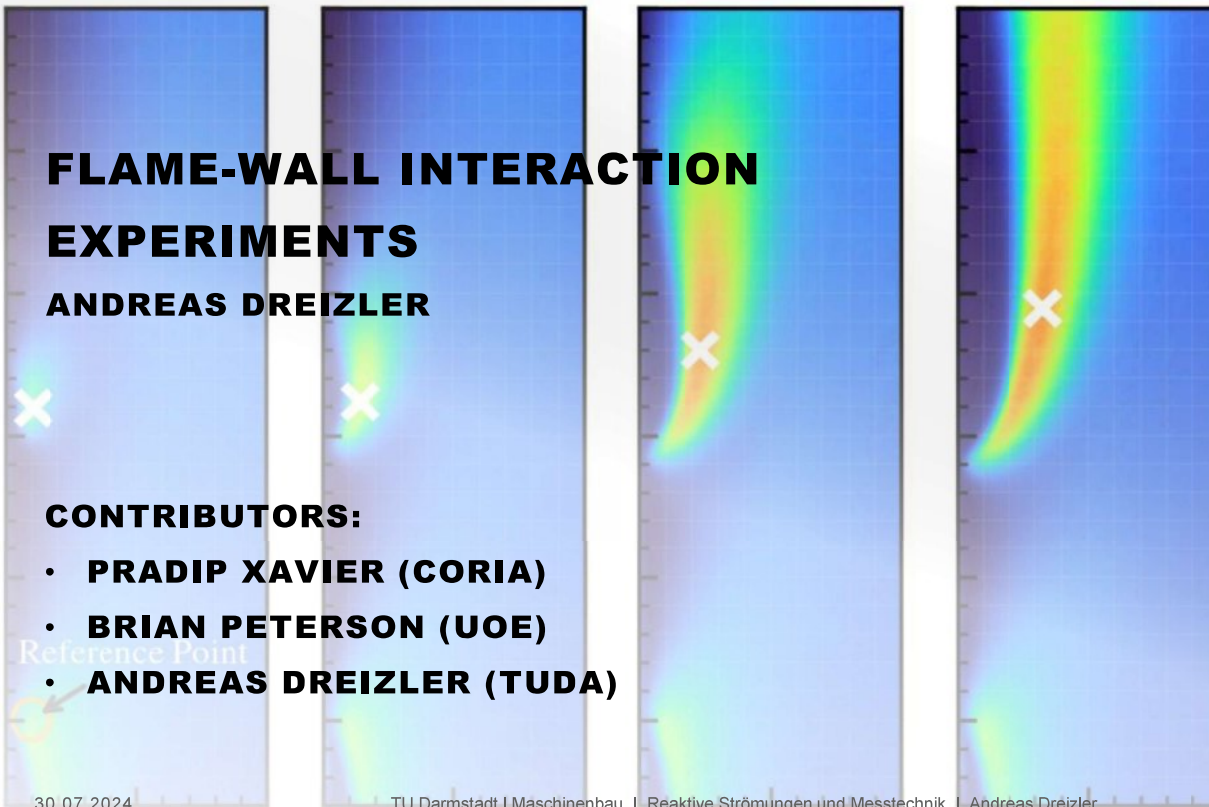
As mentioned in KC3-exp, experimental and numerical studies are usually carried out separately. With the new fuels, an expanded scope with active walls and safety, and the corresponding new configurations, there is a good opportunity to bring experiments and simulations closer together in the spirit of the TNF tradition. There is a unique opportunity for the development of LES models by the availability of DNS data sets in combination with experimental data gained with multi-parameter diagnostics from various configurations, including one- and two-sided FWI, passive and active walls, atmospheric and elevated pressures, premixed and partially premixed mixtures, and various carbonaceous and non-carbonaceous fuels.

# FLAME-WALL INTERACTION EXPERIMENTS

ANDREAS DREIZLER

## CONTRIBUTORS:

- PRADIP XAVIER (CORIA)
- BRIAN PETERSON (UOE)
- ANDREAS DREIZLER (TUDA)



30.07.2024

TU Darmstadt | Maschinenbau | Reaktive Strömungen und Messtechnik | Andreas Dreizler

1

TNF 16 Workshop

## Recent Progresses on Near-Wall Energy Processes

[Dr. Pradip Xavier \(PI\)](#)

Co-workers: Antoine Blaise (PhD student), Artémis Blondel (PhD student), Dr. Avinash Chaudhary, Dr. Sylvain Petit, & Prof. Frédéric Grisch

INSA Rouen Normandie, Univ Rouen Normandie, CNRS, Normandie Univ, CORIA UMR 6614, F-76000 Rouen, France





# Research strategy

## Near-wall energy processes @CORIA:

- Research activity in the **understanding of near-wall energy processes** (e.g. FWI, thermal aggression)
- **Academic activities** & applications in **aeronautical gas turbine combustors**
- Experimental approach using advanced **laser-based diagnostics** (CFD on-going)

## Various methods / physical processes are studied:

- Advanced laser-based diagnostics (PLIF, phosphor thermometry, PIV, etc.)
- Flame dynamics & aerodynamics (turbulent combustion)
- Pollutant formation (CO)
- Material aging and cooling strategy (e.g. thermal aggression, effusion cooling, etc.)

3

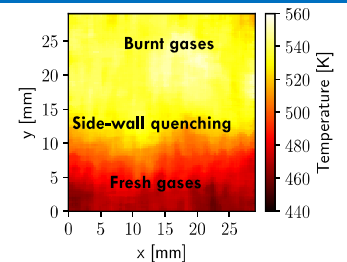
# 1 / Development of Laser-based Diagnostics

## ➤ Surface Phosphor Thermometry

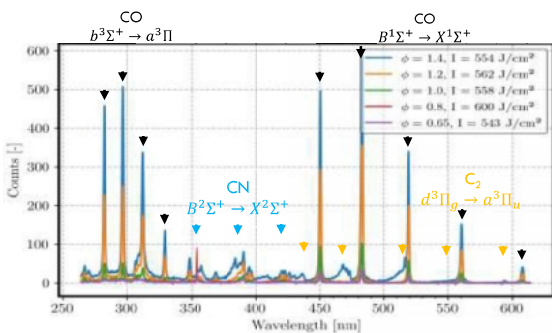
Optimization of the uncertainty w/ the time-integrated approach (2%)

Wall temperature imaging during FWI events

Coupling w/ other laser-based diagnostics (PIV, PLIF)



Mean wall temperature during sidewall FWI



CO emission spectra in reactive conditions

## ➤ Two-photon Laser-Induced Fluorescence (WiP)

Instantaneous CO imaging near walls (collection strategy, interferences)

Application to FWI

Coupling w/ other laser-based diagnostics (OH-PLIF)

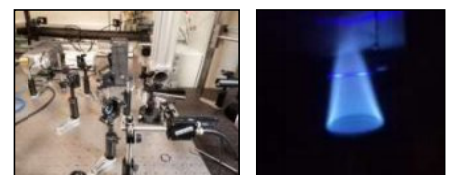
WiP (quantification of signal, detectivity threshold, etc.)

## ➤ Two-line Atomic Fluorescence on Indium (WiP)

Gas-phase temperature measurements near wall

Application to thermal aggression

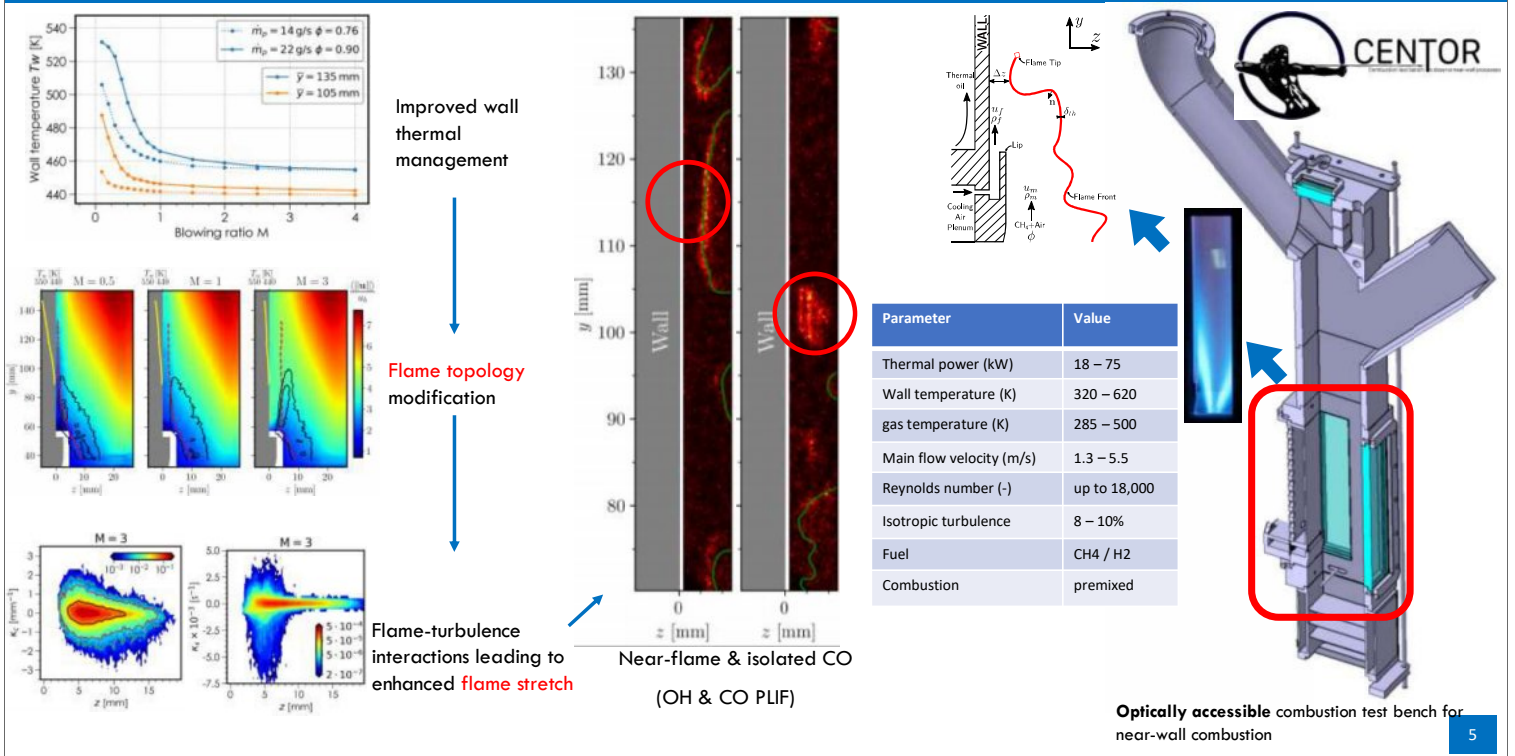
Instantaneous pointwise and imaging



Optical arrangement & fluorescence visualization in reactive conditions

4

# 2/ Flame-cooling air interaction (FCAI)

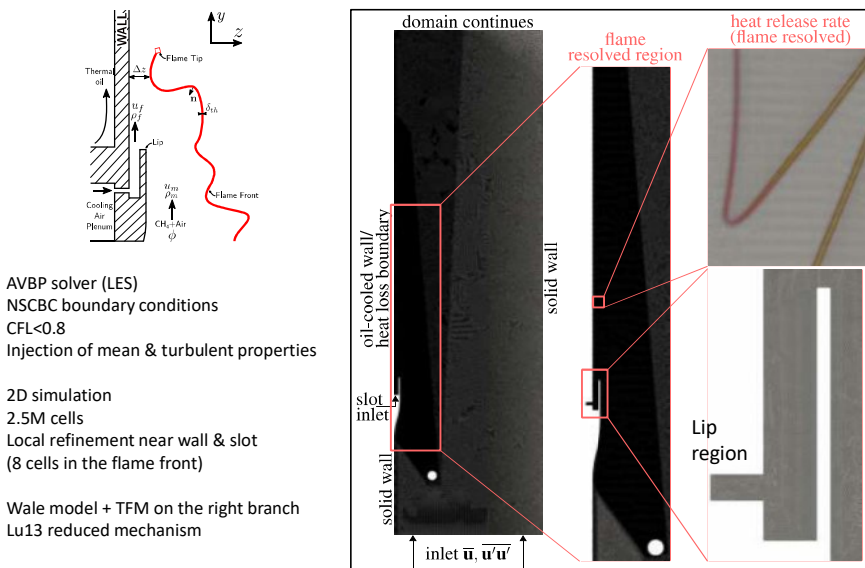


# 2'/ FCAI – EXP / CFD



Mimic the FCAI case with high-fidelity numerical simulations (LES)  
 Obtain non-accessible scalars to better understand near-wall flame dynamics & CO emissions

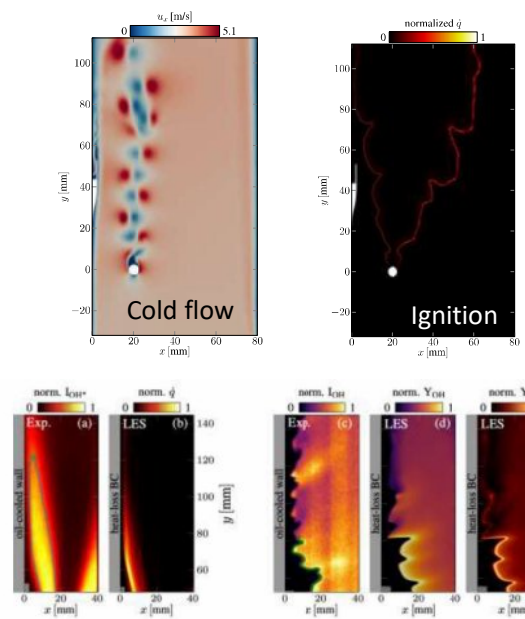
➤ Joint work w/ TU Berlin (M. Casel, A. Ghani)



AVBP solver (LES)  
 NSCBC boundary conditions  
 CFL < 0.8  
 Injection of mean & turbulent properties

2D simulation  
 2.5M cells  
 Local refinement near wall & slot  
 (8 cells in the flame front)

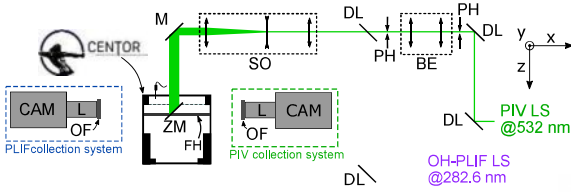
Wale model + TFM on the right branch  
 Lu13 reduced mechanism



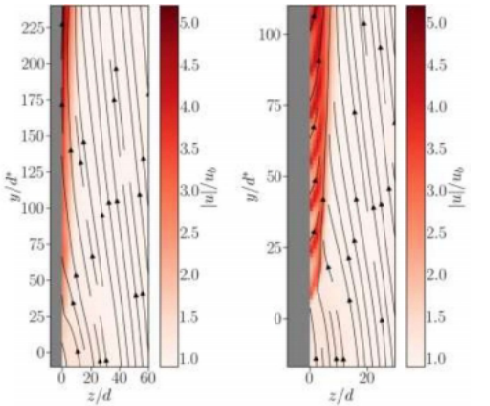
First EXP/CFD comparisons

# 3/ Flame-wall interactions w/ effusion walls

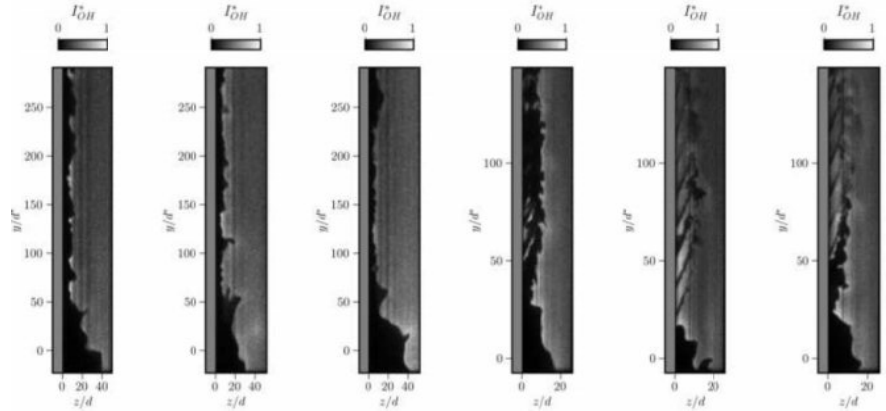
Investigation of cold-flow topology and flame dynamics w/ realistic effusion walls (< mm)  
 Multi-perforated plate from SAFRAN is inserted in the CENTOR test bench (protected geometry)



PIV (w/ solid seeding)  
 OH-PLIF  
 Variation of the hole diameter, equivalence ratio, blowing ratio



Analysis of the air-film establishment & mainstream disturbance (cold)



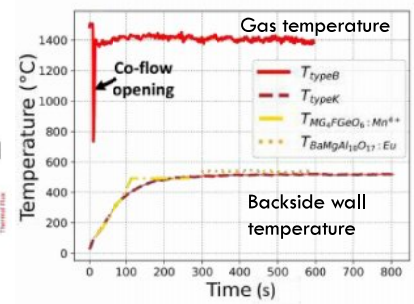
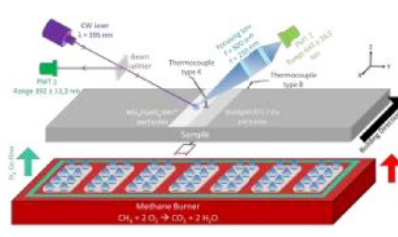
Flame dynamics with the flame penetration into the cooling air-film

# 4/ Durability of metallic walls



Influence of realistic gas thermochemistry (T, X) during thermal aggression processes Provide more quantitative information in the near-wall gas phase

➤ Joint work w/ CNRS GPM-France (B. Vieille, F. Barbe)



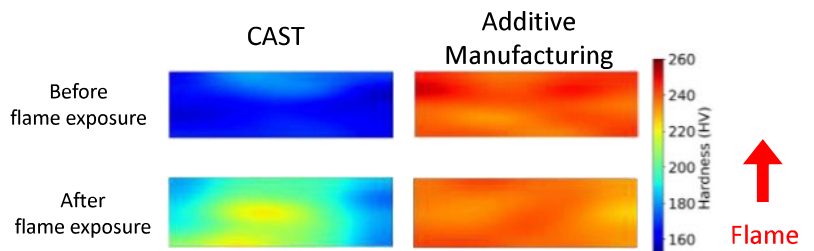
Implementation of laser-based diagnostics in the near-wall region



Uniform/stratified thermal aggression w/ laminar flames



Mechanical / microstructure properties



Comparison before-after aggression w/ the effect of manufacturing process

## More details here:

- A. Blaise, G. Godard, A. Vandel, F. Grisch, P. Xavier "Two-photon planar laser-induced fluorescence of near-wall CO during the interaction between a flame and a cooling air film", *21th Int. Symposium on applications of Laser and Imaging Techniques to Fluid Mechanics*, 2024, Lisbon, Portugal.
- A. Blaise, S. Petit, F. Grisch, P. Xavier "Effect of the blowing ratio on the interaction between a flame and an air-cooled combustor wall", *ASME Turbo Expo: Turbine Technical Conference and Exposition*, 2023, Boston, MA, USA.
- P. Xavier, A. Blaise, B. Quevreux, B. Mille, S. Pascaud, C. Viguier, F. Grisch "Experimental investigation of direct flame-cooling air interaction with an effusion cooled combustor wall", *ASME Turbo Expo: Turbine Technical Conference and Exposition*, 2023, Boston, MA, USA.
- A. Chaudhary, A. Coppalle, G. Godard, P. Xavier, B. Vieille, Phosphor thermometry for surface temperature measurements of composite materials during fire test, *International Journal of Heat and Mass Transfer*, 211, 124215, 2023 (<https://doi.org/10.1016/j.ijheatmasstransfer.2023.124215>)
- S. Petit, B. Quevreux, R. Morin, R. Guillot, F. Grisch, P. Xavier, Experimental investigation of flame-film cooling interactions with an academic test rig and optical laser diagnostics, *Journal of Turbomachinery* 145(4), 041007, 2023 (<https://doi.org/10.1115/1.4055867>)
- S. Petit, A. Blaise, G. Godard, B. Mille, T. Muller, P. Toutain, F. Grisch, P. Xavier "Experimental study of the interaction between a turbulent flame and a cooling air film", *20th Int. Symposium on applications of Laser and Imaging Techniques to Fluid Mechanics*, 2022, Lisbon, Portugal.
- S. Petit, P. Xavier, G. Godard, F. Grisch, Improving the temperature uncertainty of  $Mg_2FGeO_6:Mn^{4+}$  ratio-based phosphor thermometry by using a multi-objective optimization procedure, *Applied Physics B* 128, 57, 2022 (<https://doi.org/10.1007/s00340-021-07733-3>)
- S. Petit, P. Xavier, F. Grisch, Spatial and spectral filtering strategies for surface phosphor thermometry measurements, *Measurements Science and Technology* 33, 115022, 2022 (<https://doi.org/10.1088/1361-6501/ac894c>)
- S. Petit, P. Xavier, F. Grisch, Temperature Uncertainty Improvements of Surface Phosphor Thermometry for Imaging Applications, *Optical Sensors and Sensing Congress (AIS, LACSEA, Sensors, ES)*, LTh3E.3, 2022 (<https://doi.org/10.1364/LACSEA.2022.LTh3E.3>)

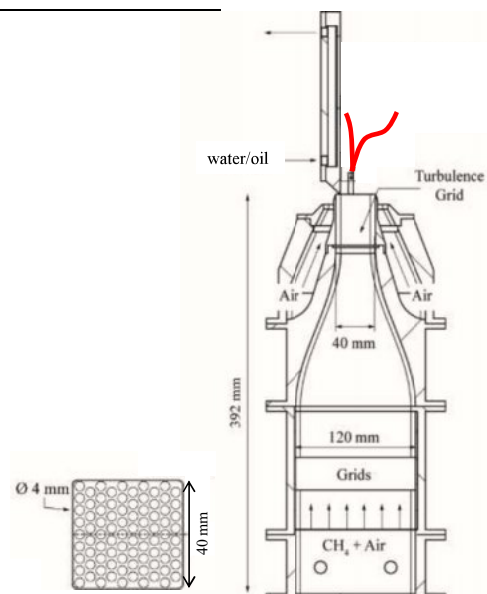
Contact: [pradip.xavier@coria.fr](mailto:pradip.xavier@coria.fr)



## Flame vortex interaction (FVI) in FWI

University of Edinburgh & TU Darmstadt

PIV, wavelet-based optical flow, OH-LIF

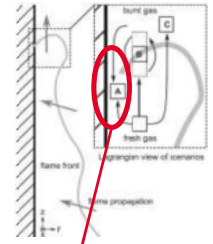
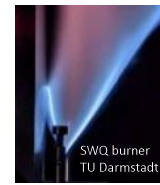




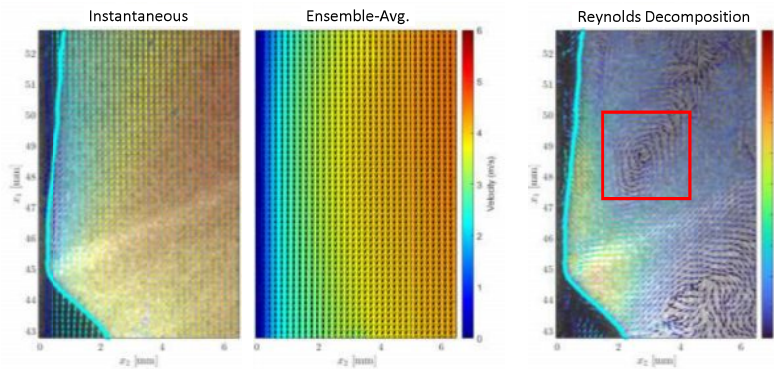
# Flame Vortex Interaction (FVI) in FWI

- High-speed PIV & OH-LIF in SWQ burner
  - $Re = 5900$ ; **turbulent**; DME-air  $\Phi = 0.83$
- Zengraf et al. - FVI is plausible mechanism for mass transport at quenching
- Lagrangian view needed to visualize FVI
  - Reynolds decomposition  $\rightarrow$  Lagrangian view in boundary layer flows.

Zengraf et al. *Combust. Flame* 111681 (2022)

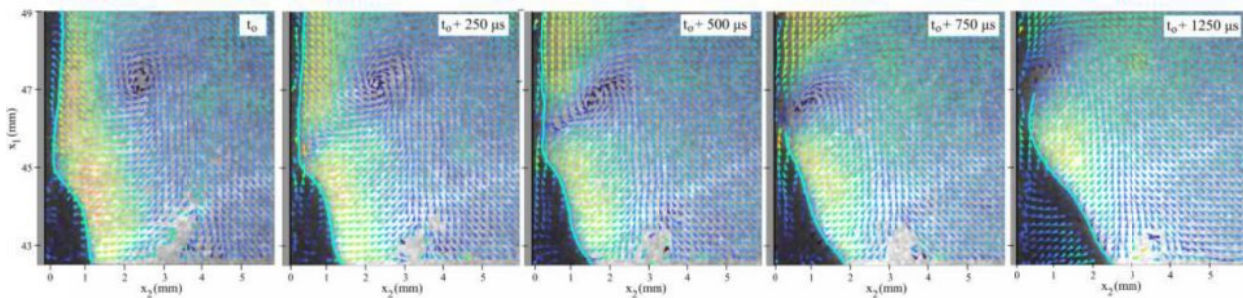
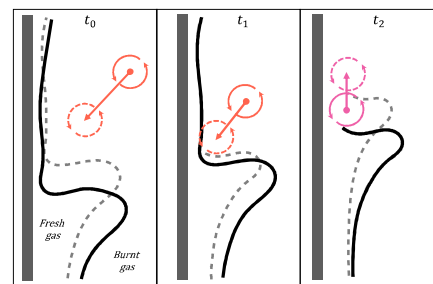


High CO<sub>2</sub> mole fractions at low T



# Flame Vortex Interaction (FVI) in FWI

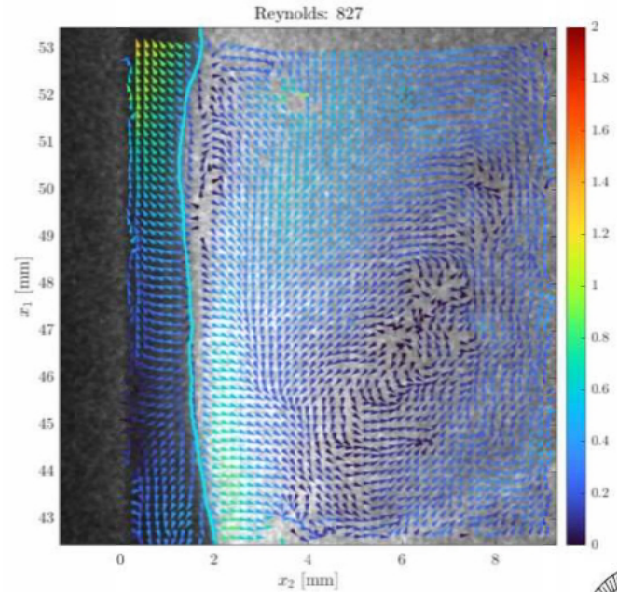
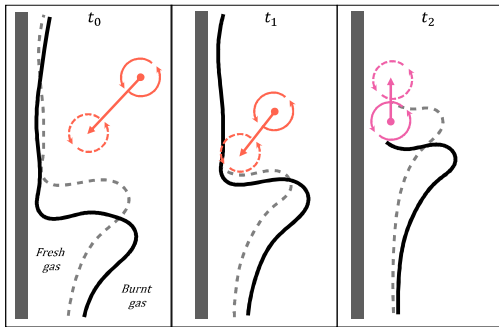
- CCW vortex emerges in burnt gas region
- Vortex approaches wall and flame quenches
  - HOQ to SWQ configuration
- Vortex remains above quenching location.





# FVI Sequence – PIV analysis

- CCW vortex emerges in burnt gas region
- Vortex approaches wall and flame quenches
  - HOQ to SWQ configuration
- Vortex remains above quenching location.



# Flame Vortex Interaction (FVI) in FWI

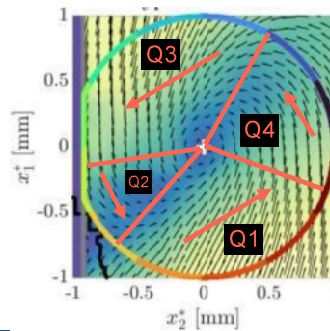
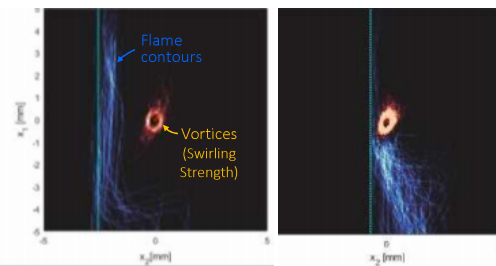
## Statistics

- 17 vortex events in 1000 image sequence (0.25 sec)
- All events: HOQ → SWQ & vortex remains above quenching

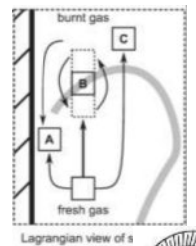
## Wavelet-based Optical Flow

- Quenching phenomena
  - FVI pushes flame towards wall. Excess heat loss & increased strain occur.
- Transport
  - Non-reacting flow = sweep & ejection events dominate (Q4, Q2)
  - FVI intensifies “in” and “out” events (Q3, Q1)
  - Flow structure supports hypothesis from Zentgraf et al.

Conditionally avg. on vortex center (17 events; ~240 images)



Q2 - Ejection $u_1 = -$ $u_2 = +$	Q1 - Outward $u_1 = +$ $u_2 = +$
Q3 - Inward $u_1 = -$ $u_2 = -$	Q4 - Sweep $u_1 = +$ $u_2 = -$

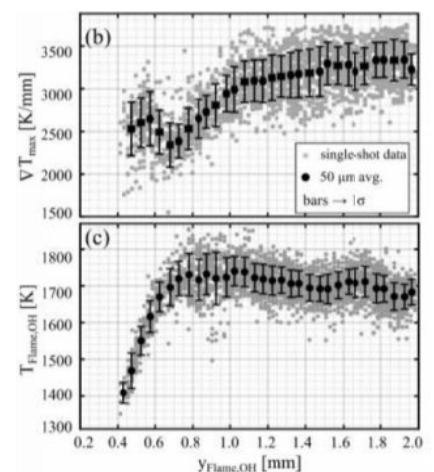
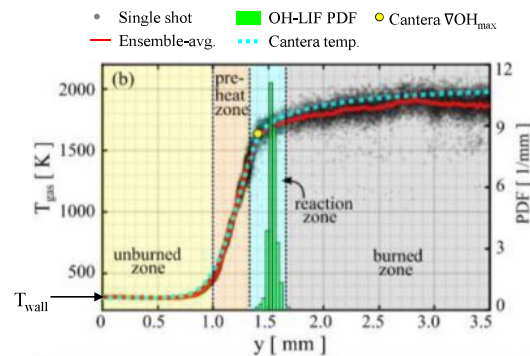
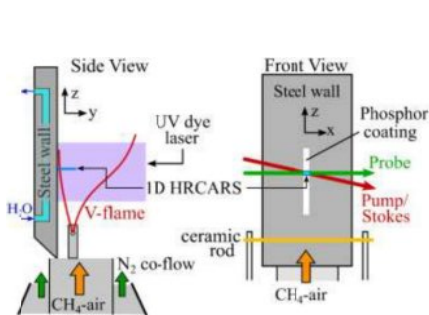


## Changes in flame thermal structure during FWI

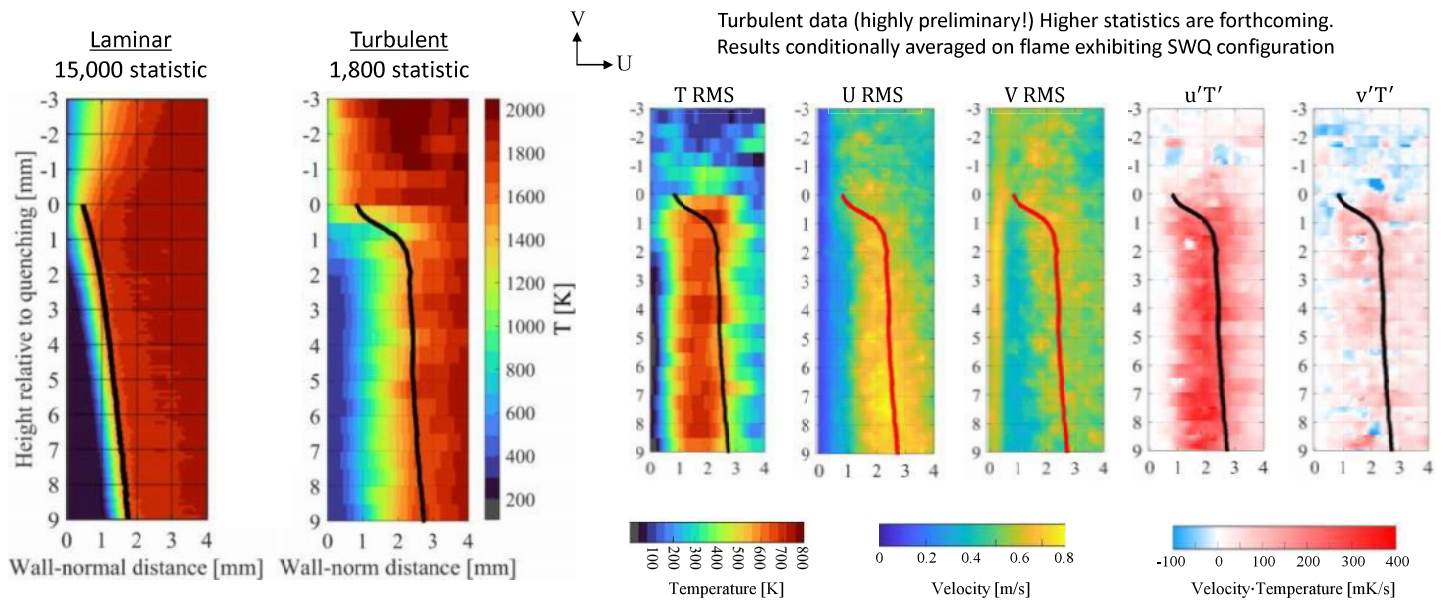
University of Edinburgh  
1D CARS, OH-LIF, Phosphor Thermometry

## Thermal flame structure

- SWQ burner:  $Re = 5900$ ; **LAMINAR**;  $CH_4$ -air  $\Phi = 0.83$
- Wall-normal temperature profiles of flame during FWI
  - Evaluate thermal flame structure as function of wall heat loss
  - $\nabla T_{max}$  (in preheat zone) and  $T_{flame}$  ( $T_{gas}$  at OH-LIF) as function of flame-wall distance



# Ensemble temperature field and flame



*FWI in two-wall passages -  
Impact of thermodiffusive instabilities on wall heat flux*

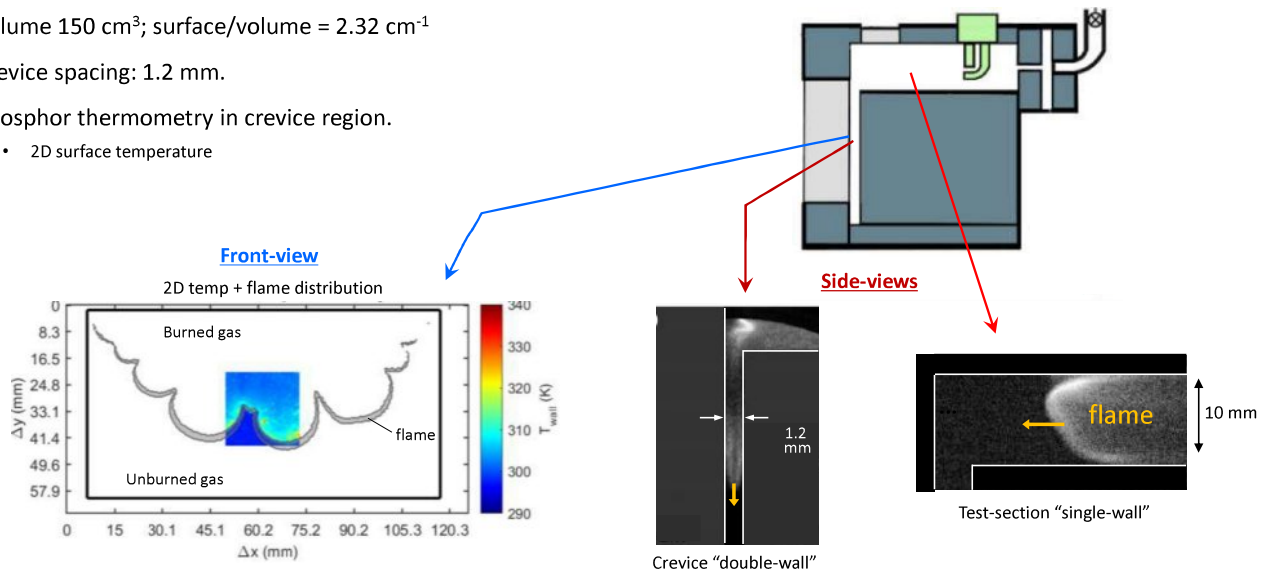
*University of Edinburgh  
Phosphor thermometry & chemiluminescence*



# FWI in Fixed Volume Chamber

- Escofet-Martin et al. *Proc. Combust. Inst.* 38 (2021)
- Ojo et al., *Combust. Flame.* 233 (2021)
- Ojo et al., *Combust. Flame* 240 (2022)
- Ojo et al., *Proc. Combust. Inst.* 39 (2023)

- Premixed charge ( $\text{CH}_4\text{-air } \Phi = 1.0$ ;  $\text{H}_2\text{-air } \Phi = 0.45$ ) filled to select pressure (1-2 bars)
- Volume  $150 \text{ cm}^3$ ; surface/volume =  $2.32 \text{ cm}^{-1}$
- Crevice spacing: 1.2 mm.
- Phosphor thermometry in crevice region.
  - 2D surface temperature



# Lean Hydrogen vs. Methane

Ojo et al., *Flow Turb. Combust.* (in review)

- Flame power
  - $\text{CH}_4\text{-air } \Phi=1.0 \rightarrow 4.5 \text{ MW}$
  - $\text{H}_2\text{-air } \Phi=0.45 \rightarrow 1.6 \text{ MW}$
- Hotter cellular structures on wall for lean  $\text{H}_2$  - thermodiffusive instabilities
- Locally higher  $T_{\text{wall}}$

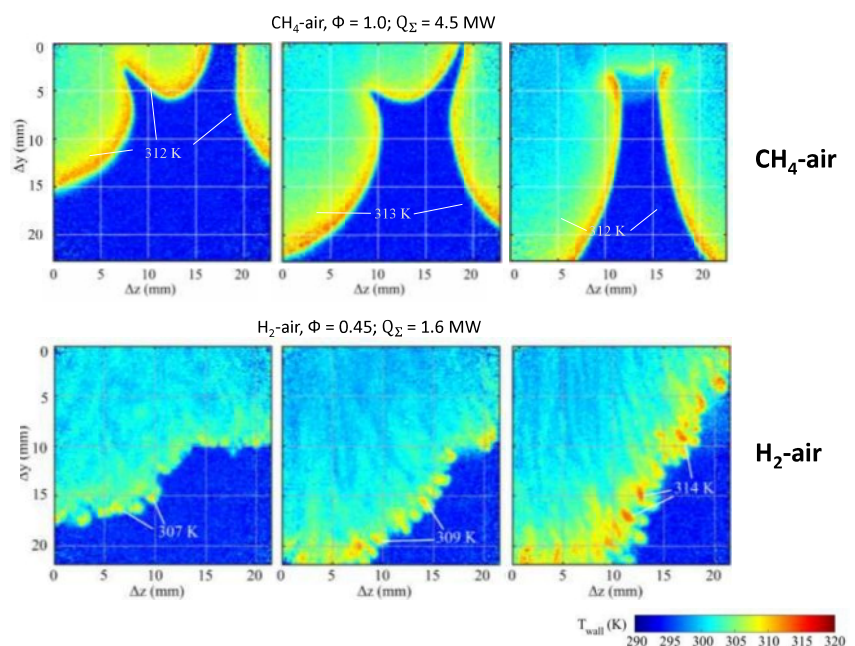
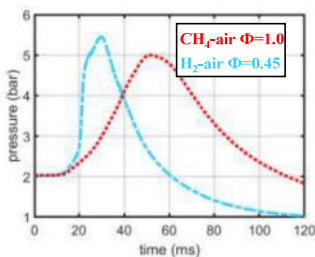
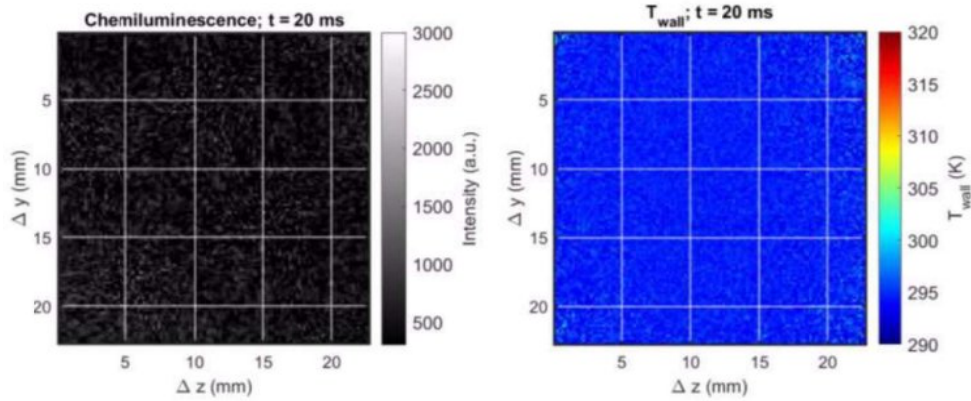




# Image sequence 1 kHz – lean hydrogen

Ojo et al., *Flow Turb. Combust.* (in review)

- Hydrogen-air ( $\Phi = 0.45$ ;  $Q_\Sigma = 1.6 \text{ MW}^*$ )
- Thermodiffusive instabilities

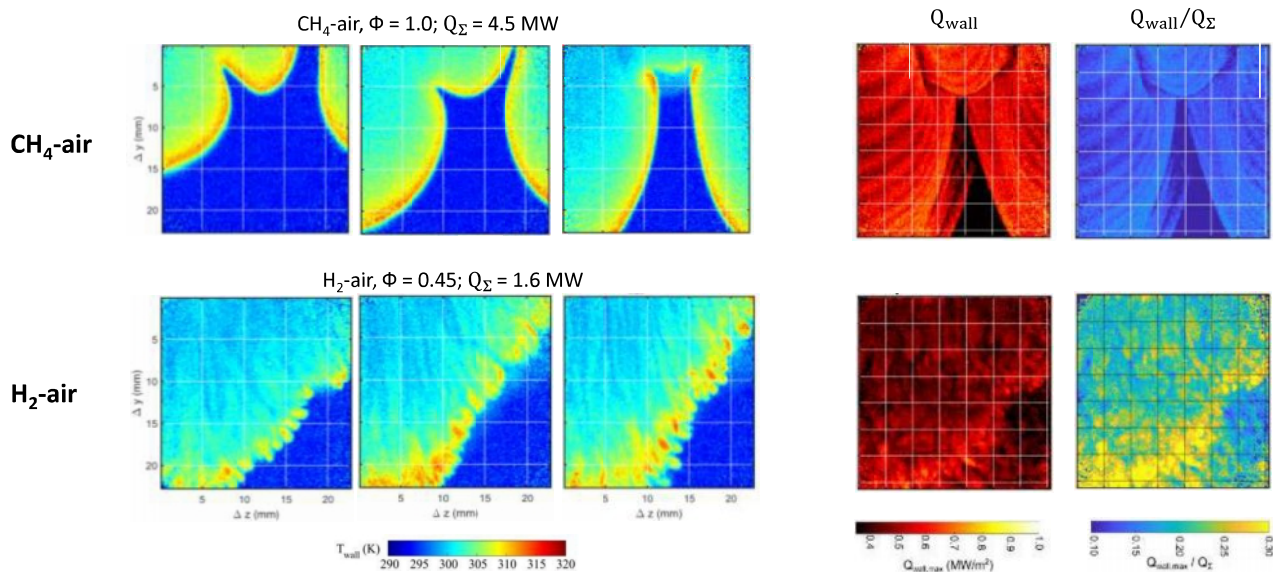


Weak signals from  $\text{OH}^*$  &  $\text{H}_2\text{O}^*$

## Wall heat flux

$$Q_{\text{wall}}(t) = \sqrt{\frac{\rho C_p k}{\pi}} \int_0^t \frac{dT_{\text{wall}}(\bar{\tau})/d\bar{\tau}}{\sqrt{t-\bar{\tau}}} d\bar{\tau}$$

Ojo et al., *Flow Turb. Combust.* (in review)





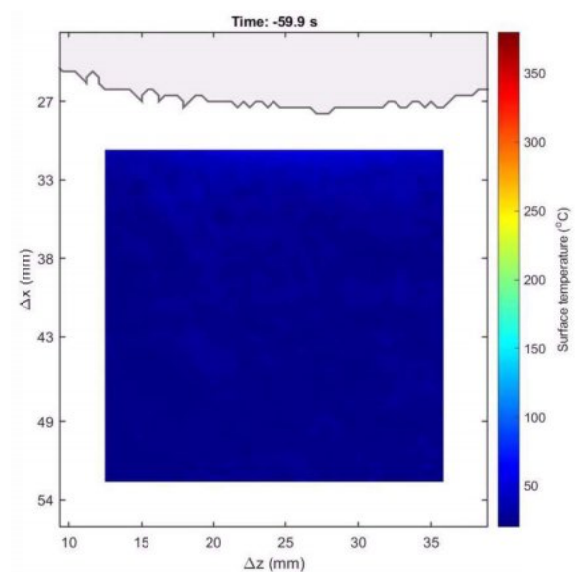
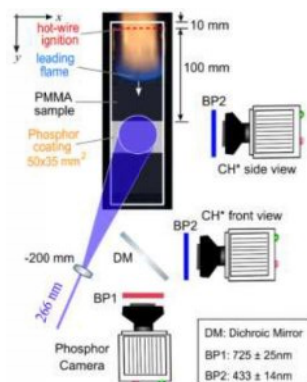
## FWI during flame spread on PMMA surfaces

University of Edinburgh  
Phosphor thermometry, CH\* imaging

## Downward flame spread

Burnford et al. Fuel 365 (2024)  
Morrisset et al. Proc. Combust. Inst. 40 (2025)

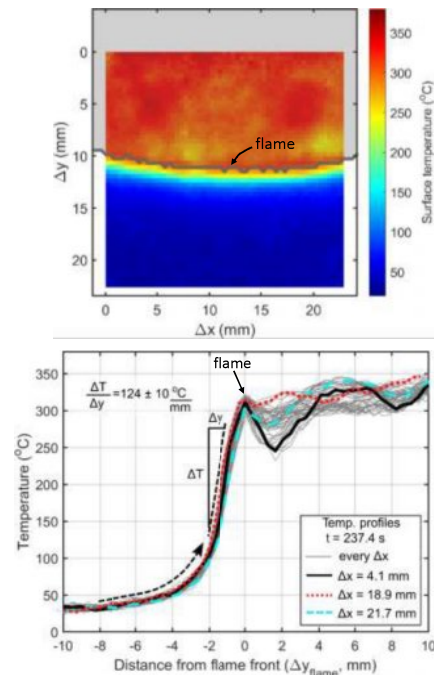
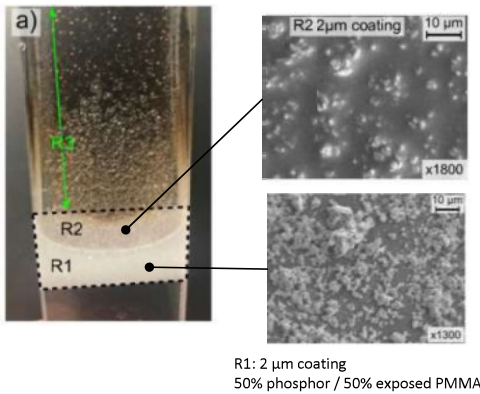
- PMMA samples –  $200 \times 50 \times 12 \text{ mm}^3$
- Surface temperature (phosphor thermometry) and CH\* imaging
  - $\text{Gd}_3\text{Ga}_5\text{O}_{12}:\text{Cr,Ce}$
  - $2 \mu\text{m}$  coating thickness



# Downward flame spread

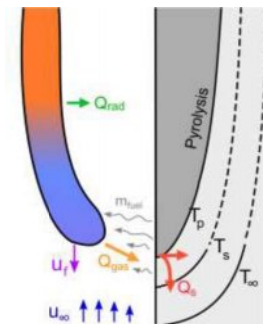
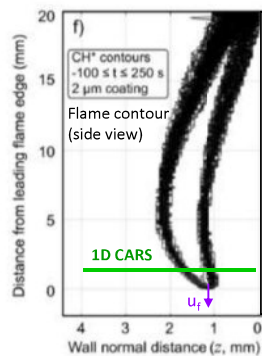
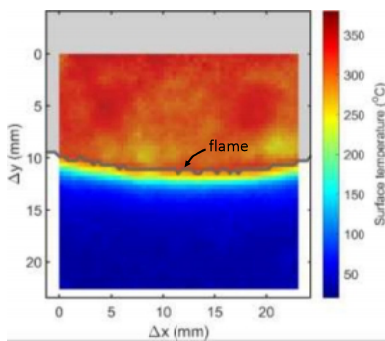
Burnford et al. Fuel 365 (2024)  
Morrisset et al. Proc. Combust. Inst. 40 (2025)

- Sharp gradients in front of flame
- Onset of pyrolysis  $\sim 1$  mm ahead of the flame
- Temperature beneath flame in burning region
  - Phosphors sink into PMMA
  - Temperature dip after flame related to endothermic reactions



# Downward flame spread

- Future work: Studying the heat transfer, chemical, and fluid mechanic processes that govern the flame spread rate ( $u_f$ )
  - 1D CARS, Phosphor thermometry,  $\text{CH}_2\text{O}$  and OH-LIF, PIV, Two-color pyrometry



# FWI STUDIES AT TU DARMSTADT

## 1 Passive walls

- FWI at elevated pressure (finished)
- FWI for H<sub>2</sub>/air flames at 1 bar (WIP)

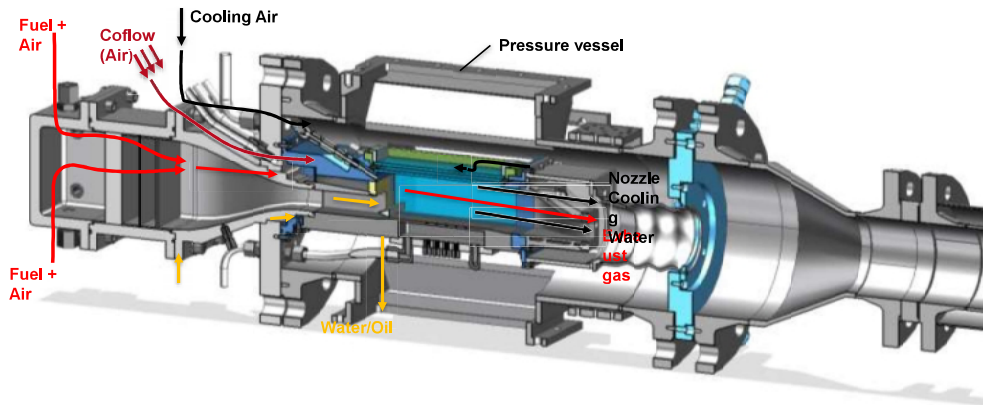
## 2 Active walls

- Flame-wall-effusion cooling air interaction 1 bar (WIP)
- Boundary layer flames and pyrolysis of polymer samples 1 bar (WIP)

# PASSIVE WALLS

Flame-wall interaction at elevated pressure

# FWI AT ELEVATED PRESSURE – NOVEL COMBUSTOR

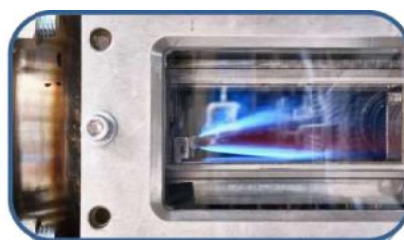


- Johe et al., Dreizler; I. J. Heat Fluid Flow 94 (2022) 108921
- Johe et al., Dreizler; Proceedings of the Combustion Institute 39, Issue (2023) 2159-2168
- Johe et al., Dreizler; Combustion and Flame 260 (2024) 113214

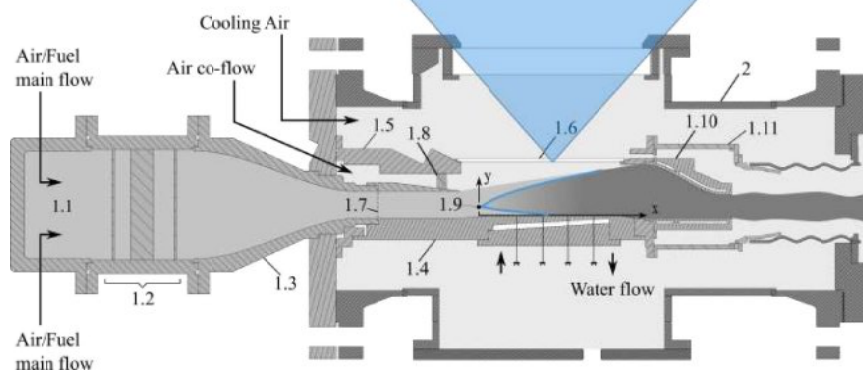
# FWI AT ELEVATED PRESSURE

## Main design features:

- Pressure vessel for up to 10 bar
- Optical access from 3 sides
- Temperature-controlled quenching wall
- V-shaped flame stabilized at ceramic rod



- 1.1 Burner plenum
- 1.2 Flow homogenization (grids & meshes)
- 1.3 Morel type nozzle
- 1.4 Quenching wall
- 1.5 Flame tube
- 1.6 Quartz glass windows



- 1.7 Turbulence-generating grid
- 1.8 Co-flow homogenization (sintered bronze structure)
- 1.9 Ceramic rod
- 1.10 Exhaust gas nozzle
- 1.11 Exhaust gas plenum
- 2 Pressure vessel

## OPERATION CONDITIONS

Pressure: 1 and 3 bar

CH<sub>4</sub>/air,  $\phi = 0.8$

Ratio  $u_B/s_L$  const to achieve mean quenching position located at similar axial position, therefore different Re-numbers

$p$ (bar)	$u_B$ (m/s)	$s_L$ (m/s)	$Re$ (–)	$T_{wall}$ (K)
1	3.8	0.27	8200	319 ± 1.6
3	2.3	0.17	15,000	359 ± 2.4

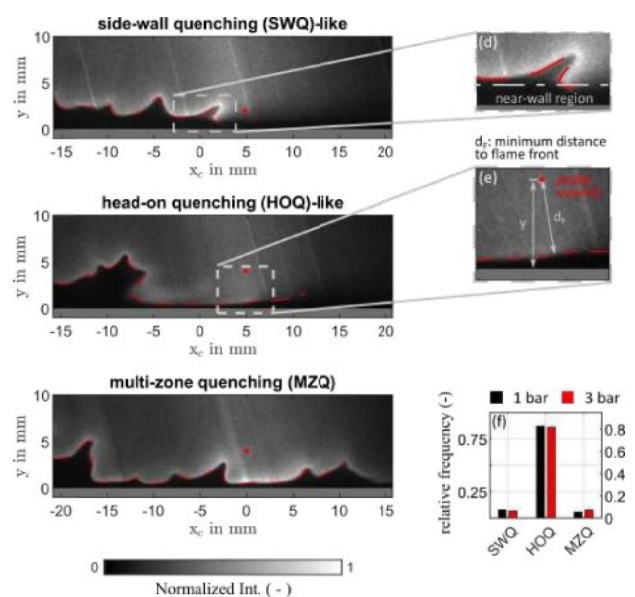
$s_L$  from 1D Cantera simulations, GRI 3.0

31

## AVAILABLE QUANTITIES

### Parameters measured by laser diagnostics

- Flow field (2C2D PIV)
- Flame front location, flame brush, flame surface density (OH-PLIF)
- Gas temperature (DP-CARS)
- CO<sub>2</sub> and CO mole fractions (DP-CARS, LIF)



Classification in SWQ, HOQ, and MZQ <sup>32</sup>

- Johe et al., Dreizler; I. J. Heat Fluid Flow 94 (2022) 108921
- Johe et al., Dreizler; PROCI39, Issue (2023) 2159-2168
- Johe et al., Dreizler; Combustion and Flame 260 (2024) 113214

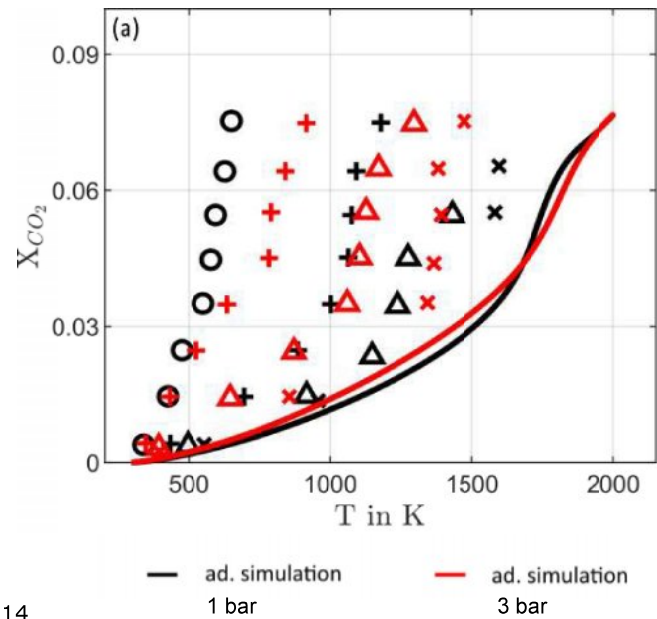


## EXEMPLARY RESULTS

### CO<sub>2</sub> – T – correlation 1 bar vs 3 bar

Conditional averages for various wall distances

1 bar		3 bar	
○	y = 0.1 mm	+	y = 0.4 mm
+	y = 0.35 mm	△	y = 0.65 mm
△	y = 0.65 mm	×	y = 0.85 mm
×	y = 0.85 mm		



- Johe et al., *Combustion and Flame* 260 (2024) 113214

33

## FWI STUDIES AT TU DARMSTADT

### 1 Passive walls

- FWI at elevated pressure (finished)
- FWI for H<sub>2</sub>/air flames at 1 bar (WIP)

### 2 Active walls

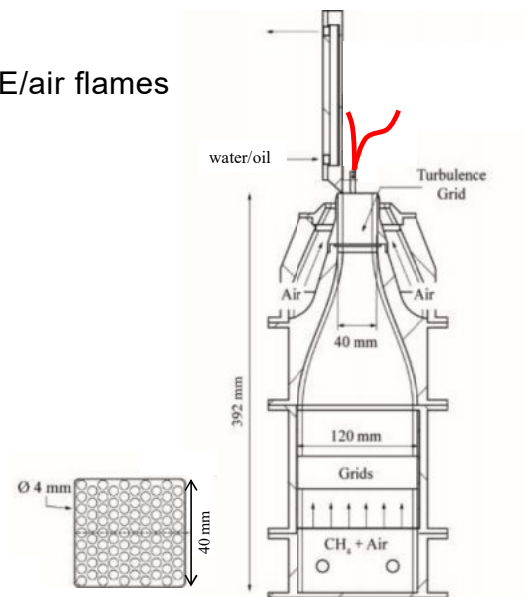
- Flame-wall-effusion cooling air interaction 1 bar (WIP)
- Boundary layer flames and pyrolysis of polymer samples 1 bar (WIP)

34

## PASSIVE WALLS

Flame-wall interaction for  $H_2$ /air flames

- Configuration adapted from previous  $CH_4$  and DME/air flames
- Work-in-progress



35

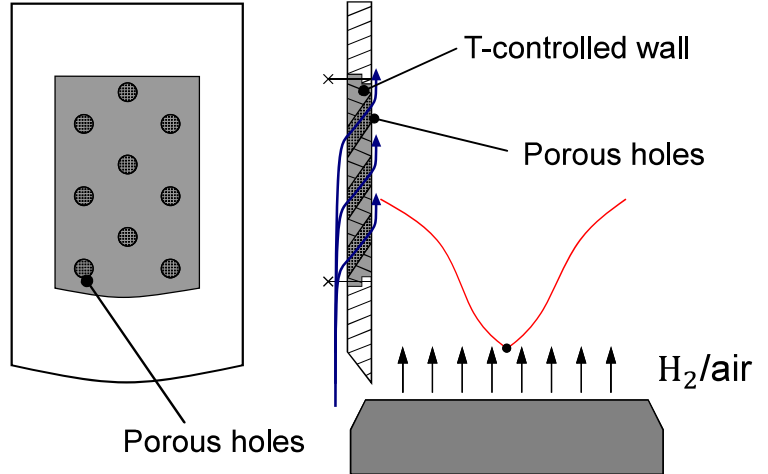
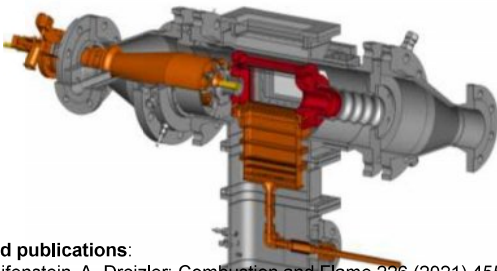
## ACTIVE WALLS

36

## ACTIVE WALLS

### Flame-wall-effusion cooling air interaction for $H_2$ /air flames

- Work-in-progress
- Complement our studies of flame-wall-effusion cooling air interaction at elevated pressure



#### Related publications:

M. Greifenstein, A. Dreizler: *Combustion and Flame* 226 (2021) 455–466

M. Greifenstein, A. Dreizler: *International Journal of Heat and Fluid Flow* 88 (2021) 108768

M. Greifenstein, J. Hermann, B. Böhm, A. Dreizler: *Experiments in Fluids* 60, Article number: 10 (2019)

J. Hermann, M. Greifenstein, B. Böhm, A. Dreizler: *Flow, Turbulence and Combustion* 102, pages 1025–1052 (2019)

37

## FWI STUDIES AT TU DARMSTADT

### 1 Passive walls

- FWI at elevated pressure (finished)
- FWI for  $H_2$ /air flames at 1 bar (WIP)

### 2 Active walls

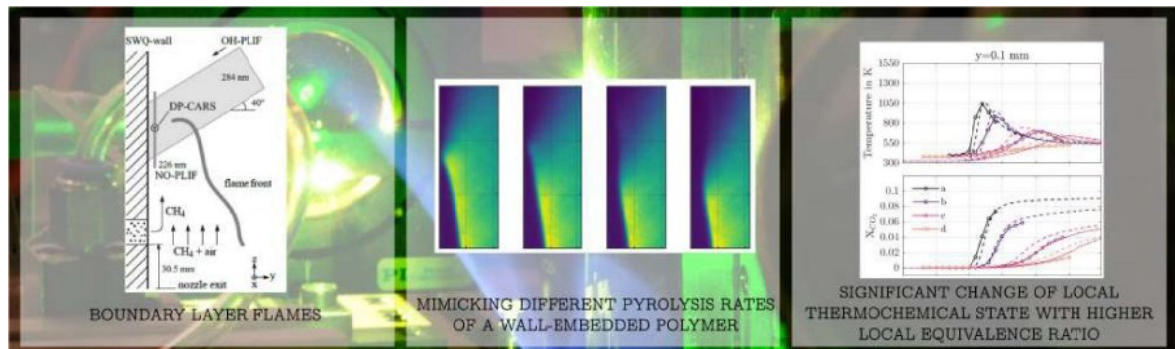
- Flame-wall-effusion cooling air interaction 1 bar (WIP)
- **Boundary layer flames and pyrolysis of polymer samples 1 bar (WIP)**

38

## ACTIVE WALLS

**Stratified boundary-layer flames, mimicking pyrolysis and combustion of a polymer**

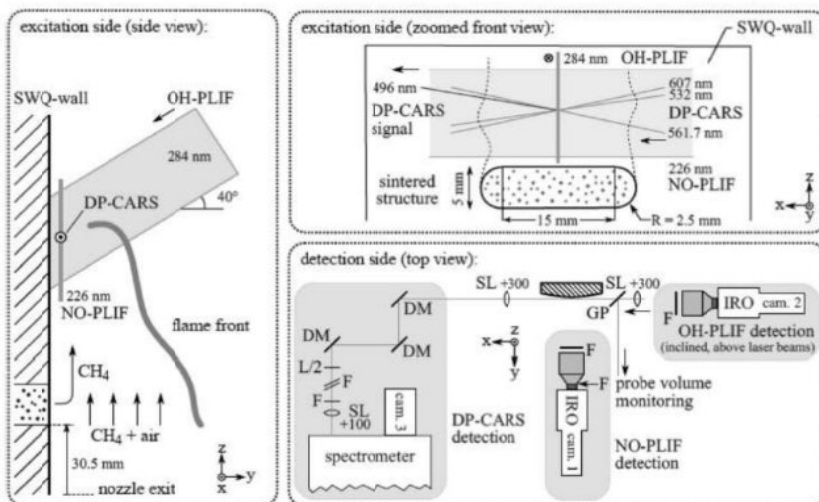
- Fuel supply upstream quenching point
- Position of reaction zone (OH-PLIF)
- Mixture fraction upstream reaction zone (NO-PLIF)
- Gas temperature and CO<sub>2</sub> mole fraction (DP-CARS)



Greifenstein et al. Dreizler; Experiments in Fluids (2024) 65:7

39

## EXPERIMENTAL SETUP, OPERATIONAL CONDITIONS



### V-flame

- CH<sub>4</sub>/air,  $\phi = 1.0$
- Re = 5900 (laminar)

### Wall

- Temperature stabilized at 60° C

### Secondary fuel supply

- CH<sub>4</sub> (upstream quenching point)
- Flow rate varied from 0 to 4.5 Lh<sup>-1</sup>

Case	a	b	c	d
$\dot{V}$	0 Lh <sup>-1</sup>	2 Lh <sup>-1</sup>	3.5 Lh <sup>-1</sup>	4.5 Lh <sup>-1</sup>

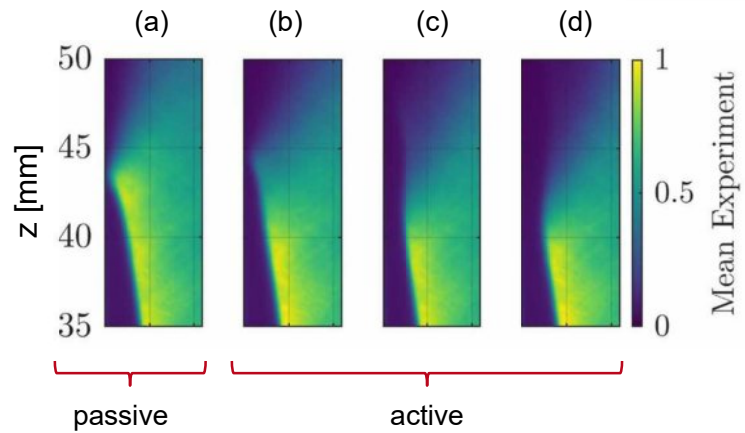
Greifenstein et al. Dreizler; Experiments in Fluids (2024) 65:7

40

## RESULTS – STRATIFIED BOUNDARY-LAYER FLAMES

Mean OH-PLIF signals (normalized)

- Change of flame topology by secondary fuel supply



Case	a	b	c	d
$\dot{V}$	$0 \text{ Lh}^{-1}$	$2 \text{ Lh}^{-1}$	$3.5 \text{ Lh}^{-1}$	$4.5 \text{ Lh}^{-1}$

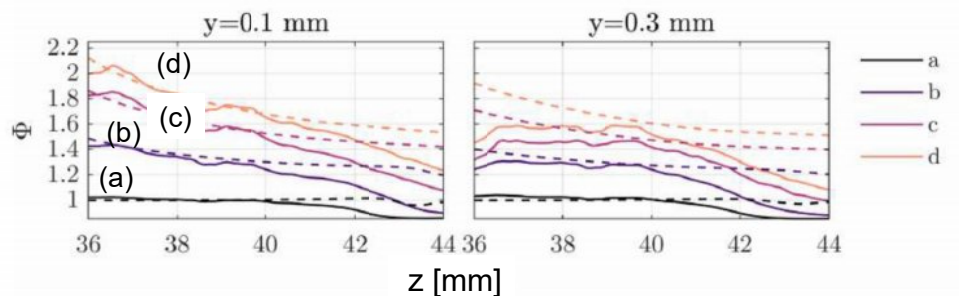
Greifenstein et al. Dreizler; Experiments in Fluids (2024) 65:7

41

## RESULTS – STRATIFIED BOUNDARY-LAYER FLAMES

Equivalence ratio in axial direction for 0.1 and 0.3 mm from the wall

- NO-LIF data only in yet non-reacted gas up to 2 mm from the flame
- Dashed lines: simulation from STFS (C. Hasse et al.)



Case	a	b	c	d
$\dot{V}$	$0 \text{ Lh}^{-1}$	$2 \text{ Lh}^{-1}$	$3.5 \text{ Lh}^{-1}$	$4.5 \text{ Lh}^{-1}$

Greifenstein et al. Dreizler; Experiments in Fluids (2024) 65:7

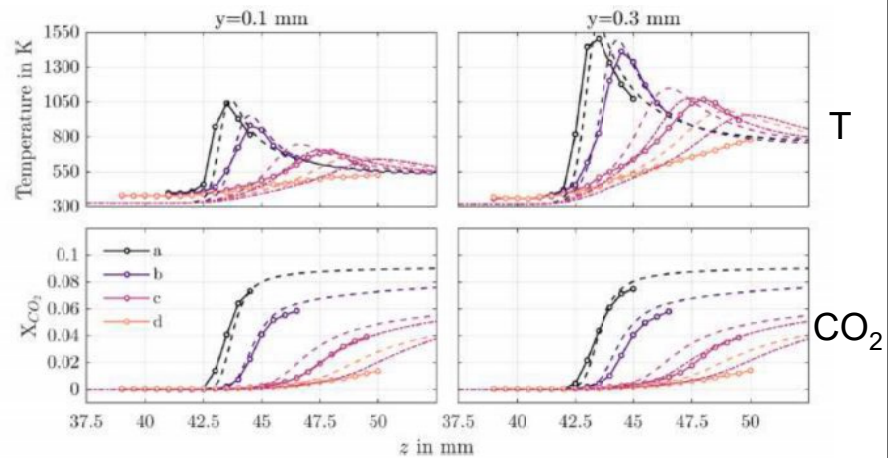
42



## RESULTS – STRATIFIED BOUNDARY-LAYER FLAMES

Wall-parallel temperature & CO<sub>2</sub> profiles

- Increasing flowrate of secondary fuel shifts the thermochemical states toward lower temperatures and lower CO<sub>2</sub> mole fractions
- Dashed lines: simulation from STFS (C. Hasse et al.)



Case	a	b	c	d
$\dot{V}$	0 Lh <sup>-1</sup>	2 Lh <sup>-1</sup>	3.5 Lh <sup>-1</sup>	4.5 Lh <sup>-1</sup>

Solid lines: EXP  
Dashed lines: SIM

Greifenstein et al. Dreizler; Experiments in Fluids (2024) 65:7

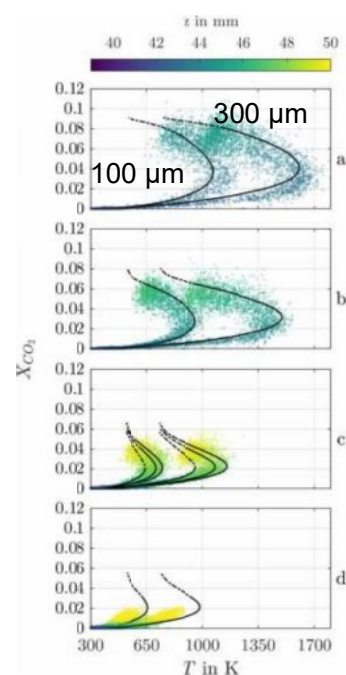
43

## RESULTS – STRATIFIED BOUNDARY-LAYER FLAMES

CO<sub>2</sub>-T-Scatter plots

Color indicates z-coordinate

- Thermochemical state strongly changed by secondary inflow
- Lines: simulation from STFS (C. Hasse et al.)



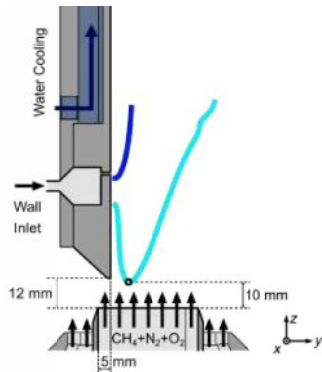
Greifenstein et al. Dreizler; Experiments in Fluids (2024) 65:7

44

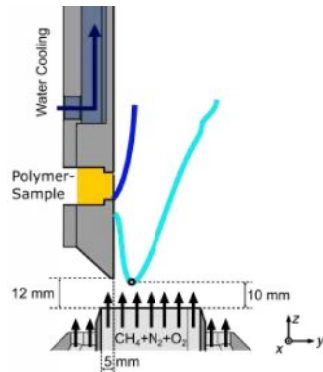
## NEW CASE – WORK IN PROGRESS

Stratified boundary-layer flames, mimicking **pyrolysis and combustion of a polymer**

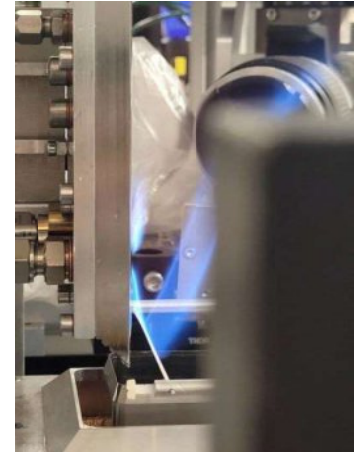
- Lean  $\text{CH}_4/\text{air}$  V-flame with excess  $\text{O}_2$
- Fuel supply **downstream** quenching point ( $\text{CH}_4$ , polymer)



Case 1:  $\text{CH}_4$  inlet



Case 2: Polymer sample



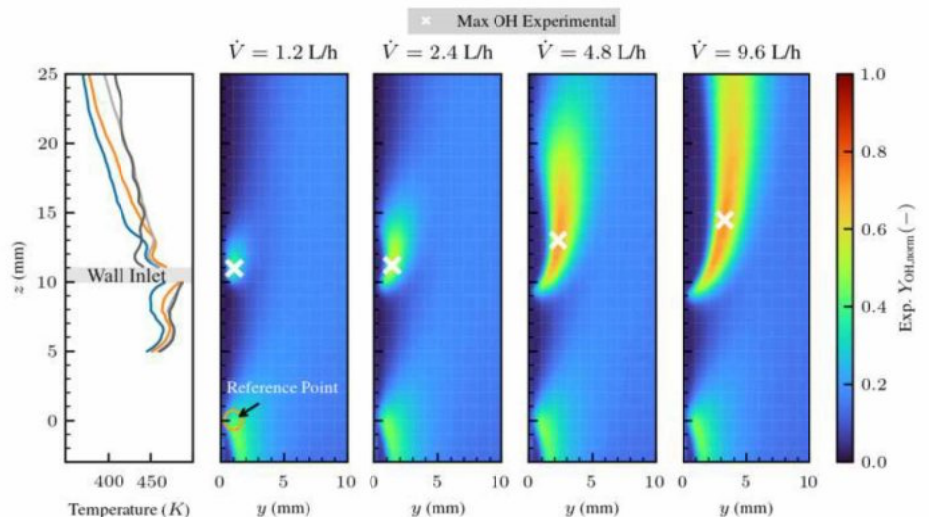
Case 1:  $\text{CH}_4$  inlet

45

## RESULTS (SELECTED)

Stratified boundary-layer flames, mimicking **pyrolysis and combustion of a polymer**

- Case 1  $\text{CH}_4$  at wall inlet
- OH-PLIF and wall temp.



46

## SUMMARY

### Benchmark configurations ready to be used in a TNF-style manner

- **Passive walls:**
  - SWQ-type configuration, open and at elevated pressure, two-wall passage
  - SWQ-H<sub>2</sub>/air flame-wall interaction is WIP
- **Active walls:**
  - Flame-effusion cooling-air interaction: enclosed available, open w/ H<sub>2</sub> is WIP
  - Stratified boundary layer flames: available, more data to come
  - Polymer near-wall combustion: WIP any interest by the TNF/PTF community?

**Thank you for your kind attention**

TNF16 2024, MILAN, ITALY

# FLAME-WALL INTERACTION (MODELING AND SIMULATION)



Special thanks to Max Schneider

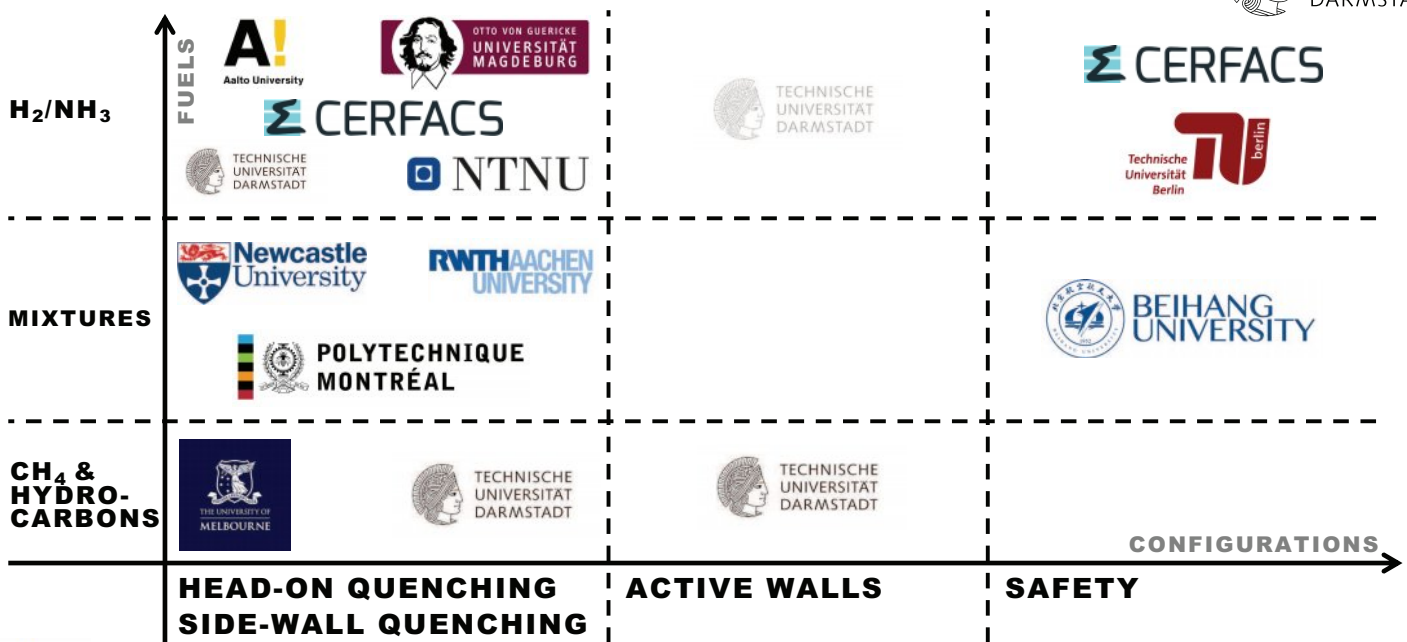
SESSION COORDINATORS: ANDREAS DREIZLER, CHRISTIAN HASSE

11.09.24

Mechanical Engineering | Simulation of reactive Thermo-Fluid Systems | Christian Hasse

1

## AGENDA / CONTRIBUTIONS



# KEY OBSERVATIONS

## PHYSICAL UNDERSTANDING

### 1: New fuels and mixtures

FWI for  $H_2/NH_3$  differs significantly from hydrocarbons ( $CH_4, \dots$ ), even in simple geometries

### 2: Beyond standard FWI

More complex configurations: effusion cooling, active walls with polymers...

New application areas: safety/flashback, ...

## METHODOLOGY

### 3: Increase in number of DNS studies

More DNS than LES

FWI → lack of knowledge for new fuels

Numerical experiments → fundamental for model development

# KEY OBSERVATIONS

## PHYSICAL UNDERSTANDING

### 1: New fuels and mixtures

FWI for  $H_2/NH_3$  differs significantly from hydrocarbons ( $CH_4, \dots$ ), even in simple geometries

### 2: Beyond standard FWI

More complex configurations: effusion cooling, active walls with polymers...

New application areas: safety/flashback, ...

## METHODOLOGY

### 3: Increase in number of DNS studies

More DNS than LES

FWI → lack of knowledge for new fuels

Numerical experiments → fundamental for model development

### Not the best example for TNF style discussion

- There is not a single aspect such as multi regime combustion but a multitude of key findings and challenges
- Many different configurations in 13 contributions
- Almost as many fuels/fuel mixtures as configurations



# KEY MESSAGES AND CHALLENGES

## HYDROCARBONS

Key Message 1: Advanced near-wall combustion models available

KM1

## H<sub>2</sub>/NH<sub>3</sub> AND MIXTURES

Key Challenge 1: Near-wall chemistry

KC1

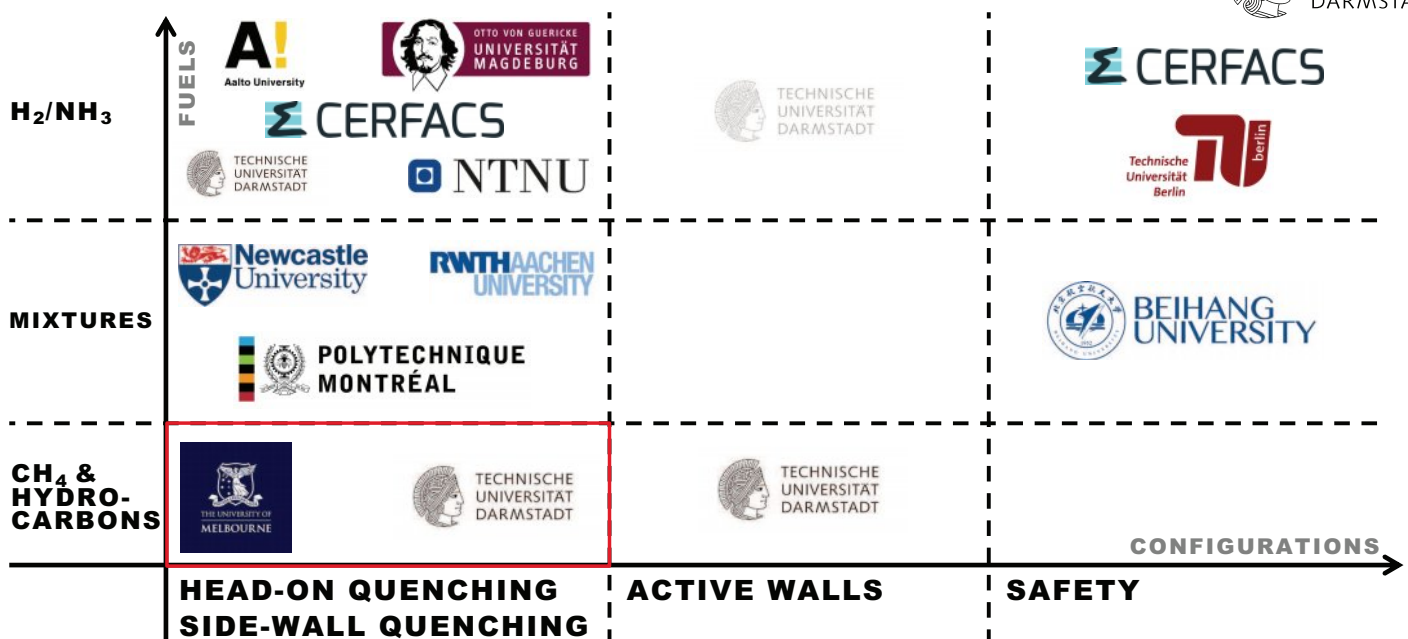
Key Challenge 2: Near-wall combustion and pollutant models

KC2

Key Challenge 3: Safety and especially flashback

KC3

# AGENDA / CONTRIBUTIONS



# FLAME-VORTEX INTERACTION DURING TURBULENT SIDE-WALL QUENCHING

Matthias Steinhausen, Thorsten Zirwes, Henning Bockhorn, Federica Ferraro,  
Arne Scholtissek, Christian Hasse

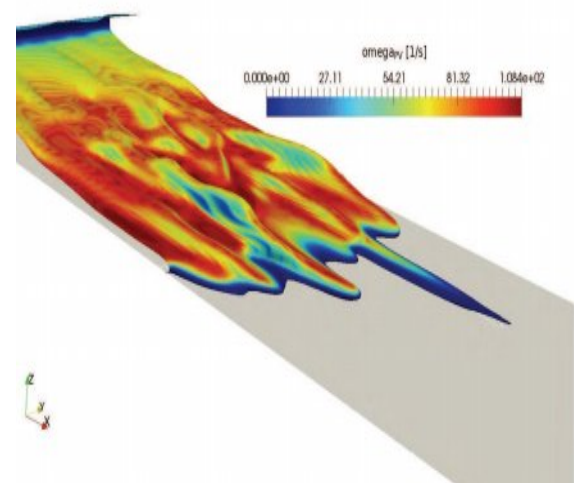
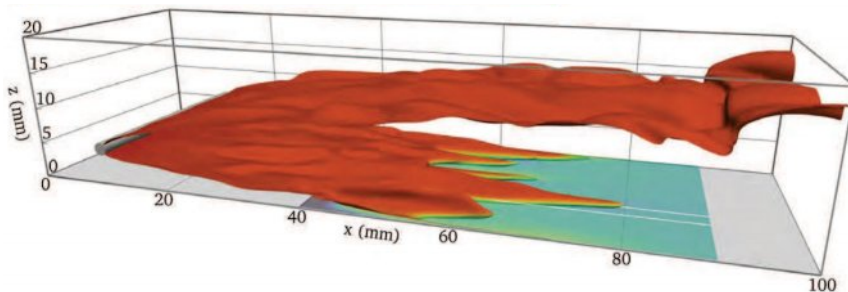
11.09.24

Mechanical Engineering | Simulation of reactive Thermo-Fluid Systems | Matthias Steinhausen

KM1

## SETUP TURBULENT METHANE-AIR V-FLAME IN SWQ

Snapshot of the Progress Variable iso-surface in the reactive quasi-DNS



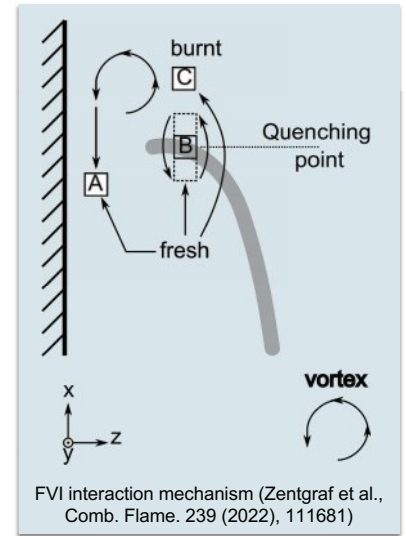
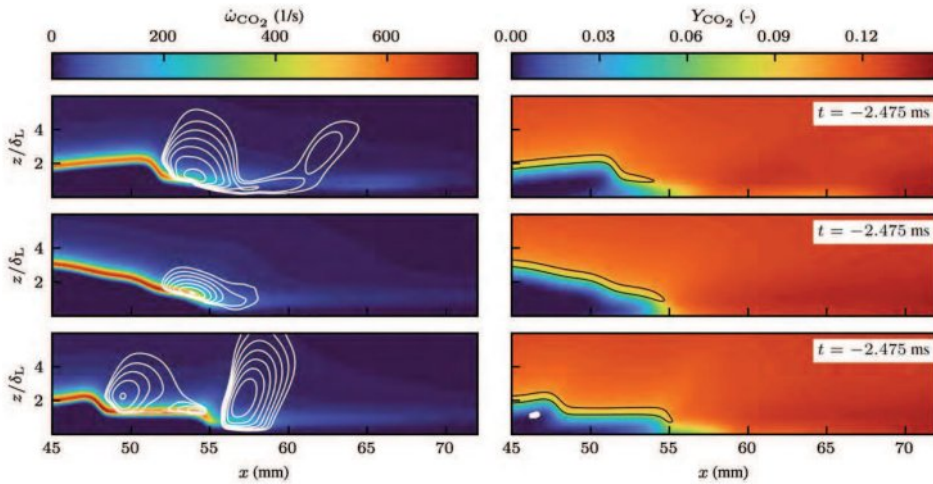
### Benchmark<sup>[1,2]</sup>

Fully developed turbulent channel flow  
> 200 Mio. cells

Stoichiometric methane-air V-flame  
Reduced CRECK-mechanism  
(24 Species, 165 Reactions)

[1] Steinhausen M, Zirwes T, Ferraro F, Popp S, Zhang F, Bockhorn H, Hasse C. Int J Heat Fluid Flow 2022;93:108913.  
[2] Steinhausen M, Zirwes T, Ferraro F, Scholtissek A, Bockhorn H, Hasse C. Proc Combust Inst 2023;39:2149–58.

# FLAME-(TIP-)VORTEX-INTERACTION MECHANISM



Flame-Vortex Interaction (FVI) mechanism in a wall-normal cut plane. Left: Vortices (Q-criterion, white); Right: flame position (black), FVI area (white)<sup>[1]</sup>.

[1] Steinhausen M, Zirwes T, Ferraro F, Scholtissek A, Bockhorn H, Hasse C. Proc Combust Inst 2023;39:2149–58.

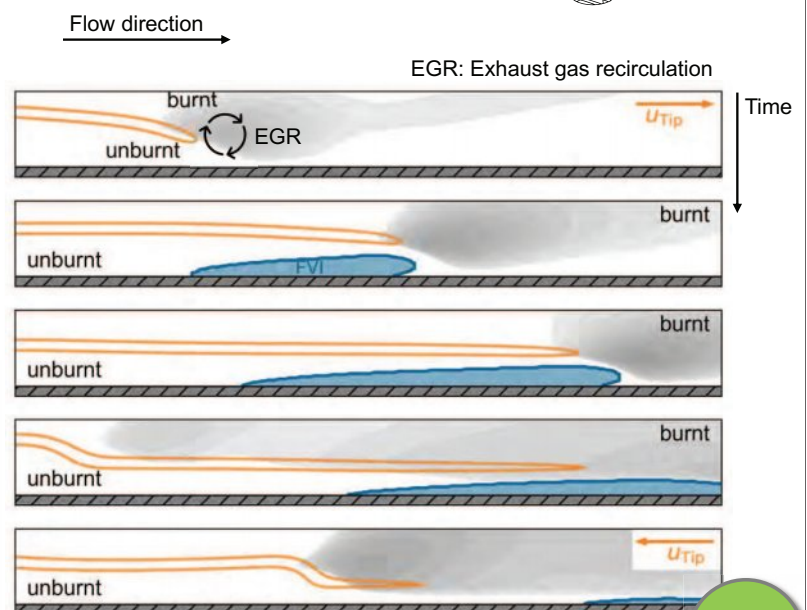
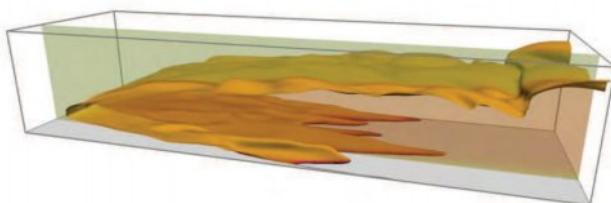


KM1

# FLAME-VORTEX INTERACTION

## FLAME-VORTEX-INTERACTION MECHANISM

- Vortex pushes burnt gases to the wall
- Flame front propagates over the burnt gases
- Mixing of fresh and cold burnt gases (blue area)
- Can also occur “out-of-plane” (next slide)



Source: Matthias Steinhausen, STFS, TU Darmstadt

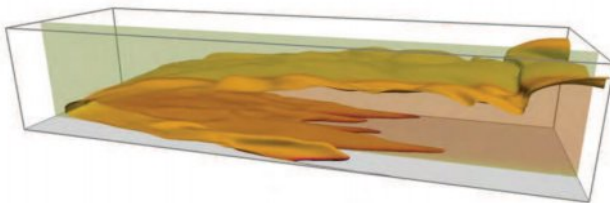


KM1

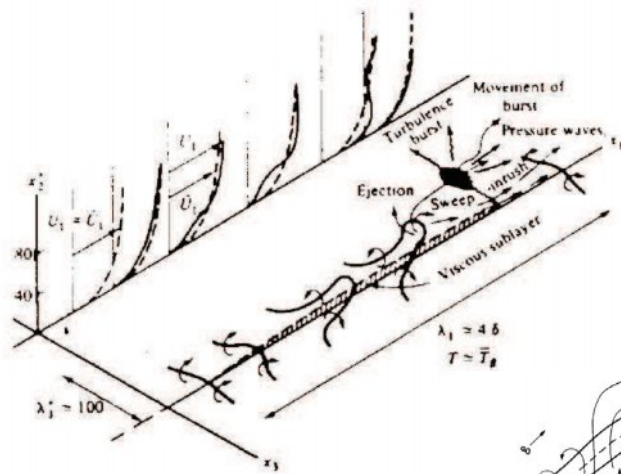
# FLAME-VORTEX INTERACTION

## FLAME-VORTEX-INTERACTION MECHANISM

- Vortex pushes burnt gases to the wall
- Flame front propagates over the burnt gases
- Mixing of fresh and cold burnt gases
- the picture on the right with ejection/sweeps is changed in reactive conditions – quadrant analysis

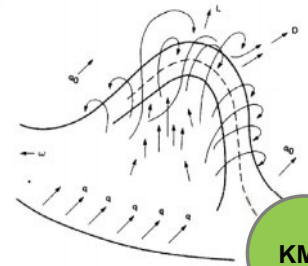


Source: Matthias Steinhausen, STFS, TU Darmstadt



Reproduced from  
Theodorsen (1952)

Reproduced from Hinze (1975)



KM1



## Flame-wall Interaction under the presence of intense turbulence

Shreshtha Gupta, Mohsen Talei

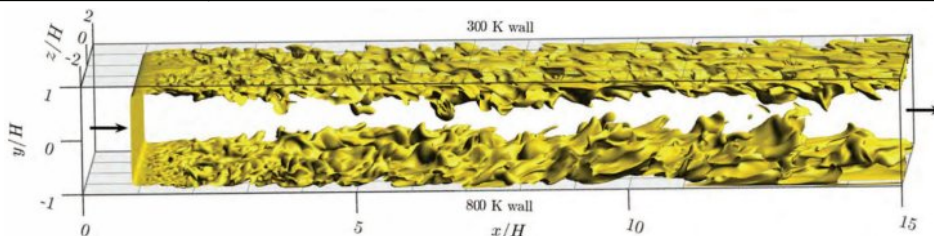
Slides have been rearranged by STFS.

KM1

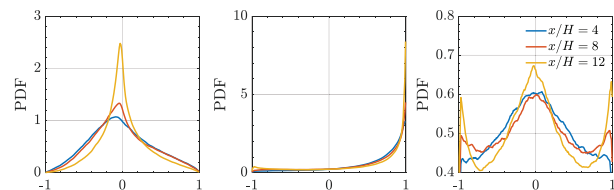
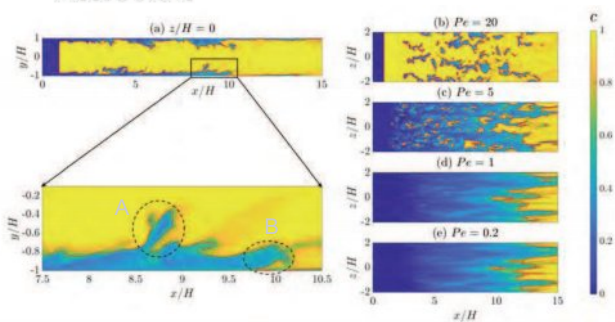


- Turbulent Flame interacting with 300 K & 800 K isothermal wall

Flame	Methane-air, $\phi = 1$ , $T_u = 800$ K, $P = 1$ atm Smooke and Giovangigli (16 species, 46 reactions) mechanism
Domain	Channel: $15H$ (streamwise) $\times$ $2H$ (wall-normal) $\times$ $4H$ (spanwise), $H = 11.3 \times \delta_{th} = 2.8$ mm
Flow	Bulk velocity $U_b = 300$ m/s Bulk Reynolds number, $Re_b = 10,000$
Boundary conditions	Inlet: Fully developed non-reacting DNS Outlet: partially non-reflecting (NSCBC) Faces: left & right: periodicity <b>top: 300 K isothermal wall</b> <b>bottom: 800 K isothermal wall</b>



KM1



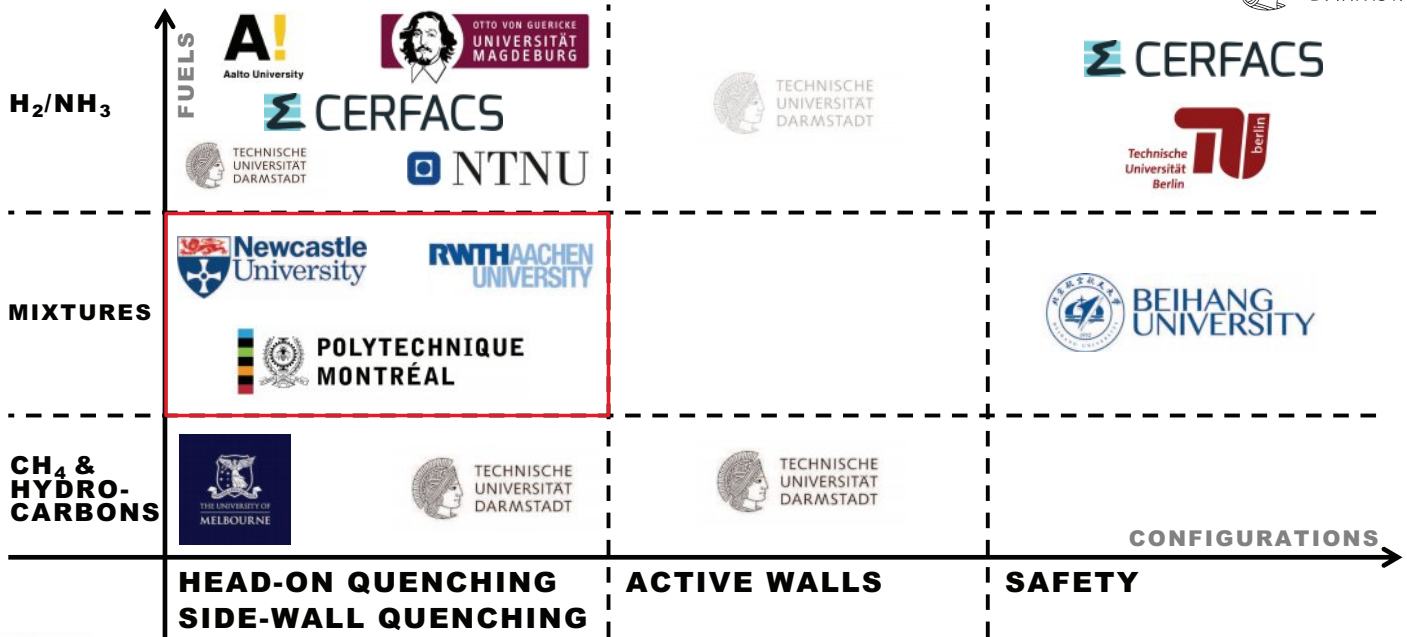
- One iso-value of  $c$  cannot represent the flame during FWI.
- Instead, the rate of consumption of fuel can be used as a flame marker near the wall.
- Figure shows the  $Pe_Q$  for 800K and 300K wall, indicating that the flame can exist for relatively small values of  $Pe$ .
- The  $Pe_Q$  of 300 K wall is slightly higher than that of 800 K wall, suggesting the impact of wall temperature.
- Turbulence has a substantial influence on pushing the flame towards the wall.

- Directional flame surface normal PDF with respect to  $x$  (streamwise),  $y$  (away from wall) and  $z$  (spanwise) is shown in the Figure.
- The PDF is shifted to  $N_x \rightarrow 0$  &  $N_y \rightarrow 1$  during FWI (at  $x/H=12$ ), indicating that the flame is more likely to be parallel to the wall.
- This suggests that 1D head-on quenching can be largely representative of the FWI in terms of flame orientation in the presence of intense turbulence.

KM1



# AGENDA / CONTRIBUTIONS



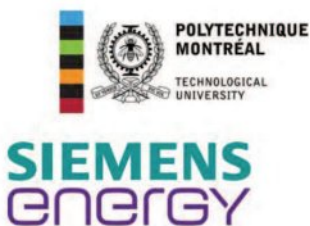
Mechanical Engineering | Simulation of reactive Thermo-Fluid Systems | Christian Hasse

15

KC2

## DNS of a laboratory lean $H_2/CH_4$ low-swirl flame impinging on an inclined wall

O. Chabot<sup>1</sup> M. Nozari<sup>1</sup> S. Jella<sup>2</sup> M. Vabre<sup>1</sup> L. Fan<sup>3</sup> M. Day<sup>4</sup> P. Vena<sup>3</sup>  
 L. Esclapez<sup>4</sup> B. Savard<sup>1</sup>



<sup>1</sup>Polytechnique Montréal  
<sup>2</sup>Siemens Energy Canada Ltd.  
<sup>3</sup>National Research Council Canada  
<sup>4</sup>National Renewable Energy Laboratory



# Target laboratory flame

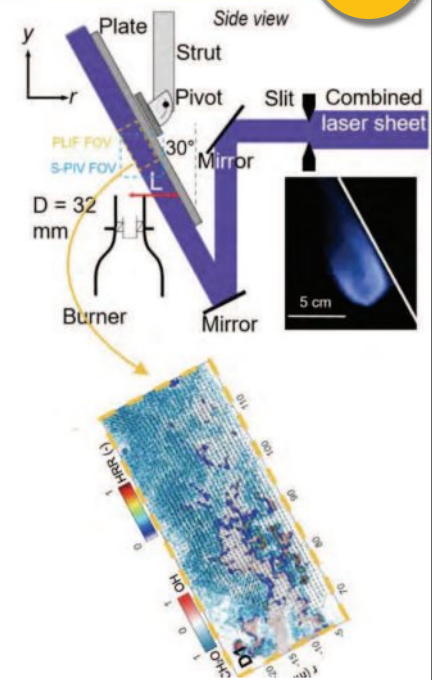
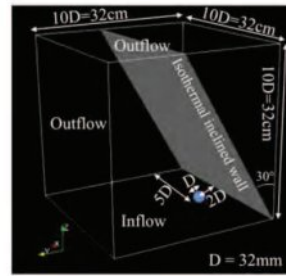
KC2

## Experimental flame<sup>1</sup>:

- ▶ Model GT swirl injector
- ▶  $Re = 20,000$
- ▶ Nominal  $Ka \approx 300$
- ▶ Fuel:  $H_2/CH_4$  (70:30 vol.)
- ▶ Near lean blow-off limit
- ▶  $\phi = 0.41$
- ▶ Water-cooled plate at 330 K
- ▶ Simultaneous stereo-PIV and  $CH_2O \times OH$  PLIF

## Simplified DNS setup:

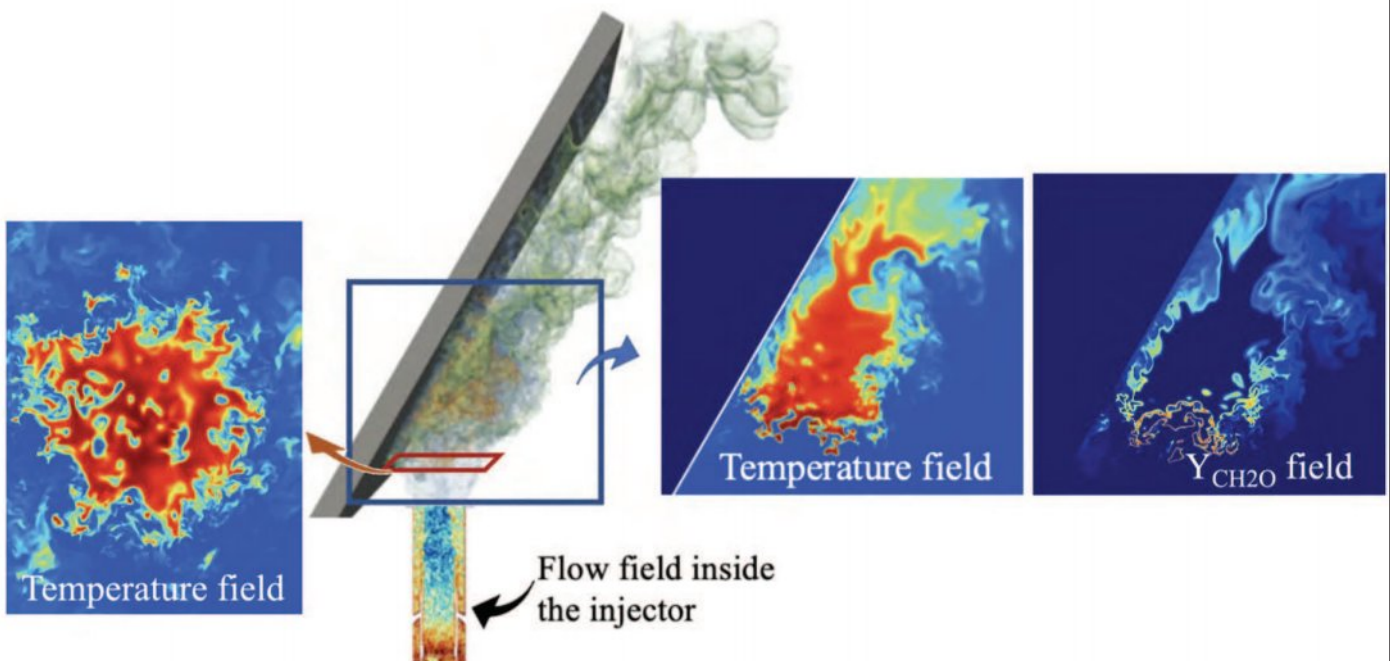
- ▶ Same dimensions,  $Re$ ,  $Ka$ , mixture
- ▶ Cuboid domain
- ▶ Inflow from separate injector LES
- ▶ Uniform, low-velocity co-flow
- ▶ Plate modeled by isothermal EB



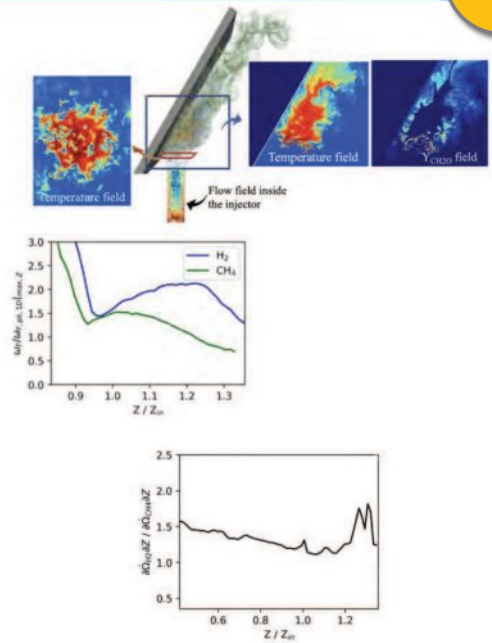
<sup>1</sup>Fan et al., Proc. Comb. Inst., 2023

# Overview

KC2



- ▶ Lab-scale flame DNS reveals complex structure
- ▶ Effect of wall heat on flame structure at low  $Z$  near the wall
- ▶ Very lean flames are sustained (back support?), but products not reached
- ▶ Relatively more  $\text{CH}_4$  slip compared to  $\text{H}_2$



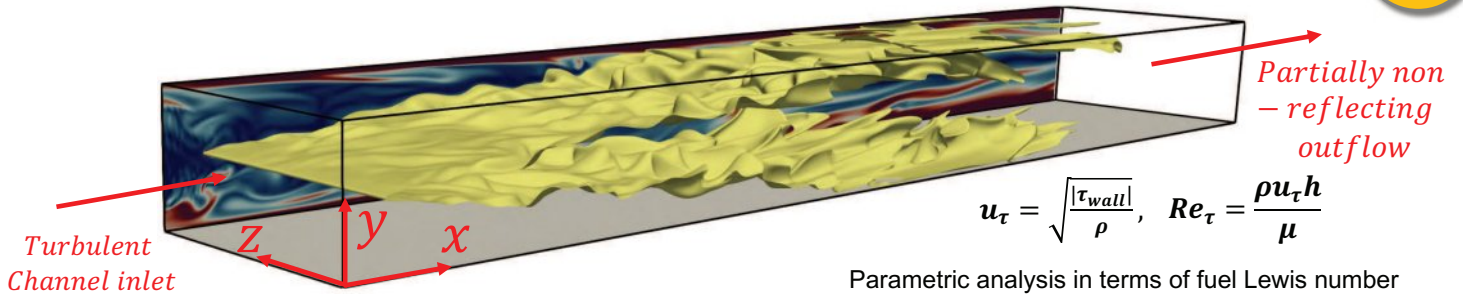
## Physics and Modelling of premixed flame-wall interaction in turbulent boundary layers using Direct Numerical Simulation data

Slides have been rearranged by STFS.



# DNS database for Oblique flame-wall interaction

KC2



$$u_\tau = \sqrt{\frac{|\tau_{wall}|}{\rho}}, \quad Re_\tau = \frac{\rho u_\tau h}{\mu}$$

Parametric analysis in terms of fuel Lewis number

Cases	Fuel Composition
$Le_F = 0.6$	25% H <sub>2</sub> and 75% CH <sub>4</sub>
$Le_F = 1.0$	100% CH <sub>4</sub>
$Le_F = 1.4$	90% C <sub>2</sub> H <sub>6</sub> and 10% CH <sub>4</sub>

Parametric analysis in terms of thermal boundary condition

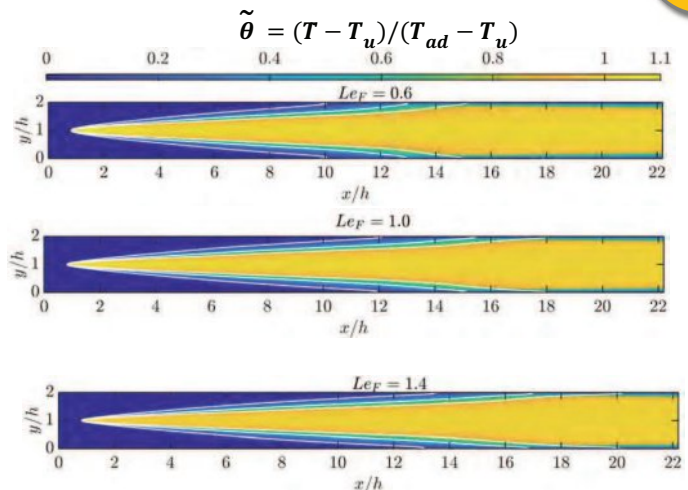
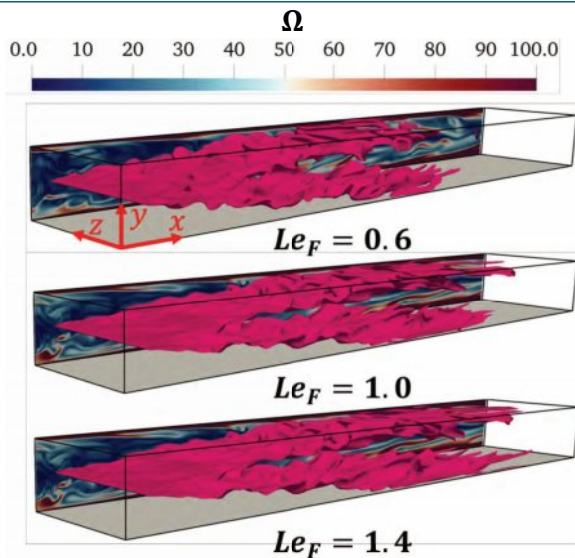
Boundary conditions	$\theta = \frac{T - T_u}{T_{ad} - T_u}$
Isothermal wall with $T_w = T_u \rightarrow \theta = 0$	
Adiabatic Wall $\rightarrow \partial/\partial y = 0$	
Isothermal wall with $T_w > T_u \rightarrow \theta = 0.3$	



- V-flame is investigated in this work with friction velocity based Reynolds number  $Re_\tau = 110$  and  $180$  in channel flow configuration with inert walls.
- Domain size of  $22.22h \times 2h \times 4h$  discretised using  $4000 \times 360 \times 720$  and  $6667 \times 600 \times 1200$  grid points for  $Re_\tau = 110$  and  $180$ , respectively.
- $y^+ \leq 0.6$  is used for the grid point adjacent to the wall and approximately two grid points are in  $y^+ \leq 1.0$  region and at least 8 grid points are within  $\delta_{th}$ .

## Effects of $Le_F$ on instantaneous and mean fields

KC2

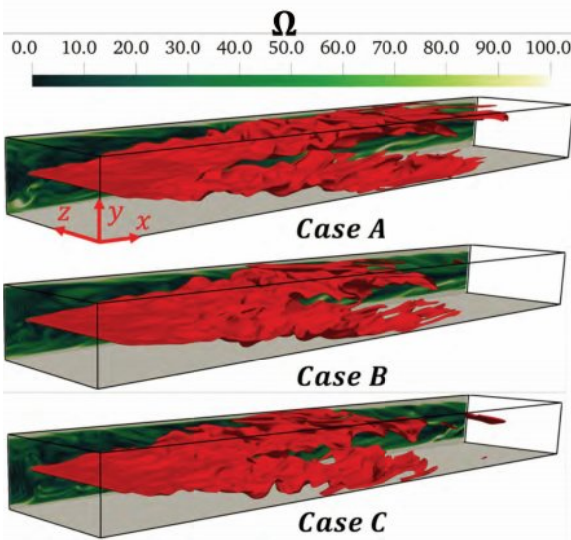


Fields of Favre-averaged temperature  $\tilde{\theta}$  along with mean reaction progress variable contour  $\tilde{c} = 0.1, 0.5$  and  $0.8$ .

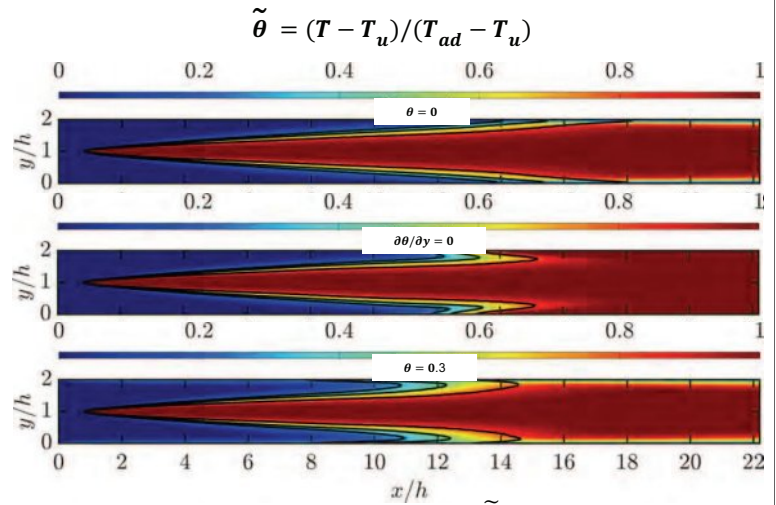
Isosurfaces of  $c = 0.5$  with distributions of normalised vorticity magnitude  $\Omega = \sqrt{w_i w_i} \times h / u_{\tau, NR}$  in the central mid-plane



# Effects of thermal boundary condition on relevant fields



Isosurfaces of  $c = 0.5$  with distributions of normalised vorticity magnitude  $\Omega = \sqrt{w_i w_i} \times h / u_{\tau, NR}$  in the central mid-plane

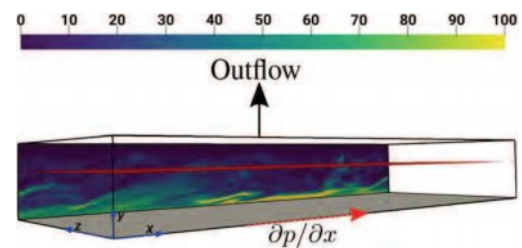
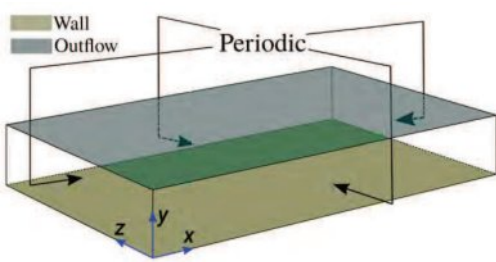


Fields of Favre-averaged temperature  $\tilde{\theta}$  along with mean reaction progress variable contour  $\tilde{c} = 0.1, 0.5$  and  $0.8$ .



# DNS database for head-on flame-wall interaction

KC2



- The Head-on interaction (HOI) configuration is considered within turbulent boundary layers.
- $Re_\tau = 110$  and  $Re_\tau = 180$  periodic boundary layer with isothermal inert walls is used.
- The reactant and isothermal wall temperature are set to  $730K$ .
- The flame is representative of methane-air  $\phi = 1.0$ ,  $Le = 1.0$  with  $S_L/u_\tau = 0.7$ .
- Domain size  $10.69h \times 1.33h \times 4h$  discretised on  $1920 \times 240 \times 720$  (for  $Re_\tau = 110$ ) and  $3200 \times 400 \times 1200$  (for  $Re_\tau = 180$ ) grid points.
- The simulation is run until the flame has fully consumed the reactants.

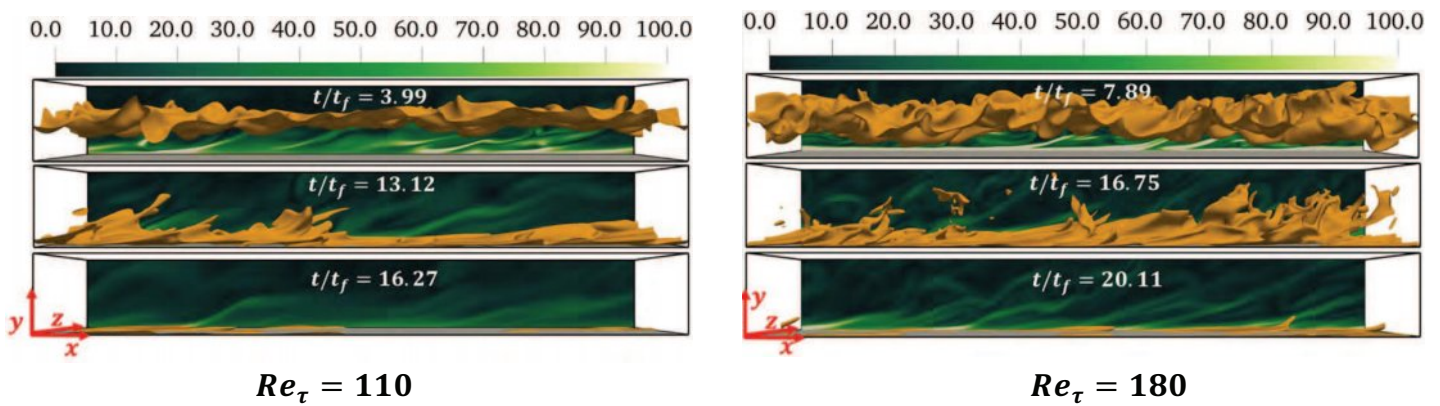




## Head-on interaction instantaneous behaviour

KC2

- Head-on quenching by cold isothermal inert walls across turbulent boundary layer is shown below



- DNS data of head-on interaction with adiabatic walls across turbulent boundary layer in the same configuration is also available.



## CO emissions in turbulent premixed methane/hydrogen jet flames interacting with isothermal walls

KC2

Kai Niemietz, Heinz Pitsch  
Institute for Combustion Technology  
RWTH Aachen University

## Turbulent jets

- Jet Reynolds number  $Re_j = 5,500$
- Jet exit velocity  $u_j = 73.5$  m/s
- Jet slot height  $h_j = 1.2$  mm
- Temperature  $T^0 = 673$  K

## Pilot

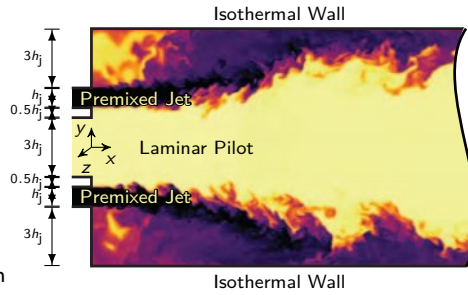
- Pilot exit velocity  $u_p = 20$  m/s
- Pilot slot height  $h_p = 3 h_j = 3.6$  mm
- Burnt exhaust gas  $T_p = T^b = 1782$  K

## Pressure $p = 4$ atm

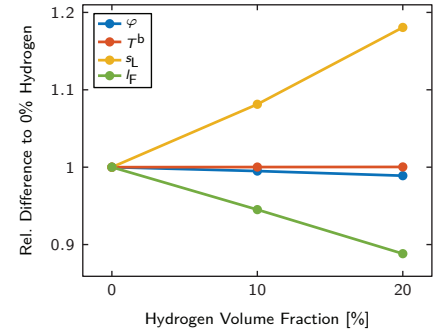
## Wall temperature $T_w = 1000$ K

## Methane/hydrogen/air mixture

- Pure methane presented at last TNF<sup>[1]</sup>
- 10%<sub>vol</sub> and 20%<sub>vol</sub> H<sub>2</sub> in the fuel
- Equivalence ratio  $\varphi \approx 0.5$



Equivalence ratio:  $\varphi_0 = 0.5$   
 Adiabatic flame temperature:  $T_0^b = 1782.42$  K  
 Laminar burning velocity:  $s_{L,0} = 26.10$  cm/s  
 Flame thickness:  $l_{F,0} = 229.36$   $\mu$ m



## Chemistry

- Finite rate skeletal methane mechanism  
25 species, 155 reactions<sup>[2]</sup>
- Detailed diffusion model

## Domain

- 100  $h_j \times 12 h_j \times 6 h_j$
- 120 mm  $\times$  14.4 mm  $\times$  7.2 mm
- 6060  $\times$  1440  $\times$  360 cells = 3.1 billion cells

27

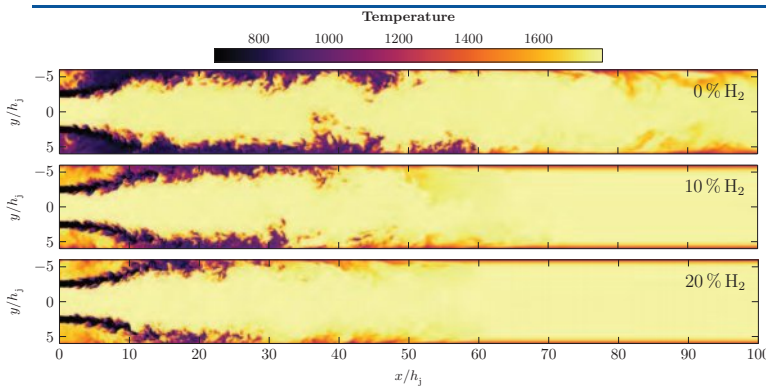
Institute for Combustion Technology | Heinz Pitsch

[1] K. Niemi et al., Proc. Combust. Inst. 39 (2) (2023) 2209–2218.

[2] L. Cai et al., Proc. Combust. Inst. 37 (1) (2019) 639–647.



# Preliminary results from ongoing simulations

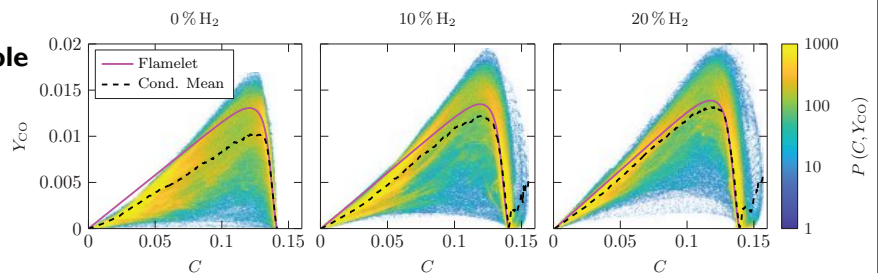


## Instantaneous temperature fields

- Shortened flame length with increasing hydrogen content
  - Higher reactivity of the fuel
- Reduced flame-wall interaction?

## JPDF of CO mass fraction and progress variable

- Conditional mean closer to unstretched flamelet with increasing H<sub>2</sub>
  - Higher flame speed compensates slower chemistry from lower temperatures?
  - Reduced FWI causes less non-flamelet combustion?



28

Institute for Combustion Technology | Heinz Pitsch



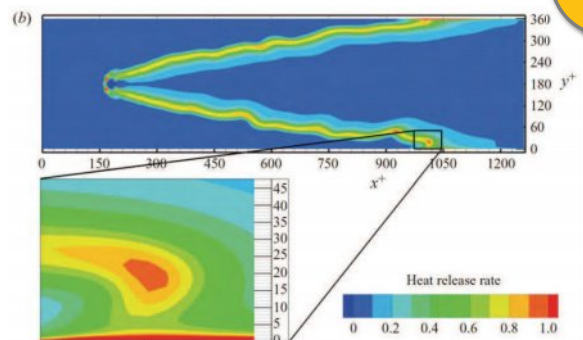
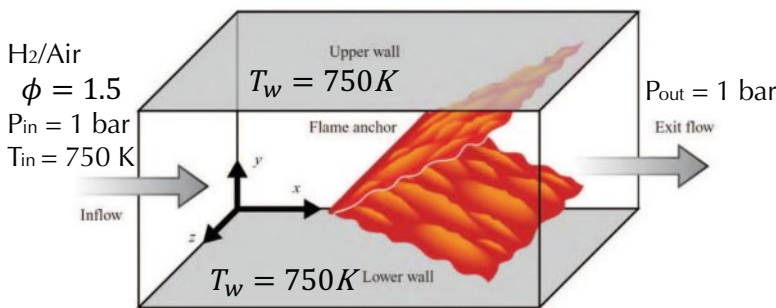
# AGENDA / CONTRIBUTIONS

<b>FUELS</b> $H_2/NH_3$  <b>MIXTURES</b>  <b>CH<sub>4</sub> &amp; HYDRO-CARBONS</b>				
	<b>HEAD-ON QUENCHING</b> <b>SIDE-WALL QUENCHING</b>		<b>ACTIVE WALLS</b>	<b>SAFETY</b>
	<b>CONFIGURATIONS</b>			



## Flame wall interaction (FWI): the limits of present chemical schemes for H<sub>2</sub> flames impacting cold walls and a model to fix this (IFHC)

L. DeNardi, O. Vermorel, Q. Douasbin, T. Poinsoot CERFACS



- ▶ Most groups studying FWI with H<sub>2</sub> know that unexpected heat release rates are observed at walls [1]. One example in the DNS of Gruber et al.
- ▶ This problem occurs for all chemical schemes we tested [2]



# A model for premixed H<sub>2</sub> FWI: IFHC

- ▶ The problem comes from the H radical at the wall. It can be fixed using a model we called IFHC, which brings  $Y_H$  to 0 at the wall:
- ▶ Infinitely Fast Heterogeneous Catalysis (IFHC) [2] activates these reactions ON THE WALL
 
$$2H + O \rightarrow H_2O$$

$$H + OH \rightarrow H_2O$$

$$4H + O_2 \rightarrow 2H_2O$$
- ▶ Eliminating H at the wall is sufficient to fix the problem

Combustion and Flame 261 (2024) 113328

Contents lists available at ScienceDirect

Combustion and Flame

journal homepage: [www.sciencedirect.com/journal/combustion-and-flame](http://www.sciencedirect.com/journal/combustion-and-flame)

ELSEVIER

Infinitely Fast Heterogeneous Catalysis Model for Premixed Hydrogen Flame-Wall Interaction

Loïc De Nardi<sup>a,\*</sup>, Quentin Douasbin<sup>a</sup>, Olivier Vermorel<sup>a</sup>, Thierry Poinso<sup>a,b</sup>

<sup>a</sup>Centre Européen de Recherche et de Formation Avancée en Calcul Scientifique (CERFACS), 42 av. Gaspard Coriolis, 31057 Toulouse, France  
<sup>b</sup>Institut de Mécanique des Fluides de Toulouse (IMFT), 2 allée du Professeur Camille Soula, 31400 Toulouse, France

ARTICLE INFO

Keywords:  
 Hydrogen  
 Laminar premixed flames  
 Flame-wall interaction  
 Head-on quenching

ABSTRACT

In most computations of reacting flows, walls are considered as inert. This approach can produce non-physical results that lead to very large values of heat release at the wall for hydrogen Flame-Wall Interaction (FWI). This paper confirms this unexpected behavior at walls for H<sub>2</sub> flames. It also explores the possibility that the problem does not come from a deficiency of the chemical scheme at low temperatures but from the wall boundary condition: due to the large amount of radical species produced by H<sub>2</sub> flames, the "inert" assumption may not be valid anymore. The purpose of this study is twofold: (1) to propose a simplified model named Infinitely Fast Heterogeneous Catalysis (IFHC) that mimics surface reactions and (2) to test it on the canonical Head-On Quenching (HOQ) configuration. A large set of parameters is investigated: a skeletal (San Diego) and a detailed (Burke) chemical schemes are tested, the grid-dependence and the influence of operating conditions ( $\phi$ ,  $T_w$ , and  $P$ ) are assessed. Results show that the IFHC model can inhibit the chemical pathways that are responsible for the heat generation peak observed on the wall in hydrogen FWI with inert surfaces. The IFHC model also allows computations to converge when the mesh is refined, a property that cannot be reached for inert wall treatments. Using IFHC, neither the predicted quenching distance nor the flame structure are altered. However, the maximum wall heat flux is significantly decreased when compared to inert walls. Over the range of operating conditions studied, the maximum wall heat flux is reached at high pressure, low wall-temperature and equivalence ratios close to the maximum of reactivity of H<sub>2</sub> flames ( $\phi \approx 1.7$ ). This study shows that, for H<sub>2</sub> FWI, walls should be at least modeled with simple surface reactions – such as IFHC – and that assuming inert walls is not possible.

[2] L. De Nardi, Q. Douasbin, O. Vermorel, and T. Poinso, "Infinitely Fast Heterogeneous Catalysis Model for Premixed Hydrogen Flame-Wall Interaction," *Combustion and Flame*, vol. 261, p. 113328, Mar. 2024, doi: [10.1016/j.combustflame.2024.113328](https://doi.org/10.1016/j.combustflame.2024.113328).

31 | CERFACS

Loïc De Nardi - [denardi@cerfacs.fr](mailto:denardi@cerfacs.fr)

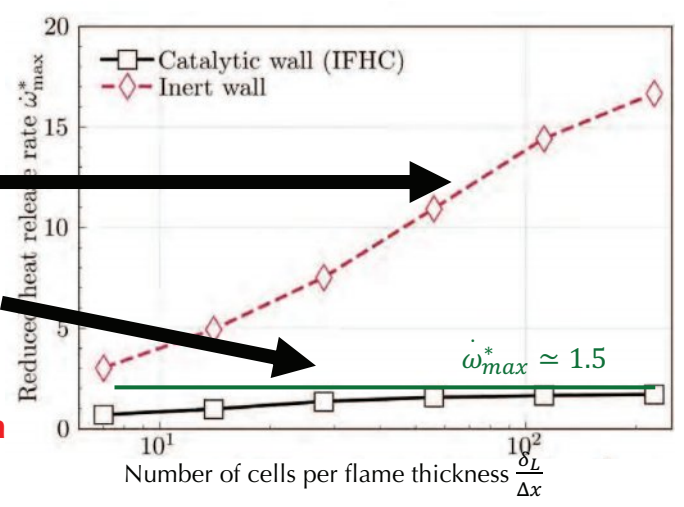


# 1D HOQ simulation: comparing solutions with and without IFHC [2]



- ▶ Without IFHC, the problem is ill posed: refining the mesh leads to values of maximum heat release on wall which never stabilize when mesh is refined
- ▶ With IFHC, the problem becomes well-posed and the heat release rate on the wall converges. Careful: it still does not go to zero !

The IFHC fixes the problem but this is probably an issue which should be tackled in the future by chemistry and catalysis experts



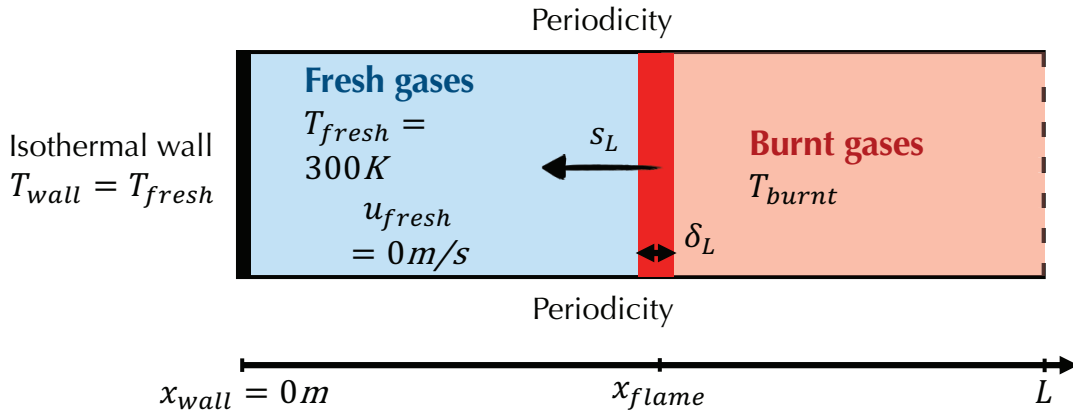
Loïc De Nardi - [denardi@cerfacs.fr](mailto:denardi@cerfacs.fr)





# Verification of IFHC model for 1D H<sub>2</sub>/Air FWI

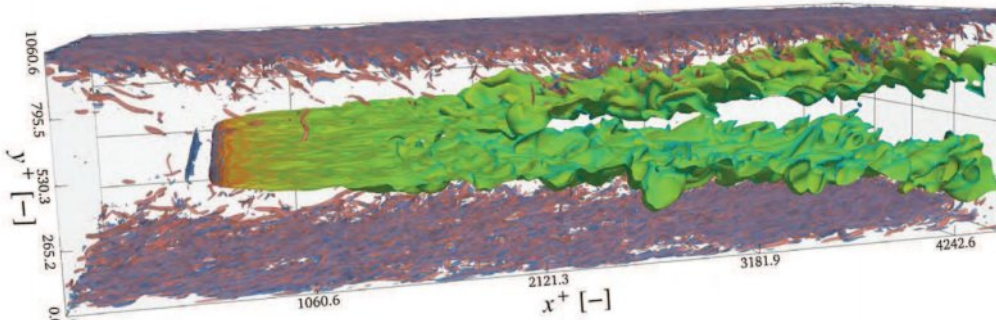
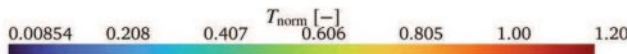
A simple test case is the unsteady interaction of a 1D premixed flame impinging on a wall: **1D Head On Quenching** [3]. Diagnostic: maximum heat release rate reached on the wall during the interaction



Performed with both **San Diego** [5] and **Burke** [6] schemes

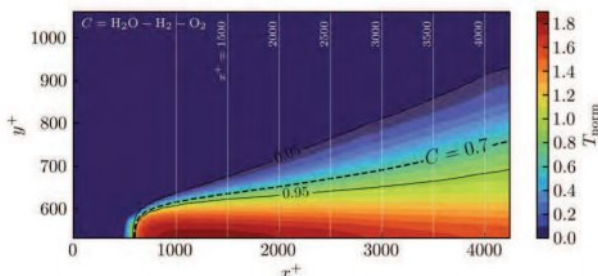


## SETUP



**Anchored V-flame in a turbulent channel flow**

$T = 750 K, p = 2 \text{ bar},$   
 $\phi = 0.25, 0.35$   
 H<sub>2</sub>-Air (Li 2004 mech.)  
 $Re_{\tau} = 530, Re_c = 11.000$



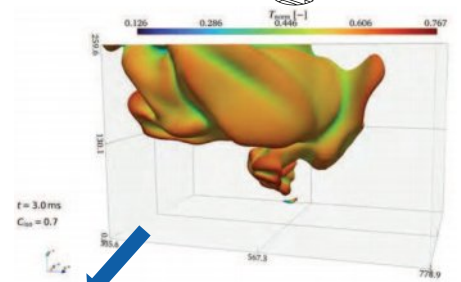
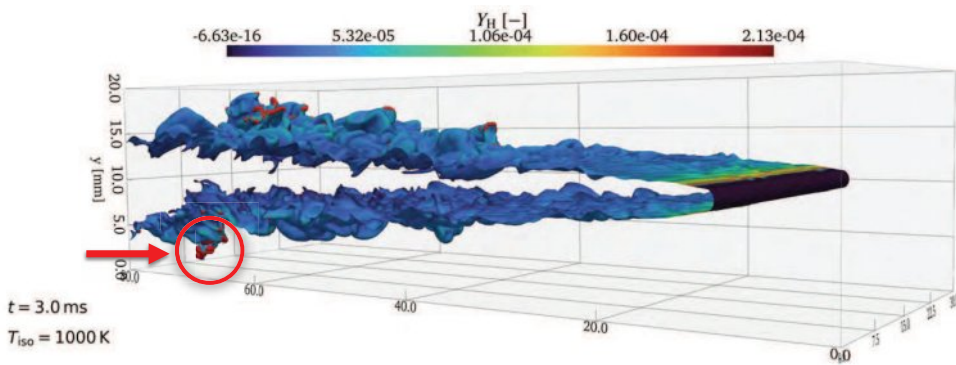
$t = 2.00 \text{ ms}$   
 iso:  $C_{norm} = 0.7$



The flame does not touch the wall for  $\phi = 0.25$

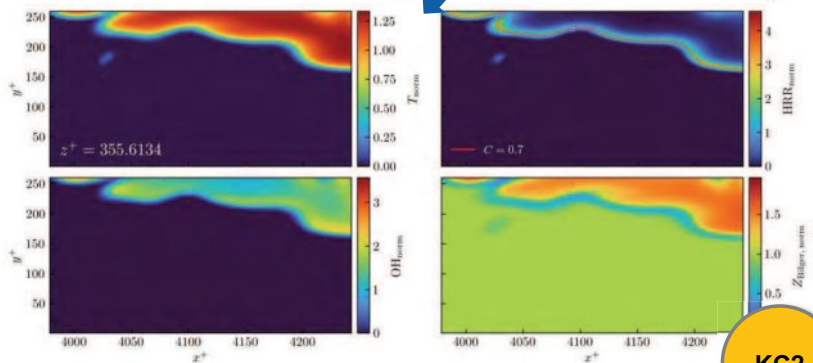






Spots with 2<sup>nd</sup> HRR-Peak at  $\kappa_c > 0$  and superadiabatic conditions ( $H_2O_{norm} > 1$ )

Burning rate variation and differential diffusion in sub-unity Lewis-number flame!  
 → Outlook: Intermittent FWI for  $\phi = 0.35$



## An analysis on flame-wall interaction of premixed laminar ammonia/air flames enriched with hydrogen

### Project Team Members:

- Prof. Ossi Kaario (Associate Professor, Aalto University)
- Dr. Parsa Tamadonfar (Post-doctoral Researcher, Aalto University)
- Prof. Ville Vuorinen (Associate Professor, Aalto University)
- Dr. Shervin Karimkashi (Academic Coordinator, Aalto University)

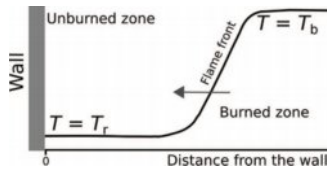
### Main Collaborator:

- Dr. Thorsten Zirwes (Deputy Director of the Institute for Combustion Technology, University of Stuttgart)

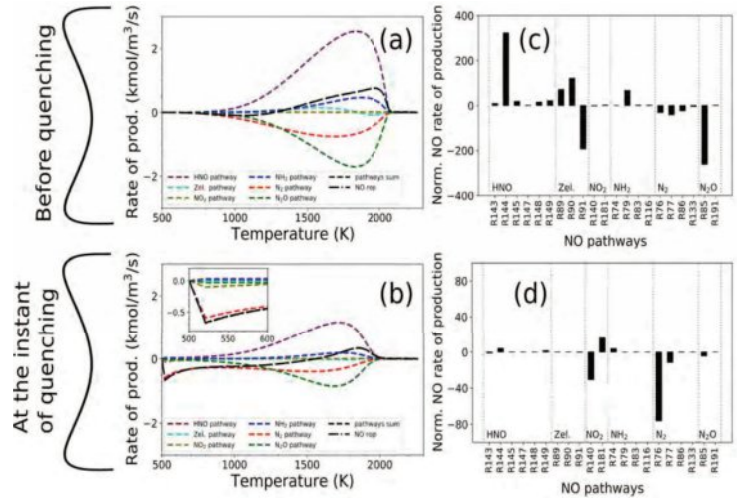
# 1-D head-on quenching of ammonia/hydrogen/air flames

KC2

Tamaddonfar et al., *Combustion and Flame*, 265, 2024, 113444.



- Premixed laminar ammonia/air flames enriched with hydrogen.
- Varying
  - blending ratios (the molar ratio of hydrogen to the ammonia/hydrogen mixture): 0.0 to 0.4.
  - equivalence ratios: 0.8 to 1.2.
  - wall temperatures: 300 to 750 K.
  - pressures: 1 to 5 atm.
- Finite rate chemistry with chemical kinetic mechanism developed by Stagni et al. [1] with 31 species and 203 reactions.



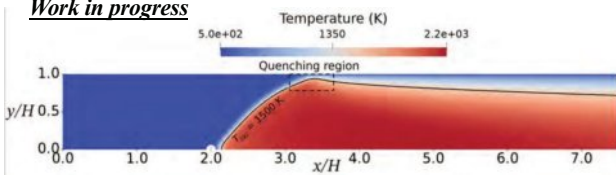
Quenching distance decreases and maximum absolute wall heat flux increases with increasing the blending ratio, the equivalence ratio, the wall temperature, and the pressure.

[1] Stagni et al., An experimental, theoretical and kinetic-modeling study of the gas-phase oxidation of ammonia. *React. Chem. Eng.*, 2020, 5: p. 696-711.

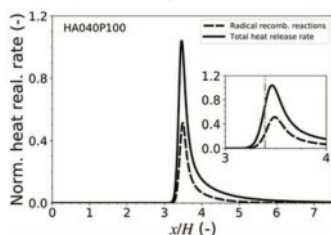
# 2-D side-wall quenching of ammonia/hydrogen/air flames

KC2

*Work in progress*

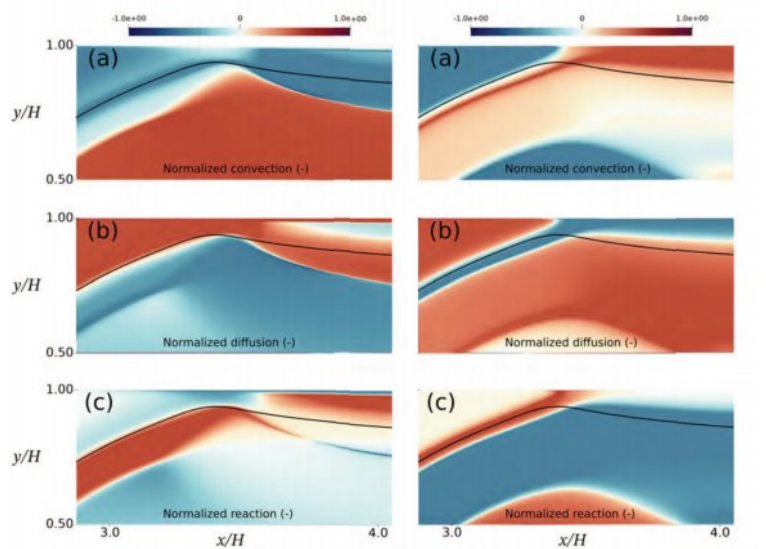


- Premixed laminar ammonia/hydrogen/air flames.
- Varying
  - blending ratios: 0.35 to 0.45.
  - equivalence ratios: 0.6 to 1.2.
- at 1 atm and reactants/wall temperature of 500 K.
- Finite rate chemistry with Stagni chemical kinetic mechanism.



NO species transport budget analysis

N<sub>2</sub>O species transport budget analysis

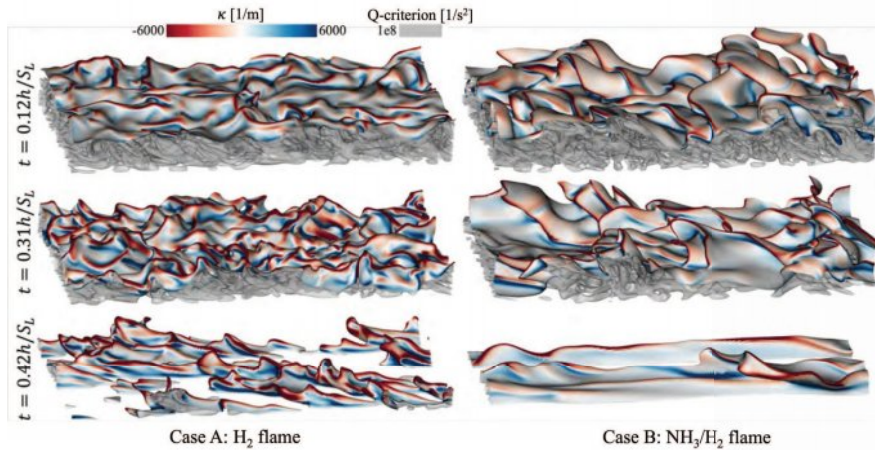




# Head-on quenching of H<sub>2</sub>/air and NH<sub>3</sub>/H<sub>2</sub>/air flames in a turbulent channel flow at $Re_\tau \approx 300$

Cheng Chi, Dominique Thévenin

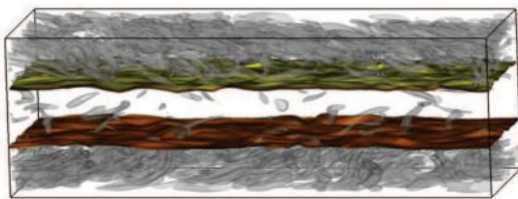
Otto von Guericke University Magdeburg



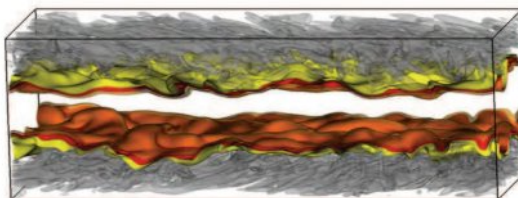
## Numerical configurations (DNS)



**Case A:** H<sub>2</sub>/air flame with  $Re_\tau = 280$  and  $Da_w = 0.167$



**Case B:** NH<sub>3</sub>/H<sub>2</sub>/air flame with  $Re_\tau = 313$  and  $Da_w = 0.004$



**Cases C and D** are with **adiabatic walls**  
**Cases E and F** are with **Le = 1** approximation

**Solver:** in-house low-Mach DNS code **DINO**

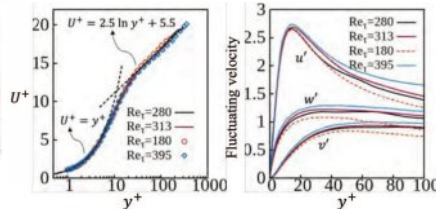
**Detailed chemical mechanism:**

- H<sub>2</sub>/air: Li mechanism (9s19r)
- NH<sub>3</sub>/H<sub>2</sub>/air flame: nitrogen subset of SD (21s64r)

**Molecular transport:** mixture-averaged diffusion

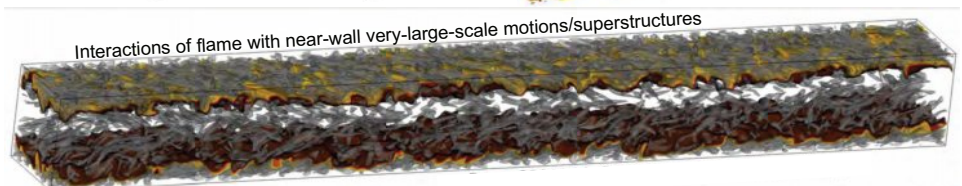
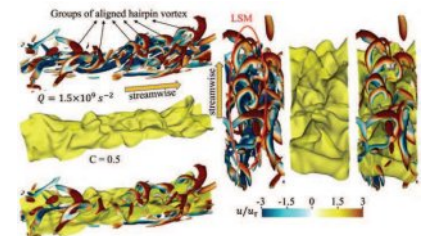
Table 1: Simulation details for the two turbulent cases.

Description (units)	Case A	Case B
Friction velocity $u_\tau$ (m/s)	6.40	5.13
Viscous length scale $l^*$ ( $\mu\text{m}$ )	17.86	15.97
Friction Reynolds number $Re_\tau$ (-)	280	313
H <sub>2</sub> volume ratio $\alpha$ (-)	1.0	0.2
Equivalence ratio $\phi$ (-)	1.5	1.0
Unburned & wall temp. $T_u$ & $T_w$ (K)	750	750
Damköhler number $Da$ (-)	0.167	0.004
Laminar flame speed $S_L$ (m/s)	14.54	0.843
Laminar flame thickness $\delta_L$ (mm)	0.243	0.661
Wall time scale $t_w$ ( $\mu\text{s}$ )	2.79	3.11
Flame time scale $t_L$ ( $\mu\text{s}$ )	16.7	784
Computational cost (million CPUh)	2.6	4.7



**Objectives:**

- Differential diffusion effects on quenching characteristics (using **Cases A/B/E/F**) [1];
- Near-wall pollutant emission characteristics for NH<sub>3</sub>/H<sub>2</sub> flame (using **Case B**) [2];
- Near-wall flame dynamics (including flame thickening mechanism, combustion regime dynamics, flame-vortex/coherent structure interactions,...) (using **Cases A/B/C/D**) [3, 4].

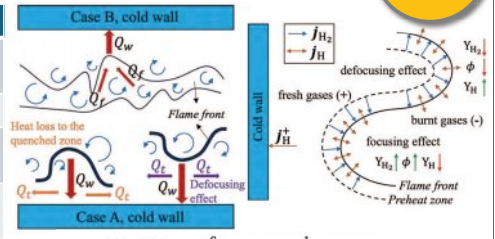


[1] Chi et al., *Proc. Combust. Inst.* 40 (2024) 105276. [2] Chi, *Combust. Flame*, in (2<sup>nd</sup> round) review. [3] Chi et al., *Eur. J. Mech. B/Fluids* 101 (2023) 167-175. [4] Chi et al., *J. Fluid Mech.* (in preparation)

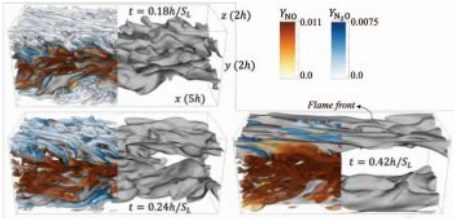
# Main results



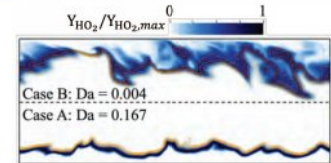
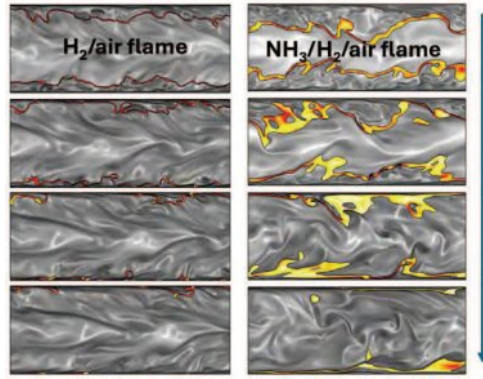
	Low Da		High Da		
Fuel mixture	All fuels	Blended or single fuel with $Le \approx 1$	Blended fuels with very different $Le$	Rich H2	Lean H2
Differential diffusion effects	suppressed	negligible	<b>differential diffusion of fuels</b>	<b>preferential diffusion of H/H2</b>	
			smaller under turb. condition	smaller under turb. condition	larger under turb. condition
Turbulence effects	higher $Fw_Q$ and lower $Pe_Q$	similar $Fw_Q$ and $Pe_Q$	lower $Fw_Q$ and $Pe_Q$	lower $Fw_Q$	higher $Fw_Q$



Thermal law at flame quenching:  $Q_w = Q_u + \int_0^{x_u} Q(x) dx - Q_t$   
 Near-wall radical recombination reactions    Wall tangential heat flux



- For low Da number flames, the  $NH_3$  slip would be substantially reduced.
- Both **flame/wall** and **flame/flame interactions** would result in accumulation of  $N_2O$  and consumption of  $NO$ .



- Flame thickening mechanism during FWI:**
- Both effects of wall heat loss and near-wall turbulent length scales are minor. **The major reason for flame thickening is due to the zero-diffusion flux boundary condition.**
  - For turbulent flames with high Da number, the effect of wall turbulence is negligible,
  - while for flames with low Da number, the flame thickness would decrease due to laminarization near the wall.



TECHNISCHE  
UNIVERSITÄT  
DARMSTADT



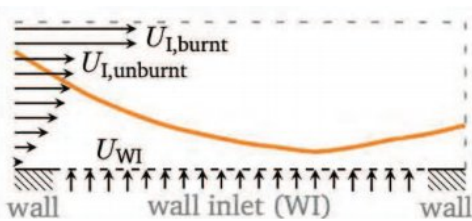
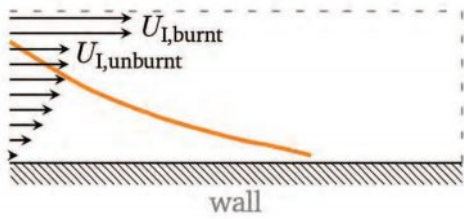
## FLAME-WALL / FLAME-EFFUSION-COOLING-AIR INTERACTION

M. SCHNEIDER, M. STEINHAUSEN, H. NICOLAI, C. HASSE



FIGURE BY C. ALANYALIOGLU

# NUMERICAL SETUP



## SIMPLIFIED 2D CONFIGURATION

Stoichiometric CH<sub>4</sub>-air mixture,  $T_{\text{gas}} = 300 \text{ K}$ ,  $p = 1 \text{ atm}$

Variable volumetric inflow rate

- $\dot{V} = 0 \text{ Lm}^{-1}\text{h}^{-1}$  (SWQ)
- .....
- $\dot{V} = 5000 \text{ Lm}^{-1}\text{h}^{-1}$

Detailed chemistry (DC) model

- $Le = 1$
- **Laminar simulations** using OpenFOAM

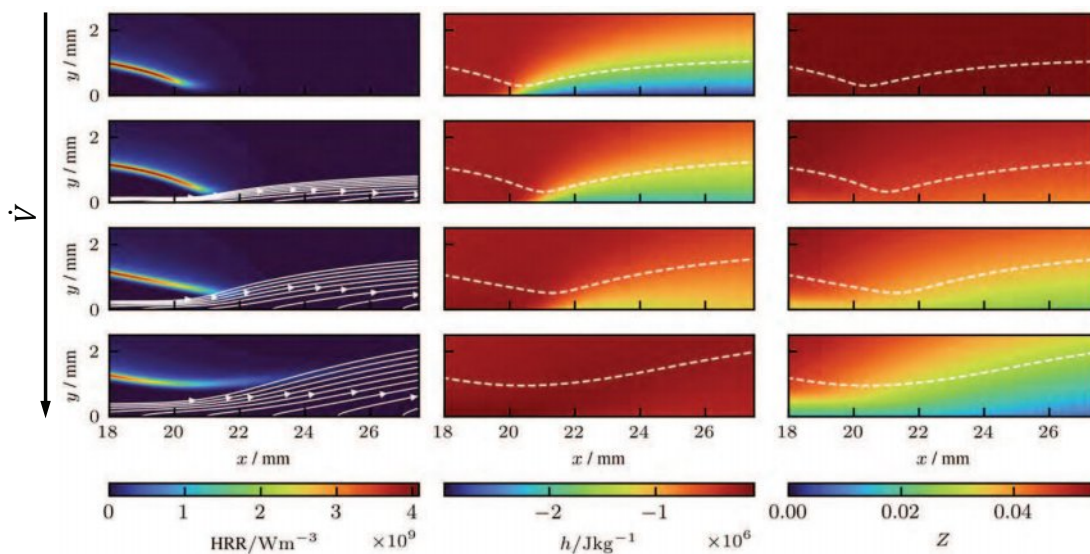
[1] Max Schneider, Matthias Steinhausen, Hendrik Nicolai, Christian Hasse, Modeling of effusion cooling air-flame interaction using thermochemical manifolds, Proceedings of the Combustion Institute, Volume 40, Issues 1–4, 2024



Mechanical Engineering | Simulation of reactive Thermo-Fluid Systems | Max Schneider

KM1

# PHYSICAL PHENOMENA



## PHYSICAL EFFECTS

- Heat loss to wall  $\rightarrow$  FWI
- Dilution of mixture  $\rightarrow$  FCAI

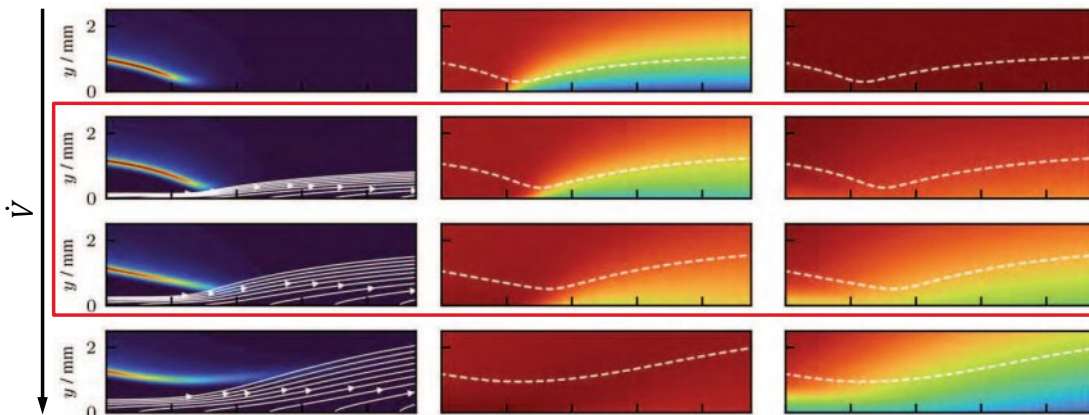


Mechanical Engineering | Simulation of reactive Thermo-Fluid Systems | Max Schneider

KM1



# PHYSICAL PHENOMENA

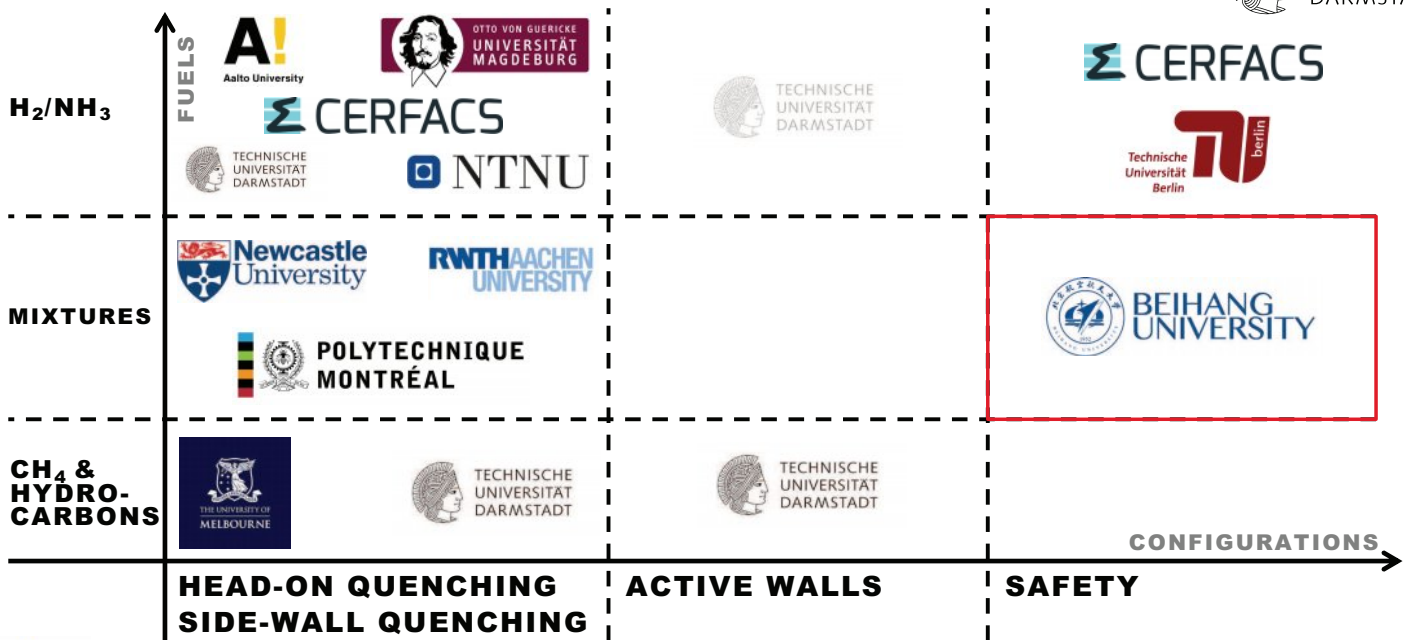


## PHYSICAL EFFECTS

- Heat loss to wall → FWI
- Dilution of mixture → FCAI

**SUPERIMPOSITION OF FWI AND FCAI EFFECTS TAKES PLACE IN DIFFERENT INTERACTION REGIMES: HEAT LOSS DOMINATED, MIXTURE DOMINATED, BOTH EFFECTS ARE DOMINANT → DETAILS SEE PAPER**

# AGENDA / CONTRIBUTIONS



Dr. Hao Xia



Prof. Wang Han

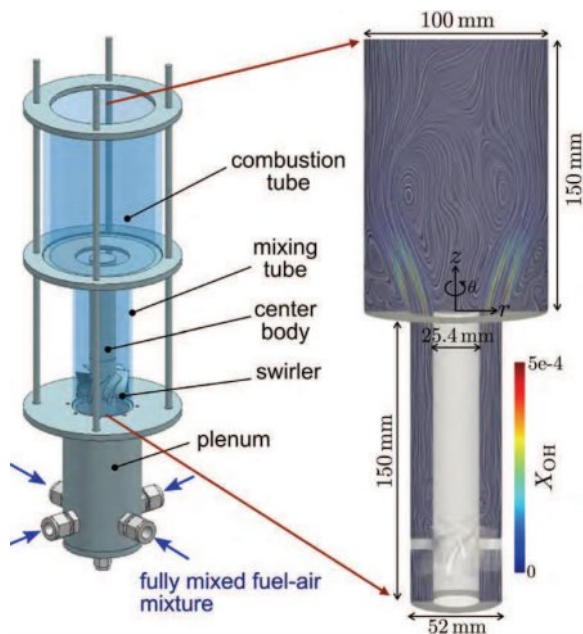


Prof. Jeroen van Oijen



Slides have been rearranged by STFS.

➤ UT Swirl burner

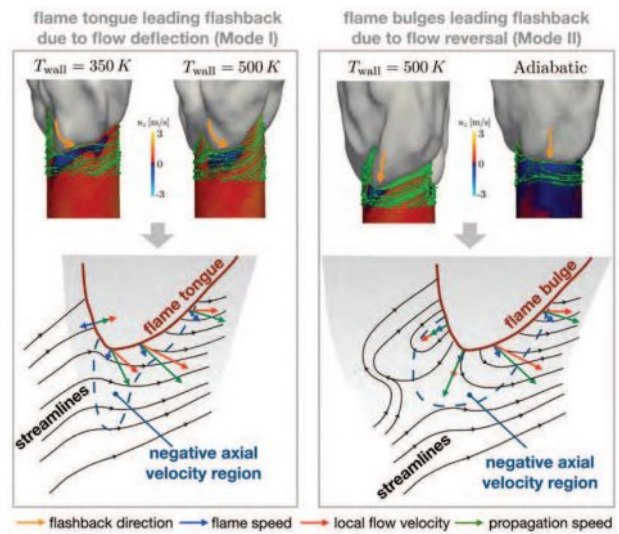
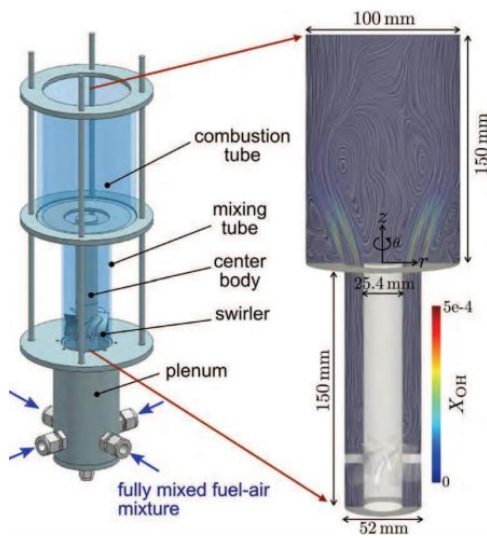


95%H2/5%CH4-air,  $\phi=0.4$



(Ebi et al., CNF2016)

## ➤ Previous results with TFLES



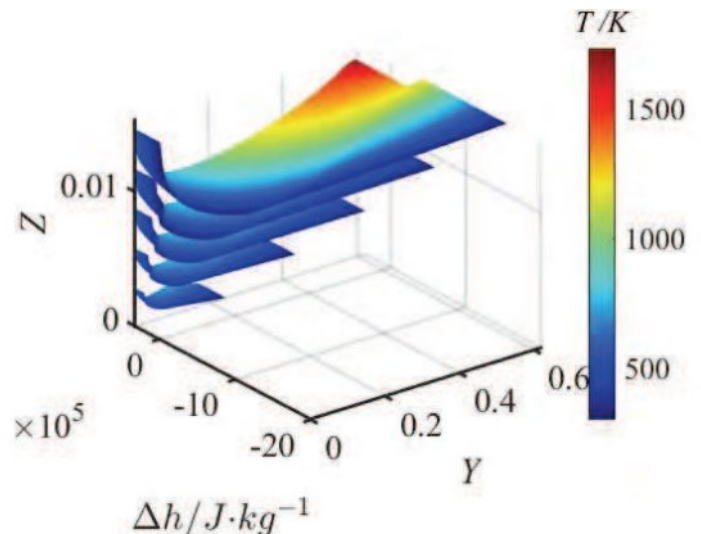
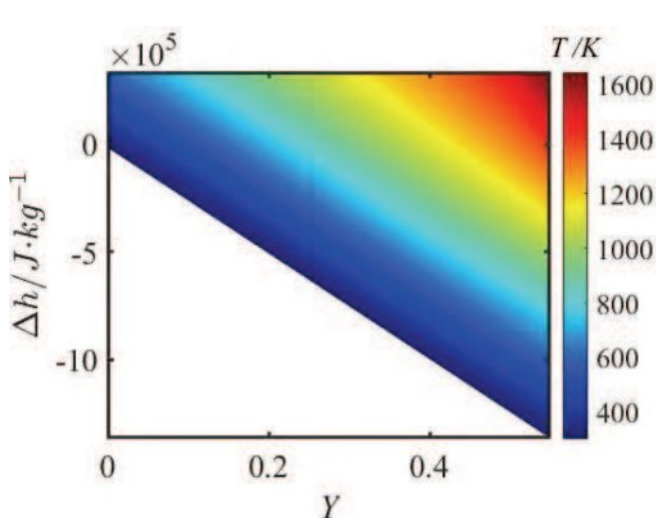
Hao Xia, Wang Han,..., C. Hasse, *PROCI*, Volume 39, 2023, 4541-4551.

- Two modes: flashback due to large-scale flame tongue, and flashback due to flame bulges.
- TFLES modeling leads to the partial loss of flame wrinkling.

## ➤ LES/FGM with differential diffusion (DD) by H. Xia, W. Han, J.A. van Oijen

Combustion model: 3D-FGM

CV1: progress variable; CV2: mixture fraction; CV3: enthalpy



FGM table of H<sub>2</sub>/CH<sub>4</sub> flame ( $\varphi = 0.4$ ) with **unity Le**

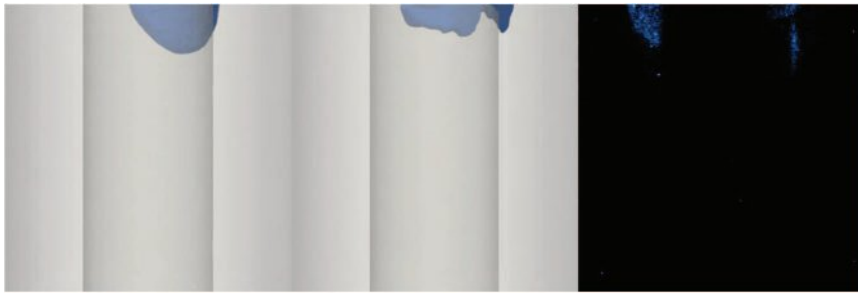
FGM table of H<sub>2</sub>/CH<sub>4</sub> flame ( $\varphi = 0.4$ ) with **DD**

Unity  $Le$  case

DD case

Experiment

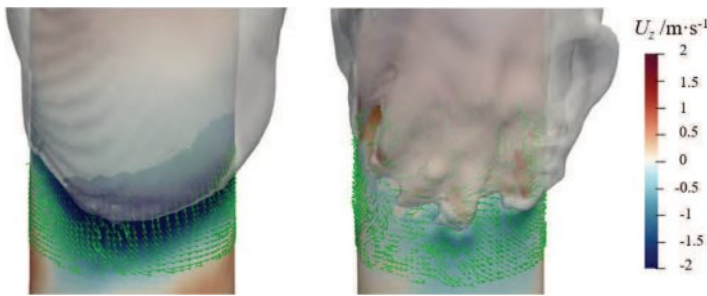
CNF under review



**Average flashback speed**

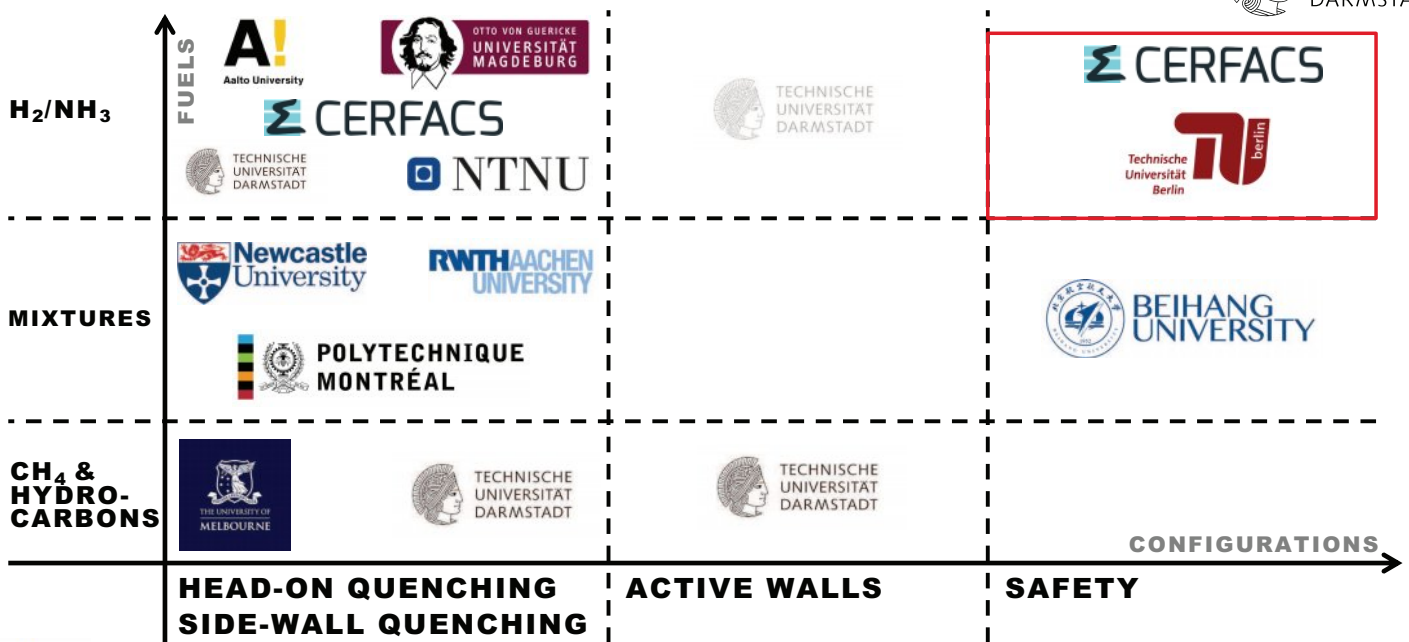
Experiment	0.94 m/s
Unity Le	0.55 m/s
DD	1.02 m/s

Flashback at  $T_{wall} = 350$  K, flame front:  $T = 1180$  K contour



- The flame tongue with DD is much more wrinkled and the flow field is inverted at an upstream location.
- The more wrinkled flame front faster accelerates the flames with  $Le$  less than unity.

**AGENDA / CONTRIBUTIONS**





# Experimental and numerical studies of high-pressure hydrogen jet flame impacting on walls

L. Gaipf, T. Jaravel, Q. Douasbin  
 CERFACS

M. Hamdaoui, T. Schuller, T. Poinsof  
 IMFT

Slides have been rearranged by STFS.

www.cerfacs.fr

KC3



## Context: leak of high pressure H<sub>2</sub> tank in a confined space

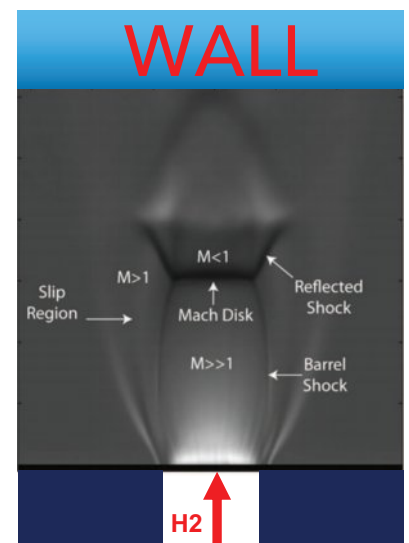
KC3

A choked H<sub>2</sub> jet in a confined space raises multiple questions needing fundamental research:

- Can it autoignite [1-3]?
- How does the flame stabilize in the shock system [4-5]?
- What is the effect of the crossflow if there is one?
- What happens for any wall in the path of the flame ?

In terms of DNS/LES, this leads to many difficulties:

- Must handle flames and shocks at high Reynolds nbr
- Premixed as well as diffusion flame zones
- High speed reacting jet impacting cold wall: law of the wall treatments ?



Ruggles and Ekoto 2012

[1] T. Mogi, Y. Wada, Y. Ogata, and A. Koichi Hayashi, *IJHE*, 2009.

[2] Y. R. Kim, H. J. Lee, S. Kim, and I.-S. Jeung, *PCI*, 2013

[3] M. Asahara, A. Yokoyama, N. Tsuboi, and A. K. Hayashi, *IJHE*, 2023

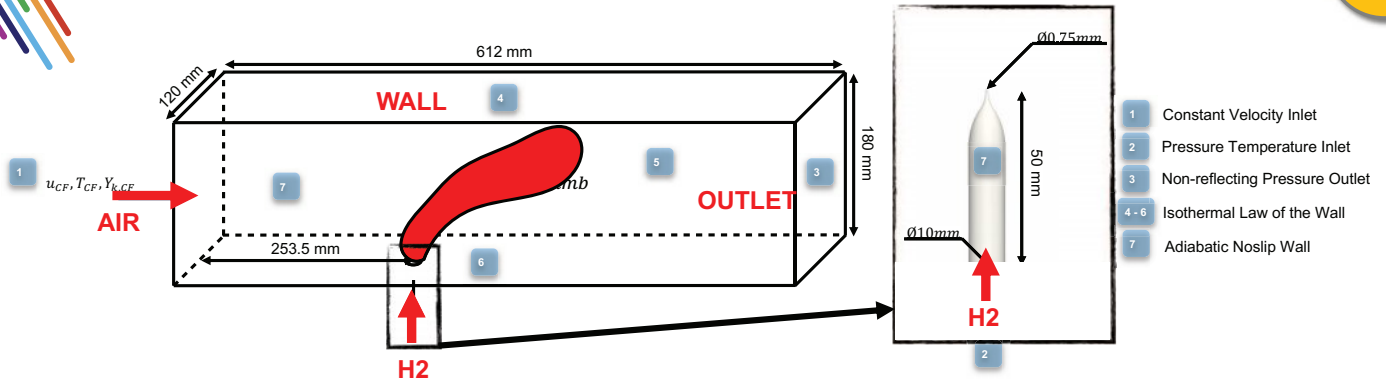
[4] D. Bradley, et al., *CNF*, 2016

[5] A. J. Ruggles and I. W. Ekoto, *IJHE*, 2012



# IMFT experimental setup for flame wall interaction:

KC3



## LES with AVBP (CERFACS):

- Turbulent Combustion Model for premixed/diffusion flames: TFLES [5]
- LES model: WALE [6]
- Shock Treatment: LAD [7]
- Convection scheme: Lax Wendroff [8]
- San Diego Mechanism [9]
- Wall Treatment: IFHC [10]



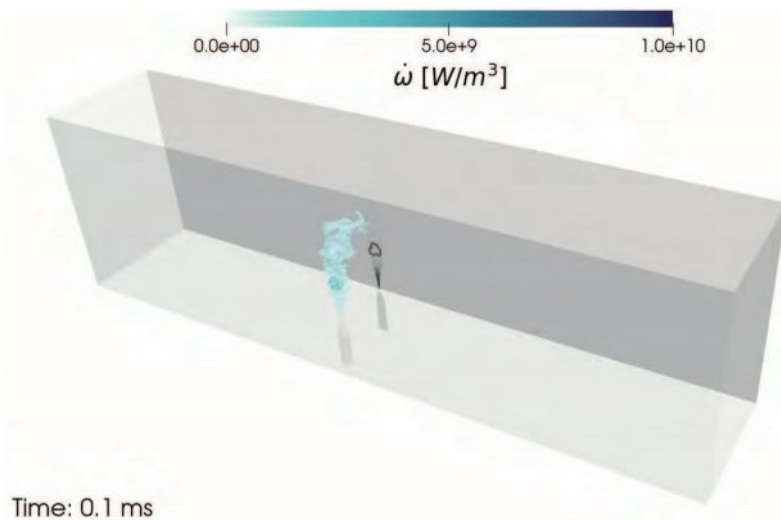
[4] T. Schonfeld, M. Rudgyard, AIAA Journal, 1999  
 [5] O. Colin, et al., PoF, 2000  
 [6] F. Nicoud and F. Ducros, FTC, 1999  
 [7] T. Schmitt, FTC, 2020  
 [8] P. Lax and B. Wendroff, CPAM, 1960  
 [9] F. Williams, 2014  
 [10] C. R. Wilke, TJCP, 1950  
 [10] L. De Nardi et al., CnF, 2024

## Preliminary results

KC3

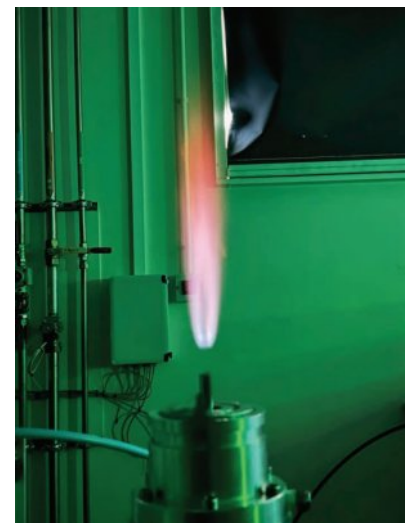
CFD: first LES results

Experimental Validation



Time: 0.1 ms

Isocontour of  $\phi_{LFL}$  in light blue  
 Isocontour coloured by  $\omega$  defined at  $Y_{OH} = 0.02 \cdot \max(Y_{OH})$



Ignited Jet Flame (IMFT)

# Turbulent premixed hydrogen flames

## Jet burner configuration

Paul Porath & Abdulla Ghani  
July 2024

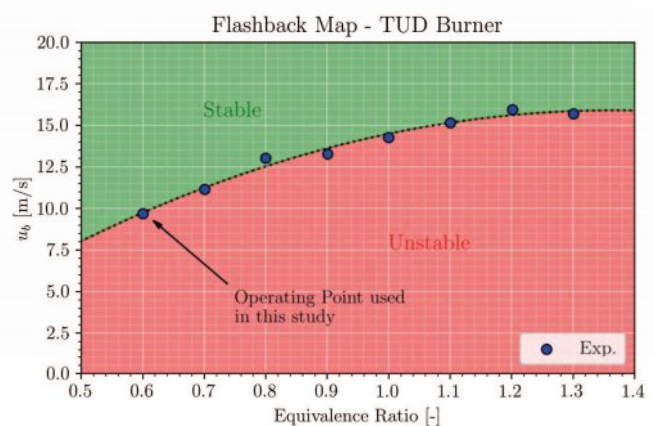
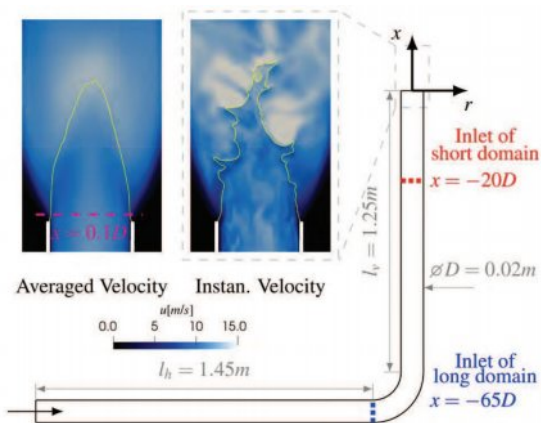
# DMF

Data Analysis and  
Modeling of Turbulent  
Flows



## Burner assembly and the modeled FB event using LES

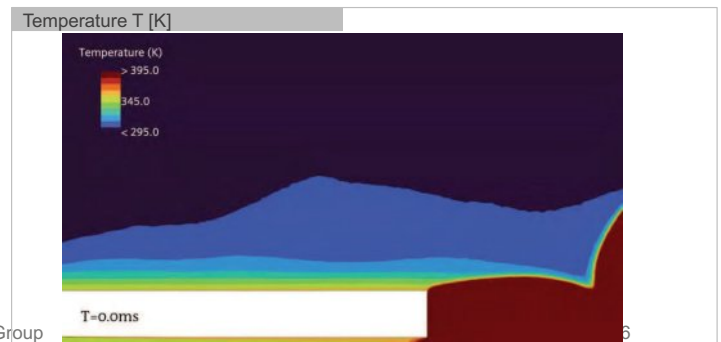
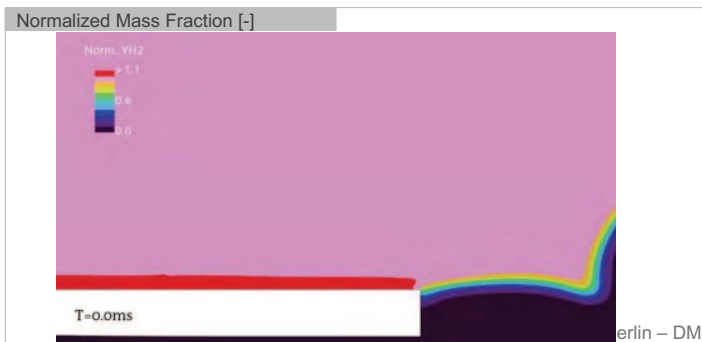
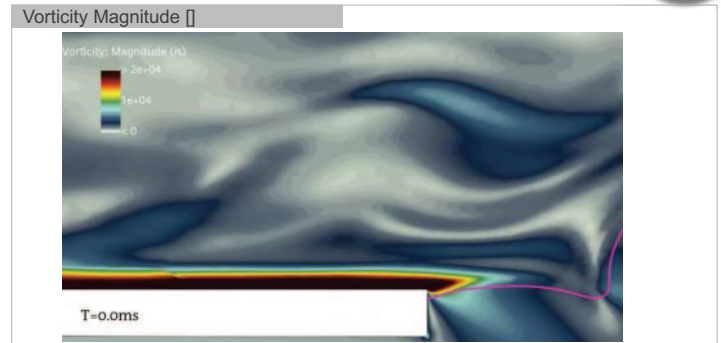
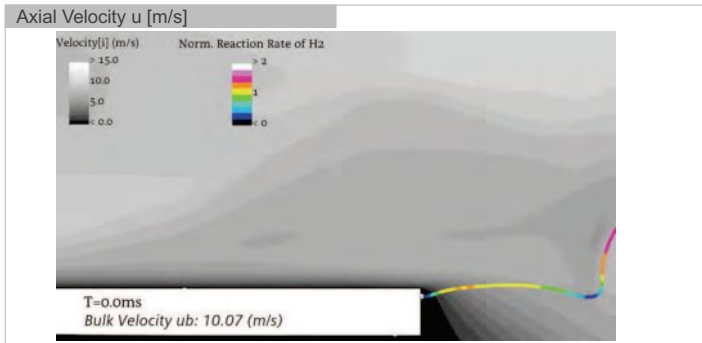
- Tube diameter:  $d = 20\text{mm}$
- Tube material: copper



Boundary Conditions (BCs)	Value
Equivalence ratio $\phi$	0.6
Preheat temperature $T_p$	295K
Pressure $p$	1bar
Reynolds Number $Re$	$\sim 11000$
Adiabatic Flame Temperature $T_{ad}$	1833K

**Flashback is triggered by a low velocity streak caused by the lift-up mechanism which transports low velocity fluid away from the wall**

KC3



Berlin – DMF Group

6

## KEY MESSAGES AND CHALLENGES



### HYDROCARBONS

Key Message 1: Advanced near-wall combustion models available

KM1

### H2/NH3 AND MIXTURES

Key Challenge 1: Near-wall chemistry

KC1

Key Challenge 2: Near-wall combustion and pollutant models

KC2

Key Challenge 3: Safety and especially flashback

KC3

# KEY MESSAGES AND CHALLENGES



## HYDROCARBONS

### Key Message 1: Advanced near-wall combustion models available

- Flamelets for hydrocarbons show good results if properly chosen; parameterization depends on complexity of configuration, e.g. active vs. passive walls.
- Reduced order models can be constructed from canonical flames - but these are somewhat more complex, e.g. head-on quenching (HOQ).
- If near-wall turbulent mixing is resolved in LES, extended flamelet models are adequate

## H<sub>2</sub>/NH<sub>3</sub> AND MIXTURES

Key Challenge 1: Near-wall chemistry

Key Challenge 2: Near-wall combustion and pollutant models

Key Challenge 3: Safety and especially flashback

# KEY MESSAGES AND CHALLENGES



## HYDROCARBONS

Key Message 1: Advanced near-wall combustion models available

## H<sub>2</sub>/NH<sub>3</sub> AND MIXTURES

### Key Challenge 1: Near-wall chemistry

Chemistry at/close to the wall should be (re)visited for H<sub>2</sub>. Do we know anything for NH<sub>3</sub>?

- Known for hydrocarbons - reaction pathways
- H<sub>2</sub> - gas phase and/or catalytic/heterogeneous reactions?

Key Challenge 2: Near-wall combustion and pollutant models

Key Challenge 3: Safety and especially flashback

# KEY MESSAGES AND CHALLENGES

## HYDROCARBONS

Key Message 1: Advanced near-wall combustion models available

## H<sub>2</sub>/NH<sub>3</sub> AND MIXTURES

Key Challenge 1: Near-wall chemistry

### Key Challenge 2: Near-wall combustion and pollutant models

- Reduced order models for H<sub>2</sub>/NH<sub>3</sub> not yet available
  - First DNS datasets available, experiments to be expected
  - Can canonical configurations such as HOQ be used for reduced order models?
- Near-wall stratification/superadiabatic conditions/pollutants: Imposed from the main flame or caused by near-wall processes... or both?
- CO and NO<sub>x</sub> (incl. N<sub>2</sub>O) near wall not yet understood

KC2

Key Challenge 3: Safety and especially flashback

# KEY MESSAGES AND CHALLENGES

## HYDROCARBONS

Key Message 1: Advanced near-wall combustion models available

## H<sub>2</sub>/NH<sub>3</sub> AND MIXTURES

Key Challenge 1: Near-wall chemistry

Key Challenge 2: Near-wall combustion and pollutant models

### Key Challenge 3: Safety and especially flashback

Turbulent flashback scenario for H<sub>2</sub> not fully (...) understood.

- Differential diffusion highly relevant near the wall... something we know!
- Multiple flashback scenarios already in laminar case - Only very little turbulent DNS and experimental data available.
- Impact on flashback: uncertainty in near-wall chemistry, conjugate heat transfer?

KC3



## Summary: Piloted Ammonia Jet Flame: Experimental Results and Initial Model Comparison

*Coordinators: Gaetano Magnotti and Hong Im*

The objective of the session was to compare recent experimental measurements and numerical simulations of a series of partially premixed,  $H_2/N_2/NH_3$ -air, turbulent flames. The flames were stabilized over the Sydney inhomogeneous piloted burner, modified by removing the inner fuel-pipe and using the full length of the burner to guarantee uniform mixing between fuel and air, as in the original Sandia/Sydney piloted flame. The burner was operated with a mixture of 43% simulated cracked ammonia and air, with an equivalence ratio  $\Phi = 3$  in the central jet. A pilot flame (a mixture of 43% simulated cracked ammonia and air, with an equivalence ratio  $\Phi = 0.9$ , and power of 520 W) ensures flame stabilization over a wide range of Reynolds numbers, and a co-flow air velocity of 0.8 m/s provides a controlled boundary condition. Experimental data (Raman/Rayleigh, OH and  $NH_2$ ) were obtained for three flames with central jet Reynolds numbers of 24000 (Flame D), 32000 (Flame E), and 36000 (Flame F) corresponding to 59%, 79%, and 89% of the global extinction Reynolds number.

The flame series offers several challenges to numerical simulations. The large amount of hydrogen in the mixture may require the inclusion of differential diffusion effects, especially in the near field of Flame D. Flame E and Flame F are designed to challenge the models in predicting localized extinction events. Laminar counterflow burner simulations show a complex flame structure, with three heat release peaks, corresponding to the peak in OH, temperature, and  $NH_2$ . Experimental results show that for Flame F extinction starts from the lean side (drop in OH at the mixture fraction of peak OH) and then propagates to the rich side (drop in  $NH_2$  at the mixture fraction corresponding to peak  $NH_2$ ). Re-ignition follows the same pattern, starting from the lean side, 6 diameters from the nozzle, and propagates to the rich side at the axial location 15 diameters downstream. In Flame E, re-ignition is faster, and there is no region with extinction limited only to the rich side.

Nine teams were involved in the simulations of Flame D: KAUST/HUST, Loughborough University/Imperial College, Peking University (PKU), Stanford University, Paris Seclay/CNRS (EM2C), Zhejiang University (ZJU), University of Stuttgart/University of Sydney, Argonne National Lab, and Kyoto University/Zhejiang University (KYU/ZJU). Five groups used OpenFOAM, and five used in-house codes (PIPER, YALES2, CharlesX, an in-house LES solver for ZJU, and an in-house DNS code from KYU/ZJU). All the simulations were LES, except for a DNS (KYU/ZJU) and a URANS (Loughborough/Imperial). Several combustion modelling approaches were employed including tabulated chemistry, moment closure models, and stochastic particle methods. Most simulations employed the Stagni chemical kinetics model (31 species), and the remaining used the KAUST mechanism, an updated mechanism from Lindstedt, the Okafor mechanism, and the Shrestha mechanism. Molecular transport was modeled using a mixture average approach (3 simulations), a unity Lewis number approach (3 simulations) and assigned Schmidt (0.7), and turbulent Schmidt number (0.4 or 0.7). The temporal and spatial schemes are 2<sup>nd</sup> order in time and space for five of the simulations, 3<sup>rd</sup> order for the Stanford simulation, 4<sup>th</sup> order for the YALES 2 and for the DNS simulations, and first order in time, second order in space for the Lboro/IC and the PKU simulations.

Previous simulations of the Sandia piloted jet flame series, were sensitive to the boundary conditions. Velocity measurements were not available for this series, and strategies to simulate the turbulence of the central jet included 10% random fluctuation, turbulent-library-based methods, and velocity fluctuations from Sandia flame D, rescaled to the new bulk velocity. The pilot was modeled with a uniform velocity (6.8 m/s) and equilibrium combustion products, except for the EM2C simulation where the pilot holes were simulated.

All the simulations were at a preliminary stage, as the data were released only a few months before the workshop, and therefore it is not possible to obtain definite conclusions from this initial exercise. The comparison of mixture fraction profiles in physical space shows that all simulations fail to capture

the early decay observed in the experiments at  $X/D=1$ . All the simulations show a unity mixture fraction (no mixing) until 3 mm, whereas the experiment shows a decay after 2.5 mm. Simulations match the experiments in predicting the location of peak rms of mixture fraction representative of the shear layer between the fuel jet and the pilot flame. Uncertainties in the provided boundary conditions could be responsible for the mismatch in the profile, but it is worth noting that turbulence level cannot be the sole responsible, as the three experimental mixture fraction profiles at  $x/D=1$  are perfectly overlapped, despite a factor 2 difference in the Reynolds number. Similarly, the asymmetry in the pilot, affects the pilot region, but does not significantly alter the experimental mixture fraction distribution at the first axial location. Further downstream, simulations continue to underpredict the mixing up to  $x/D=15$ . At  $z/D=30$  the spread among simulations is large, and most simulations have underpredicted mixing, except for the EM2C and the KYU/ZJU simulation that overpredict it. Overall, none of the simulation was able to mimic the experimental profile at all heights. Further comparisons in physical space are dominated by the mismatch in the mixture fraction profiles, and therefore the rest of the presentation focused on results in mixture fraction space. The PKU and KYU/ZJU correctly capture the measured superadiabatic temperature at  $x/D=1$ , which is missed by other simulations including differential diffusion (KAUST, Loughborough), and by the simulations using unity Lewis number. At  $Z/D=2$  and above, all the simulated temperature profiles agree reasonably well with the experiments, although some discrepancies remain for the ITV and IITK simulations. Profiles of  $H_2$  and  $NH_3$  reveal that the simulations systematically overestimate  $H_2$  and underestimate  $NH_3$ . The simulation from PKU appears to be in better agreement. OH profiles are reasonably well captured. Note that the measured OH in the rich region is probably an artifact of the measurements, possibly caused by other radicals associated to ammonia combustion ( $NH_2$ ,  $N_2H_2$ , ...).

Fewer groups (KAUST, ZJU, PKU, ITV and Loughborough) attempted the simulation of Flame F. In physical space, all simulations underpredict the mixing, as already observed for Flame D. In mixture fraction space, experimental temperature profiles are dominated by localized extinction, that appears as early as  $X/D=2$ . All simulations underestimate the amount of localized extinction, with presumed PDF models performing generally worse. PKU and ITV simulations perform relatively well in predicting localized extinction at  $Z/D=6$  and  $Z/D=10$ , but underpredict it closer to the nozzle. Experiments show that localized extinction start on the lean side, characterized by a drop in the OH at  $Z/D=2$  that only appears at  $X/D=4$  for the PKU model. PDF distributions of  $NH_2$  shows generally narrower distributions in the simulation but correctly predict the appearance of  $NH_2$  in lean samples, in the presence of localized extinction.

Overall, this dataset is deemed interesting by the TNF community, and the large number of groups involved despite the short time available for the simulation promises that in-depth analysis, conditioned on the type of models used will be possible. To go further with the analysis, most numerical simulations must be consolidated, and a significant improvement of the mixture fraction field is necessary prior to analyzing the effect of different turbulence-combustion models. Velocity measurements, especially in the near field, would be desirable to help converge to common and more detailed boundary conditions for all the simulations.



## NH<sub>3</sub>/H<sub>2</sub>/N<sub>2</sub>/air partially premixed piloted jet flame

TNF 2024

Presenter: Gaetano Magnotti

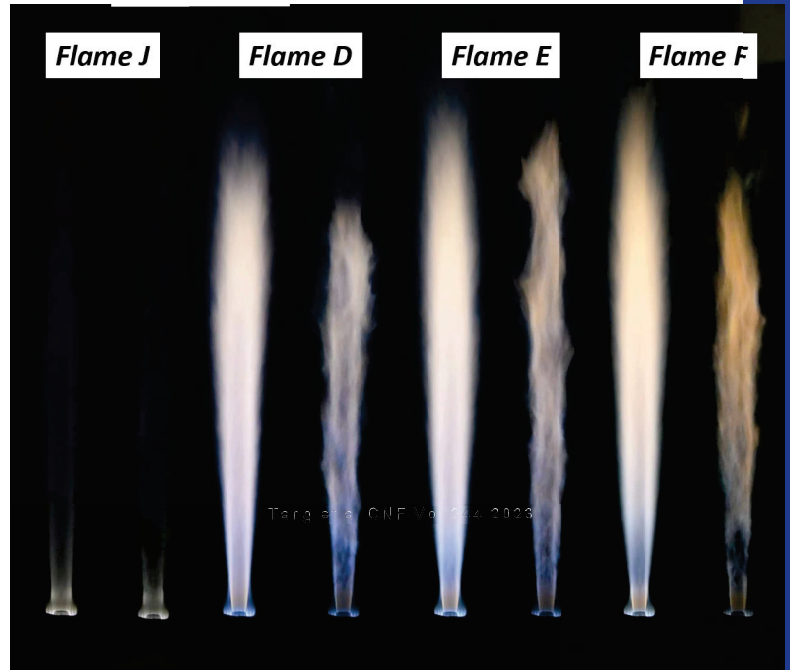
1



## Partially premixed NH<sub>3</sub>/H<sub>2</sub>/air piloted jet flames at atmospheric pressure

## Partially premixed, NH<sub>3</sub>/H<sub>2</sub>/N<sub>2</sub> piloted flames

- Four partially premixed piloted jet flames
- Modified Sydney piloted burner
- Raman/Rayleigh+OH/NH<sub>2</sub> LIF
- Fuel: Simulated partially cracked ammonia (43%), and air with  $\Phi = 3$
- Flame J with 100% cracking
- Pilot jet: Simulated partially cracked ammonia (43%), and air with  $\Phi = 0.9$  520W
- **Turbulence-chemistry interaction, localized extinction/re-ignition**
- **Differential diffusion**
- Three Reynolds numbers
  - Flame D Re=24000 (59% Re<sub>extinction</sub>)
  - Flame E Re=32000 (79% Re<sub>extinction</sub>)
  - Flame F Re=36000 (89% Re<sub>extinction</sub>)
  - Flame J Re=36000 (N<sub>2</sub>:H<sub>2</sub>=1:3)



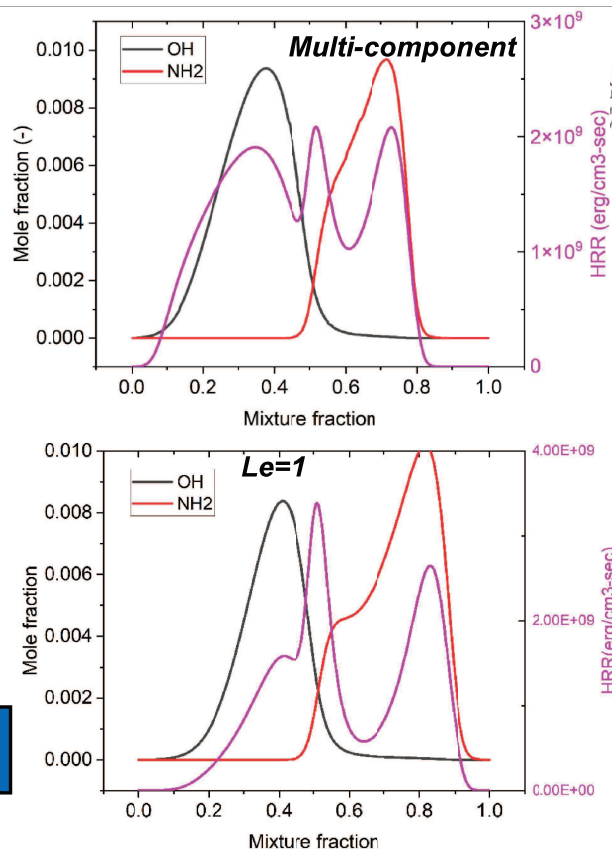
3

## Cracked ammonia piloted flames

- Laminar flame structure from counterflow flames
- Three peaks of heat release identified
  - A peak near  $\zeta = 0.75$  from the premixed, stratified region
  - A peak near  $\zeta = 0.5$  corresponding to the peak temperature
  - A peak near the OH peak
- For unity Lewis number
  - Reduced heat release near the peak of OH
  - Increased heat release near stoichiometric mixture fraction

Poster F05 at the  
symposium on  
Friday

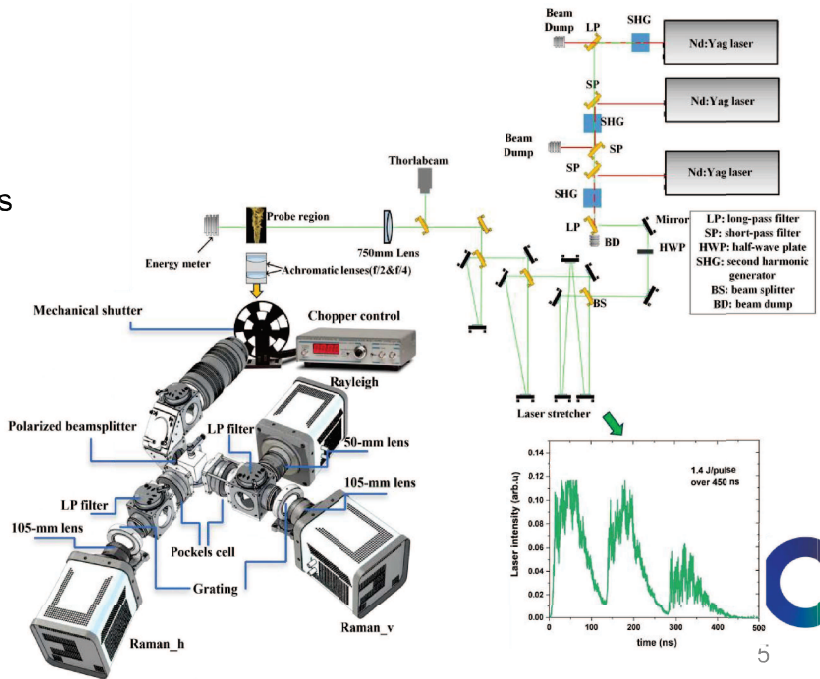
Tang et al. PROCI 40  
(1-4), 105472



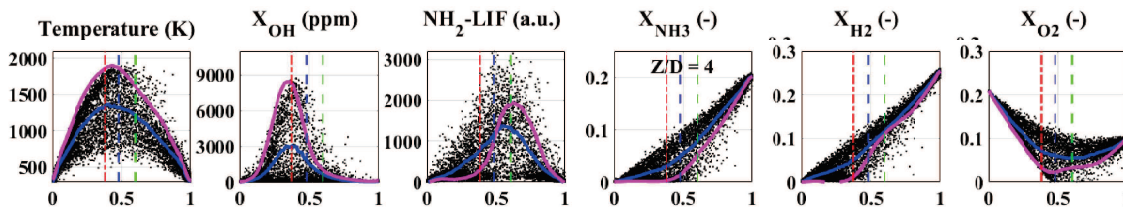
4

# Experimental set-up

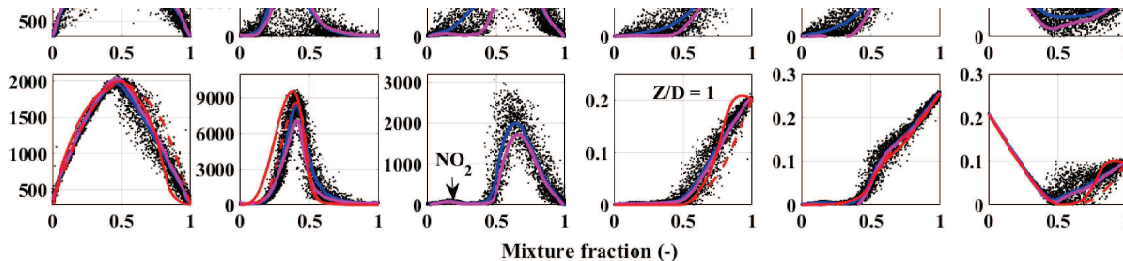
- 1D Raman/Rayleigh scattering for temperature and major species measurements
  - Mole fractions within 0.01
  - Temperature within 40 K
- Semi-quantitative NH<sub>2</sub> measurements from fluorescence interference at 532 nm
  - NH<sub>2</sub> within 10% of predicted value over 23 laminar flames
  - ~ 100 ppm standard deviation at peak temperature, ~ 50 ppm elsewhere
- Saturated OH-LIF
  - Temperature from Raman/Rayleigh



# Ammonia piloted flames: near field



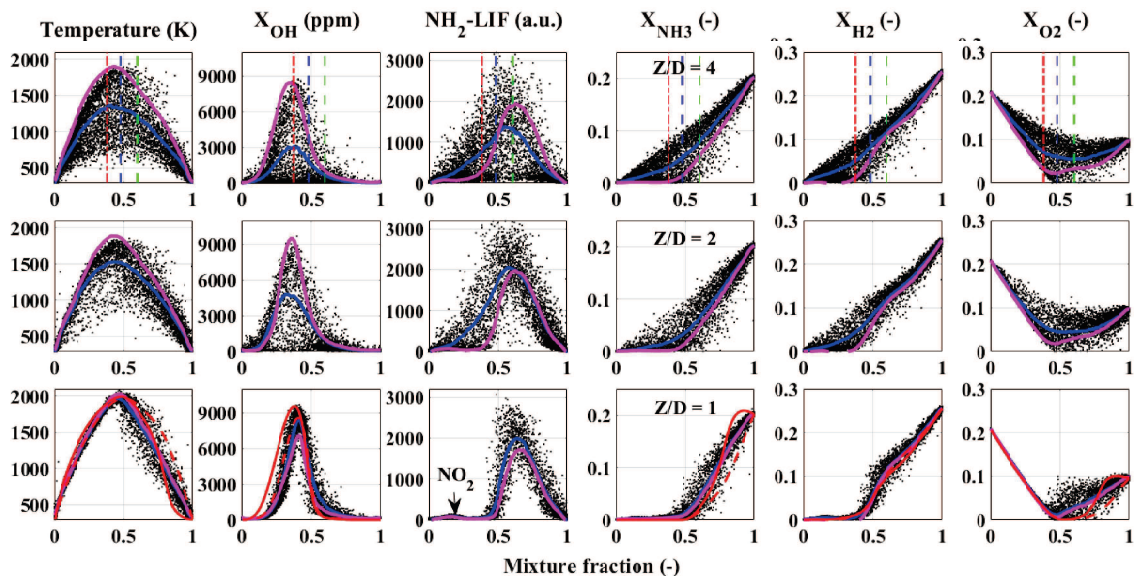
Small differences between Flame D and F at  $z/D=1$ . Intermediate between unity  $Le$  and full multi-component simulation



Tang et al. *PROCI* 40  
(1-4), 105472



# Ammonia piloted flames: near field

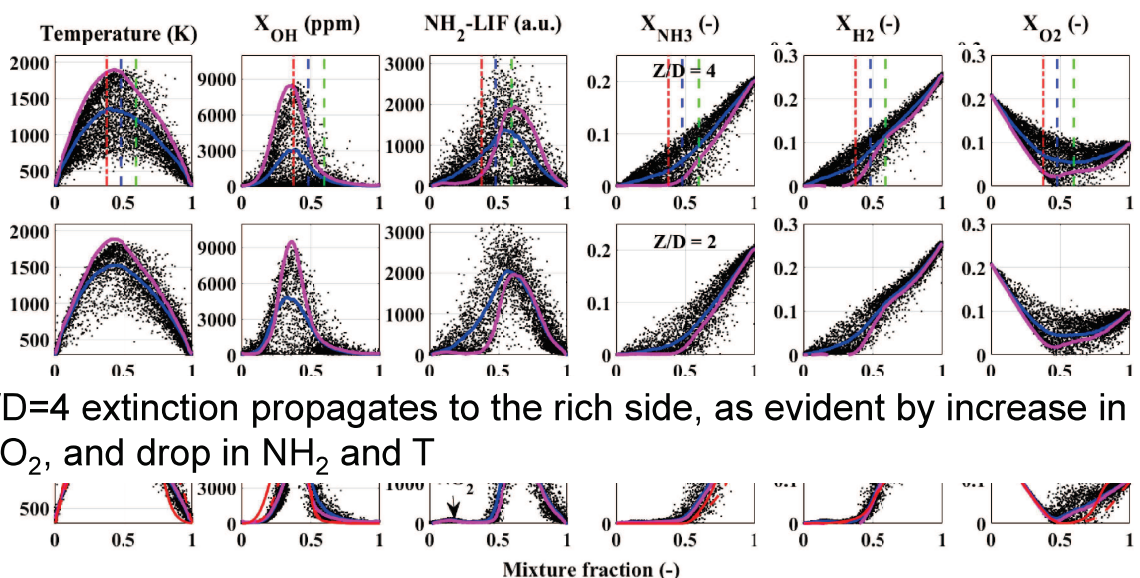


- At  $z/D=2$  local extinctions starts on lean side. Note drop in OH, and  $\text{NH}_2$ , and the appearance of  $\text{NH}_3$  and  $\text{H}_2$  for lean mixture fractions

Tang et al. *PROCI* 40 (1-4), 105472

7

# Ammonia piloted flames: near field

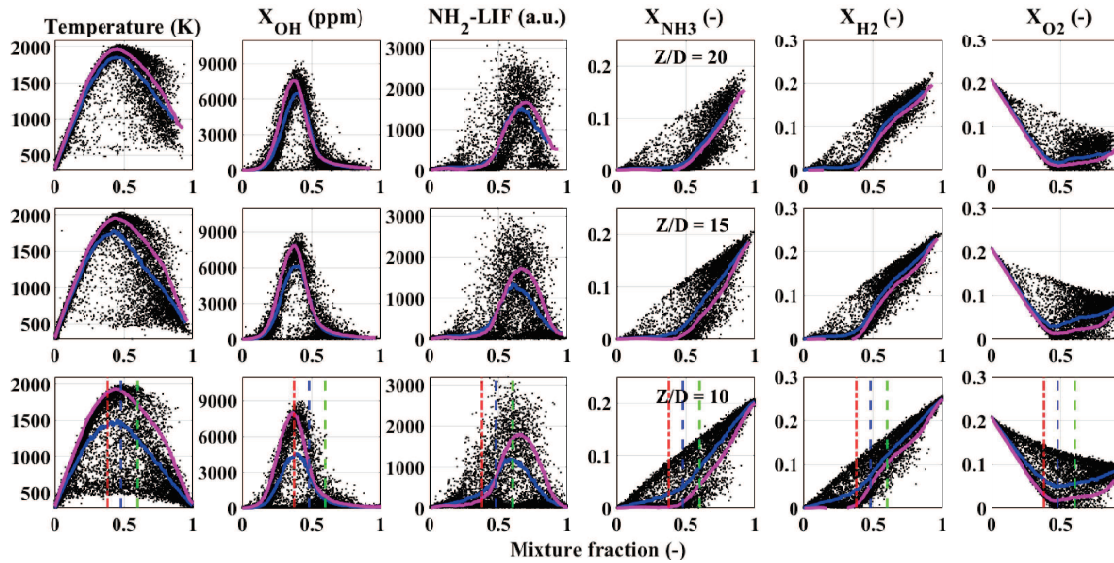


At  $z/D=4$  extinction propagates to the rich side, as evident by increase in  $\text{NH}_3$ , and  $\text{O}_2$ , and drop in  $\text{NH}_2$  and T

Tang et al. *PROCI* 40 (1-4), 105472

8

# Ammonia piloted flames: far field

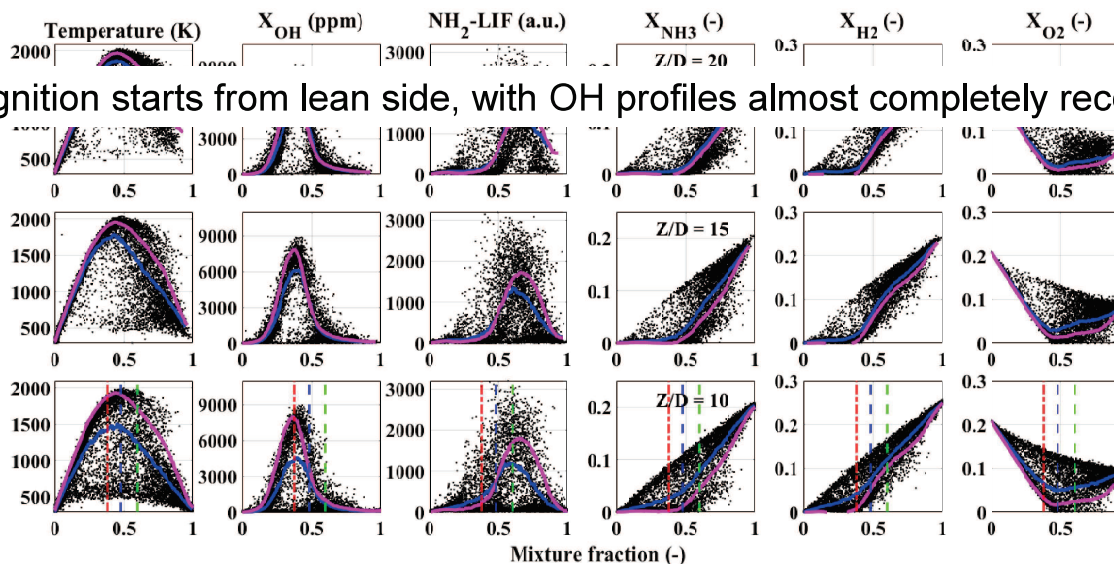


- $z/D=10$  continues to show extensive localized extinction

9

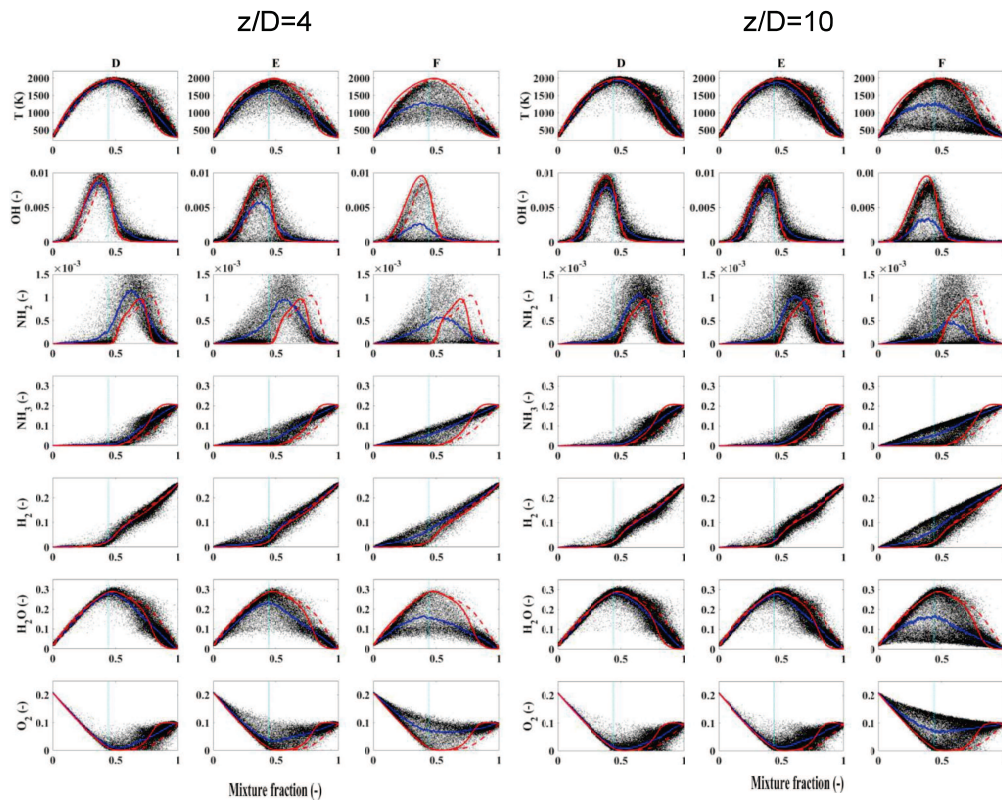
# Ammonia piloted flames: far field

Re-ignition starts from lean side, with OH profiles almost completely recovered



10

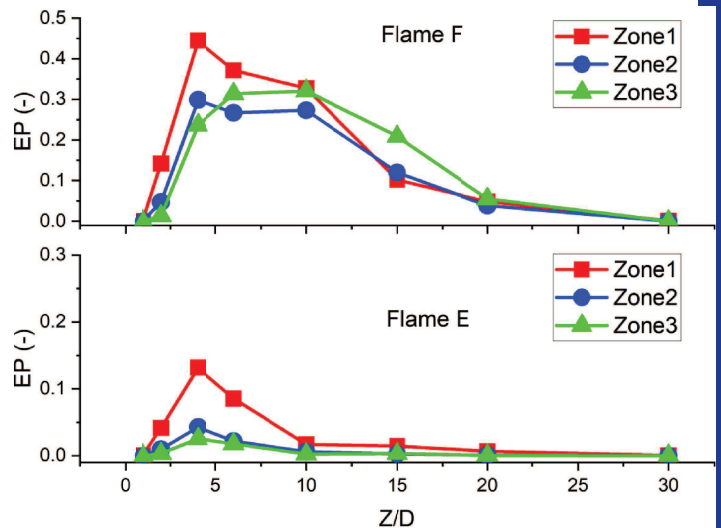
## Scatter plots



11

## Analysis of local extinction

- Extinction probability computed based on the mixture fraction corresponding to the OH, T and  $\text{NH}_2$  peak
- Zone 1: OH concentrations below 1500 ppm for  $\xi=0.38$
- Zone 2: temperature below 1100 K for  $\xi=0.48$
- Zone 3:  $\text{NH}_2$ -LIF intensity below 400 counts for  $\xi=0.60$
- Extinction and re-ignition start from the lean side (zone 1) and propagate to the rich side
- Flame E does not show persistence of extinction in the rich region (zone 3)



Can simulation capture this behavior and provide more insight?

TNF16 workshop

# KAUST Piloted $\text{NH}_3/\text{H}_2/\text{N}_2$ /air flames Joint experimental-numerical comparisons

Junjun Guo, Hao Tang, Francisco Hernandez Perez,  
Gaetano Magnotti, Hong G. Im

King Abdullah University of Science and Technology (KAUST), Thuwal 23955, Saudi Arabia



July 21, 2024



## Objectives

- ❖ It is not about getting a perfect match with the experiments
- ❖ Assess the performances of the current simulations using the state of the art sub-models
- ❖ Identify experimental observations that are not well captured by the majority of the modeling strategies

2



## 10 dataset from 9 contributing teams



Junjun Guo  
Francisco Hernandez Perez  
Zhaohui Liu  
Hong G. Im  
**(KAUST/HUST)**



Yicun Wang, Xinzhou Tang,  
Jiangkuan Xing, Kun Luo, Qingqing  
Xue, Jianren Fan  
**(ZJU-DMC and ZJU-FGM)**



Lu Tian  
R. Peter Lindstedt  
**(lboro/IC)**



Sergio Gutiérrez,  
Thorsten Zirwes,  
Andreas Kronenburg,  
Matthew Cleary  
**(ITV)**



Han Li, Ke Xiao, Zhi X. Chen  
**(PKU)**



Shobhit Gautam,  
Santanu De,  
Eshan Sharma  
**(IIT-K)**



Jenzen Ho, Guillaume Vignat,  
Matthias Ihme  
**(Stanford)**



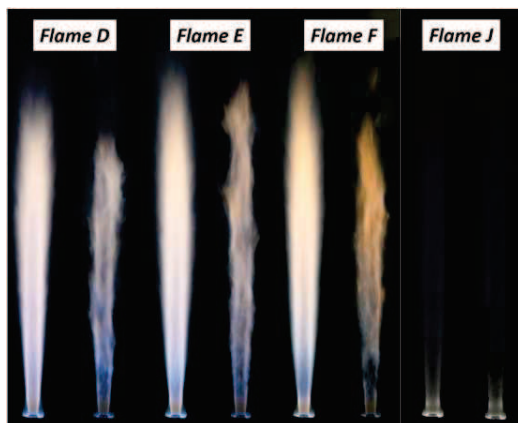
Samuel Dillon, Etienne Espada,  
Benoit Fiorina  
Renaud Mercier  
**(EM2C)**



Jiangkuan Xing,  
Ryoichi Kurose,  
Kun Luo  
**(KYU/ZJU)**

3

## Target flames



43% cracked ammonia      100%  
**KAUST Piloted  $\text{NH}_3/\text{H}_2/\text{N}_2/\text{air}$  flames**

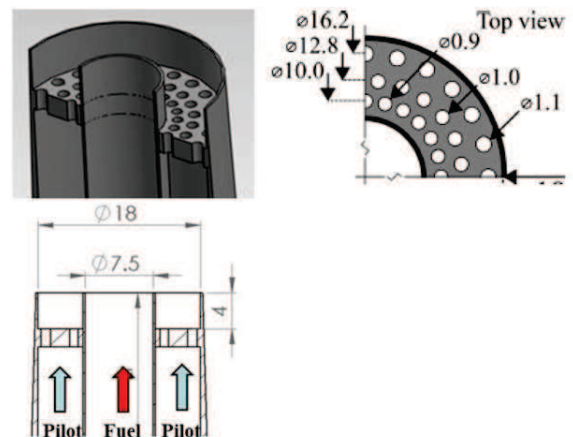


Figure 2: Schematic of the Sydney "inhomogeneous" burner

**Modified pilot-assisted jet burner**

*From Prof. Gaetano Magnotti's group at KAUST*

4





## Flame D and F

Flame conditions	D	F
NH <sub>3</sub> :H <sub>2</sub> :N <sub>2</sub> ratio (Vol.)	40:45:15	40:45:15
$\phi$ of fuel jet	3.0	3.0
Bulk jet velocity (m/s)	61.07	91.60
Coflow velocity (m/s)	0.80	0.80
Pilot power (W)	520	520
$\phi$ of Pilot	0.9	0.9
Re @ setpoint	24,000	36,000
Re @ blowoff	40,500	40,500
Inlet fuel Temp. (K)	293.5	293.5
Inlet coflow Temp. (K)	295.6	295.6
Pressure (bar)	1.0	1.0

(43% simulated cracked NH<sub>3</sub>)

5



## Flame D and F

### Boundary conditions for the **central jet**

Table 6 Nominal and measured mole fractions of the central fuel/air mixture for flames D, E, F.

Flame	Nominal (by volume)	Measured	Difference	Nominal with NH <sub>3</sub> adjusted	Difference after adjustment
O <sub>2</sub>	0.0953	0.0960	0.0007	0.097	0.001
N <sub>2</sub>	0.4415	0.4456	0.0041	0.449	0.0034
NH <sub>3</sub>	0.2179	0.2031	0.0148	0.2031	0
H <sub>2</sub>	0.245	0.2553	0.0103	0.2507	-0.0046

6



# Flame D and F

## Boundary conditions for the pilot inlet

Table 2: Pilot nominal flow rates

Pilot	By Vol.	Velocity	Phi	Flow rate (SLM @ 20 C)	Pilot Power
NH3:H2:N2	40:45:15	1.03 m/s	0.9	1.33 : 1.5 : 0.5, air 9.26	520 W

Table 2 shows measurements at the peak-temperature location for a case with air in the main jet, and only the pilot ignited.

Table 3: Pilot composition and temperature. Adiabatic calculations, and measured values at peak temperature for Z/D=1

Pilot	Temperature	$x_{O_2}$	$x_{N_2}$	$x_{H_2O}$	$x_{OH}$
Adiabatic	2047	0.016	0.698	0.285	0.0026
Measured	1960	0.0155	0.6955	0.292	0.0023

7

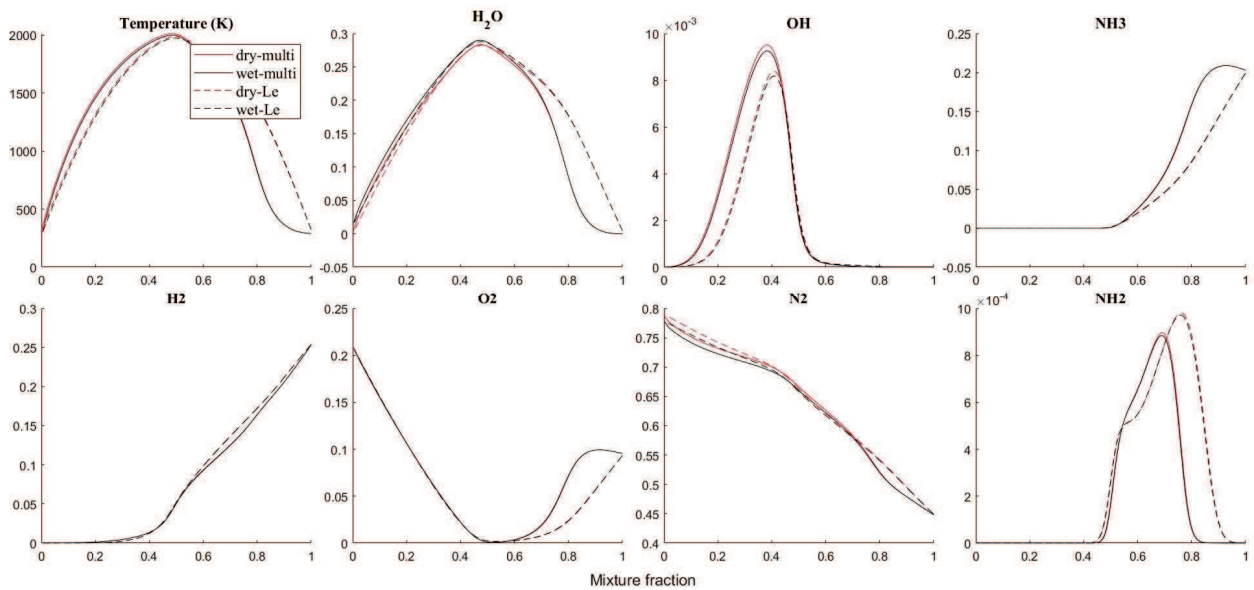


# Flame D and F

Counterflow diffusion flame calculated by Dr. Hao Tang

## Boundary conditions for the coflow

## Effect of humidity (1.5% H<sub>2</sub>O)



8

## Modeling approaches

	Code	Turbulence	Combust.	Chemistry	Molecular transport	Temporal and spatial scheme
KAUST/HUST	OpenFOAM	Dyn. Smagorinsky	Species-weighted FPV (diffusion)	KAUST(38 sp)	Mixture-averaged	2 <sup>nd</sup> order; 2 <sup>nd</sup> order
ZJU	in-house LES solver	Smagorinsky	Direct moment closure	Stagni (31 sp)	Unity-Le	2 <sup>nd</sup> order; 2 <sup>nd</sup> order
ZJU	OpenFOAM	One-equation eddy	FGM (premixed)	Stagni (31 sp)	Unity-Le	1 <sup>st</sup> order; 2 <sup>nd</sup> order
Ibora/IC	PIPER (parabolic solver)	URANS with second moment closure	Joint-Scalar PDF	updated Lindstedt's mech. (21 sp)	McDermott and Pope's model	2 <sup>nd</sup> order
PKU	DeepFlame	Sigma	Laminar	Okafor (25 sp)	Mixture-averaged	1 <sup>st</sup> order; 2 <sup>nd</sup> order
EM2C	YALES2	WALE	F-TACLES (diffusion)	Stagni (31 sp)	Unity-Le	4 <sup>th</sup> order; 4 <sup>th</sup> order
IITK	OpenFOAM	Smagorinsky	Multiple mapping conditioning (MMC)	Stagni (31 sp)	Sc = 0.7 Sct = 0.4	2 <sup>nd</sup> order; 2 <sup>nd</sup> order
ITV	OpenFOAM	Sigma	Multiple mapping conditioning (MMC)	Stagni (31 sp)	Sc = 0.7 Sct = 0.4	2 <sup>nd</sup> order; 2 <sup>nd</sup> order
Stanford	CharlesX	Vreman	FPV (diffusion)	Stagni (31 sp)	Sc = 0.7 Pr = 0.7	3 <sup>rd</sup> order; 3 <sup>rd</sup> order
KYU/ZJU	in-house DNS code	None	Laminar	Shrestha (33 sp)	Mixture-averaged	4 <sup>th</sup> order; 4 <sup>th</sup> order

## Modeling approaches

	Code	Turbulence	Combust.	Chemistry	Molecular transport	Temporal and spatial scheme
KAUST/HUST	OpenFOAM	Dyn. S	Species-weighted / (diffusion)	KAUST(38 sp)	Mixture-averaged	2 <sup>nd</sup> order; 2 <sup>nd</sup> order
ZJU	in-house LES solver	Smag		Stagni (31 sp)	Unity-Le	2 <sup>nd</sup> order; 2 <sup>nd</sup> order
ZJU	OpenFOAM	One-equation eddy	FGM (premixed)	Stagni (31 sp)	Unity-Le	1 <sup>st</sup> order; 2 <sup>nd</sup> order
Ibora/IC	PIPER (parabolic solver)	URAN mome	Joint-Scalar PDF	updated Lindstedt's mech. (21 sp)	McDermott and Pope's model	2 <sup>nd</sup> order
PKU	DeepFlame	Sigma	Laminar	Okafor (25 sp)	Mixture-averaged	1 <sup>st</sup> order; 2 <sup>nd</sup> order
EM2C	YALES2	WALE	F-TACLES (diffusion)	Stagni (31 sp)	Unity-Le	4 <sup>th</sup> order; 4 <sup>th</sup> order
IITK	OpenFOAM	Smagorinsky	Multiple mapping conditioning (MMC)	Stagni (31 sp)	Sc = 0.7 Sct = 0.4	2 <sup>nd</sup> order; 2 <sup>nd</sup> order
ITV	OpenFOAM	Sigma	Multiple mapping conditioning (MMC)	Stagni (31 sp)	Sc = 0.7 Sct = 0.4	2 <sup>nd</sup> order; 2 <sup>nd</sup> order
Stanford	CharlesX	Vrema	FPV (diffusion)	Stagni (31 sp)	Sc = 0.7 Pr = 0.7	3 <sup>rd</sup> order; 3 <sup>rd</sup> order
KYU/ZJU	in-house DNS code	None		Shrestha (33 sp)	Mixture-averaged	4 <sup>th</sup> order; 4 <sup>th</sup> order

## Modeling approaches

	Code	Turbulence	Combust.	Chemistry	Molecular transport	Temporal and spatial scheme
KAUST/HUST	OpenFOAM	Dyn. Smagorinsky	Species-weighted FPV (diffusion)	KAUST(38 sp)	Mixture-averaged	2 <sup>nd</sup> order; 2 <sup>nd</sup> order
ZJU	in-house LES solver	Smagorinsky	Direct moment closure <b>8 LES</b>	Stagni (31 sp)	Unity-Le	2 <sup>nd</sup> order; 2 <sup>nd</sup> order
ZJU	OpenFOAM	One-equation eddy	FGM (premixed)	Stagni (31 sp)	Unity-Le	1 <sup>st</sup> order; 2 <sup>nd</sup> order
Iboro/IC	PIPER (parabolic solver)	URANS with second moment closure	<b>1 URANS</b>	updated Lindstedt's mech. (21 sp)	McDermott and Pope's model	2 <sup>nd</sup> order
PKU	DeepFlame	Sigma	Laminar	Okafor (25 sp)	Mixture-averaged	1 <sup>st</sup> order; 2 <sup>nd</sup> order
EM2C	YALES2	WALE	F-TACLES (diffusion)	Stagni (31 sp)	Unity-Le	4 <sup>th</sup> order; 4 <sup>th</sup> order
IITK	OpenFOAM	Smagorinsky	Multiple mapping conditioning (MMC)	Stagni (31 sp)	Sc = 0.7 Sct = 0.4	2 <sup>nd</sup> order; 2 <sup>nd</sup> order
ITV	OpenFOAM	Sigma	Multiple mapping conditioning (MMC)	Stagni (31 sp)	Sc = 0.7 Sct = 0.4	2 <sup>nd</sup> order; 2 <sup>nd</sup> order
Stanford	CharlesX	Vreman	FPV (diffusion)	Stagni (31 sp)	Sc = 0.7 Pr = 0.7	3 <sup>rd</sup> order; 3 <sup>rd</sup> order
KYU/ZJU	in-house DNS code	None	<b>1 DNS</b>	Shrestha (33 sp)	Mixture-averaged	4 <sup>th</sup> order; 4 <sup>th</sup> order

## Modeling approaches

	Code	Turbulence	Combust.	Chemistry	Molecular transport	Temporal and spatial scheme
KAUST/HUST	OpenFOAM	Dyn. Smagorinsky	Species-weighted FPV (diffusion)	KAUST(38 sp)	<b>4 Tabulated chemistry method</b>	2 <sup>nd</sup> order; 2 <sup>nd</sup> order
ZJU	in-house LES solver	Smagorinsky	Direct moment closure	Stagni (31 sp)	<b>1 Moment closure model</b>	2 <sup>nd</sup> order; 2 <sup>nd</sup> order
ZJU	OpenFOAM	One-equation eddy	FGM (premixed)	Stagni (31 sp)	Unity-Le	1 <sup>st</sup> order; 2 <sup>nd</sup> order
Iboro/IC	PIPER (parabolic solver)	URANS with second moment closure	Joint-Scalar PDF	updated Lindstedt's mech. (21 sp)	<b>3 Stochastic particle method</b>	2 <sup>nd</sup> order
PKU	DeepFlame	Sigma	Laminar	Okafor (25 sp)	<b>2 Laminar</b>	Mixture-averaged
EM2C	YALES2	WALE	F-TACLES (diffusion)	Stagni (31 sp)	Unity-Le	4 <sup>th</sup> order; 4 <sup>th</sup> order
IITK	OpenFOAM	Smagorinsky	Multiple mapping conditioning (MMC)	Stagni (31 sp)	Sc = 0.7 Sct = 0.4	2 <sup>nd</sup> order; 2 <sup>nd</sup> order
ITV	OpenFOAM	Sigma	Multiple mapping conditioning (MMC)	Stagni (31 sp)	Sc = 0.7 Sct = 0.4	2 <sup>nd</sup> order; 2 <sup>nd</sup> order
Stanford	CharlesX	Vreman	FPV (diffusion)	Stagni (31 sp)	Sc = 0.7 Pr = 0.7	3 <sup>rd</sup> order; 3 <sup>rd</sup> order
KYU/ZJU	in-house DNS code	None	Laminar	Shrestha (33 sp)	Mixture-averaged	4 <sup>th</sup> order; 4 <sup>th</sup> order

## Modeling approaches

	Code	Turbulence	Combust.	Chemistry	Molecular transport	Temporal and spatial scheme
KAUST/HUST	OpenFOAM	Dyn. Smagorinsky	Species-weighted FPV (diffusion)	KAUST(38 sp)	Mixture-averaged	2 <sup>nd</sup> order; 2 <sup>nd</sup> order
ZJU	in-house LES solver	Smagorinsky	Direct moment closure	Stagni (31 sp)	Unity-Le	2 <sup>nd</sup> order; 2 <sup>nd</sup> order
ZJU	OpenFOAM	One-equation eddy	FGM (premixed)	Stagni (31 sp)	Unity-Le	1 <sup>st</sup> order; 2 <sup>nd</sup> order
Iboro/IC	PIPER (parabolic solver)	URANS with second moment closure	Joint-Scalar PDF	updated Lindstedt's mech. (21 sp)	McDermott and Pope's model	2 <sup>nd</sup> order
PKU	DeepFlame	Sigma	Laminar	Okafor (25 sp)	Mixture-averaged	1 <sup>st</sup> order; 2 <sup>nd</sup> order
EM2C	YALES2	WALE	F-TACLES (diffusion)	Stagni (31 sp)	Unity-Le	4 <sup>th</sup> order; 4 <sup>th</sup> order
IITK	OpenFOAM	Smagorinsky	Multiple mapping conditioning (MMC)	Stagni (31 sp)	Sc = 0.7 Sct = 0.4	2 <sup>nd</sup> order; 2 <sup>nd</sup> order
ITV	OpenFOAM	Sigma	Multiple mapping conditioning (MMC)	Stagni (31 sp)	Sc = 0.7 Sct = 0.4	2 <sup>nd</sup> order; 2 <sup>nd</sup> order
Stanford	CharlesX	Vreman	FPV (diffusion)	Stagni (31 sp)	Sc = 0.7 Pr = 0.7	3 <sup>rd</sup> order; 3 <sup>rd</sup> order
KYU/ZJU	in-house DNS code	None	Laminar	Shrestha (33 sp)	Mixture-averaged	4 <sup>th</sup> order; 4 <sup>th</sup> order

## Modeling approaches

	Code	Turbulence	Combust.	Chemistry	Molecular transport	Temporal and spatial scheme
KAUST/HUST	OpenFOAM	Dyn. Smagorinsky	Species-weighted FPV (diffusion)	KAUST(38 sp)	Mixture-averaged	2 <sup>nd</sup> order; 2 <sup>nd</sup> order
ZJU	in-house LES solver	Smagorinsky	Direct moment closure	Stagni (31 sp)	Unity-Le	2 <sup>nd</sup> order; 2 <sup>nd</sup> order
ZJU	OpenFOAM	One-equation eddy	FGM (premixed)	Stagni (31 sp)	Unity-Le	1 <sup>st</sup> order; 2 <sup>nd</sup> order
Iboro/IC	PIPER (parabolic solver)	URANS with second moment closure	Joint-Scalar PDF	updated Lindstedt's mech. (21 sp)	McDermott and Pope's model	2 <sup>nd</sup> order
PKU	DeepFlame	Sigma	Laminar	Okafor (25 sp)	Mixture-averaged	1 <sup>st</sup> order; 2 <sup>nd</sup> order
EM2C	YALES2	WALE	F-TACLES (diffusion)	Stagni (31 sp)	Unity-Le	4 <sup>th</sup> order; 4 <sup>th</sup> order
IITK	OpenFOAM	Smagorinsky	Multiple mapping conditioning (MMC)	Stagni (31 sp)	Sc = 0.7 Sct = 0.4	2 <sup>nd</sup> order; 2 <sup>nd</sup> order
ITV	OpenFOAM	Sigma	Multiple mapping conditioning (MMC)	Stagni (31 sp)	Sc = 0.7 Sct = 0.4	2 <sup>nd</sup> order; 2 <sup>nd</sup> order
Stanford	CharlesX	Vreman	FPV (diffusion)	Stagni (31 sp)	Sc = 0.7 Pr = 0.7	3 <sup>rd</sup> order; 3 <sup>rd</sup> order
KYU/ZJU	in-house DNS code	None	Laminar	Shrestha (33 sp)	Mixture-averaged	4 <sup>th</sup> order; 4 <sup>th</sup> order



## Modeling approaches

	Code	Turbulence	Combust.	Chemistry	Molecular transport	Temporal and spatial scheme
KAUST/HUST	OpenFOAM	Dyn. Smagorinsky	Species-weighted FPV (diffusion)	KAUST(38 sp)	Mixture-averaged	2 <sup>nd</sup> order; 2 <sup>nd</sup> order
ZJU	in-house LES solver	Smagorinsky	Direct moment closure	Stagni (31 sp)	Unity-Le	2 <sup>nd</sup> order; 2 <sup>nd</sup> order
ZJU	OpenFOAM	One-equation eddy	FGM (premixed)	Stagni (31 sp)	Unity-Le	1 <sup>st</sup> order; 2 <sup>nd</sup> order
Iboro/IC	PIPER (parabolic solver)	URANS with second moment closure	Joint-Scalar PDF	updated Lindstedt's mech. (21 sp)	McDermott and Pope's model	2 <sup>nd</sup> order
PKU	DeepFlame	Sigma	Laminar	Okafor (25 sp)	Mixture-averaged	1 <sup>st</sup> order; 2 <sup>nd</sup> order
EM2C	YALES2	WALE	F-TACLES (diffusion)	Stagni (31 sp)	Unity-Le	4 <sup>th</sup> order; 4 <sup>th</sup> order
IITK	OpenFOAM	Smagorinsky	Multiple mapping conditioning (MMC)	Stagni (31 sp)	Sc = 0.7 Sct = 0.4	2 <sup>nd</sup> order; 2 <sup>nd</sup> order
ITV	OpenFOAM	Sigma	Multiple mapping conditioning (MMC)	Stagni (31 sp)	Sc = 0.7 Sct = 0.4	2 <sup>nd</sup> order; 2 <sup>nd</sup> order
Stanford	CharlesX	Vreman	FPV (diffusion)	Stagni (31 sp)	Sc = 0.7 Pr = 0.7	3 <sup>rd</sup> order; 3 <sup>rd</sup> order
KYU/ZJU	in-house DNS code	None	Laminar	Shrestha (33 sp)	Mixture-averaged	4 <sup>th</sup> order; 4 <sup>th</sup> order

## Modeling approaches (continue)

	Cells	Comp. time [CPU-hrs/ms]	Central jet boundary conditions	Pilot boundary conditions
KAUST/HUST	4.6 M	150	Turbulent library-based methods	uniform velocity of 6.8 m/s
ZJU-DMC	1.89 M	736	10% Random fluctuation	uniform velocity of 6.55 m/s
ZJU-FGM	7.2 M	111 (Flame D) 180 (Flame F)	10% Random fluctuation	uniform velocity of 6.55 m/s
Iboro/IC	284 X n	720-2400 (in total)	1/7th power profile	uniform velocity of 6.7 m/s
PKU	16 M	~4,000	Internal recycling-mapping method	uniform velocity of 6 m/s equilibrium state gas
EM2C	17.8 M tetrahedral	52	No turbulence injection	Pilot holes were meshed
IITK	2.24 M	191 322 (with sampling)	Turbulent library-based methods	uniform velocity of 6.46 m/s equilibrium state gas
ITV	1.98 M	125 (Flame D) 89 (Flame F)	Turbulent library-based methods Nominal species component	uniform velocity of 6.8 m/s equilibrium state gas
Stanford	5 M	~900 (Flame D)	Velocity and velocity fluctuations from Sandia Flame D rescaled to new bulk velocity	constant mass flow rate experimental burnt mixture at z/D=1
KYU/ZJU	112 M	36,354 (Flame D)	Turbulent library-based methods	Uniform velocity of 6.55 m/s Adiabatic burnt mixture

## Modeling approaches (continue)

	Cells	Comp. time [CPU-hrs/ms]	Central jet boundary conditions	Pilot boundary conditions
KAUST/HUST	4.6 M	150	Turbulent library-based methods	uniform velocity of 6.8 m/s
ZJU-DMC	1.89 M	736	10% Random fluctuation	uniform velocity of 6.55 m/s
ZJU-FGM	7.2 M	111 (Flame D) 180 (Flame F)	10% Random fluctuation	uniform velocity of 6.55 m/s
Ibora/IC	284 X n	720-2400 (in total)	1/7th power profile	uniform velocity of 6.7 m/s
PKU	16 M	~4,000	Internal recycling-mapping method	uniform velocity of 6 m/s equilibrium state gas
EM2C	17.8 M tetrahedral	52	No turbulence injection	Pilot holes were meshed
IITK	2.24 M	191 322 (with sampling)	Turbulent library-based methods	uniform velocity of 6.46 m/s equilibrium state gas
ITV	1.98 M	125 (Flame D) 89 (Flame F)	Turbulent library-based methods Nominal species component	uniform velocity of 6.8 m/s equilibrium state gas
Stanford	5 M	~900 (Flame D)	Velocity and velocity fluctuations from Sandia Flame D rescaled to new bulk velocity	constant mass flow rate experimental burnt mixture at z/D=1
KYU/ZJU	112 M	36,354 (Flame D)	Turbulent library-based methods	Uniform velocity of 6.55 m/s Adiabatic burnt mixture

## Modeling approaches (continue)

	Cells	Comp. time [CPU-hrs/ms]	Central jet boundary conditions	Pilot boundary conditions
KAUST/HUST	4.6 M	150	Turbulent library-based methods	uniform velocity of 6.8 m/s
ZJU-DMC	1.89 M	736	10% Random fluctuation	uniform velocity of 6.55 m/s
ZJU-FGM	7.2 M	111 (Flame D) 180 (Flame F)	10% Random fluctuation	uniform velocity of 6.55 m/s
Ibora/IC	284 X n	720-2400 (in total)	1/7th power profile	uniform velocity of 6.7 m/s
PKU	16 M	~4,000	Internal recycling-mapping method	uniform velocity of 6 m/s equilibrium state gas
EM2C	17.8 M tetrahedral	52	No turbulence injection	Pilot holes were meshed
IITK	2.24 M	191 322 (with sampling)	Turbulent library-based methods Measured species at z/D = 1	uniform velocity of 6.46 m/s equilibrium state gas
ITV	1.98 M	125 (Flame D) 89 (Flame F)	Turbulent library-based methods Nominal species component	uniform velocity of 6.8 m/s equilibrium state gas
Stanford	5 M	~900 (Flame D)	Velocity and velocity fluctuations from Sandia Flame D rescaled to new bulk velocity	constant mass flow rate experimental burnt mixture at z/D=1
KYU/ZJU	112 M	36, 354 (Flame D)	Turbulent library-based methods	Uniform velocity of 6.55 m/s Adiabatic burnt mixture



## Mean and RMS radial profiles in physical space

### Conditional mean in mixture fraction space

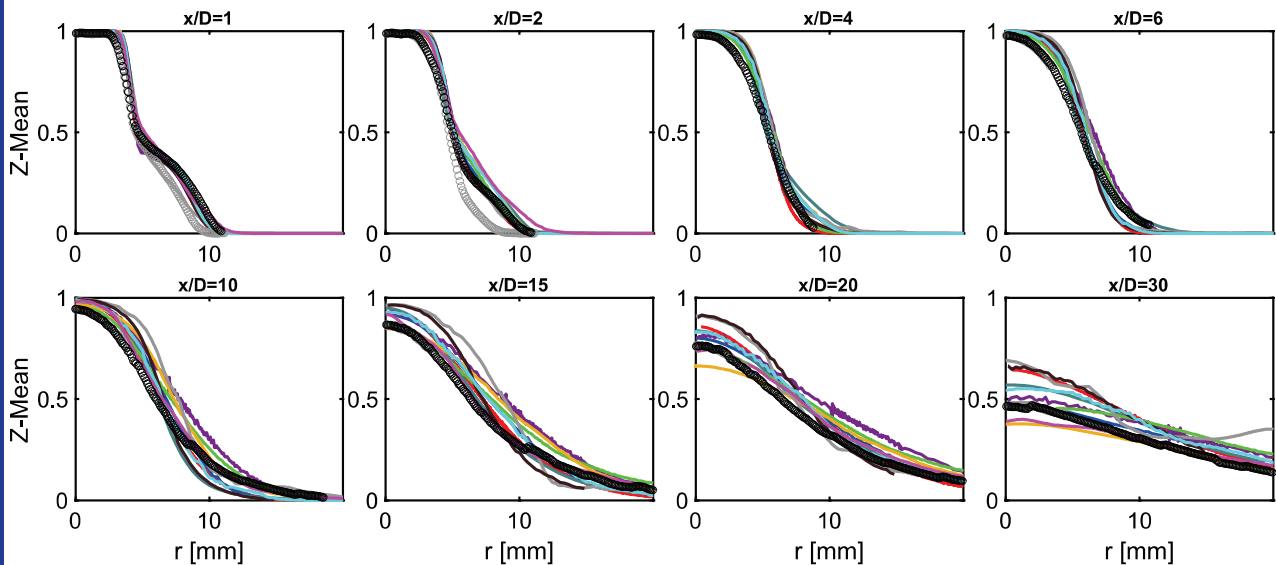
#### Flame D

19



## Flame D: Mean mixture fraction

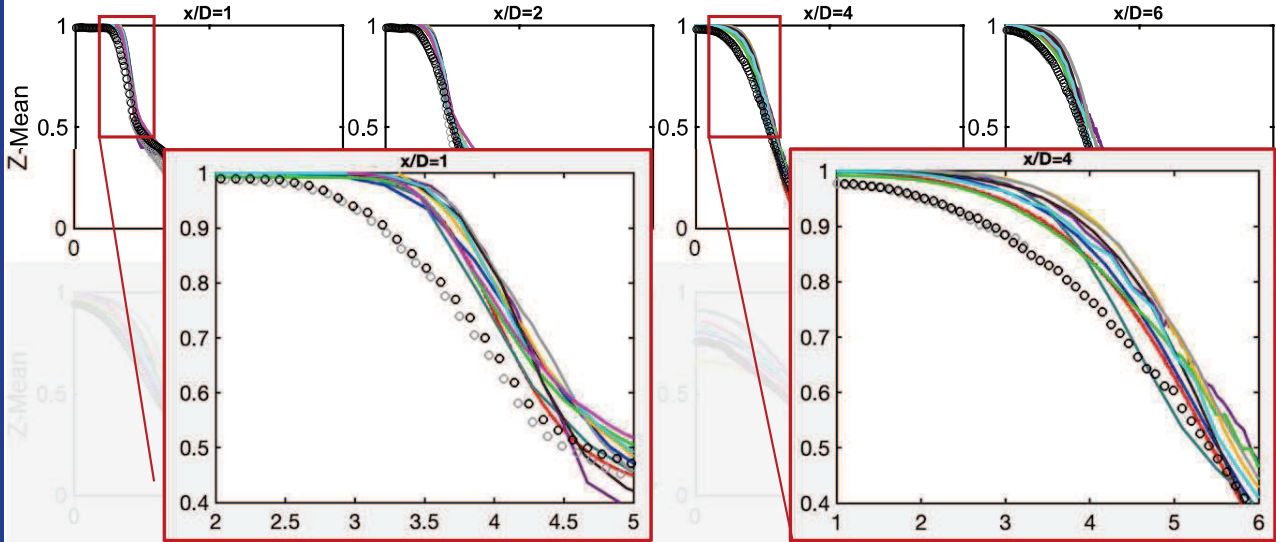
- Exp.(right) KAUST/HUST ZJU-DMC ZJU-FGM Iboro/IC PKU
- Exp.(left) EM2C IITK ITV Stanford KYU/ZJU





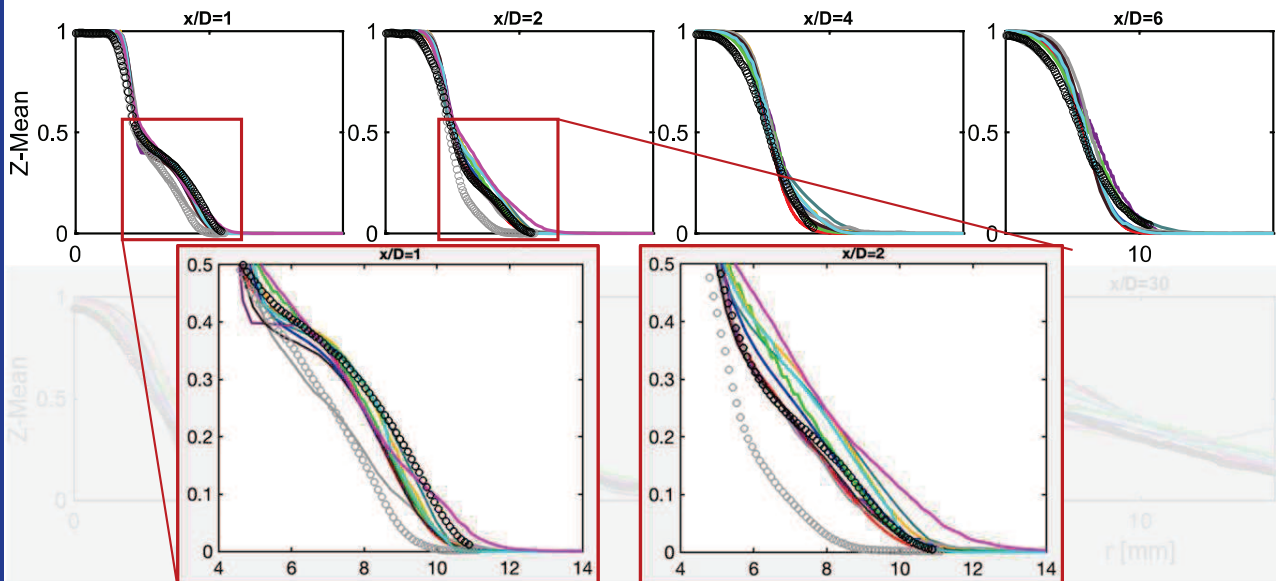
## Flame D: Mean mixture fraction

- Exp.(right) KAUST/HUST ZJU-DMC ZJU-FGM Iboro/IC PKU
- Exp.(left) EM2C IITK ITV Stanford KYU/ZJU



## Flame D: Mean mixture fraction

- Exp.(right) KAUST/HUST ZJU-DMC ZJU-FGM Iboro/IC PKU
- Exp.(left) EM2C IITK ITV Stanford KYU/ZJU

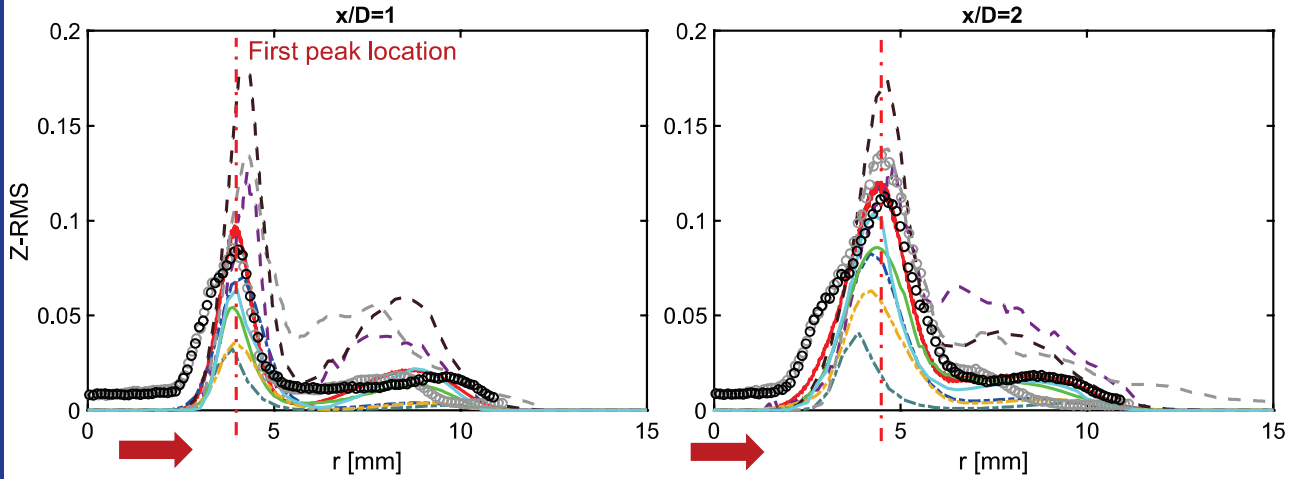




## Flame D: RMS Mixture fraction

- Exp.(right) — KAUST/HUST — PKU — Stanford
- Exp.(left) — ZJU-DMC — ZJU-FGM — EM2C
- Iboro/IC — IITK — ITV

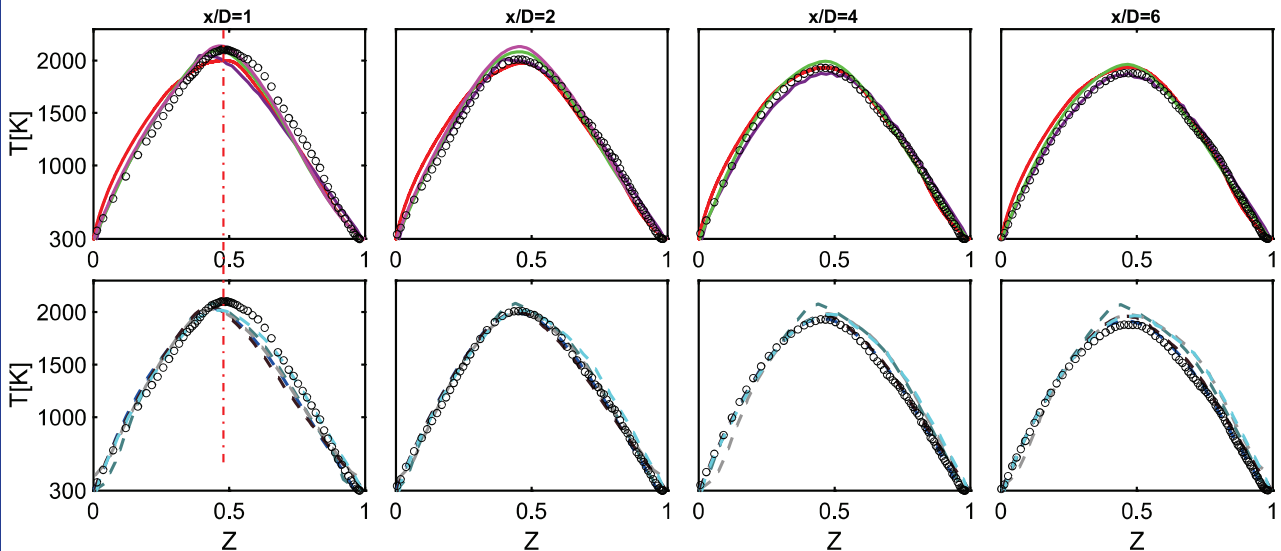
Library-based; Mapping; Scaled measurement  
10% Random fluctuation; No turbulence  
PDF-based models



## Flame D: Temperature (near-field: 1D-6D)

- Exp. — KAUST/HUST — Iboro/IC — PKU — KYU/ZJU
- ZJU-DMC — ZJU-FGM — IITK — ITV — Stanford

Considering differential diffusion  
Using unity Lewis number



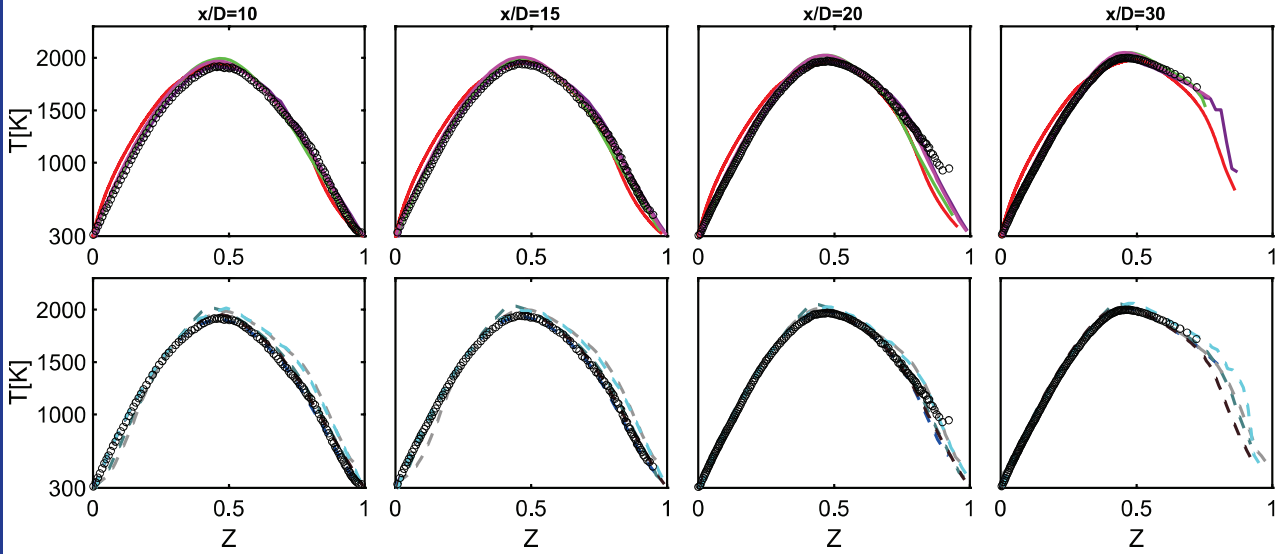
24





## Flame D: Temperature (downstream: 10D-30D)

○ Exp.    — KAUST/HUST    — Iboro/IC    — PKU    — KYU/ZJU  
— ZJU-DMC    — ZJU-FGM    — IITK    — ITV    — Stanford

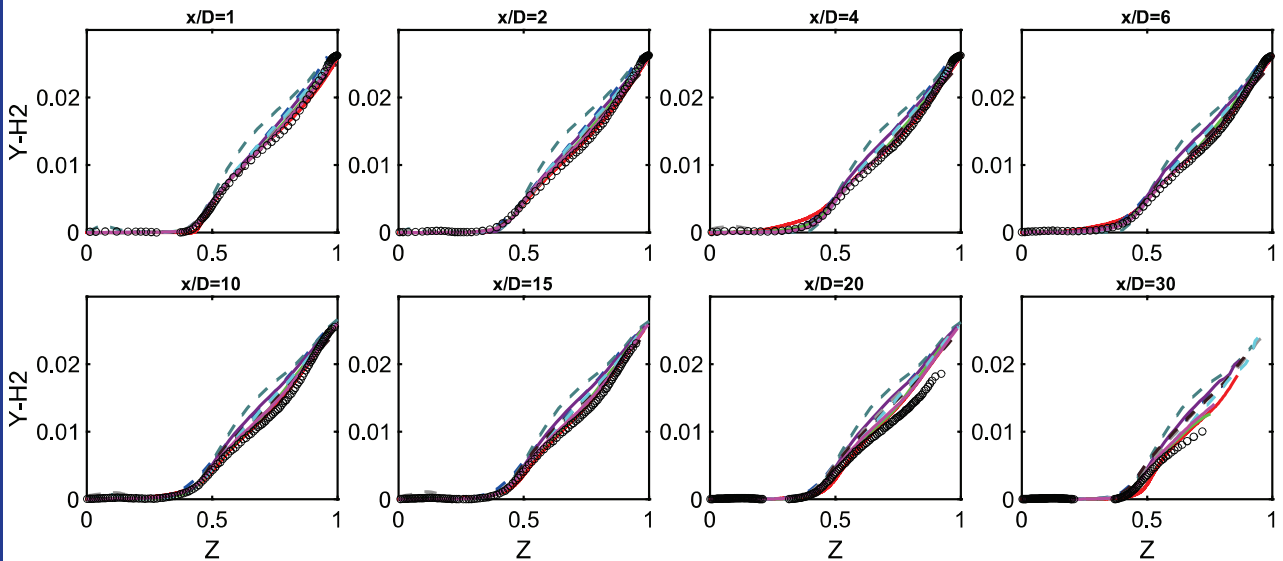


25



## Flame D: H<sub>2</sub> mass fraction

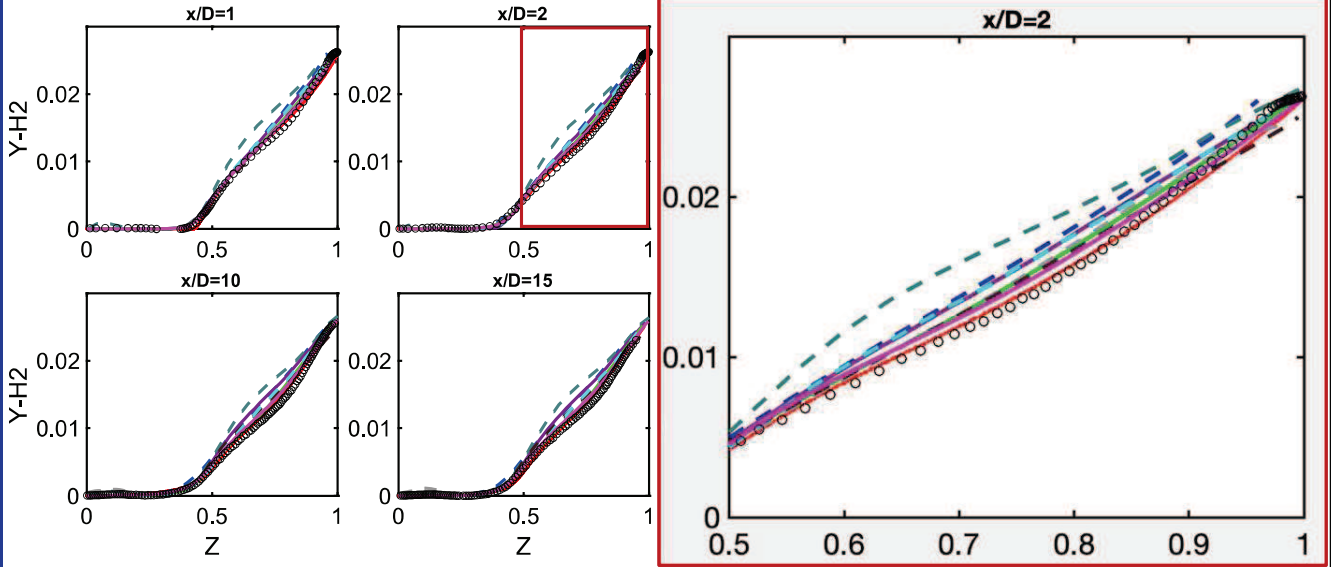
○ Exp.    — KAUST/HUST    — Iboro/IC    — PKU    — KYU/ZJU  
— ZJU-DMC    — ZJU-FGM    — IITK    — ITV    — Stanford



26

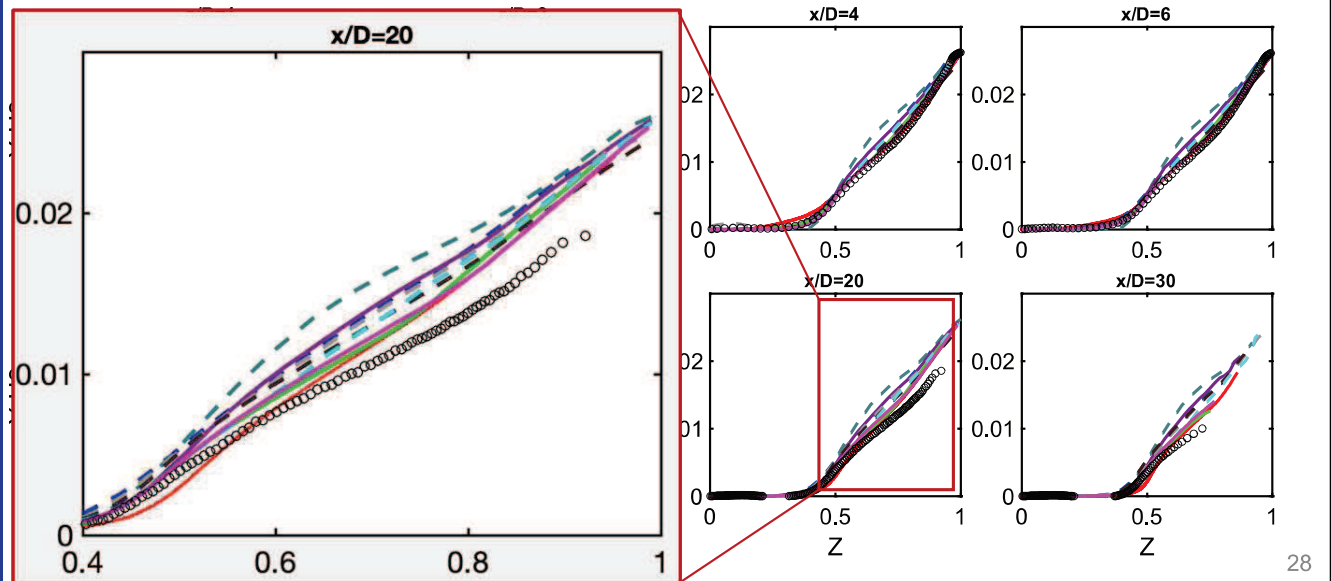
## Flame D: H<sub>2</sub> mass fraction

◦ Exp.    — KAUST/HUST    — Iboro/IC    — PKU    — KYU/ZJU  
 - - ZJU-DMC    - - ZJU-FGM    - - IITK    - - ITV    - - Stanford



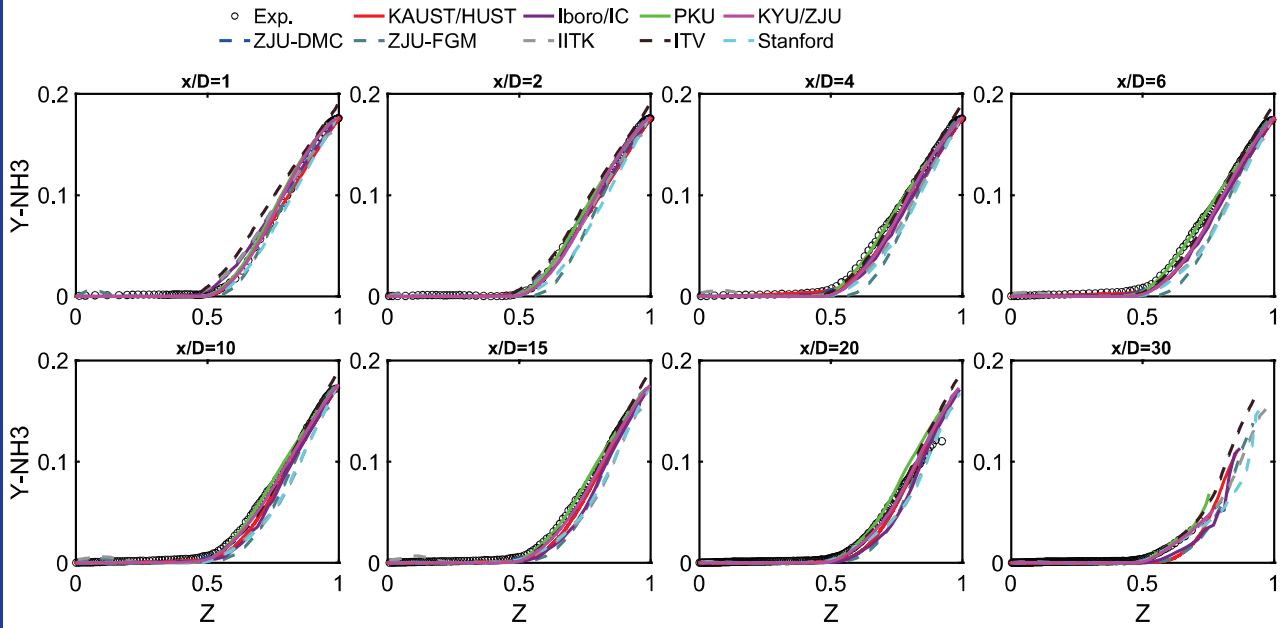
## Flame D: H<sub>2</sub> mass fraction

◦ Exp.    — KAUST/HUST    — Iboro/IC    — PKU    — KYU/ZJU  
 - - ZJU-DMC    - - ZJU-FGM    - - IITK    - - ITV    - - Stanford

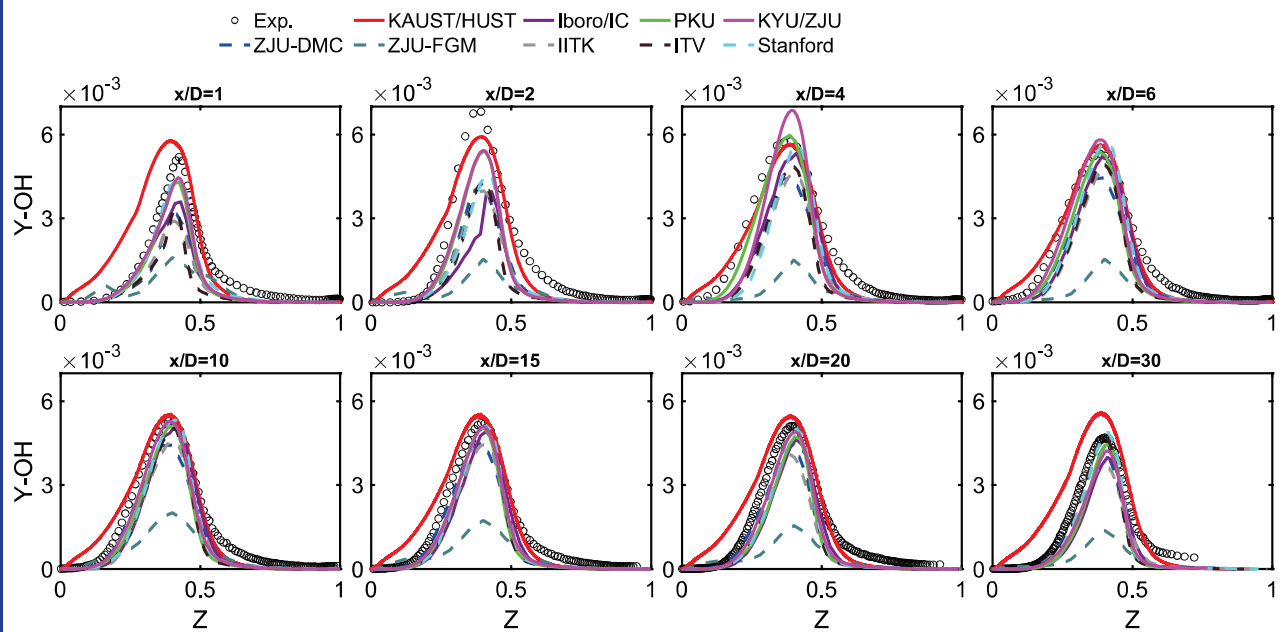




## Flame D: $\text{NH}_3$ mass fraction



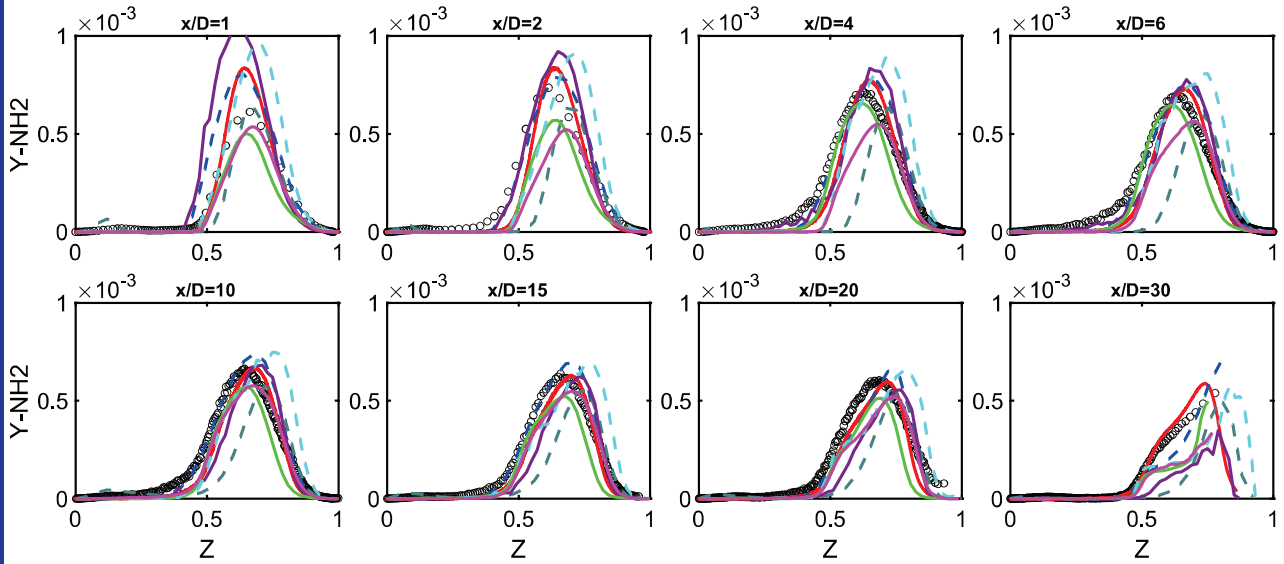
## Flame D: OH mass fraction





## Flame D: $\text{NH}_2$ mass fraction

○ Exp.    — KAUST/HUST    — Iboro/IC    — PKU    — KYU/ZJU  
— ZJU-DMC    — ZJU-FGM    — IITK    — ITV    — Stanford



31



Mean and RMS radial profiles in physical space

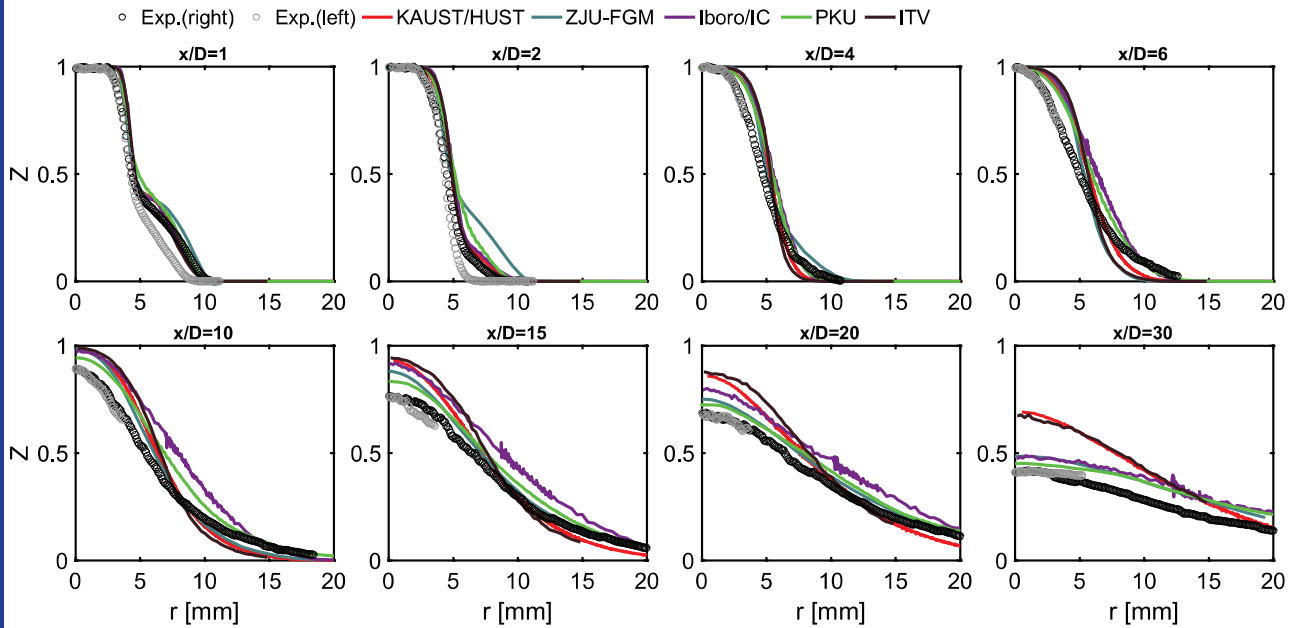
Conditional mean in mixture fraction space

Flame F

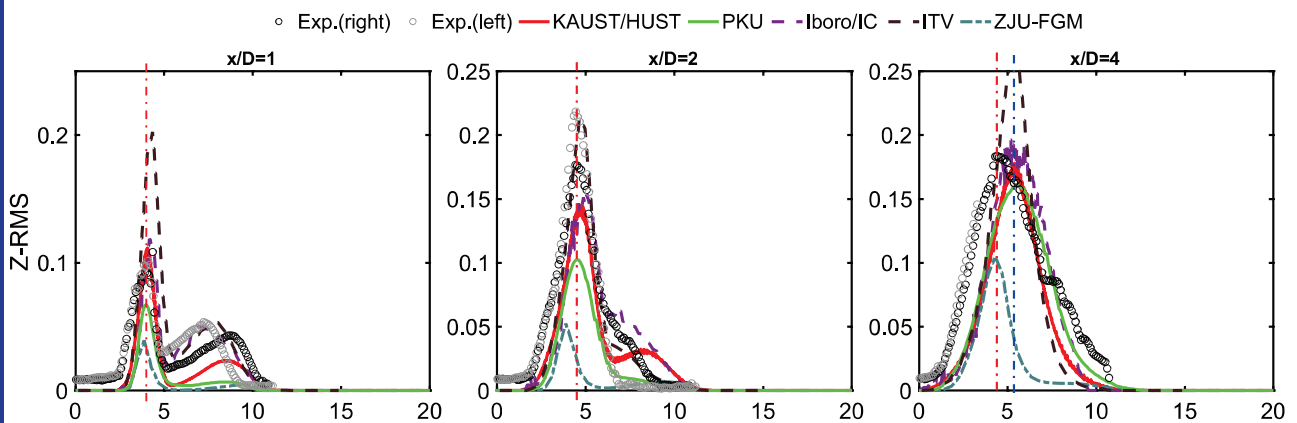
32



## Flame F: Mean Mixture fraction



## Flame F: RMS of Mixture fraction (1D-4D)

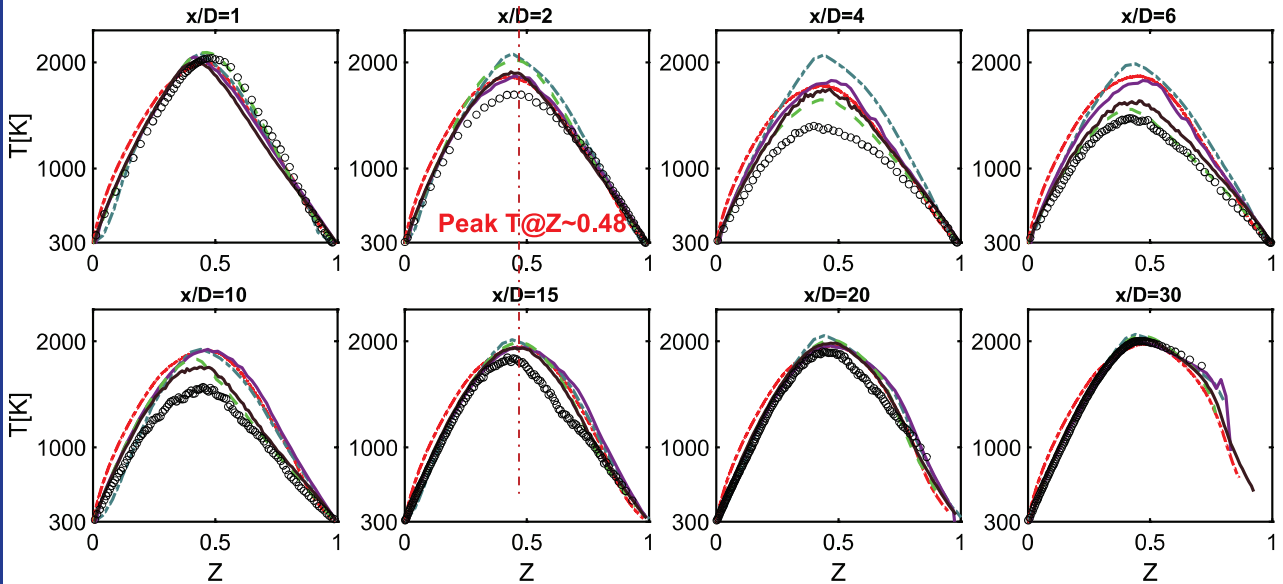


- ❖ First peak was captured at 1D and 2D, but shifted at 4D
- ❖ PDF-based models provided higher RMS values



# Flame F: Temperature

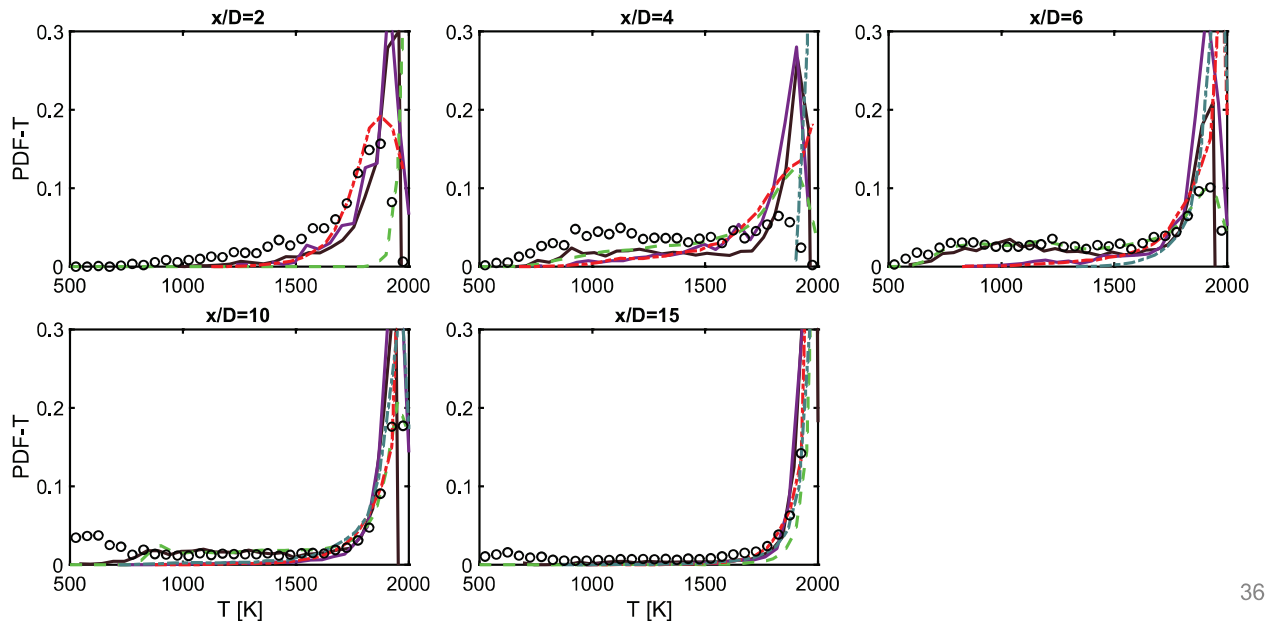
Tran. PDF    Laminar    Presumed PDF  
 ◦ Exp. — ITV — Iboro/IC — PKU — KAUST/HUST — ZJU-FGM



35

# Flame F: PDF of T in Z [0.46 0.50]

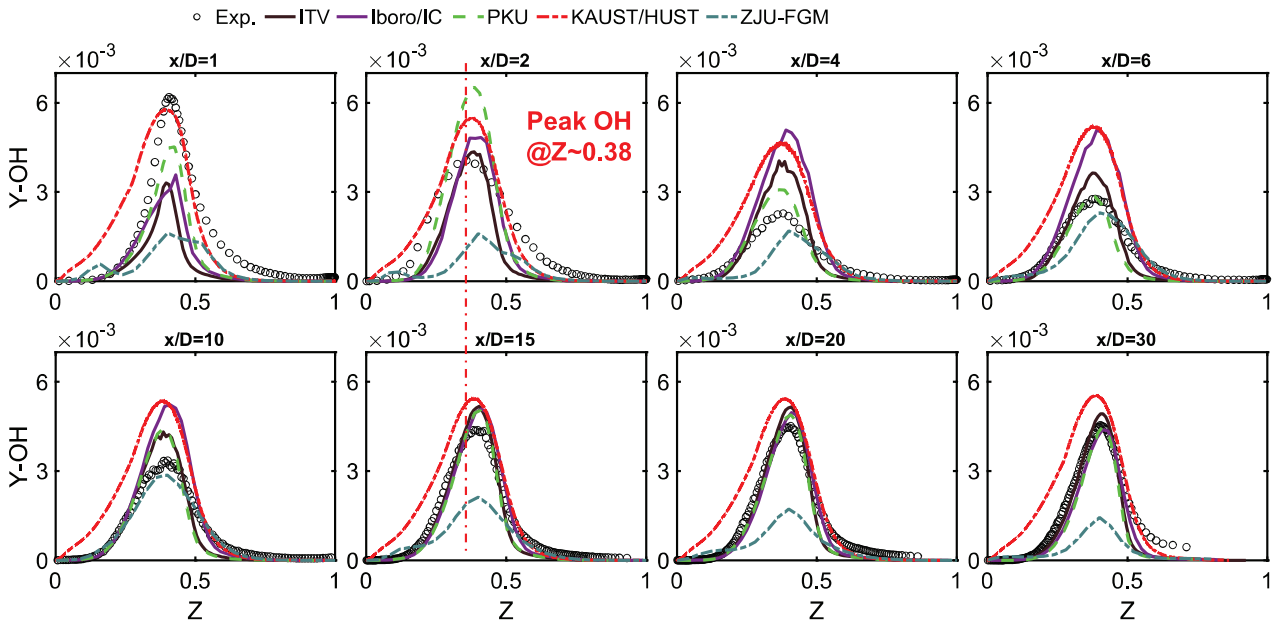
◦ Exp. — ITV — Iboro/IC — PKU — KAUST/HUST — ZJU-FGM



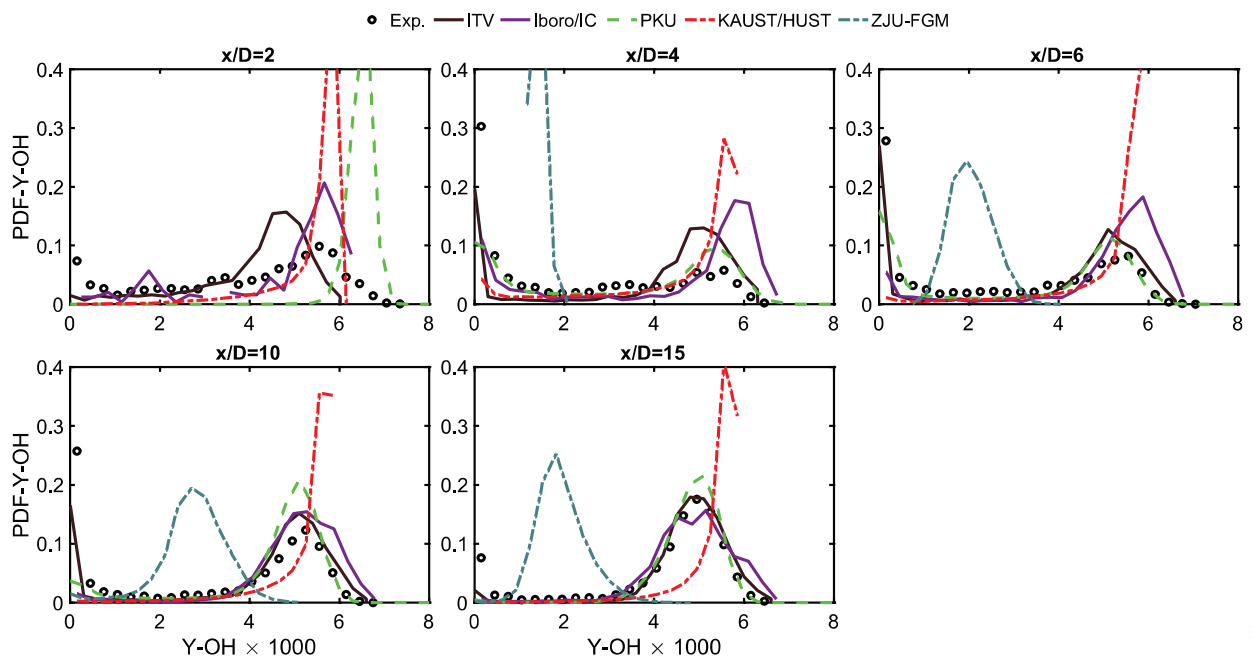
36



## Flame F: OH mass fraction



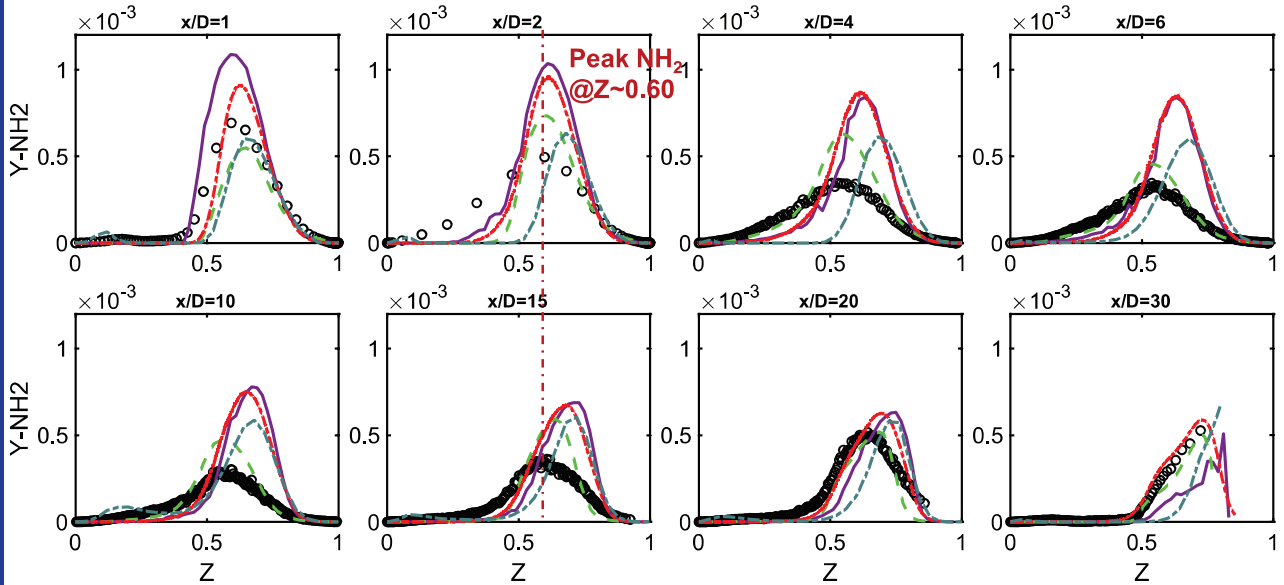
## Flame F: PDF of OH in Z [0.36 0.40]





## Flame F: $\text{NH}_2$ mass fraction

• Exp. — Iboro/IC — PKU — KAUST/HUST — ZJU-FGM

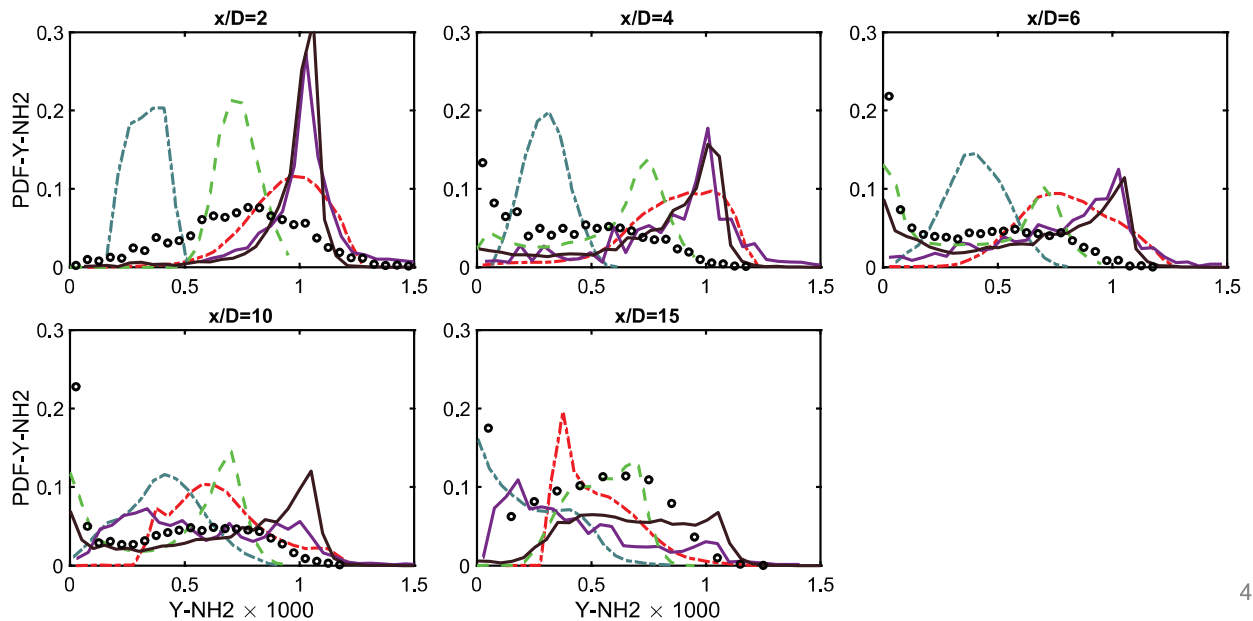


39



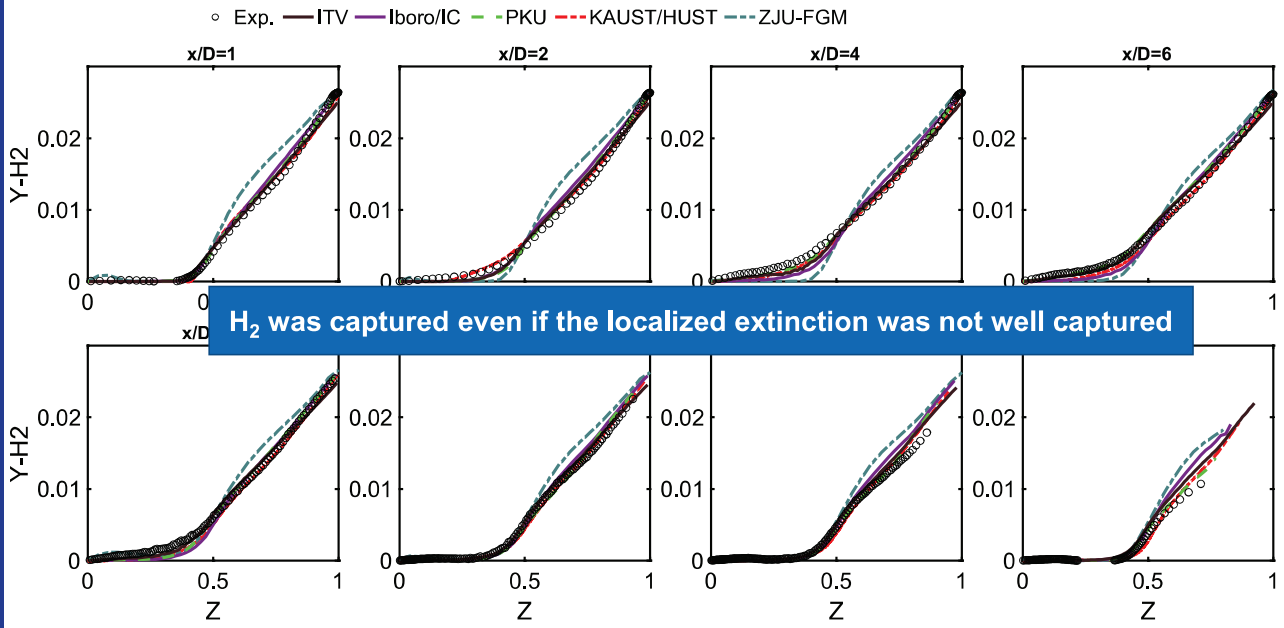
## Flame F: PDF of $\text{NH}_2$ in Z [0.58 0.62]

• Exp. — ITV — Iboro/IC — PKU — KAUST/HUST — ZJU-FGM

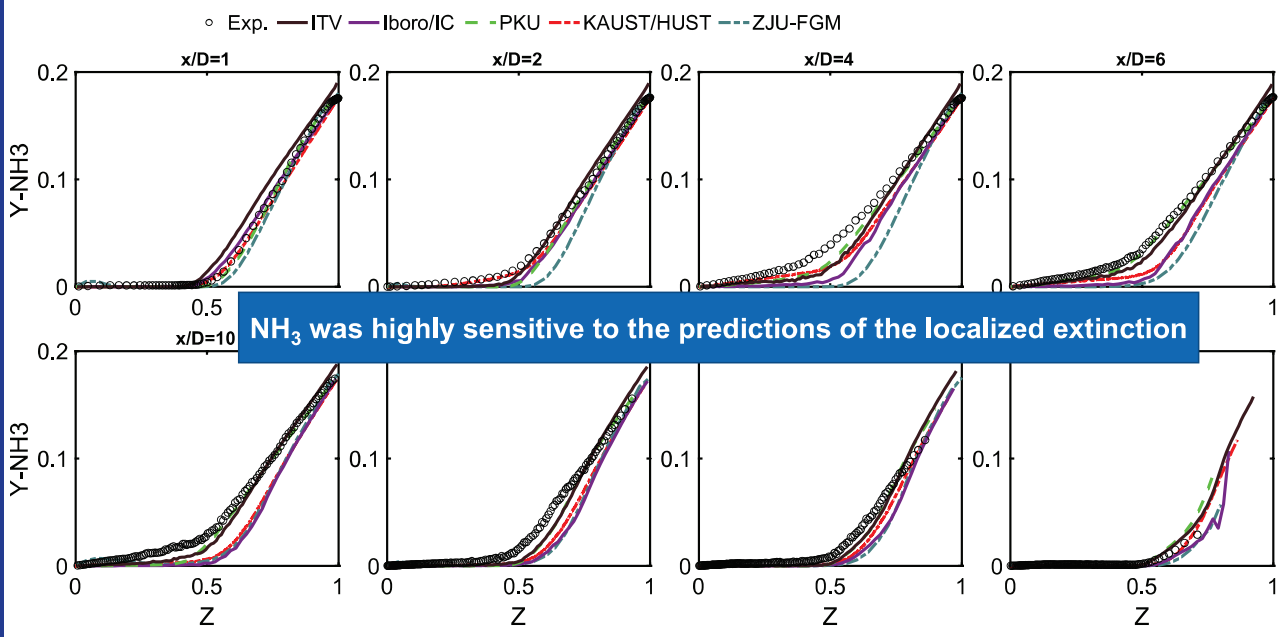


40

## Flame F: H<sub>2</sub> mass fraction



## Flame F: NH<sub>3</sub> mass fraction



## Summary and Discussion

- ❖ What are particular modelling challenges for cracked ammonia flames, compared to hydrocarbon flames?
- ❖ What experimental observations are not well captured by the majority of the modeling strategies?  
(Mixing process near burner; localized extinction in Flame F;.....)
- ❖ .....

43



جامعة الملك عبدالله  
للعلوم والتقنية  
King Abdullah University of  
Science and Technology

CCRC

شكراً  
THANK YOU!



*Powering a sustainable energy future.*



[ccrc.kaust.edu.sa](http://ccrc.kaust.edu.sa)

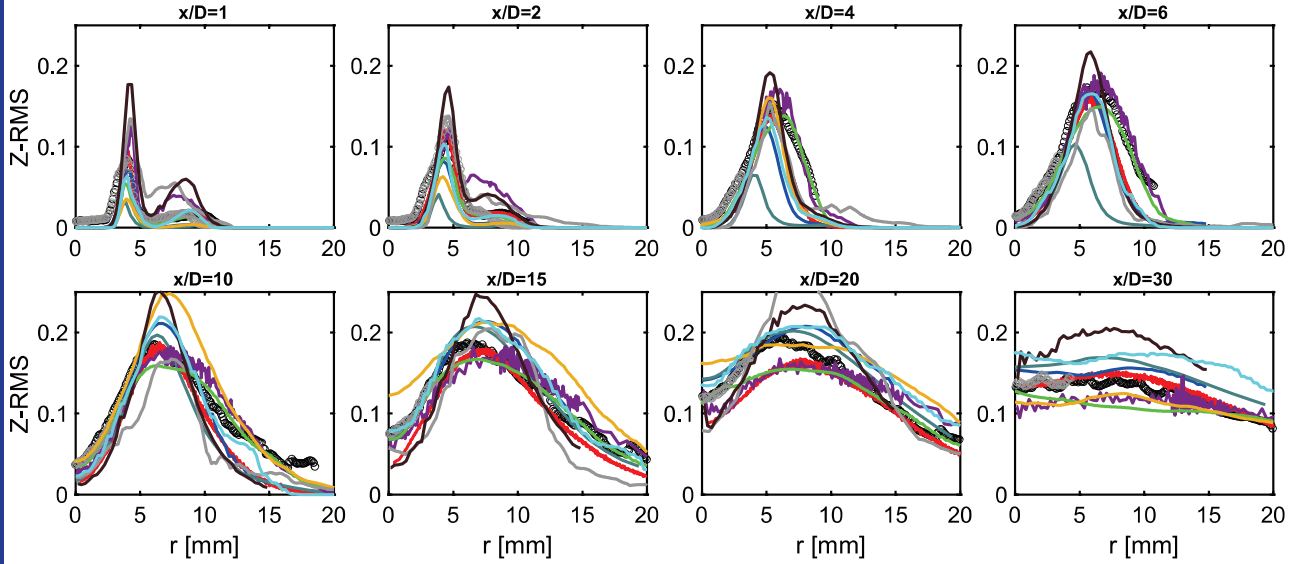
44





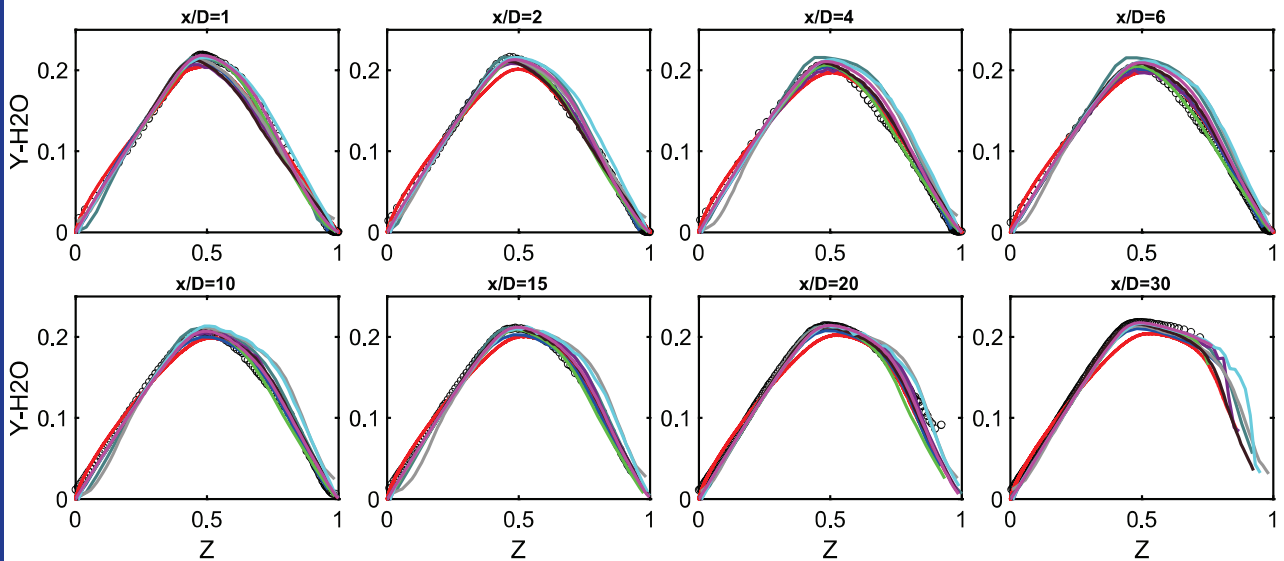
## Flame D: RMS of Mixture fraction

- Exp.(right) — KAUST/HUST — ZJU-DMC — ZJU-FGM — Iboro/IC — PKU
- Exp.(left) — EM2C — IITK — ITV — Stanford — KYU/ZJU



## Flame D: H<sub>2</sub>O mass fraction

- Exp. — KAUST — ZJU-DMC — ZJU-FGM — Iboro/IC
- PKU — IITK — ITV — Stanford — KYU/ZJU

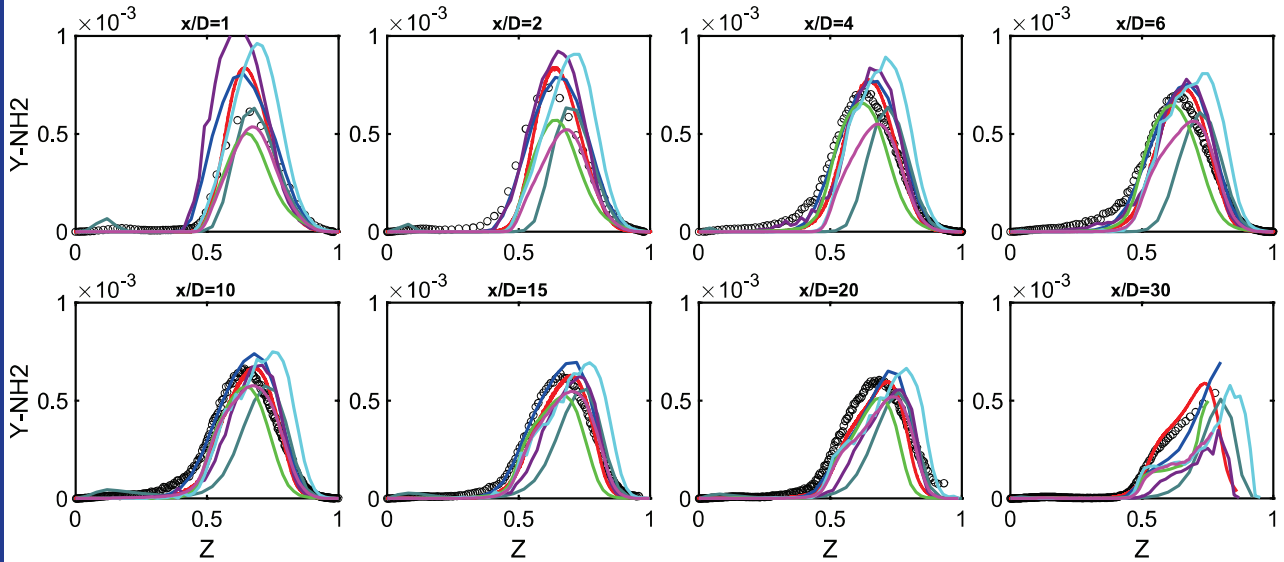


46



## Flame D: $\text{NH}_2$ mass fraction

○ Exp. — KAUST — ZJU-DMC — ZJU-FGM — Iboro/IC  
— PKU — Stanford — KYU/ZJU

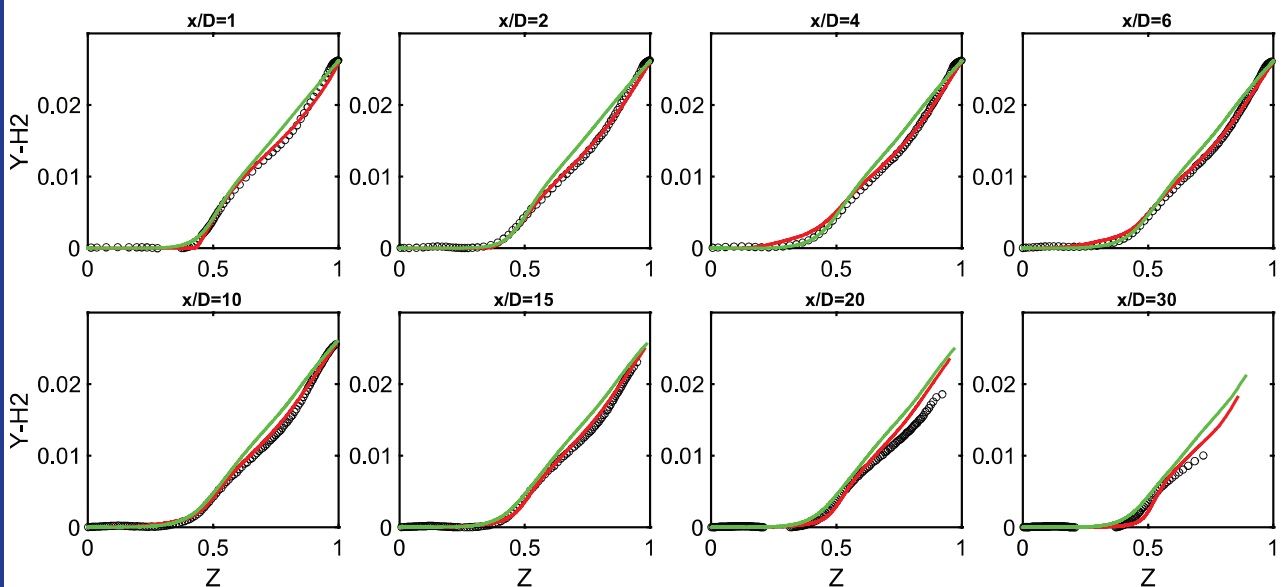


47



## Flame D: Differential diffusion

○ Exp. — FPV with Diff-Diff — FPV with Unity Lewis

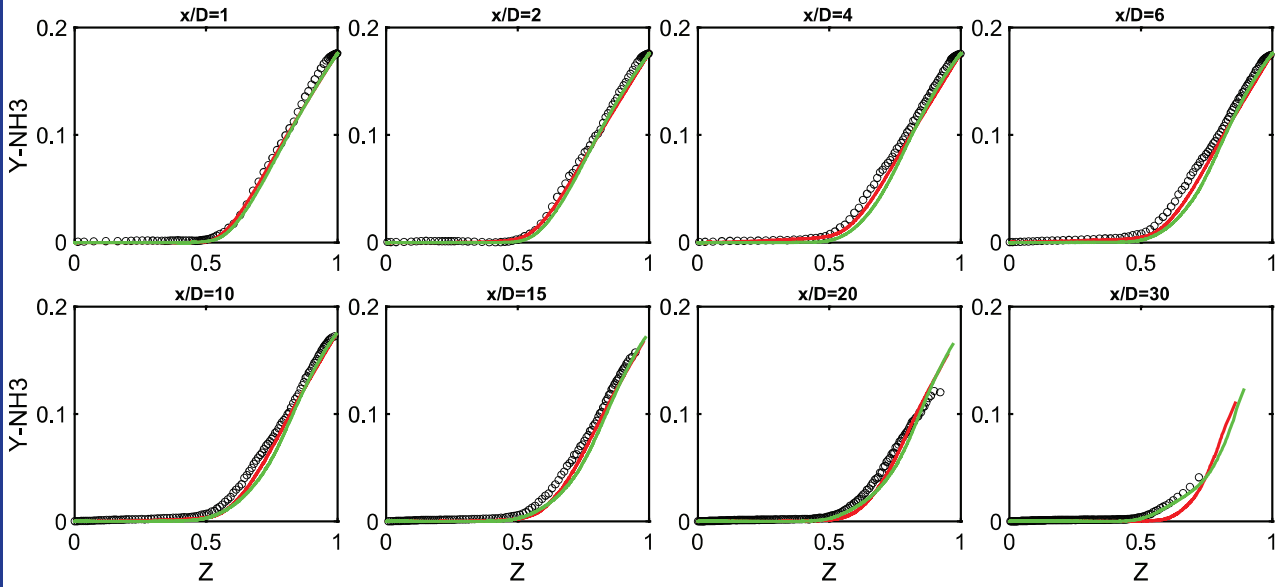


48



## Flame D: Differential diffusion

○ Exp. — FPV with Diff-Diff — FPV with Unity Lewis

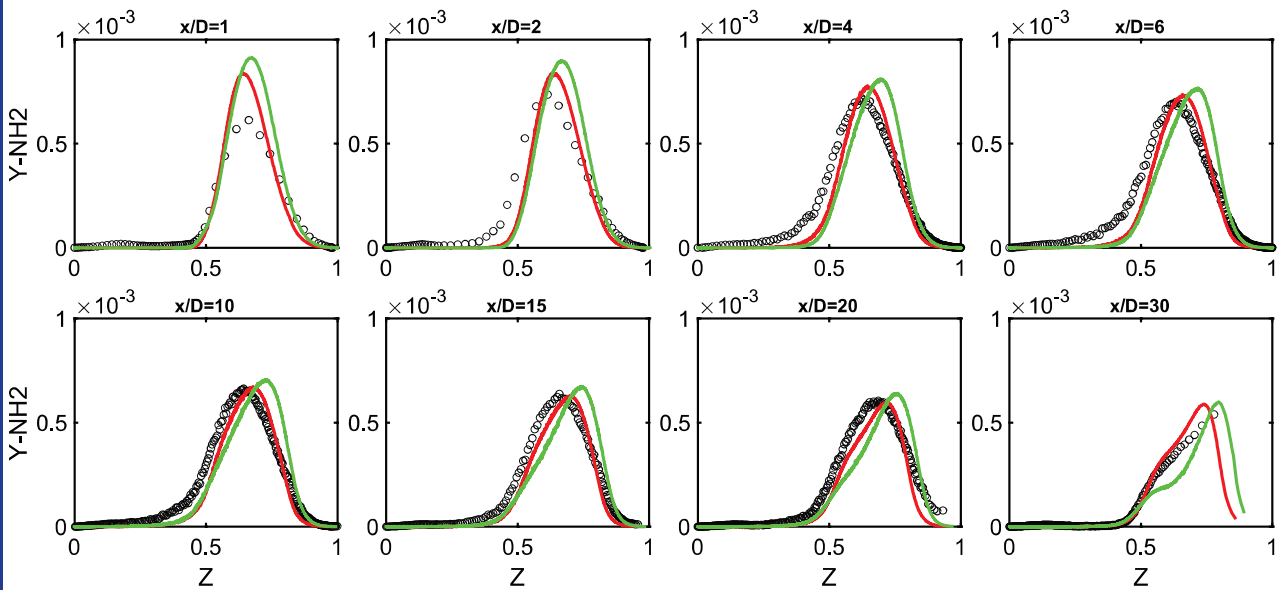


49



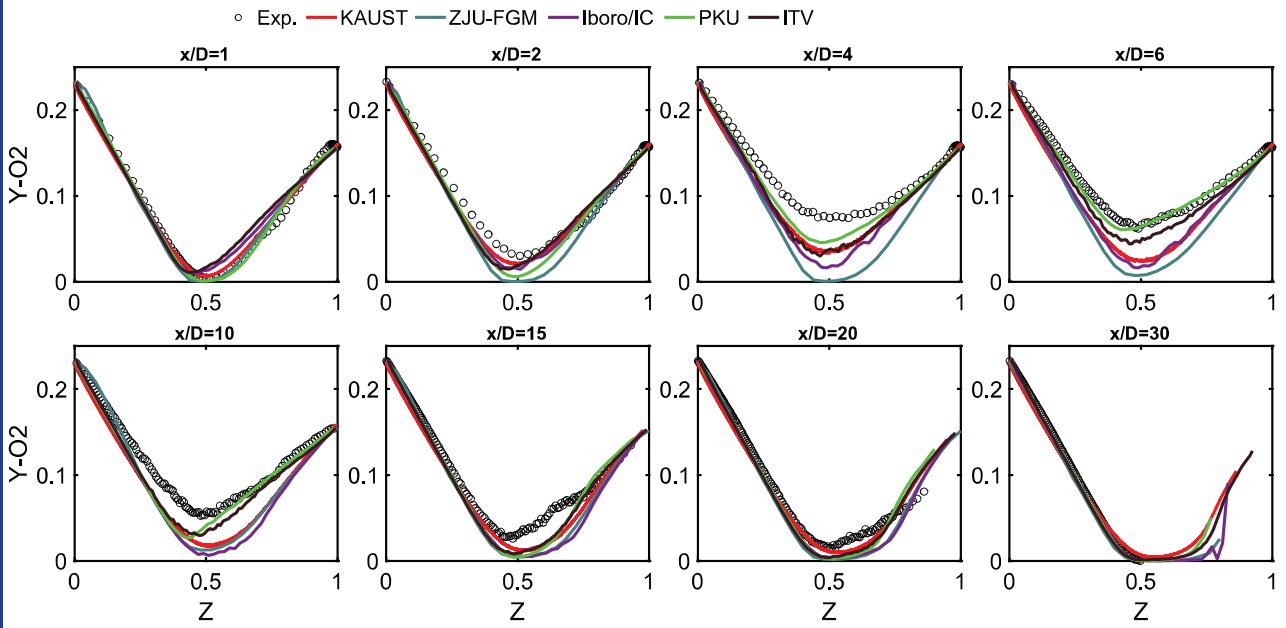
## Flame D: Differential diffusion

○ Exp. — FPV with Diff-Diff — FPV with Unity Lewis



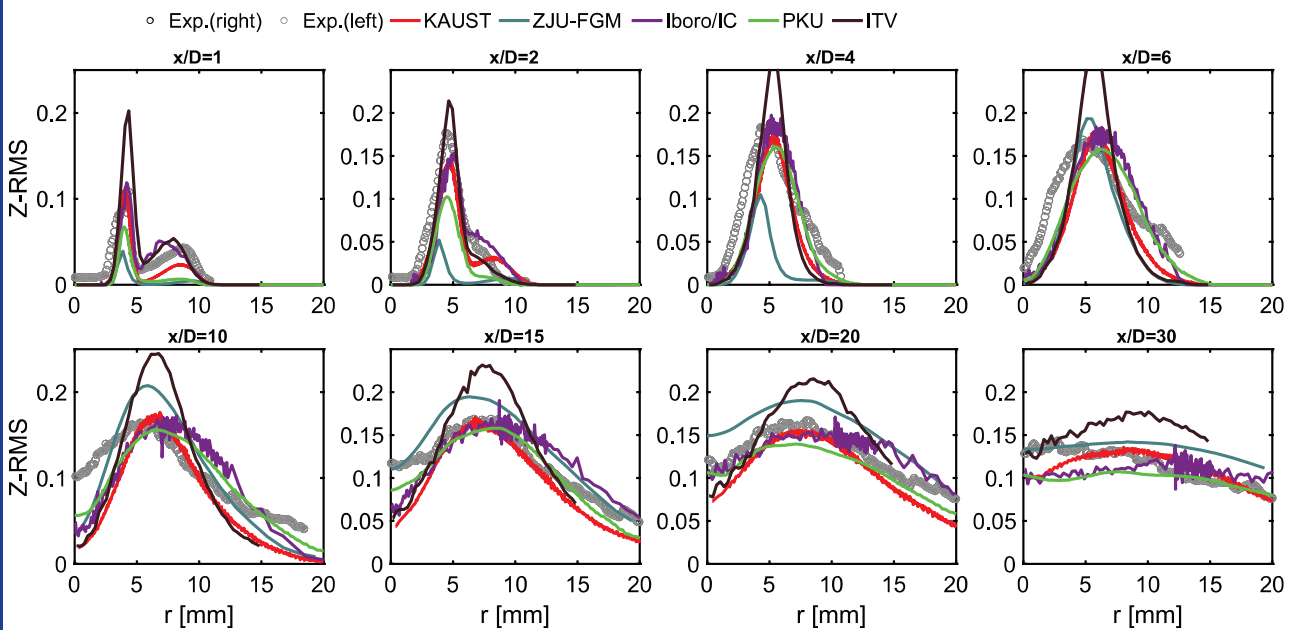
50

## Flame F: O<sub>2</sub> mass fraction



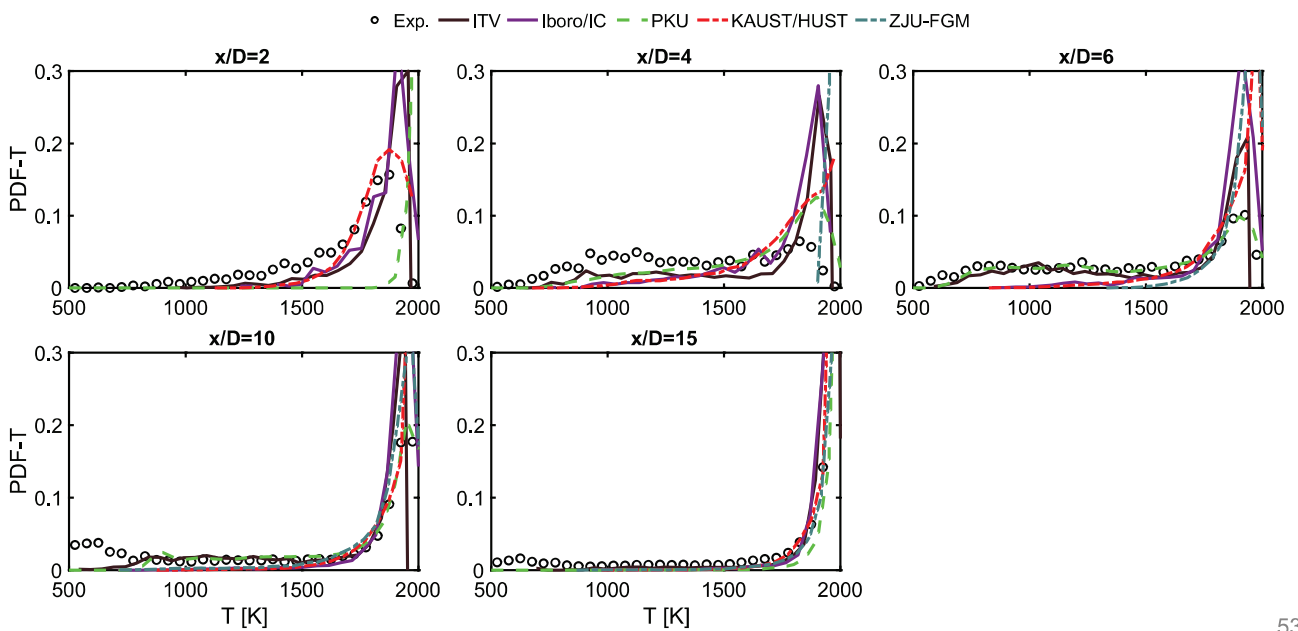
51

## Flame F: RMS of Mixture fraction





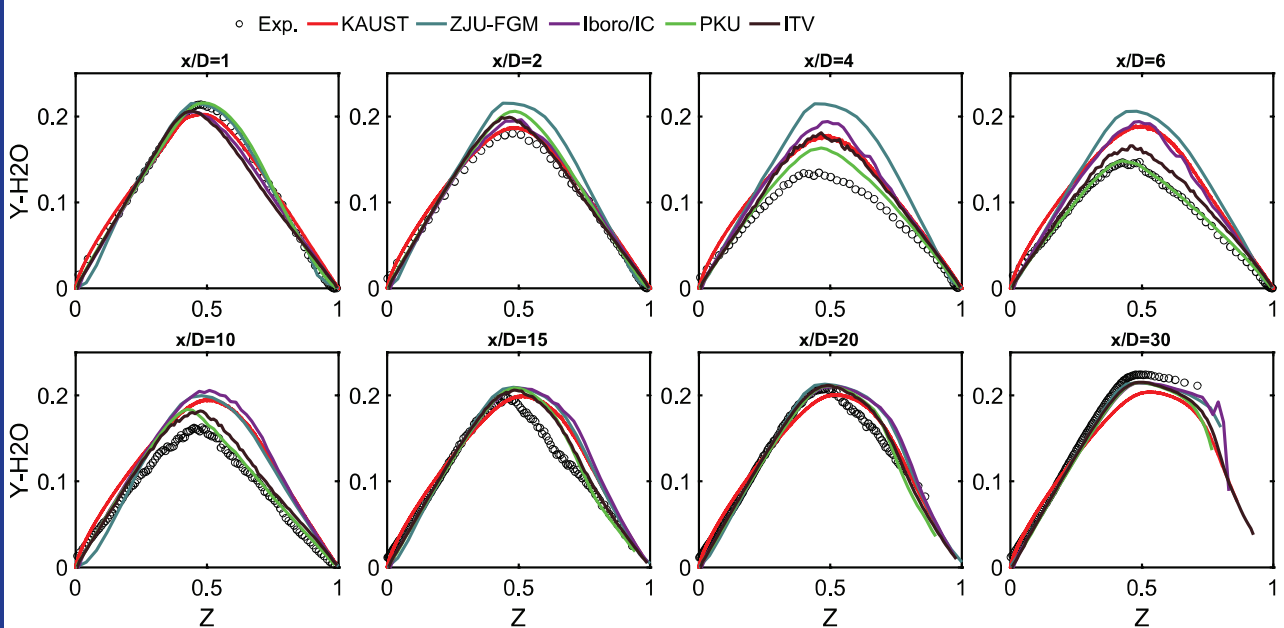
## Flame F: PDF of T in Z [0.46 0.50]



53



## Flame F: H<sub>2</sub>O mass fraction



54



TNF/PTF Workshops

Blank Page

## TNF Session: Possible Future TNF Target Cases

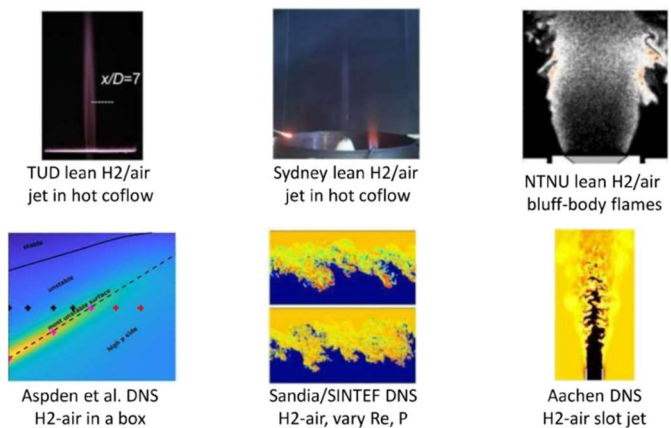
Coordinators: Robert Barlow, Matt Dunn, Gaetano Magnotti

### Summary

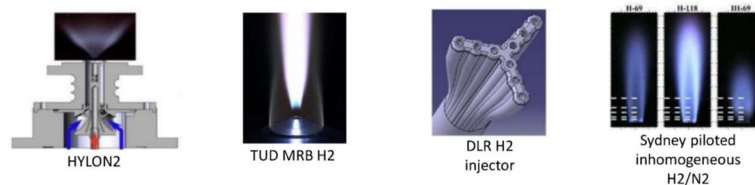
The purpose of this session was to present a brief overview of a number data sets that might be considered as target cases for the next TNF Workshop. The list includes the HYLON configurations and the KAUST piloted flames of cracked ammonia, which are already expected to targets for 2026. Several configurations, including both experimental and DNS data sets, were introduced during earlier sessions, and several additional configurations from Sydney University, KAUST, TU Darmstadt, and DLR Stuttgart were introduced during this Future Targets session. Most cases burn H<sub>2</sub> or NH<sub>3</sub>/H<sub>2</sub> blends.

All candidates were categorized according to fuel and combustion mode, as shown below and in the final two slides of the presentation.

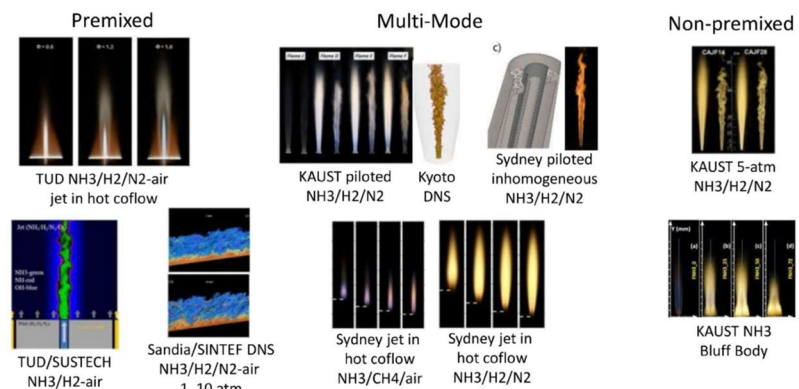
### Hydrogen, Premixed



### Hydrogen, Multi-Mode



### Ammonia, All Modes



Discussion of the selection of cases to be used for collaborative comparisons was deferred to the Final Discussion, during which a process for distributing information and polling community interest was outlined.



## Future Target Flames

- Session objectives
  - Introduce more candidates for future collaborative comparisons
  - Clarification questions; what TCI physics are probed?
- “Good” TNF targets:
  - Relatively simply geometry and fuel
  - Well-defined bc’s
  - Variation of sensitive parameters to test TCI models (not single case)
  - Detailed measurements of velocity and scalars (0D, 1D, 2D, but maybe not *Everything, Everywhere, All at Once*)
- Next session (among other things):
  - Which cases to target for TNF 2026
  - Identify things that could/should be done in common (e.g., chemical mech, precalculated inflows, wall bc’s, ...)



## Discussion Points

- Clarification questions on specific cases?
- Additional measurements that may be needed?
- Which cases attract high interest?
- Which cases to prioritize for collaborative comparisons?

# Future TNF target flames from The University of Sydney

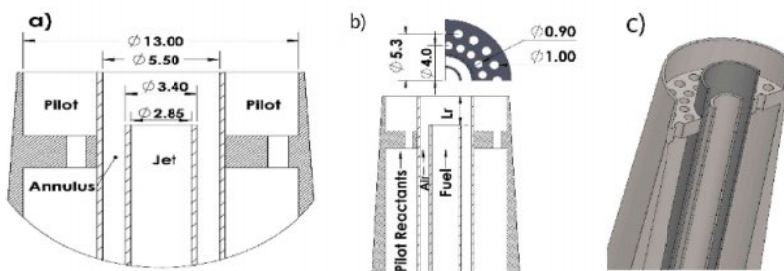
Matthew J. Dunn<sup>1</sup>, Andrew R.W. Macfarlane<sup>1</sup> and Assaad R. Masri<sup>1</sup>

<sup>1</sup> School of Aerospace, Mechanical and Mechatronics Engineering, The University of Sydney

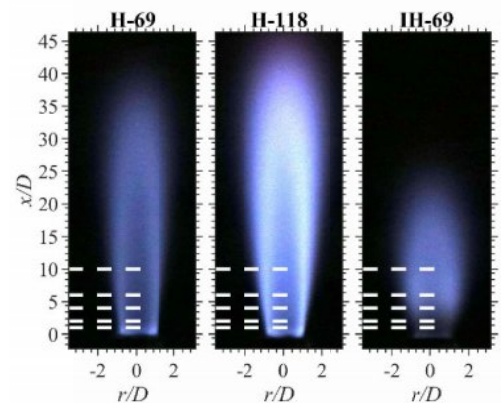


TNF Workshop  
 Satellite workshop of the 40<sup>th</sup> International  
 Combustion Symposium  
 Politecnico di Milano, Italy  
 20<sup>th</sup>-21<sup>st</sup> July 2024

## Sydney Inhomogeneous burner H<sub>2</sub>/N<sub>2</sub> flames

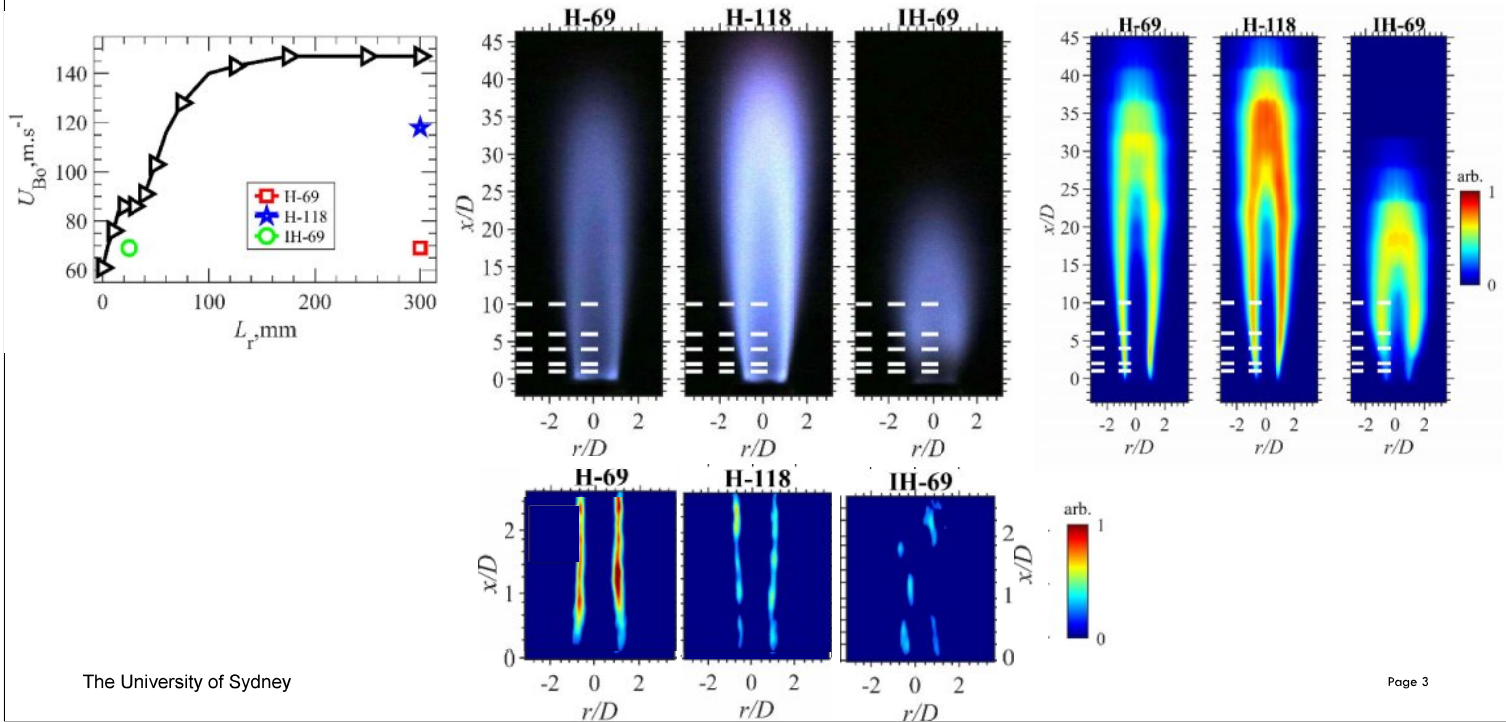


**Jet: 40% H<sub>2</sub>, 60% N<sub>2</sub>**



Name	$L_r$ , mm	$U_{Bo}$ , m.s <sup>-1</sup>	$\phi_{Global}$	$U_{Exp}$ , m.s <sup>-1</sup>	$Re$	$U_{Bo}$ , %	$U_j/U_A$	$\dot{Q}_{Pilot}$ , W
H-69	300	147	4.76	69	17,980	58	10	114
H-118	300	147	4.76	118	30,595	80	10	114
IH-69	25	86	4.76	69	17,980	80	10	114

# Sydney Inhomogeneous burner H<sub>2</sub>/N<sub>2</sub> flames



The University of Sydney

Page 3

# Sydney Inhomogeneous burner H<sub>2</sub>/N<sub>2</sub> flames

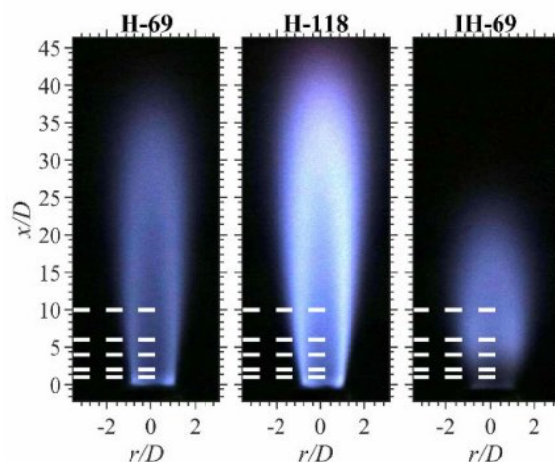
## Line Raman/Rayleigh measurements at KAUST



Prof. Gaetano Magnotti



Dr Hao Tang

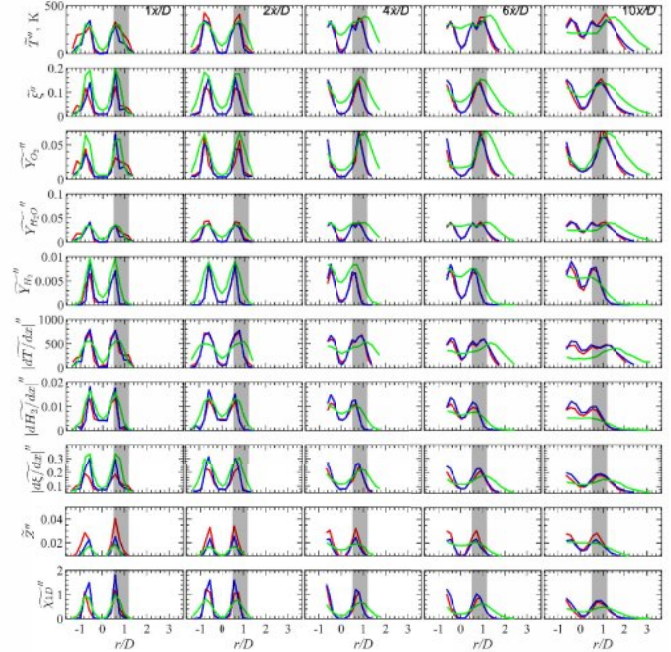
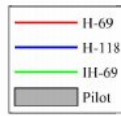
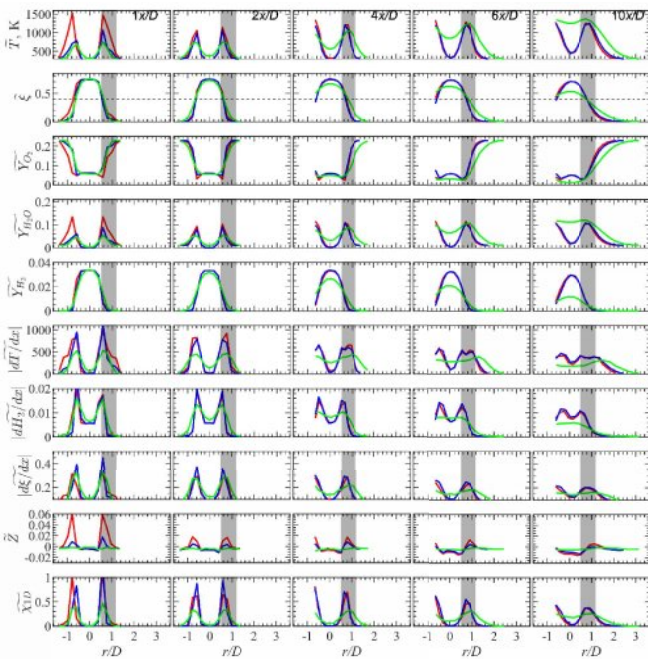


The University of Sydney

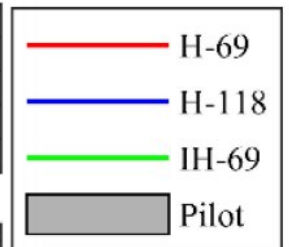
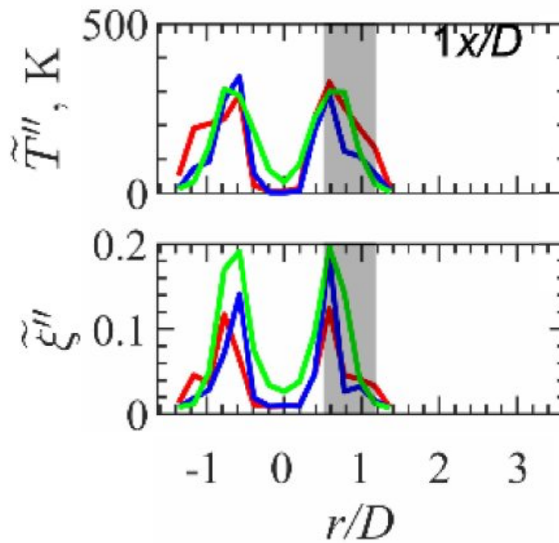
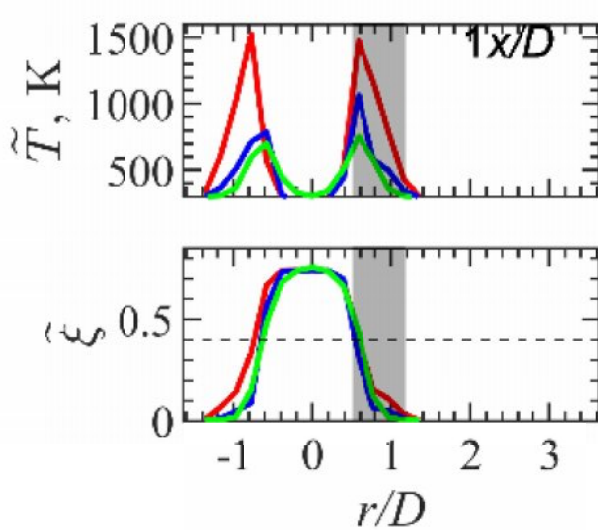
Page 4



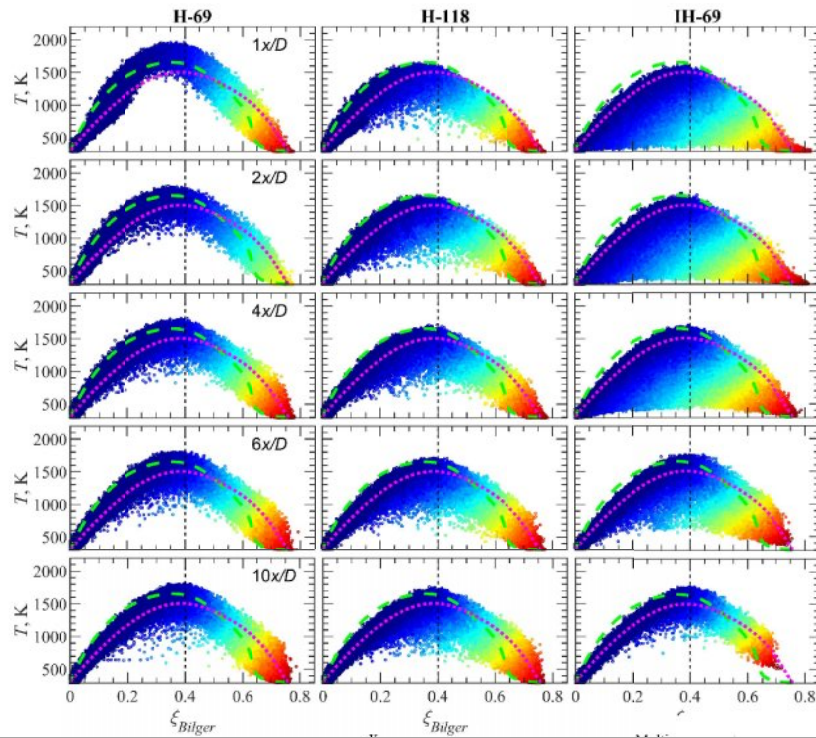
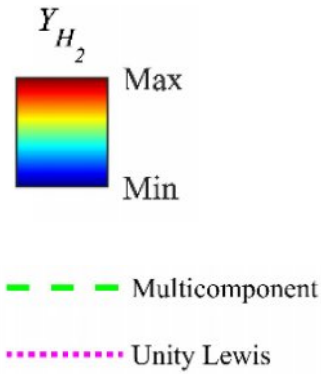
# Sydney Inhomogeneous burner $H_2/N_2$ flames



# Sydney Inhomogeneous burner $H_2/N_2$ flames



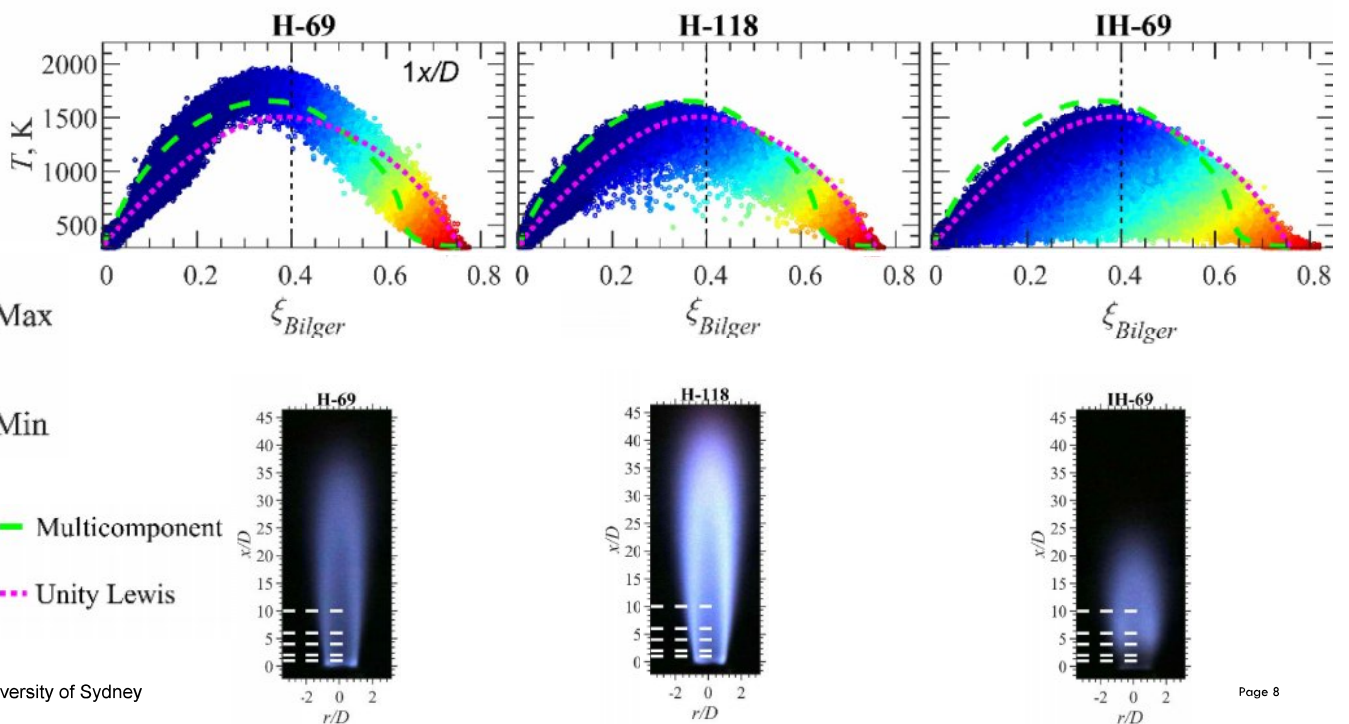
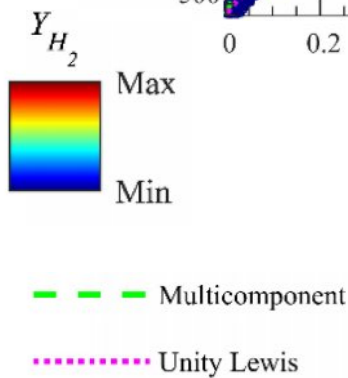
# Sydney Inhomogeneous burner H<sub>2</sub>/N<sub>2</sub> flames



The University of Sydney

Page 7

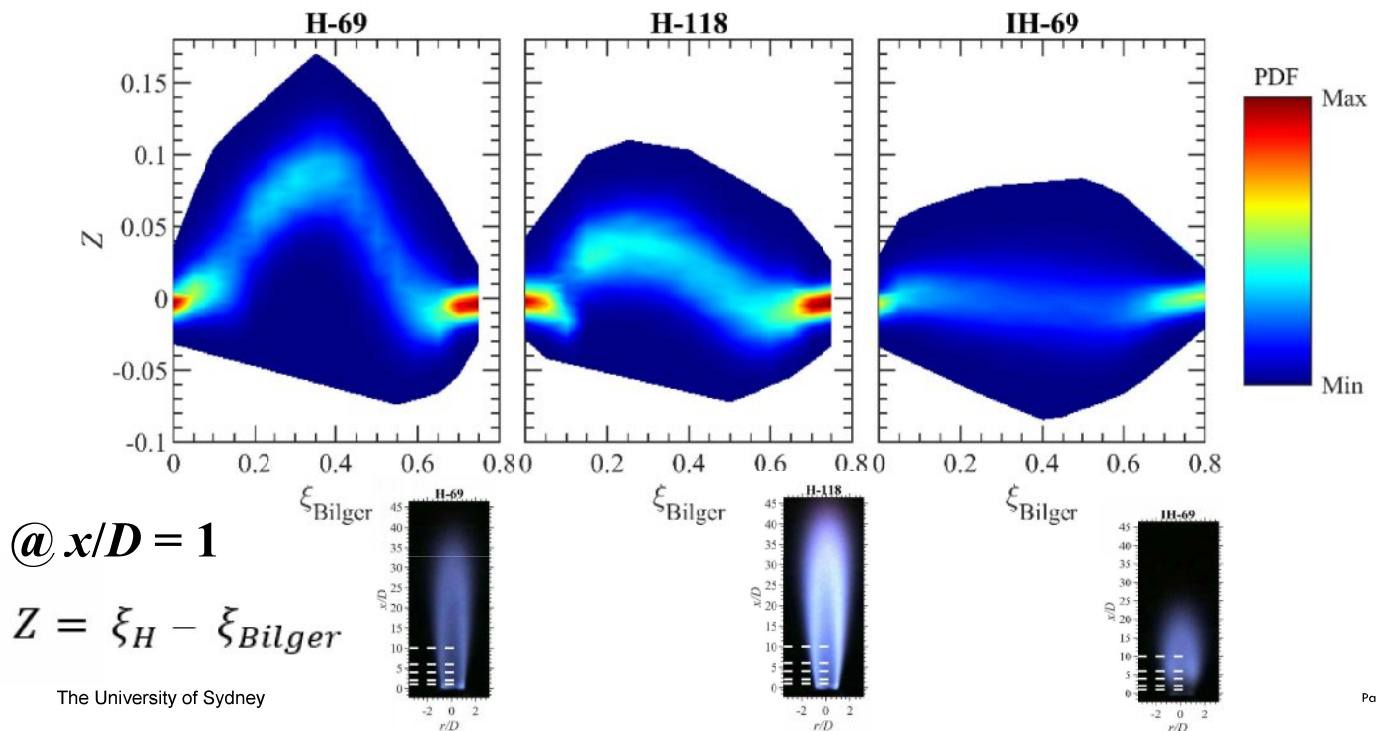
# Sydney Inhomogeneous burner H<sub>2</sub>/N<sub>2</sub> flames



The University of Sydney

Page 8

## Sydney Inhomogeneous burner H<sub>2</sub>/N<sub>2</sub> flames



## Sydney Inhomogeneous burner H<sub>2</sub>/N<sub>2</sub> flames

Well posed BC, good experience from previous TNF on CH<sub>4</sub> inhomogeneous burner flames

H<sub>2</sub> jet diffusion flames near blow off (80%) without compressibility effects

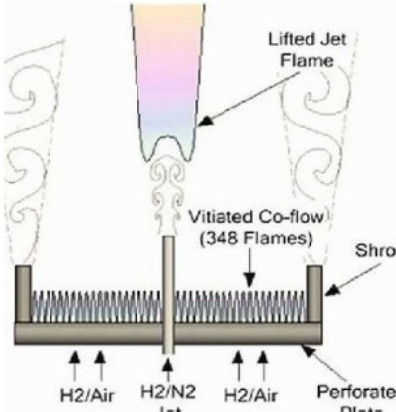
Detailed scalar data available now, publication under review



# Berkeley "Cabra" hot coflow burner

$H_2/N_2$  3:1 jet, 107 m/s

$T_c = 1020-1080$  K



Simultaneous laser Raman-Rayleigh-LIF measurements and numerical modeling results of a lifted turbulent  $H_2/N_2$  jet flame in a vitiated coflow

R Cabra, T Myhrvold, JY Chen, RW Dibble... - Proceedings of the ..., 2002 - Elsevier

An experimental and numerical investigation is presented of a lifted turbulent  $H_2/N_2$  jet flame in a coflow of hot vitiated gases. The vitiated coflow burner emulates the coupling of ...

☆ Save Cite Cited by 468 Related articles All 9 versions ACNP Holdings

$CH_4$ /air 2:1 jet, 100 m/s

$T_c = 1400-1550$  K

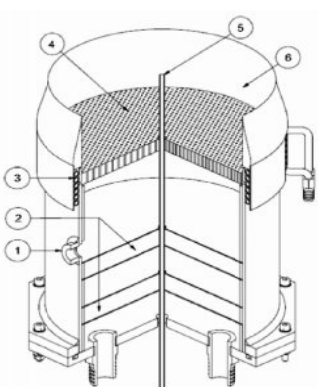
[HTML] Lifted methane-air jet flames in a vitiated coflow

R Cabra, JY Chen, RW Dibble, AN Karpetis... - Combustion and ..., 2005 - Elsevier

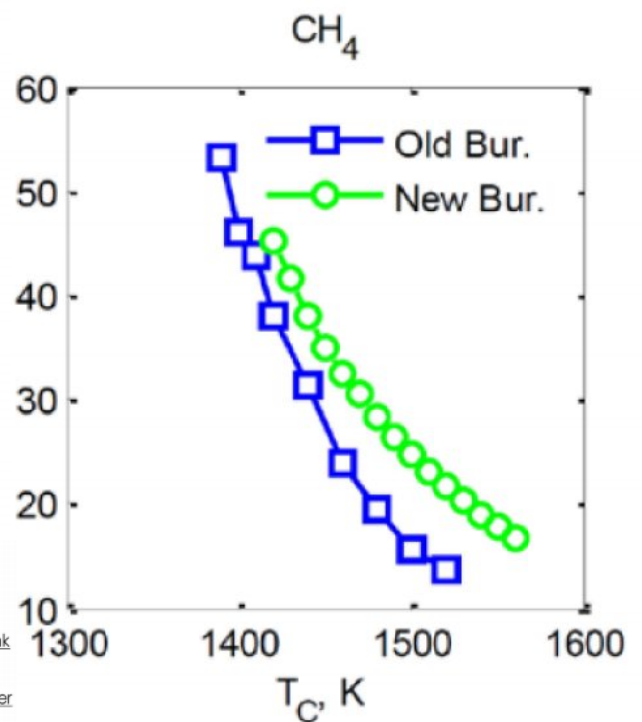
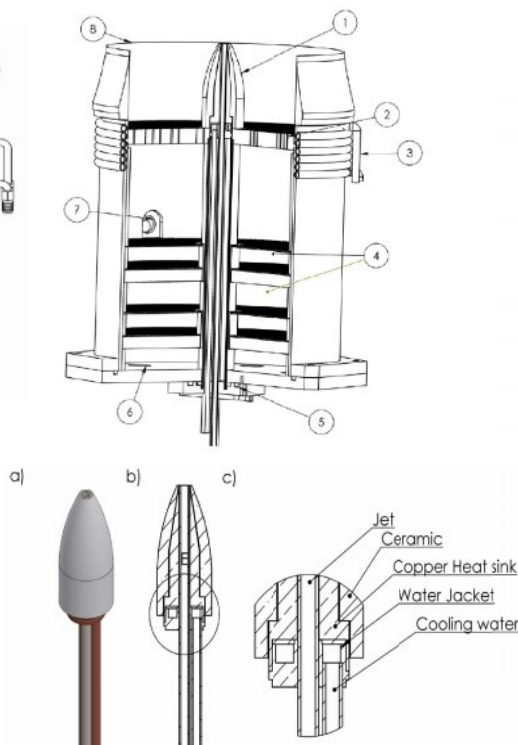
The present vitiated coflow flame consists of a lifted jet flame formed by a fuel jet issuing from a central nozzle into a large coaxial flow of hot combustion products from a lean premixed ...

☆ Save Cite Cited by 401 Related articles All 10 versions

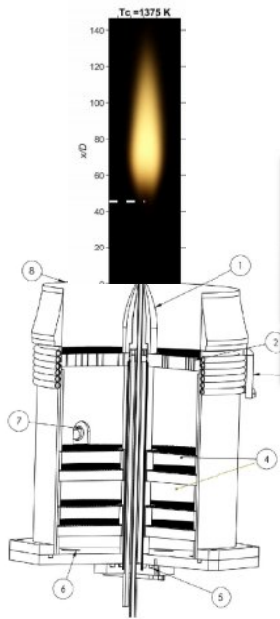
# Sydney hot coflow burner



$\Phi_{ID,jet} = 4.57$  mm,  
70 mm long



# Sydney cracked ammonia jet in hot coflow cases



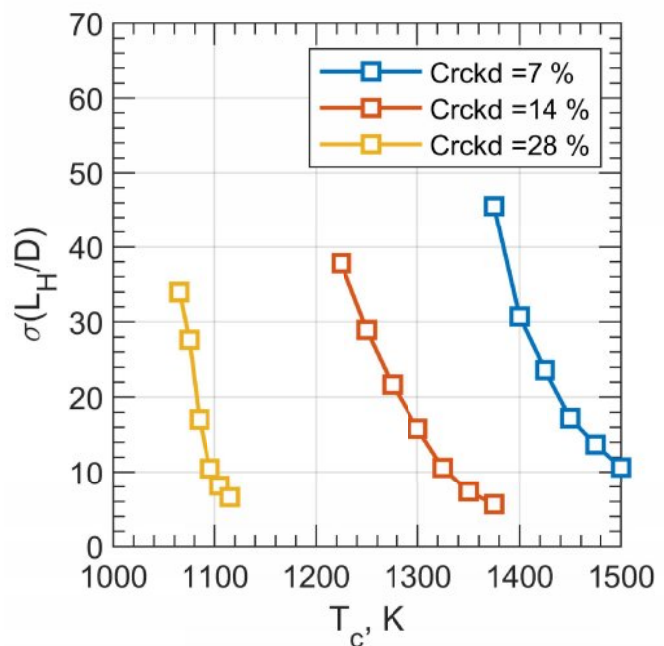
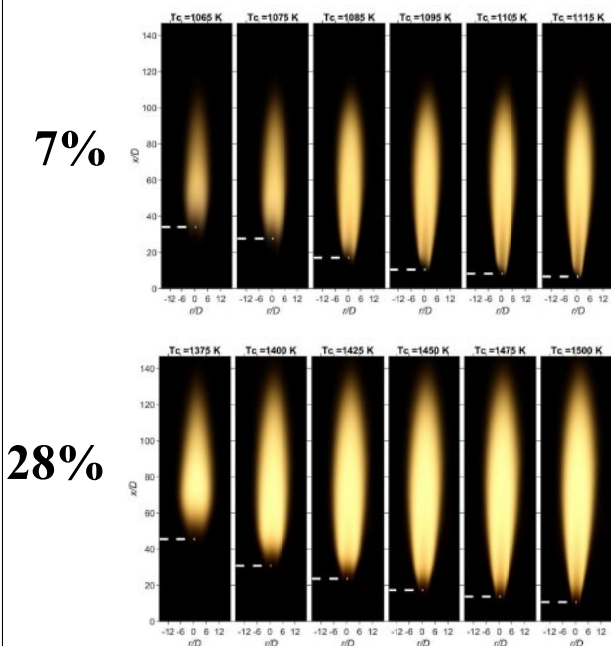
% Cracked NH <sub>3</sub>	$X_{\text{jet, NH}_3}$	$X_{\text{jet, H}_2}$	$X_{\text{jet, N}_2}$	$T_{\text{coflow (K)}}$
7%	0.869159	0.098131	0.03271	1060-1120 K
14%	0.754386	0.184211	0.061404	1220-1380 K
28%	0.5625	0.328125	0.109375	1370-1500 K
6-12%	0.887-0.786	0.0849-0.161	0.0283-0.0536	1400 K

$$D_{\text{jet}} = 4.45 \text{ mm}, U_{\text{jet}} = 100 \text{ m/s}, U_{\text{burnt, coflow}} = 4 \text{ m/s}$$

The University of Sydney

Page 13

# Sydney cracked ammonia jet in hot coflow

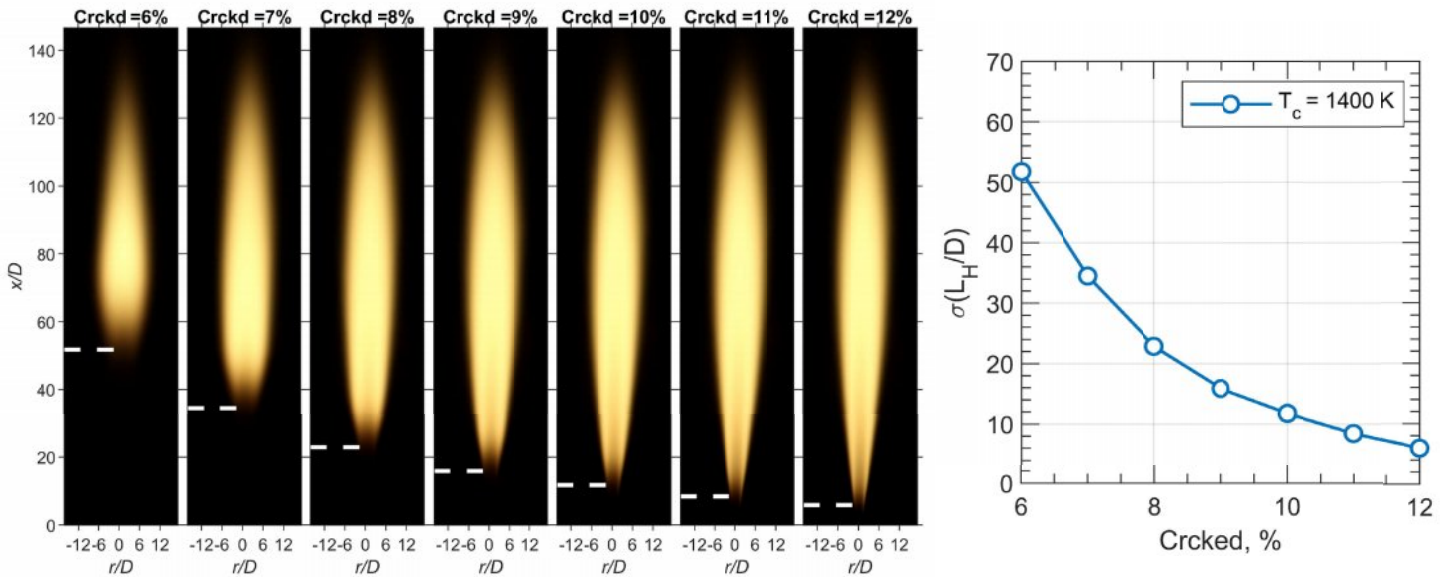


The University of Sydney

Page 14



## Sydney cracked ammonia jet in hot coflow cases

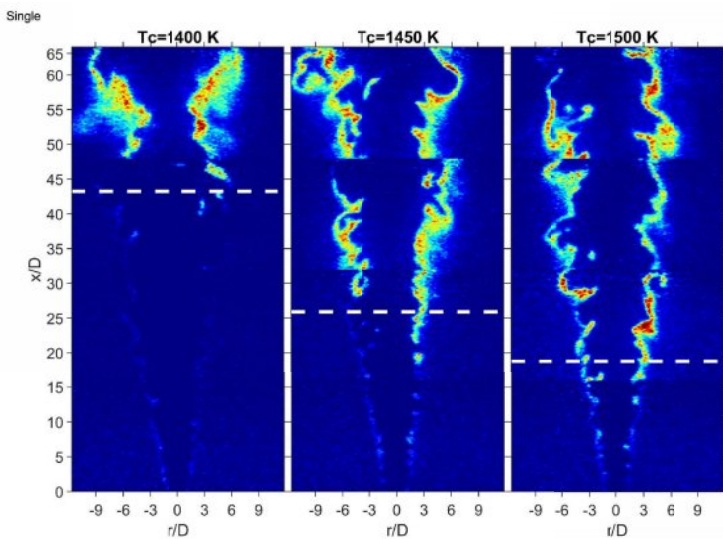


The University of Sydney

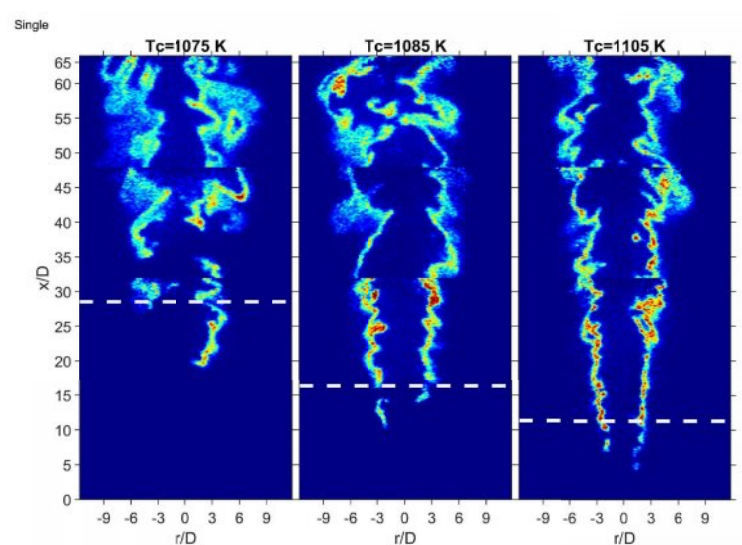
Page 15

## Sydney cracked ammonia jet in hot coflow cases

7% cracked  $\text{NH}_3$ , vary  $T_c$



28% cracked  $\text{NH}_3$ , vary  $T_c$



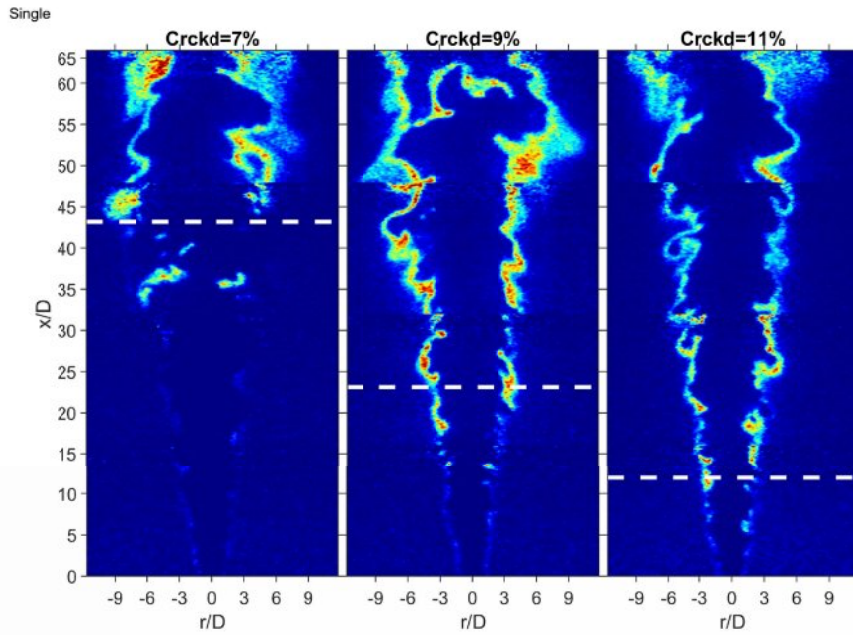
Not shown here: 14% cracked  $\text{NH}_3$ , vary  $T_c$

The University of Sydney

Page 16

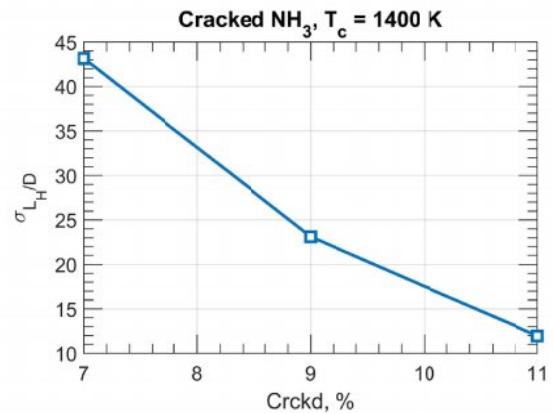
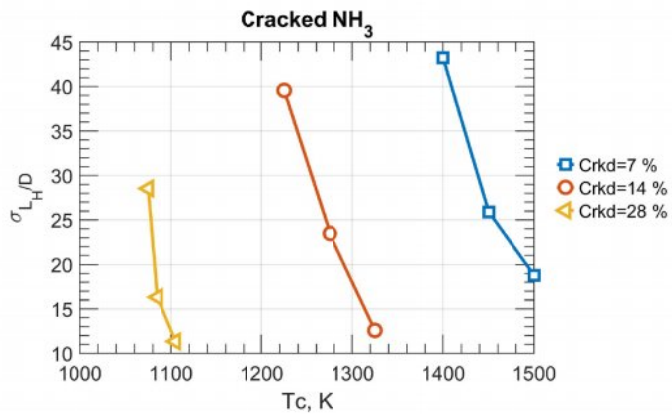
# Sydney cracked ammonia jet in hot coflow cases

Vary % cracked  $\text{NH}_3$ , fixed  $T_c = 1400 \text{ K}$



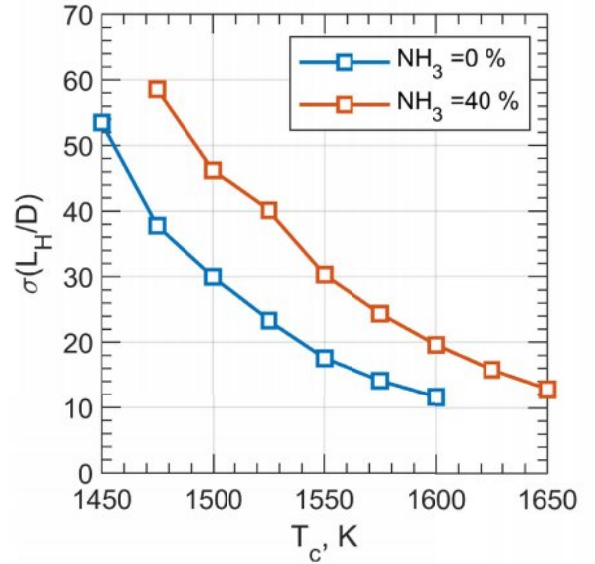
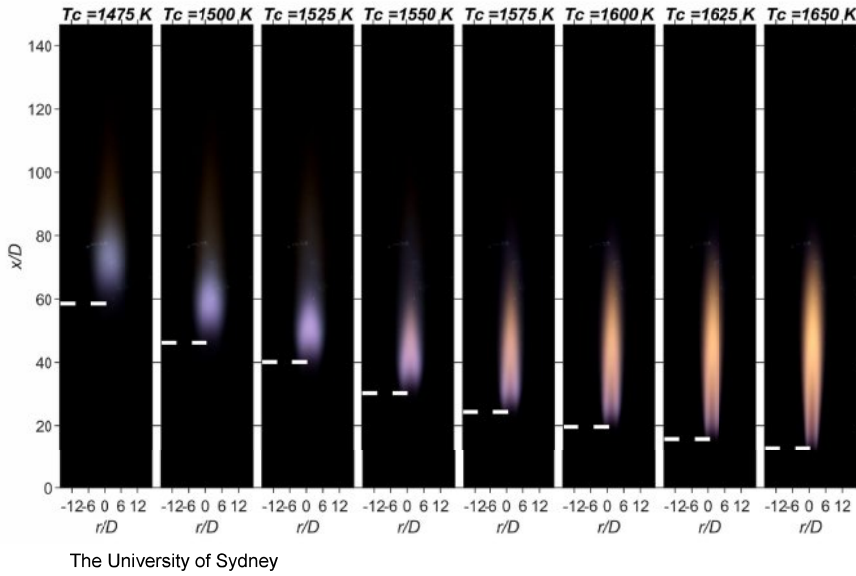
# Sydney cracked ammonia jet in hot coflow cases

Proposed 11 validation cases



# Sydney partially premixed NH<sub>3</sub>/CH<sub>4</sub> jet in hot coflow

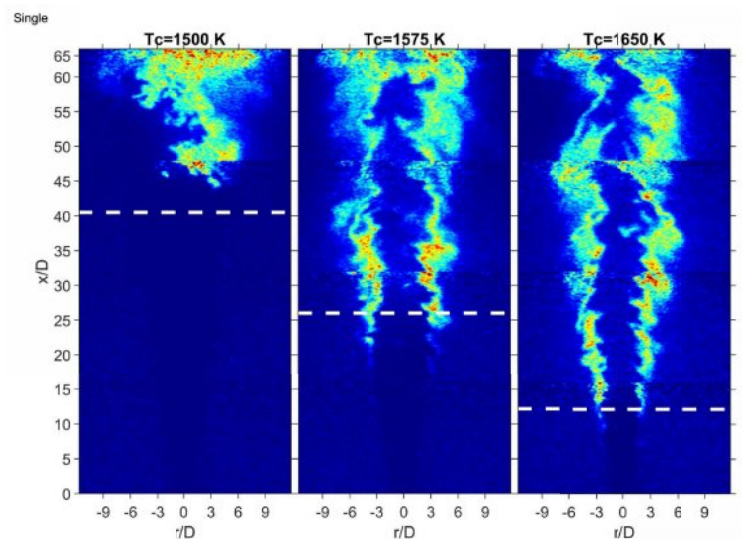
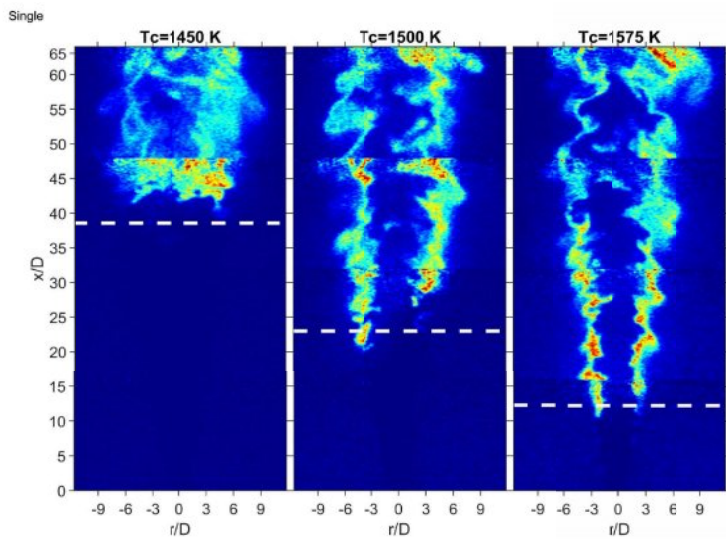
Fuel: 40% NH<sub>3</sub>, 60% CH<sub>4</sub>  
 Jet: 2:1 air:fuel, 100 m/s



# Sydney partially premixed NH<sub>3</sub>/CH<sub>4</sub> jet in hot coflow

Fuel: 100% CH<sub>4</sub>,  
 Jet: 2:1 air:fuel, 100 m/s

Fuel: 40% NH<sub>3</sub>, 60% CH<sub>4</sub>,  
 Jet: 2:1 air:fuel, 100 m/s



## Sydney cracked ammonia jet in hot coflow cases

Narrowed down a large parameter space of cracked ammonia flames to ~12 flames

Narrowed down a large parameter space of partially premixed  $\text{NH}_3/\text{CH}_4$  (40%  $\text{NH}_3$ , 60%  $\text{CH}_4$ ) flames to 3 flames

OH measured and easily computed from simulations

Alternate paradigm for model validation

Present trends of  $L_H$  varying  $T_C$  and % cracked for validation, rather than scatter plots and mean and rms profiles

## Sydney lean premixed $\text{H}_2$ jet in hot coflow

Utilise the Sydney premixed jet in hot coflow previously developed for lean  $\text{CH}_4$ +air

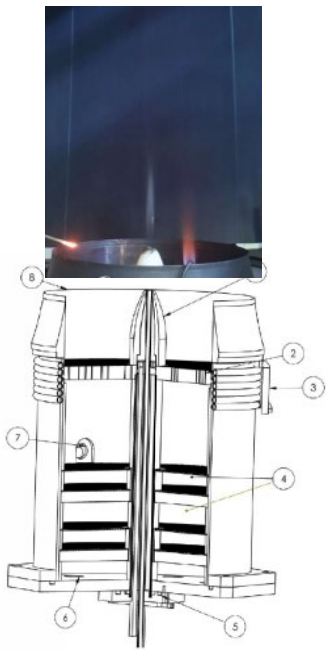
Consider the case of a lean premixed  $\text{H}_2$  jet issuing into a hot coflow of the same equivalence ratio

System defined by a single progress variable

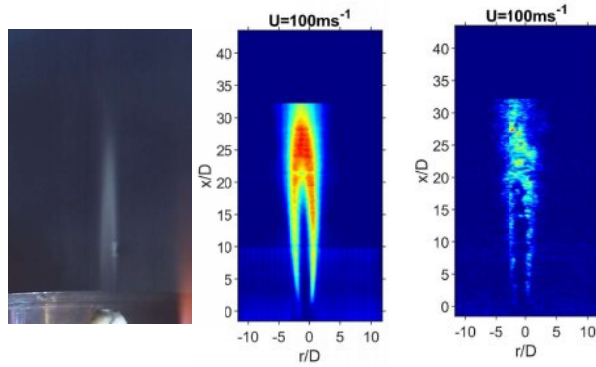
Incorporate compressibility



## Sydney lean premixed H<sub>2</sub> jet in hot coflow



The University of Sydney



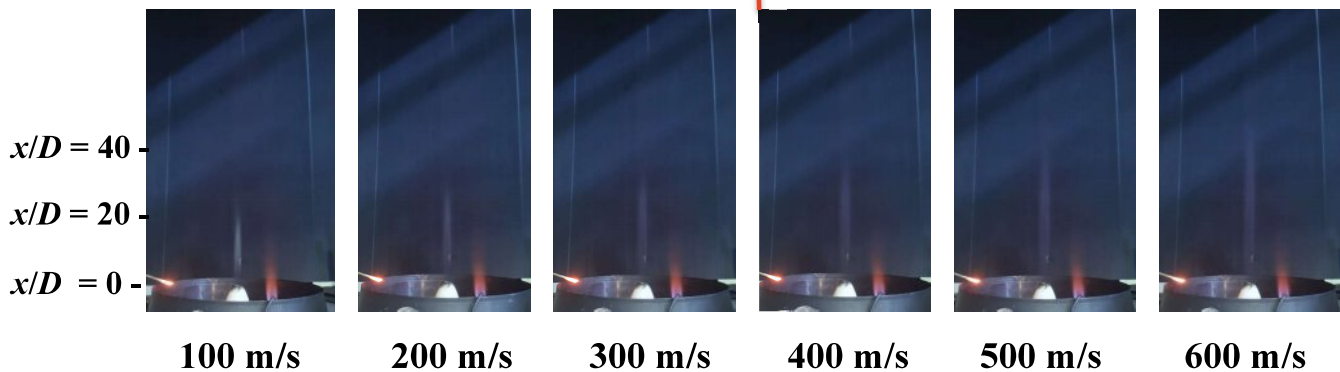
$T_{\text{coflow}} = T_{\text{ad}}$	$\Phi_{\text{coflow}} = \Phi_{\text{jet}}$	$U_{\text{jet}}$ range (m/s)	$X_{\text{H}_2, \text{jet}}$	$X_{\text{O}_2, \text{coflow}}$	$c$ (m/s)
1200 K	0.307	100-600	0.129	0.137	363.6
1300 K	0.348	100-600	0.146	0.128	366.2
1500 K	0.435	100-600	0.183	0.109	371.5

Page 23

## Sydney lean premixed H<sub>2</sub> jet in hot coflow

$$T_{\text{ad}} = T_{\text{coflow}} = 1500 \text{ K}, \phi_{\text{jet}} = \phi_{\text{coflow}} = 0.435$$

$$M_{\text{jet}} = 1$$



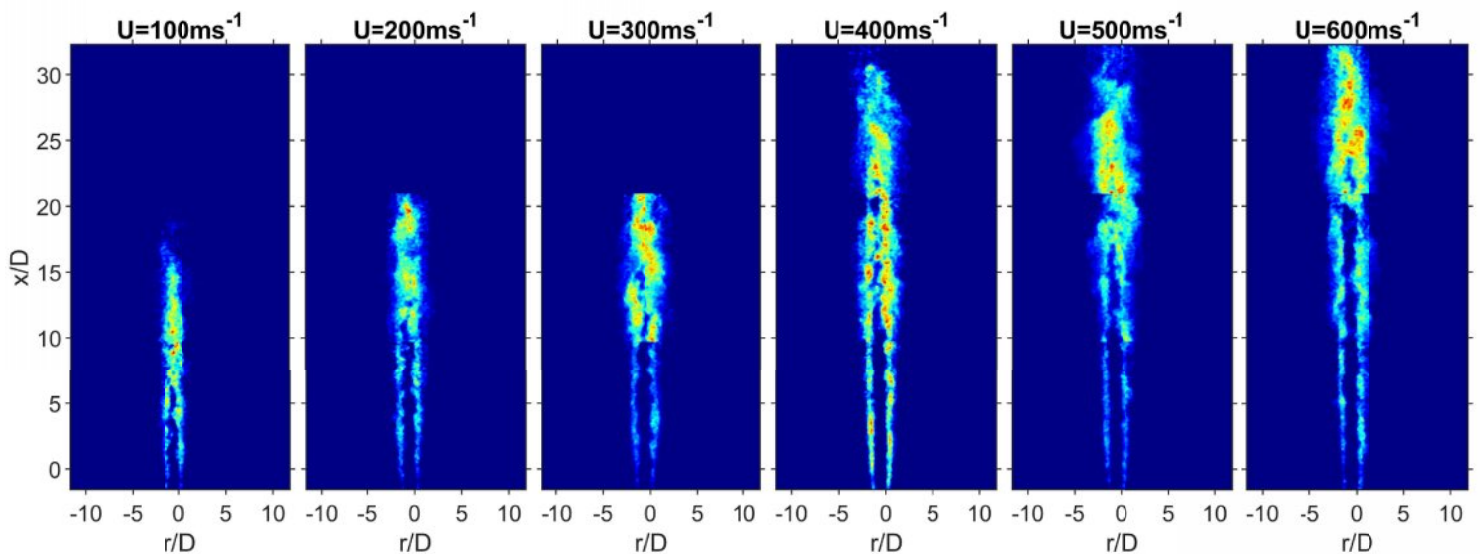
The University of Sydney

Page 24



## Sydney lean premixed H<sub>2</sub> jet in hot coflow (PJB)

$$T_{\text{ad}} = T_{\text{coflow}} = 1500 \text{ K}, \phi_{\text{jet}} = \phi_{\text{coflow}} = 0.435$$

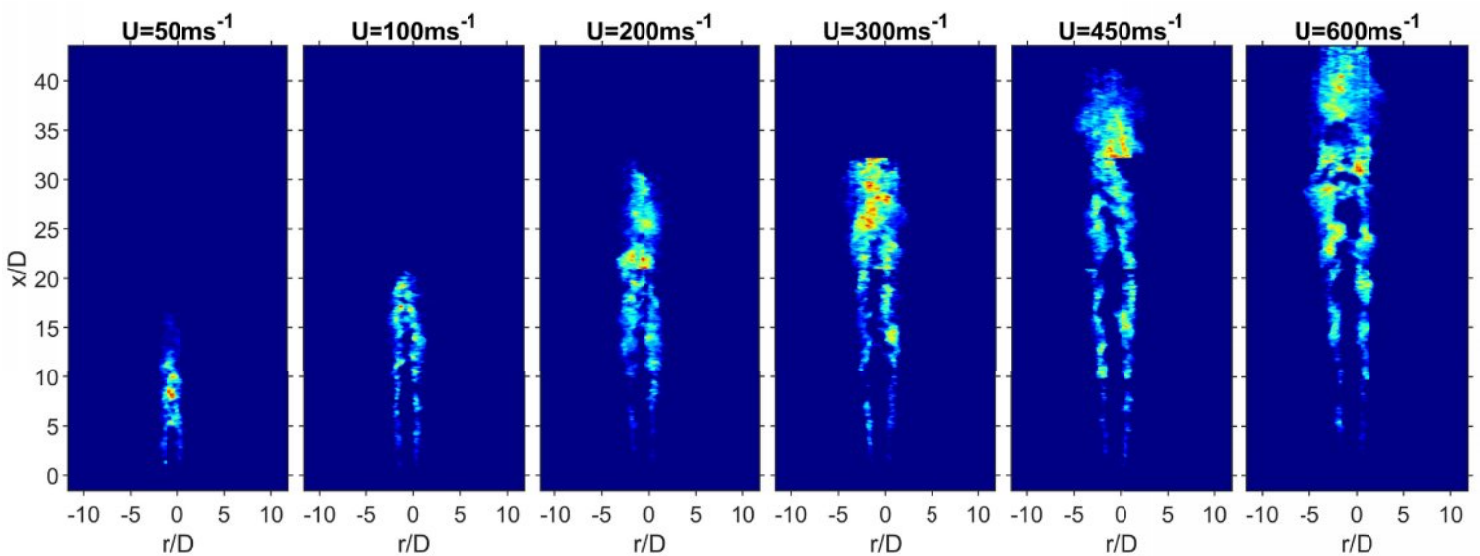


The University of Sydney

Page 25

## Sydney lean premixed H<sub>2</sub> jet in hot coflow (PJB)

$$T_{\text{ad}} = T_{\text{coflow}} = 1300 \text{ K}, \phi_{\text{jet}} = \phi_{\text{coflow}} = 0.348$$

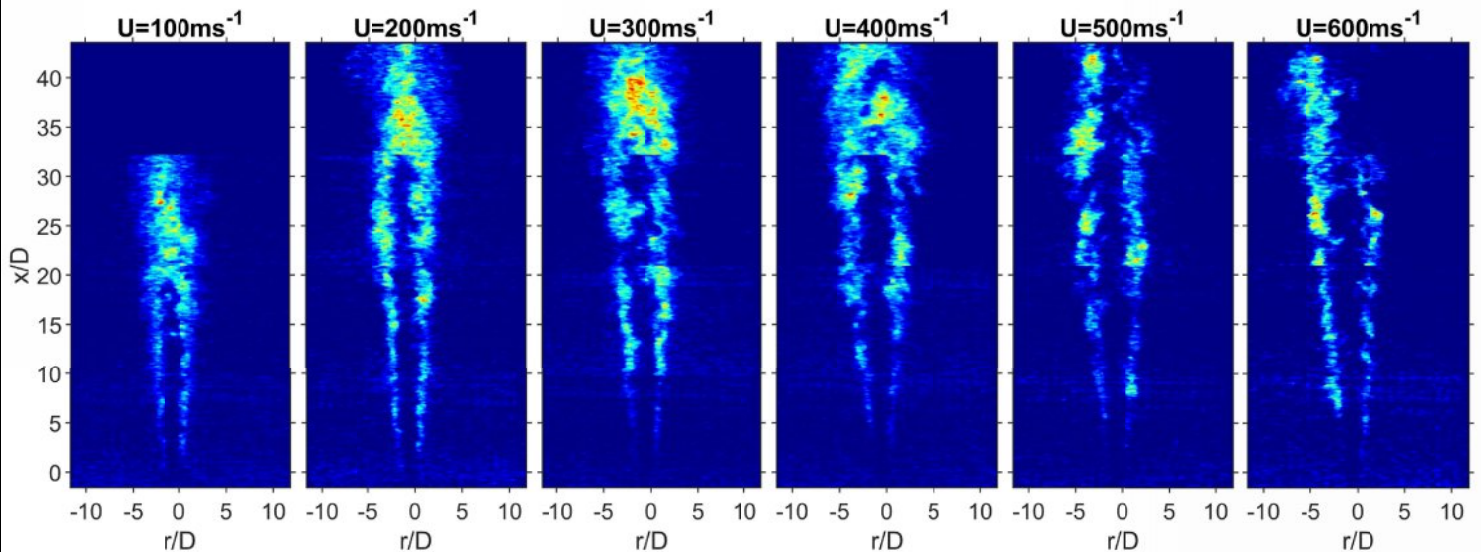


The University of Sydney

Page 26

## Sydney lean premixed H<sub>2</sub> jet in hot coflow (PJB)

$$T_{\text{ad}} = T_{\text{coflow}} = 1200 \text{ K}, \phi_{\text{jet}} = \phi_{\text{coflow}} = 0.307$$



The University of Sydney

Page 27

## Sydney lean premixed H<sub>2</sub> jet in hot coflow (PJB)

Simple single progress variable jet in hot coflow configuration

Near lean limit cases

Cases with and without compressibility and shocks

Local extinction evident in all cases

Flame length, FSD and OH comparison possible now

The University of Sydney

Page 28



جامعة الملك عبد الله  
للعلوم والتقنية  
King Abdullah University of  
Science and Technology

CCRC



## Available TNF datasets from KAUST

TNF 2024

Presenter: Gaetano Magnotti

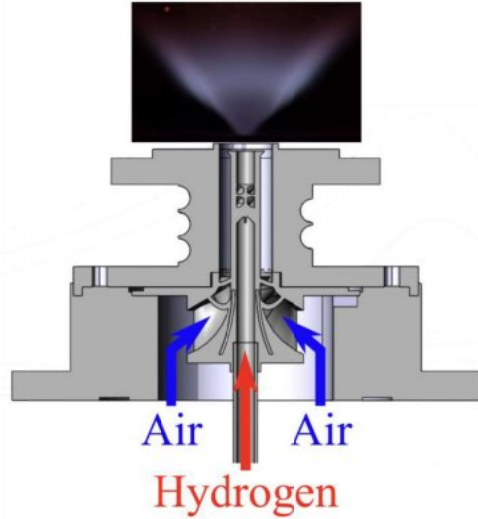
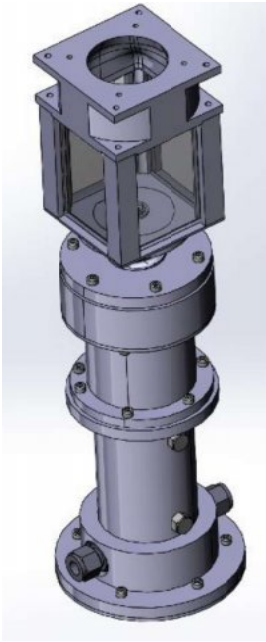
1



## Hylon 2 IMFT/KAUST



# Final geometry of the HYLON TNF v2 injector



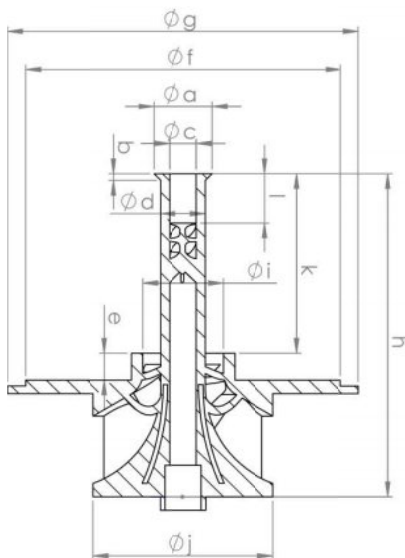
- Diameter annular channel: 18 mm
- Diameter central channel: 6 mm
- Thickness central channel: 2 mm
- Size central channel deflector: 1.5 mm
- Recess central injector: 4.3 mm
- Swirl number air flow: 0.9
- Swirl number hydrogen flow: 0.9
- Width combustion chamber: 78 mm
- Length combustion chamber: 149 mm
- Contraction ratio exhaust: 0.51

3

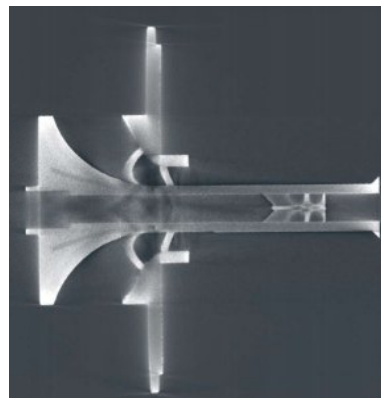
# Validation of the manufactured geometry

a) Verifications with caliper measurements

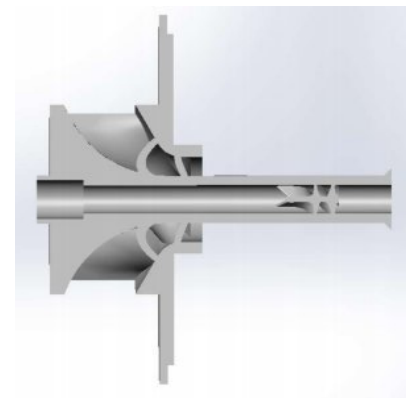
b) X-Ray tomography of the injector



X-Ray picture



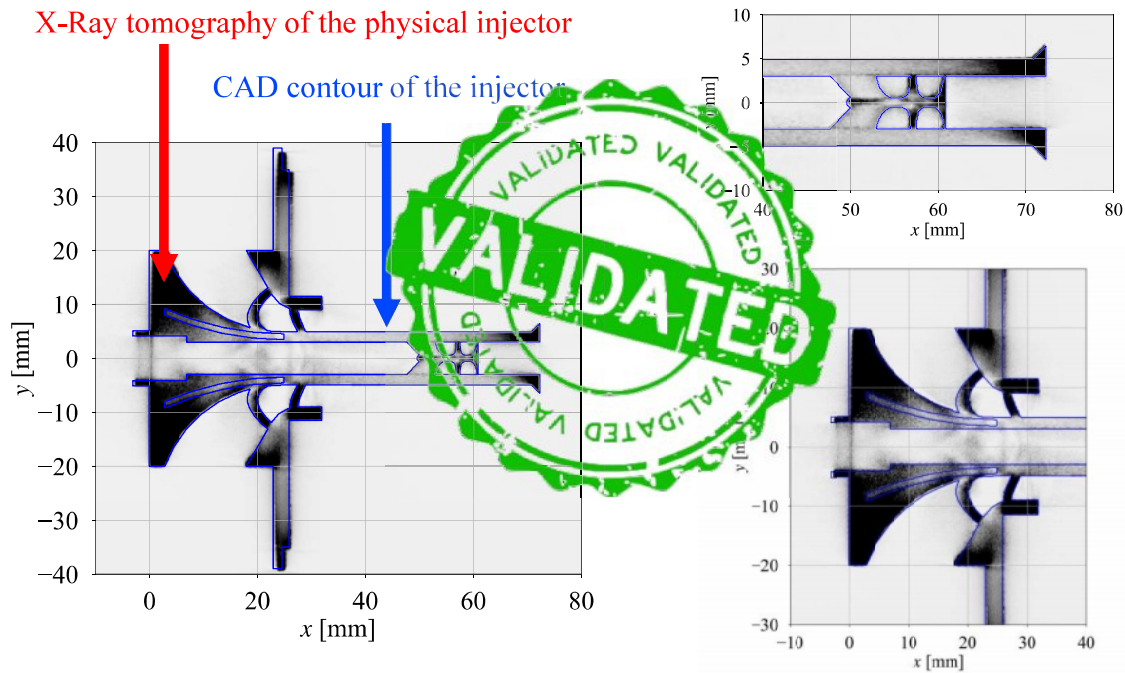
CAD picture



4

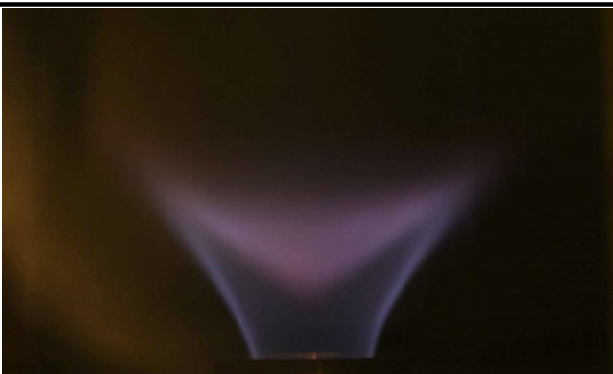


## Validation of the manufactured geometry

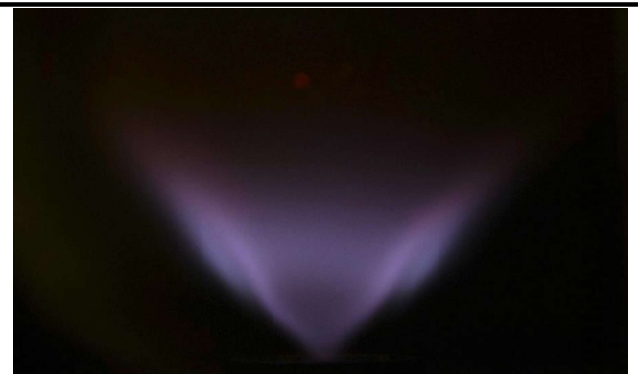


## Raman/Rayleigh/OH/NO-LIF at 1 bar

FLAME	$V_{air}$ (SLM)	$V_{H_2}$ (SLM)	$\phi$	P (Watts)	$U_{air}$ (m/s)	$U_{H_2}$ (m/s)	$Re_{air}$	$Re_{H_2}$
A	85	15	0.42	2696	12.5	9.5	4003.1	517.6
L	170	30	0.42	5393	25	19	8006.2	1035.2



Flame A



Flame L

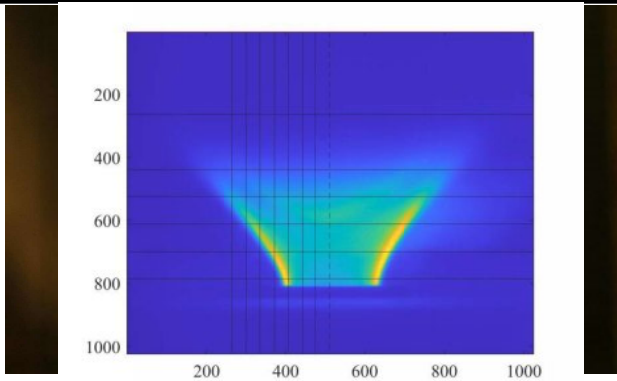
6





# Raman/Rayleigh/OH/NO-LIF at 1 bar

FLAME	$V_{air}$ (SLM)	$V_{H_2}$ (SLM)	$\phi$	P (Watts)	$U_{air}$ (m/s)	$U_{H_2}$ (m/s)	$Re_{air}$	$Re_{H_2}$
A	85	15	0.42	2696	12.5	9.5	4003.1	517.6
L	170	30	0.42	5393	25	19	8006.2	1035.2



Flame A

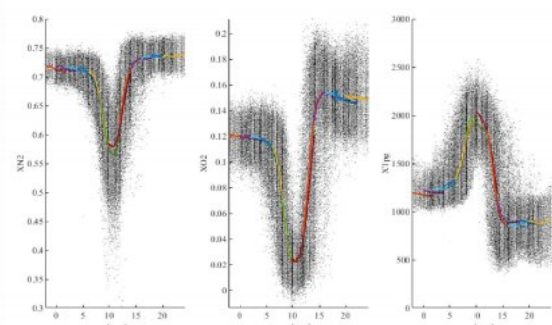
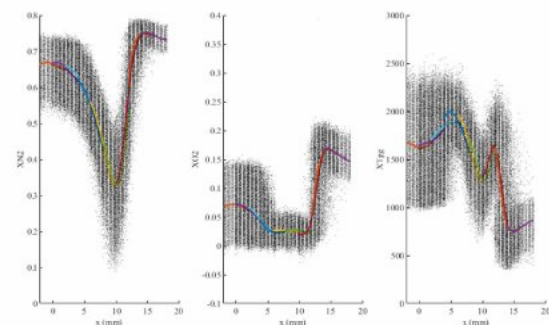
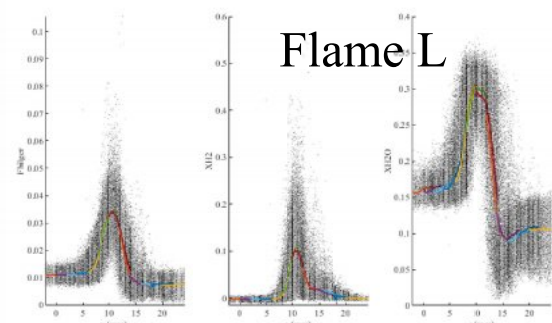
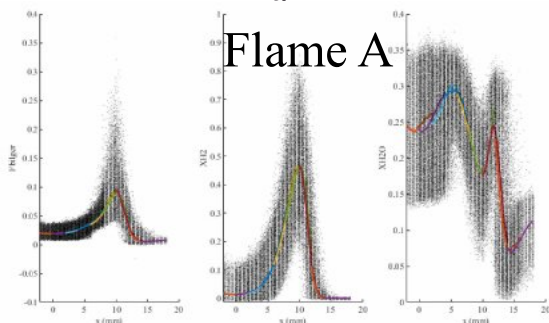


Flame L

7



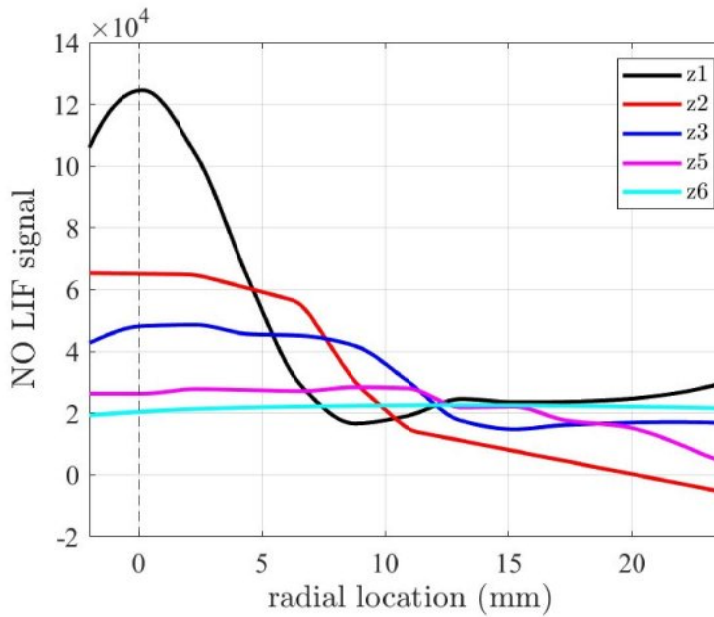
# Preliminary results for axial location 3



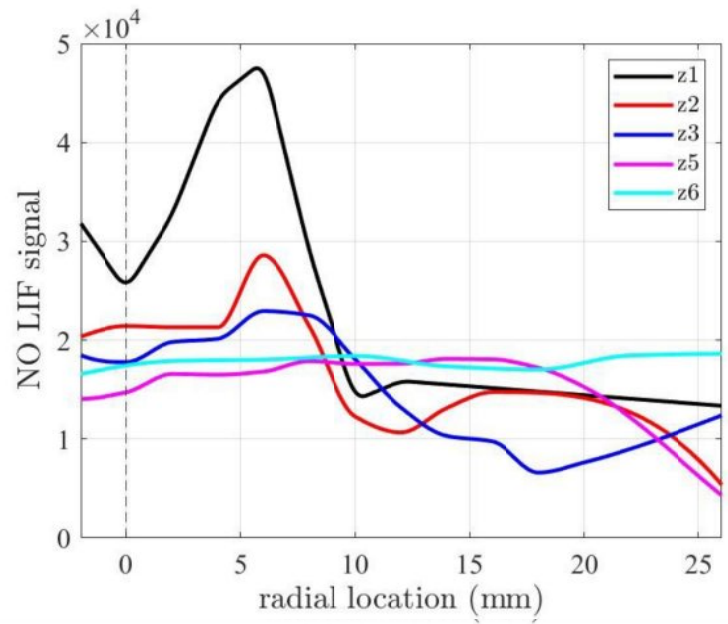
8

# Preliminary results: OH and NO LIF profiles

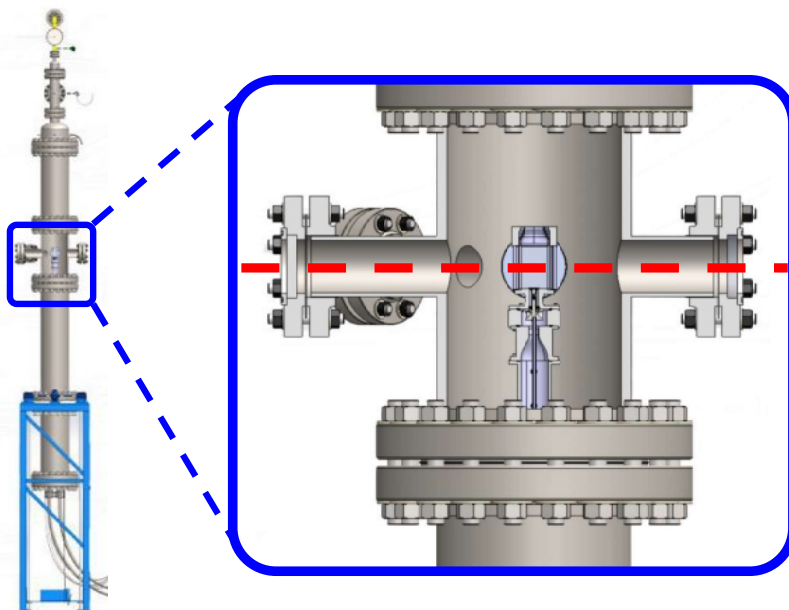
## Flame A



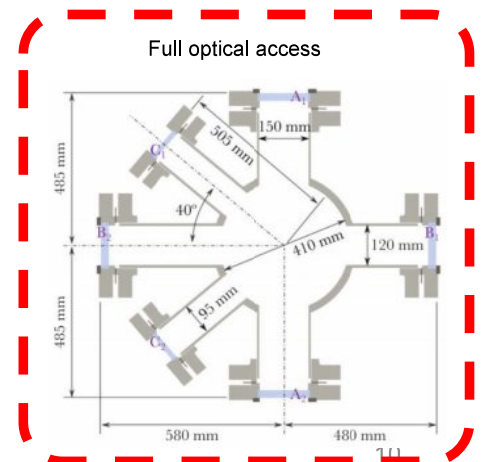
## Flame L



# Installation inside the HPCD test bench

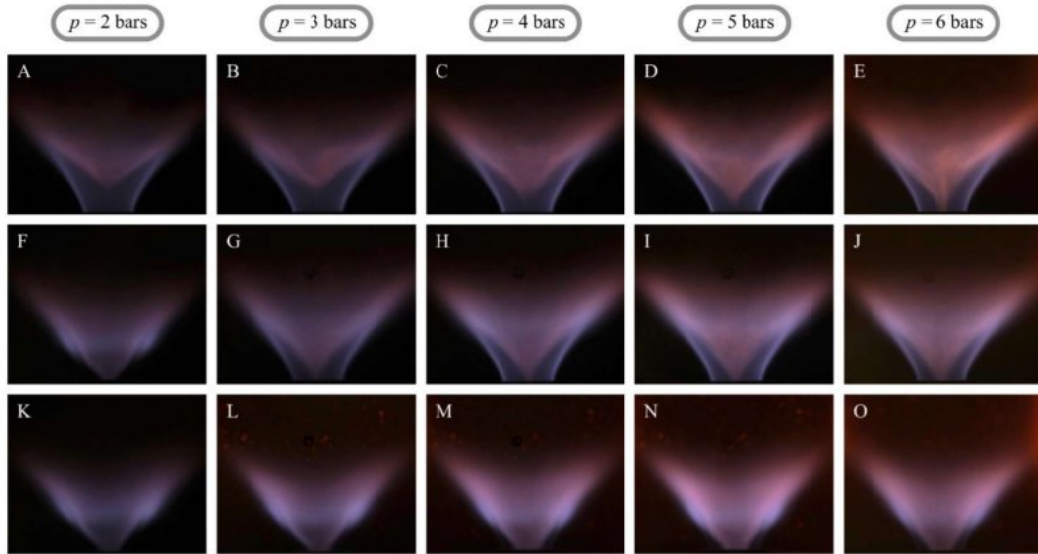


- Thermal power range: 0 to 70 kW
- Overall pressure range: 1 to 15 bars
- Pre-heated air system: currently in implementation





# High-pressure flames



The injector both anchored and lifted flame stabilization regimes (and some other interesting cases!)

11

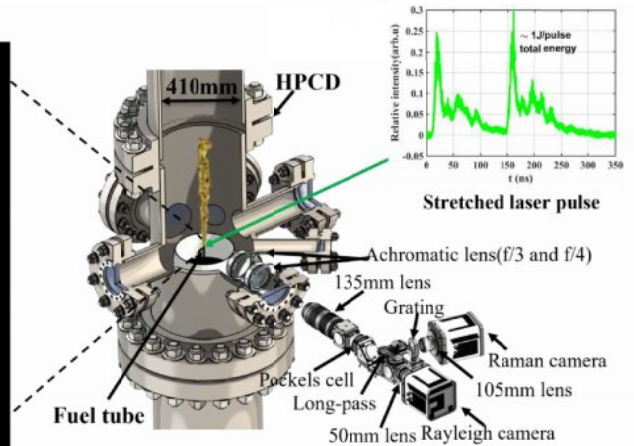
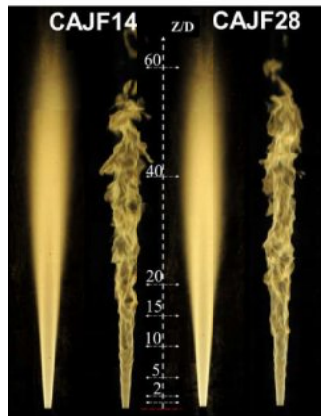


## Partially cracked ammonia jet flames at elevated pressure



## High-pressure cracked ammonia jet flames

- Fuel simulating 14% and 28% cracked ammonia
- Non-premixed jet in air co-flow
- 3.35 mm inner diameter
- **5 bar operating pressure**
- **Reynolds number of 11000** for the turbulent flames
- Simultaneous Raman and NO LIF
- **Velocity measurements** (cold-gas PIV)
- T, major species, NO and velocity data available
- Mean, RMS, PDF...



*Tang et al. Combustion and Flame*  
244, 112292

*Tang et al. Experimental Thermal and Fluid Science* 149, 111020

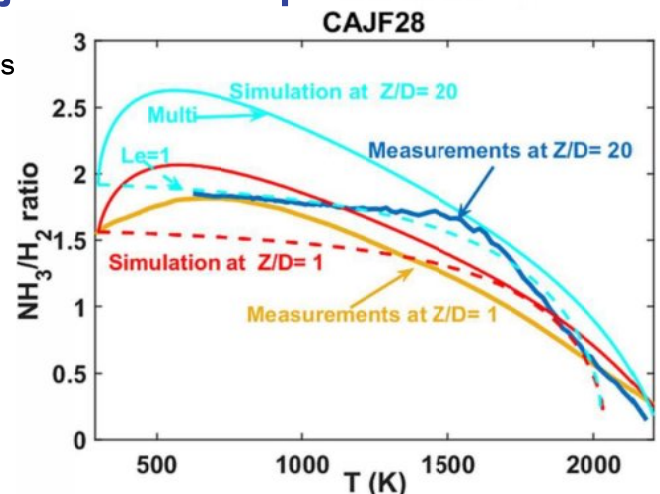
*Wang et al. Proceedings of the Combustion Institute* 39 (1), 1465-1474

13



## High-pressure cracked ammonia jet flames: experiments

- Dataset useful to evaluate differential diffusion effects
- Diff-diff parameter negligible above 15D
- Differential diffusion affects centerline  $\text{NH}_3/\text{H}_2$  ratio across the entire flame



*Tang et al. Combustion and Flame*  
244, 112292

*Tang et al. Experimental Thermal and Fluid Science* 149, 111020

*Wang et al. Proceedings of the Combustion Institute* 39 (1), 1465-1474

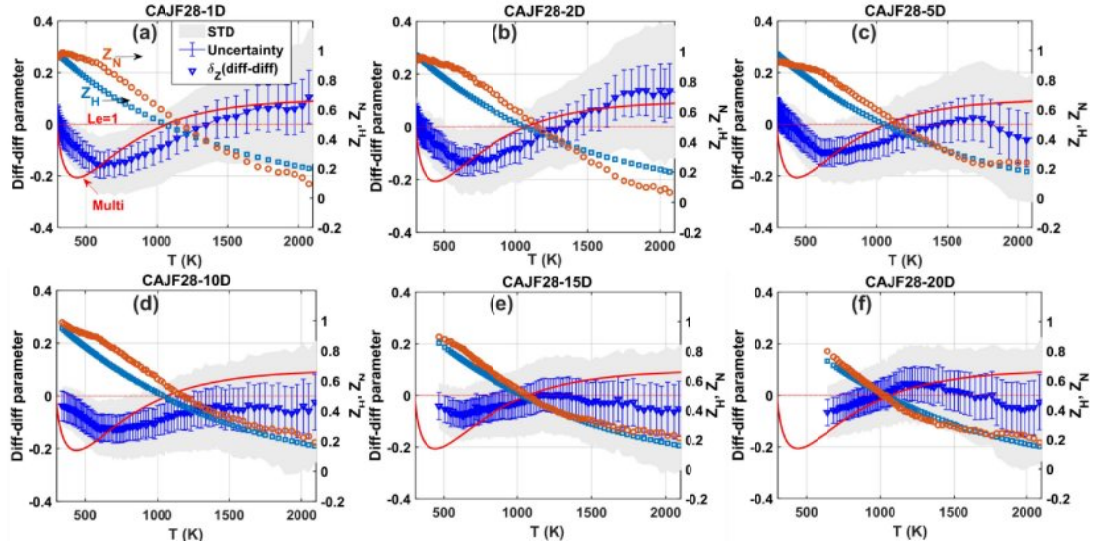
14





# High-pressure cracked ammonia jet flames: experiments

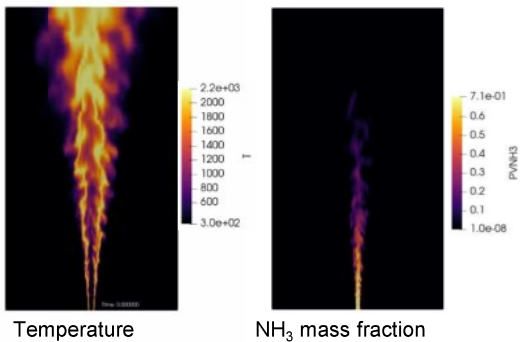
- Dataset useful to evaluate differential diffusion effects
- Diff-diff parameter negligible above 15D
- Differential diffusion affects centerline NH3/H2 ratio across the entire flame



15

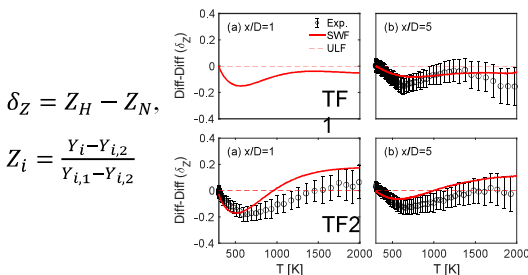


# Simulation of KAUST pressurized NH<sub>3</sub>/H<sub>2</sub> flame

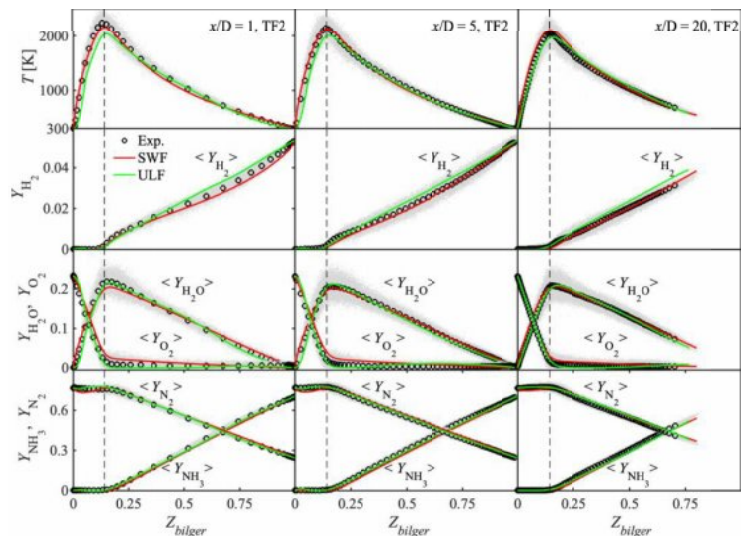


Temperature

NH<sub>3</sub> mass fraction



Comparison of differential diffusion parameter



SWF: species weighted FPV model with differential diffusion

ULF: unity Lewis number FPV model

Comparison of conditional mean temperature and species mass fraction in mixture fraction space

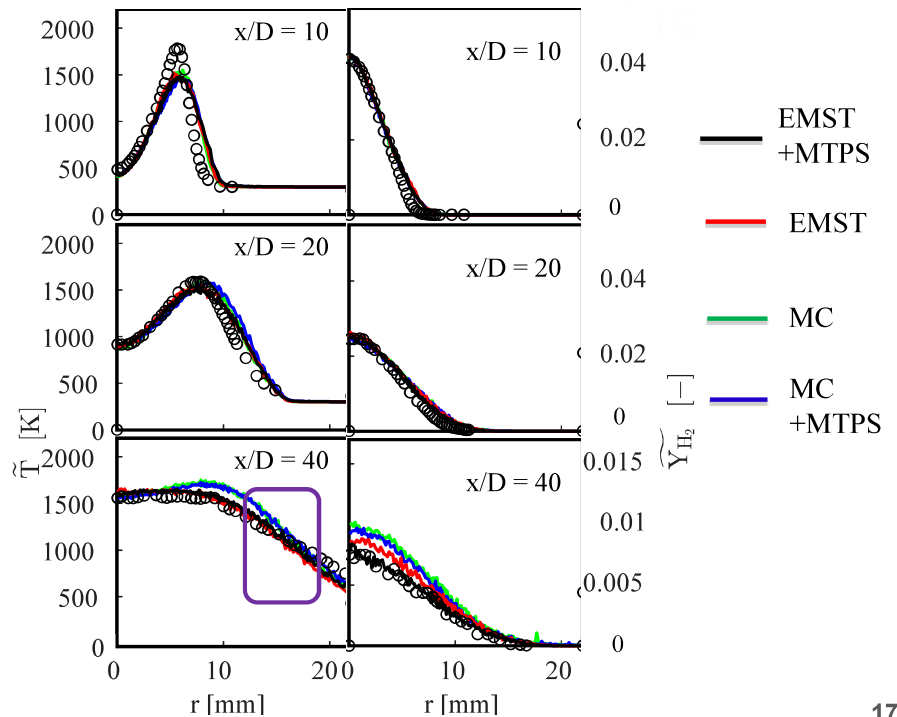
Gao et al, CNF 2024 under review

6



# High-pressure cracked ammonia jet flames: simulations of CAJF28

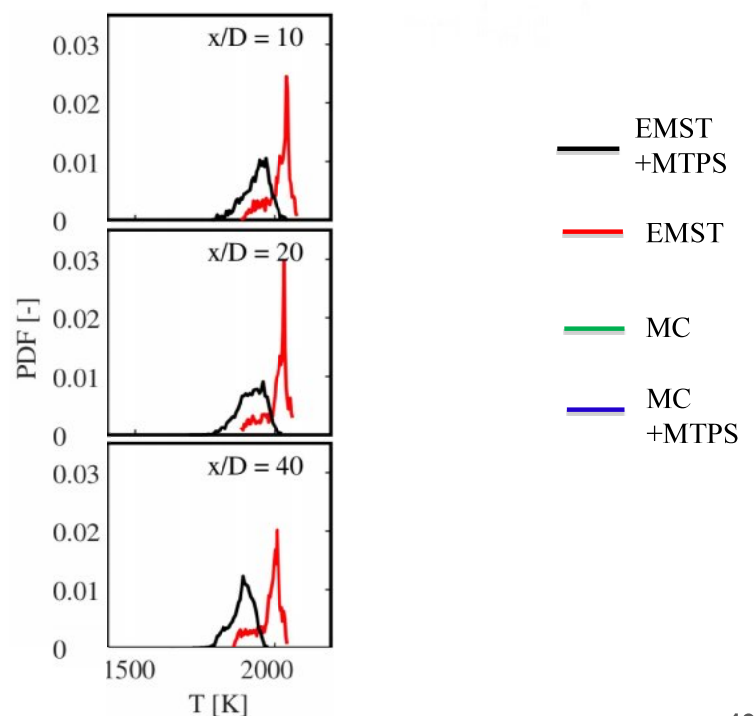
- $P = 5 \text{ atm}$  and  $Re = 11,200$  - CAJF28
- Method: Joint-Scalar Transported PDF approach that two mixing models are compared (MC vs. EMST)
- Molecular diffusion is considered via Molecular Transport in Physical Space model (MTPS) (McDermott and Pope, JCP, 226, 2007)
- **Molecular diffusion** can be observed at  $x/D = 40$  for  $H_2$  (Left)
- PDF of temperature (Middle) shows a shift due to MTPS although radial profiles of mean values are similar.



17

# High-pressure cracked ammonia jet flames: simulations of CAJF28

- $P = 5 \text{ atm}$  and  $Re = 11,200$  - CAJF28
- Method: Joint-Scalar Transported PDF approach that two mixing models are compared (MC vs. EMST)
- Molecular diffusion is considered via Molecular Transport in Physical Space model (MTPS) (McDermott and Pope, JCP, 226, 2007)
- **Molecular diffusion** can be observed at  $x/D = 40$  for  $H_2$  (Left)
- PDF of temperature (Middle) shows a shift due to MTPS although radial profiles of mean values are similar.

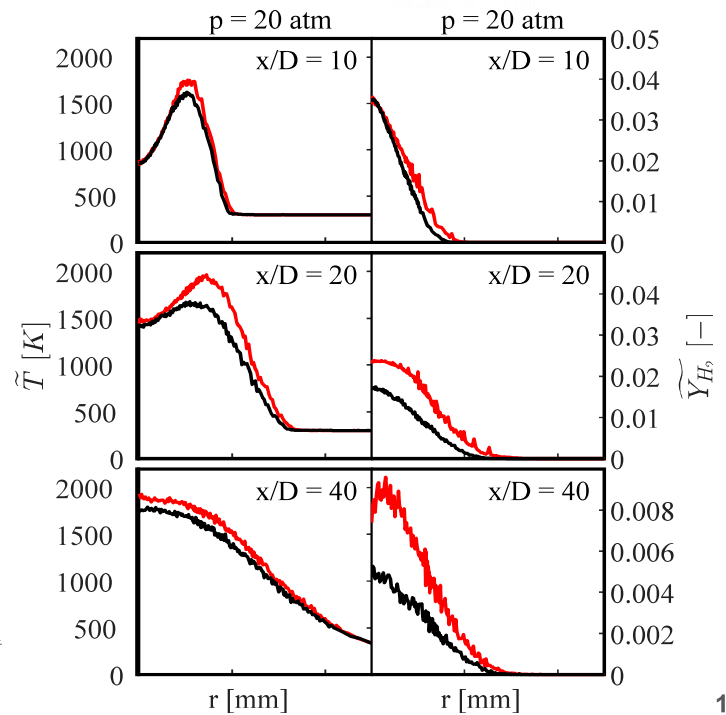


18

# High-pressure cracked ammonia jet flames: simulations: effect of pre-heating and higher pressure

- Computational explorations at enhanced pressure (**20 atm**) and preheated fuel mixtures (600 K) show a **stronger** effect of **differential diffusion** (Right).

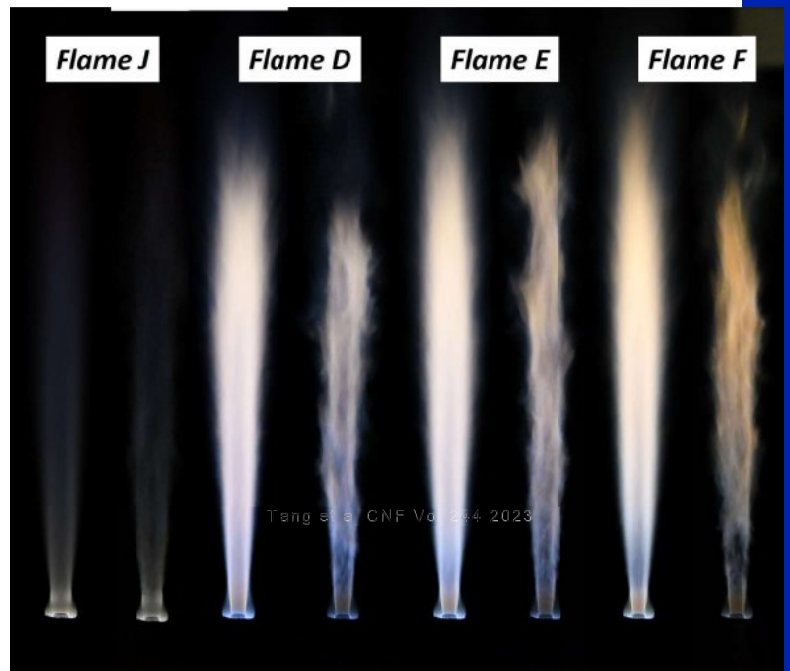
*Lu Tian*  
*R Peter Lindstedt*



## Partially premixed NH<sub>3</sub>/H<sub>2</sub>/air piloted jet flames at atmospheric pressure

## Partially premixed, NH<sub>3</sub>/H<sub>2</sub>/N<sub>2</sub> piloted flames

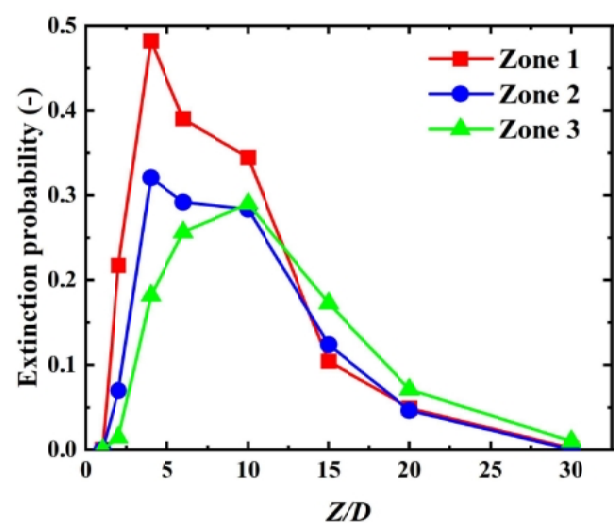
- Four partially premixed piloted jet flames
- Modified Sandia piloted burner
- Raman/Rayleigh+OH/NH<sub>2</sub> LIF
- Fuel: Simulated partially cracked ammonia (43%), and air with  $\Phi = 3$
- Flame J with 100% cracking
- Pilot jet: Simulated partially cracked ammonia (43%), and air with  $\Phi = 0.9$  520W
- **Turbulence-chemistry interaction/localized extinction/re-ignition**
- **Differential diffusion**
- Three Reynolds numbers
  - Flame D Re=24000 (59%  $Re_{extinction}$ )
  - Flame E Re=32000 (79%  $Re_{extinction}$ )
  - Flame F Re=36000 (89%  $Re_{extinction}$ )
  - Flame J Re=36000 (N<sub>2</sub>:H<sub>2</sub>=1:3)



21

## Partially premixed, NH<sub>3</sub>/H<sub>2</sub>/N<sub>2</sub> piloted flames

- 10 numerical datasets collected from 9 groups
- 8 LES, 1 URANS, 1 DNS. Simulations still being refined
- Only Flame D and Flame F
- All groups struggles in capturing flame length
- No group correctly captured the extinction behavior
- Flame E and Flame J data will be fully released within the next 6 months.
- More extensive comparison expected for TNF 2026.
- **We need NO and PIV data (message received)**



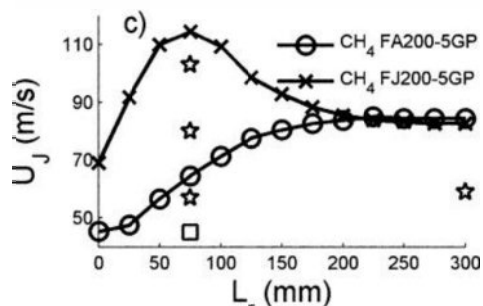
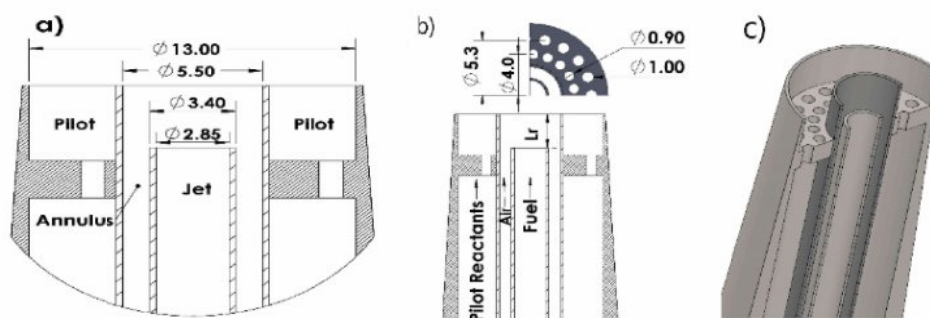
22



# Sydney inhomogeneous burner with ammonia in the fuel blend

## Sydney inhomogeneous burner: background

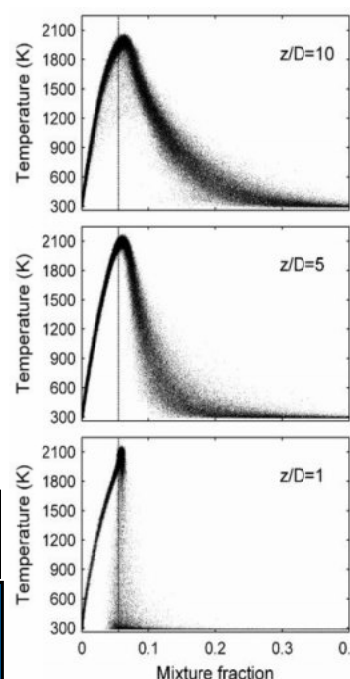
- Designed to target role of fuel stratification
- TNF target flame using CH<sub>4</sub> as fuel



*Barlow et al. Combustion and Flame 162, 3516*

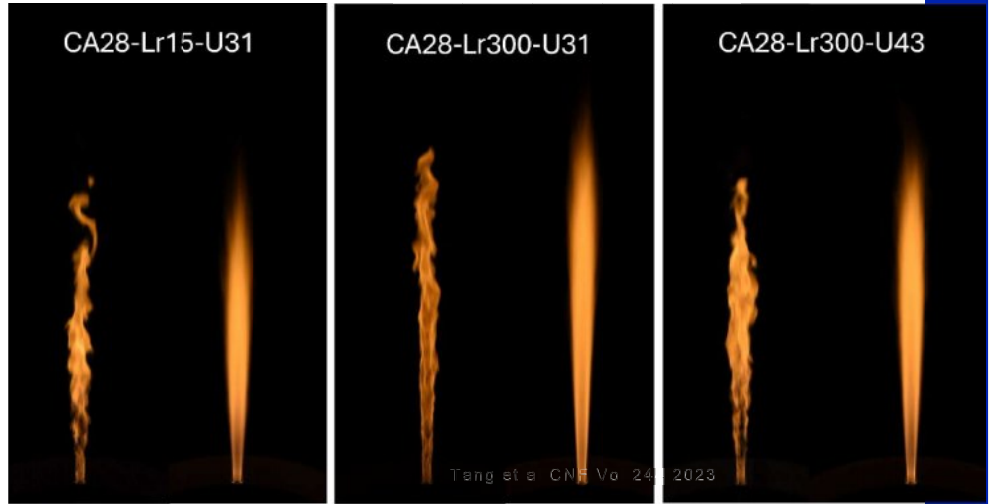
*Meares et al. Proceedings of the Combustion Institute 35 (2), 1477-1484*

### FJ-5GP-Lr75-80



## Sydney inhomogeneous burner: 28% cracking

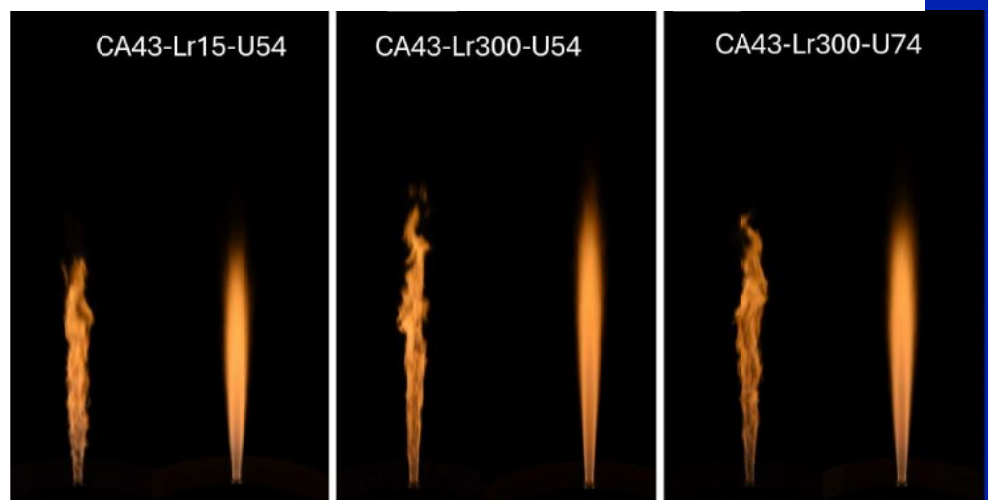
- Designed to target role of fuel stratification
- 1D Raman/Rayleigh
- $\phi_{global} = 4.76$ , Pilot 114W
- 28% Cracked ammonia series: effect of recess and Re
  - $NH_3:H_2:N_2=56:33:11$  (28% cracking)
  - $Lr=15/U=31$  ( $Re=10319$ , 80%  $Re_{extinction}$ )
  - $Lr=300/U=31$  ( $Re=10319$ , 58%  $Re_{extinction}$ )
  - $Lr=300/U=43$  ( $Re=14347$ , 80%  $Re_{extinction}$ )
- **Data collected** Expected availability: Spring 2025



25

## Sydney inhomogeneous burner: 43% cracking

- 43% cracked ammonia series: effect of recess and Re
  - $NH_3:H_2:N_2=40:45:15$   
 $\phi_{global} = 4.76$
  - $Lr=15/U=54$  ( $Re=17816$ , 80%  $Re_{extinction}$ )
  - $Lr=300/U=54$  ( $Re=17816$ , 58%  $Re_{extinction}$ )
  - $Lr=300/U=74$  ( $Re=24367$ , 80%  $Re_{extinction}$ )
- **Data collected.** Expected availability to modelers Spring 2025

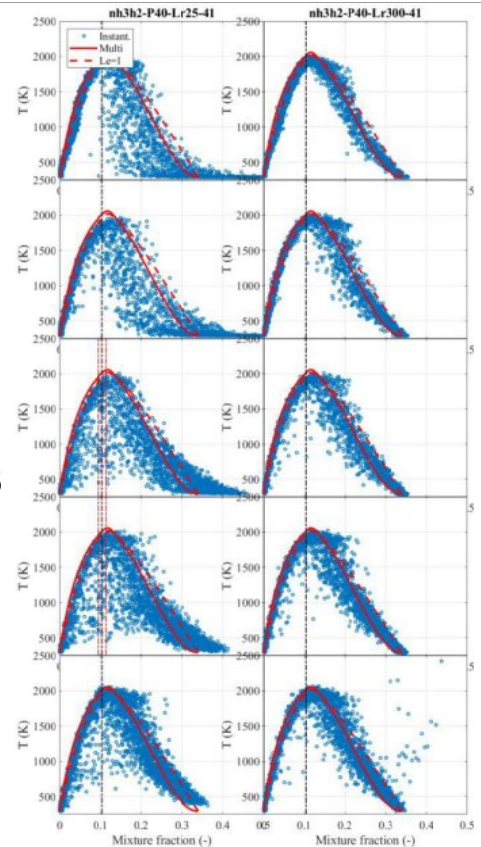
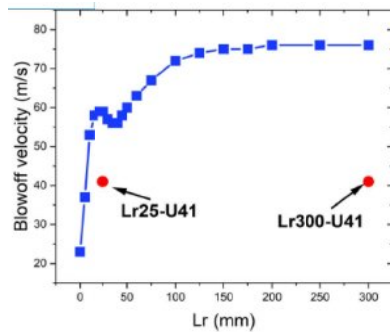


26



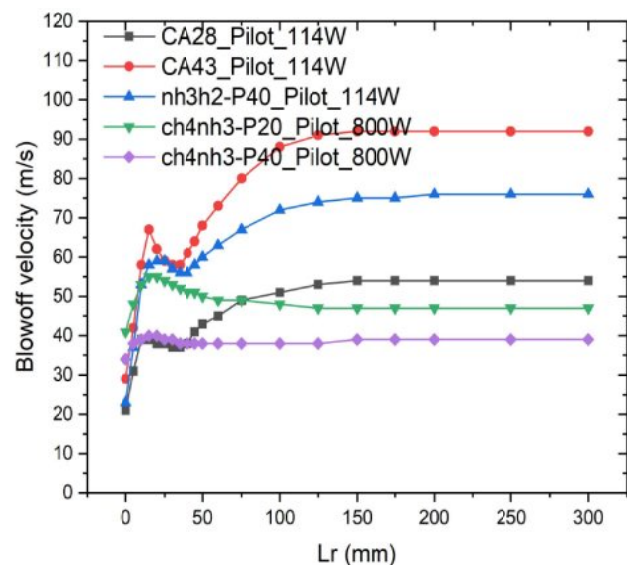
## Sydney inhomogeneous burner: NH<sub>3</sub>/H<sub>2</sub>=60:40

- Effect of recess length
  - $\phi_{global} = 4.76$ , Pilot 114 W
  - Lr=25/U=41 (Re=13399, 70% Re<sub>extinction</sub>)
  - Lr=300/U=41 (Re=17816, 54% Re<sub>extinction</sub>)
- **Polarization separation for improved fluorescence suppression**
- **Data collected.** Expected availability to modelers Spring 2025



## Sydney inhomogeneous burner: methane addition

- Effect of methane addition
  - Lr=15, Pilot 800W
  - CH<sub>4</sub>:NH<sub>3</sub>=8:2, U=42 (Re=14322, 77% Re<sub>extinction</sub>)
  - CH<sub>4</sub>:NH<sub>3</sub>=6:4, U=32 (Re=10910, 80% Re<sub>extinction</sub>)
- Effect of recess length
  - Lr=300 CH<sub>4</sub>:NH<sub>3</sub>=6:4, U=31 (Re=10569, 80% Re<sub>extinction</sub>)
- **Polarization separation essential for fluorescence suppression**
- **Data collected.** Expected availability to modelers Spring 2025

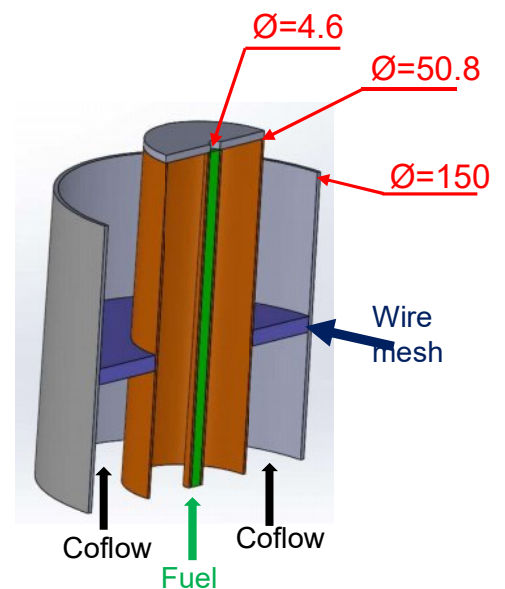
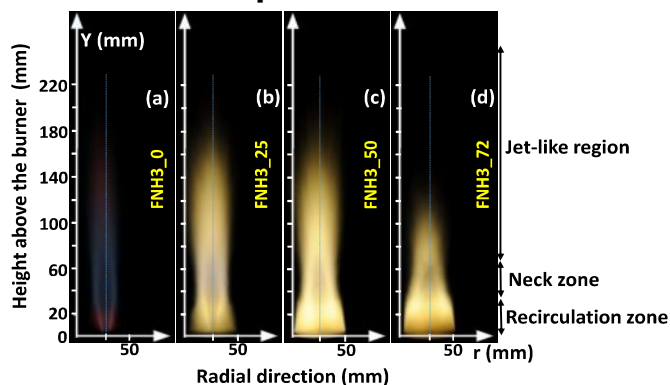




# Bluff-body stabilized flames

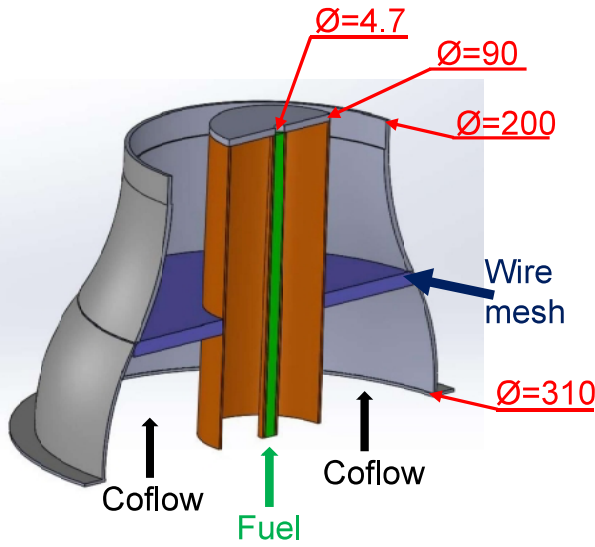
## Bluff-body ammonia burner

- Evaluate the role of the products recirculation in partial cracking of ammonia
- Raman/Rayleigh data available for variable cracking ratios
- Initial design was limited in momentum ratio by max air flow-rate
  - **Unable to burn pure ammonia**



Alfazazi et al, CNF Volume 258, Part 2, December 2023, 113066

# New bluff-body ammonia burner



Alfazazi et al, PROC-S-23-01104

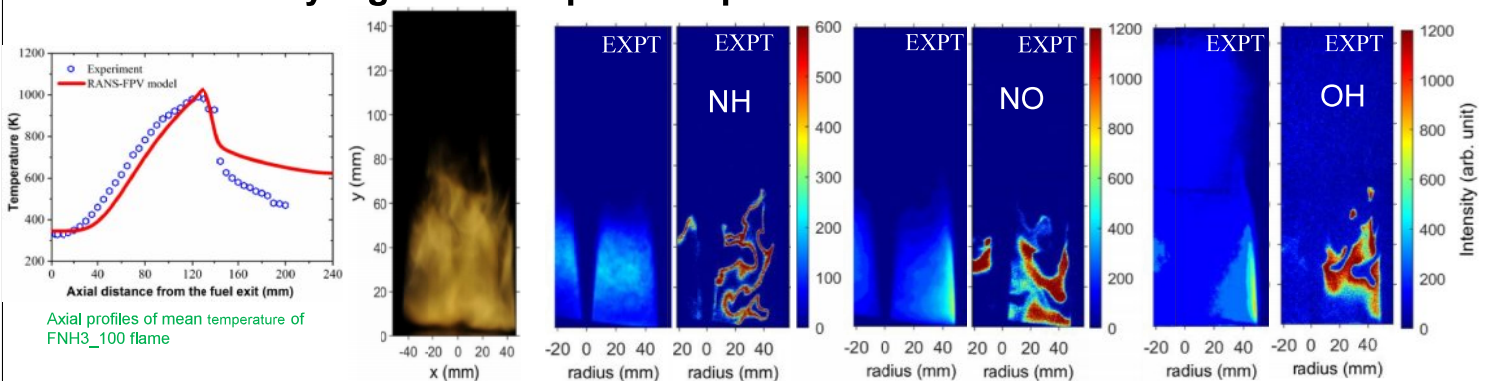
Case Name	Fuel composition (% by Volume)			Fuel exit velocity (m/s)	Reynolds number $Re_{jet}$	Momentum flux ratio	Power (KW)
	NH3	H2	N2				
FNH3_0	0	75	25	92.6	9000	2.5	13.5
FNH3_25	25	56.25	18.75	63.2	9000	2.5	11.0
FNH3_50	50	37.5	12.5	46.6	9000	2.5	9.5
FNH3_75	75	18.75	6.25	36.2	9000	2.5	8.4
FNH3_100	100	0	0	29.2	9000	2.5	7.6

- Reynold number fixed at 9000
- Momentum flux ratio  $((\rho v^2)_{jet} / (\rho v^2)_{co-flow})$  fixed at 2.5
- Reduced ratio of jet diameter to bluff-body diameter (0.051 vs 0.091)
- **Capable of 100% ammonia combustion**

31

## MILD combustion behavior

- Peak temperature past the visible region, suggesting MILD combustion regime downstream
- NH, NO and OH are localized in the visible flame region
- **OH persists in the non-luminous region, but more uniformly distributed, suggesting a volumetric combustion**
- Axial and Radial distribution of NO, N2O, NH3, H2, and O2 using the GC and FTIR
- Raman/Rayleigh data acquisition planned for Fall 2024/



# 1-D LASER RAMAN SPECTROSCOPY & INJECTOR DEVELOPMENT

A quantitative study of hydrogen-air mixing ratio for a novel fuel injection concept in a non-premixed single nozzle FLOX® combustor with 1-D Laser Raman spectroscopy

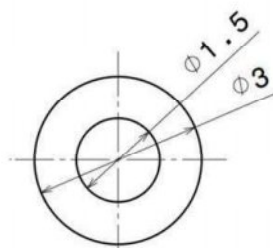


## Fuel injector geometry FuelTube & BMV006



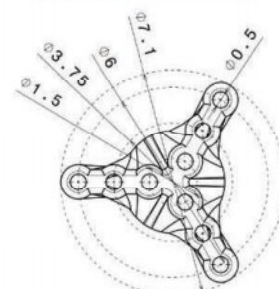
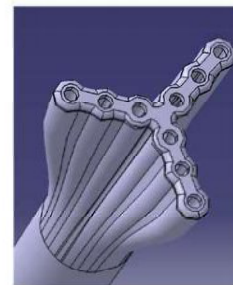
### FuelTube:

○  $A_{\text{eff}} = 1.76 \text{ mm}^2$



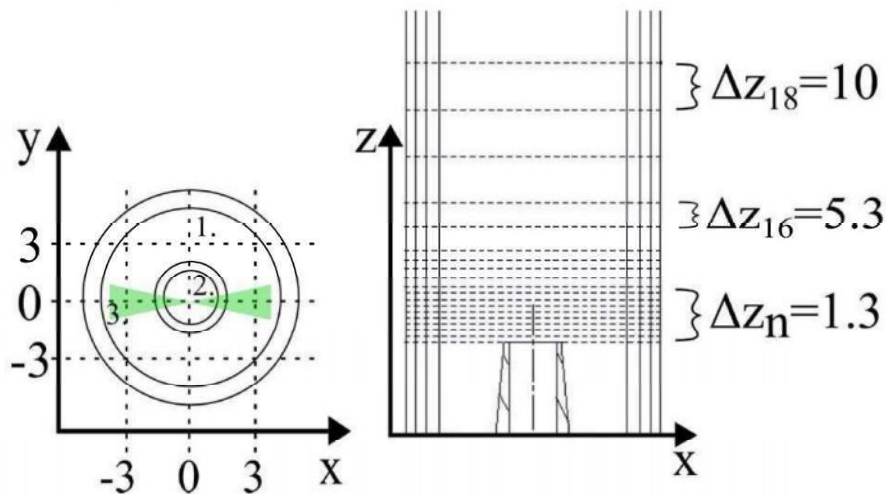
### BMV006:

○  $A_{\text{eff}} = 1.76 \text{ mm}^2$





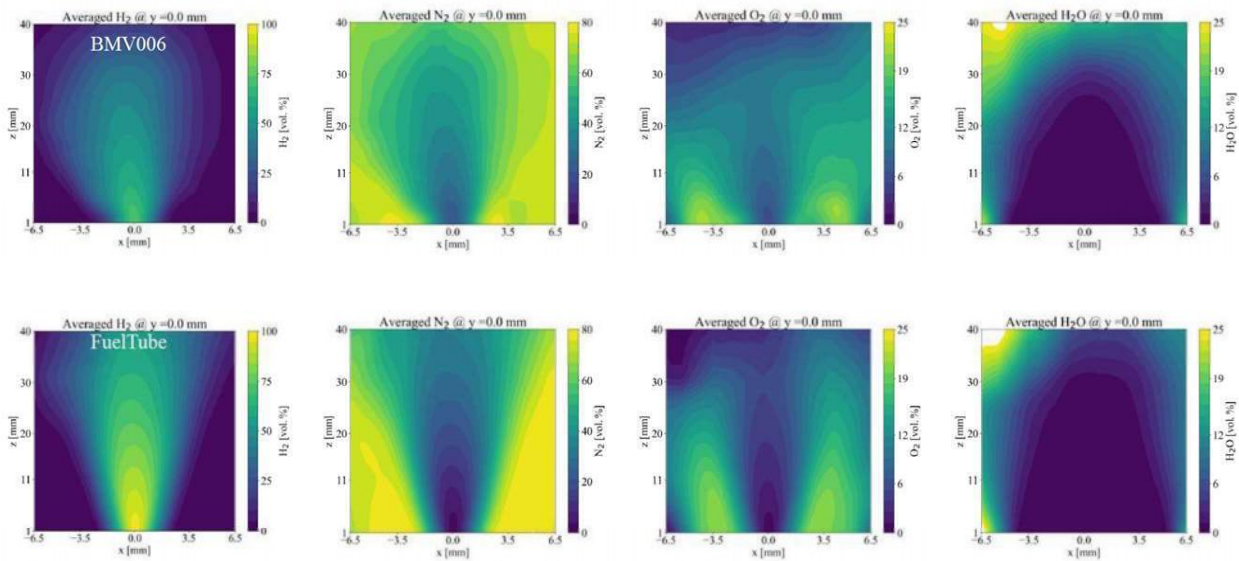
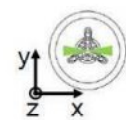
# Measurement positions 1-D Laser Raman Spectroscopy



1. Co-flow Air 2. Fuel H<sub>2</sub> 3. Laser beam ( $\lambda = 532$  nm)

6

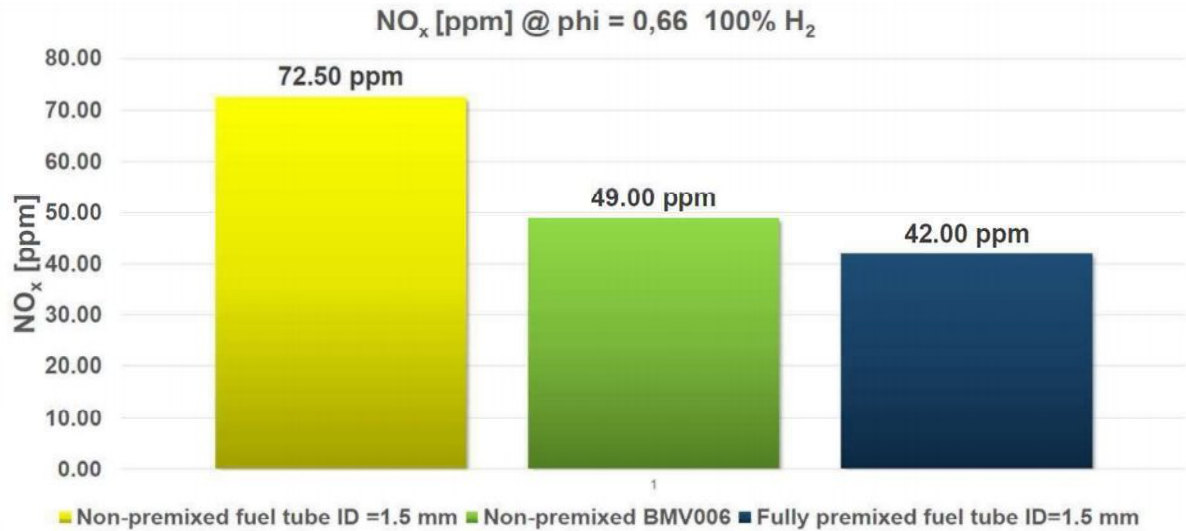
# Results Averaged major species concentration @ $y = 0.0$ mm



8



## Exhaust gas measurements NO<sub>x</sub> values (uncorrected)



16

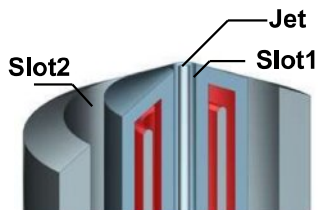
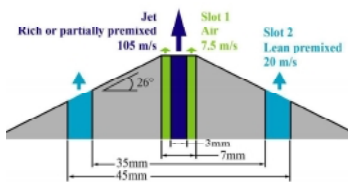
DARMSTADT HYDROGEN FLAMES



## MULTI-REGIME BURNER (MRB)

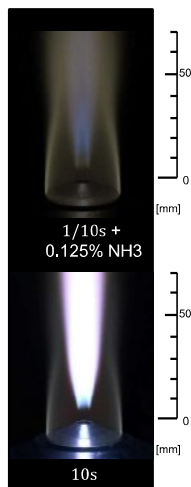
1D06

### Geometry



T. Li et al. *Combustion and Flame* 257, 113036

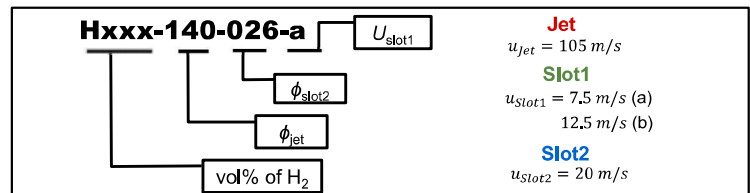
### H<sub>2</sub> Flames



### Operating Conditions

Case	Fuel	$\phi_{jet}$	$\phi_{slot1}$	$\phi_{slot2}$	OH-LIF	PIV	Raman
H000-140-080-a	CH <sub>4</sub>	1.4	0	0.8	✓	✓	
H000-220-080-a	CH <sub>4</sub>	2.2	0	0.8	✓	✓	✓
H000-350-080-a	CH <sub>4</sub>	3.5	0	0.8	✓	✓	
H100-140-026-a	H <sub>2</sub>	1.4	0	0.26	✓	✓	✓
H100-220-026-a	H <sub>2</sub>	2.2	0	0.26	✓	✓	✓
H100-350-026-a	H <sub>2</sub>	3.5	0	0.26	✓	✓	✓

### Hxxx-140-026-a



**Jet**  
 $u_{jet} = 105 \text{ m/s}$   
**Slot1**  
 $u_{slot1} = 7.5 \text{ m/s (a)}$   
 $12.5 \text{ m/s (b)}$   
**Slot2**  
 $u_{slot2} = 20 \text{ m/s}$



Mechanical Engineering | Reactive Flows and Diagnostics | Andreas Dreizler

8

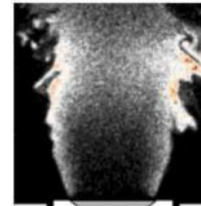
## Candidates: Premixed H<sub>2</sub>



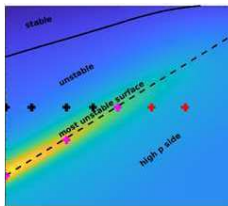
TUD lean H<sub>2</sub>/air  
jet in hot coflow



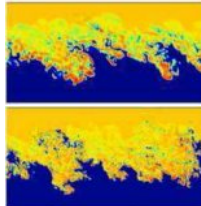
Sydney lean H<sub>2</sub>/air  
jet in hot coflow



NTNU lean H<sub>2</sub>/air  
bluff-body flames



Aspden et al. DNS  
H<sub>2</sub>-air in a box

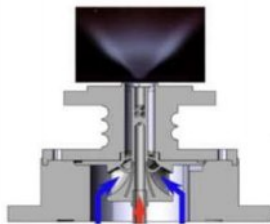


Sandia/SINTEF DNS  
H<sub>2</sub>-air, vary Re, P



Aachen DNS  
H<sub>2</sub>-air slot jet

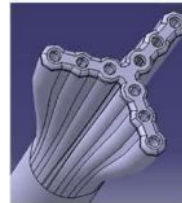
## Candidates: Multi-Mode H<sub>2</sub>



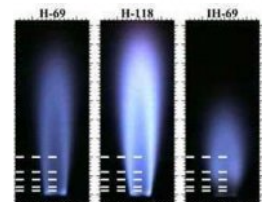
HYLON2



TUD MRB H<sub>2</sub>



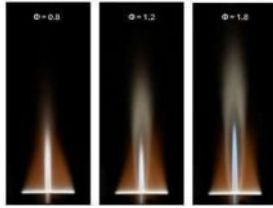
DLR H<sub>2</sub>  
injector



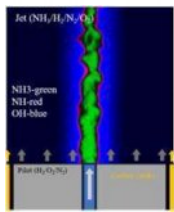
Sydney piloted  
inhomogeneous  
H<sub>2</sub>/N<sub>2</sub>

# Candidates: Ammonia

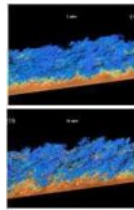
## Premixed



TUD NH<sub>3</sub>/H<sub>2</sub>/N<sub>2</sub>-air  
jet in hot coflow

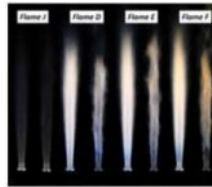


TUD/SUSTECH  
NH<sub>3</sub>/H<sub>2</sub>-air



Sandia/SINTEF DNS  
NH<sub>3</sub>/H<sub>2</sub>/N<sub>2</sub>-air  
1, 10 atm

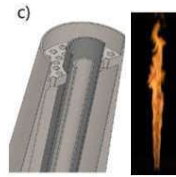
## Multi-Mode



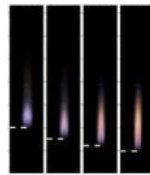
KAUST piloted  
NH<sub>3</sub>/H<sub>2</sub>/N<sub>2</sub>



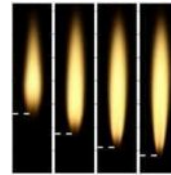
Kyoto  
DNS



Sydney piloted  
inhomogeneous  
NH<sub>3</sub>/H<sub>2</sub>/N<sub>2</sub>

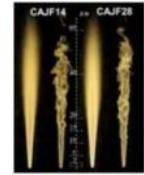


Sydney jet in  
hot coflow  
NH<sub>3</sub>/CH<sub>4</sub>/air

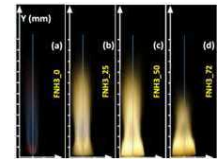


Sydney jet in  
hot coflow  
NH<sub>3</sub>/H<sub>2</sub>/N<sub>2</sub>

## Non-premixed



KAUST 5-atm  
NH<sub>3</sub>/H<sub>2</sub>/N<sub>2</sub>



KAUST NH<sub>3</sub>  
Bluff Body

## Summary and Closing Discussion TNF 16

### *Back to the Future – Towards TNF17*

*Christian Hasse (TU Darmstadt)*

This is a summary for the TNF16 workshop, which was partially held together with the Premixed Turbulent Flames (PTF) workshop at Politecnico di Milano on 20-21 July 2024.

### **TNF Scope and History**

The TNF workshop focuses on fundamental issues of turbulence chemistry interactions in gaseous flames. The objectives are to:

- Establish a library of well-documented flames that advance fundamental scientific understanding of turbulent combustion and are appropriate for testing and extending models for complex combustion systems.
- Provide a framework for collaborative comparisons of reference data from experiments and DNS with modeled results from LES.
- Identify priorities for further experimental and computational research.

One TNF USP/legacy is – among others – the availability of instantaneous and averaged thermochemical states from Raman/Rayleigh that is crucial for turbulent combustion model development and validation. Up to TNF14 in Dublin in 2018, a wide range of flames with different modes (premixed, stratified, partially premixed, non-premixed) and regimes ( $Re$ ,  $Da$ ,  $Ka$  number) were investigated mostly for  $CH_4$ , with only small excursions to DME and very early also to  $H_2$ . TNF sessions evolved around data sets from target flames, and the numerical results from different groups were compared to experimental data. Preliminary and work-in-progress data was submitted. The open discussion atmosphere allowed discussions on the physics of the flames and how the models could be improved. Modeling results usually improved substantially from workshop to workshop, and new experimental configurations were discussed to challenge the models.

At TNF15 in Vancouver in 2022, there was substantially fewer TNF-style discussions on burners and model deficiencies. The interest decreased for pure hydrocarbon target flames, and there was only one session on the Darmstadt Multi Regime Burner. Despite the large interest in  $H_2$ , experimental data were not yet available, only first DNS data had been generated. While this did not allow for a TNF-style comparison, the discussion session on modeling was very intense and engaging. That clearly showed the need for reference data sets.

At TNF15 joint sessions with the PTF workshop were organized for the first time as a practical response to lower overall attendance due to lingering effects of the COVID pandemic. The PTF workshop aims to have presentations on particular topics, not on data sets and comparisons. Joint TNF-PTF sessions were also part of the TNF16 program as a combination of TNF-style topical discussions and PTF-style talks on premixed  $H_2$  flames, chemical kinetics, AI/ML.

### **Topics at TNF16**

The TNF16 topics can be categorized into four groups. More details can be found in the attached slides.

1. Target flames – Experiments and/or DNS
2. Turbulent combustion models
3. Kinetic mechanisms including diagnostics
4. ML, community tools and data sharing

## 1. Target flames – Experiments and/or DNS

The availability of reference data has substantially improved over the last two years. Data were presented for the Hylon and Hylon2 (incl. KAUST measurements) burner, the KAUST Piloted NH<sub>3</sub>/H<sub>2</sub> Jet Flames, the Darmstadt McKenna and MRB (H<sub>2</sub>, NH<sub>3</sub>/H<sub>2</sub> flames), and the NTNU lean H<sub>2</sub>/air burner. Several additional potential target flames were presented on the second day. TNF-style comparisons were presented for the Hylon burner and the KAUST Piloted NH<sub>3</sub>/H<sub>2</sub> Jet Flames.

With the availability of different DNS data sets, the TNF community discussed options to use these data for model development and validation. As a result, it was suggested to plan for a sequence of cases with increasing complexity.

Finally, near wall flames continue to be of interest for the TNF community. New aspects such as active walls (effusion cooling, polymers in wall) will be considered in the future. Near-wall H<sub>2</sub>/NH<sub>3</sub> flames under pressure are particularly relevant for safety, in particular flashback is a topic of interest.

## 2. Turbulent combustion models

The review of turbulent H<sub>2</sub> flames and the subsequent discussion were very engaging and identified several open scientific questions especially for lean H<sub>2</sub> flames. These include among others:

- How does the thermo-diffusive instability (TDI) interact with turbulence? Is the interaction synergistic?
- How does the interaction of turbulence and TDI change for high Ka numbers?
- What are the governing parameters?  $Ze$ ,  $Ka$ ,  $Pe$  and/or others?
- How to model flames under high pressure. Do the observed differences between high- and low-pressure laminar flames carry over to turbulent flames?

This non-exhaustive list clearly demonstrates the need for TNF-style target flames from experiments and DNS to systematically address these scientific questions.

## 3. Kinetic mechanisms including diagnostics

The availability of reliable kinetic mechanisms for NH<sub>3</sub> was already addressed at TNF15. Peter Lindstedt gave a comprehensive review on NH<sub>3</sub> kinetics. There are current uncertainties for some key fundamental reaction sequences and these need to be addressed by the kinetics community. Thus, chemical mechanisms for DNS and LES are likely to evolve over the next years. This needs to be considered in the planning of the numerical work.

It is crucial for the TNF community to agree on a small number of mechanisms to allow for consistent comparisons. This will be addressed between TNF16 and TNF17, see below.

Another topic of relevance is the near-wall chemistry of rich H<sub>2</sub> flames. This was discussed in the FWI session. This topic will also be addressed before TNF17, and suggestions are expected to be released.

## 4. ML, community tools and data sharing

The field has advanced significantly, evidenced by the first coupled *a posteriori* applications as compared to the previous *a priori* analyses. The next key challenges are:

- Data, benchmarks, and metrics
- Common models, methods, and approaches
- Best practice

It was suggested to identify benchmark problems for ML-applications following the TNF approach. This will allow to evaluate ML-based approaches, e.g., for manifold parameterization or combustion



modeling in general. There is interest in sharing ML-models through TNF/PTF infrastructure and by this establish best practice guidelines for ML-model selection, ML-training, and ML-evaluation.

## Final discussion and decisions

Turbulent H<sub>2</sub> and NH<sub>3</sub> flames at atmospheric and pressurized conditions are still poorly understood, and turbulence chemistry interaction models are still in the early stages. The dynamics of hydrogen flames change substantially under pressure, so the extrapolation of atmospheric results to technically relevant conditions is more challenging than previously for hydrocarbon flames. Experiments and DNS for pressurized flames remain a formidable challenge that needs to be coordinated between TNF16 and TNF17. The increasing availability of high-quality experimental and numerical data for target flames will allow for TNF-style comparisons at TNF17 aiming to *first break and then advance the model*.

Flashback and Flame-Wall Interaction continue to be relevant topics in the TNF scope. Effusion cooling and active walls are to be considered in the future.

The availability of reliable NH<sub>3</sub> kinetics and H<sub>2</sub> near-wall chemistry remains an open issue. The use of chemical mechanisms for TNF target flames should be coordinated to ensure a consistent comparison at TNF17.

**The TNF community expressed its strong commitment to return to the more original TNF format (back to the future) with discussion evolving around target flame data sets.** In contrast to previous workshops, this will feature not only experimental but also numerical DNS data sets. It is expected that more target flame sessions are required for TNF17 compared to TNF15 and TNF16. Consequently, the number of PTF-style mini-symposia organized as shared TNF-PTF sessions might decrease due to time restrictions.

The following four next steps were agreed upon to prepare for TNF17.

## Next Steps for TNF17

### 1. Provide an overview of experimental target flames and data sets

TU Darmstadt will prepare brief description (one-pager) for their experimental configurations. That includes a short description of the setup, the employed diagnostics and the data. This can include both available data and future data with an approximate date when it can be shared with the TNF community. Data can also include supporting numerical data, e.g., detailed flow conditions from an inflow-LES.

This description will be used as template for all other groups to describe their target flames. These descriptions will be shared among the TNF participants and eventually be published via the TNF website.

Research Data Management has become an important aspect for most funding schemes and recommended data repositories may vary within the TNF community. It was decided that data will be made available by the individual groups using their preferred platform. The data will be assigned a DOI as a unique identifier. New DOIs will be continuously added to the experimental one-pager and published on the TNF website.

Coordinators: Dreizler, Hasse (TU Darmstadt)

## 2. Provide an overview of DNS target flames and data sets

Similarly to the experimental data, University of Edinburgh will prepare a one-pager for the DNS configurations. Following this template, TNF participants working on DNS are invited to provide the description of their configuration. The aim is to identify a sequences of DNS configurations with increasing complexity, e.g., flame in a box → flame in a temporally evolving shear layer → shear flame.

Sharing the descriptions and the data will follow the approach outlined above for the experimental data.

Coordinator: Attili (University of Edinburgh)

## 3. Aligning experimental/DNS work with modeling/LES between TNF16 and TNF17

The one-pagers for experiments and DNS will be shared with the TNF community interested in model turbulent combustion model development and LES. These groups will indicate which flames they will be working on for TNF17. This information will be helpful for both the experimental and DNS groups to better plan their next steps.

The planning should be available spring 2025 and should be updated towards the end of 2025 around the submission deadline for the 41<sup>st</sup> Symposium.

Coordinators: Dreizler, Hasse (TU Darmstadt)

## 4. Chemical kinetics for TNF target flames

The current uncertainty in  $\text{NH}_3$  kinetics and near-wall  $\text{H}_2$  kinetics is a challenge for a consistent comparison of experiments/DNS and LES. It is expected that mechanisms will improve in the near future and new versions will be released.

**$\text{NH}_3$ :** When comparing to DNS data, the same mechanism should be used in LES. When comparing to experimental TNF data, a few suitable TNF mechanisms will be identified and suggested for LES use. The suggestions will be shared with the TNF community and be published on the TNF website. The TNF community can also support the mechanism development with thermochemical states from Raman/Rayleigh/LIF in laminar counterflow flames. This can also include data at higher pressures of up to 5 bars at KAUST.

**$\text{H}_2$  near-wall:** Several TNF participants indicated their interest to discuss the issue with colleagues, e.g. from Material Sciences.

Feedback concerning  $\text{NH}_3$  and  $\text{H}_2$  near-wall should be given to A. Stagni, who will summarize potential next steps.

Coordinators: Stagni (Politecnico di Milano), Magnotti (KAUST)



**TNF16 2024, MILAN, ITALY**

# **SUMMARY AND CLOSING DISCUSSION**

**CHRISTIAN HASSE**

11.09.2024

Mechanical Engineering | Simulation of reactive Thermo-Fluid Systems | Christian Hasse

1



**TNF16 2024, MILAN, ITALY**

# **SUMMARY AND CLOSING DISCUSSION**

**CHRISTIAN HASSE**

11.09.2024

Mechanical Engineering | Simulation of reactive Thermo-Fluid Systems | Christian Hasse

2

# TNF SCOPE

The emphasis is on fundamental issues of turbulence-chemistry interactions in gaseous flames. The objectives are to:

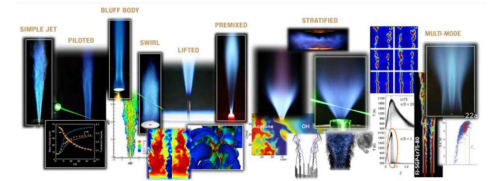
- Establish a library of well-documented flames\* that advance fundamental scientific understanding of turbulent combustion and are appropriate for testing and extending models for complex combustion systems.
- Provide a framework for collaborative comparisons of measured and modeled results.
- Identify priorities for further experimental and computational research.

\* Experiments: One TNF USP/legacy is – among others – the availability of instantaneous and averaged thermochemical state from Raman/Rayleigh

## TNF Workshop

International Workshop on Measurement and Comparison of Turbulent Flames

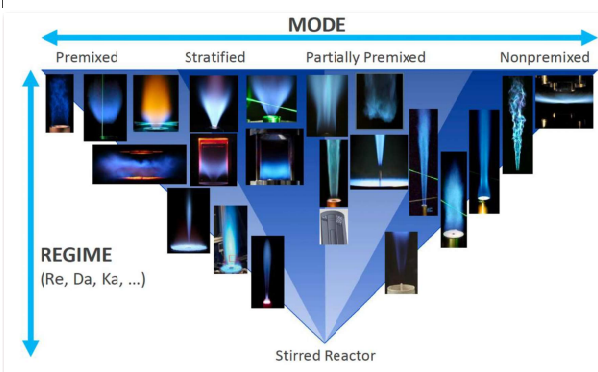
HOME TNF16 - MILAN 2024 DATA ARCHIVE WORKSHOP PROCEEDINGS CONTACT



The TNF Workshop is an open and ongoing international collaboration among experimental and computational researchers in turbulent combustion. The emphasis is on fundamental issues of turbulence-chemistry interactions in gaseous flames. The objectives are to:



# UP TO TNF14 (DUBLIN 2018)



A wide range of different flames

- Sydney/Sandia piloted jet flame series
- bluff body stabilized
- swirled flames
- stratified flames
- opposed jet
- inhomogeneous inlets/multi regime burner
- Sessions for different flames: introduction to the burner, comparison of numerical results from different groups
- Discussion on how to “break the model”, progress in modeling from meeting to meeting
- New burners to challenge models
- CH<sub>4</sub> as fuel with small excursions to DME

Barlow et al., TNF Workshop  
Barlow, 11th Mediterranean Combustion Symposium, 2019



# TNF15 IN VANCOUVER



## HOW I REMEMBER IT

- Substantially less TNF-style discussion on particular burners and model deficiencies (“break the model”).

### Possible reasons

- Interest decreased for pure hydrocarbon target flames. One session on Multi Regime Burner
- Large interest in  $H_2$ , but experimental data not available. First DNS data appearing
- $NH_3$  discussion, outlook on technology. Planning for experiments, first DNS datasets
- Further discussion on compressible and multi-phase combustion
- **In short: The largest interest for the future was in  $H_2$  and also  $NH_3$ . But the experimental target flame data was not yet available and only a few DNS data sets appeared. The discussion on modeling was very intense and engaging.**



# FROM TNF15 TO TNF 16



## IMPORTANT TOPICS IDENTIFIED AT TNF15

1. Transport processes/differential diffusion in turbulent flames (esp. new fuels)
2. Experimental and DNS configurations that build on TNF heritage
3. Consolidated chemistry for  $NH_3$  – use in DNS and LES

ad 1+2

- identification of target datasets - HIT and shear driven turbulent cases.
- TD instability: “do we worry from an application points of view?”  
→ the understanding clearly evolved over the last two years.
- DNS for data validation → now clearly established
- Modeling of subfilter behavior of instabilities ==> first papers at the symposium
- In addition to pure  $H_2/NH_3$  fuel mixtures  $CH_4/H_2$  and  $NH_3/H_2$  are clearly relevant; many studies investigate variable mixing ratios

ad 3:

- to be discussed further – see the next slides





# TNF16



## TNF AND PTF – JOINT SESSIONS IN 2022 AND 2024

- TNF aim: discussion evolve around datasets
- PTF aim: more presentations on particular topics

## WHAT IS THE SITUATION IN 2024?

- Joint sessions as a combination of TNF-style topical discussions and PTF-style talks on premixed  $H_2$  flames, chemical kinetics, AI/ML
- Joint discussion on  $H_2$  target flames
- Joint session on FWI
- TNF discussion KAUST Piloted  $NH_3/H_2$  Jet Flames
- TNF discussion on future target flames



# FUTURE OF TNF



- **TNF15:** Severe lack of  $H_2$  and  $NH_3$  target flames and data
  - **TNF16:** Hylon Burner, Kaust Piloted  $NH_3/H_2$  Jet Flame + many more data sets (Darmstadt, NTNU, ..) are becoming available
  - **TNF16:** More DNS data sets are available ... and more to come
  - Target flame discussion for **TNF17** (and who can deal with high pressures)
- Opportunity to have a more original TNF-style workshop in 2026 – if we want that..
- I personally would like to re-introduce more TNF-style discussions
    - Turbulent combustion models for  $H_2$ ,  $NH_3$  and fuel blends will rely on high-quality target flame data either from experiments or DNS
    - Open TNF discussion was key to advance understanding and models – there are a lot of open questions for  $H_2$  and  $NH_3$

→ discussion at the end



# TNF16

## FOUR TOPICS

1. Target flames – Experiments and/or DNS
2. Turbulent combustion models
3. Kinetic mechanisms including diagnostics
4. ML, community tools and data sharing

# TARGET FLAMES – EXP

## Situation has improved significantly in the last two years

- Hylon and Hylon2 (incl. KAUST measurements)
- KAUST Piloted  $\text{NH}_3/\text{H}_2$  Jet Flames
- Darmstadt McKenna/MRB ( $\text{H}_2$ ,  $\text{NH}_3/\text{H}_2$ )
- NTNU lean  $\text{H}_2/\text{air}$

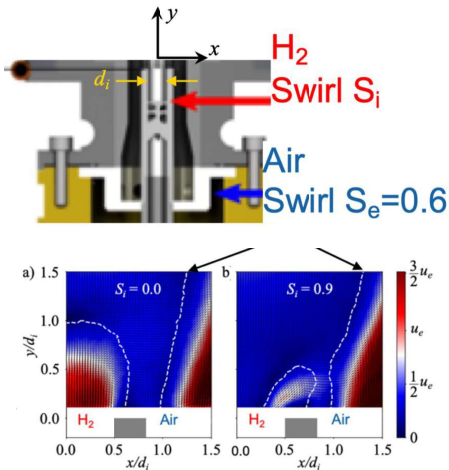
## Flames discussed in the previous session (RB, GM, MD, BD)

- Hylon and Hylon2 (incl. KAUST measurements)
- Pressurized  $\text{NH}_3/\text{H}_2$  flame
- Sydney inhomogeneous inlet with  $\text{NH}_3/\text{H}_2$  with recessed inlet
- Bluff-body  $\text{NH}_3$  burner (available and future version)
- Sydney Inhomogeneous inlets  $\text{H}_2/\text{N}_2$
- Sydney hot coflow burner  $\text{NH}_3/\text{H}_2$
- Partially premixed  $\text{CH}_4/\text{NH}_3$  cases
- Lean premixed  $\text{H}_2$  in hot coflow
- more candidates by Rob (DLR FLOX)  
→ sorted by Rob: premixed ⇔ multi-mode ⇔ non-premixed

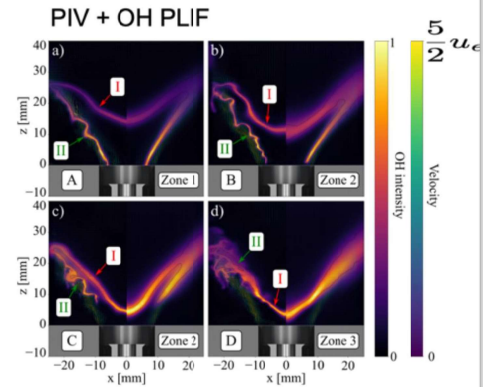
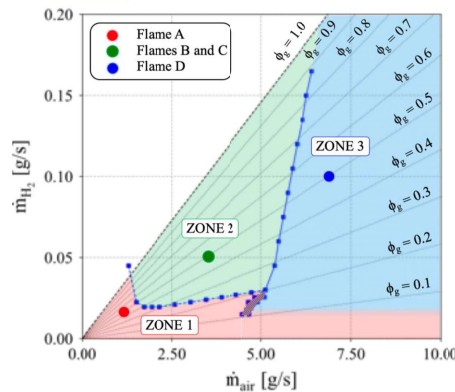
# HYLON

## TNF-style discussion of the main characteristics

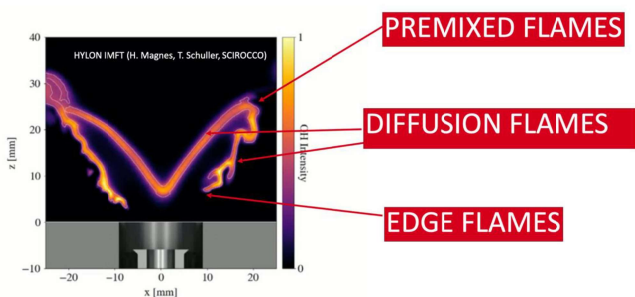
- attached and detached flames: flames A-D
- selection target flame named A and L
- premixed, non-premixed and edge flames



## Stabilization chart @ p=1 bar, T=300 K



# HYLON

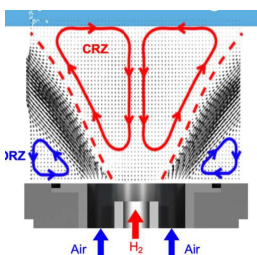


## TNF-style comparison of experimental and numerical data

- Sequence from cold flow field → cold mixing → hot conditions
- TP: “more complex than TNF style flames”.... I disagree
- 26 groups have begun working on the case

## Outlook for Hylon2:

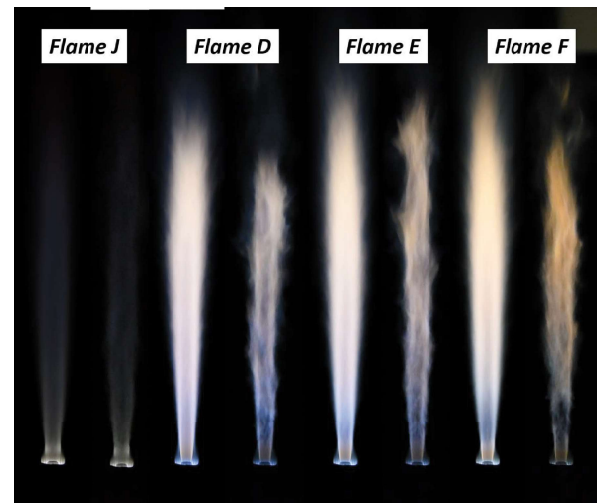
- Higher pressure
- New geometry



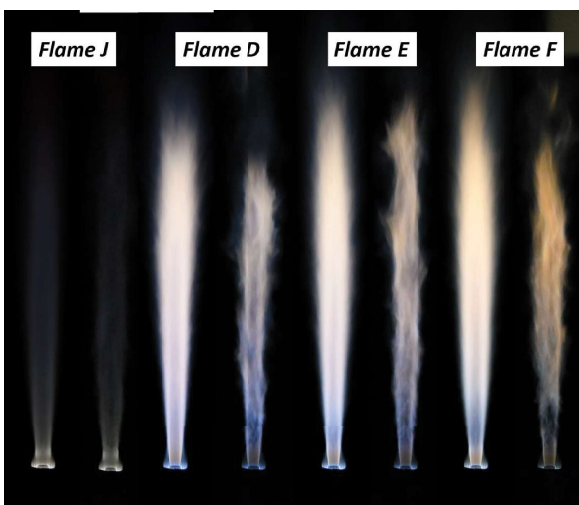
Turbulent combustion model will become even more important at high pressure, cannot resolve the 30µm flame thickness

# KAUST NH3/H2 JET FLAME

- **Four partially premixed piloted jet flames**
- Modified Sandia piloted burner
- Raman/Rayleigh+OH/NH<sub>2</sub> LIF
- Fuel: Simulated partially cracked ammonia (43%), and air with  $\Phi=3$ , Flame J with 100% cracking
- Pilot jet: Simulated partially cracked ammonia (43%), and air with  $\Phi=0.9$  520W
- **Turbulence-chemistry interaction/localized extinction/re-ignition**
- **Differential diffusion**
- Three Reynolds numbers
  - Flame D Re=24000 (59% Reextinction)
  - Flame E Re=32000 (79% Reextinction)
  - Flame F Re=36000 (89% Reextinction)
  - Flame J Re=36000 (N<sub>2</sub>:H<sub>2</sub>=1:3)



# KAUST NH3/H2 JET FLAME



## TNF-style comparison of experimental and numerical data

- First discussion on the main physics based on experiments, e.g. extinction.
- 10 numerical contributions.
- Discussion of experiments vs. numerical (D and F) identifies deficiencies in modeling but also issues in the experiment → asymmetry, velocity measurement needed.
- DD important for Flame D, local extinction in Flame F not predicted well

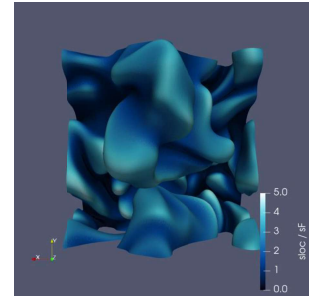
## Outlook for TNF17:

- Advances in modeling – more insights into physics
- Experimental data, PIV +... NO<sub>x</sub> (?)

# TARGET FLAMES – DNS

Different DNS configurations have been shown

- Flame-in-a-box
  - Temporally evolving shear layer
  - Shear flame
- Suggestion: Modelers should look at a succession of cases



## Things to discuss

1. Do we have DNS for DNS configurations or is it becoming realistic to perform DNS of "close-to-the-target flame" conditions ( $Z_e, K_a, Pe$  geometry)?
2. If we want to use succession of DNS data – do we need to align them (transport, chemistry etc.)?
3. Can we define a TNF-DNS set – similar to a target flame?
4. Who could lead/organize this? Do we need a small working group?



# TARGET FLAMES – EXTENSIONS



Other topics of interest – an updated view on flame wall interaction

1. Flame wall interaction for  $H_2$  and  $NH_3$  – pressure?
2. Flashback for  $H_2$  and  $NH_3$  – pressure?
3. Effusion cooled walls
4. Polymers in walls

## Things to discuss

1. What is the interest to look at these topics 1-4?
2. Can we agree on a target flame?





# TNF16

## FOUR TOPICS

1. Target flames – Experiments and/or DNS
2. **Turbulent combustion models**
3. Kinetic mechanisms including diagnostics
4. ML, community tools and data sharing

# TURBULENT H<sub>2</sub> COMBUSTION MODELS

## A NON-EXCLUSIVE LIST OF IMPRESSIONS/QUESTIONS

- Topic has advanced substantially over the last two years
- Predicting the laminar flame speed enhancement is the tricky part (TDI).
- Synergistic (is it synergistic?) effect of turbulence and TDI not fully understood. How can it be modelled ... simple multiplication?
- The combustion model becomes very important at higher pressures.
- High-pressure is very challenging – both in experiment and simulation. But it is also extremely important.
- What is high pressure?
- Already laminar flames significantly differ between low and high p.
- Higher reactant temperatures must be considered.

# TURBULENT H<sub>2</sub> COMBUSTION MODELS

## A NON-EXCLUSIVE LIST OF IMPRESSIONS/QUESTIONS

- Interaction of turbulence and TDI at high turbulence levels not entirely clear, influence of especially high pressure, high Ka number.
- It is not clear what the impact of chemistry/uncertain reactions for very lean conditions can be on TDI.
- Flashback driven by fine scale effects, hot walls, Soret effect.
- DNS: Do we need detailed transport models or are constant non-unity Le-numbers sufficient. Does it matter for model development
- What are the governing parameters?  $Ze$ ,  $Ka$ ,  $Pe$  and/or others?

**My summary:** We need TNF-style target flames from experiments and DNS to systematically address these

**Discussion:** Things to add?

# TNF16

## FOUR TOPICS

1. Target flames – Experiments and/or DNS
2. Turbulent combustion models
3. **Kinetic mechanisms including diagnostics**
4. ML, community tools and data sharing

# NH3 KINETICS

- The need for NH3 kinetics was already discussed at TNF15
- Review of NH3 kinetics by Peter Lindstedt
- Chemical kinetic mechanisms for ammonia are advancing rapidly.
- An exceptionally wide range of chemical mechanisms have been produced.

Kinetic model	Species concentration							Ignition delay time	Laminar burning velocity	Overall mean
	Pyrolysis	Oxidation			Thermal DeNO <sub>x</sub>	Mean				
		High T	Intermediate T	Low T						
NUIG_2023	0.741	0.778	0.841	0.894	0.909	0.833	0.842	0.888	0.854	
KAUST_2023	0.734	0.763	0.903	0.890	0.910	0.840	0.820	0.897	0.852	
KAUST_2021	0.734	0.759	0.887	0.890	0.901	0.834	0.823	0.894	0.851	
Polimi_2023	0.687	0.769	0.850	0.883	0.908	0.819	0.822	0.888	0.843	
Polimi_2020	0.715	0.737	0.848	0.885	0.906	0.818	0.817	0.892	0.842	
Mei_2021	0.673	0.759	0.848	0.850	0.921	0.810	0.818	0.882	0.837	
Polimi_2022	0.715	0.736	0.848	0.869	0.906	0.815	0.801	0.892	0.836	
Thomas_2022	0.636	0.769	0.848	0.834	0.898	0.797	0.814	0.889	0.833	
Mei_2020	0.633	0.736	0.851	0.811	0.917	0.790	0.819	0.891	0.833	
Manna_2022	0.708	0.720	0.887	0.848	0.910	0.814	0.823	0.833	0.823	
Lindstedt_2023	0.707	0.689	0.832	0.865	0.898	0.798	0.821	0.841	0.820	
Shrestha_2021	0.678	0.685	0.815	0.797	0.712	0.737	0.818	0.890	0.815	
Gotama_2022	0.589	0.748	0.825	0.845	0.731	0.748	0.804	0.880	0.810	
Marshall_2023	0.718	0.712	0.829	0.840	0.892	0.798	0.793	0.831	0.807	
Glarborg_2018	0.624	0.699	0.809	0.816	0.892	0.768	0.823	0.810	0.801	
Han_2020	0.095	0.752	0.843	0.831	0.859	0.676	0.810	0.899	0.795	
Otomo_2018	0.652	0.591	0.808	0.858	0.819	0.746	0.805	0.818	0.790	

Girhe et al. 2024

# NH3 KINETICS

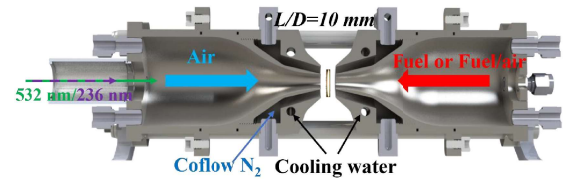
Summary (for a more complete version see slides by P. Lindstedt)

- There are current uncertainties for some key fundamental reaction sequences and these need to be addressed
- Inaccurate validation data poses a problem when assessing model performance.
- **Accurate speciation data is king** and the prospects for fundamental “chemistry experiments” featuring time resolved shock tube data are gradually improving
- Flames are not suitable for determining chemical kinetic data. There is, however, a major role for accurate flame data use in the context of validation.

# DIAGNOSTICS FOR NH<sub>3</sub> KINETICS

## Suggestion by Gaetano Magnotti:

- Detailed temperature and species measurements in flames can complement 0D and 1D reactors
- Counterflow flames well suited for this task
- Raman/Rayleigh/LIF for minor species profiles in temperature and mixture fraction space
- Optically accessible counterflow flames already extensively tested at elevated pressures (5 bar)
- No intrinsic challenge in varying the inlet temperature and O<sub>2</sub> content, and bath gas (water vapor addition?)
- Flexible platform to develop LIF of additional species (NH, N<sub>2</sub>O, NO<sub>2</sub>)



# OUTLOOK KINETICS FOR TNF

## Discussion NH<sub>3</sub>

- How do we deal with the current varieties in NH<sub>3</sub> mechanisms in DNS and also in LES?
- Should we define one/a few TNF mechanisms?
- Can we connect to the kinetic groups? Does it make sense to have them provide updates/stable releases every 6-12 months?

## Discussion H<sub>2</sub>

- How do we deal with the current varieties in NH<sub>3</sub> mechanisms in DNS and also in LES?
- Who can help us with (close to) surface chemistry of H<sub>2</sub>? Homogeneous or heterogeneous chemistry?

# TNF16

## FOUR TOPICS

1. Target flames – Experiments and/or DNS
2. Turbulent combustion models
3. Kinetic mechanisms including diagnostics
4. **ML, community tools and data sharing**

# REVIEW OF ML FOR COMBUSTION

## ML for combustion modeling and experimental analysis

- Review of contributions from 10 groups -- similar challenge as in FWI due to very different objectives
- In summary, the field has advanced significantly. M. Ihme: “Over the last two years - from a priori to a posteriori”

## Key challenges

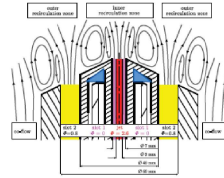
- Data, benchmarks, and metrics
- Common models, methods, and approaches
- Best practice



# REVIEW OF ML FOR COMBUSTION

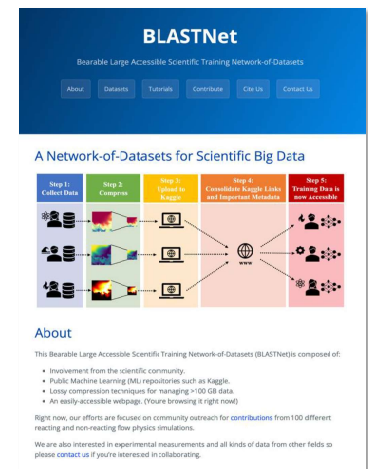
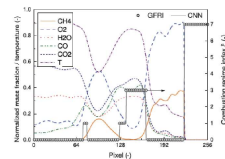
## Benchmark problems for ML-applications

- Combustion-regime identification
- Manifold parameterization
- Combustion modeling



## TN/PF participation

- ML-model benchmark
- Share ML-models through TN/PF infrastructure
- Establish best practice



<https://blastnet.github.io>

# FUTURE OF TNF... REVISITED

- **TNF15:** Severe lack of H2 and NH3 target flames
- **TNF16:** Hylon Burner, Kaust Piloted NH3/H2 Jet Flame + many more data sets (Darmstadt, NTNU, ..) become available
- **TNF16:** More DNS data set are available
- Target flame discussion for **TNF17** (and who can deal with high pressures)
- Opportunity to have a more original TNF-style workshop in 2026 – if we want that.. do we want that?
- I personally would like to re-introduce more TNF-style discussions
  - Turbulent combustion models for H2, NH3 and fuel blends will rely on high-quality target flame data either from experiments or DNS
  - Open TNF discussion was key to advance understanding and models – there are a lot of open questions for H2 and NH3

## Opinions?

TNF/PTF Workshops

Blank Page

## TNF Poster Authors and Titles

First Author	Affiliation	Poster Title
Al-Kassar, Sofiane	Uni. Edinburgh	Turbulent lean premixed hydrogen flames at high pressure and high temperature
Berger, Lukas	Uni. Edinburgh	A priori and a posteriori analysis of an LES combustion model for turbulent hydrogen flames with thermodiffusive instabilities
Brouzet, Davy	Stanford	Effect of sustainable aviation fuel on the direct and indirect noise of a next-generation aviation gas turbine
Cassese, Biagio	IST Napoli	Preferential diffusion effects on tabulated chemistry methods for hydrogen/methane and hydrogen/ammonia blends
Chi, Cheng	Uni. Magdeburg	Flame thickening during turbulent flame-wall interactions
Chu, Hongchao	RWTH Aachen	Interactions of differential diffusion and mixture inhomogeneities in hydrogen and iso-octane flame kernels under engine conditions
Cohen, Samuel	Uni. Southern California	Calculating Temperature and Species Concentration from Quasi-2D Combustion Video Data using Physics-Informed Neural Networks
Dillon, Samuel	Uni. Paris-Saclay	Filtered tabulated chemistry for multi-regime combustion with application to dual-swirl HYLON injector
Jose, Basil	Uni. Stuttgart	ML-augmented diagnostics for feature extraction incorporating deep learning and GPU acceleration methods
Kaddar, Driss	TU Darmstadt	Ammonia-hydrogen combustion modelling enabled by high-performance GPU computing
Kang, Yeonse	Uni. Stuttgart	Effect of swirl-afflicted turbulence on pressure swirl spray in high-momentum jet-stabilised burners
Mao, Runze	Peking Uni.	An open-source community platform for multi-fidelity reacting flow simulation
Niemietz, Kai	RWTH Aachen	CO emissions in turbulent premixed methane/hydrogen jet flames interacting with isothermal walls
Palulli, Rahul	KTH	Analysis of NO formation pathways based on extended proper orthogonal decomposition in a swirl-stabilised, hydrogen-fuelled gas turbine combustor
Petry, Niklas	DLR Stuttgart	Investigation of hydrogen-air mixing behavior in an atmospheric jet-stabilized single nozzle combustor using 1-D laser Raman spectroscopy
Richter, Martin	NTNU/TU Da	Measurements of NO in the product gases of laminar premixed NH <sub>3</sub> /H <sub>2</sub> /N <sub>2</sub> -air and NH <sub>3</sub> /CH <sub>4</sub> -air flames using laser induced fluorescence
Schneider, Max	TU Darmstadt	Near-wall H <sub>2</sub> combustion
Schuh, Vinzenz	TU Darmstadt	Model extension for the artificially thickened flame approach for lean hydrogen-ammonia flames
Tang, Xinzhou	Zhejiang Uni.	Large eddy simulation of the KAUST piloted ammonia flame with the flamelet-generated manifold method
Tian, Lu	Loughborough Uni.	The impact of mixing models and molecular transport in turbulent non-premixed NH <sub>3</sub> /H <sub>2</sub> /N <sub>2</sub> / jet flames at elevated pressure
Walia, Gunvir Singh	IIT Kanpur	Direct Numerical Simulation of flames in high-speed flows
Wang, Yicun	Zhejiang Uni.	Large eddy simulation of the KAUST piloted ammonia flame with the direct moment closure model
Xing, Jiangkuan	Zhejiang Uni.	A direct numerical simulation study on the KAUST piloted cracked ammonia flames with detailed chemistry

# Turbulent lean premixed hydrogen flames at high pressure and high temperature

Sofiane Al Kassar, William Lauder, Geveen Arumapperuma, Antonio Attili\*  
Institute for Multiscale Thermofluids, School of Engineering, University of Edinburgh, Edinburgh EH9 3FD,  
United Kingdom

\* Corresponding author: antonio.attili@ed.ac.uk

Premixed hydrogen flames are susceptible to thermo-diffusive instabilities, which manifest themselves with super-adiabatic temperatures and alternating regions of enhanced reactivity and extinction in highly curved regions of the flame surface. They lead to complex patterns and up to a five-fold increase of flame speed in laminar conditions [1–3]. In the turbulent regime, they interact synergistically with the flow field and cause even larger effects [4, 5]. In this work, the effect of elevated pressure and temperature on thermodiffusive instabilities in turbulent hydrogen flames is investigated using large-scale Direct Numerical Simulations (DNS). A 3D DNS of a turbulent lean premixed hydrogen/air jet flame, at a jet Reynolds number of 11000, has been performed using an elevated pressure of 20 atm and a temperature of 700K in the unburned mixture, similar to the typical conditions of gas turbines for electricity production. The results are compared with a low-pressure/low-temperature DNS similar to that presented by Berger et al. [4]. The two flames have the same Reynolds number and a very similar Karlovitz number to isolate the effect of increased temperature and pressure. It is worth noting that the increase of pressure tends to enhance thermodiffusive effects and the instability, while the increase of temperature has the opposite effect [2, 3]; therefore, it is of interest to investigate the simultaneous change of the two parameters to support the extrapolation of data from ambient conditions to gas-turbine settings.

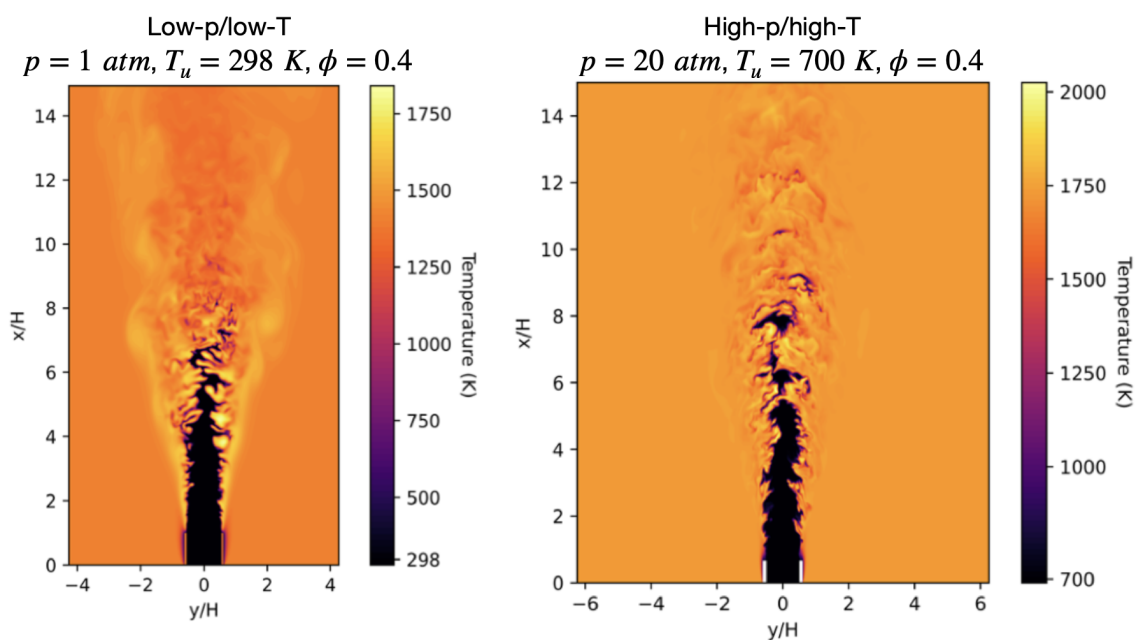


Figure 1: Visualisation of the temperature field in a 2D slice for the DNS of the flames at low and high pressure.

A comparison of the temperature field in the two cases is shown in Fig. 1. The temperature field is similar, with superadiabatic temperatures that exceed the temperature in the coflow, in both cases; however, the low-pressure case shows slightly higher temperature overshoots, in particular in the finger regions typical of thermodiffusively unstable flames. On the other hand, the high-pressure case shows a smaller size for the typical structures related to the thermodiffusive instability, consistently with the analysis in both the linear and non-linear regimes for laminar flames at high pressure [2, 3].

Figure 2 shows the joint probability density function (jPDF) of the progress variable  $C$  with the normalised temperature  $T$  and the mixture fraction  $Z$ , the corresponding conditional means, and the solution in 1D laminar unstretched freely propagating flames at the same conditions. It is observed that the scatter is smaller in the high

pressure conditions, while the deviation of the conditional means from the 1D solution is larger for the high-pressure case. This suggests that the impact of turbulence on the local burning behaviour is weaker in the high-pressure case, probably due to a different impact of curvature on the local burning rate, while the overall mean, which has been shown to be strongly related to the mean turbulent strain by Berger et al. [5], is more affected at high pressure. This last observation is quantified more clearly in Fig 3, which shows the deviation of mixture fraction from the 1D solution. For the high-pressure case, the mean mixture fraction deviates more from the 1D solution compared to the low-pressure flame.

It is concluded that thermodiffusive instabilities are enhanced at elevated pressures and temperature. The relative increase of the average mixture fraction in the turbulent flames compared to the mixture fraction in a laminar 1D flame, which is a reliable measure of thermodiffusive effects, was found to be larger in the high-pressure/high-temperature case in comparison to that at low pressure and low temperature. These observations suggest that the synergistic interactions between thermodiffusive instabilities and turbulence is enhanced at high-pressure conditions.

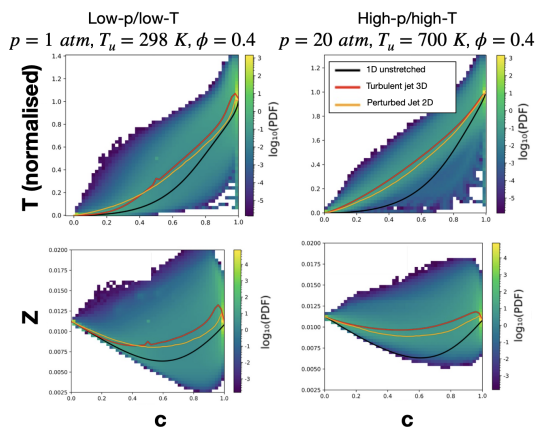


Figure 2: Joint probability density functions of the progress variable  $C$  with the normalised temperature  $T$  and the mixture fraction  $Z$  for the two flames at low and high pressure. The lines are conditional means for the 3D DNS and for 2D laminar unstable flames at the same conditions and are compared with the solution in 1D laminar unstretched freely propagating flames.

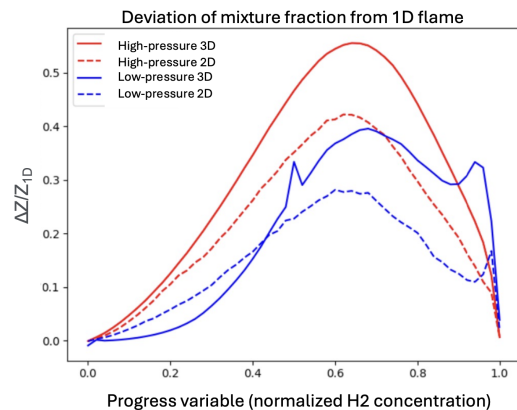


Figure 3: Deviation of the conditional mean of mixture fraction from the solution in 1D laminar unstretched freely propagating flames at the same conditions. The results are shown for the 3D DNS of the flames at low and high pressure and for 2D laminar unstable flames at the same conditions.

## References

- [1] L. Berger, K. Kleinheinz, A. Attili, and H. Pitsch. Characteristic patterns of thermodiffusively unstable premixed lean hydrogen flames. *Proc. Combust. Inst.*, 37(2):1879–1886, 2019.
- [2] L. Berger, A. Attili, and H. Pitsch. Intrinsic instabilities in premixed hydrogen flames: Parametric variation of pressure, equivalence ratio, and temperature. Part 1 - Dispersion relations in the linear regime. *Combust. Flame*, 240:111935, 2022.
- [3] L. Berger, A. Attili, and H. Pitsch. Intrinsic instabilities in premixed hydrogen flames: parametric variation of pressure, equivalence ratio, and temperature. Part 2 - Non-linear regime and flame speed enhancement. *Combust. Flame*, 240:111936, 2022.
- [4] L. Berger, A. Attili, and H. Pitsch. Synergistic interactions of thermodiffusive instabilities and turbulence in lean hydrogen flames. *Combust. Flame*, 244:112254, 2022.
- [5] L. Berger, A. Attili, M. Gauding, and H. Pitsch. Effects of Karlovitz number variations on thermodiffusive instabilities in lean turbulent hydrogen jet flames. *Proc. Combust. Inst.*, 40:105219, 2024.



# A priori and a posteriori analysis of an LES combustion model for turbulent hydrogen flames with thermodiffusive instabilities

Lukas Berger<sup>a</sup>, Antonio Attili<sup>b,\*</sup>, Michael Gauding<sup>a</sup>, Heinz Pitsch<sup>a</sup>

<sup>a</sup> Institute for Combustion Technology, RWTH Aachen University, Aachen 52056, Germany

<sup>b</sup> Institute for Multiscale Thermofluids, School of Engineering, University of Edinburgh, Edinburgh EH9 3FD, United Kingdom

\* Corresponding author: antonio.attili@ed.ac.uk

Hydrogen flames are prone to thermodiffusive instabilities, which are caused by the strong differential diffusion between hydrogen and the other species and the consequent disparity between the diffusion of heat and fuel mass. In laminar flames, thermodiffusive instabilities cause strong flame wrinkling, significant fluctuations of the local burning rate, and an important increase of the overall flame speed [1–3]. In the turbulent regime, thermodiffusive instabilities can interact with turbulence synergistically, showing effects that are even larger than those observed in the laminar regime at the same thermochemical conditions [4, 5]. This results from high curvature and strain rate values in the turbulent environment, which further enhance the effects of differential diffusion.

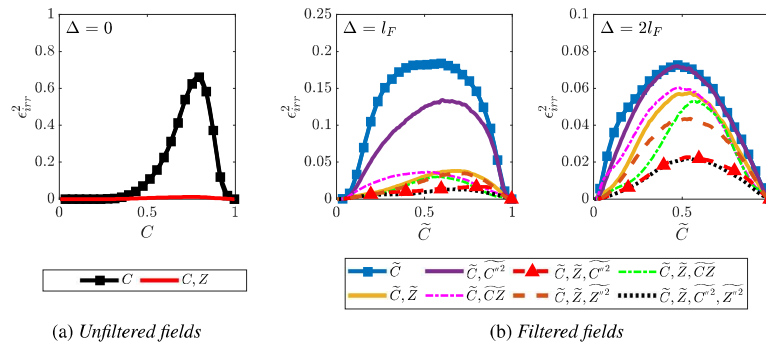


Figure 1: Irreducible errors of progress variable source term using different sets of parameters: Analysis for (a) unfiltered fields and (b) filtered fields with two different filter sizes  $\Delta$ . Note that  $\Delta = l_F$  and  $\Delta = 2l_F$  correspond to filtering of 10 and 20 grid points in the DNS, respectively.

Reproducing these instabilities in Large Eddy Simulation (LES), where their effects are only partially resolved, is challenging. Combustion models that account for differential diffusion effects have been proposed by Bastiaans et al. [6], Böttler et al. [7], Regele et al. [8], Schlup and Blanquart [9], employing a reduced set of transport equations coupled with a flamelet tabulation, which included at least two scalars in order to consider differential diffusion in the LES. While these approaches have been tested in laminar conditions, to utilize them in LES, models for the turbulence/flame subfilter interactions are required. To pursue model development in a systematic way, we followed the approach presented by Trisjono and Pitsch [10]; the DNS data of Berger et al. [4] are employed. From the DNS data, model hypotheses for the subfilter closure in LES are formulated and tested in an a priori analysis. Thereafter, the performance of the proposed models is assessed in an a posteriori analysis by conducting LES of the DNS configuration.

The results of the a priori analysis are summarised in Fig. 1. The irreducible error for the progress variable source term obtained in an optimal estimator analysis [11] is shown conditioned on the progress variable using different sets of candidate parameters to be employed in the LES for the flamelet table parametrization. Progress variable  $\tilde{C}$ , progress variable variance  $\tilde{C}''^2$ , and mixture fraction  $\tilde{Z}$  are identified as suitable model input parameters, while the addition of the mixture fraction variance  $\tilde{Z}''^2$  does not show significant improvements.

Following these observations, an LES combustion model based on pre-tabulated unstretched premixed flamelets with varying equivalence ratio is formulated and tested in a posteriori analysis using a grid that is eight times coarser than

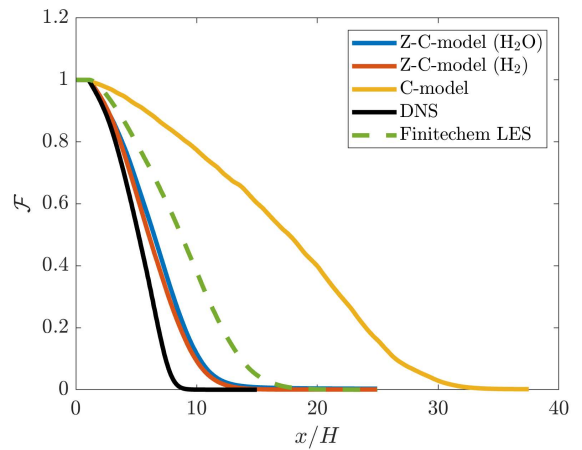


Figure 2: Fuel mass flux along axial direction ( $x$ ) for the DNS and the different LES models.

the DNS grid. Subfilter closure is achieved via a presumed probability density function, using a  $\beta$  – PDF to capture subgrid fluctuations of the progress variable. This combustion model shows significant improvements in predicting the flame length and local phenomena, such as super-adiabatic temperature, compared to combustion models that either neglect differential diffusion effects or consider these effects but neglect the subfilter closure. Two variants of the model formulation with a water- or hydrogen-based progress variable have been tested, yielding overall similar predictions. An LES based on the same models of the DNS (finite-rate detailed chemistry) is considered; this case is performed on the same grid used for all the other LES and does not include any subgrid combustion model. A quantitative assessment of the a posteriori performance is shown in Fig. 2, where the fuel mass flux  $\mathcal{F}$  along the axial direction computed from the different LES results is compared with the DNS. A qualitative overview of the flame shape obtained with the different LES models is shown in Fig. 3, which confirms the observations made above.

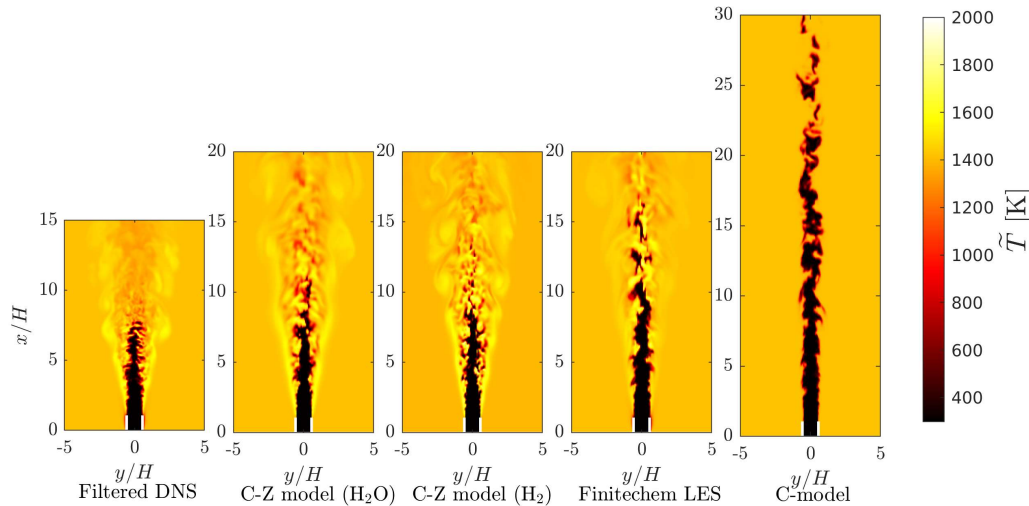


Figure 3: Two-dimensional cuts of the temperature field for the filtered DNS data and those obtained with the different LES models.

## References

- [1] L. Berger, K. Kleinheinz, A. Attili, and H. Pitsch. Characteristic patterns of thermodynamically unstable premixed lean hydrogen flames. *Proc. Combust. Inst.*, 37(2):1879–1886, 2019.
- [2] L. Berger, A. Attili, and H. Pitsch. Intrinsic instabilities in premixed hydrogen flames: Parametric variation of pressure, equivalence ratio, and temperature. part 1 - dispersion relations in the linear regime. *Combust. Flame*, 240:111935, 2022.
- [3] L. Berger, A. Attili, and H. Pitsch. Intrinsic instabilities in premixed hydrogen flames: parametric variation of pressure, equivalence ratio, and temperature. part 2 - non-linear regime and flame speed enhancement. *Combust. Flame*, 240:111936, 2022.
- [4] L. Berger, A. Attili, and H. Pitsch. Synergistic interactions of thermodynamically instabilities and turbulence in lean hydrogen flames. *Combust. Flame*, 244:112254, 2022.
- [5] L. Berger, A. Attili, M. Gauding, and H. Pitsch. Effects of karlovitz number variations on thermodynamically instabilities in lean turbulent hydrogen jet flames. *Proc. Combust. Inst.*, 40, 2024 (Accepted).
- [6] R.J.M. Bastiaans, A.W. Vreman, and H. Pitsch. Dns of lean hydrogen combustion with flamelet-generated manifolds. *CTR Annual Research Briefs*, pages 195–206, 2007.
- [7] Hannes Böttler, Haris Lulic, Matthias Steinhausen, Xu Wen, Christian Hasse, and Arne Scholtissek. Flamelet modeling of thermo-diffusively unstable hydrogen-air flames. *Proceedings of the Combustion Institute*, 2022.
- [8] J. D. Regele, E. Knudsen, H. Pitsch, and H. Blanquart. A two-equation model for non-unity lewis number differential diffusion in lean premixed laminar flames. *Combust. Flame*, 160(2):240–250, 2013.
- [9] J. Schlup and G. Blanquart. A reduced thermal diffusion model for h and h2. *Combust. Flame*, 191:1–8, 2018.
- [10] P. Trisjono and H. Pitsch. Systematic analysis strategies for the development of combustion models from dns: A review. *Flow, Turbulence and Combustion*, 95:231–259, 2015.
- [11] L. Berger, K. Kleinheinz, A. Attili, F. Bisetti, H. Pitsch, and M. E. Mueller. Numerically accurate computational techniques for optimal estimator analyses of multi-parameter models. *Comb Theory and Mod*, 22(3):480–504, 2018.

# Effect of sustainable aviation fuel on the direct and indirect noise of a next-generation aviation gas turbine

Davy Brouzet<sup>a</sup>, Jen Zen Ho<sup>a</sup>, Duane McCormick<sup>b</sup>, C. Aaron Reimann<sup>b</sup>, Jeff Mendoza<sup>b</sup>, Lance Smith<sup>b</sup>, Matthias Ihme<sup>a,c</sup>

<sup>a</sup> Department of Mechanical Engineering, Stanford University, Stanford, 94305, CA, USA

<sup>b</sup> RTX Technology Research Center, East Hartford, 06108, CT, USA

<sup>c</sup> Department of Photon Science, SLAC National Accelerator Laboratory, Menlo Park, 94025, CA, USA

Corresponding author: jzho@stanford.edu

A large eddy simulation of a next-generation aviation gas turbine combustor fueled with a sustainable aviation fuel is performed and the effect of the differences between this fuel and conventional Jet-A fuel on the indirect and direct noise is measured. A Green's function is used to compute the contribution of the unsteady heat release rate to the direct noise while the entropy fluctuations downstream of the combustor are used to estimate the indirect noise. The overall sound spectral level as a function of downstream location are very similar. The direct noise was found to be approximately 1-2 dB lower than conventional jet fuel which was due to the lower root mean square fluctuation of the heat release rate peak. In contrast, the indirect noise was 3-4 dB higher, which was due to a longer temperature inhomogeneity field.

C1 fuel modelled by the HyChem mechanism [1] was simulated and compared against conventional Jet A fuel in a next-generation N+3 aviation combustor. The geometry details can be found in [2], and detailed computational methodology is described in [3]. This simulation was conducted without the VRASC tube.

Figure 1 shows the OverAll Sound Pressure Level (OASPL) from the direct and indirect noise. Direct noise was approximately 1-2 dB lower compared to the Jet-A fuel through the streamwise direction,  $z$ , of the combustor, while the indirect noise was 3-4 dB higher.

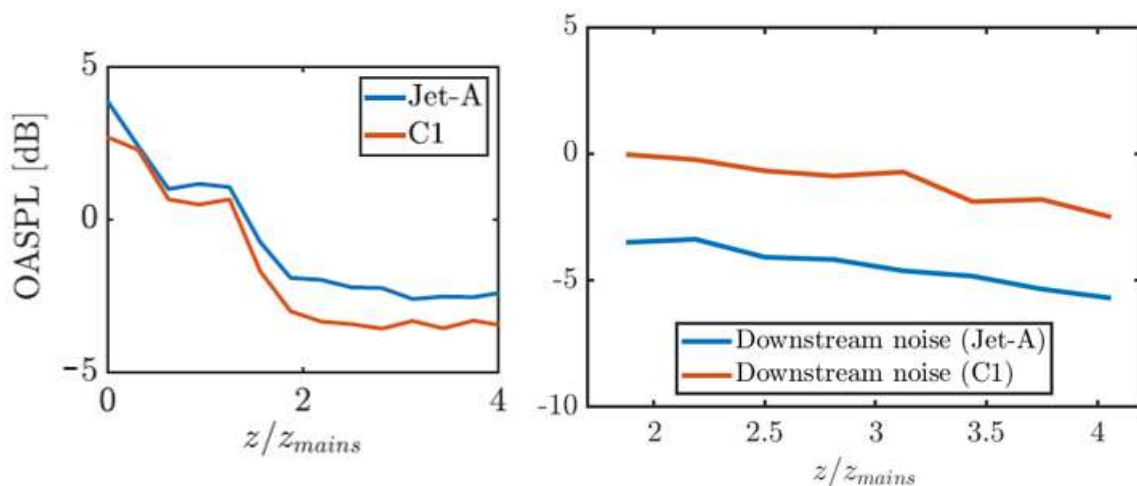


Figure 1: OASPL of the direct noise (left) and indirect noise (right).

Figure 2 shows the root mean square (rms) values of the temperature,  $T$ . The longer temperature rms field shows that with the C1 fuel the temperature inhomogeneities extend further into the combustor. This results in larger indirect noise caused by the supersonic exit nozzle when these inhomogeneities are accelerated through the outlet.

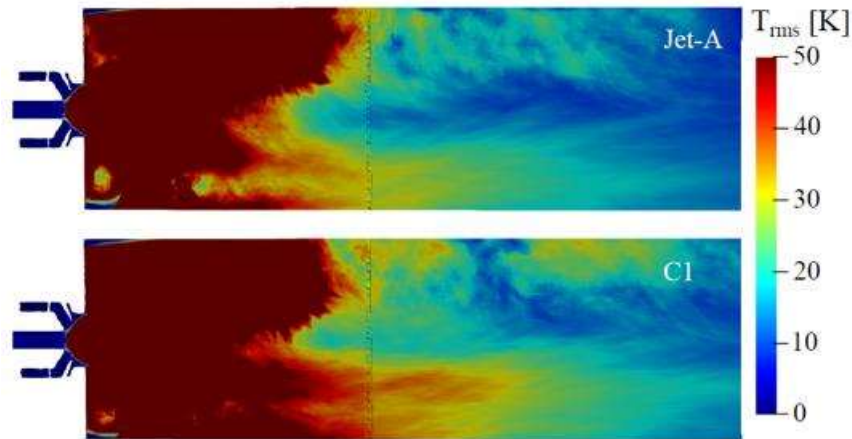


Figure 2: Root mean square of  $T$ .

## References

- [1] K. Wang, R. Xu, T. Parise, J. Shao, A. Movaghar, D. J. Lee, J.-W. Park, Y. Gao, T. Lu, F. N. Egolfopoulos, D. F. Davidson, R. K. Hanson, C. T. Bowman, H. Wang, A physics-based approach to modeling real-fuel combustion chemistry – IV. HyChem modeling of combustion kinetics of a bio-derived jet fuel and its blends with a conventional Jet A, *Combustion and Flame* 198 (2018) 477–489.
- [2] D. McCormick, J. Snyder, W. Kim, J. Mendoza, Volume 1: Final Report, 2020.
- [3] D. Brouzet, B. Krisna, D. McCormick, C. A. Reimann, J. Mendoza, M. Ihme, Analysis of direct and indirect noise in a next-generation aviation gas turbine combustor, *Combustion and Flame* 260 (2024).

# Preferential diffusion effects on tabulated chemistry methods for hydrogen/methane and hydrogen/ammonia blends

B. Cassese<sup>1,2</sup>, G. Sorrentino<sup>1</sup>, M. De Joannon<sup>1</sup>, R. Ragucci<sup>1</sup>

biagio.cassese@stems.cnr.it

1. Istituto di Scienze e Tecnologie per l'Energia e la Mobilità sostenibili - Consiglio Nazionale delle Ricerche, Napoli, Italy.

2. Università degli Studi di Napoli, Dipartimento di Ingegneria Industriale, Napoli, Italy.

## Abstract

Advancements in more efficient combustion systems heavily rely on understanding the fundamental combustion characteristics of the different energy carriers and numerical simulation has a fundamental role in that. However, detailed chemistry simulation can be computationally prohibitive for industrial design workflows. Tabulated chemistry methods stand out as a promising approach, offering a cost-effective method for maintaining accuracy in simulations. Manifold generation is a pivotal aspect of tabulated chemistry methods as it delineates the range of thermochemical states accessible during the simulation. Preferential diffusion is one of the dominant effects that must be included when hydrogen is used as a fuel. The present work aims at numerically investigate the effect of preferential diffusion on flamelet-generated manifolds for different hydrogen-methane and hydrogen-ammonia blends. Extinguish counterflow diffusion flames are used for the generation of the manifold, solved by CHEM1D with two different transport models. As expected, preferential diffusion effects are predominant at high hydrogen molar fractions and become negligible at concentrations lower than 0.5. Preferential diffusion affects the shape of the manifold, i.e. higher diffusion of the progress variable species towards leaner and richer mixture fractions. Contours of the progress variable source term show higher peaks for the unity-Lewis case, due to the absence of diffusive transport, while a wider reaction zone is observed for the mixture-averaged case, as it can be seen from figures 1 and 2. These effects are even more predominant for the hydrogen/ammonia blends compared to hydrogen methane blends. Hence, manifolds are deeply affected by preferential diffusion, emphasizing the necessity of its incorporation into flamelet equations.

## Acknowledgements

This research was partly funded by the European Union, NextGenerationEU in the framework of the National Sustainable Mobility Center - MOST, CN00000023, Italian Ministry of University and Research Decree n. 1033— 17/06/2022, Spoke 12, CUP B43C22000440001 and by the National Recovery and Resilience Plan (NRRP), Mission 4, Component 2, Investment 1.1, Call for tender No. 1409 published on 14.9.2022 by the Italian Ministry of University and Research (MUR), funded by the European Union – NextGenerationEU – Project Title REACTANT –



CUP B53D23026970001, Grant Assignment Decree No. 1385 adopted on 01/09/2023 by the Italian Ministry of University and Research (MUR).

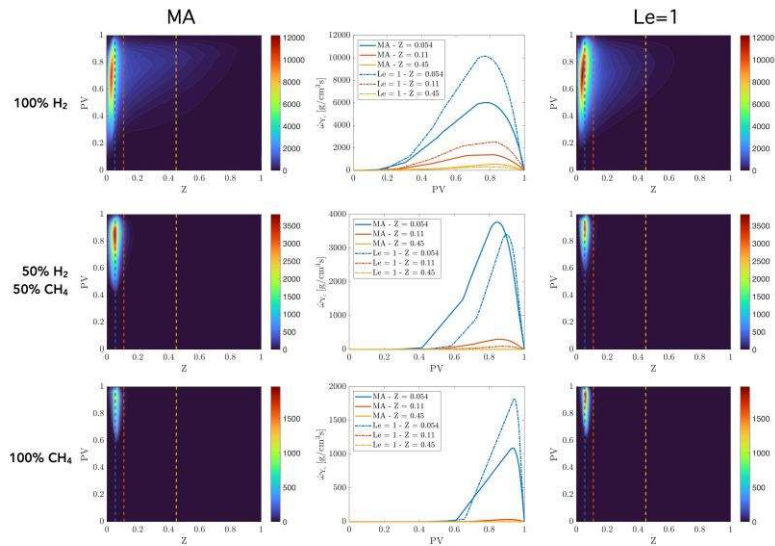


Figure 1- Progress variable source term for different hydrogen/methane blends and transport model

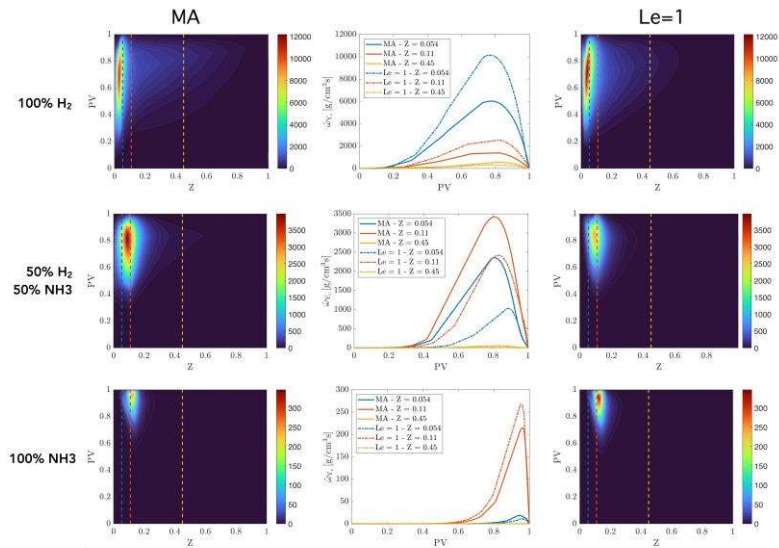


Figure 2- Progress variable source term for different hydrogen/ammonia blends and transport model

# Flame thickening mechanism during flame-wall interactions

Cheng Chi<sup>1,\*</sup>, Bénédicte Cuenot<sup>2</sup>, Dominique Thévenin<sup>1</sup>

<sup>1</sup>University of Magdeburg “Otto von Guericke”, Magdeburg, D-39106, Germany

<sup>2</sup>CERFACS, 42 avenue Gaspard Coriolis, Toulouse, 31047, France

(\*corresponding email: cheng.chi@ovgu.de)

It has been observed in [1, 2] that the flame thickness would increase as the boundary layer is approached during the flame-wall interaction (FWI) process. Such thickened flame thickness is critical for reduced modeling of FWI, as the combustion regime might change dramatically. Gruber et al. [1] briefly explained the flame thickness increase by two reasons: 1) the increased unsteadiness and wrinkling of the flame brush results in an increase of the averaged flame thickness; 2) the turbulent length and time scales decreases as the distance from the wall is reduced, while the chemical time scales become larger due to heat loss. These two reasons can be summarized into two effects: heat loss effect and turbulence length scale effect. Detailed investigation of these two effects on flame thickening has not been done.

In this study, the objective is to reveal the underlying mechanisms controlling flame thickening near the wall boundary layer. Effects of heat loss and turbulence length scale are investigated. Head-on quenching of laminar premixed NH<sub>3</sub>/H<sub>2</sub>/air flames have been firstly simulated, using the in-house DNS solver DINO [3], to investigate the effect of heat loss. Then head-on flame quenching in a fully developed turbulent channel flow has been simulated, to check the effect of turbulence length scales. Details of the 3D turbulent cases can be found in [4]. Both isothermal and adiabatic walls are checked.

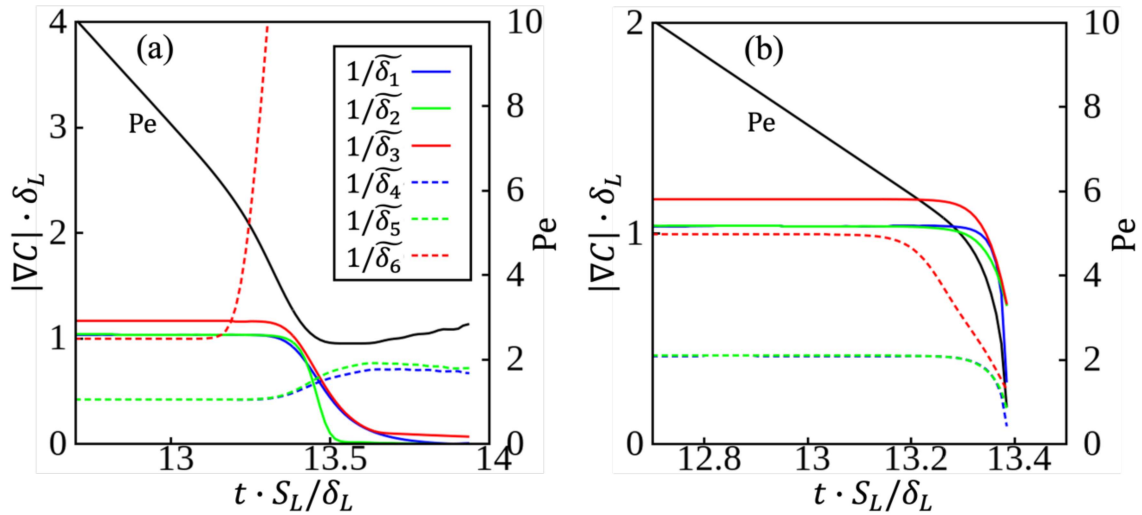


Figure 1: Time evolution of the surface density function defined on different isosurfaces during FWI for (a) the isothermal wall and (b) the adiabatic wall.

Before discussion of the simulation results, there are several definitions of the flame thickness, which need to be clarified. Flame thickness can be usually defined based on  $\delta_f = \frac{1}{|\nabla C|}$  on a certain isosurface. If the progress variable  $C$  is defined thermally based on temperature, then  $\delta_f$  is the thermal thickness. On the

other hand, if  $C$  is defined based on species mass fractions, then  $\delta_f$  is the chemical thickness. Figure 1 shows the time evolution of the surface density function (SDF) defined on different isosurfaces during FWI for the isothermal and adiabatic walls.  $\delta_1, \delta_2,$  and  $\delta_3$  are chemical thickness, while  $\delta_4, \delta_5,$  and  $\delta_6$  are thermal thickness. As is seen, with isothermal wall, all chemical thicknesses are increasing during FWI, while the thermal thicknesses are decreasing. With adiabatic wall, all thicknesses are increasing. To analyze the controlling mechanism, we will focus on  $\delta_2$  and  $\delta_5$ . The controlling equation of SDF is

$$\frac{1}{|\nabla C|} \frac{d|\nabla C|}{dt} = -(a_n + n \cdot \nabla S_d) = -a_{n,eff}$$

where  $a_{n,eff}$  is the effective normal strain rate,  $a_n$  is the normal strain rate and  $S_d$  is the flame displacement speed. Figure 2(a) shows the time evolutions of  $a_n, n \cdot \nabla S_d$  and  $a_{n,eff}$  in the adiabatic wall case. As is seen,  $a_{n,eff}$  is mainly controlled by  $n \cdot \nabla S_d$ . The decrease of  $|\nabla C|$  is mainly due to the rapid increase of  $\nabla S_d$  as the flame approaches to the wall. Figure 2(b) shows the time evolutions of  $\nabla S_d, \nabla S_{d,diff}$  and  $\nabla S_{d,react}$ . As is seen, change of  $|\nabla C|$  is dominated by the reaction term  $\nabla S_{d,react}$ . Finally, Fig. 2(c) shows the distributions of  $S_{d,react}$  and  $|\nabla C|$  on the flame front at different time instants. It is observed that rapid increase of  $\nabla S_{d,react}$  is because of the zero diffusion flux  $|\nabla C| = 0$  at the wall. This also explains why the thermal thickness decreases in the isothermal wall case, because  $|\nabla T| \neq 0$  in that case. Therefore, It is concluded that increase of the flame thickness near the wall is mainly due to the zero diffusion flux for species on the wall boundary.

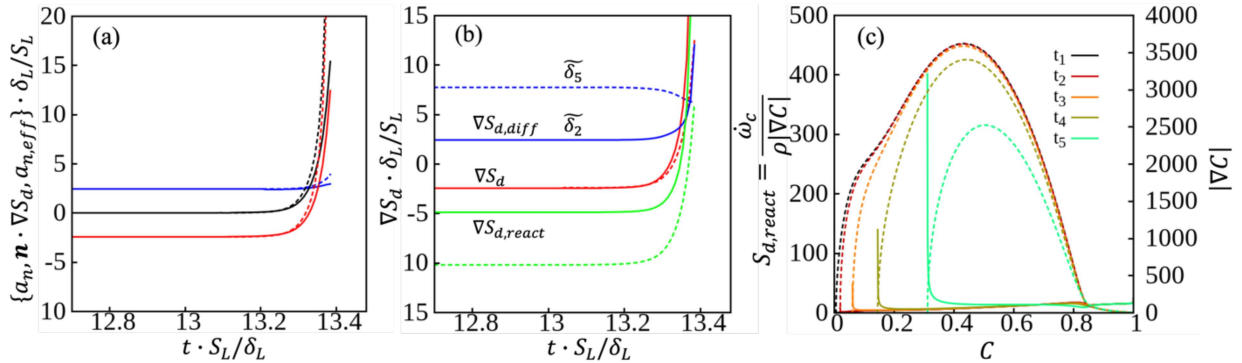


Figure 2: Time evolution of (a)  $a_n, n \cdot \nabla S_d$  and  $a_{n,eff}$  and (b)  $\nabla S_d, \nabla S_{d,diff}$  and  $\nabla S_{d,react}$  in the adiabatic wall case. (c) Distributions of  $S_{d,react}$  and  $|\nabla C|$  on the flame front at different time instants.

## Reference

- [1] A. Gruber, R. Sankaran, E. R. Hawkes, J. H. Chen, J. Fluid Mech. 658 (2010) 5-32.
- [2] P. Zhao, L. Wang, N. Chakraborty, J. Fluid Mech. 848 (2018) 193-218.
- [3] A. Abdelsamie, G. Fru, T. Oster, F. Dietzsch, G. Janiga, D. Thévenin, Comput. Fluids 131 (2016) 123-141.
- [4] C. Chi, C. Yu, B. Cuenot, U. Maas, D. Thévenin, Proc. Combust. Inst. 40 (2024) 105276.

# Preferential diffusion effects on hydrogen and iso-octane flames in inhomogeneous mixtures

Hongchao Chu\*, Lukas Berger, Michael Gauding, Sebastian Pieper, Heinz Pitsch

*Institute for Combustion Technology, RWTH Aachen University, 52056 Aachen, Germany*

\*Corresponding author: h.chu@itv.rwth-aachen.de

## Introduction

In direct-injection spark-ignition engines, the in-cylinder fuel-air equivalence ratio field at the time of ignition is often inhomogeneous, which can significantly influence the flame kernel development and thus the entire combustion stroke. This can be particularly important for ultra-lean combustion concepts applied for increasing thermal efficiencies. For mixtures of species with different diffusivities, the flame kernel development can be significantly influenced by preferential diffusion. Both the inhomogeneous fuel distribution in the unburned gas and preferential diffusion alter the equivalence ratio in the reaction zone, thus influencing the combustion process. This study aims to investigate the interactions of preferential diffusion and mixture inhomogeneities in hydrogen and iso-octane flame kernels under engine conditions.

## DNS database

In this study, the existing DNS database [1] of homogeneous premixed iso-octane and hydrogen flames was extended with early flame kernels in lean mixtures with inhomogeneous initial fuel distributions. Detailed descriptions of the configuration and numerical methods can be found in the study [1]. In addition to the standard finite-rate-chemistry DNS equation systems, a passive scalar  $Z_F$  is solved in the DNS, serving as an indicator for mixture inhomogeneity. The transport equation of  $Z_F$  is the same as the fuel species but with the chemical source term set to zero. The flame kernels are ignited in a decaying homogeneous isotropic turbulent (HIT) field. Characteristic parameters of the DNS are listed in Table 1. The thermodynamic parameters were specified to represent the hydrogen and gasoline engine conditions. The flow parameters, such as the Reynolds number  $Re_t$  and the Damköhler number  $Da$ , are specified as closely as possible to typical SI engine conditions.

Table 1: Conditions and characteristic parameters of DNS: Turbulent Reynolds number  $Re_t = l_t u' / \nu$ , turbulent velocity fluctuation  $u'$ , turbulent integral length scale  $l_t = u'^3 / \bar{\epsilon}$ , mean dissipation rate  $\bar{\epsilon}$ , kinematic viscosity  $\nu$ , Karlovitz number  $Ka = t_f / t_\eta$ , Damköhler number  $Da = t_t / t_f$ , chemical time  $t_f = l_f / s_1^0$ , Kolmogorov time  $t_\eta = (\nu / \bar{\epsilon})^{1/2}$ , turbulent integral time  $t_t = l_t / u'$ , flame thickness  $l_f$  computed from the maximum temperature gradient, unstretched laminar flame speed  $s_1^0$ , Kolmogorov length  $\eta$ , initial pressure  $p$ , and temperature  $T_u$ , fuel-air equivalence ratio  $\phi$ , effective Lewis number  $Le_{eff}$ , and ignition radius  $R_{ign}$ .

Case name	H <sub>2</sub> THom	H <sub>2</sub> TInHom	H <sub>2</sub> LHom	H <sub>2</sub> LInHom	iso-C <sub>8</sub> H <sub>18</sub> THom	iso-C <sub>8</sub> H <sub>18</sub> TInHom
Fuel	hydrogen	hydrogen	hydrogen	hydrogen	Iso-octane	Iso-octane
$\phi(\tilde{Y}_F)$	0.4	0.4	0.4	0.4	0.8	0.8
$RSTD$ of $\phi$	0	0.30	0	0.15	0	0.36
$p$ [bar]	40	40	40	40	6	6
$T_u(\tilde{Y}_F)$ [K]	800	800	800	800	600	600
$Le_{eff}(\tilde{Y}_F)$	0.3	0.3	0.3	0.3	2.5	2.5
Flow field	HIT	HIT	Quiescent	Quiescent	HIT	HIT
$Re_t$	385	385	-	-	385	385
$Ka(\tilde{Y}_F)$	18	18	-	-	18	18
$Da(\tilde{Y}_F)$	1.1	1.1	-	-	1.1	1.1
Grid size	1440 <sup>3</sup>	1440 <sup>3</sup>	720 <sup>3</sup>	1080 <sup>3</sup>	960 <sup>3</sup>	960 <sup>3</sup>
Realizations	3	3	1	1	8	8
$R_{ign}/l_t$	0.4	0.4	0.4	0.4	0.4	0.4

## Results

To assess the interactions between the mixture inhomogeneity and thermodiffusive instability, the correlation between the Bilger mixture fraction  $Z$  [2], which also considers demixing due to preferential diffusion, and  $Z_F$  is shown in Fig. 1. If the thermodiffusive instabilities are enhanced by mixture inhomogeneity, an increase in  $Z$  is expected for the hydrogen flame kernels in the inhomogeneous mixture compared to those in the homogeneous

mixture. However, as shown in Fig. 1, an approximately linear correlation between  $Z$  and  $Z_F$  is observed for both fuels and the conditional mean  $\overline{Z|Z_F}$  at  $\phi = 0.4$  for hydrogen and  $\phi = 0.8$  for iso-octane agrees well with the corresponding homogeneous cases, which are displayed as circles.  $f(Z_F)$  denotes the lines with a slope of unity passing through these circles. The good agreement of the conditional mean  $\overline{Z|Z_F}$  with  $f(Z_F)$  for the inhomogeneous cases demonstrates that preferential diffusion leads to the same amount of demixing, independent of  $Z_F$ . Thus, the effects of preferential diffusion on the mean values  $\overline{Z|Z_F}$  are not influenced by mixture inhomogeneity.

To assess the effects of mixture inhomogeneity on the preferential diffusion-induced fluctuations in the local mixture fraction, the PDF of  $(Z - f(Z_F))$  is shown in Fig. 2. The fluctuations are almost identical for flame kernels in homogeneous and inhomogeneous mixtures. This indicates that, under the investigated conditions, no enhancement of the preferential diffusion by the mixture inhomogeneity can be identified in the turbulent flame kernels, which can be attributed to the distinctly different characters of these two effects. Preferential diffusion is an intrinsic effect strongly associated with local flame topology. However, the effects of mixture inhomogeneity represent an external disturbance for the flame, which is not necessarily strongly correlated with local flame topology.

**Acknowledgement** H. C. and H. P. acknowledge the funding by the Deutsche Forschungsgemeinschaft (DFG, German Research Foundation) under Research Unit FOR2687. M. G. and H. P. have received funding from the European Research Council (ERC) under the European Union’s Horizon 2020 research and innovation program (grant agreement No 101054894).

The authors gratefully acknowledge the Gauss Centre for Supercomputing e.V. ([www.gauss-centre.eu](http://www.gauss-centre.eu)) for funding this project by providing computing time on the GCS Supercomputer Super-MUC at Leibniz Supercomputing Centre (LRZ, [www.lrz.de](http://www.lrz.de)). The authors gratefully acknowledge the computing time provided to them at the NHR Center NHR4CES at RWTH Aachen University (project number p0021021).

## References

- [1] H. Chu, L. Berger, T. Grenga, M. Gauding, L. Cai, H. Pitsch, Effects of turbulence on variations in early development of hydrogen and iso-octane flame kernels under engine conditions, *Combust. Flame* 255 (2023) 112914.
- [2] R. Bilger, S. Stårner, R. Kee, On reduced mechanisms for methane-air combustion in nonpremixed flames, *Combust. Flame* 80 (1990) 135–149.

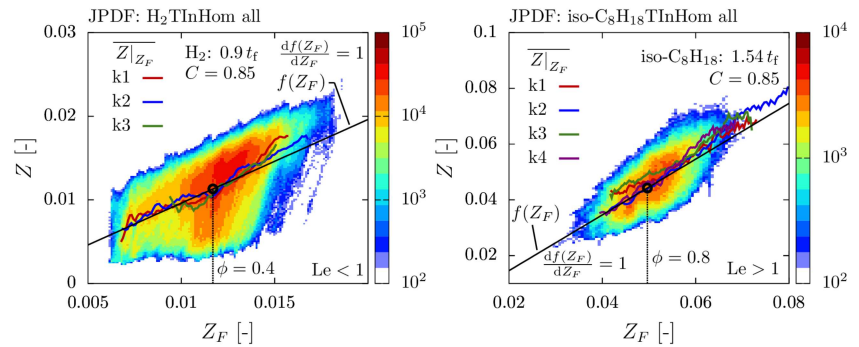


Figure 1: Correlation of  $Z$  and  $Z_F$  in the reaction zone defined by  $C = 0.85$ . The color shows the logarithm of the joint probability density function (PDF) considering all corresponding realizations. Lines represent the conditional mean for different realizations.

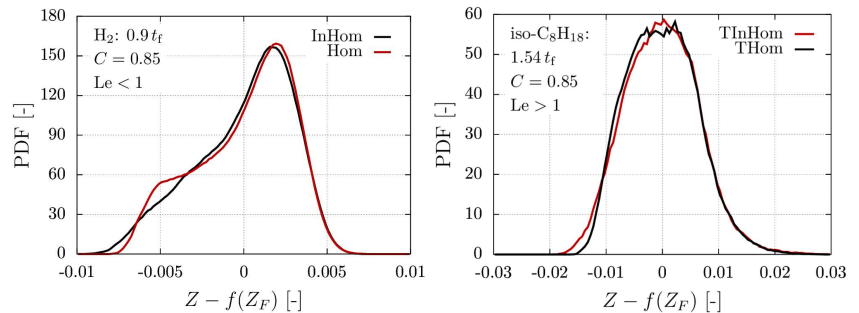


Figure 2: PDF of  $(Z - f(Z_F))$  in the reaction zone defined by  $C = 0.85$  considering all turbulent kernels of each fuel.



# Calculating Temperature and Species Concentration from Quasi-2D Combustion Video Data using Physics-Informed Neural Networks

Benjamin L. Cohen<sup>1,\*</sup>, Zhenghong Zhou<sup>1</sup>, and Paul D. Ronney<sup>1</sup>

<sup>1</sup>*Aerospace and Mechanical Engineering, University of Southern California, Los Angeles, CA 90007, United States*

*\*Corresponding Author Email: blcohen@usc.edu*

The field of complex reacting flows occupies a unique academic niche, characterized by partial theoretical knowledge and imperfect data measurements. Physics-Informed Neural Networks (PINNs) bridge this gap, fusing limited theoretical understanding with incomplete datasets to construct a more comprehensive picture. This is particularly relevant in the study of quasi-2D combustion processes, which are prevalent in high aspect ratio environments such as car engines. Our study focuses on a dilute hydrogen flame observed through a Hele-Shaw apparatus, with particular attention to the cellular instabilities and unique sawtooth shapes formed under specific conditions. The video analysis component is critical, as it challenges us to discern meaningful data from high-frame-rate videos, where visibility issues arise due to the diminished signal-to-noise ratio at increased frame rates. This problem underscores the need for sophisticated processing techniques to enhance video clarity and extract valuable data. By applying PINNs to this video data, we have constructed detailed profiles of temperature, species concentration, and velocity, offering a new lens through which to view combustion dynamics. This methodology not only allows for the deconstruction of video data into a richer dataset but also offers a lower-cost alternative to traditional experimental and computational approaches. The continuous nature of the function provided by PINNs, as opposed to discrete datasets, presents a significant advantage in analyzing these complex systems.

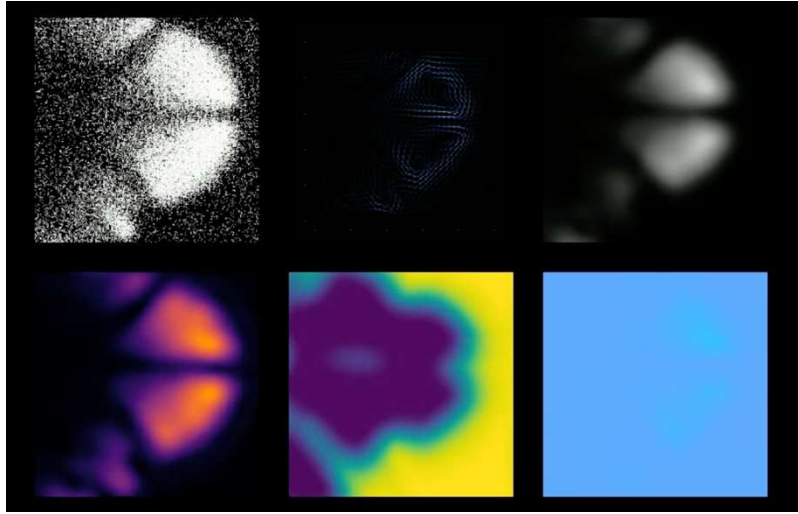


Figure 1: Combustion dynamics visualized in six segments. Top left: Original video footage. Top middle: Velocity profile. Top right: Brightness reconstructed using PINNs. Bottom left: Temperature profile. Bottom middle: Concentration profile. Bottom right: Pressure profile.

In our Physics informed neural network model,  $\Pi$  symbolizes the predicted profiles, ( $p$  – pressure,  $T$  – temperature,  $Y$  – fuel concentration) across all points in time and space. This is achieved through the sequential application of dense neural network layers, denoted as  $A$ , which serve as linear operators on the preceding layer, followed by an activation function,  $\sigma$ . The final activation function is specifically tailored within the context of the domain to ensure the boundary conditions are satisfied for all potential weight configurations.

$$\Pi(x, y, t) \equiv \sigma^{D-SAF} \circ A^N \sigma^N \circ \dots \circ A^1 \sigma^1 \circ A^0(x, y, t) = p, T, Y \quad (1)$$

The domain-specific activation function,  $\sigma^{D-SAF}$ , is defined as:

$$\sigma^{D-SAF}(w) = \epsilon_0(w_0) + \bar{\alpha}_i \bar{w}_{ij} \bar{\beta}_j^T \quad (2)$$

Here  $w_0$  and  $\bar{w}$  are the features or nodes of the penultimate layer, while  $\epsilon_0$ ,  $\bar{\alpha}$ , and  $\bar{\beta}^T$  are coefficients derived from the zeroth and first-order terms of a Fourier approximation of the boundary conditions.

D-SAF equations for Hele-Shaw (quasi-2D with one open wall):

$$\beta_i(y) = \alpha_0(2iy)^2 : \alpha_i(x) = 4\alpha_{i-1}(x) - 4\alpha_{i-1}(x)^2 \quad (3)$$

$$\epsilon_0 = \alpha_0(x)w_0(1,0) + \alpha_0(y)^2\alpha_0(x)(w_0(1,1) - w_0(1,0)) + \alpha_0(x)w_0(1,y) \quad (4)$$

Planck's law of spectral radiance is applied to deduce how temperature and concentration profiles result in near-infrared light detected by the camera, specifically at a wavelength of 823 nm, indicative of heated water vapor. By averaging over intervals aligned with the camera's shutter speed, we can predict how a PINN-derived profile would manifest in captured footage.

$$B(Y, T) \propto \frac{1 - Y}{e^{T_p/T'} - 1} : T_p = \frac{hc}{\lambda k_B} \quad (5)$$

A Variational Autoencoder was pretrained to encode the shape of the light intensity flame profile into an 8-dimensional latent space. A loss function on the data portion compares the L2 norm of the latent space of the brightness from a provided video and a brightness profile from our brightness model, composed with  $\Pi$ .

A Physics-Informed Loss is leveraged to construct detailed temperature, pressure, and concentration profiles by integrating video data with relevant physical laws. The foundation is built upon governing equations akin to the Poisson-like and Euler-Darcy equations, as described by Daniel Fernández-Galisteo et al [1]. These equations (6-8) are expressed in their residual forms:

$$\mathcal{L}_p \equiv \nabla^2 p - \sigma q \rho T_x p_x - \sigma q \rho T_y p_y + q \mu^2 [T_{xx} + T_{yy}] + \sigma \rho q^2 \mu^2 [T_x^2 + T_y^2] + q \mu \omega = 0 \quad (6)$$

$$\mathcal{L}_T \equiv T_t - \frac{\mu}{\rho} [T_{xx} + \sigma q \rho T_x^2 + T_{yy} + \sigma q \rho T_y^2] + \frac{1}{\mu} [p_x T_x + p_y T_y] + \frac{\omega}{\rho} = 0 \quad (7)$$

$$\mathcal{L}_Y \equiv Y_t - \frac{\mu}{\rho L e} [Y_{xx} + \sigma q \rho Y_x^2 + Y_{yy} + \sigma q \rho Y_y^2] + \frac{1}{\mu} [p_x Y_x + p_y Y_y] - \frac{\omega}{\rho} = 0 \quad (8)$$

Training and hyperparameter tuning are conducted using the frameworks established by Paris Perdikaris [2] [3] and Rose Yu [4], which involve specific sampling strategies and adaptive spatial weights.

Training was performed on an NVIDIA A100, utilizing half an hour of computational time for a square domain 20 times the thermal flame thickness. The physics-informed loss was minimized until the conservation laws were obeyed 98.9% of the time using the L-infinity norm, showing room for improvement but still providing an acceptable reconstruction given the low computational cost.

- [1] D. Fernandez-Galisteo, V. N. Kurdyumova and P. D. Ronneyb, "Analysis of premixed ame propagation between two closely-spaced parallel plates," *Combustion and Flame*, vol. 190, no. April 2018, pp. 133-145, 2018.
- [2] S. Wang, S. Sankaran, H. Wang and P. Perdikaris, "An Expert's Guide to Training Physics-Informed Neural Networks," arXiv: Preprint , Philadelphia, PA, 2023.
- [3] S. Wang, X. Yu and P. Perdikaris, "When and Why PINNs Fail to Train: A Neural Tangent Kernel Perspective," arXiv: Preprint, Philadelphia, PA, 2020.
- [4] R. Wan, D. Maddix, C. Faloutsos, Y. Wang and R. Yu, "Bridging Physics-based and Data-driven modeling for Learning Dynamical Systems," Proceedings of Machine Learning Research, San Diego, CA, 2021.

# Filtered tabulated chemistry for multi-regime combustion with application to the HYLON injector

Samuel Dillon<sup>a,b,\*</sup>, Renaud Mercier<sup>b</sup>, Benoit Fiorina<sup>a</sup>

<sup>a</sup>EM2C Laboratory, CNRS, CentraleSupélec, Université Paris-Saclay, 8-10 rue Joliot-Curie, 91190 Gif-sur-Yvette, France

<sup>b</sup>Safran Tech, Digital Sciences & Technologies Department, Rue des Jeunes Bois, Châteaufort, Magny-Les-Hameaux 78114, France

## 1. Introduction

Flamelet-type approaches for modelling turbulent combustion remain popular due to their low-cost and ability to incorporate detailed chemistry effects [1]. These approaches aim at modelling the turbulent flame brush using a collection of thin flamelets where it is assumed that turbulence does not impact the inner flame structure and that the high-dimensional composition space of turbulent flames are confined to a lower dimensional subspace [2]. One-dimensional flamelet equations are usually restricted to a single regime and/or flow configuration, for example 1D freely-propagating (1DFP) flamelet archetypes cannot accurately be used for non-premixed flames where diffusive fluxes exist across iso-equivalence ratio surfaces [3]. For multi-regime flamelet methods, one of the main challenges is distinguishing between combustion regimes [4]. The approach proposed by Franzelli et al. [5] maps the partially-premixed thermochemical subspace by incorporating partially-premixed counterflow flames computed in the physical space. While this extra degree-of-freedom requires the use of an extra tabulation coordinate, the mixture scalar dissipation rate, it does not require the use of a flame sensor. Coupling tabulated chemistry with the LES method for reactive flow raises the problem of resolving flame fronts. Indeed, in practical mesh conditions, the flame thickness is in general smaller than the grid size. To avoid numerical artefacts caused by a poor resolution of the flame thickness, explicit flame filtering approaches can be used [6]. Among them, the F-TACLES (Filtered tabulated chemistry for LES) model couples flame filtering with tabulated chemistry through the filtering of 1D flamelets. F-TACLES was initially developed for premixed combustion by filtering 1D premixed flames [7] and was more recently extended to non-premixed and multi-regime combustion by filtering 1D counterflow diffusion and partially-premixed flames [8–11]. This abstract shows the recently obtained results for the HYLON injector using the new F-TACLES multi-regime model.

## 2. Coupling tabulated chemistry with LES using F-TACLES

Coupling tabulated chemistry with LES requires the modelling of filtered thermochemical quantities  $\tilde{\phi}$ . The F-TACLES formalism is based on the filtering of 1-D flames, either premixed, diffusion or partially-premixed. These quantities are tabulated as a function of the filtered progress variable  $\tilde{Y}_c$  and filtered mixture fraction  $\tilde{Z}$  for premixed and non-premixed flames. For multi-regime combustion, both  $\tilde{Y}_c$  and  $\tilde{Z}$  are used in conjunction with the resolved scalar dissipation rate  $\chi_{\tilde{Z}}^n$  to distinguish between flame regimes [11]. Transport equations for  $\tilde{Y}_c$  and  $\tilde{Z}$  and the resolved scalar dissipation rate  $\chi_{\tilde{Z}}^n$  are outlined below.

$$\frac{\partial \tilde{\rho} \tilde{Y}_c}{\partial t} + \nabla \cdot (\tilde{\rho} \tilde{\mathbf{u}} \tilde{Y}_c) = \nabla \cdot (\rho_0 D_0 \nabla \tilde{Y}_c) + \tilde{\rho} \tilde{\omega}_{Y_c}^{\text{TAB}} + \alpha_{Y_c}^{\text{TAB}} + \Omega_{Y_c}^{\text{TAB}} \quad (1)$$

$$\frac{\partial \tilde{\rho} \tilde{Z}}{\partial t} + \nabla \cdot (\tilde{\rho} \tilde{\mathbf{u}} \tilde{Z}) = \nabla \cdot (\tilde{\rho} D_{\tilde{Z}}^{\text{TAB}} \nabla \tilde{Z}) \quad (2)$$

$$\chi_{\tilde{Z}}^n = |\nabla_n \tilde{Z}|^2 \quad (3)$$

The superscript TAB represents a quantity closed from a chemical look-up table.  $\alpha_{\phi}^{\text{TAB}} = \nabla \cdot (\overline{\rho D \nabla \phi} - \rho_0 D_0 \nabla \tilde{\phi})$  is the unresolved diffusive flux of scalar  $\phi$ , where  $\phi$  denotes either  $Z$  or  $Y_c$  coordinate.  $\Omega_{\phi}^{\text{TAB}} = \nabla \cdot (\overline{\rho \mathbf{u} \phi} - \tilde{\rho} \tilde{\mathbf{u}} \tilde{\phi})$  is the unresolved convective flux of scalar  $\phi$  and  $\tilde{\omega}_{Y_c}$  is the filtered progress variable source term.  $\rho_0$  and  $D_0$  are the reference density and diffusivity.

## 3. Controlling the resolved flame thickness with variable filter size $\Delta$

In LES, it is crucial to sufficiently resolve the inner reactive flame thickness  $\delta_{\tilde{r}}$  (defined as the full-width at half maximum [12]), in order to accurately predict flame consumption rates. Within the F-TACLES framework, it means that the filter width of the look-up table should be chosen so that the filtered reactive thickness is resolved over  $n$  grid points, i.e.  $\delta_{\tilde{r}} = n \Delta_x$ , irrespective of variations in the local strain rate. In practice, the value of  $n$  depends on the numerical schemes

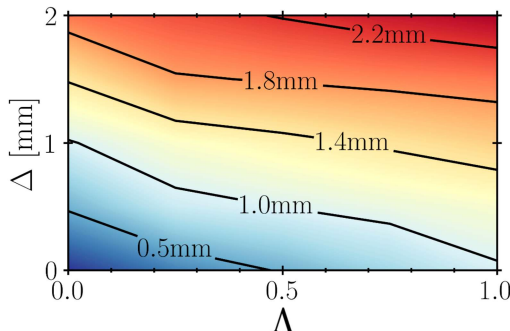


Fig. 1: Iso-contours of  $H_2$ -Air flames filtered reactive thickness  $\delta_{\tilde{r}}$

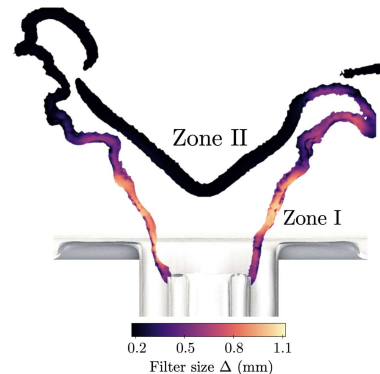


Fig. 2: Instantaneous view of filter size on HYLON A flame

used in the CFD solver [7]. Figure 1 shows the iso-line of  $\delta_{\tilde{\tau}}$ , expressed in  $(\Lambda, \Delta)$  subspace, where  $\Lambda = \tilde{Y}_c(z_{st}, a) / \tilde{Y}_c^{eq}(z_{st})$  is the generalised progress variable computed at stoichiometric conditions. In order to control the reactive flame thickness, the 1-D flamelets are filtered for a given iso-contour of  $\delta_{\tilde{\tau}}$ . Precisely, the required  $\Delta$  can be extracted for each flamelet  $\Delta = \Delta(a, \delta_{\tilde{\tau}})$  (or equivalently  $\Delta = \Delta(\Lambda, \delta_{\tilde{\tau}})$ ). Figure 2 shows a practical implementation of the variable- $\Delta$  case. In regions of high strain, the filter is larger whereas in regions of low strain (wake of  $H_2$  injector), the filter size is naturally lower.

#### 4. Numerical application to dual-swirl HYLON injector

The target configuration is the dual-swirled coaxial injector HYLON designed and experimented at IMFT [13]. Two operating conditions are given in the framework of the TNF workshop, an attached flame A and a lifted flame L. Simulations are performed using the YALES2 solver developed by the CORIA laboratory [14]. The numerical setup consists of a fourth-order time integration scheme TFV4A. Fourth-order accurate spatial integration is utilised with central finite-volume schemes, with the MUSCL scheme used for scalar transport. The SGS reynolds stresses are computed using the WALE model. The mesh consists of 13.7 million tetrahedral elements. Sub-grid scale wrinkling is not included in this study due to the lack of wrinkling models dedicated to pure diffusion flame regimes. Figure 3 shows the LES versus the experimental flame shapes for the F-TACLES multi-regime model. The model successfully retrieves the correct flame structures for both attached and lifted flames.

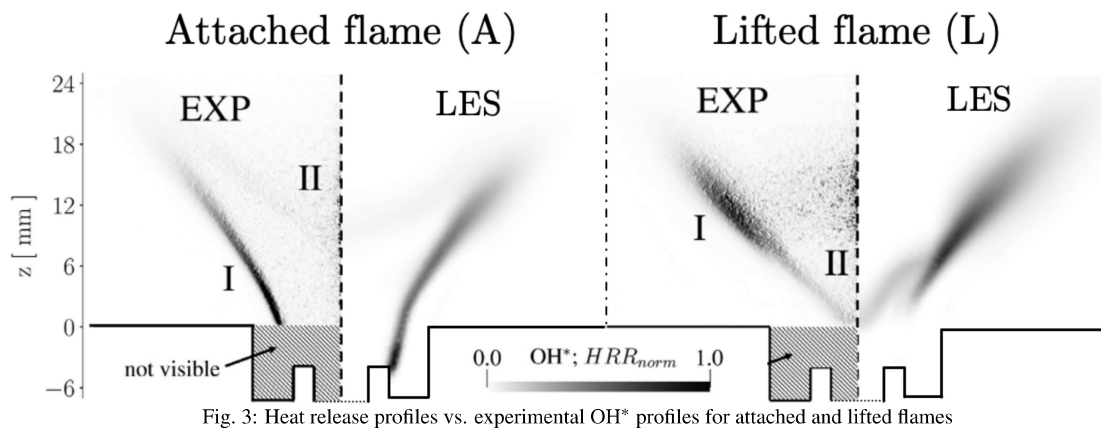


Fig. 3: Heat release profiles vs. experimental  $OH^*$  profiles for attached and lifted flames

#### References

- [1] O. Gicquel, N. Darabiha, D. Thévenin, Liminar premixed hydrogen/air counterflow flame simulations using flame prolongation of ildm with differential diffusion, *Proceedings of the Combustion Institute* 28 (2) (2000) 1901–1908.
- [2] N. Peters, *Turbulent combustion*, Cambridge university press, 2000.
- [3] B. Fiorina, O. Gicquel, L. Vervisch, S. Carpentier, N. Darabiha, Approximating the chemical structure of partially premixed and diffusion counterflow flames using fpi flamelet tabulation, *Combustion and flame* 140 (3) (2005) 147–160.
- [4] E. Knudsen, H. Pitsch, Capabilities and limitations of multi-regime flamelet combustion models, *Combustion and Flame* 159 (1) (2012) 242–264.
- [5] B. Franzelli, B. Fiorina, N. Darabiha, A tabulated chemistry method for spray combustion, *Proceedings of the Combustion Institute* 34 (1) (2013) 1659–1666.
- [6] M. Boger, D. Veynante, H. Boughanem, A. Trouvé, Direct numerical simulation analysis of flame surface density concept for large eddy simulation of turbulent premixed combustion, in: *Symposium (International) on Combustion*, Vol. 27, Elsevier, 1998, pp. 917–925.
- [7] B. Fiorina, R. Vicquelin, P. Auzillon, N. Darabiha, O. Gicquel, D. Veynante, A filtered tabulated chemistry model for les of premixed combustion, *Combustion and Flame* 157 (3) (2010) 465–475.
- [8] A. Coussement, T. Schmitt, B. Fiorina, Filtered tabulated chemistry for non-premixed flames, *Proceedings of the Combustion Institute* 35 (2) (2015) 1183–1190.
- [9] S. Dillon, R. Mercier, B. Fiorina, Large-Eddy-Simulation of Turbulent Non-Premixed Hydrogen Combustion Using the Filtered Tabulated Chemistry Approach, *Journal of Engineering for Gas Turbines and Power* (2023) 1–25.
- [10] S. Dillon, R. Mercier, B. Fiorina, Controlling the resolved flame thickness of non-premixed flames in les with filtered tabulated chemistry, *Proceedings of the Combustion Institute* 40 (2024).
- [11] S. Dillon, R. Mercier, B. Fiorina, A new filtered tabulated chemistry model for multi-regime combustion: A priori validation on a laminar triple flame, *Proceedings of the Combustion Institute* 40 (1) (2024) 105301.
- [12] P. Auzillon, B. Fiorina, R. Vicquelin, N. Darabiha, O. Gicquel, D. Veynante, Modeling chemical flame structure and combustion dynamics in les, *Proceedings of the Combustion Institute* 33 (1) (2011) 1331–1338.
- [13] A. Aniello, D. Laera, S. Marragou, H. Magnes, L. Selle, T. Schuller, T. Poinso, Experimental and numerical investigation of two flame stabilization regimes observed in a dual swirl h2-air coaxial injector, *Combustion and Flame* 249 (2023) 112595.
- [14] V. Moureau, P. Domingo, L. Vervisch, Design of a massively parallel cfd code for complex geometries, *Comptes Rendus Mécanique* 339 (2-3) (2011) 141–148.



# ML-augmented diagnostics for feature extraction

Basil Jose, Fabian Hampp

Institute of Combustion Technology for Aerospace Engineering (IVLR)  
Pfaffenwaldring 38-40, University of Stuttgart  
fabian.hampp@ivlr.uni-stuttgart.de

The combustion performance and non-CO<sub>2</sub> emissions of highly turbulent spray flames is driven by the involved interactions between gas phase turbulence, atomization, evaporation, mixture formation and chemical reactions. To enhance our understanding of turbulent reacting multi-phase flows (or subsets) based on experimental data, advanced data processing methods become necessary. This involves accurate feature segregation, i.e. detection and masking of signal from background, to determine, for example, conditional statistics and in turn provide a quantitative delineation of the involved interactions. Such fundamental understanding facilitates the innovation of injection and combustor hardware that is equipped for future fuel flexible markets and close-to zero non-CO<sub>2</sub> emissions.

A wide range of optical diagnostics such as particle image velocimetry (PIV), shadowgraphy, laser-induced fluorescence (LIF) and laser induced incandescence (LII), amongst others, are available to effectively capture the underlying phenomena. While the acquisition of such data sets often takes only seconds to days, the experimental preparation and high-level data processing is often of the order of weeks to years. In this context, precise, efficient and reusable (following the FAIR principles) methodologies to analyse heaps of data generated from such measurements become increasingly inevitable. Conventional data analysis methods are frequently sensitive to domain parameters, e.g. experimental conditions, thus limiting their transferability between datasets and hardware configurations. By contrast, machine learning (ML)-based methods are highly generalisable and thereby adaptable to unknown domain variations with enhanced transferability to new domains. Thus, ML-augmented data analysis tools with domain invariance can significantly reduce the re-calibration and tuning effort of experimental data post-processing methodologies. In the current work, we present our ML-augmented diagnostic data analysis framework including the model development approach to enhance and accelerate the processing from raw image-based data to high-level statistical information. The general framework flow schematic to create the ML models is depicted in Fig. 1. A limiting factor in the preparation of such models is the time requirement for generating labelled training data. In order to reduce this effort, a new strategy based on domain randomisation [1] is adopted to produce synthetic training data semi-automatically.

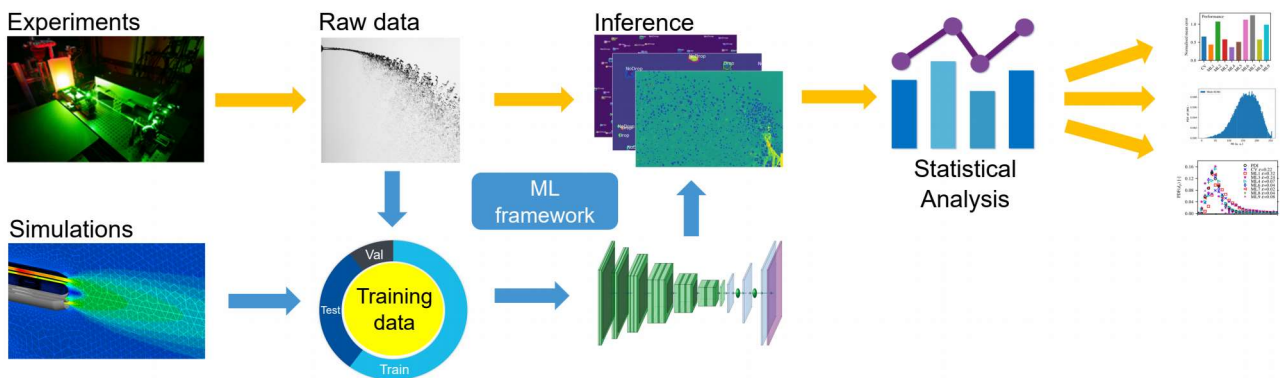


Figure 1: ML-augmented diagnostic data analysis framework. State-of-the-art machine learning models are integrated to conventional framework to obtain high accuracy and generalisation. Additional strategies for reducing labelling effort by using signal from experimental, simulated and generative data are adopted.

Domain randomisation involves training the model on diluting the specifications of object classes that are not of interest with the objective to render the ML-based detection models domain invariant. During inference of real data, i.e. the segregation of signal in noisy experimental data, the model ignores arbitrary domain variations. In the context of computer vision of image-based diagnostic data, this involves realising a model that is invariant to conceivable background or other interferences. For generating synthetic training data without manual labelling, first the objects of interest (e.g. soot filaments, ligaments, flame fronts) are extracted from experimental and simulated data frames using conventional methods creating an objects' database. The ground truth database is augmented by means of diffusion models to enhance the diversity in the training data and improve general model applicability.



Ground truth instances are subsequently randomly selected, positioned, geometrically augmented (e.g. rotation, scaling, distortion) and fused onto synthetic background. The latter consists of a mosaic of random patches of various domain images. In the positioning process, the instances are simultaneously labelled and the images along with the annotations stored. The training dataset is generated by repeating these steps and an appropriate DNN architecture is selected for the specific experimental method. This is followed typically by a transfer-learning approach, hyperparameter optimisation and extensive validation. The models performance is validated using training metrics, periodic manual inference on real data and, if possible, validated using different diagnostics, analysis methods or quantitative comparison with hand-labelled independent data. Once a model is found adequate, it is incorporated into the model database of our data analysis tool (EDACS) for contextual detections, modularity and MPI performance enhancements to analyse complete experimental campaign and infer high-level statistics.

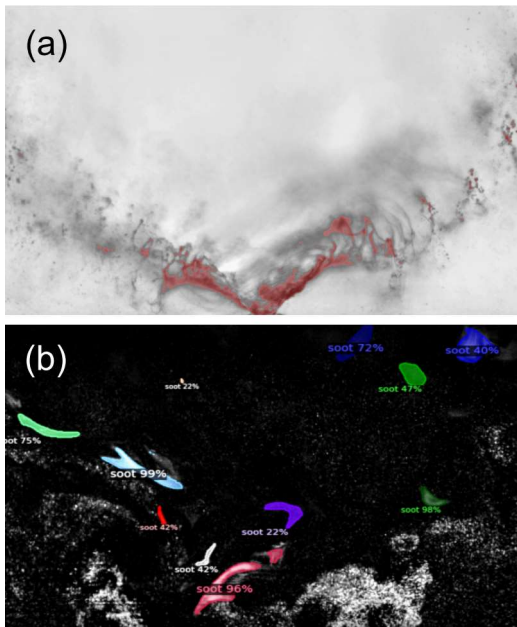


Figure 3: Inference from different models (a) Spray segmentation model, (b) Soot detection model.

transfer and reinforced learning approaches to enhance the generality, robustness, transferability and accuracy of the developed ML-models.

### Acknowledgments

The authors acknowledge the funding by the Deutsche Forschungsgemeinschaft (DFG, German Research Foundation) - project numbers: 456687251. We further acknowledge the support by the German Aerospace Center (DLR) Stuttgart and the Stuttgart Center for Simulation Science (SimTech).

### References

- [1] J. Tobin, R. Fong, A. Ray, J. Schneider, W. Zaremba, P. Abbeel, Domain randomisation for transferring deep neural networks from simulation to the real world, *IEEE/RSJ IROS* (2017) 23-30.
- [2] B. Jose, F. Hampp, Machine learning based spray process quantification, *Int. J. Multiphase Flow* 172 (2024) 104702.
- [3] B. Jose, F. Hampp, IVLR DataVerse on ML-augmented diagnostics, *DaRUS* (2024) <https://doi.org/10.18419/darus-4147>.
- [4] K. He, G. Gkioxari, P. Dollár, R. Girshick, Mask R-CNN, *IEEE/ICCV* (2017) 2980-2988.
- [5] T. Cheng, X. Wang, S. Chen, W. Zhang, Q. Zhang, C. Huang, Z. Zhang, W. Liu, Sparse Instance Activation for Real-Time Instance Segmentation, *IEEE/CVPR* (2022) 4423-4432.
- [6] A. Kirillov, R. Girshick, K. He, P. Dollár, Panoptic Feature Pyramid Networks, *IEEE/CVF* (2019) 6392-6401.

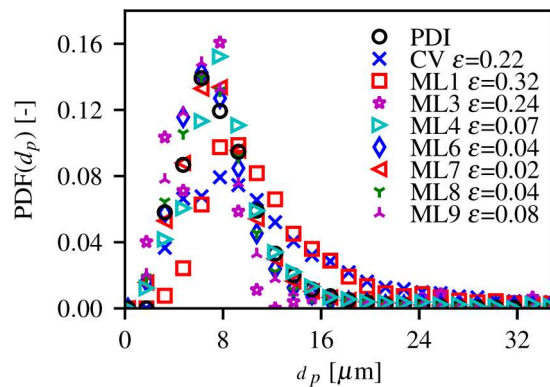


Figure 2: Spray droplet size distribution (PDF) comparing conventional (CV) and machine learning (ML) models against PDI measurements [2].

We have developed the proposed methodology for quantitative droplet sizing using a commercial pressure swirl injector. The accuracy has been validated against independently conducted phase Doppler interferometry (PDI) measurements and the transferability evaluated for a wide range of spray parameter (see Fig. 2) [2]. For this purpose, a total of nine trained ML models (based on state-of-the-art instance segmentation model architectures, Mask R-CNN [4] and SparseInst [5]) are evaluated. The experiments show good agreement between the ML models and the PDI measurements in comparison to conventional methods, thus validating our approach. We have generalised the approach by developing spray detection models (SemanticFPN [6]) via semantic segmentation that can accurately trace gas-liquid-interfaces of various types of technical fuel sprays without parameter tuning and thus enabling a quantitative description of turbulence-spray atomization interactions (Fig. 3 (a)).

We are currently also working on a ML detection model that can segment individual soot filaments from Mie scattering images / PIV flow fields by means of highly accurate masks for a future quantification of strain effects on formation, transport and oxidation regions (Fig. 3 (b)). We are currently extending the methodology to other image-based diagnostics such as LIF, chemiluminescence, LII and, in the long run also to 0D and 1D diagnostics, with the ambition to create an open-source repository of trained models with corresponding objects' databases [3]. Amongst other steps, we currently explore the capacity for physics-informed

# AMMONIA-HYDROGEN COMBUSTION MODELLING ENABLED BY HIGH-PERFORMANCE GPU COMPUTING

D. KADDAR<sup>1</sup>, H. NICOLAI<sup>1</sup>, C. E. FROUZAKIS<sup>2</sup>, M. BODE<sup>3</sup>, C. HASSE<sup>1</sup>

<sup>1</sup> Technical University of Darmstadt (TUDa), Department of Mechanical Engineering, Simulation of reactive Thermo-Fluid Systems (STFS), Darmstadt, Germany

<sup>2</sup>Swiss Federal Institute of Technology (ETH Zurich), Laboratory for Aerothermochemistry and Combustion Systems, Zurich, Switzerland

<sup>3</sup> Forschungszentrum Jülich (FZJ), Jülich Supercomputing Centre (JSC), Institute for Advanced Simulation (IAS), Jülich, Germany  
e-mail: kaddar@stfs.tu-darmstadt.de

## 1 INTRODUCTION

To address the pressing issue of climate change, society confronts the formidable task of transitioning away from fossil fuels in our energy system. However, these fuels present fundamental challenges due to their distinct combustion and emission characteristics compared to hydrocarbon fuels. Hydrogen's high diffusivity and reactivity drive its strong turbulent burning rate, influenced by turbulent fluctuations and intense thermo-diffusive instabilities from differential diffusion (1). Conversely, ammonia, a promising hydrogen carrier, requires precise NOx emission control during partial decomposition. This study aims to fill the knowledge gap on these fuels, focusing on staged combustion with controlled flame propagation. By leveraging advanced high-performance computing tools, we seek to unlock the potential of fuel-flexible, high-power density combustion systems for zero-carbon gas turbines.

To fully exploit the potential of current and future HPC architectures, a recently developed extension to the GPU-capable spectral element method solver nekRS (2) for reactive flows, nekCRF, is employed, enabling high-fidelity direct numerical simulations (DNS) of configurations at technically relevant operating conditions.

## 2 CONFIGURATION

The setup involves a turbulent premixed  $\text{NH}_3/\text{H}_2/\text{N}_2$  jet flame operating under slightly rich conditions. This configuration, illustrated in Fig. 1, is adapted from a McKenna burner studied experimentally at TU Darmstadt.

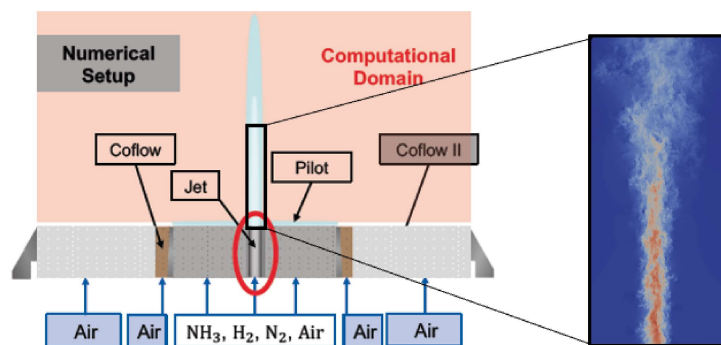


Figure 1: Schematic depiction of the McKenna burner configuration. Zoom shows the jet-flow field.

## 3 RESULTS

Figure 2 showcases the high-fidelity data from these DNS studies, illustrating flame structures as a function of temperature for the main fuel species ( $\text{NH}_3$ ,  $\text{H}_2$ ), and the OH and H

radicals. Additionally, one-dimensional freely propagating flames with unity Lewis number and mixture averaged transport models are displayed, which are used to build manifold-based combustion models (1). The scatter in the DNS data demonstrates reasonable agreement with both models. To establish a better comparison, temperature conditional averaging of the DNS data is performed, shown in the bottom row of Fig. 2. This comparison shows a favourable match of the conditional average with the mixture-averaged flamelets for both fuel species, with high-temperature differences attributed to unmodeled mixing with the surrounding co-flow of burnt gases, and low-temperature deviations due to turbulent mixing with ammonia pre-cracking. Notably, the radicals OH and H also align well with the mixture-averaged flamelet. As these species are markers for curvature and strain impacts on turbulent flame structures, it can be concluded that  $\text{NH}_3/\text{H}_2$  flames are less sensitive to curvature and strain than hydrogen flames, as reported in previous studies (1).

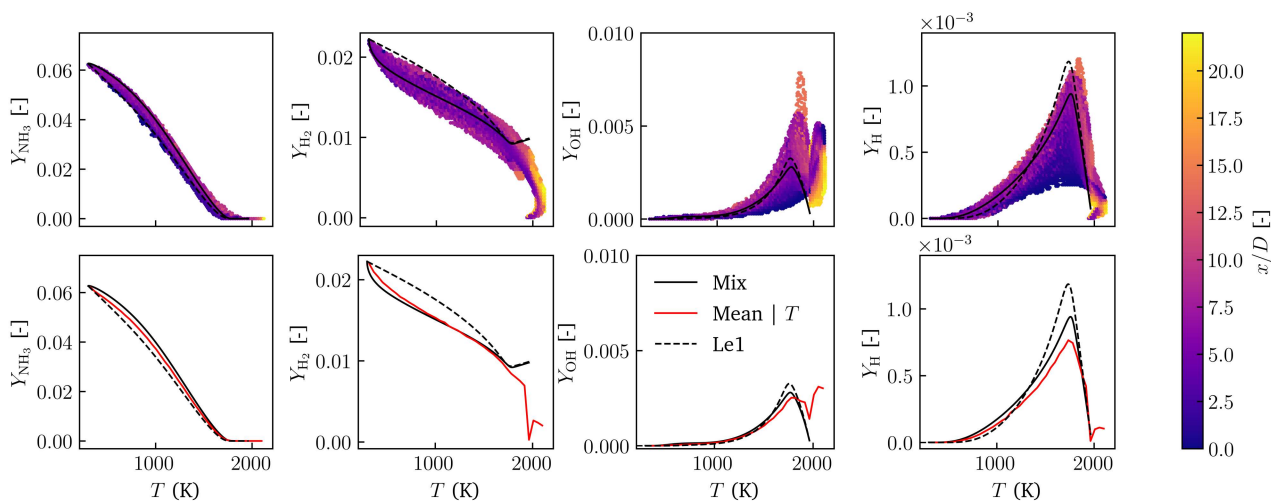


Figure 2: Top: Instantaneous scatters of the thermochemical state together with unity Lewis numbers and mixture-averaged flamelets. Bottom row: Conditional averaged of DNS data.

## 4 ACKNOWLEDGMENTS

This project has received funding from the European High-Performance Computing Joint Undertaking (JU) under grant agreement No 101118139. The JU receives support from the European Union’s Horizon Europe Program. The authors gratefully acknowledge the German Federal Ministry of Education and Research (BMBF) and state of Hesse for supporting this work as part of the NHR funding and the Gauss Centre for Supercomputing e.V. for funding this project by providing computing time on the GCS Supercomputer JUWELS at Jülich Supercomputing Centre (JSC).

## References

- [1] H. Böttler, D. Kaddar, T. J. P. Karpowski, F. Ferraro, A. Scholtissek, H. Nicolai, and C. Hasse, “Can flamelet manifolds capture the interactions of thermo-diffusive instabilities and turbulence in lean hydrogen flames?—An a-priori analysis,” *International Journal of Hydrogen Energy*, vol. 56, pp. 1397–1407, 2024.
- [2] P. Fischer, S. Kerkemeier, M. Min, Y.-H. Lan, M. Phillips, T. Rathnayake, E. Merzari, A. Tomboulides, A. Karakus, N. Chalmers, and T. Warburton, “NekRS, a GPU-accelerated spectral element Navier–Stokes solver,” *Parallel Computing*, vol. 114, p. 102982, 2022.

# Effect of swirl afflicted turbulence on pressure swirl spray in high-momentum jet-stabilised burners

Yeonse Kang<sup>1</sup>, Fabian Hampp<sup>1†</sup>

<sup>1</sup> Institute of combustion technology for aerospace engineering, University of Stuttgart, Germany

† fabian.hampp@ivlr.uni-stuttgart.de

Modern gas turbines (GT) assume a pivotal role in the decarbonisation of the energy, transportation and industrial sectors through the use of sustainable fuels including hydrogen (H<sub>2</sub>), ammonia (NH<sub>3</sub>) and sustainable aviation fuel (SAF) [1, 2]. To further reduce non-CO<sub>2</sub> emissions, future GTs require a co-optimisation of chemical energy vector and injection and combustor hardware to fulfil the fuel flexibility needs while offering low emissions. High-momentum jet-stabilised combustion systems (FLOX) are well known for their excellent fuel flexibility, being capable of utilising 100% H<sub>2</sub>, low calorific syngas as well as liquid fuels such as heating oil and kerosene, while ensuring wide operational flexibility and low emissions [3–6]. These advantages arise from the interaction of intense jet streams of radicals and heat, which promote robust exhaust gas recirculation within the combustor [4, 7]. However, the scalability of liquid fuel-operated FLOX burners towards compact designs, as required for hybrid aero-engine concepts and micro gas turbine systems, has been impeded by the lack of suitable injection concepts and axially elongated structure of the flame. The latter can be addressed by the implementation of swirler concepts. Low-swirl designs offer a promising approach featuring an open centre passage while realising divergent flow in the absence of an inner recirculation zone with short residence time. This aerodynamic flow relationship ensures reliable load flexibility and low emissions for various fuels [8, 9]. In related studies, Koyama and Tachibana [10] investigated liquid-operated low-swirl fuel nozzles in a 290 kW industrial GT combustor using kerosene. More recently, Kang et al. [11] integrated a low-swirl concept into a dual airblast atomizer, enhancing droplet atomization and mixture homogeneity and thereby expanding the operational range and reducing NO<sub>x</sub> emissions. Yet, the above studies emphasise the need to enhance the understanding of the interaction between highly turbulent air flow and liquid sprays systems to optimise atomization, mixture formation and combustion and ultimately reduce emissions.

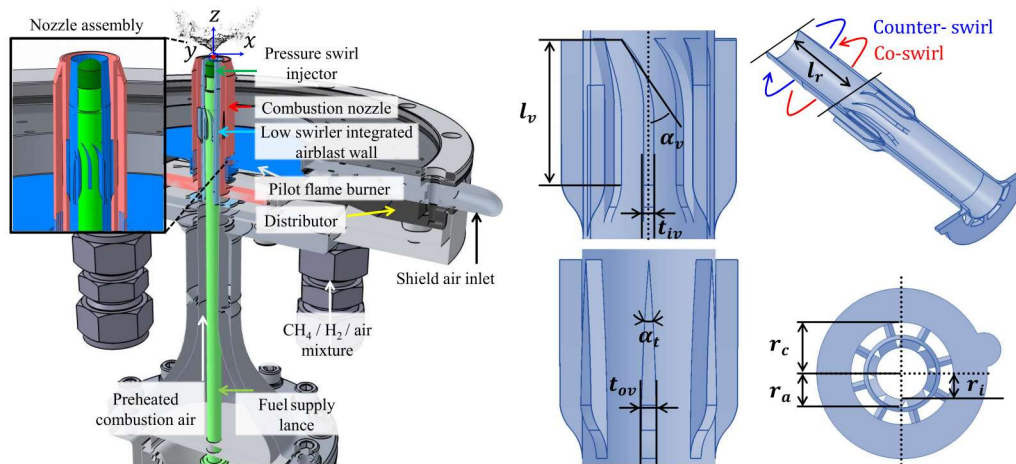


Figure 1: Single nozzle piloted jet spray flame burner schematic. Low swirl concepts are mounted and located with a recess length ( $l_r = 18$  mm) from the combustor nozzle exit with the coordinate system origin fixed to its centre. The right side sketches show the developed AM low swirl elements integrated into an airblast wall, featuring both straight and curved vanes. The bottom support plate serves to maintain the position and orientation.

To address the aforementioned, the current work investigates the interactions between low-swirl afflicted air flow and hollow cone pressure swirl spray in a high-momentum jet flame configuration. The left-hand side of Fig. 1 illustrates a schematic of the piloted jet-stabilised burner equipped with a modular additive manufactured low-swirl configuration, that is detailed in the right-hand side sketch [11]. The main air flow is geometrically split into outer (straight vanes, high-momentum flow) and inner (curved vanes, swirl-afflicted) air flow. To evaluate the influence of swirl on high-momentum airflow and spray behaviour, seven different low-swirl nozzles, ranging from  $-45^\circ$  to  $45^\circ$  vane angles in  $15^\circ$  increments, are used. Atomization performance is characterised using phase Doppler interferometry and shadowgraphy measurements. The combustion process is measured by means of OH\* chemiluminescence imaging and exhaust gas analysis. The data are analysed across a wide range of jet velocities ( $80 \leq u_j$  (m/s) < 160) and fuel mass flow rates ( $0.1 \leq \dot{m}_l$  (g/s)  $\leq 0.5$ ) to evaluate the aerodynamic and liquid loading effects. The influence of swirl-afflicted air on the high-momentum jet-stabilised flame is delineated from the perspectives of both spray and combustion behaviours



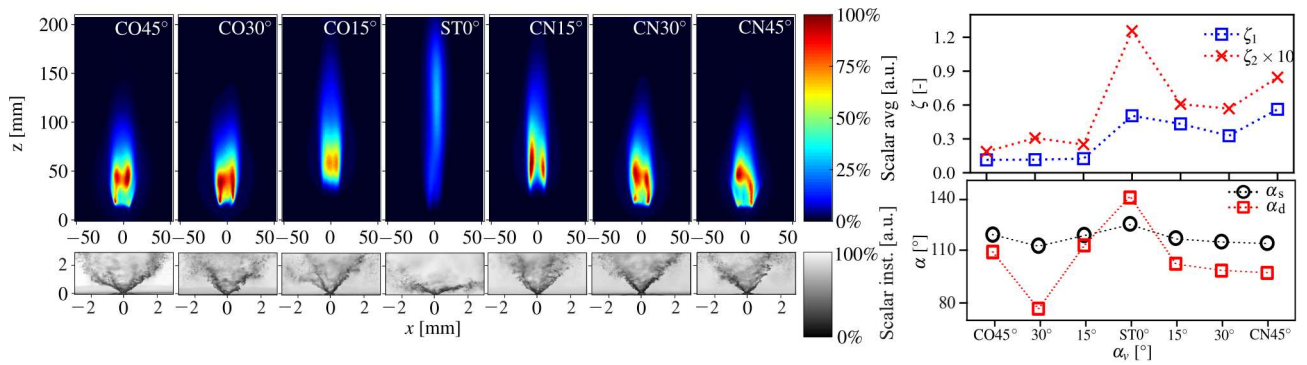


Figure 2: Left: Series of time averaged OH\*-CL and instantaneous shadowgraphy images for the low-swirl variation. Right: Low-Swirl effect on flame symmetry (top) and spray sheet and dispersion angle (bottom).

Figure 2 displays time averaged OH\* and instantaneous shadowgraphy images as a function of low-swirl directions and angles to provide a global view of the flame and pressure swirl spray behaviour. For the conventional injector, ST0° shows a notably elongated flame structure (flame lift-off height of 20 mm and penetration of 200 mm) and low OH\* chemiluminescence (CL) intensity. The introduction of circumferential gaseous flow velocity around the hollow cone pressure swirl spray results in a more compact and spatially broadened heat release zone, as indicated by the OH\*-CL distribution, with improved axial symmetry. Regarding spray behaviour, the ST0° case exhibits a significantly widened spray dispersion angle with a pronounced flapping mode due to the interaction of the high momentum coaxial gaseous flow with the bluff body geometry of the injector creating a wake. Conversely, swirl-afflicted air flow gradually restores the nominal hollow cone spray angle as the swirl number increases. While turbulent dispersion inherently promotes homogeneous mixture formation, periodic vortex shedding in the spray wake can lead to fluctuating mixture stratification with elevated emissions. Besides resulting in modestly improved atomization and distinctly enhanced radial droplet dispersion, low-swirl afflicted air flow acts stabilising on the liquid spray sheet surface by suppressing such flow features. These effects are further quantified by means of spray sheet statistics, e.g. growth rates, curvature, as well as droplet size and dispersion statistics. The transition from jet stabilised over multi-mode to swirl influenced combustion, analysed via POD, is further supported by flame lift-off height and penetration measurements. The improved spray dispersion results, despite the significantly more compact heat release zone, in reduced NO<sub>x</sub> emissions and a predominant absence of soot in the studied direct injection kerosene flames. These results underline the necessity to co-optimize practical liquid fuel injection systems in application related highly turbulent flow environments.

### Acknowledgments

The authors acknowledge the funding by the Deutsche Forschungsgemeinschaft (DFG, German Research Foundation) - project numbers: 456687251. We further acknowledge the support by the German Aerospace Center (DLR) Stuttgart.

### References

- [1] M. Molière, The fuel flexibility of gas turbines: A review and retrospective outlook, *Ener.* 16 (2023) 3962.
- [2] M. Huth, A. Heilos, Fuel flexibility in gas turbine systems: impact on burner design and performance, in: Y. Sakai, C. Vassilicos (Eds.), *Modern Gas Turbine Systems*, Woodhead Publishing, 2013.
- [3] H. Schütz, R. Lückcrath, B. Noll, M. Aigner, Complex Chemistry Simulation of : Flameless Oxidation Combustion, *Clean Air International Journal on Energy for a Clean Environment* 8 (3) (2007) 239.
- [4] R. Lückcrath, W. Meier, M. Aigner, Combustion at High Pressure with Different Fuel Compositions, *Journal of Engineering for Gas Turbines and Power* 130 (1) (2008) 011505.
- [5] F. Hampp, J. D. Gounder, H. Ax, R. Lückcrath, O. Lammel, M. Hase, B. Janus, High momentum jet flames at elevated pressure, E: Quantification of droplet size distribution and transport, *ASME* (2020) GT2020-14619.
- [6] F. Hampp, D. Schäfer, O. Lammel, Spray flame characterization of a duel injector for compact combustion systems, *Comb. Sci. Tech.* (2023) DOI: 10.1080/00102202.2023.2249222.
- [7] O. Lammel, H. Schütz, G. Schmitz, R. Lückcrath, M. Stöhr, B. Noll, M. Aigner, M. Hase, W. Krebs, Combustion at High Power Density and High Flame Temperatures, *Journal of Engineering for Gas Turbines and Power* 132 (12) (2010) 121503.
- [8] R. K. Cheng, Low swirl combustion, *The Gas Turbine Handbook*, 2006.
- [9] R. Cheng, D. Littlejohn, W. Nazeer, K. Smith, Laboratory studies of the flow field characteristics of low-swirl injectors for application to fuel-flexible turbines, *J. Eng. Gas Turb. Power* 130 (2008) 021501.
- [10] M. Koyama, S. Tachibana, Technical applicability of low-swirl fuel nozzle for liquid-fueled industrial gas turbine combustor, *Fuel* 107 (2013) 766-776.
- [11] Y. Kang, J. Ahn, F. Hampp, Low swirl effect on compact spray and combustion systems using additive manufactured dual airblast injectors, *ASME* (2024) GT2024-125618.



# CO emissions in turbulent premixed methane/hydrogen jet flames interacting with isothermal walls

Kai Niemietz\*, Heinz Pitsch

*Institute for Combustion Technology, RWTH Aachen University, 52056 Aachen, Germany*

\*Corresponding author: k.niemietz@itv.rwth-aachen.de

## Introduction

The low load operating range of stationary gas turbines is often limited by the carbon monoxide (CO) concentration. Due to low temperatures, CO is not fully oxidized and kinetically controlled, non-equilibrium CO remains in the exhaust gas. Flame-wall interactions (FWI) strongly influence the CO chemistry and thus the downstream concentration [1, 2]. The addition of small amounts of hydrogen (H<sub>2</sub>) to the methane (CH<sub>4</sub>) fuel may be able to reduce the exhaust CO concentration by increasing the mixtures' reactivity [3]. The small amounts of hydrogen substitution are not expected to cause characteristic thermodiffusive instabilities in the flame but do increase the flame speed and the radical pool available for CO oxidation. In this investigation, we will evaluate the influence of hydrogen substitution in turbulent premixed methane jet flames with flame-wall interaction. Three direct numerical simulations (DNS) are analyzed. The first case is the reference without hydrogen, introduced at the previous TNF workshop [2]. Two additional DNS are being performed, where 10% and 20% of the fuel volume are substituted by hydrogen, while keeping the adiabatic flame temperature constant.

## Methodology

The simulation domain is set up to capture the most relevant effects in gas turbine combustion including high strain rates due to the turbulent flow, large areas of strong FWI, and two distinct recirculation regions, where cooled burnt gas interacts with the flame. As shown in Figure 1, the inlet consists of two parallel turbulent slot jets separated by a laminar pilot. Isothermal, no-slip walls enclose the domain in the crosswise direction; periodic boundary conditions are implemented in the spanwise direction. The simulation grid contains 3.1 billion cells. The reactive, unsteady Navier-Stokes equations are solved in the low-Mach limit using the in-house finite-differences solver CIAO [4]. The unburnt gas in the pure methane case is a methane/air mixture with an equivalence ratio of  $\varphi = 0.5$ . In the two cases containing hydrogen, the equivalence ratio is slightly lowered ( $\varphi \approx 0.495$ ) to maintain a constant adiabatic flame temperature. The unburnt temperature is  $T = 673$  K and the simulations are performed at an elevated pressure of  $p = 4$  atm. The bulk inlet velocity of the jets is  $u_j = 73.5$  m/s and the jet width is  $h_j = 1.2$  mm resulting in a jet Reynolds number ( $Re_j = u_j h_j / \nu$ ) of 5500, where  $\nu$  is the kinematic viscosity of the reactants. Finite rate chemistry is employed, using a skeletal methane mechanism with 25 species which was derived from the full mechanism of Cai et al. [5]. The crosswise walls have a constant wall temperature of  $T_w = 1000$  K and the inlets are enclosed by adiabatic walls.

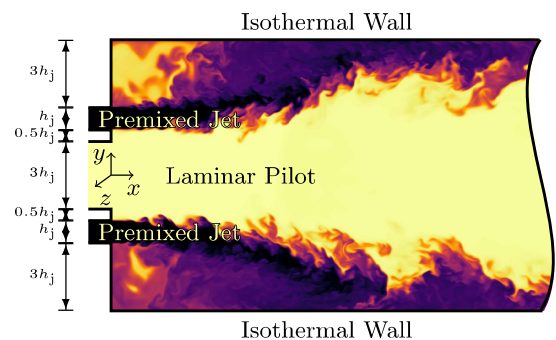


Figure 1: Sketch of the simulation domain. Color indicates the temperature field. The inflow consists of two turbulent jets with a laminar pilot in the center [2].

## Results

The preliminary results indicate that the influence of hydrogen addition in turbulent flames is stronger than in laminar flames. Both the global flame parameters and emissions show distinct changes. It must be noted that the images are not taken at the same time, as the simulations are currently still running and not converged. Results are intended as indications only and may still change.

Instantaneous images of the temperature fields are shown in Figure 2. The three cases (0%, 10%, and 20% H<sub>2</sub>) are shown top to bottom. The flame becomes considerably shorter with increasing hydrogen content. This additionally reduces the intensity of the flame-wall interaction which may further shorten the flame. Joint probability density functions (JPDF) of the CO mass fraction  $Y_{CO}$  and the progress variable  $C$  are presented in Figure 3. Some progress variable overshoots are observed in the hydrogen cases which are not present in the pure methane case.

With increasing  $H_2$  concentrations, the conditional means of the DNS data become closer to the results of the unstretched flamelet solution. One possible explanation is the increasing flame speed which compensates the slower chemistry due to lower temperatures. Additionally, the reduced FWI may also reduce the non-flamelet behavior. Further analysis is necessary to understand these phenomena in greater detail.

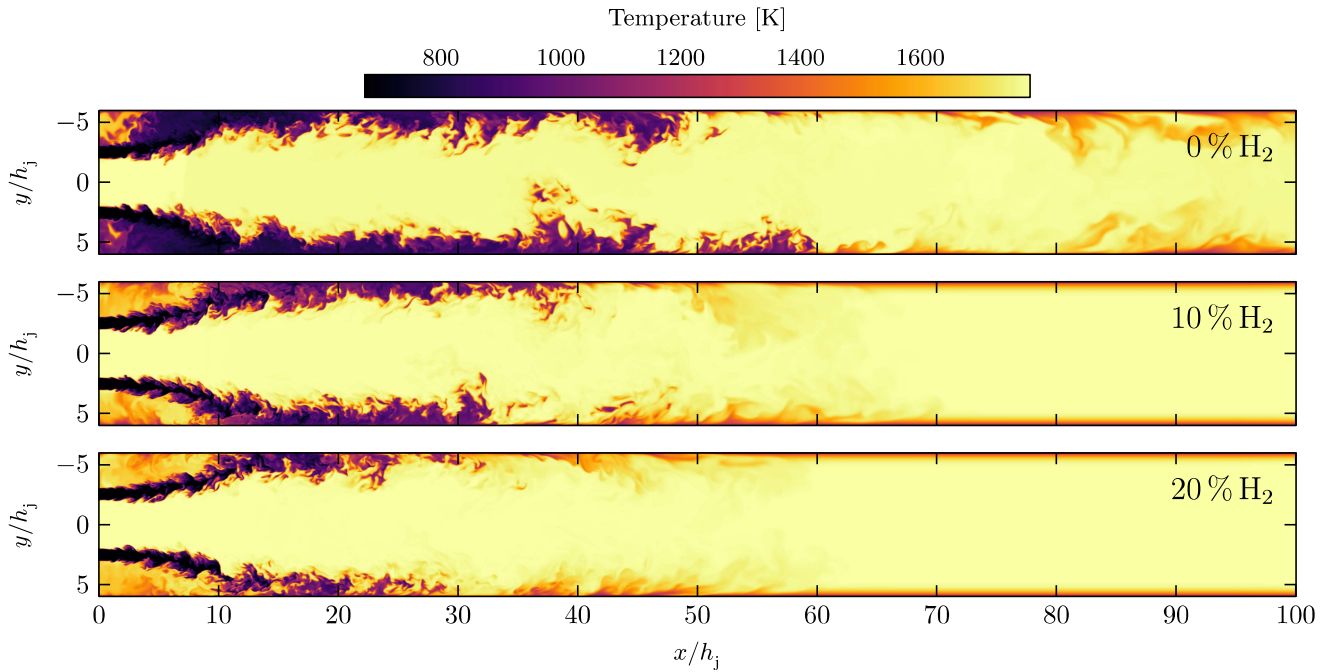


Figure 2: Instantaneous temperature fields for the three fuel ratios.

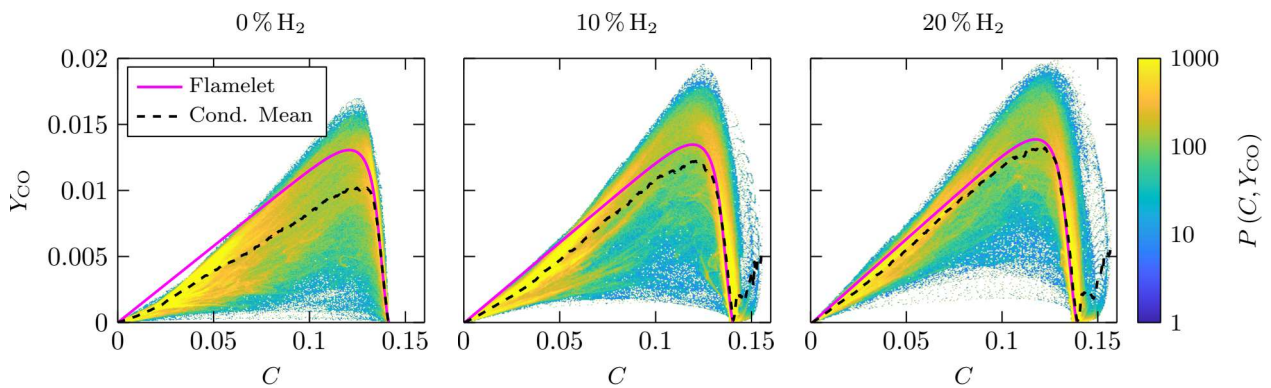


Figure 3: JPDF of CO mass fraction and progress variable. The color plots show the JPDF in logarithmic scale; the conditional mean and the unstretched flamelet solution are included in the figures.

## References

- [1] H. Kosaka, F. Zentgraf, A. Scholtissek, L. Bischoff, T. Häber, R. Suntz, B. Albert, C. Hasse, A. Dreizler, *Int. J. Heat Fluid Flow* 70 (2018) 181–192.
- [2] K. Niemi, L. Berger, M. Huth, A. Attili, H. Pitsch, *Proc. Combust. Inst.* 39 (2) (2023) 2209–2218.
- [3] A. Biber, C. Wieland, H. Spliethoff, in: 30. Deutscher Flammentag, Hannover-Garbsen, 28–29 September, 2021.
- [4] O. Desjardins, G. Blanquart, G. Balarac, H. Pitsch, *J. Comput. Phys.* 227 (15) (2008) 7125 – 7159.
- [5] L. Cai, A. Ramalingam, H. Minwegen, K. A. Heufer, H. Pitsch, *Proc. Combust. Inst.* 37 (1) (2019) 639–647.

# Analysis of $NO$ formation pathways based on extended proper orthogonal decomposition in a swirl-stabilised, hydrogen-fuelled gas turbine combustor.

Rahul Palulli, Christophe Duwig

Department of Chemical Engineering, KTH Royal Institute of Technology, Brinellvagen 8, Stockholm 114 28, Sweden

Contact email: [palulli@kth.se](mailto:palulli@kth.se) (Rahul Palulli)

Use of hydrogen fuel offers a promising solution in the journey towards decarbonisation as it does not produce carbon-based emissions. However, hydrogen combustion features other harmful emissions such as the oxides of nitrogen ( $NO_x$ ). A detailed comprehension of these  $NO_x$  emissions and its formation pathways is necessary to facilitate its mitigation. This study aims to present a methodology to analyse the  $NO$  formation pathways in a swirl-stabilised, hydrogen-fuelled gas turbine combustor.

In this study, large-eddy simulations (LESs) are performed on the AHEAD burner developed at TU Berlin [1], the details of which are available in the TNF workshop's website [2]. The computational domain used is shown in Figure 1 where the green arrows represent the air inlet flow and the red arrows indicate fuel inlet flow. The fuel streams enter the domain through two plenums and are then injected into the mixing tube through numerous small orifices. The air stream enters the domain through axial and radial slots. The fuel and air mix in the mixing tube before entering the combustion chamber. The sudden expansion into the combustion chamber forms recirculation regions near the centreline and near the walls at the combustor inlet which also facilitate flame stabilisation. A hydrogen/air flame with an equivalence ratio of 0.6 is simulated in this study.

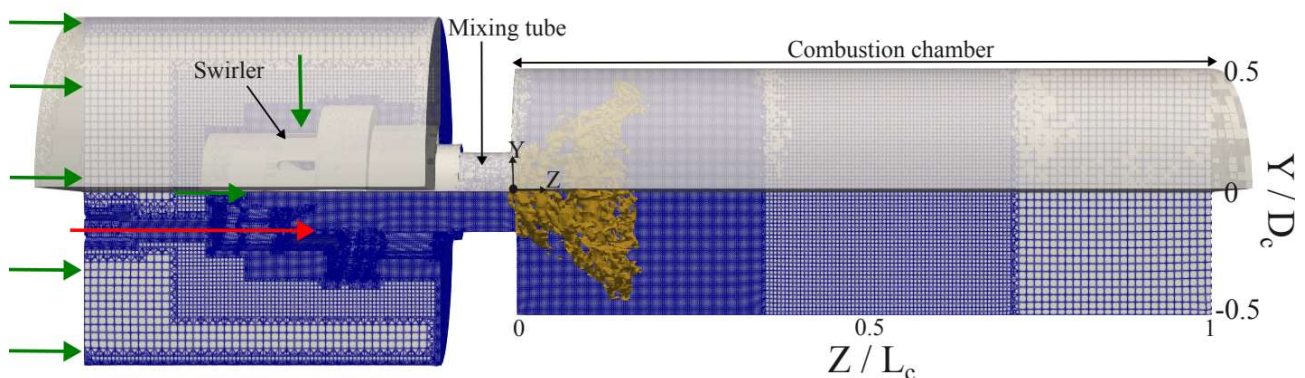


Figure 1: The computational domain [3].

The objective of this study is to combine the LES results, extended proper orthogonal decomposition (EPOD) analysis and zero-dimensional (0D) perfectly-stirred reactors (PSRs) to shed more light on the  $NO$  formation pathways in this swirl-stabilised, hydrogen-fuelled gas turbine combustor. This provides an efficient combination of high-fidelity LES simulation and a zero-

dimensional (0D) ideal reactor analysis aided by the use of EPOD. While the LES simulation reveals the flow and flame characteristics in detail, the 0D ideal reactor analysis provides a useful tool to understand the underlying chemistry in detail. Moreover, application of EPOD on the LES results helps one to identify the spatial locations and time instants which feature significant fluctuations of a variable of interest. Therefore, the 0D analysis can be limited to those spatial-temporal combinations thus reducing the number of points where a detailed chemistry analysis needs to be performed.

First, LES simulations are performed for the conditions mentioned above. Then, EPOD is performed on the LES results based on rate of production of *NO* ( $ROP_{NO}$ ). These results provide directions to identify the points which feature maximum variations in *NO* production rate. The species compositions and temperature at these identified points obtained using LES are exported to a 0D PSR to perform detailed chemical pathway analysis. This 0D PSR analysis reveals the contribution of individual reactions to the *NO* production and consumption. Furthermore, a pathway diagram also facilitates visualisation of the various *NO* formation pathways. The *NO* formation pathway obtained at the identified points and the contribution of individual reactions towards *NO* production and consumption will be presented at the TNF workshop 2024.

#### References:

1. T. G. Reichel, S. Terhaar, O. Paschereit, Increasing Flashback Resistance in Lean Premixed Swirl-Stabilized Hydrogen Combustion by Axial Air Injection, *J. Eng. Gas Turbine. Power* 137(7) 071503.
2. <https://tnfworkshop.org/ahead-lean-premixed-swirl-stabilized-hydrogen-burnertu-berlin/>
3. R. Palulli, K. Zhang, C. Duwig, Extended proper orthogonal decomposition based investigation of *NO* formation pathways in a non-premixed, hydrogen-fuelled, gas turbine combustor, *Advances in Appl. Energy* [manuscript to be submitted].



# Investigation of hydrogen-air mixing behavior in an atmospheric jet-stabilized single nozzle combustor using 1-D laser Raman spectroscopy

Niklas Petry, Zhiyao Yin, Holger Ax, Klaus-Peter Geigle, Oliver Lammel, Andreas Huber

German Aerospace Center (DLR), Institute of Combustion Technology, Pfaffenwaldring 38-40, 70569 Stuttgart, Germany

niklas.petry@dlr.de

## 1. Introduction

In the present study, 1-D laser Raman spectroscopy is employed to investigate the mixing of fuel ( $H_2$ ) and oxidizer (air) in jet-stabilized turbulent non-premixed flames. Extensive research has explored the mixing dynamics of coaxial jets with hydrocarbon fuels [1]. However, there remains a scarcity of experimental data in the literature concerning turbulent and differential diffusive mixing in hydrogen-air turbulent non-premixed flames (TNF), one of very few is [2]. Notably, the significance of molecular diffusivity in TNF is increased with hydrogen as fuel [3]. To concurrently measure the absolute concentrations of major species, such as  $H_2$ ,  $O_2$ ,  $N_2$ , and  $H_2O$ , and temperature, 1-D laser Raman spectroscopy is currently deemed the most suitable method. The calculation of the mixture fraction, as proposed by Bilger [3], accounts for both turbulent and molecular diffusive mixing mechanisms.

The importance of jet-stabilized combustion has grown significantly in the past decade and represents a beneficial combustor design for stationary gas turbines [4]. However, in the context of utilizing hydrogen as a fuel in aircraft engines, achieving homogeneous and efficient mixing over short distances is particularly desirable. Additionally, stringent security requirements pertaining to combustion stability must be met, with flame flashback strictly prohibited. Hence, a non-premixed fuel-air nozzle configuration, as depicted in Fig. 1, is ideally suited. Figure 1 also illustrates the measurement positions both across and downstream of the nozzle, where 1-D laser Raman spectroscopy was performed.

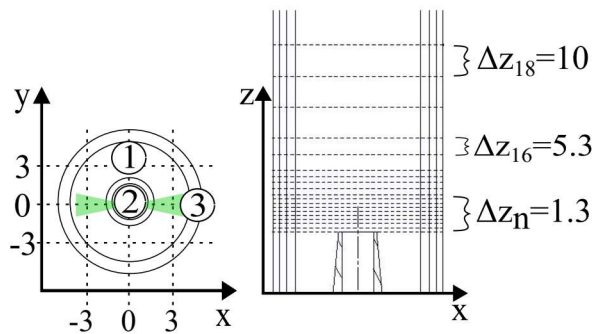


Fig. 1: Measurement positions for 1-D laser Raman spectroscopy. (1) air nozzle (2) fuel injector, (3) the laser beam path is visualized in green

hibited a temporal energy distribution resembling a classical rectangular pulse shape. In Fig. 2 the 1-D laser Raman setup is shown, where the Raman scattering from the 6 mm sample length was collected by an apochromatic lens ( $f = 230$  mm, diameter = 150 mm) and directed into the entrance slit of a spectrometer (Acton Research SpectrPro 300i;  $f = 300$  mm;  $f/4.2$ , 420 lines/mm, slit: 1 mm  $\times$  14 mm). A narrow-band filter ( $\lambda = 532$  nm) placed before the entrance slit removed surface scattered light. An image-intensified ICCD (Princeton Instruments PI-Max; 1340  $\times$  1300 pixels, 16 bit/pixel) was positioned at the spectrometer's exit aperture. Pixel binning into superpixels significantly reduced noise, resulting in a final digital resolution of 268  $\times$  28 superpixels for each single-shot image (spatial resolution: 0.214 mm per superpixel). 300 single-shot spectra were recorded for each measurement position. For enhancing the signal-to-noise ratio, background correction is performed on each single-shot spectrum with an averaged background spectrum. This involves the use of a  $\lambda/2$  plate to modify the laser beam's polarization, effectively reducing the Raman signal in the background. Quantifying major species concentrations from 1-D Raman measurements involves post-processing. This includes applying the ideal gas law and temperature-dependent calibration coefficients unique to each species. These coefficients are determined

## 2. Measurement technique

This study evaluates mixing quality using two injectors: a conventional straight pipe and a novel annular contour injector. Both were tested within a non-premixed nozzle configuration in a confined atmospheric single-nozzle ( $D_{air, nozzle} = 10$  mm) combustor, featuring the pronounced recirculation zone typical of FLOX systems. 1-D laser Raman scattering was used for one-dimensional quantitative measurement of burned and unburned species ( $O_2$ ,  $H_2$ ,  $H_2O$ , and  $N_2$ ) concentrations, alongside temperature. The laser beam, with a pulse duration of  $\tau_{pulse} = 1$   $\mu$ s and pulse energy of  $E_{pulse} = 1$  J/pulse at  $\lambda = 532$  nm, exhibited a temporal energy distribution resembling a classical rectangular pulse shape.



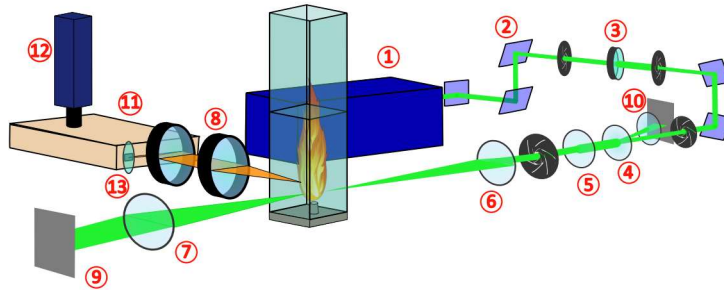


Fig. 2: *Experimental setup for the 1-D Raman laser spectroscopy. 1 = Nd:YAG laser; 2 = mirror; 3 =  $\lambda/2$  plate; 4 = plano concave lens; 5 = biconvex lens; 6, 7 = plano convex; 8 = achromatic lens; 9/10 = energy detector; 11 = spectrograph; 12 = ICCD camera; 13 = notch filter ( $\lambda = 532$  nm)*

through prior calibration measurements of the respective species or their mixtures at known concentrations and temperatures.

### 3. Results and Discussions

The results depicted in Fig. 3 present exemplarily a 2-D reconstruction of the averaged concentration for hydrogen and the mixture fraction downstream of the nozzle exit. The entire dataset, including  $H_2$ ,  $O_2$ ,  $N_2$ ,  $H_2O$ , and mixture fraction, was obtained at the center plane ( $y = 0$  mm) of the nozzle. The 2-D reconstructed absolute data for the 18 measurement positions are interpolated onto a grid of 255x255 pixels with a relative error of less than 2 % of the absolute value.

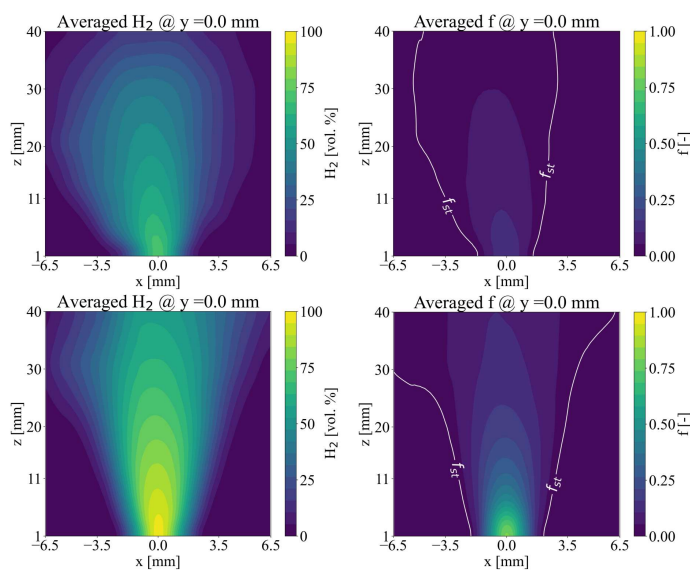


Fig. 3: *2-D reconstruction of experimentally measured  $H_2$  and mixture fraction. Upper row:  $H_2$  concentration (left) and mixture fraction (right) for novel injector design; bottom row: mean  $H_2$  concentration and mixture fraction for fuel tube*

The recorded dataset is expected to be valuable for CFD model validation.

### References

1. H. Eickhoff et al., "Experimental investigation on the stabilization mechanism of jet diffusion flames," Symposium (International) on Combust. **20**, 311–318 (1985).
2. A. Vranos et al., "An experimental study of the stability of hydrogen-air diffusion flames," Combust. Flame **12**, 253–260 (1968).
3. R. Bilger, "The structure of turbulent nonpremixed flames," Symposium (International) on Combust. **22**, 475–488 (1989).
4. W. Krebs et al., "Advanced Combustion System for High Efficiency (ACE) of the New SGT5/6- 9000HL Gas Turbine," ASME Proc. **GT2022-82299** (2022).

# Measurements of NO in the product gases of laminar premixed NH<sub>3</sub>/H<sub>2</sub>/N<sub>2</sub>-air and NH<sub>3</sub>/CH<sub>4</sub>-air flames using laser induced fluorescence.

M. Richter<sup>a,b,c,\*</sup>, J. Lill<sup>b,c</sup>, R.S. Barlow<sup>d</sup>, A. Gruber<sup>e</sup>, A. Dreizler<sup>c</sup>, J.R. Dawson<sup>a</sup> and D. Geyer<sup>b</sup>

<sup>a</sup> Department of Energy and Process Engineering (EPT), Norwegian University of Science and Technology, Trondheim, Norway  
<sup>b</sup> Laboratory for Optical Diagnostics and Renewable Energies (ODEE), University of Applied Sciences Darmstadt, Darmstadt, Germany  
<sup>c</sup> Reactive Flows and Diagnostics (RSM), Technical University of Darmstadt, Darmstadt, Germany  
<sup>d</sup> Barlow Combustion Research, Livermore, USA  
<sup>e</sup> Thermal Energy, SINTEF Energy Research, Trondheim, Norway

\* Corresponding author: martin.richter@ntnu.no

Ammonia-based fuels have been identified as a promising zero-carbon energy carriers due to their high energy density, relative to hydrogen, and simpler logistics. However, a potential disadvantage is the presence of fuel-bound nitrogen which can lead to order of magnitude higher emissions of undesired nitrogen oxides (NO<sub>x</sub>) compared to conventional fuels. Presently, chemical kinetics schemes for ammonia combustion still show large differences in the prediction of nitric oxide (NO). Quantitative experimental data are therefore needed to validate and optimize these reaction mechanisms. This study presents measurements of NO in the product gases of laminar premixed NH<sub>3</sub>/H<sub>2</sub>/N<sub>2</sub>-air (27 - 45 % H<sub>2</sub>) flames, which mimics partially dissociated ammonia, and NH<sub>3</sub>/CH<sub>4</sub>-air (40 - 80 % CH<sub>4</sub>) flames. These flames are stabilized on a flat-flame burner. NO is probed in its A-X(0,1) system near 236 nm using linear laser induced fluorescence (LIF). A calibration approach based on the addition of NO to a lean premixed CH<sub>4</sub> flame is presented. The LIF signals are corrected for changes in the Boltzmann fraction, line overlap, number density, and quenching. Temperature measurements using N<sub>2</sub> thermometry [1] allow characterization of the adiabaticity of the operating conditions and adjustment of the signal corrections to the local temperature. Major species are extracted from 1-D simulations.

The temperatures obtained from the Raman thermometry N<sub>2</sub> fits [1] are 0-4% below the adiabatic flame temperature. Signal corrections based on changes in number density, Boltzmann fraction, absorption line broadening and quenching combined are in the order of 10 %. The highest NO mole fractions were 1.3 % for NH<sub>3</sub>/H<sub>2</sub>/N<sub>2</sub> (at 45 % H<sub>2</sub>) and 0.9 % for NH<sub>3</sub>/CH<sub>4</sub> (at 50 % CH<sub>4</sub>). The measured NO mole fractions are compared with different chemical kinetic schemes, depending on the fuel mixture. For NH<sub>3</sub>/H<sub>2</sub>/N<sub>2</sub>, the tested models show good agreement for rich mixtures and a slight underprediction of NO for lean mixtures. For NH<sub>3</sub>/CH<sub>4</sub>, experimental data and tested models show good agreement for intermediate levels of CH<sub>4</sub>, whereas significant deviations are found for rich mixtures at higher levels of CH<sub>4</sub> in the fuel. The present study provides a comprehensive data set of NO mole fractions measured in the product gases of NH<sub>3</sub>/H<sub>2</sub>/N<sub>2</sub>-air and NH<sub>3</sub>/CH<sub>4</sub>-air flames. Comparison with recent chemical kinetic models indicates that none of the models can predict NO mole fractions over the full range of fuel mixtures and equivalence ratios investigated here. The data presented can be used to validate and optimize chemical kinetic models.

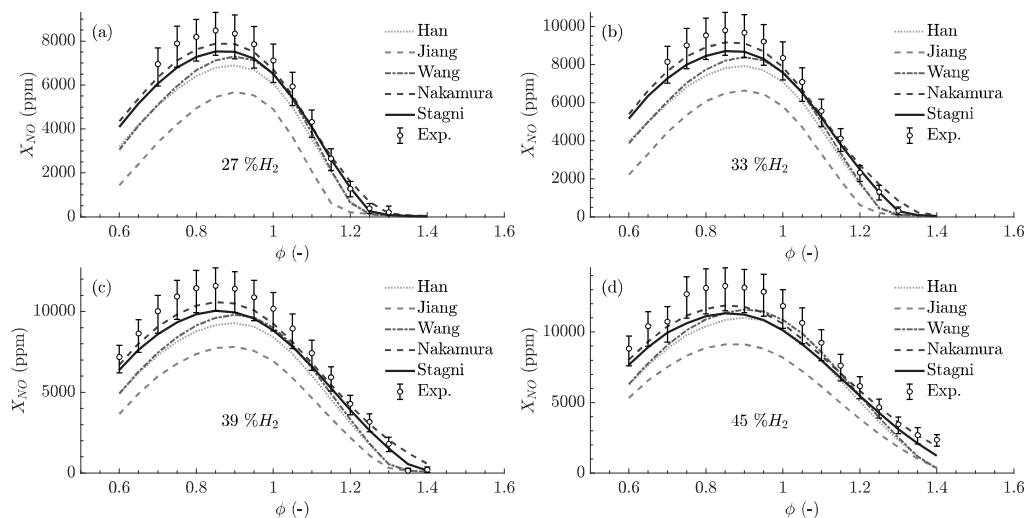


**Figure 1:** Experimental and numerical mole fractions of NO for four different NH<sub>3</sub>/H<sub>2</sub>/N<sub>2</sub> blends ranging from 27 % to 45 % H<sub>2</sub>. Error bars combine stochastic uncertainties (1 $\sigma$ ), uncertainties from the calibration measurement and systematic errors. Chemical kinetic models by Han et al. [2], Jiang et al. [3], Wang et al. [4], Nakamura et al. [5] and Stagni et al. [6].

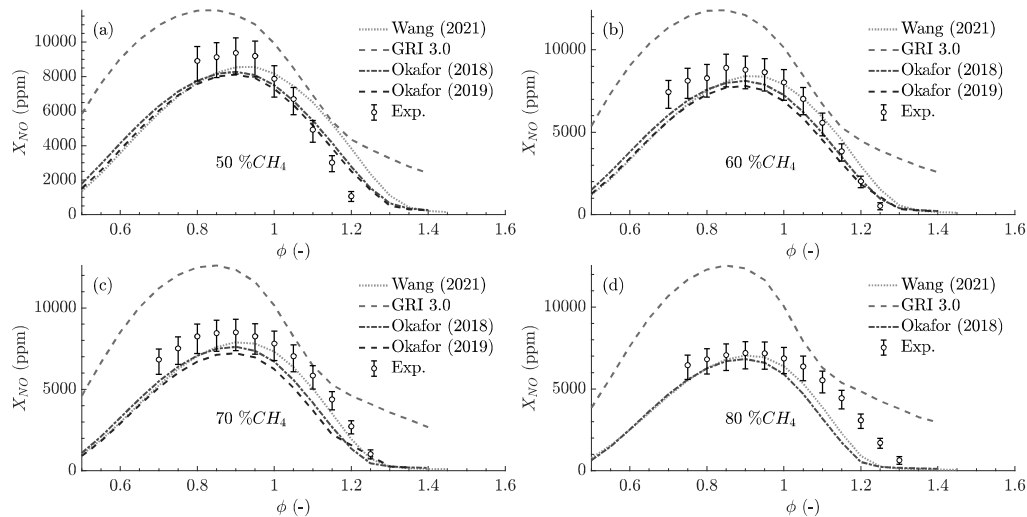


**Figure 2:** Experimental and numerical mole fractions of NO for four different NH<sub>3</sub>/CH<sub>4</sub> blends ranging from 50 % to 80 % CH<sub>4</sub>. Chemical kinetic models: Wang et al. [4], GRI 3.0 [7], Okafor et al. [8,9].

## References

- [1] J. Lill, K. Dieter, K. Koschnick, A. Dreizler, G. Magnotti, D. Geyer, Measurement and simulation of temperature-dependent spontaneous Raman scattering of O<sub>2</sub> including P and R branches, *J. Quant. Spectrosc. Radiat. Transf.* 297 (2023) 108479. <https://doi.org/10.1016/j.jqsrt.2022.108479>.
- [2] X. Han, Z. Wang, Y. He, Y. Zhu, K. Cen, Experimental and kinetic modeling study of laminar burning velocities of NH<sub>3</sub>/syngas/air premixed flames, *Combust. Flame* 213 (2020) 1–13. <https://doi.org/10.1016/j.combustflame.2019.11.032>.
- [3] Y. Jiang, A. Gruber, K. Seshadri, F. Williams, An updated short chemical-kinetic nitrogen mechanism for carbon-free combustion applications, *Int. J. Energy Res.* 44 (2020) 795–810. <https://doi.org/10.1002/er.4891>.
- [4] Z. Wang, X. Han, Y. He, R. Zhu, Y. Zhu, Z. Zhou, K. Cen, Experimental and kinetic study on the laminar burning velocities of NH<sub>3</sub> mixing with CH<sub>3</sub>OH and C<sub>2</sub>H<sub>5</sub>OH in premixed flames, *Combust. Flame* 229 (2021) 111392. <https://doi.org/10.1016/j.combustflame.2021.02.038>.
- [5] H. Nakamura, S. Hasegawa, T. Tezuka, Kinetic modeling of ammonia/air weak flames in a micro flow reactor with a controlled temperature profile, *Combust. Flame* 185 (2017) 16–27. <https://doi.org/10.1016/j.combustflame.2017.06.021>.
- [6] A. Stagni, S. Arunthanayothin, M. Dehue, O. Herbinet, F. Battin-Leclerc, P. Bréquigny, C. Mounaïm-Rousselle, T. Faravelli, Low- and intermediate-temperature ammonia/hydrogen oxidation in a flow reactor: Experiments and a wide-range kinetic modeling, *Chem. Eng. J.* 471 (2023) 144577. <https://doi.org/10.1016/j.cej.2023.144577>.
- [7] G.P. Smith, D.M. Golden, M. Frenklach, N.W. Moriarty, B. Eiteneer, M. Goldenberg, T.C. Bowman, R.K. Hanson, S. Song, W.C. Gardiner, V.V. Lissianski, Z. Qin, [http://www.me.berkeley.edu/gri\\_mech/](http://www.me.berkeley.edu/gri_mech/).
- [8] E.C. Okafor, Y. Naito, S. Colson, A. Ichikawa, T. Kudo, A. Hayakawa, H. Kobayashi, Experimental and numerical study of the laminar burning velocity of CH<sub>4</sub>–NH<sub>3</sub>–air premixed flames, *Combust. Flame* 187 (2018) 185–198. <https://doi.org/10.1016/j.combustflame.2017.09.002>.
- [9] E.C. Okafor, Y. Naito, S. Colson, A. Ichikawa, T. Kudo, A. Hayakawa, H. Kobayashi, Measurement and modelling of the laminar burning velocity of methane-ammonia-air flames at high pressures using a reduced reaction mechanism, *Combust. Flame* 204 (2019) 162–175. <https://doi.org/10.1016/j.combustflame.2019.03.008>.

# NEAR-WALL COMBUSTION OF PREMIXED UNSTABLE H<sub>2</sub>-AIR FLAMES

M. SCHNEIDER<sup>1</sup>, H. NICOLAI<sup>1</sup>, C. HASSE<sup>1</sup>

<sup>1</sup> Technical University of Darmstadt (TUDA)

Department of Mechanical Engineering, Simulation of reactive Thermo-Fluid Systems

Otto-Berndt-Str. 2, 64287 Darmstadt, Germany

e-mail: schneider@stfs.tu-darmstadt.de

## 1 INTRODUCTION

Green hydrogen is a promising carbon-free energy carrier for electricity, propulsion, and the chemical industry. Integrating hydrogen into existing energy systems is effectively done through thermochemical energy conversion (1). Fuel-lean premixed combustion generates less NO<sub>x</sub> emissions compared to non-premixed or stoichiometric combustion due to lower exhaust gas temperatures (2).

However, lean premixed hydrogen/air flames face challenges, mainly due to combustion instabilities affecting flame dynamics, heat release rates, and flame speeds. In lean premixed hydrogen flames, the low Lewis number of hydrogen causes strong differential diffusion effects, leading to wrinkled flame fronts and increased fuel conversion rates, known as thermodiffusive instability.

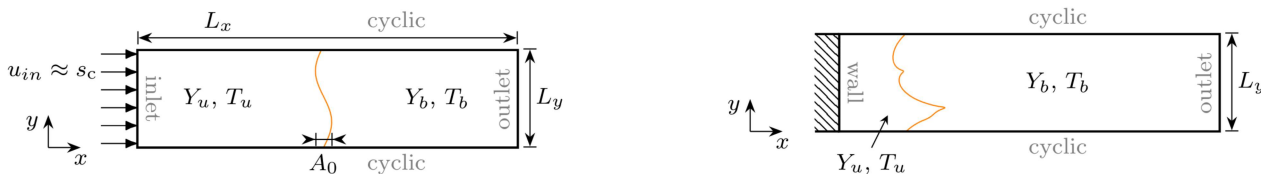
Another challenge is the design of combustion chambers, such as engines and turbines, which are enclosed by walls (3). Hydrogen's high reactivity leads to higher wall heat fluxes and thermal loads compared to hydrocarbons (4). Flame-wall interactions (FWI) generally lower combustion efficiency, affect pollutant formation, and can cause flashback.

Though thermodiffusive instabilities and FWI have been studied separately, their combined effects on near-wall flame quenching remain unexplored. Thermodiffusive instabilities impact flame structure, speed, and heat release, likely influencing FWI. Welch et al. (5) showed that lean hydrogen flame instabilities occur in real, wall-enclosed configurations, such as in spark-ignition engines.

Hence, this study aims to connect the research of thermodiffusive instabilities and flame-wall interactions by investigating two-dimensional head-on quenching of thermodiffusively unstable flames in a numerical study.

## 2 CONFIGURATION

In Fig. 1a and 1b, the numerical configuration used to generate thermodiffusively unstable flames as initial conditions for the subsequent simulations of two-dimensional HOQ and the numerical configuration used for the two-dimensional HOQ itself are shown.



(a) Schematic of the 2D computational domain for generating the thermodiffusively unstable flames. The initial flame front consists of weakly perturbed one-dimensional unstretched flames. The domain height  $L_y$  is varied.

(b) Schematic of the 2D computational domain for the HOQ of the thermodiffusively unstable flames. The flame front is mapped from the initial simulations.

Figure 1: Computational setup.

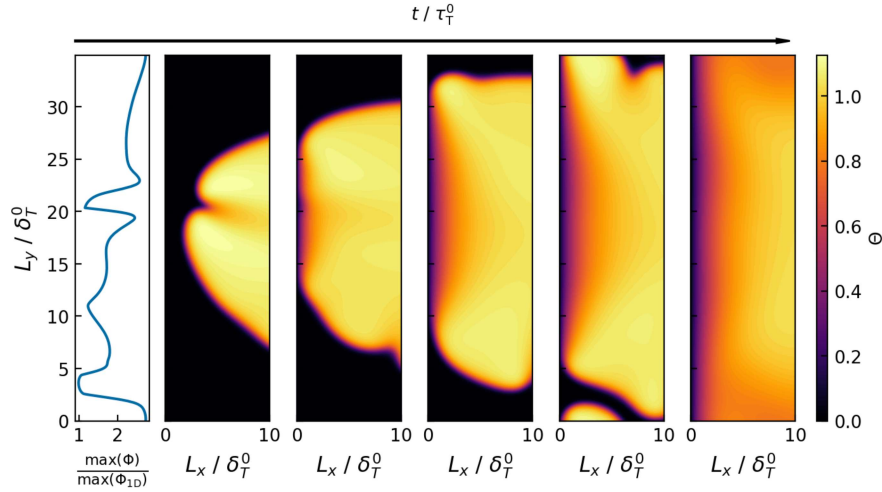


Figure 2: Left: Maximum wall heat flux  $\Phi$  of a thermodiffusively unstable flame quenching at a wall normalized by the maximum wall heat flux  $\Phi_{1D}$  of a 1D freely-propagating flame at the same conditions along the wall parallel direction. Right: Time series of a two-dimensional thermodiffusively unstable flame quenching at a wall. The colorbar shows the normalized temperature  $\Theta = \frac{T - T_{\text{unburned}}}{T_{\text{ad}} - T_{\text{unburned}}}$ .

### 3 RESULTS

In Fig. 2, a time series of a two-dimensional thermodiffusively unstable flame quenching at a wall is visualized. Compared with a one-dimensional head-on quenching under the same conditions, the maximum and the mean wall heat flux averaged along the wall parallel axis are increased.

### 4 ACKNOWLEDGMENTS

This work has been funded by the Deutsche Forschungsgemeinschaft (DFG, German Research Foundation) – Project Number 523792378 - SPP2419. The simulations were performed on the Lichtenberg high-performance computer at TU Darmstadt.

### References

- [1] S. Verhelst and T. Wallner, “Hydrogen-fueled internal combustion engines,” *Progress in Energy and Combustion Science*, vol. 35, p. 490–527, Dec. 2009.
- [2] S. M. Correa, “A review of noxformation under gas-turbine combustion conditions,” *Combustion Science and Technology*, vol. 87, p. 329–362, Jan. 1993.
- [3] A. Dreizler and B. Böhm, “Advanced laser diagnostics for an improved understanding of premixed flame-wall interactions,” *Proceedings of the Combustion Institute*, vol. 35, no. 1, p. 37–64, 2015.
- [4] L. De Nardi, Q. Douasbin, O. Vermorel, and T. Poinso, “Infinitely fast heterogeneous catalysis model for premixed hydrogen flame-wall interaction,” *Combustion and Flame*, vol. 261, p. 113328, Mar. 2024.
- [5] C. Welch, J. Erhard, H. Shi, A. Dreizler, and B. Böhm, “An experimental investigation of lean hydrogen flame instabilities in spark-ignition engines,” *Proceedings of the Combustion Institute*, vol. 40, no. 1–4, p. 105391, 2024.



# Model extension for the artificially thickened flame approach for lean hydrogen-ammonia flames

Vinzenz Schuh<sup>a,\*</sup>, Driss Kaddar<sup>a</sup>, Hendrik Nicolai<sup>a</sup>, Christian Hasse<sup>a</sup>

<sup>a</sup>*Technical University of Darmstadt (TUDa), Simulation of reactive Thermo-Fluid Systems*

*Otto-Berndt-Str. 2, 64287 Darmstadt, Germany*

*\*Email: schuh@stfs.tu-darmstadt.de*

---

## 1 Introduction

Green ammonia is a promising energy carrier for electricity generation, propulsion, and the chemical industry. Integrating ammonia into energy systems requires effective thermochemical energy conversion. However, the combustion of ammonia is limited due to, e.g., the narrow flammability limits and slow flame speed. To compensate, partial pre-cracking of ammonia to hydrogen can improve these combustion characteristics. However, hydrogen combustion poses challenges due to combustion instabilities in lean premixed flames. These instabilities can significantly impact flame dynamics, heat release rates and flame speeds, affecting safety and thermal efficiency. In lean premixed hydrogen-ammonia flames, instabilities can arise due to hydrogen's low Lewis number. Studies on 2D planar flames have characterized the impact of thermodiffusive and hydrodynamic instabilities using dispersion relations focusing on the instability development during the linear early stage [1, 2]. Additionally, research has focused on the non-linear long-term evolution of unstable flame propagation [3]. Modeling lean premixed hydrogen flames presents challenges, particularly in chemistry reduction for large eddy simulations (LES) and combustion models to reduce resolution requirements. Recent studies have explored reduced mechanisms and chemistry tabulation for chemistry reduction [4], as well as approaches like the artificially thickened flame (ATF) model [5] and filtering methods [6, 7]. In a previous study, a novel efficiency function, based on fractal theory, is derived which accurately predicts the flame consumption speed of the unstable thickened flame in the non-linear regime [8]. This study applies the model extension to turbulent conditions using the well-established slot flame [4, 9].

## 2 Results

The model extension for the ATF approach, presented in our previous study [8], is based on the scaling behavior of the instabilities relative to the thickening factor  $F$ . The characteristic length scales of thickened and unthickened flame fronts were quantified through dispersion relation analyses and statistical investigation of the length scales of the instability structures. A linear scaling relationship between instabilities and the thickening factor  $F$  was identified. It was found that the domain size where the respective instability structures arise expands with increasing  $F$ , leading to modified consumption speed increases for thickened flames. These relations were summarized in a regime map based on flame intrinsic and outer geometric length scales, which defined the requirements of the model extension. A novel efficiency formulation, leveraging the fractal-like characteristics of the instabilities, was derived from identified requirements. The model was successfully employed and evaluated in a fully coupled manner. Additionally, a dynamic formulation for determining model parameters on the fly was introduced and validated, demonstrating promising results for 2D freely propagating flames [8].

In this study, we consider the well-established turbulent slot flame to assess the performance of the developed model. To this extent, the slot flame is simulated in a fully resolved manner as well as using the traditional ATF approach. Fig. 1 shows that the original ATF formulation underpredicts the flame speed and, thus, overestimates the flame length. Applying the ATF extension significantly improves the flame length, indicating that the flame speed matches the fully resolved simulation more accurately. Additionally, the extension of the proposed model to ammonia-hydrogen flames is discussed by including an analysis of the 2D freely propagating flames with intrinsic instabilities using an ammonia-hydrogen blend.

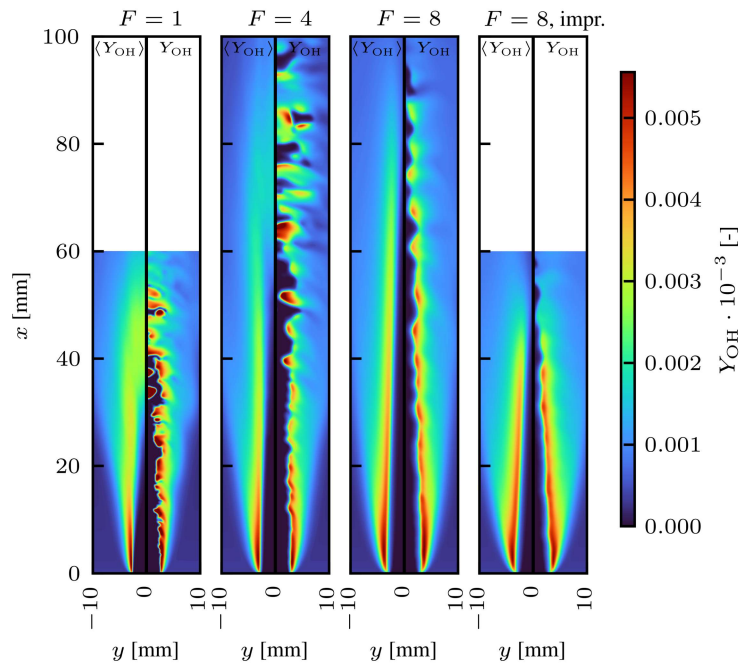


Figure 1: Results of the turbulent slot flame, fully resolved ( $F = 1$ ) [4] and applying the ATF approach with  $F = 4$  and  $F = 8$  (left to right), shown by the time-averaged and instantaneous OH mass fraction. Additionally, the model extension ("impr.") is applied to the thickened flame with  $F = 8$  on the very right flame.

### 3 Acknowledgments

This research has been funded by the German Federal Ministry for Education and Research under grant 03SF0640B. The authors gratefully acknowledge the computing time provided to them at the NHR Center NHR4CES at RWTH Aachen University (project p0020682).

### References

- [1] C. Altantzis, C. E. Frouzakis, A. G. Tomboulides, M. Matalon, K. Boulouchos, [Hydrodynamic and thermodiffusive instability effects on the evolution of laminar planar lean premixed hydrogen flames](#), J. Fluid Mech. 700 (2012) 329–361.
- [2] S. Kadowaki, T. Hasegawa, [Numerical simulation of dynamics of premixed flames: flame instability and vortex–flame interaction](#), Prog. Energ. Combust. 31 (3) (2005) 193–241.
- [3] L. Berger, K. Kleinheinz, A. Attili, H. Pitsch, [Characteristic patterns of thermodiffusively unstable premixed lean hydrogen flames](#), Proc. Combust. Inst. 37 (2019) 1879–1886.
- [4] H. Böttler, D. Kaddar, T. J. P. Karpowski, F. Ferraro, A. Scholtissek, H. Nicolai, C. Hasse, [Can flamelet manifolds capture the interactions of thermo-diffusive instabilities and turbulence in lean hydrogen flames? - An a-priori analysis](#), Int. J. Hydrog. Energy 56 (2024) 1397–1407.
- [5] H. Nicolai, L. Dressler, J. Janicka, C. Hasse, [Assessing the importance of differential diffusion in stratified hydrogen–methane flames using extended flamelet tabulation approaches](#), Phys. Fluids 34 (8) (2022) 085118.
- [6] P. E. Lapenna, R. Lamioni, F. Creta, [Subgrid modeling of intrinsic instabilities in premixed flame propagation](#), Proc. Combust. Inst. 38 (2021) 2001–2011.
- [7] P. E. Lapenna, A. Remiddi, D. Molinaro, G. Indelicato, F. Creta, [A-posteriori analysis of a data-driven filtered wrinkled flamelet model for thermodiffusively unstable premixed flames](#), Combust. Flame 259 (2024) 113126.
- [8] V. Schuh, C. Hasse, H. Nicolai, [An extension of the artificially thickened flame approach for premixed hydrogen flames with intrinsic instabilities](#), submitted to: Proc. Combust. Inst. (2024).
- [9] L. Berger, A. Attili, H. Pitsch, [Synergistic interactions of thermodiffusive instabilities and turbulence in lean hydrogen flames](#), Combust. Flame 244 (2022) 112254.

# Large eddy simulation of the KAUST piloted ammonia flame with the flamelet-generated manifold method

Xinzhou Tang, Jiangkuan Xing, Kun Luo\*, Yicun Wang, Qingqing Xue, Jianren Fan

State Key Laboratory of Clean Energy Utilization, Zhejiang University, Hangzhou, China

\*Author to whom correspondence should be addressed: [zjulk@zju.edu.cn](mailto:zjulk@zju.edu.cn)

## ABSTRACT

In this work, large eddy simulations (LES) of the KAUST piloted NH<sub>3</sub>/H<sub>2</sub> flames are conducted using the flamelet-generated manifold (FGM) method. The prediction results of LES-FGM are compared with the experimental data and satisfactory agreement between them is observed. Overall, this work demonstrates the potential of LES-FGM in predicting turbulent ammonia combustion.

## INTRODUCTION

As a carbon-free fuel, ammonia (NH<sub>3</sub>) is receiving increasing attention due to its potential to replace traditional fossil fuels. Turbulent ammonia combustion research benefits significantly from the use of large eddy simulation (LES). To accurately simulate turbulent ammonia combustion, the detailed chemical mechanism needs to be taken into account. As a well-known tabulation method, flamelet-generated manifold (FGM) [1] is an efficient method for considering detailed chemical mechanisms. The aim of this work is to explore the capability of LES-FGM method to simulate turbulent ammonia combustion. To this end, LESs of flames D and F using the FGM method are conducted and validated against the detailed experiment data.

## METHODOLOGY

For constructing the flamelet library, a total of 22 solutions of 1D freely propagating flames with various equivalence ratios are obtained using Cantera [2]. To describe the detailed chemical system, a comprehensive kinetic model of ammonia oxidation from the work of Stagni et al. [3] is adopted. All the simulations are performed using an in-house LES solver, where a one-equation eddy viscosity model [4] is used to close the subgrid stress. Flames D and F are simulated in this work and their jet configurations are listed in Table 1. The turbulent inlet of the fuel jet is constructed by imposing random turbulence with a fluctuation scale of 10% on the time-averaged velocity profile of a pipe flow. Approximately 7.2 million mesh cells are used to discretize the computational domain. The first 0.05 seconds of simulation time are used to develop turbulent structures and another 0.05 seconds are used to obtain time-averaged and root mean square (RMS) statistics. The whole simulation for flame D and flame F used 256 cores and took about 43.4 and 70.3 hours, respectively.

**Table 1** Velocities and mole fractions of the central fuel/air jet.

Flame	Bulk velocity [m/s]	$X_{O_2}$	$X_{N_2}$	$X_{NH_3}$	$X_{H_2}$
D	61.07	0.096	0.4456	0.2031	0.2553
F	91.60	0.096	0.4456	0.2031	0.2553

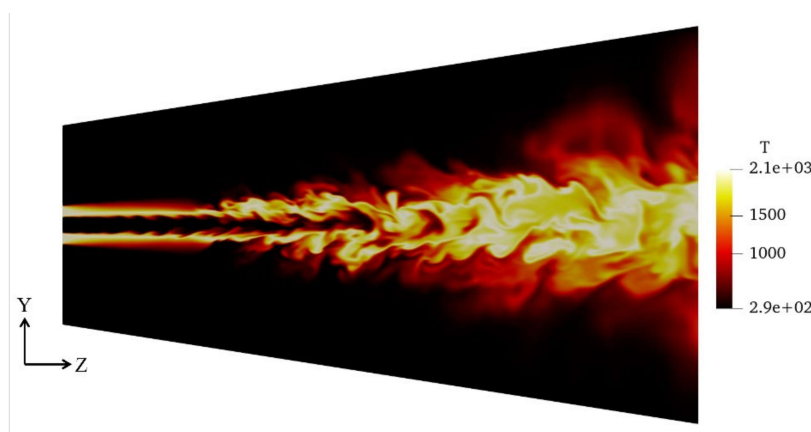


**Fig. 1** Instantaneous temperature distribution on the vertical cross-section of flame D.

## RESULTS AND DISCUSSION

The instantaneous temperature distribution on the vertical cross-section of flame D is displayed in Fig. 1. In the upstream region, the high-temperature pilot flame extends straight from the annular inlet. The fresh fuel/air mixture enters through the central nozzle and is ignited by the pilot flame at a certain distance from the nozzle. With fully developed turbulent structures, the entire flame exhibits a wrinkled front. As shown in Fig. 2, the predicted radial profiles of time-averaged values and RMS of temperature for flame D are compared with the experimental data. An overall consistency is achieved in the distribution of time-averaged temperature. There is a slight overestimation of the peak at  $Z/D = 2$ ,  $Z/D = 4$ , and  $Z/D = 6$  while the temperature near the axis is underestimated at  $Z/D = 10$ ,  $Z/D = 15$ , and  $Z/D = 20$ . This could be attributed to the weaker turbulence intensity in the simulation compared with that in the experiment, resulting in slower heat exchange between the pilot flame and the central jet. This fact can also be observed from the RMS distribution of temperature. In the upstream region, the predicted temperature fluctuations are lower than those measured experimentally. Along the flow direction, the deviations gradually decrease. Ultimately, both the time-averaged values and RMS of temperature show good agreement with the experimental measurements at  $Z/D = 30$ .

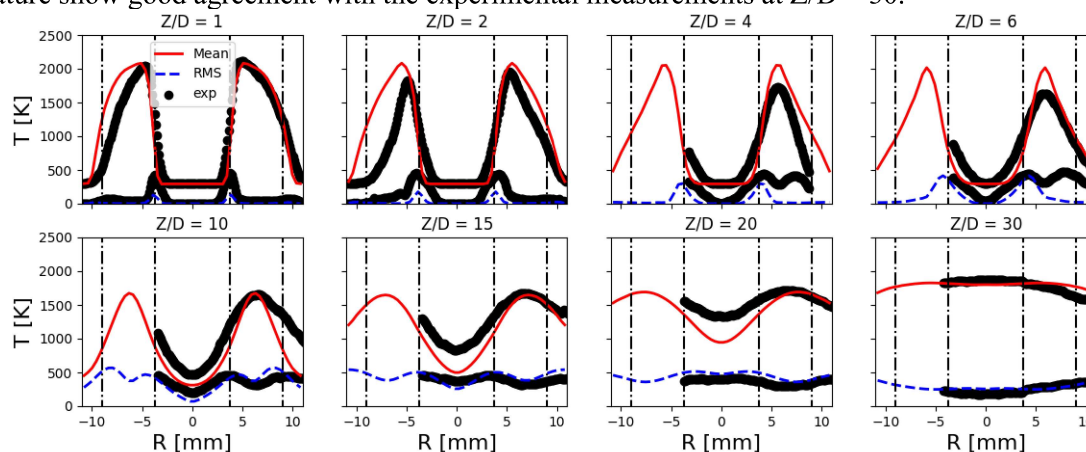


**Fig. 2** Comparisons of time-averaged values and RMS of temperature for flame D between the simulation and experiment.

In addition to temperature, comparisons between the simulation and experiment are also performed for the mixture fraction and species mole fractions. The results show that the distributions of mixture fraction, fuel, oxidizer, and major products are generally consistent with the experimental measurements. Similar results are also observed for flame F. In summary, although there are some local deviations, the simulations overall reproduce the experimental observations well.

## CONCLUSIONS

In this work, the LESs of flames D and F from the KAUST piloted ammonia flame series are conducted with the FGM method. The predicted radial distributions of temperature, mixture fraction, and species at different axial positions are compared with the experimental data. The results show that the predictions are in a good agreement with the experimental measurements. It suggests that the LES-FGM method can be applied to investigate turbulent ammonia combustion.

## REFERENCES

- [1] Oijen JAV, Goey LPHD. Modelling of Premixed Laminar Flames using Flamelet-Generated Manifolds. *Combustion Science and Technology* 2000;161:113–37.
- [2] Goodwin DG, Moffat HK, Speth RL. *Cantera: An object-oriented software toolkit for chemical kinetics, thermodynamics, and transport processes*, vol. 124. Pasadena, CA: Caltech; 2009.
- [3] Stagni A, Cavallotti C, Arunthanayothin S, Song Y, Herbinet O, Battin-Leclerc F, et al. An experimental, theoretical and kinetic-modeling study of the gas-phase oxidation of ammonia. *React Chem Eng* 2020;5:696–711.
- [4] Yoshizawa A. Statistical theory for compressible turbulent shear flows, with the application to subgrid modeling. *Physics of Fluids* 1986;29:2152–64.

# The impact of molecular mixing in composition space and differential diffusion in physical space on turbulent non-premixed $\text{NH}_3/\text{H}_2/\text{N}_2$ jet flames at elevated pressures

Lu Tian<sup>1,2</sup> and R. Peter Lindstedt <sup>\*2</sup>

<sup>1</sup>Department of Aeronautical and Automotive Engineering, Loughborough University, LE11 3RS, United Kingdom

<sup>2</sup>Department of Mechanical Engineering, Imperial College London, SW7 2AZ, United Kingdom

Green ammonia may provide an attractive alternative carbon-free fuel despite unfavourable combustion properties. The latter include slow chemistry resulting in low flame speeds and long ignition delay times coupled with potentially high emissions of oxides of nitrogen. The modelling challenges become particularly acute in practical applications featuring turbulent flows due to dominant turbulence-chemistry interactions that make the use of presumed combustion mode based models with limited time-scale linkages between flow and chemistry inappropriate. Transported joint probability density function (JPDF) methods can incorporate detailed chemistry without approximation and accurately represent turbulence-chemistry interactions [1]. Significant amounts of hydrogen are formed from the cracking of ammonia leading to more reactive mixtures and the need to consider differential molecular diffusion at low to intermediate Reynolds numbers. McDermott and Pope [2] delineated Molecular Transport in Physical Space (MTPS) and molecular mixing in composition space. The former is usually neglected at higher Reynolds numbers with molecular mixing commonly treated using the modified Curl's (MC) [3], Euclidean Minimum Spanning Tree (EMST) [4] or Multiple Mapping Closures (MMC) [5] closures. Simatos et al. [6] included MTPS into JPDF computations of an auto-ignition stabilised methane flame at a Reynolds number of 28,000 and showed a strong influence on computed  $\text{H}_2$  levels. The current study uniquely considers the impact of molecular mixing models combined with MTPS on the modelling of the elevated pressure (5 atm) KAUST  $\text{NH}_3/\text{H}_2/\text{N}_2$  CAJF14 and CAJF28 flames ( $\text{Re} = 11,200$ ) [7]. Detailed chemistry [8] is included without approximation through the JPDF approach. The impact of MTPS is further explored via pre-heated fuel mixtures over a pressure range from 10 to 20 atm while maintaining the Reynolds numbers. Results for CAJF28 ( $\text{NH}_3:\text{H}_2:\text{N}_2=0.563:0.328:0.109$ ) are presented to explore the impact of differential diffusion of hydrogen. The impact of MTPS is explored via a coupling with either MC or EMST as illustrated in Fig. 1. It can be seen that EMST provides better agreement with measurements for both mean and RMS of temperature at  $x/D = 40$  and  $x/D = 60$ . The impact of MTPS on mean temperatures is modest, but tends to lead to an underprediction of the RMS far downstream. This discrepancy was not consistent for other scalars. The radial profiles of the hydrogen mass fraction are presented in Fig. 1 with MTPS improving both mean and RMS – particularly at  $x/D = 40$ . The current study also explored the IEM mixing model as an alternative to MC and EMST and it was found to require much stronger flame ignition and to overestimate the hydrogen mass fraction. Practical applications (e.g., gas turbines) usually feature much higher pressures and preheated fuel mixtures. The current study uses the same fuel composition as CAJF28, but increases the temperature of the fuel mixture to 600 K at higher pressures from 10 to 20 atm while maintaining the same Reynolds number of 11,200. The impact of MTPS on temperature and the hydrogen mass fraction at 10 and 20 atm is presented in Fig. 2. The impact of MTPS remains modest at 10 atm with a more notable impact beyond  $x/D = 10$  at 20 atm. At 10 atm, MTPS provides a marginally lower peak mean hydrogen mass fraction at  $x/D = 40$ . The impact is estimated to be significant at 20 atm with a factor of two difference at  $x/D = 40$ . Further data, including statistics at different pressure conditions will be presented in the poster.

## References

- [1] S.B. Pope, Prog. Energy Combust. Sci. 11 (1985) 119–192.

\*Corresponding author: r.p.lindstedt@imperial.ac.uk



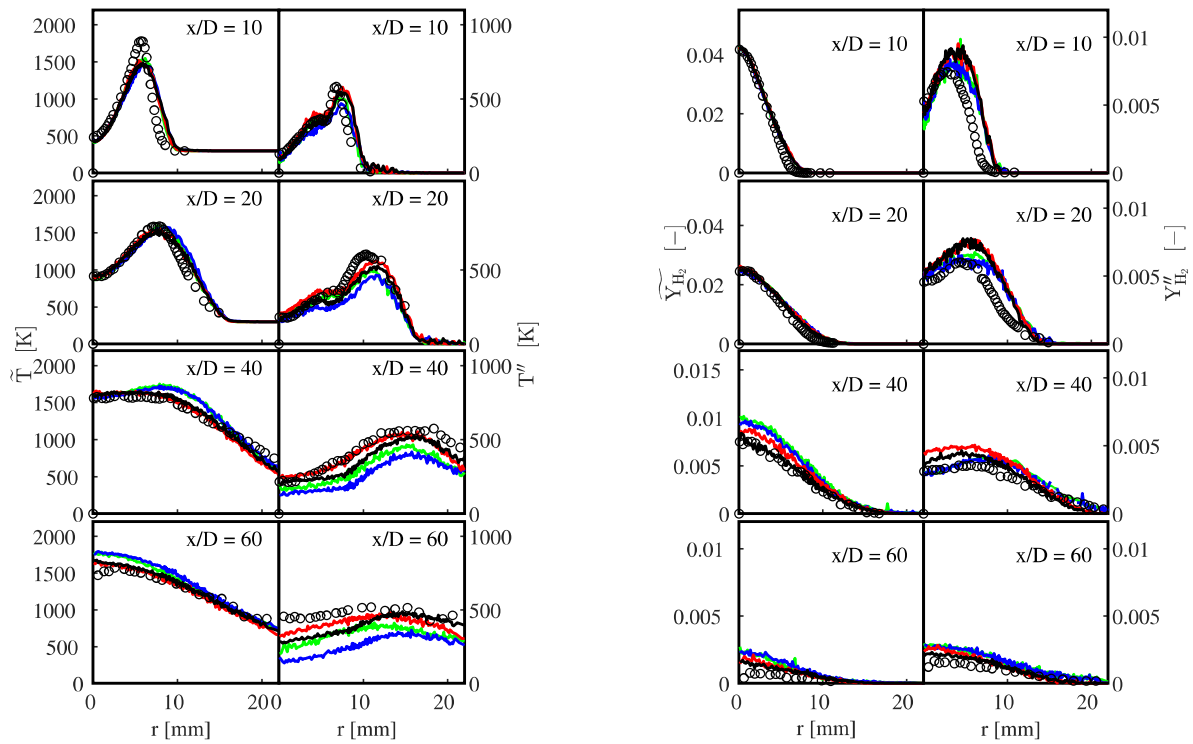


Figure 1: Radial profiles of mean and RMS of temperature (left) and  $H_2$  mass fraction (right) for CAJF28. Symbols: (o) Measurements [7]; Lines: (—) EMST + MTPS; (—) EMST; (—) MC + MTPS; (—) MC.

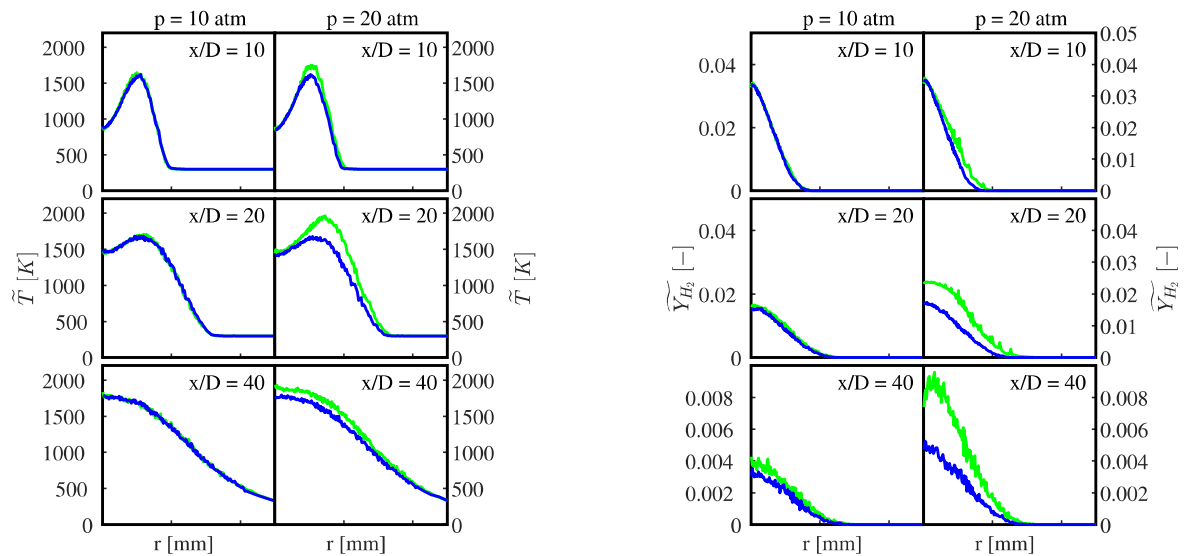


Figure 2: Radial profiles of predicted mean temperatures (left) and mean  $H_2$  mass fractions (right) at  $p = 10$  and  $20$  atm (composition as CAJF28) based on EMST. Lines: (—) MTPS; (—) without MTPS.

- [2] R. McDermott, S.B. Pope, *J. Comput. Phys.* 226 (2007) 947–993.
- [3] J. Janicka, W. Kolbe, W. Kollmann, *J of Non-Equil. Thermody.* 4 (1979) 47–66.
- [4] S. Subramaniam, S.B. Pope, *Combust. Flame* 115 (1998) 487–514.
- [5] A.P. Wandel, R.P. Lindstedt, *Proc. Combust. Inst.* 37 (2019) 2151–2158.
- [6] P. Simatos, L. Tian, R.P. Lindstedt, *Combust. Flame* 239 (2022) 111665.
- [7] H. Tang, C. Yang, G. Wang, Y. Krishna, T.F. Guiberti, W.L. Roberts, G. Magnotti, *Combust. Flame* 244 (2022) 112292.
- [8] D. Greenblatt, L. Tian, R. Lindstedt, *Combust. Flame* (2023) 112733.

# Direct Numerical Simulation of Flames in high-speed flows

Gunvir Singh Walia<sup>1,\*</sup>, Sebastian Galindo-Lopez<sup>2</sup>, Matthew J. Cleary<sup>2</sup> and Santanu De<sup>1</sup>

<sup>1</sup> Department of Mechanical Engineering, Indian Institute of Technology, Kanpur, India

<sup>2</sup> School of Aerospace, Mechanical and Mechatronic Engineering, The University of Sydney, NSW 2006, Australia

Email: [gunvirs@iitk.ac.in](mailto:gunvirs@iitk.ac.in)<sup>1,\*</sup>

Scalar mixing and combustion in high-speed aerospace propulsion devices like Rotating Detonation Engines (RDE) and Scramjets involve the presence of both low and high-speed flow features along with discontinuities like shocks and contact surfaces. Accurate resolution of the intricate low Mach turbulent flow features along with a good resolution of shocks and contacts prevalent in such flows pose challenges for most of the conventional shock capturing schemes exhibiting higher numerical dissipation. To this end, an OpenFOAM based solver using an all-speed AUSM<sup>+</sup>up (Advection Upstream Splitting Method) flux scheme (Liou 2006) has been developed and validated by performing a Direct Numerical Simulation (DNS) of an available temporally evolving supersonic reacting shear layer configuration. The computational domain under consideration has been adopted from the supersonic reacting shear layer simulated previously by Gibbons et al. (2019). The database of Gibbons was generated by University of Minnesota's well-established compressible finite volume CFD solver *US3D* having a 6<sup>th</sup> order gradient reconstruction for the inviscid fluxes and therefore it serves as a good validation test case. In the present work, the three-dimensional instantaneous Navier-Stokes equations along with the multicomponent species and energy transport equations are solved in conservative, finite volume form using the AUSM<sup>+</sup>up methodology. The Lewis Number is set to 1.4 similar to Gibbons et al. (2019). The simulations are validated using spatially averaged mean quantities against the simulations of Gibbons et al. (2019) and our results (Fig. 1) show a good agreement with the results of Gibbons. The effect of inclusion of the enthalpy diffusion flux (inter-diffusion flux) term in the energy transport for non-unity Lewis number is also assessed, demonstrating a low sensitivity to its inclusion in comparison to the results neglecting it.

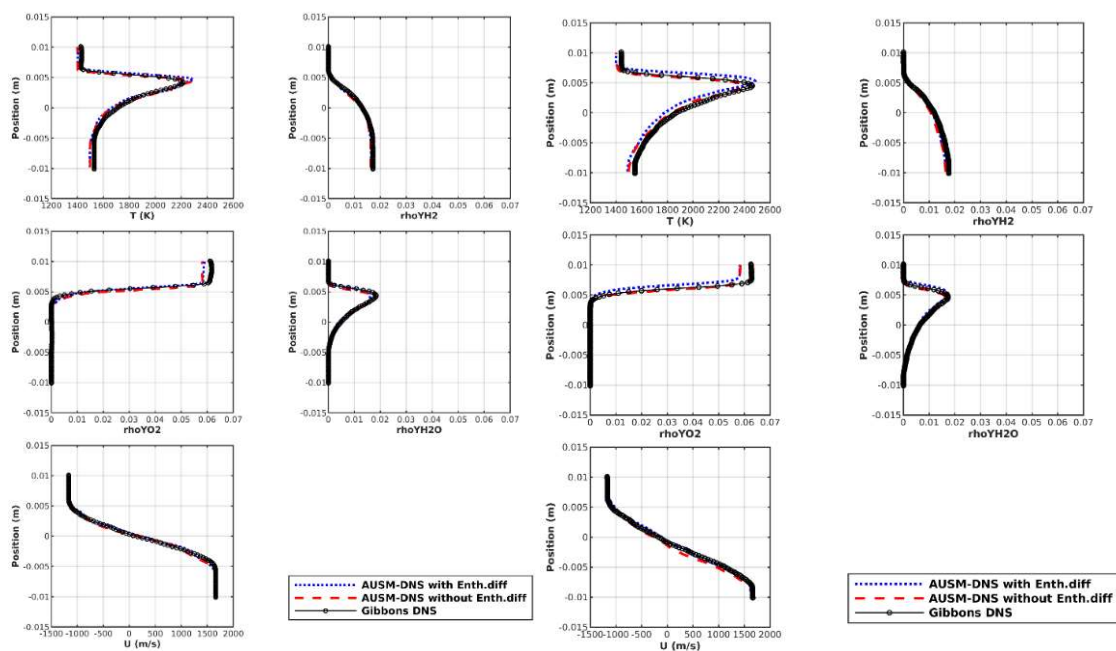


Figure 1. Validation with Gibbons' DNS at 40 (left) and 80 (right)  $\mu$ s time instants with the present simulation (AUSM-DNS) with and without enthalpy diffusion flux term in the energy transport equation.

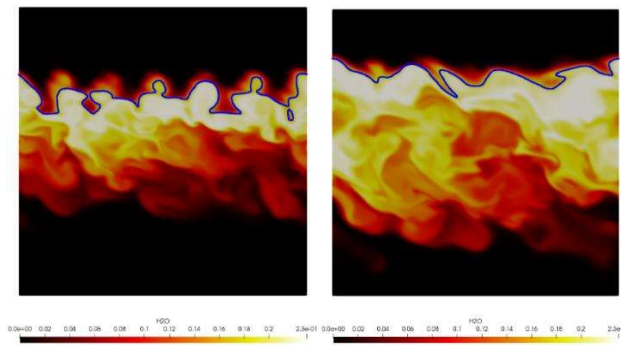


Figure 2. Snapshots of product (water) specie mass fractions at 40 (left) and 80 (right)  $\mu$ s time instants. Blue line shows the iso-line of stoichiometric mixture fraction.

Further, the generated DNS database was used to gain some insights to support the future model development for such flames. The flame structure was analysed which revealed a distinct compressive pressure-work heating effect along with the usual chemical heat release, which is evident through the significant pressure induced fluctuations in the temperature (T) and sensible enthalpy (h) conditional scatter plots in Fig.3. This indicates the necessity of accurate modelling of the physics of pressure-work effect in turbulence-chemistry interaction models for such flames. Overall, a fully burning diffusion flame structure was observed. Good correlation of the sensible enthalpy (h) with mixture fraction (Z) was observed, indicating the suitability of Z as a marker of localness in the composition space for the case under consideration. This is particularly relevant for deciding the reference or conditioning variable for the Generalised Multiple Mapping Conditioning (MMC) and Conditional Moment Closure (CMC) based turbulent combustion modelling approaches.

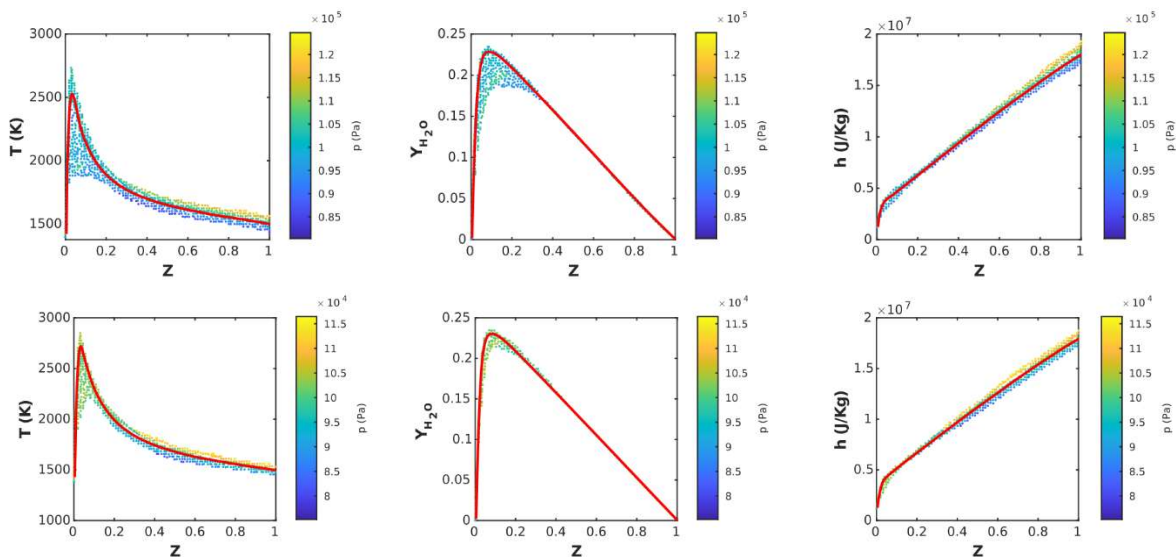


Figure 3. Scatter plots of Temperature (left), water specie mass fraction (middle) and sensible enthalpy (right) conditioned on mixture fraction (Z) coloured by pressure (p). Red line shows the conditional mean. 40 (top row) and 80 (bottom row)  $\mu$ s time instants.

## References

- Gibbons N., Wheatley V. Combustion Regime Analysis of a Supersonic Turbulent Mixing Layer. *Australian Combustion Symposium 2019*.
- Liou, M.S., 2006. A sequel to AUSM, Part II: AUSM+-up for all speeds. *Journal of Computational Physics*, 214 (1), pp.137-170.

# Large eddy simulation of the KAUST piloted ammonia flame with the direct moment closure model

Yicun Wang, Jiangkuan Xing, Kun Luo\*, Xinzhou Tang, Qingqing Xue, Jianren Fan

State Key Laboratory of Clean Energy Utilization, Zhejiang University, Hangzhou, China

\*Author to whom correspondence should be addressed: [zjulk@zju.edu.cn](mailto:zjulk@zju.edu.cn)

## ABSTRACT

In this study, our previously proposed direct moment closure (DMC) model is applied to the large eddy simulation (LES) of the KAUST piloted ammonia flame from the TNF workshop. The simulation results are compared with the experimental data for model validation. The LES-DMC results show a good agreement with the experimental measurements in terms of the quantitative statistics of temperature and mixture fraction. The simulation results validate the predictive capability of the DMC model for ammonia combustion.

## INTRODUCTION

Ammonia ( $\text{NH}_3$ ) is considered a promising hydrogen carrier and carbon-free fuel to achieve the goals of reducing carbon emissions and sustainable energy use. Large eddy simulation (LES) is an important tool for the research of turbulent ammonia combustion. To accurately simulate turbulent ammonia combustion, high-fidelity turbulent combustion models need to be developed to account for the complex turbulence-chemistry interactions. In our previous studies, we proposed a direct moment closure (DMC) model [1, 2], originally from the second-order moment model [3]. The DMC model is methodologically applicable to different combustion regimes and has been extended to multi-step reactions with higher-order moments closed. The previous validation of the DMC model focused on flame configurations of conventional hydrocarbon fuels. In this study, the DMC model is further applied to simulate a benchmark configuration of KAUST piloted  $\text{NH}_3/\text{H}_2$  flame [4] from the TNF workshop.

## METHODOLOGY

The KAUST piloted  $\text{NH}_3/\text{H}_2$  flame D [4] from the TNF workshop is selected as the target configuration, which is composed of three inlet streams, i.e. jet, pilot, and coflow. The computational domain is a cylinder with a diameter of  $20D$  and a length of  $40D$ , which is discretized by a grid number of  $1.89 \times 10^6$ . The skeletal chemistry mechanism [5] containing 31 species and 203 reactions is used. The subgrid-scale stress tensor is modeled using the Smagorinsky model. The direct moment closure (DMC) model [1, 2] is utilized for the modeling of turbulence chemistry interactions (TCI). The boundary conditions are velocity inlet and pressure outlet. The velocities of the pilot and coflow are set to the fixed value of 6.55 m/s and 0.8 m/s, respectively. The inlet boundary of the fuel jet velocity is set as the turbulent inlet with a fluctuation scale of 10%. The inlet boundary conditions for temperature and species mass fractions are summarized in Table 1. The simulation end time is 0.08 s and the last 0.04 s is used to make statistics to get the mean and RMS values. The total computational cost is 58880 core-hours.

**Table 1** Inflow parameters of the KAUST piloted  $\text{NH}_3/\text{H}_2$  flame D.

Parameters	Jet	Pilot	Coflow
$T$ [K]	293.5	2047	296.6
$Y_{\text{O}_2}$ [-]	0.1574	0.0203	0.232
$Y_{\text{N}_2}$ [-]	0.6394	0.7746	0.768
$Y_{\text{NH}_3}$ [-]	0.1770	0	0
$Y_{\text{H}_2}$ [-]	0.0262	0	0
$Y_{\text{H}_2\text{O}}$ [-]	0	0.2033	0
$Y_{\text{OH}}$ [-]	0	0.0018	0

## RESULTS AND DISCUSSION

Only partial results are shown here for simplicity. Figures 1 and 2 show the radial profile of the time-averaged values and *rms* fluctuations of temperature and mixture fraction for flame D. In the statistics of the mean temperature, the DMC model can accurately capture the peak values and spatial distribution at the upstream locations of  $z/D = 1 \sim 10$ . The temperature near the axis is underestimated at locations of  $z/D = 15$  and 20, which

is attributed to the insufficient development of turbulence in the simulation compared with the experiments. This can also be supported by the underprediction of *rms* fluctuations of temperature. Compared to the temperature prediction, the simulation results of the mixture fraction show a better agreement with the experimental measurements, as shown in Fig. 2. Overall, the DMC model exhibits excellent performance in predicting the spatial distribution of temperature and mixture fraction.

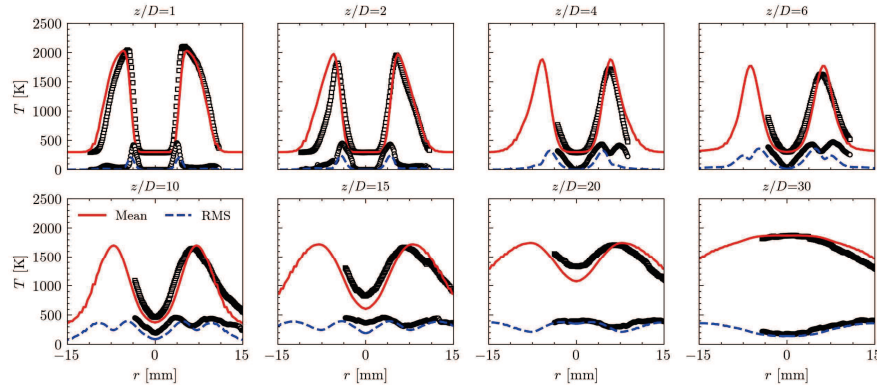


**Fig. 1** Radial profiles of time-averaged values and *rms* fluctuations of temperature for the flame D at various axial locations. Lines: LES mean (solid), LES *rms* (dash-dot); symbols: experimental data.

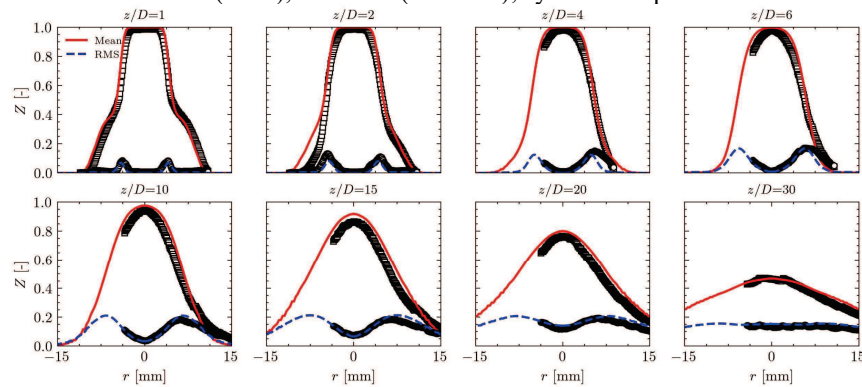


**Fig. 2** Radial profiles of time-averaged values and *rms* fluctuations of mixture fraction for the flame D at various axial locations. Lines: LES mean (solid), LES *rms* (dash-dot); symbols: experimental data.

## CONCLUSIONS

In this work, the DMC model has been incorporated with LES and used to simulate the KAUST piloted ammonia flame. The simulation results using the LES-DMC method are compared with experimental data for model validation. The LES-DMC results show good agreement with the experiment data in terms of the radial distribution of mean and fluctuation values of the temperature and mixture fraction. The mass fractions of major and minor species at different axial locations are also well predicted. Overall, the DMC model is well-validated and shows great potential for future application in ammonia combustion modeling.

## REFERENCES

- [1] R. Z. Liu, K. Luo, C. C. Song, T. Jin, M. Chai, and J. R. Fan, "Large eddy simulation of a turbulent supercritical hydrothermal flame with a novel direct moment closure model," *Fuel*, 332, (2023).
- [2] K. Luo, R. Liu, Y. Bai, A. Attili, H. Pitsch, F. Bisetti, and J. Fan, "A-priori and a-posteriori studies of a direct moment closure approach for turbulent combustion using DNS data of a premixed flame," *Proc. Combust. Inst.*, 38, pp. 3003-3011, (2021).
- [3] L. X. Zhou, L. Y. Hu and F. Wang, "Large-eddy simulation of turbulent combustion using different combustion models," *Fuel*, 87, pp. 3123-3131, (2008).
- [4] Magnotti G., Tang H., Barlow R., Piloted NH<sub>3</sub>/H<sub>2</sub>/N<sub>2</sub>/air flames J, D-E and F. Pre-release 1.0, Feb. 7th, 2024.
- [5] A. Stagni, C. Cavallotti, S. Arunthanayothin, Y. Song, O. Herbinet, F. Battin-Leclerc, and T. Faravelli, "An experimental, theoretical and kinetic-modeling study of the gas-phase oxidation of ammonia," *REACT. CHEM. ENG.*, 5, pp. 696-711, (2020).



# A direct numerical simulation study on the KAUST piloted cracked ammonia flame with detailed chemistry

Jiangkuan Xing<sup>a,\*</sup>, Kun Luo<sup>b</sup>, Ryoichi Kurose<sup>a</sup>

<sup>a</sup>Department of Mechanical Engineering and Science, Kyoto University, Kyoto daigaku-Katsura, Nishikyo-ku, Kyoto, Japan

<sup>b</sup>State Key Laboratory of Clean Energy Utilization, Zhejiang University, Hangzhou, China

\*Corresponding email address: [xing.jiangkuan.6h@kyoto-u.ac.jp](mailto:xing.jiangkuan.6h@kyoto-u.ac.jp)

## Abstract

This study reports a direct numerical simulation (DNS) on the KAUST piloted cracked ammonia flame D with detailed chemistry, using 112 million computational grids. The reaction mechanism developed by Shrestha et al. [Pro. Combust. Inst. 2021, 38(2), 2163-2174] is used to account for the combustion chemistry. The species diffusivity is considered with the mixture-averaged approach. The predicted radial mean and *rms* profiles of temperature and mass fractions of NH<sub>3</sub>, H<sub>2</sub>O, and H<sub>2</sub> are compared with the experimental data. Overall, good agreements can be achieved for both the upstream and downstream locations for the mean profiles, while for the *rms* profiles, more statistics are needed. The DNS data will also be used to develop advanced turbulent combustion models in future work.

## Introduction

The low combustion intensity is one of the main challenges for using ammonia as a fuel for combustion [1]. Cracked ammonia (NH<sub>3</sub>) is considered a promising strategy to enhance NH<sub>3</sub> combustion [2,3], which features a fuel mixture of NH<sub>3</sub>, N<sub>2</sub>, and H<sub>2</sub>. Prior efforts mainly focused on measuring the fundamental combustion properties and establishing the reaction kinetics. Recently, KAUST has performed a detailed measurement of piloted turbulent cracked ammonia flames [4]. As a complicated dual-fuel mixture, accurate and efficient modeling of cracked ammonia is still an open question. Direct numerical simulation (DNS) has proven to be an effective approach to study combustion physics and useful for developing turbulent combustion models, as demonstrated in many previous studies [5,6]. In the present study, we performed a direct numerical simulation for the target flame D. The results are compared with the experimental data, including the radial mean and *rms* profiles of species and temperatures.

## Methodology

The target KAUST flame D is investigated using DNS with detailed chemistry. No turbulence or combustion models are used. The computational domain is a cylinder with a length of 40D, and its diameter gradually varies from 15D to 25 D. This design is based on the fact that the Kolomogrov scale is small in the upper stream and gradually increases with jet expansion. The minimum grid size is about 20 μm in the jet edge region and gradually increases to 50 μm at downstream locations. The reaction mechanism developed by Shrestha et al. [7] is used to account for the combustion kinetics. The mixture-averaged approach is used to consider species diffusivity. For the central fuel stream, a fully developed turbulent pipe flow, which is obtained by performing cold flow DNS calculations, is used. For the pilot stream and air coflow stream, a laminar uniform profile is used due to the high viscosity and low velocity, respectively. It is noted that here the pilot stream is set as a fully-burnt mixture, and the velocity is adjusted based on the provided mass flow rate. The boundary conditions of scalar variables are consistent with the experimental data. The whole simulation time is 40 ms. The first 25 ms are used to develop the flow, and the rest 15 ms are used to make statistics. The DNS calculation is performed with an in-house solver on the supercomputer Fugaku by parallel computation using 8920 cores for 840 hours.

## Results and discussion

Due to the page limitation, only part of the results are presented here. Figure 1 shows the flame structure and instantaneous distribution of temperature, oxygen, and ammonia at different streamwise locations. Figure 1 shows the comparison of the radial mean and *rms* profiles of the temperature and mass fractions of interested species (only NH<sub>3</sub>, H<sub>2</sub>, and H<sub>2</sub>O are shown for brevity). For the upperstream location  $Z/D=1$ , the radial mean and *rms* profiles of temperature and species can be well reproduced. While for the  $Z/D=2$ , the pilot flame region is overestimated. For the downstream locations, including  $Z/D=10$  and  $Z/D=15$ , good agreements can also be achieved for the predictions of mean temperature and mass fractions of NH<sub>3</sub>, H<sub>2</sub>, and H<sub>2</sub>O. However, the *rms* profiles are largely underestimated, especially in the jet-central locations. This indicates that more statistical time is needed, and we are now performing the further calculations.

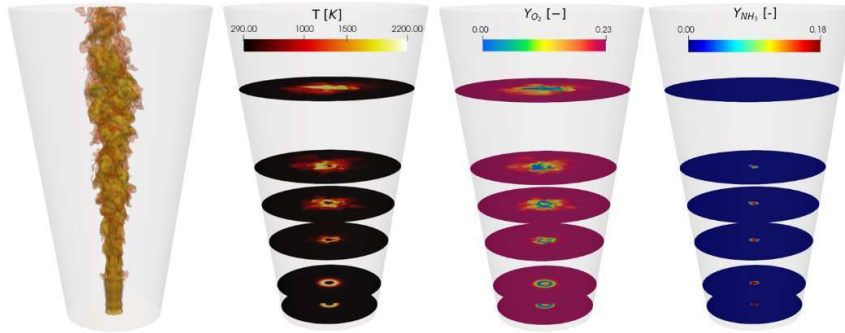


**Figure 1** Flame structure represented by temperature iso-value surfaces and instantaneous distribution of temperature, oxygen and ammonia at different streamwise locations

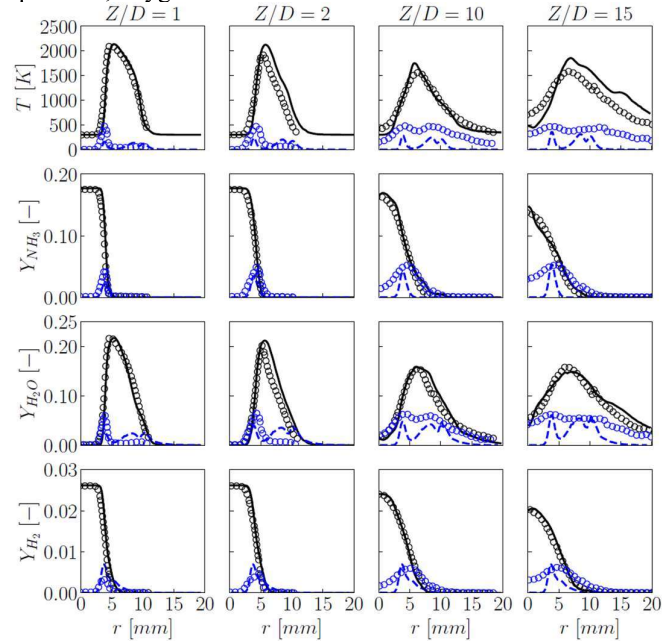


**Figure 2** Radial mean (black) and *rms* (blue) profiles of the temperature and mass fractions of interested species measured in the experiments (scatter) and predicted in the DNS (line).

## Conclusion

In the present work, a DNS study on the KAUST cracked flame D with detailed chemistry is reported. The DNS results are compared with the experimental data. Overall, the DNS can well reproduce the experimental data. Specifically, the radial mean profiles of temperature and species mass fractions can be well reproduced by the DNS. The *rms* profiles can be well reproduced at upper-stream locations but underestimated at downstream locations, indicating the need for a longer statistical time. In our future work, we will further use the DNS data to develop advanced turbulent combustion models.

## References

- [1] Xing J., Pillai A.L., Kurose R., *Appl. Energy Combust. Sci.*, 2023, 15, 100193.
- [2] An Z., Zhang W.J., Zhang M., et al., *Energy Fuels*, 2024, 38 (8), 7412-7430.
- [3] Mei B., Zhang J., Shi X., et al., *Combust. Flame*, 2021, 231, 111472.
- [4] Tang H., Yang C., Wang G., et al., *Combust. Flame*, 2022, 244, 112292.
- [5] Xing J., Luo K., Kurose R., et al., *Pro. Combust. Inst.*, 2023, 39 (3), 3227-3237
- [6] Domingo P., Vervisch L., *Pro. Combust. Inst.*, 2023, 39(2), 2055-2076.
- [7] Shrestha K.P., Lhuillier C., Barbosa A.A., et al., *Pro. Combust. Inst.*, 2021, 38(2), 2163-2174.